ITERATIVE LEARNING CONTROL OF MULTIVARIABLE PLANTS

by

Samir Sami Mohamed

A Thesis submitted for the Degree of Doctor of Philosophy

of the

University of Salford

Department of Aeronautical and Mechanical Engineering

April 1992

ACKNOWLEDGEMENTS

I wish to express my sincere appreciation and thanks to my supervisor, Professor B. Porter, for his friendship, supervision and encouragement during the course of the research, and for his patience and understanding during the writing of this thesis.

Many thanks are due to Professor A.S. Hassan at the University of Baghdad for his support.

I would also like to thank my wife and my parents for their moral support throughout the course of this research, and I therefore dedicate this thesis to them.

Finally, I wish to express my thanks to the Iraqi Government for offering me the scholarship to pursue my higher education.

SYNOPSIS

In recent years, many researchers have proposed different iterative learning controllers, which unfortunately mostly require that the plants under control be regular. Therefore, in order to remove this limitation, various analogue and digital iterative learning controllers are proposed in this thesis.

Indeed, it is shown that analogue iterative learning controllers can be designed for plants with any order of irregularity using initial state shifting or initial impulsive action. However, such analogue controllers have to be digitalised for purpose of implementation. In addition, in the synthesis of their control laws, such controllers require some knowledge of the plants' Markov parameters. Therefore, new digital iterative learning controllers are proposed. Such digital controllers circumvent the need for detailed mathematical models of the plants in any form. Indeed, the proposed digital iterative learning controllers rely on input/output data in the synthesis of their control laws. It is shown that digital iterative learning controllers can be readily designed for multivariable plants of any order or irregularity using only such input/output data in the form of step-response matrices.

The learning rates achievable in both the analogue and digital iterative learning control of linear multivariable plants are investigated. It is shown that the irregularity and stability characteristics of the plants under control impose severe constrains on the achievable learning rates. Indeed, it is shown that the learning parameter in the case of digital iterative learning controllers increases as the order of plant irregularity increases. This increase in the learning parameter affects the learning performance and the speed of convergence adversely. This discovery led to the introduction of compensators in the design of digital iterative learning controllers for irregular plants

which help to improve the learning performance and convergence by reducing the effective learning parameter. Since such digital iterative learning controllers use step-response matrices in the synthesis of their control laws and since the step-response characteristics can be identified in real time, it is shown in this thesis that iterative learning controllers can readily be rendered adaptive in case plant dynamics are initially unknown or time-varying.

In order to demonstrate the applicability of these results to the control of robotic manipulators, both analogue and digital iterative learning controllers are designed for a two-link manipulator in both joint and task spaces. Finally, digital iterative learning controllers are designed and practically implemented in the real-time positional control of a dc servo actuator.

CONTENTS

PART I

INTRODUCTION TO ITERATIVE LEARNING CONTROL

CHAPTER 1

1.1 INTRODUCTION

In recent years, control has played a vital role in the progress of engineering and science. It has become an important part of modern manufacturing and industrial processes. Thus, for example, control systems are found in all sectors of industry, such as computer-controlled machine tools, automatic assembly lines, aerospace systems, power systems, robotics, and many others. In addition, developments in the theory and practice of control have provided improvements in the quality of products, decreases in the costs of production, and increases in production rates. These various control systems are different in their design, principle, and methodology. Indeed, from the viewpoint of principle of operation, control systems can be classified into three categories as follows:

(a) non-adaptive systems;

(b) adaptive systems;

(c) learning systems.

Thus, for example, non-adaptive control systems are systems mainly associated with feedback control techniques, whereby the actual output of the plant is compared with the desired output and then an actuating error signal is formed. The controller then takes an appropriate action based on that signal so as to reduce the error and bring the output of the plant to a desired value. However, in order to design such controllers, prior knowledge of the plant dynamics is required. This is usually obtained by using some form of off-line identification scheme whereby the plant parameters are estimated. In addition, such controllers can be designed and implemented for plants

with either non-repetitive or repetitive tasks. However, implementing such controllers on plants with repetitive tasks will never progressively eliminate any error which might exist in the first trial. In other words, these devices do not improve their performance as the plant repeats its task.

Adaptive control sytems are systems which have the ability to self-adjust by tuning their own parameters so as to accommodate large changes in the plant parameters and environment, in order to maintain optimal performance. However, designing adaptive controllers does not require prior knowledge of the plant dynamics. This knowledge is usually obtained by using some form of on-line identification scheme whereby the plant parameters are estimated. Thus, adaptive control is closely related to the problem of system identification. Indeed, an adaptive controller can be viewed as being composed of two parts: the first part is where some or all of the plant parameters under control are identified and the second part is where such identified parameters are used to design and form a control law. Thus, in adaptive control systems, the dynamic plant characteristics must be identified at all times so that the controller parameters can be adjusted in order to maintain optimal performance. This means that the adaptive controller will not work without knowing the plant dynamics. However, even with such knowledge, adaptive controllers are in general unable to improve their performance as the plant repeats its task.

Learning control systems are systems in which the controller has the ability to learn from past experience and accordingly improve its performance progressively, just like a human operator. Various intelligent control schemes have been investigated and implemented practically, such as fuzzy logic control, expert system control, iterative learning control, and most recently neural control. The feature which makes investigating and implementing intelligent control schemes worthwhile is that there are now so many industrial processes where plants cannot be well-controlled using non-

adaptive or adaptive control because of the absence of plant models (for instance, metal-cutting machines, production systems, and steel furnaces, etc (Ward et al, 1990)). Therefore, in such cases some form of intelligent control is required. Moreover, modern industry requires machines to be more intelligent in order to lower the cost of production, improve safety standards in hazardous environments, and indeed increase rates of production.

In this thesis, new iterative learning controllers are investigated and practically implemented. These controllers embody iterative learning algorithms in which the $(k+1)th$ input to the plant, $u_{k+1}(t)$, consists of the kth input, $u_k(t)$, together with an increment formed from the difference between the desired output, $v(t)$, and the kth actual output of the plant $y_k(t)$. Thus, such controllers are designed and implemented for plants with repetitive tasks only. Furthermore, designing such controllers requires little or no information about the plant dynamics. In fact, the only information which might be required is input/output information concerning the step-response matrix of the plant under control. This step-response matrix can be obtained by performing an open-loop test on the plant. Thus, unlike non-adaptive and adaptive controllers, these iterative learning controllers have the ability to improve their performance progressively as the machines repeat their tasks. In addition, these controllers have the edge over adaptive controllers in controlling plants with significant non-linear characteristics. This is because adaptive control systems usually exhibit some delay while they are adjusting themselves in response to newly identified plant characteristics. This delay arises because it often takes several control intervals to detect and account for significant variations in the plant dynamical characteristics (e.g, due to nonlinearity). This results in degradation in the system performance because of the lack of the correct information at the right time. However, in the case of repetitive tasks, this heavy burden of trying to identify the non-linear part of the plant dynamics by the use of adaptive controllers can

frequently be eliminated by using iterative learning controllers. This is because such controllers provide excellent feedforward compensation for the plant dynamics as the machine repeats its motion.

However, it might be argued that good adaptive controllers can be designed to deal with all types of plant dynamic variations in the case of either repetitive or unrepetitive tasks. But why design a very complicated and probably expensive adaptive controller when a simpler and cheaper iterative learning controller can perform even better? After all, in industry today many machines repeat their task over and over in cycles, so why not learn from past experience and minimise, if not eliminate, the error in the system performance altogether? These considerations motivate the study of iterative learning control.

1.2 LITERATURE SURVEY OF ITERATIVE LEARNING CONTROLLERS

Human beings have the ability to learn from past experience and through practice. Athletes improve their form of body motion by learning through repeated training, babies begin their course of learning from the beginning of their lives, learning how to talk, walk, communicate, etc, and skilled human operators master the operation of machines by acquiring skill in practice and gaining knowledge from experience. By taking all this into account, it is widely believed that humans can learn from experience but that machines cannot. In order to make robots and machines able to learn from their previous trials, such devices have to be provided with some of the attributes of human beings, such as sensors and memory. Therefore, in recent years much attention has been devoted to the design of new controllers called 'iterative learning controllers' which improve their performance progressively as machines repeat their tasks. These controllers embody iterative learning algorithms in which the $(k+1)th$ input to the plant consists of the kth input together with an increment formed

from the difference between the pre-specified desired trajectory and *kth* output from the plant. In this way, machines are able to improve their performance as they repeat their tasks without the help of human operators.

Uchiyama (1978) was the first researcher to investigate and implement iterative learning control on a real mechanical arm. He realised that, at high speed, the desired trajectory of motion of the robotic arm cannot be obtained simply by applying the desired trajectory functions to the servo system as the reference input because the time lag in the servo system is not negligible. Uchiyama (1978) found a solution to this problem by applying a compensating computed torque to the servo system. However, it is very difficult to obtain this torque since it takes a great deal of effort to obtain the correct torque history in view of the difficulty of modelling the arm. Therefore, Uchiyama (1978), realising that an alternative must be found to avoid this difficulty, discovered that by repeating a proper process of trial and correction the reference input which realises the desired pattern of trajectory can be obtained. However, in the correction scheme of Uchiyama (1978) there is no precise proof of convergence. In addition, the plants under control are restricted to having transfer function of relative order zero.

This work was accordingly extended by Arimoto et al (1984) who gave, for the first time, details of a controller that improved its performance progressively. This controller was represented by a learning algorithm with control law of the form

$$e_k(t) = v(t) - y_k(t) \quad , \qquad \text{...(1.1)}$$

$$u_{k+1}(t) = u_k(t) + \Gamma\, \dot{e}_k(t) \quad . \qquad \text{...(1.2)}$$

This algorithm has proved to be effective and practically implementable. However, it has the following limitations:

(a) The plants under control must be regular. This means that linear time-invariant multivariable plants must have full-rank first Markov parameters. Therefore, in robotic applications, velocity variables must be chosen to be controlled rather than position variables.

(b) The plants under control must have known time-invariant state-space models.

(c) The algorithm is analogue and therefore has to be digitalised for purposes of implementation.

However, in addition, Arimoto et al (1985, 1986) and Arimoto (1986) proposed different learning algorithms with control laws of the form

$$u_{k+1}(t) = u_k(t) + \Phi\, e_k(t) \quad , \qquad \text{...(1.3a)}$$

$$u_{k+1}(t) = u_k(t) + \left(\Phi + \Gamma\, \frac{d}{dt}\right) e_k(t) \quad , \qquad \text{...(1.3b)}$$

and

$$u_{k+1}(t) = u_k(t) + \left(\Phi + \Psi \int dt + \Gamma\, \frac{d}{dt}\right) e_k(t) \quad . \qquad \text{...(1.3c)}$$

Such control laws have been called *P*, *PD*, and *PID* iterative learning control laws, respectively.

However, all these control laws have the same limitations mentioned earlier although they differ in their effectiveness and in their speed of convergence. Kawamura et al (1985) have nevertheless obtained excellent practical results using such iterative learning controllers in the hybrid position/force control of complicated robotic manipulators. However, the contribution of Kawamura et al (1985) to the theory of

iterative learning control is that they tried to modify the plant input for the next iteration by using position, velocity error or both, but not acceleration error in robotic control. Indeed, Kawamura (1985, 1988) stated that "*it may be difficult to realise the desired motion with high accuracy when acceleration and velocity signals are contaminated by noise*". Moreover, Kawamura et al (1988) realised that, in the positional control of robotic manipulators, using only the position error signal would not guarantee that the error would converge to zero. In fact, it was found that using such modifications the position and velocity errors diverged. Various other types of analogue iterative learning controllers have been proposed by Furuta and Yamakita (1986, 1987), Atkenson and McIntyre (1986), Craig (1984), Mita et al (1984,1985), and Ahn and Choi (1990). These controllers are different in their design methodology, effectiveness, and indeed in their emphasis. Thus, for example, in all these researches the stability of the learning algorithm is investigated but the convergence rate is discussed only by Atkenson and McIntyre (1986). The results of Ahn and Choi (1990) confirm the results of Chapters 2 and 3 of this thesis with respect to the design of general analogue iterative learning controllers for arbitrary orders of irregularity. However, in the design of Ahn and Choi (1990) it is necessary for learning to occur that the desired trajectory is $(q\text{-}1)$ times continuously differentiable, where q is the relative degree of the plant.

Recently, Arimoto (1990, 1991a, 1991b) proposed a new analogue iterative learning control algorithm with forgetting factor. The introduction of this forgetting factor helped the learning algorithm to be more robust with respect to initialisation errors, disturbances, and measurement noise. However, this new learning algorithm has the same limitations mentioned earlier. Several more analogue learning controllers were proposed by Messner et al (1991) and Sugie and Ono (1987), Bien and Huh (1989), and Oh et al (1988). In fact, Messner et al (1991) and Oh et al (1988) used adaptive control to identify some system parameters and some disturbance functions in order to

achieve good system performance and good disturbance rejection. Bien and Huh (1989) proposed iterative learning algorithms in which the data for several previous iterations have to be remembered in order to modify the control signal for the next iteration. In other words, the control signal at the $(k+1)th$ iteration is formed from the information at the kth iteration, together with the information at the $(k-1)th$ iteration. This method, although effective, requires that many controller gains must be tuned in order to achieve good learning performance and speedy convergence. Furthermore, as a result of using information from more than one previous iteration, more memory space is required.

Mita et al (1984, 1985) discussed the stability of learning algorithms in the frequency domain. Since the frequency-domain analysis is valid only for continuous systems and since, in real life, digital controllers are used to control automatic machines, the use of discrete-system analysis is more appropriate than either the continuous-system analysis or the frequency-domain analysis. Moreover, since the learning control scheme requires the storage of the previous iteration's data, it is rather natural from an implementational point of view that the control algorithm be given in the discrete-time domain. Thus, several digital iterative learning algorithms have been proposed by Togai and Yamano (1985a, 1985b, 1986), Shouresh et al (1988, 1989), Ishihara et al (1986), and Hwang et al (1991). However, in all these algorithms (except that of Ishihara et al (1986)), the state error was used to modify the control signal for the next iteration. It follows therefore that all the states must be observable. Moreover, a condition for convergence was obtained for each algorithm. Thus, for example, Togai et al (1985a) obtained a convergence condition based on an optimisation concept, whilst Ishihara et al (1986) obtained a condition based on preventing excessive increase of the output error in the transient trial stages.

In order to obtain speedy convergence, the generalised inverse of the discrete-time input matrix must be used as a controller gain in all these proposed algorithms except that of Ishihara et al (1986) which uses the finite sequence of impulse responses of the plant to determine the controller gain. Moreover, Hwang et al (1991) used an identification technique to obtain the discrete-time plant and input matrices which are then used as important and essential parts of the learning algorithm. Miller et al (1987a, 1987b, 1990) and Kuc and Nam (1989) proposed a different form of learning control, where learning is based on using the 'CMAC' module (cerebeller model arithmetic computer) developed by Albus (1972).

Finally, many researchers have implemented their learning algorithms on robotic manipulators, eg, Arimoto et al (1984), Togai et al (1985a), Craig (1984), and Kuc et al (1991). However, in these implementations the learning algorithm is used as part of a control system which utilises classical feedback control as well as gravity compensation. In addition, the gain matrices of the feedback controller must be high enough to bring the robot arm to the neighbourhood of the desired trajectory. In other words, the learning controller is used to provide compensation only for the unmodelled (ie, the non-linear) part of the robot dynamics.

1.3 OBJECTIVES

In order to design highly-effective iterative learning controllers for multivariable plants, it is required to develop a realistic methodology that provides practical procedures for the on-line implementation of such controllers. Therefore, design algorithms for such controllers should circumvent the need for detailed mathematical models of complex multivariable plants in either state-space or transfer-function forms. Moreover, the controllers associated with the design methodology should be easily realised by utilising data directly obtained from input/output measurements in

the time domain. Furthermore, such controllers should be easily rendered adaptive so that the time-varying and non-linear behaviour involved in the operation of the plants can be accommodated. These are the main features that represent the guidelines within which the required design methodology is chosen. Both analogue and digital iterative learning control design methodologies are proposed in this thesis, although the analogue design methodology does not accord with all of the guidelines mentioned earlier whilst the digital design methodology accords with all these guidelines. However, the analogue design methodology is proposed initially in order to avoid the most important limitation imposed by Arimoto et al (1984) and many others in that their iterative learning controllers can only be designed for regular plants. The analogue and digital design methodologies proposed in this thesis are investigated in order to demonstrate the effectiveness and the efficiency of these methodologies in designing iterative learning controllers for plants with abritrary irregularity characteristics. Furthermore, these newly proposed methodologies are used to design and implement iterative learning controllers for robotic manipulators. The digital design methodology proposed in this thesis is further illustrated by designing and implementing practically digital iterative learning controllers for a dc servo-actuator.

This digital design methodology is introduced for the following reasons :

(a) The indirect process of digitalising the analogue controllers for purposes of implementation is unsatisfactory since finite-difference approximations of the derivative action used by such analogue controllers can give rise to inaccuracies and instabilities.

(b) Since the learning control scheme requires the storage of the previous iteration's data, it is rather natural and effective from an implementational point of view that the learning algorithm be digital.

(c) These digital iterative learning controllers can be easily and directly designed

using only input/output representations in the form of the step-response matrices of the multivariable plants under control. Moreover, these controllers can easily be rendered adaptive by identifying in real time the step-response matrices of plant under control.

1.4 OUTLINE OF THE THESIS

This thesis is divided into six parts in order to explain fully the design and implementation of analogue and digital iterative learning controllers. Thus, Part I (Chapter 1) briefly introduces the control problem, presents and discusses various methods that exist in the field of iterative learning control, and states the objectives of this thesis.

Part II (Chapters 2 and 3) is concerned with the design of analogue iterative learning controllers for linear multivariable plants using initial state-shifting and initial impulsive action, respectively, for plants with arbitrary orders of irregularity. Thus, this part solves the fundamental problem faced by Arimoto et al (1984) and many others who concluded that iterative learning controllers cannot be designed for irregular plants. It is shown that the introduction of initial state-shifting or initial impulsive action is necessary in case the plant is subject to a command with initial discontinuity.

Part III (Chapters 4 and 5) is concerned with the design of non-adaptive and adaptive digital iterative learning controllers for linear multivariable plants. Thus, Chapter 4 presents a design methodology for digital iterative learning controllers using only input/output data in terms of step-response matrices. In addition, this design methodology is significantly extended to design digital iterative learning controllers for plants with arbitrary orders of irregularity by the incorporation of digital

compensators. Chapter 5 explains how such controllers can easily be rendered adaptive by identifying on-line the step-response matrices of plants, thus avoiding performance degradation in the control of initially unknown plants.

Part IV (Chapters 6, 7, and 8) is concerned with the design of analogue and digital iterative learning controllers for robotic manipulators. Thus, Chapters 6 and 7 present analogue and digital model-based iterative learning controllers for robotic manipulators, respectively, in both Cartesian and joint spaces. The computed torque method is used to reduce the non-linear robot to a linear time-invariant plant, so that the theories developed in Chapters 2, 3, and 4 can be readily implemented. Moreover, an actuator is used with different reduction gear ratios in order to investigate the effects of not knowing the full dynamical details of the robotic manipulator. Chapter 8 discusses the design of adaptive digital iterative learning controllers for robotic manipulators in both Cartesian and joint spaces. The step-response matrices of robotic manipulators are identified in real-time along their trajectories in both spaces, so that such manipulators are thus rendered amenable to adaptive digital iterative learning control.

Part V (Chapter 9) is concerned with the design and practical implementation of digital iterative learning controllers in the real-time positional control of a dc servo-actuator.

Finally, Part VI (Chapter 10) provides conclusions and recommendations for further work.

PART II

DESIGN OF ANALOGUE ITERATIVE LEARNING CONTROLLERS FOR LINEAR MULTIVARIABLE PLANTS

CHAPTER 2

DESIGN OF ITERATIVE LEARNING CONTROLLERS USING INITIAL STATE-SHIFTING

2.1 INTRODUCTION

In this chapter, the design of iterative learning controllers using initial state-shifting for linear time-invariant mulitivariable plants is considered. It is shown that these controllers do not require detailed estimates of the dynamical parameters of the plants under control and are therefore extremely attractive for application to complex industrial plants.

The existing theory of iterative learning control (Arimoto et al, 1984) requires that the plants under control be regular. This means that linear time-invariant plants must have full-rank first Markov parameters, and therefore that velocity variables must be chosen as outputs rather than positional variables in robotic applications. In order to remove this limitation, iterative learning controllers with initial state-shifting were characterised by Porter and Mohamed (1990a) for a class of completely irregular linear time-invariant plants, ie, plants with null first Markov parameters but full-rank second Markov parameters. It was further shown by Porter and Mohamed (1991a) that these results can be extended so as to embrace iterative learning controllers for ℓth-order partially irregular linear time-invariant multivariable plants, ie, plants with rank-defective first, second, ...,ℓth Markov parameter but full-rank $(\ell+1)$th Markov parameters $(\ell = 1,2,3,...)$. These theoretical results are presented in this chapter and their effectiveness is illustrated by the design of iterative learning controllers for typical first-order partially and completely irregular plants and also for a typical second-order completely irregular plant.

2.2 ANALYSIS

The linear time-invariant multivariable plants under consideration are assumed to be governed on the continuous-time set by state and output equations of the respective forms

$$\dot{x}(t) = Ax(t) + Bu(t) \qquad \ldots(2.1a)$$

and

$$y(t) = Cx(t) \quad , \qquad \ldots(2.1b)$$

where $x(t) \in R^n$ is the state vector, $u(t) \in R^m$ is the input vector, $y(t) \in R^m$ is the output vector, $A \in R^{n \times n}$ is the plant matrix, $B \in R^{n \times m}$ is the input matrix, and $C \in R^{m \times n}$ is the output matrix. In addition, it is assumed that

$$\text{rank } CB = m - p \qquad \ldots(2.2)$$

and

$$\text{rank } CAB = m \qquad (2.3)$$

where $p \in [0, m]$ is the rank defect of the first Markov parameter CB. Such plants are first-order partially irregular when $p > 0$ and therefore fail to satisfy the fundamental requirement of Arimoto et al (1984) that $p = 0$ for the existence of iterative learning controllers.

However, the results presented in this chapter indicate that it is possible to control such first-order partially irregular plants using an appropriately generalised iterative learning controller together with initial state-shifting.

In these controllers, the ultimate objective is to generate an input vector $u(t) \in R^m$ that produces a plant output vector $y(t) \in R^m$ that conicides with the desired plant output vector $v(t) \in R^m$ over a fixed finite time interval $[0,T_t]$. It is assumed that the iterative learning process begins by subjecting the plant to an arbitrary continuous input vector $u_0(t) \in R^m$ and by storing $u_0(t) \in R^m$ on $[0,T_t]$ together with the resulting error vector $e_0(t) = v(t) - y_0(t) \in R^m$ between the desired output vector and the actual output vector $y_0(t) \in R^m$ caused by the input vector $u_0(t) \in R^m$. The iterative learning process continues by adjusting the initial state vector of the plant, by subjecting the plant to a new input vector $u_1(t) \in R^m$ formed from $u_0(t) \in R^m$ and $e_0(t) \in R^m$, and by storing $u_1(t) \in R^m$ on $[0,T_t]$ together with the resulting error vector $e_1(t) = v(t) - y_1(t) \in R^m$ between the desired output vector and the actual output vector $y_1(t) \in R^m$ caused by the input vector $u_1(t) \in R^m$. This iterative process continues indefinitely thus producing a sequence of output vectors $\{y_0(t), y_1(t), \ldots, y_k(t), \ldots\}$ on $[0,T_t]$ corresponding to a sequence of initial state vectors $\{x_0(t), x_1(t), \ldots, x_k(t), \ldots\}$ and a sequence of input vectors $\{u_0(t), u_1(t), \ldots, u_k(t), \ldots\}$ on $[0,T_t]$.

In order to establish the precise conditions under which learning occurs in the case of plants governed by equations of the form (2.1), it is first necessary to introduce the following vector and matrix norms:

$$\| \dot{e}_k(t) \|_\infty = \max_{1 \le i \le m} |\dot{e}_k^{(i)}(t)| \quad , \qquad \ldots(2.4a)$$

and

$$\| G \|_\infty = \max_{1 \le i \le m} \{ \sum_{j=1}^{m} |g^{(i,j)}| \} \quad . \qquad (2.4b)$$

In these norms, $\dot{e}_k^{(i)}(t)$ is the ith element of $\dot{e}_k(t) \in R^m$, and $g^{(i,j)}$ is the i,jth element of $G \in R^{m \times m}$.

The following fundamental result can now be proved for first-order partially irregular linear time-invariant multivariable plants.

Theorem 2.1

In the case of the plant with state and output equations

$$\dot{x}_k(t) = Ax_k(t) + Bu_k(t)$$

and

$$y_k(t) = Cx_k(t)$$

under the action of the control law

$$u_{k+1} = u_k(t) + K_1\dot{e}_k(t) + K_2\ddot{e}_k(t)$$

where $K_1 \in R^{m\times m}$, $K_2 \in R^{m\times m}$ and

$$e_k(t) = v(t) - y_k(t)$$

assume that

(i) $u_0(t)$ is continuous on $[0,T_t]$ and $v(t)$, $\dot{v}(t)$ are continuously differentiable on $[0,T_t]$;

(ii) $CBK_2 = 0$;

(iii) $x_0(0)$ is such that $y_0(0) = v(0)$;

(iv) $x_{k+1}(0) = x_k(0) + BK_2\dot{e}_k(0)$ $(k = 0,1,2,...)$;

(v) $\| I_m - CBK_1 - CABK_2 \|_\infty < 1$.

Then,

$$y_k(t) \rightarrow v(t)$$

uniformly in $t \in [0, T_t]$ as $k \rightarrow \infty$.

Proof

The solution of the governing equation of the plant implies that

$$y_{k+1}(t) = CAe^{At} x_{k+1}(0) + CBu_{k+1}(t) + \int_0^t CAe^{A(t-\tau)} Bu_{k+1}(\tau) d\tau \quad .$$

Hence, it follows that

$$\dot{e}_{k+1}(t) = \dot{v}(t) - \left[CAe^{At} x_{k+1}(0) + CBu_{k+1}(t) + \int_0^t CAe^{A(t-\tau)} Bu_{k+1}(\tau) d\tau \right] .$$

This, using (iv) and substituting the control law, indicates that

$$\dot{e}_{k+1}(t) = \dot{v}(t) - [CAe^{At} x_k(0) + CAe^{At} BK_2 \dot{e}_k(0) + CBu_k(t) + CBK_1 \dot{e}_k(t)$$

$$+ CBK_2 \ddot{e}_k(t) + \int_0^t CAe^{A(t-\tau)} Bu_k(\tau) d\tau + \int_0^t CAe^{A(t-\tau)} BK_1 \dot{e}_k(\tau) d\tau$$

$$+ \int_0^t CAe^{A(t-\tau)} BK_2 \ddot{e}_k(\tau) d\tau]$$

and therefore, using (ii), that

$$\dot{e}_{k+1}(t) = \dot{v}(t) - [\dot{y}_k(t)+CAe^{At}BK_2\dot{e}_k(0)+CBK_1\dot{e}_k(t) + \int_0^t CAe^{A(t-\tau)}BK_1\dot{e}_k(\tau)d\tau$$

$$+ \int_0^t CAe^{A(t-\tau)}BK_2\ddot{e}_k(\tau)d\tau]$$

But integration by parts indicates that

$$\int_0^t CAe^{A(t-\tau)}BK_2\ddot{e}_k\ (\tau)d\tau = [CABK_2\dot{e}_k(t)-CAe^{At}BK_2\dot{e}_k(0)] + \int_0^t CAe^{A(t-\tau)}ABK_2\dot{e}_k(\tau)d\tau$$

so that

$$\dot{e}_{k+1}(t) = (I_m - CBK_1 - CABK_2)\dot{e}_k(t) - \int_0^t CAe^{A(t-\tau)}(BK_1 + ABK_2)\dot{e}_k(\tau)d\tau \ .$$

Now, taking the norm of both sides of the equation indicates that

$$\|\dot{e}_{k+1}(t)\|_\infty \ \leq \ \|I_m - CBK_1 - CABK_2\|_\infty \cdot \|\dot{e}_k(t)\|_\infty$$

$$+ \sup_{0 \leq t \leq T_t} \int_0^t \|CAe^{A(t-\tau)}(BK_1 + ABK_2)\|_\infty \cdot \|\dot{e}_k(\tau)\|_\infty d\tau$$

$$\leq \rho\|\dot{e}_k(t)\|_\infty + \sigma \sup_{0 \leq t \leq T_t} \int_0^t \|\dot{e}_k(\tau)\|_\infty d\tau$$

where

$$\rho = \| I_m - CBK_1 - CABK_2 \|_\infty \qquad \ldots(2.5)$$

and

$$\sigma = \sup_{0 \le t \le T_t} \| CAe^{At}(BK_1 + ABK_2) \|_\infty \quad . \qquad \ldots(2.6)$$

Therefore,

$$\| \dot{e}_1(t) \|_\infty \le \rho \| \dot{e}_0(t) \|_\infty + \sigma \int_0^t \| \dot{e}_0(\tau) \|_\infty d\tau \le \rho\beta + \sigma\beta t \le (\rho + \sigma t)\beta$$

where

$$\beta = \sup_{0 \le t \le T_t} \| \dot{e}_0(t) \|_\infty \quad ,$$

$$\| \dot{e}_2(t) \| \le \rho \| \dot{e}_1(t) \|_\infty + \sigma \int_0^t \| \dot{e}_1(\tau) \|_\infty d\tau \le (\rho^2 + \rho\sigma t)\beta + \sigma \int_0^t (\rho + \sigma\tau)\beta d\tau$$

$$\le (\rho^2 + \sigma\rho t)\beta + \sigma\rho\beta t + \frac{\sigma^2 t^2}{2!}\beta \le \left[\rho^2 + 2\sigma\rho t + \frac{\sigma^2 t^2}{2!}\right]\beta \quad ,$$

. . . . . .

$$\| \dot{e}_k(t) \| \le [\rho^k + k\rho^{k-1}\sigma t + \frac{k(k-1)}{2!} \cdot \rho^{k-2} \frac{\sigma^2 t^2}{2!} + \frac{k(k-1)(k-2)}{3!} \rho^{k-3} \frac{\sigma^3 t^3}{3!}$$

$$+ \frac{k(k-1)(k-2)(k-3)}{4!} \rho^{k-4} \frac{\sigma^4 t^4}{4!} + \ldots\ldots$$

$$+ k\rho \frac{\sigma^{k-1} \ell^{k-1}}{(k-1)!} + \frac{\sigma^k \ell^k}{k!}]\beta \quad ,$$

or in closed form,

$$\| \dot{e}_k(t) \|_\infty \leq \beta \sum_{q=0}^{k} \frac{k!}{q!(k-q)!} \rho^{k-q} \frac{\sigma^q \ell^q}{q!} \quad . \qquad \ldots(2.7)$$

It is found that each individual term in the right-hand side of the inequality (2.7) is positive. Therefore, in order for $\| \dot{e}_k(t) \|_\infty$ to vanish as $k \to \infty$, each term must vanish as $k \to \infty$. Indeed, the only way to make these terms vanish is by satisfying condition (v) of Theorem 2.1 that $\rho < 1$. This can be proved by noting that

$$\lim_{k \to \infty} \quad k^s \rho^k \to 0$$

for any integer $s > 0$ provided that $|\rho| < 1$. This fact is best appreciated by considering the ratio of the kth term to the $(k-1)th$ term in the *series* $K^s \rho^k$. Thus,

$$\frac{\tau_k}{\tau_{k-1}} = \frac{(k)^s \rho^k}{(k-1)^s \rho^{k-1}} = \left(\frac{k}{k-1} \right)^s \rho \quad .$$

Hence,

$$\lim_{k \to \infty} \quad \frac{\tau_k}{\tau_{k-1}} = \rho \quad .$$

This means that

$$\lim_{k\to\infty} \tau_k = 0$$

provided that $|\rho| < 1$.

However, the last term of the inequality (2.7) will vanish in a different fashion, because the speed of the factorial function's progress is more rapid than the speed of the exponential function's progress. In other words, the denominator of $(\sigma^k t^k/k!)$ increases faster than the numerator so that this term vanishes as k increases. Indeed, the speed at which this term disappears depends on the magnitude of the parameter, σ. The smaller this parameter, the faster the term will disappear.

It therefore follows from these considerations that $\|\dot{e}_k(t)\|_\infty \to 0$, as $k \to \infty$ which implies that $\dot{y}_k(t) \to \dot{v}(t)$ uniformly in $t \in [0, T_t]$ as $k \to \infty$. But

$$y_{k+1}(0) = Cx_{k+1}(0)$$

from which it follows, using (ii) and (iv), that

$$y_{k+1}(0) = Cx_k(0) + CBK_2\dot{e}_k(0) = Cx_k(0) = y_k(0)$$

and therefore, using (iii), that

$$y_k(0) = v(0)$$

for all $k = 0,1,2,....$ It is therefore finally evident that

$$y_k(t) \to v(t)$$

uniformly in $t \in [0,T_t]$ as $k \to \infty$.

It is clear from condition (iv) of Theorem 2.1 that the state must be shifted by the amount given by $BK_2\dot{e}_k(0)$ at the beginning of each successive iteration for learning to occur. (See Appendix A for more details.) The iterative learning processes characterised by Theorem 2.1 are depicted in Figure 2.1. It is important to note that, since CB has full rank in the special case of regular plants, condition (iii) of Theorem 2.1 then indicates that $K_2 = 0$ so that conditions (iv) and (v) then reduce to the corresponding results of Arimoto et al (1984) for regular plants.

It is evident that, although the parameter σ defined in equation (2.6) is not involved in the sufficient conditions for learning enunciated in Theorem 2.1, the value of σ nevertheless affects the rate at which learning occurs. This parameter is accordingly called the learning parameter of the plant/controller combination and its effect is investigated in Section 2.4. Moreover, according to equation (2.6) the value of this parameter depends on the stability characteristics of the plant under control because of the presence of e^{At}.

In addition, it is clearly impossible to satisfy condition (v) of Theorem 2.1 in the case of plants with second- or higher-order irregularities, i.e. plants with rank-defective CB, CAB,...,$CA^{\ell-1}B$ Markov parameters and full-rank $CA^{\ell}B$ Markov parameter ($\ell \geq 2$). In such cases, the following generalised result can be proved by means of the same arguments as were used in the case of Theorem 2.1.

Theorem 2.2

In the case of the plant with state and output equations

$$\dot{x}_k(t) = Ax_k(t) + Bu_k(t)$$

and

$$y_k(t) = Cx_k(t)$$

under the action of the control law

$$u_{k+1} = u_k(t) + \sum_{i=1}^{\ell+1} K_i e_k^{(i)}(t) \qquad \ldots(2.8)$$

where $K_i \in R^{m\times m}$ $(i = 1,2,\ldots,\ell+1)$ and

$$e_k(t) = v(t) - y_k(t)$$

assume that

(i) $u_0(t)$ is continuous on $[0,T_t]$ and $v(t)$, $\dot{v}(t)$ are continuously differentiable on $[0,T_t]$;

(ii) $\sum_{i=j}^{\ell+1} CA^{i-j}BK_i = 0$ $(j = 2,3,\ldots,\ell+1)$;

(iii) $x_0(0)$ is such that $y_0(0) = v(0)$;

(iv) $x_{k+1}(0) = x_k(0) + \sum_{j=2}^{\ell+1}\sum_{i=j}^{\ell+1} A^{i-j}BK_i e_k^{(i-1)}(0)$;

(v) $\| I_m - \sum_{i=1}^{\ell+1} CA^{i-1}BK_i \|_\infty < 1.$

Then,

$$y_k(t) \to v(t)$$

uniformly in $t \in [0, T_t]$ as $k \to \infty$.

It transpires, in the course of the proof that,

$$\| \dot{e}_k(t) \|_\infty \leq \beta \sum_{q=0}^{k} \frac{k!}{q!(k-q)!} \rho^{(k-q)} \frac{\sigma^q t^q}{q!} \qquad \ldots(2.9)$$

where $k > 0$.

It is clear by comparing the inequality (2.7) with (2.9) that both inequalities are identical except that in the inequality (2.9) the parameters ρ and σ are

$$\rho = \| I_m - \sum_{i=1}^{\ell+1} CA^{i-1} B K_i \|_\infty \qquad \ldots(2.10)$$

and

$$\sigma = \sup_{0 \leq t \leq T_t} \| CAe^{At} \sum_{i=1}^{\ell+1} A^{i-1} B K_i \|_\infty \ . \qquad \ldots(2.11)$$

Thus, Theorem 2.2 establishes the conditions under which the iterative learning controller governed by equation (2.8) generates an input vector $u(t) \in R^m$ that produces an output vector $y(t) \in R^m$ which coincides with the command vector $v(t) \in R^m$ over the time interval $[0, T_t]$ for higher-order irregular plants.

Finally, it is important to mention that the quantity on the right-hand side of the inequalities (2.7) and (2.9) represents an upper bound on the rate of change of error. This bound can be used as a guide to show how the parameters ρ and σ affect the learning rates in the case of iterative learning control with initial state shifting. However, this bound does not indicate how many iterations are required for the

plant's output to coincide with the desired command over the desired time interval. Nevertheless, this bound does indicate whether the learning rate is rapid or not depending on the parameters ρ and σ. It is worth mentioning that the inequalities (2.7) and (2.9) become

$$\| \dot{e}_k(t) \|_\infty \leq \beta \frac{\sigma^k t^k}{k!} \qquad \ldots(2.12)$$

when $\rho = 0$.

The rate of change of error given by equation (2.12) is investigated in Example 2.6 with different values of σ corresponding to different SISO plants.

2.3 SYNTHESIS

It is clear that learning will occur, in the sense that $e_k \to 0$ as $k \to \infty$ in Theorem 2.1, provided condition (v) is satisfied, i.e. $\rho < 1$. However, the speed with which the plant learns is determined by the values of the parameters ρ and σ. The smaller these parameters the faster the learning rate will be (see Section 2.4). The values of both parameters ρ and σ depend on the choice of the controller gain matrices; in addition, σ depends on whether the stability characteristics of the plant under control. Thus, the controller gain matrices must be designed so that both parameters are as small as possible. Therefore, in the case of first-order partially irregular plants, the controller gain matrices must be

$$K_1 = \lambda(CB + CABD)^{-1} \qquad \ldots(2.13)$$

and

$$K_2 = DK_1 \quad , \qquad \ldots(2.14)$$

where $\lambda \epsilon R^+$ and $D \epsilon R^{m \times m}$. It is then clear from equation (2.5) that

$$\rho = |1-\lambda| \qquad \ldots(2.15)$$

which implies that the crucial condition (v) of Theorem 2.1 will be satisfied provided that $0 < \lambda < 2$. In addition, D must be chosen so that $CBD = 0$ (see Appendix A).

However, it is also clear from equation (2.6) that the choice of the controller gain matrices given by equations (2.13) and (2.14) implies that the corresponding value of the learning parameter is given by

$$\underline{\sigma}_{\lambda} = \sup_{0 \leq t \leq T_t} \| CAe^{At} (B + ABD)(CB + CABD)^{-1} \|_{\infty} \quad . \qquad \ldots(2.16)$$

It is thus evident from equation (2.16) that the value of the right-hand member of equation (2.16) depends upon the stability characteristics of the plant under control. Indeed, it follows from equation (2.16) that

$$\underline{\sigma}_{\lambda} \geq \| CA(B + ABD)(CB + CABD)^{-1} \|_{\infty} \qquad \ldots(2.17)$$

in the case of open-loop stable plants.

The effects of the parameters ρ and σ on the learning rate are investigated in Section 2.4 for various plants with different irregularity and stability characteristics. Similar synthesis considerations apply in the case of plants with higher-order irregularities when Theorem 2.2 is used with ρ and σ as defined in equations (2.10) and (2.11).

2.4 ILLUSTRATIVE EXAMPLES

The use of iterative learning controllers can be conveniently illustrated by designing iterative controllers with initial state shifting for an open-loop stable, unstable, and neutrally stable first-order irregular plants. In addition, the design of such controllers is extended so as to embrace an open-loop stable plant with second-order irregularity using the control-law proposed in Theorem 2.2 Furthermore, the upper bound of the rate of error is investigated for different stable SISO plants. In all these examples, in the iteration corresponding to $k = 0$ neither the inputs nor the outputs have been plotted since both are zero.

Example 2.1

The state and output equations of a linear time-invariant plant on the continuous-time set are

$$\begin{bmatrix} \dot{x}_1(t) \\ \dot{x}_2(t) \\ \dot{x}_3(t) \end{bmatrix} = \begin{bmatrix} -3 & , & 1 & , & 0 \\ -2 & , & -1 & , & 2 \\ 0 & , & 1 & , & -2 \end{bmatrix} \begin{bmatrix} x_1(t) \\ x_2(t) \\ x_3(t) \end{bmatrix} + \begin{bmatrix} 0 & , & 0 \\ 2 & , & 1 \\ 1 & , & 3 \end{bmatrix} \begin{bmatrix} u_1(t) \\ \\ u_2(t) \end{bmatrix} \quad \ldots(2.18a)$$

and

$$\begin{bmatrix} y_1(t) \\ \\ y_2(t) \end{bmatrix} = \begin{bmatrix} 1 & , & 0 & , & -1 \\ & & & & \\ 1 & , & 0 & , & 0 \end{bmatrix} \begin{bmatrix} x_1(t) \\ x_2(t) \\ x_3(t) \end{bmatrix} \quad . \quad \ldots(2.18b)$$

In this case, the plant is asymptotically stable but first-order partially irregular since its first Markov parameter

$$CB = \begin{bmatrix} -1 & , & -3 \\ 0 & , & 0 \end{bmatrix} \qquad \text{...(2.19a)}$$

is rank defective whilst its second Markov parameter

$$CAB = \begin{bmatrix} 2 & , & 6 \\ 2 & , & 1 \end{bmatrix} \qquad \text{...(2.19b)}$$

evidently has full rank. So, the plant is first-order irregular and therefore cannot be controlled by the iterative learning controller of Arimoto et al (1984).

It is required that the output vector of this plant track the command vector

$$v(t) = \begin{bmatrix} 12t \\ -12t \end{bmatrix} (t \in [0, T_t]) \qquad \text{...(2.20)}$$

on the time interval $[0, 1]$ *sec.*

In case

$$x_0(0) = \begin{bmatrix} 0 \\ 0 \\ 0 \end{bmatrix} \qquad \text{...(2.21)}$$

and

$$u_0(t) = \begin{bmatrix} 0 \\ 0 \end{bmatrix} \quad , \qquad \text{...(2.22)}$$

the learning characteristics of the iterative learning controller with different controller gain matrices given by equation (2.13) and (2.14) when

$$D = \begin{bmatrix} 0 & , & -3 \\ 0 & , & 1 \end{bmatrix} \qquad \text{...(2.23)}$$

so that $CBD = 0$ are shown in Figure 2.2. Indeed, the results in Figures 2.2(a,b) corresponding to the choice $\lambda = 1, \rho = 0\ \sigma = 5$ show rapid learning; those in Figures 2.2 (c,d) to the choice $\lambda = 0.8, \rho = 0.2, \sigma = 4$ show less rapid learning; and those in Figures 2.2 (e,f) to the choice $\lambda = 0.5, \rho = 0.5, \sigma = 2.5$ show even less rapid learning.

In all these cases, $v(t)$ is such that

$$\dot{e}_0(0) = \begin{bmatrix} 12 \\ -12 \end{bmatrix} \neq 0 \qquad \text{...(2.24)}$$

and therefore initial state shifting is required.

Example 2.2

The state and output equations of a linear time-invariant plant on the continuous-time set are

$$\begin{bmatrix} \dot{x}_1(t) \\ \dot{x}_2(t) \\ \dot{x}_3(t) \\ \dot{x}_4(t) \end{bmatrix} = \begin{bmatrix} 0 & , & 0.5 & , & 0 & , & 0 \\ 0 & , & 0.1 & , & 0.75 & , & 0 \\ -1.5 & , & 0.5 & , & 1.25 & , & 0 \\ 2.5 & , & 0 & , & -2.5 & , & 0 \end{bmatrix} \begin{bmatrix} x_1(t) \\ x_2(t) \\ x_3(t) \\ x_4(t) \end{bmatrix}$$

$$+ \begin{bmatrix} 0 & , & 0 \\ 1 & , & 2 \\ 3 & , & 1 \\ 0 & , & 0 \end{bmatrix} \begin{bmatrix} u_1(t) \\ \\ \\ u_2(t) \end{bmatrix} \qquad \ldots(2.25a)$$

and

$$\begin{bmatrix} y_1(t) \\ \\ y_2(t) \end{bmatrix} = \begin{bmatrix} 1 & , & 0 & , & 0 & , & 0 \\ & & & & & & \\ 0 & , & 0 & , & 0 & , & 1 \end{bmatrix} \begin{bmatrix} x_1(t) \\ x_2(t) \\ x_3(t) \\ x_4(t) \end{bmatrix} \quad . \qquad \ldots(2.25b)$$

In this case, the plant is unstable and is first-order completely irregular since its first Markov parameter

$$CB = \begin{bmatrix} 0 & , & 0 \\ 0 & , & 0 \end{bmatrix} \qquad \ldots(2.26a)$$

is clearly null whilst its second Markov parameter

$$CAB = \begin{bmatrix} 0.5 & , & 1 \\ -7.5 & , & -2.5 \end{bmatrix} \qquad \text{...(2.26b)}$$

evidently has full rank. Therefore the plant is first order completely irregular and so cannot be controlled by the iterative learning controller of Arimoto et al (1984).

It is required that the output vector of this plant track the command vector

$$v(t) = \begin{bmatrix} 12t \\ -12t \end{bmatrix} \quad (t \in [0, T_t]) \qquad \text{...(2.27)}$$

on the time interval [0, 1] *sec.*

In case

$$x_0(0) = \begin{bmatrix} 0 \\ 0 \\ 0 \\ 0 \end{bmatrix} \qquad \text{...(2.28)}$$

and

$$u_0(t) = \begin{bmatrix} 0 \\ 0 \end{bmatrix} \quad , \qquad \text{...(2.29)}$$

the learning characteristics of the iterative controller with different controller gain matrices given by equations (2.13) and (2.14) when $D = I_2$ are shown in Figure 2.3.

In this case, the plant is unstable, and equation (2.16) accordingly indicates that the large value of σ corresponds to the end of the task. The results in Figures 2.3(a,b) correspond to the choice $\lambda = 1$, $\rho = 0$, $\sigma = 9.58$; those in Figures 2.3(c,d) to the choice $\lambda = 0.5$, $\rho = 0.5$, $\sigma = 4.79$; and those in Figure 2.3(e,f) to the choice $\lambda = 0.1$, $\rho = 0.9$, $\sigma = 0.958$. It is clear from these figures that, because of the instability of the plant under control, learning is slow and violent as shown in Figures 2.3(a,b) when $\lambda = 1$; that learning is slower but less violent as shown in Figures 2.3(c,d) when $\lambda = 0.5$; and that learning is even slower but even less violent as shown in Figures 2.3(e,f) when $\lambda = 0.1$. These results confirm that the instability of plants under control imposes unavoidable limits on the learning rates achievable in the iterative learning control. In all these cases, $v(t)$ is such that

$$\dot{e}_0(0) = \begin{bmatrix} 12 \\ \\ -12 \end{bmatrix} \neq 0 \qquad \ldots(2.30)$$

and therefore initial state shifting is required.

Example 2.3

The state and output equations of a linear time-invariant plant on the continuous-time set are

$$\begin{bmatrix} \dot{x}_1(t) \\ \dot{x}_2(t) \\ \dot{x}_3(t) \\ \dot{x}_4(t) \end{bmatrix} = \begin{bmatrix} 0 & , & 0 & , & 1 & , & 3 \\ 0 & , & 0 & , & 0 & , & 1 \\ 0 & , & 0 & , & 0 & , & 0 \\ 0 & , & 0 & , & 0 & , & 0 \end{bmatrix} \begin{bmatrix} x_1(t) \\ x_2(t) \\ x_3(t) \\ x_4(t) \end{bmatrix}$$

$$+\begin{bmatrix} 0 & , & 0 \\ 0 & , & 0 \\ 2 & , & 0 \\ 0 & , & -3 \end{bmatrix}\begin{bmatrix} u_1(t) \\ \\ \\ u_2(t) \end{bmatrix} \qquad \text{...(2.31a)}$$

and

$$\begin{bmatrix} y_1(t) \\ \\ y_2(t) \end{bmatrix} = \begin{bmatrix} 1 & , & 0 & , & 0 & , & 0 \\ & & & & & & \\ 0 & , & 1 & , & 0 & , & 0 \end{bmatrix}\begin{bmatrix} x_1(t) \\ x_2(t) \\ x_3(t) \\ x_4(t) \end{bmatrix} . \qquad \text{...(2.31b)}$$

In this case, the plant is clearly neutrally stable but first-order completely irregular since its first Markov parameter

$$CB = \begin{bmatrix} 0 & , & 0 \\ & & \\ 0 & , & 0 \end{bmatrix} \qquad \text{...(2.32a)}$$

is clearly null whilst its second Markov parameter

$$CAB = \begin{bmatrix} 2 & , & -9 \\ & & \\ 0 & , & -3 \end{bmatrix} \qquad \text{...(2.32b)}$$

evidently has full rank. Therefore, the plant is first order completely irregular and so cannot be controlled by the iterative learning controller of Arimoto et al (1984).

It is required that the output vector of this plant track the command vector

$$v(t) = \begin{bmatrix} 12t \\ \\ -12t \end{bmatrix} \quad (t \in [0, T_t]) \qquad \ldots(2.33)$$

on the time interval [0, 1] *sec.*

In case

$$x_0(0) = \begin{bmatrix} 0 \\ 0 \\ 0 \\ 0 \end{bmatrix} \qquad \ldots(2.34)$$

and

$$u_0(t) = \begin{bmatrix} 0 \\ \\ 0 \end{bmatrix} \quad , \qquad \ldots(2.35)$$

the learning characteristics of the iterative controller with different controller gain matrices given by equations (2.13) and (2.14) are shown in Figure 2.4.

Figures 2.4(a,b),(c,d) and (e,f) show the learning controllers when $\lambda = \{1, 0.5, 0.2\}$, $\rho = \{0, 0.5, 0.8\}$ and $\sigma = \{1, 0.5, 0.2\}$ respectively. It is clear from these figures that, learning is fast but violent as shown in Figures 2.4(a,b) when $\lambda = 1$; that learning is slower but less violent as shown in Figures 2.4(c,d) when $\lambda = 0.5$; and that learning is even slower but even less violent as shown in Figures 2.4(e,f) when $\lambda = 0.1$.

In all these cases, $v(t)$ is such that

$$\dot{e}_0(0) = \begin{bmatrix} 12 \\ \\ -12 \end{bmatrix} \neq 0 \qquad \ldots(2.36)$$

and therefore initial state shifting is required.

It is evident from the previous example that plants with small learning parameters can be controlled best using iterative learning controllers. This is because good learning performance and rapid convergence can be obtained in controlling such plants. Indeed, the results of this example confirm that plants whose eigenvalues all lie at the origin of the s-plane produce the smallest learning parameters.

Example 2.4

In the previous examples, the effects of open-loop stability characteristics on the learning parameter and the learning rate were investigated. In this example, the effect of the design parameter D in the controller gain matrices on the learning parameter is investigated. This investigation is carried out in the hope of finding ways to reduce the parameter σ without affecting the parameter ρ in order to obtain better learning rates.

The state and output equations of linear time-invariant plant on the continuous-time set are

$$\begin{bmatrix} \dot{x}_1(t) \\ \dot{x}_2(t) \\ \dot{x}_3(t) \\ \dot{x}_4(t) \end{bmatrix} = \begin{bmatrix} 0 & 5 & 0 & 0 \\ 0 & -8 & -6 & 0 \\ 3 & 2 & -3 & 0 \\ 5 & 0 & -5 & -6 \end{bmatrix} \begin{bmatrix} x_1(t) \\ x_2(t) \\ x_3(t) \\ x_4(t) \end{bmatrix}$$

$$+\begin{bmatrix} 0 & , & 0 \\ 1 & , & 2 \\ 3 & , & 1 \\ 0 & , & 0 \end{bmatrix}\begin{bmatrix} u_1(t) \\ \\ \\ u_2(t) \end{bmatrix} \qquad \text{...(2.37a)}$$

and

$$\begin{bmatrix} y_1(t) \\ \\ y_2(t) \end{bmatrix} = \begin{bmatrix} 1 & , & 0 & , & 0 & , & 0 \\ & & & & & & \\ 0 & , & 0 & , & 0 & , & 1 \end{bmatrix}\begin{bmatrix} x_1(t) \\ x_2(t) \\ x_3(t) \\ x_4(t) \end{bmatrix}. \qquad \text{...(2.37b)}$$

In this case, the plant is asymptotically stable but first-order completely irregular since its first Markov parameter

$$CB = \begin{bmatrix} 0 & , & 0 \\ 0 & , & 0 \end{bmatrix} \qquad \text{...(2.38a)}$$

is clearly null whilst its second Markov parameter

$$CAB = \begin{bmatrix} 5 & , & 10 \\ -15 & , & -5 \end{bmatrix} \qquad \text{...(2.38b)}$$

evidently has full rank. Therefore, the plant is first-order completely irregular and so cannot be controlled by the iterative learning controller of Arimoto et al (1984).

It is required that the output vector of this plant track the command vector

$$v(t) = \begin{bmatrix} 12t \\ -12t \end{bmatrix}, (t \in [0, T_t]) \qquad \text{...(2.39)}$$

on the time interval $[0, 1]$ *sec.*

In case

$$x_0(0) = \begin{bmatrix} 0 \\ 0 \\ 0 \\ 0 \end{bmatrix} \qquad \text{...(2.40)}$$

and

$$u_0(t) = \begin{bmatrix} 0 \\ 0 \end{bmatrix} \quad , \qquad \text{...(2.41)}$$

the learning characteristics of the iterative controller with controller gain matrices given by equations (2.13) and (2.14) when $\lambda = 1$, $\rho = 0$ are shown in Figure 2.5. Indeed the results presented in Figures 2.5(a,b) correspond to $D = -I_2$, $\sigma = 15$; those in Figure 2.5(c,d) correspond to $D = 0.1\, I_2$, $\sigma = 8$; and those in Figures 2.5(e,f) correspond to $D = -(CA^2B)^{-1}(CAB)$, $\sigma = 4.92$. The last choice of D is made so that $\sigma = 0$ at $t = 0$, but the largest value of σ according to equation (2.6) corresponds to $t = 0.21$ *sec.* In addition, all these choices of D guarantee that $CBD = 0$, since CB is null. Thus it is clear from Figure 2.5 that the best learning performance and most

rapid convergence is obtained when $D = -(CA^2B)^{-1}(CAB)$ (see Figures 2.5(e,f)). Finally, in all these cases $v(t)$ is such that

$$\dot{e}_0(0) = \begin{bmatrix} 12 \\ \\ -12 \end{bmatrix} \neq 0 \qquad \text{...(2.42)}$$

and therefore initial state shifting is required.

Example 2.5

The state and output equations of a linear time-invariant plant on the continuous-time set are

$$\begin{bmatrix} \dot{x}_1(t) \\ \dot{x}_2(t) \\ \dot{x}_3(t) \\ \dot{x}_4(t) \\ \dot{x}_5(t) \\ \dot{x}_6(t) \end{bmatrix} = \begin{bmatrix} 0 & 0 & 1 & 0 & 0 & 0 \\ 0 & 0 & 0 & 1 & 0 & 0 \\ -4 & -1 & 1 & 2 & -4 & 2 \\ 1 & -2 & -3 & -2 & 1 & -3 \\ 0 & 0 & 0 & 0 & -3 & 0 \\ 0 & 0 & 0 & 0 & 0 & -2 \end{bmatrix} \begin{bmatrix} x_1(t) \\ x_2(t) \\ x_3(t) \\ x_4(t) \\ x_5(t) \\ x_6(t) \end{bmatrix}$$

$$+ \begin{bmatrix} 0 & 0 \\ 0 & 0 \\ 0 & 0 \\ 0 & 0 \\ 3 & 0 \\ 0 & 2 \end{bmatrix} \begin{bmatrix} u_1(t) \\ \\ \\ \\ u_2(t) \end{bmatrix} \qquad \text{...(2.43a)}$$

and

$$\begin{bmatrix} y_1(t) \\ \\ y_2(t) \end{bmatrix} = \begin{bmatrix} 1 & , & -2 & , & 0 & , & 0 & , & 0 & , & 0 \\ 1 & , & 2 & , & 0 & , & 0 & , & 0 & , & 0 \end{bmatrix} \begin{bmatrix} x_1(t) \\ x_2(t) \\ x_3(t) \\ x_4(t) \\ x_5(t) \\ x_6(t) \end{bmatrix}. \qquad \text{...(2.43b)}$$

In this case, the plant is asymptotically stable but second-order completely irregular, since its first and second Markov parameters

$$CB = \begin{bmatrix} 0 & , & 0 \\ 0 & , & 0 \end{bmatrix} \qquad \text{...(2.44a)}$$

and

$$CAB = \begin{bmatrix} 0 & , & 0 \\ 0 & , & 0 \end{bmatrix} \qquad \text{...(2.44b)}$$

are clearly null whilst its third Markov parameter

$$CA^2B = \begin{bmatrix} -18 & , & 16 \\ -6 & , & -8 \end{bmatrix} \qquad \text{...(2.44c)}$$

evidently has full rank.

It follows therefore that such plants cannot be controlled using either the iterative learning controller proposed by Arimoto et al (1984), or the controller proposed in Theorem 2.1. However, such plants can be controlled using the iterative learning controller proposed in Theorem 2.2.

It is required that the output vector of this plant track the command vector

$$v(t) = \begin{bmatrix} 12t \\ \\ -12t \end{bmatrix} \quad (t \in [0, T_t]) \qquad \ldots(2.45)$$

on the time interval [0, 1] *sec.*

In case

$$x(0) = \begin{bmatrix} 0 \\ 0 \\ 0 \\ 0 \\ 0 \\ 0 \end{bmatrix} \qquad \ldots(2.46)$$

and

$$u_0(t) = \begin{bmatrix} 0 \\ \\ 0 \end{bmatrix} \quad , \qquad \ldots(2.47)$$

the learning characteristics of the iterative learning controller with the controller gain matrices

$$K_1 = \lambda\,(CB + CABD_1 + CA^2BD_2)^{-1} \quad , \qquad \text{...(2.48a)}$$

$$K_2 = D_1 K_1 \quad , \qquad \text{...(2.48b)}$$

and

$$K_3 = D_2 K_1 \qquad \text{...(2.48c)}$$

are shown in Figure 2.6, where $\lambda \in R^+$ and $D_1, D_2 \in R^{m \times m}$. D_1 and D_2 can be arbitrary since $CB = CAB = 0$, but, in this example, $D_1 = D_2 = I_2$ are chosen.

The results presented in Figures 2.6(a,b),(c,d) and (e,f) correspond to $\lambda = (1, 0.5, 0.2)$, $\rho = (0, 0.5, 0.8)$ and $\sigma = (6.6, 3.3, 1.32)$, respectively.

It is clear from these figures that learning is rapid as shown in Figures 2.6(a,b) when $\lambda = 1$; that learning is less rapid as shown in Figures 2.6(c,d) when $\lambda = 0.5$; and that learning is even less rapid as shown in Figures 2.6(e,f) when $\lambda = 0.2$.

Finally, in all these cases, $v(t)$ is such that

$$\dot{e}_0(0) = \begin{bmatrix} 12 \\ \\ -12 \end{bmatrix} \neq 0 \qquad \text{...(2.49a)}$$

and

$$\ddot{e}_0\,(0) = \begin{bmatrix} 0 \\ \\ 0 \end{bmatrix} \qquad \text{...(2.49b)}$$

and therefore initial state shifting is required.

Example 2.6

This example is given to illustrate the conservativeness (or otherwise) of the bound on the rate of change of error given by the inequality (2.7). This illustration is affected by considering two SISO plants governed by state and output equations of the respective forms

$$\dot{x}(t) = a\, x\,(b) + b\, u(t) \qquad \text{...(2.50a)}$$

and

$$y(t) = c\, x(t) \qquad \text{...(2.50b)}$$

for which

$$a = -1$$

$$b = 1$$

$$c = 1$$

and

$$a = -10$$

$$b = 1$$

$$c = 1$$

respectively.

In addition, these plants are controlled using an iterative learning controller with a control law of the form

$$u_{k+1}(t) = u_k(t) + K_1\, \dot{e}_k(t) \qquad \text{...(2.51)}$$

Since both these SISO plants are regular, this control law is obtained as a special case of either Theorem 2.1 or Theorem 2.2. The learning behaviour of this iterative controller is accordingly governed by the appropriate special cases of the inequalities involved in Theorems 2.1 and 2.2 (i.e. inequality (2.7) and inequality (2.9)). In addition, in this iterative learning controller if the controller gain matrix K_1 is chosen so that $\rho = 0$, inequalities (2.7) and (2.9) will be reduced to

$$\frac{\| \dot{e}_k(t) \|_\infty}{\beta} \leq \frac{\sigma^k\, t^k}{k!}$$

Therefore, it is required to investigate the relation between this inequality and $\frac{\| \dot{e}_k(t) \|_\infty}{\beta}$ of the actual process for ($t \in [0,2]$ *sec*).

It is clear from Figures 2.7(a,b) that the bound is non-conservative when σ is small; on the other hand the results represented in Figures 2.7(c,d) confirm that the bound is loose and conservative when σ is large. In addition, it is clear by comparing Figures 2.7(b,d) that learning is slow when σ is large. This is confirmed in Figures 2.7(a,c).

2.5 CONCLUSION

It has been shown in this chapter that iterative learning controllers with initial state shifting can be characterized for a class of first-order irregular linear time-invariant multivariable plants. In addition, these results have been extended so as to embrace plants with higher-orders irregularity. Furthermore, it has been shown that these results can be used to obtain important information concerning the learning rates achievable by such controllers. Indeed, it has been found that the stability characteristics of the plants under control impose severe constraints on these achievable learning rates. In addition, the upper bound of the rate of change of error

has been investigated.

Finally, these general results have been illustrated by the presentation of numerical results for the iterative control of different linear multivariable plants with various stability and irregularity characteristics.

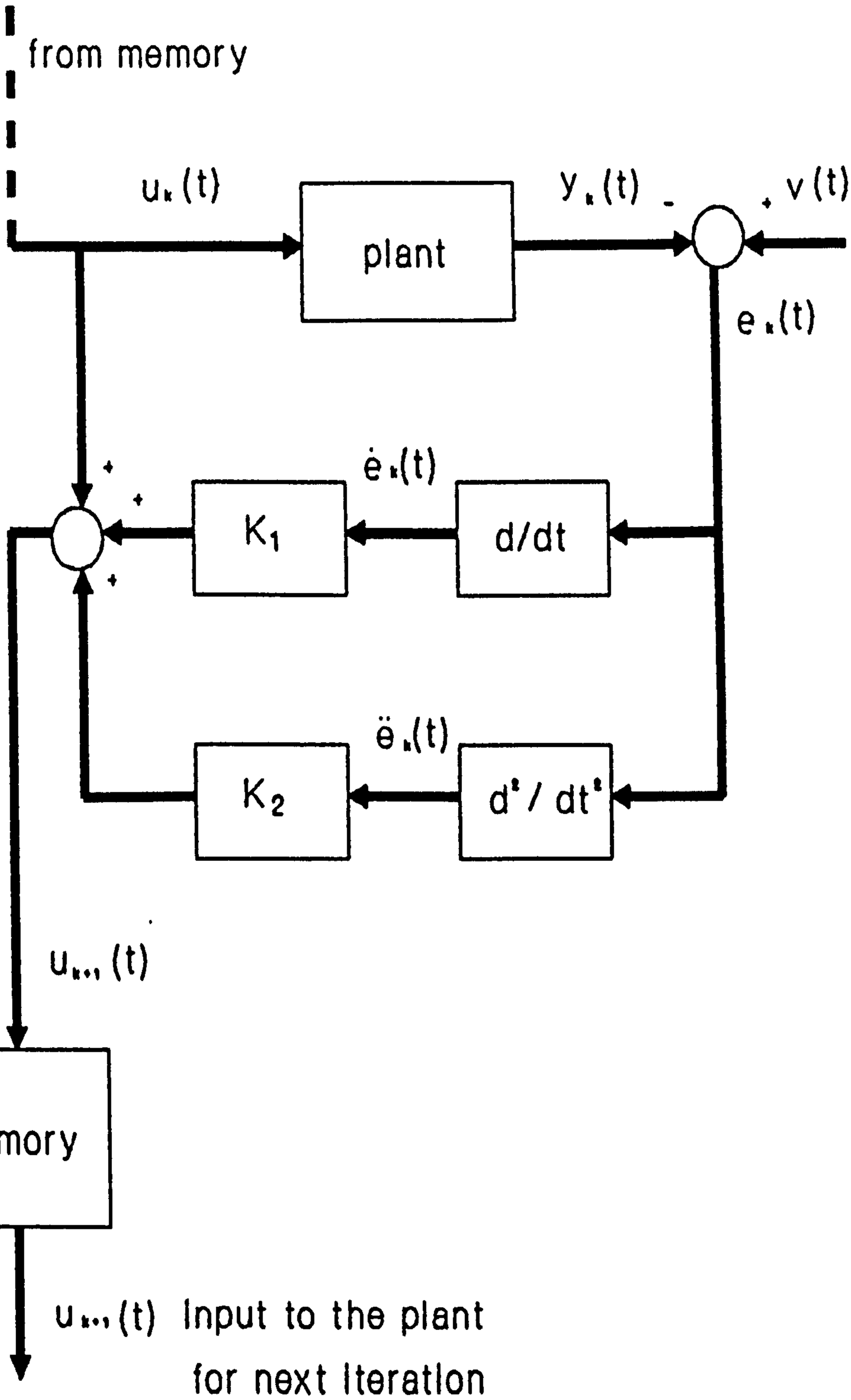

Fig.2.1 Iterative Learning Process For
First-Order Irregular Plant.

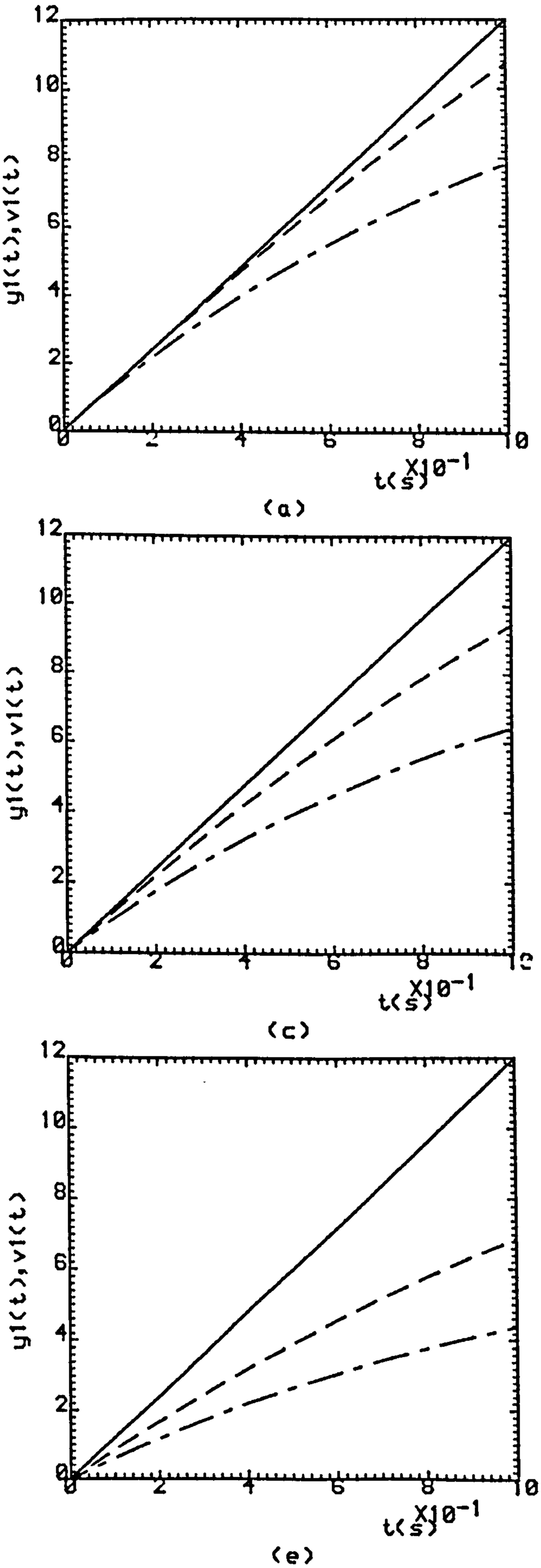

Fig.2.2 (a,b) (rho=0.0,sigma=5.0).
(c,d) (rho=0.2,sigma=4.0).
(e,f) (rho=0.5,sigma=2.5).
-·-·- K=1 , ----- K=2

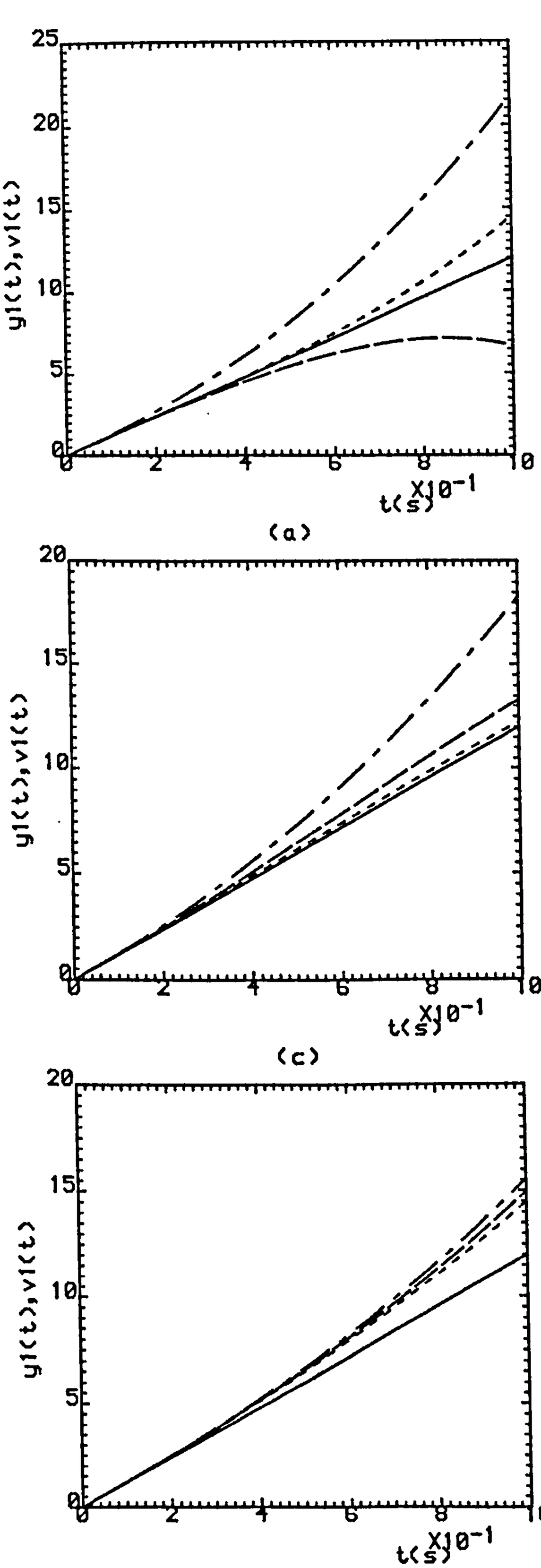

Fig.2.3 (a,b) (rho=0.0,sigma=9.58).
(c,d) (rho=0.5,sigma=4.79).
(e,F) (rho=0.9,sigma=0.958).
-·-·- K=1 , ----- K=2 , ... K=3

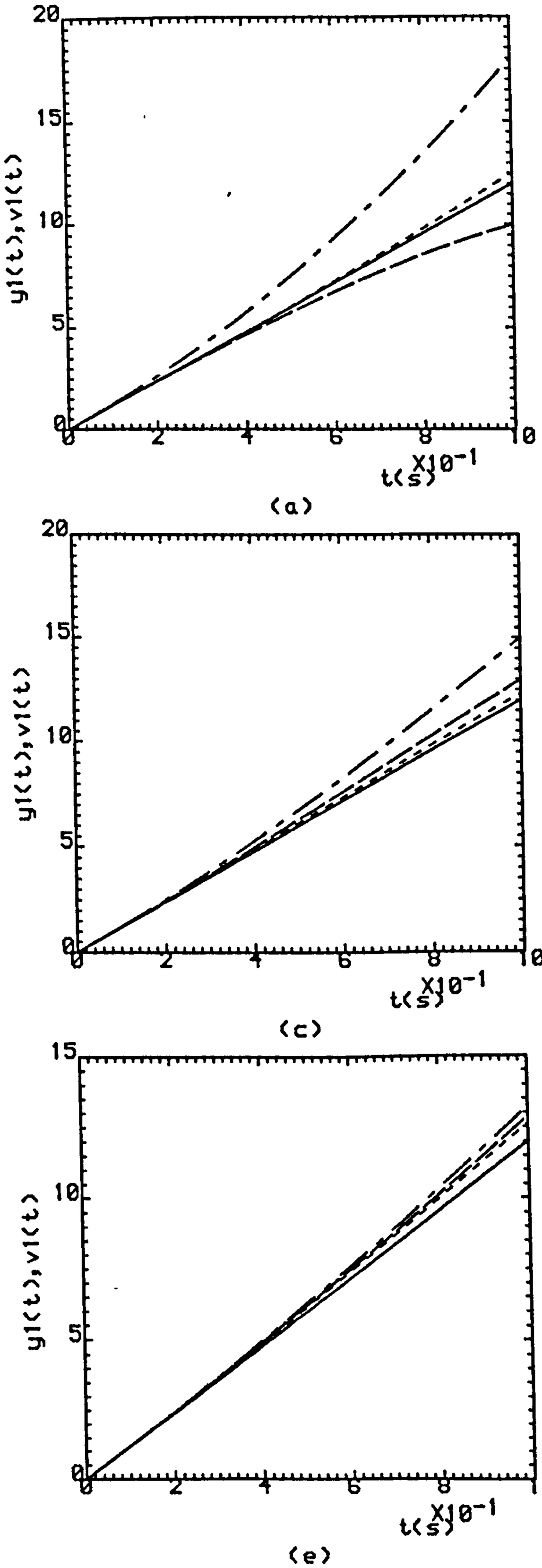

Fig.2.4 (a,b) (rho=0.0,sigma=1.0).
(c,d) (rho=0.5,sigma=0.5).
(e,F) (rho=0.8,sigma=0.2).
-.-.- K=1 , ----- K=2 , ... K=3

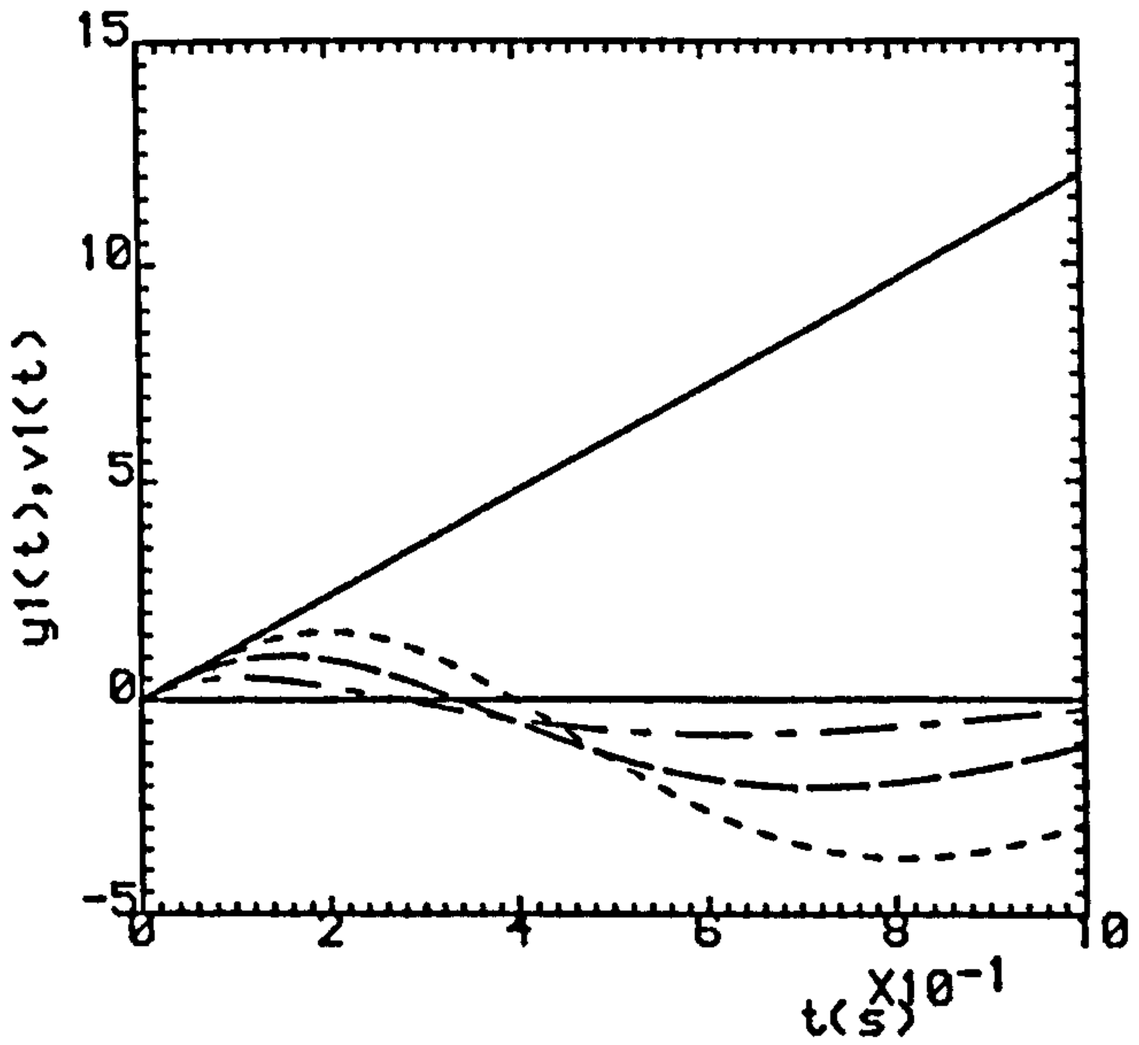

(a)

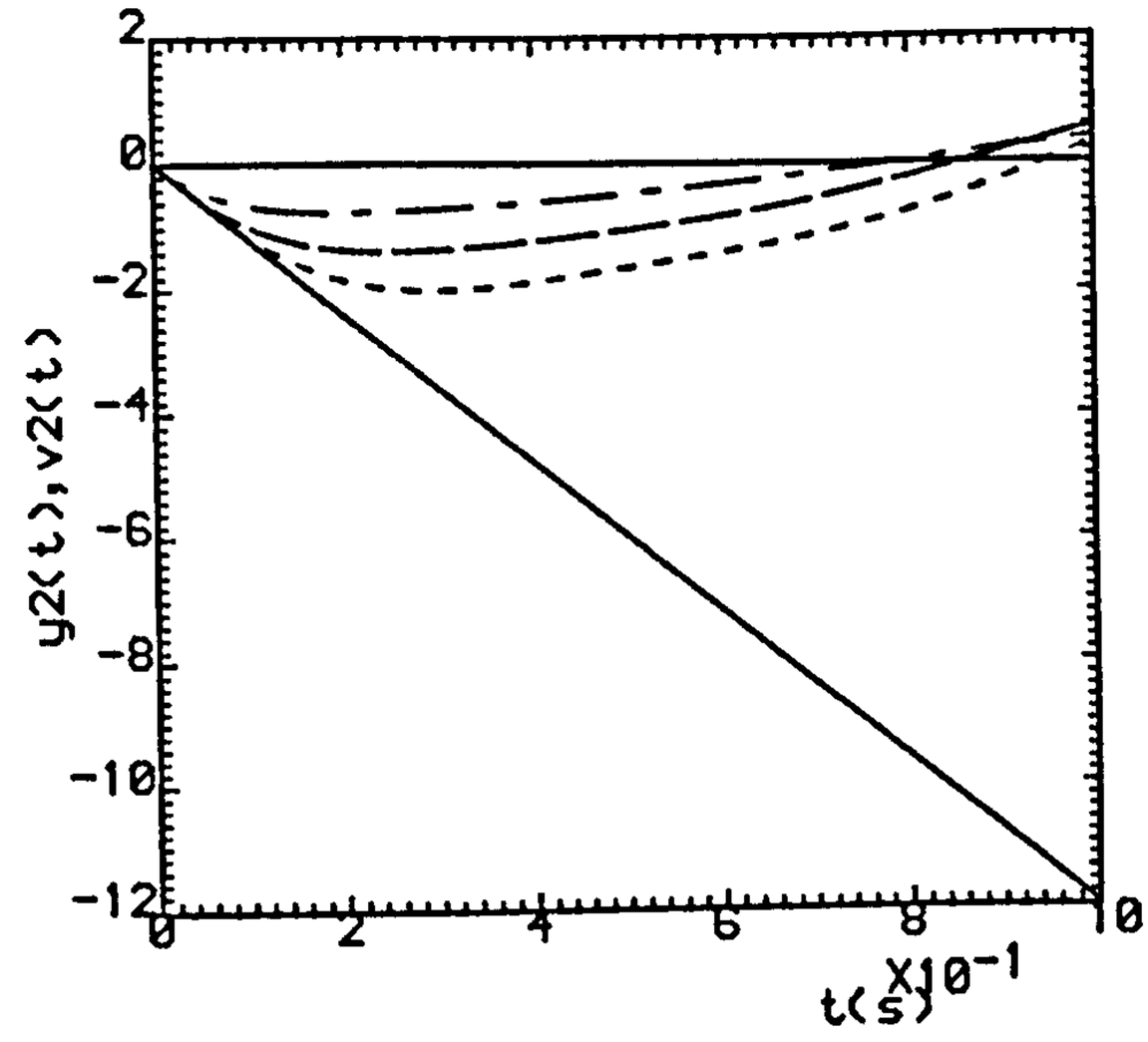

(b)

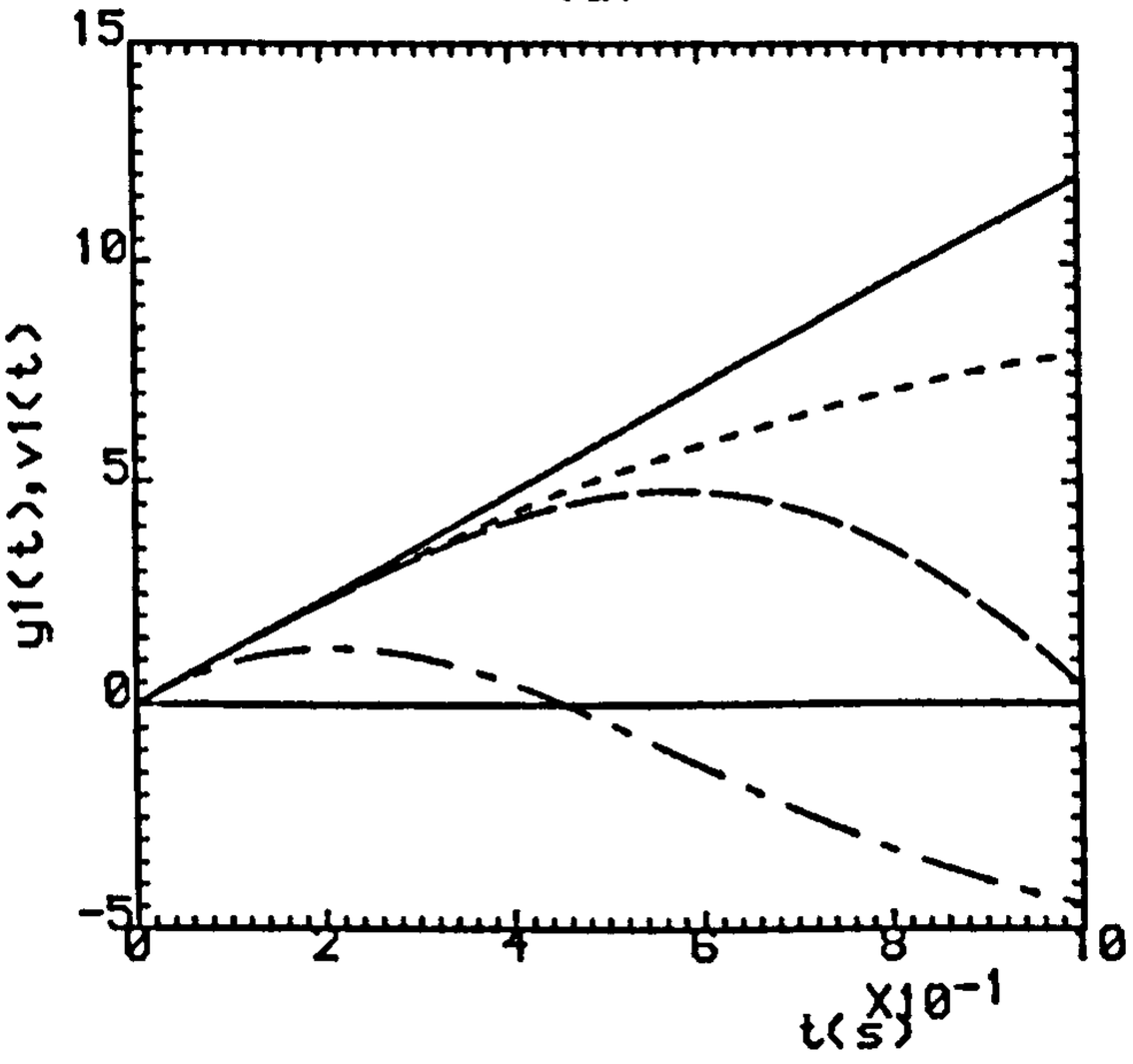

(c)

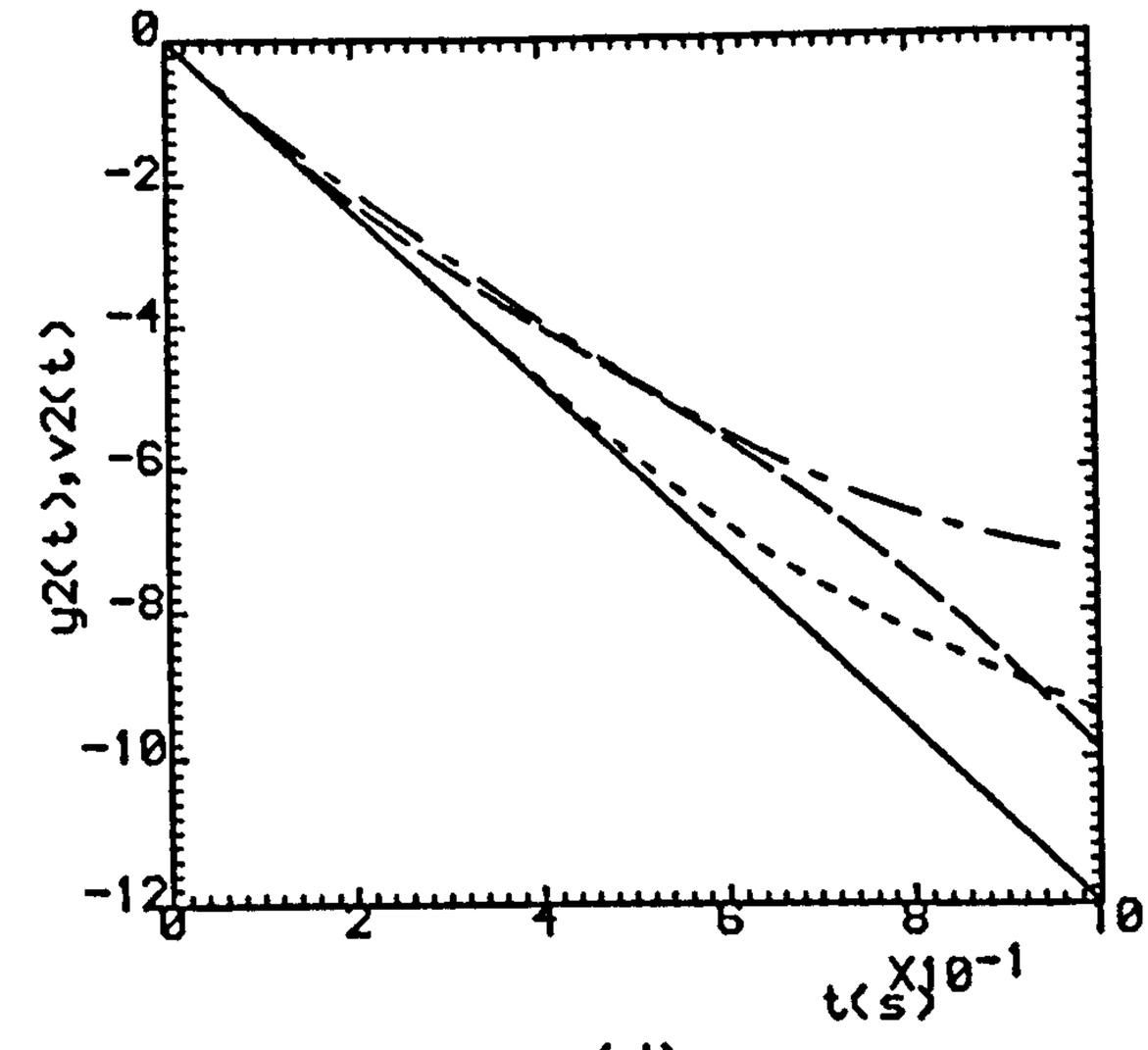

(d)

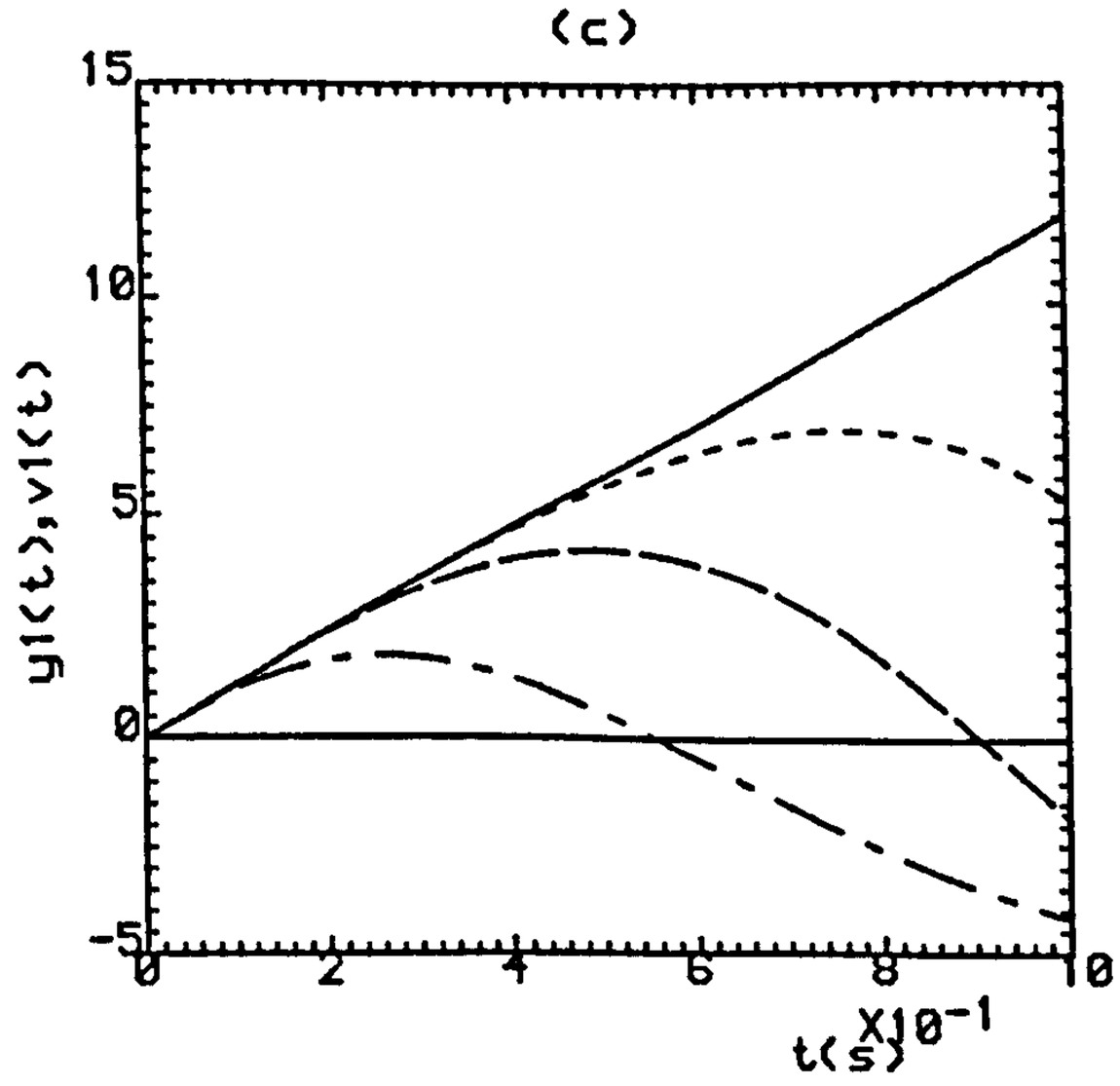

(e)

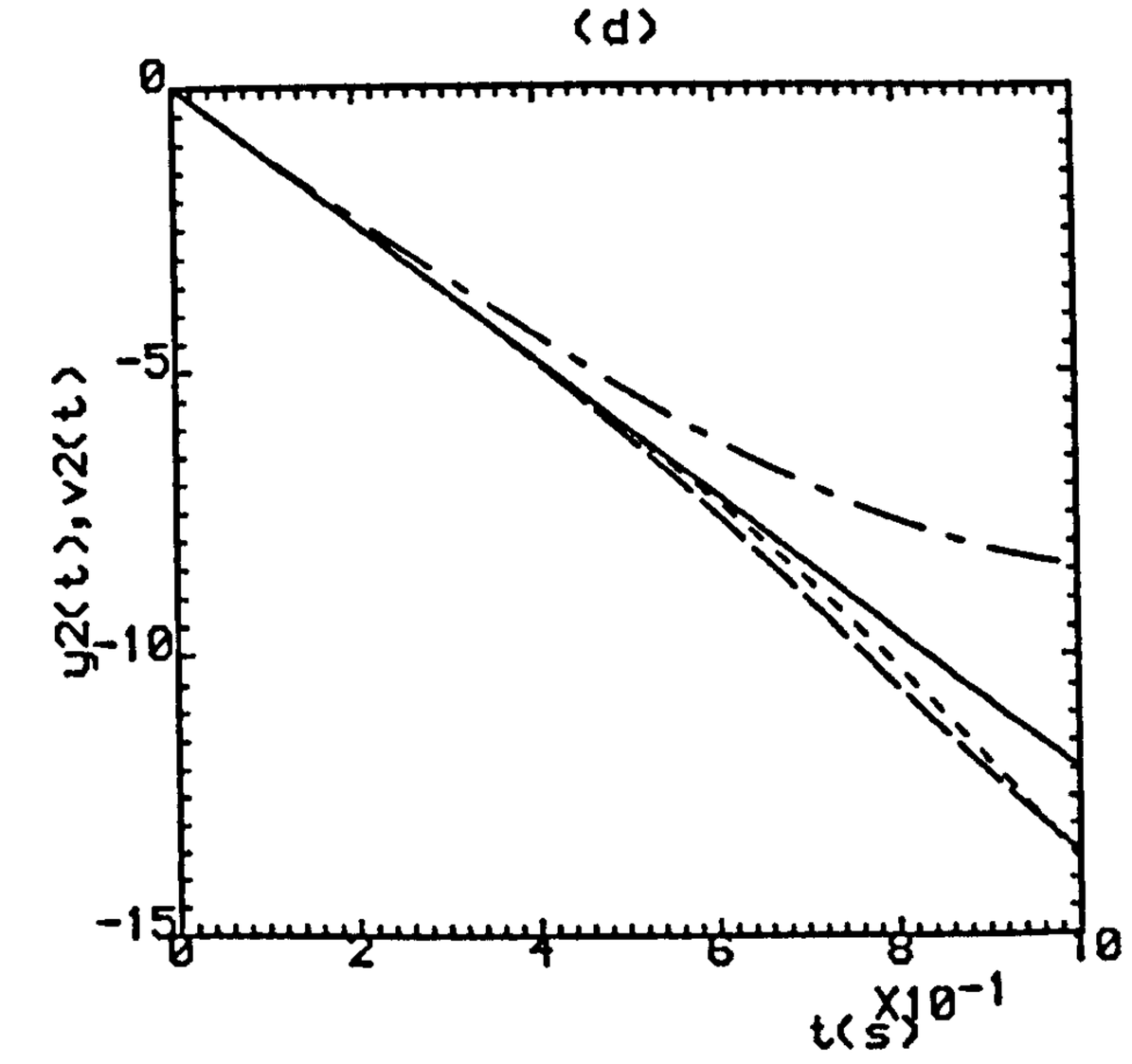

(F)

Fig.2.5 (a,b) (rho=0.0,sigma=15.0).
(c,d) (rho=0.0,sigma=8.0).
(e,f) (rho=0.0,sigma=4.92).
-·-·- K=1 , ----- K=2 , ... K=3

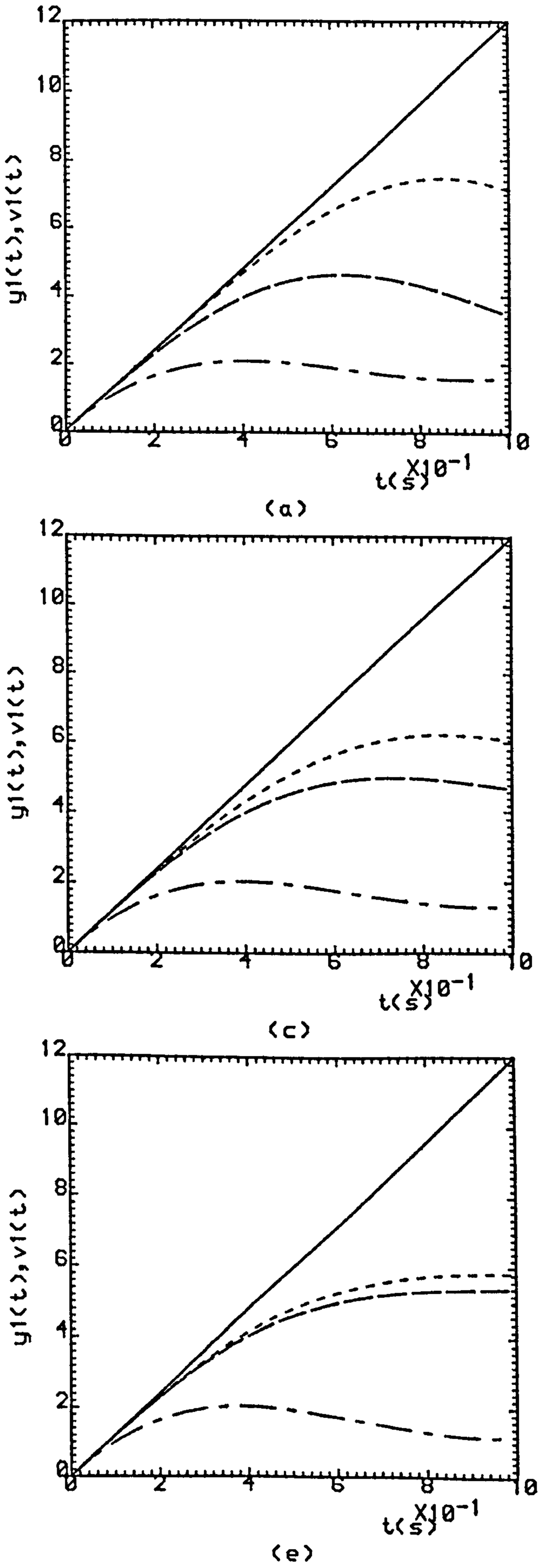

Fig.2.6 (a,b) (rho=0.0,sigma=6.6).
(c,d) (rho=0.5,sigma=3.3).
(e,f) (rho=0.8,sigma=1.32).
-·-·- K=1 , ----- K=2 , ... K=3

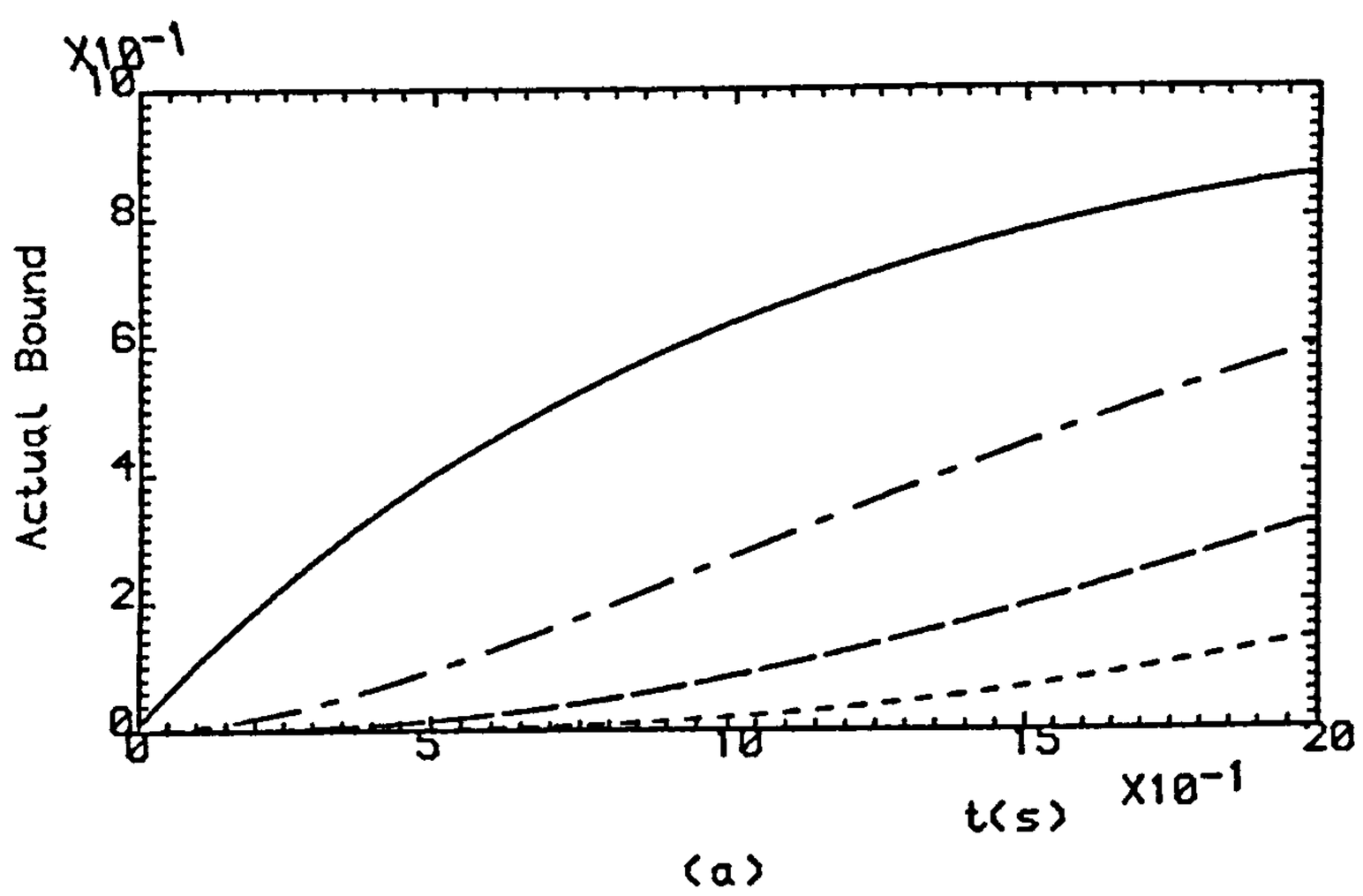

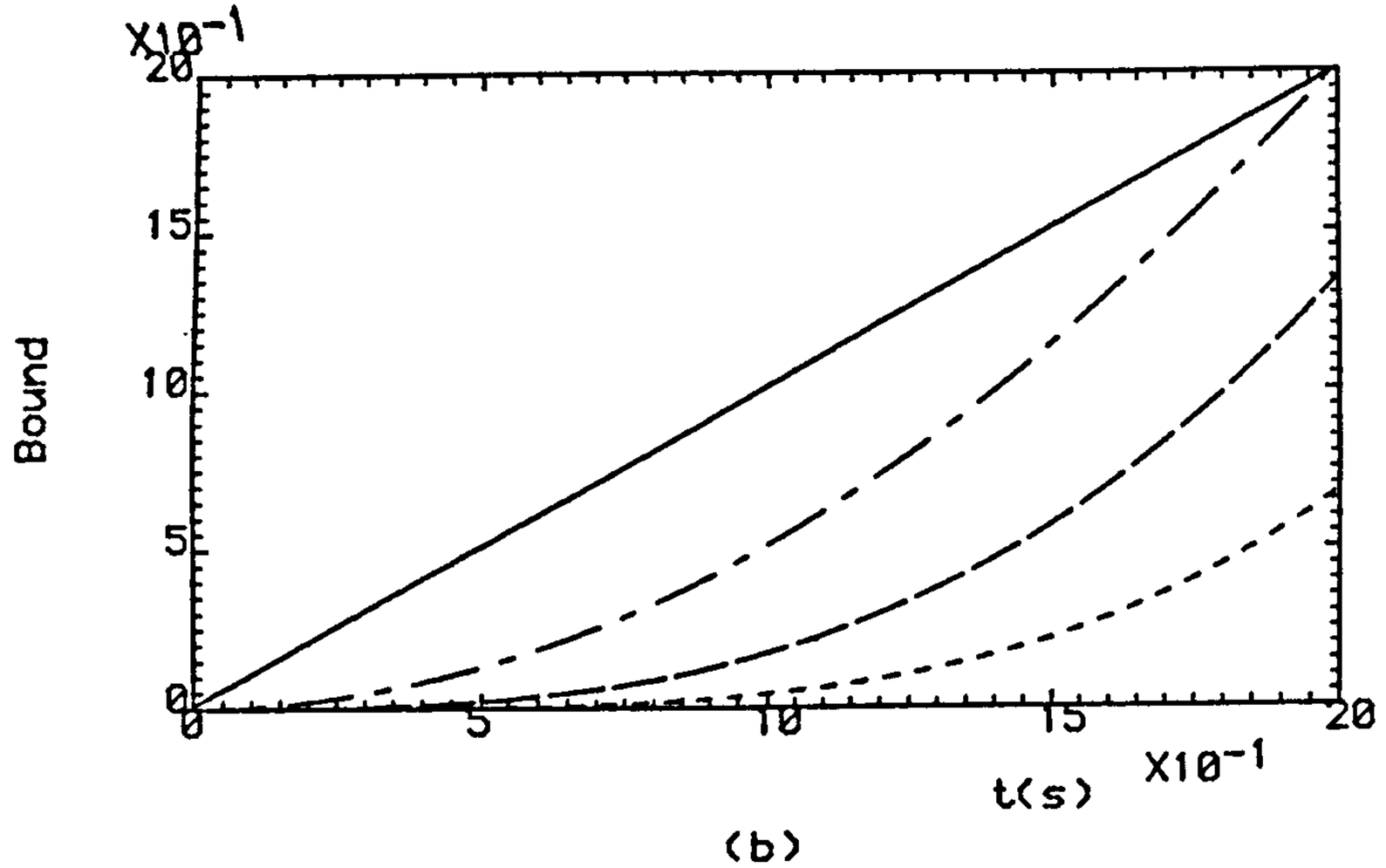

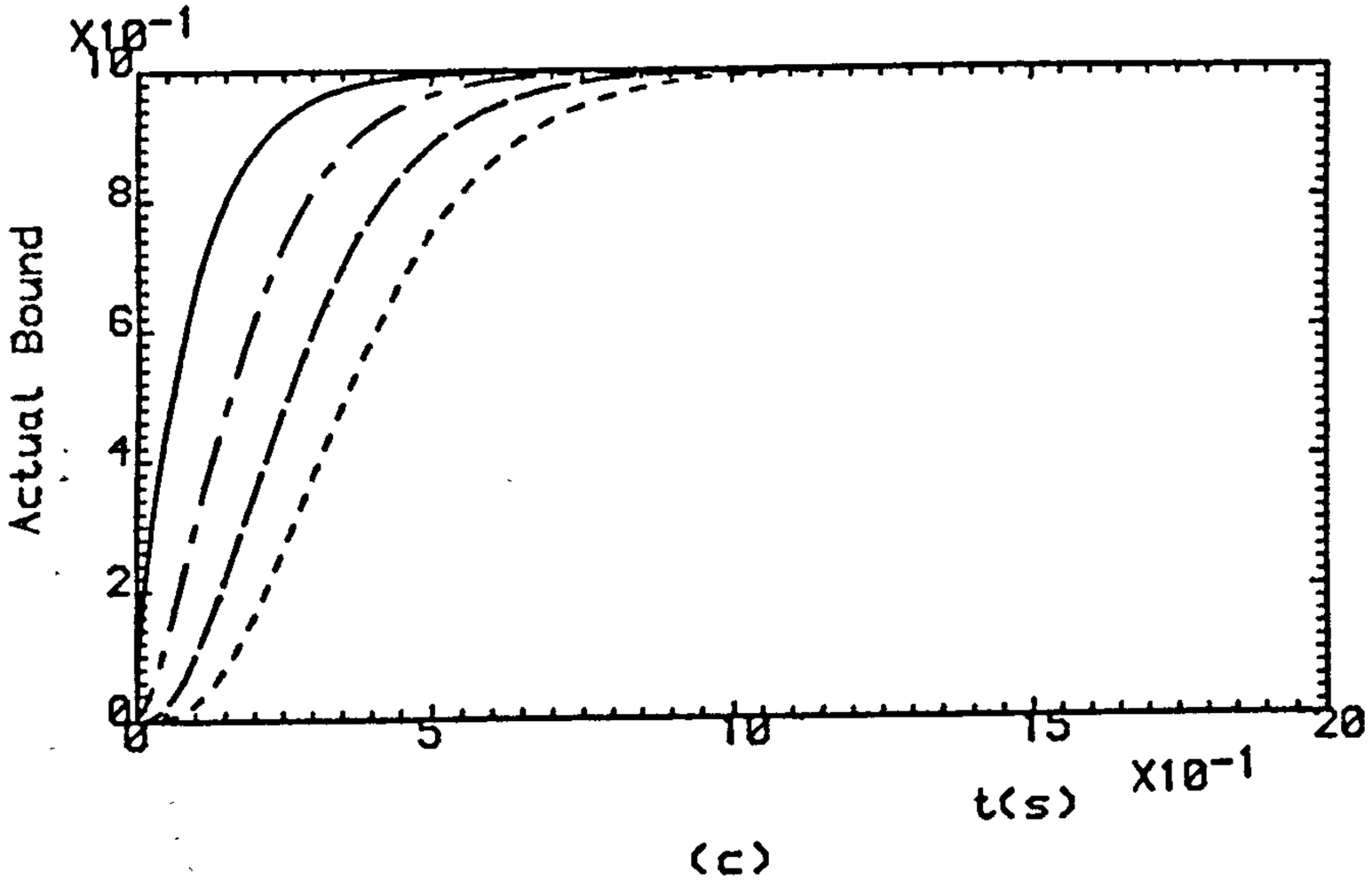

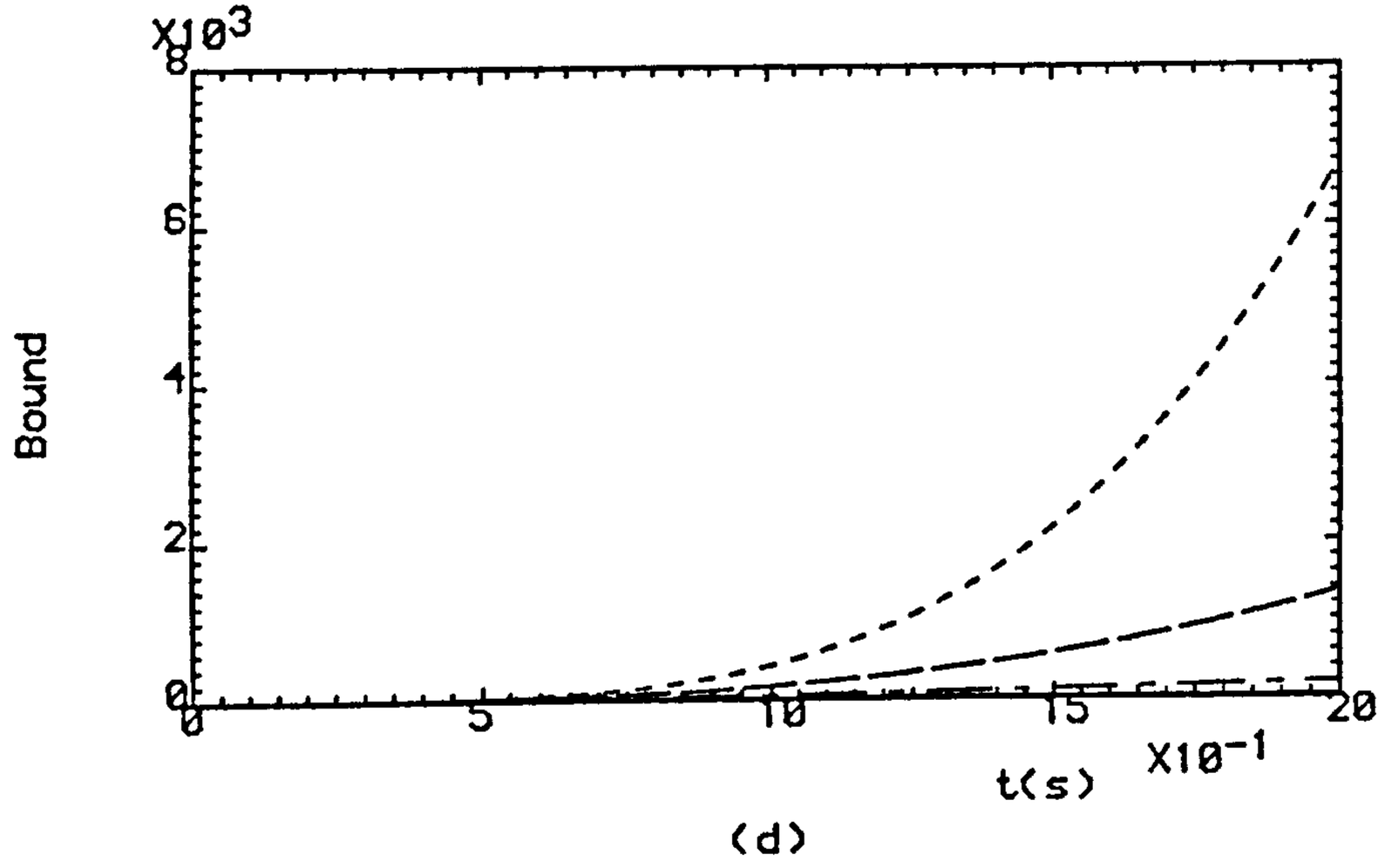

Fig.2.7 (a,b) (rho=0.0,sigma=1.0).
(c,d) (rho=0.0,sigma=10.0).

——— K=1 , -·-·- K=2 , ----- K=3 , ... K=4

CHAPTER 3

DESIGN OF ITERATIVE LEARNING CONTROLLERS USING INITIAL IMPULSIVE ACTION

3.1 INTRODUCTION

In the previous chapter, the design of iterative learning controllers with initial state shifting was considered. Due to the possible practical difficulties of implementing such controllers - namely, the difficulties involved in shifting the states at the beginning of each successive iteration for learning to occur - such controllers perhaps need to be modified. It is therefore shown in this chapter that such practical difficulties can be circumvented using iterative learning controllers with initial impulsive action. However, as was the case in Chapter 2, it is shown that these controllers do not require detailed estimates of plant parameters and are therefore extremely attractive for application to complex industrial plants. Nevertheless, it is important to note that impulsive action must be implemented practically by using pulses of short duration and large amplitude.

It was explained in Chapter 2 that the existing theory of iterative learning control (Arimoto et al 1984) requires that the plants under control be regular. In order to remove this limitation, iterative learning controllers with initial impulsive action were characterized by Porter and Mohamed (1990b) for a class of completely irregular linear time-invariant multivariable plants, i.e. plants with rank-defective first Markov parameters but full-rank second Markov parameters. It was also shown by Porter and Mohamed (1991b) that these results can be extended so as to embrace iterative learning controllers for ℓth-order partially irregular linear time-invariant multivariable

plants, i.e. plant with rank-defective first, second,.....,ℓth Markov parameters but full-rank (ℓ+1)th Markov parameter, (ℓ = 1,2,3....).

These theoratical results are presented in this chapter and their effectiveness is illustrated by the design of iterative learning controllers for typical first-order partially and completely irregular plants and also for a typical second-order completely irregular plant with various stability characteristics.

3.2 Analysis

The linear time-invariant multivariable plants under consideration are assumed to be governed on the continuous-time set by state and output equations of the respective forms

$$\dot{x}(t) = Ax(t) + Bu(t) \qquad \text{...(3.1a)}$$

and

$$y(t) = C\,x(t) \quad , \qquad \text{...(3.1b)}$$

where $x(t) \in R^n$ is the state vector, $u(t) \in R^m$ is the input vector, $y(t) \in R^m$ is the output vector, $A \in R^{n\times n}$ is the plant matrix, $B \in R^{n\times m}$ is the input matrix and $C \in R^{m\times n}$ is the output matrix. In addition, it is assumed that

$$\text{rank } CB = m - p \qquad \text{...(3.2)}$$

and

$$\text{rank } CAB = m \qquad \text{...(3.3)}$$

where $p \in [0,m]$ is the rank defect of the first Markov parameter CB. Such plants are first-order partically irregular when $p > 0$ and therefore fail to satisfy the

fundamental requirements of Arimoto et al (1984) that $p = 0$ for the existence of iterative learning controllers. However, the results presented in this chapter indicate that it is possible to control such first-order partially irregular plants using an appropriately generalized iterative learning controller together with intial impulsive action

In these controllers, the ultimate objective is to generate an input vector $u(t) \epsilon R^m$ that produces a plant output vector $y(t) \epsilon R^m$ that concides with the desired plant output vector $v(t) \epsilon R^m$ over a fixed finite time interval $[0,T_t]$. It is assumed that the iterative learning process begins by subjecting the plant to an arbitrary continuous input vector $u_0(t) \epsilon R^m$ and by storing $u_0(t) \epsilon R^m$ on $[0,T_t]$ together with the resulting error vector $e_0(t) = v(t) - y_0(t) \epsilon R^m$ between the desired output vector and the actual output vector $y_0(t) \epsilon R^m$ caused by the input vector $u_0(t) \epsilon R^m$. The iterative learning process continues by adjusting the initial state vector of the plant, by subjecting the plant to a new input vector $u_1(t) \epsilon R^m$ formed from $u_0(t) \epsilon R^m$ and $e_0(t) \epsilon R^m$, and by storing $u_1(t) \epsilon R^m$ on $[0,T_t]$ together with the resulting error vector $e_1(t) = v(t) - y_1(t) \epsilon R^m$ between the desired output vector and the actual output vector $y_1(t) \epsilon R^m$ caused by the input vector $u_1(t) \epsilon R^m$. This iterative process continues indefinitely producing a sequence of output vectors $\{y_0(t), y_1(t), ..., y_k(t), ...\}$ on $[0,T_t]$ corresponding to a sequence of initial state vectors $\{x_0(0), x_1(0), ..., x_k(0), ...\}$ and a sequence of initial input vectors $\{u_0(0), u_1(0), ..., u_k(0), ...\}$ on $[0,T_t]$.

In order to establish the precise conditions under which learning occurs in the case of plants governed by equations of the form (3.1), it is first necessary to introduce the vector and matrix norms

$$\| \dot{e}_k(t) \|_\infty = \max_{1 \le i \le m} |\dot{e}_k^{(i)}(t)| \qquad \text{...(3.4a)}$$

and

$$\| G \|_\infty = \max_{1 \le i \le m} \left\{ \sum_{j=1}^{m} |g^{(i,j)}| \right\} \qquad \text{...(3.4b)}$$

In these norms, $\dot{e}_k^{(i)}(t)$ is the ith element of $\dot{e}_k(t) \in R^m$ and $g^{(i,j)}$ is the i,jth element of $G \in R^{m \times m}$.

The following fundamental result can now be proved, for first-order partially irregular linear time-invariant multivariable plants.

Theorem 3.1

In the case of plant with state and output equations

$$\dot{x}_k(t) = Ax_k(t) + Bu_k(t)$$

and

$$y_k(t) = Cx_k(t)$$

under the action of the control law

$$u_{k+1}(t) = u_k(t) + K_1 \dot{e}_k(t) + K_2 \ddot{e}_k(t) + K_2 \dot{e}_k(0)\, \delta(t) \qquad \text{...(3.5)}$$

where $K_1 \in R^{m \times m}$, $K_2 \in R^{m \times m}$, $\delta(t)$ is the Dirac delta function, and

$$e_k(t) = v(t) - y_k(t)$$

assume that

(i) $u_0(t)$ is continuous on $[0,T_t]$ and $v(t)$, $\dot{v}(t)$ are continuously differentiable on $[0,T_t]$;

(ii) $CBK_2 = 0$;

(iii) $x_0(0)$ is such that $y_0(0) = v(0)$;

(iv) $x_{k+1}(0) = x_k(0) \quad (k = 0,1,2,...)$;

(v) $\| I_m - CBK_1 - CABK_2 \|_\infty < 1$.

Then,

$$y_k(t) \to v(t)$$

uniformly in $t \in [0,T_t]$ as $k \to \infty$.

Proof

The solution of the governing equation of the plant implies that

$$y_{k+1}(t) = CAe^{At} x_{k+1}(0) + CBu_{k+1}(t) + \int_0^t CAe^{A(t-\tau)} Bu_{k+1}(\tau)d\tau \ .$$

Hence, it follows that

$$\dot{e}_{k+1}(t) = \dot{v}(t) - \left[CAe^{At} x_{k+1}(0) + CBu_{k+1}(t) + \int_0^t CAe^{A(t-\tau)} Bu_{k+1}(\tau)d\tau \right] \ .$$

This, using (iv) and substituting the control law, indicates that

$$\dot{e}_{k+1}(t) = \dot{v}(t) - [CAe^{At} x_k(0) + CBu_k(t) + CBK_1\ \dot{e}_k(t)$$

$$+ CBK_2 \ddot{e}_k\ \ (t) + CBK_2\ \dot{e}_k(0)\ \delta(t) + \int_0^t CAe^{A(t-\tau)}\ Bu_k(\tau)d\tau$$

$$+ \int_0^t CAe^{A(t-\tau)}\ BK_1\ \dot{e}_k(\tau)d\tau + \int_0^t CAe^{A(t-\tau)}\ BK_2 \ddot{e}_k(\tau)d\tau$$

$$+ \int_0^t CAe^{A(t-\tau)}\ BK_2\ \dot{e}_k(0)\ \delta(\tau)d\tau]$$

and therefore, using (ii), that

$$\dot{e}_{k+1}(t) = \dot{v}(t) - [\dot{y}_k(t) + CBK_1\dot{e}_k(t) + \int_0^t CAe^{A(t-\tau)}BK_1\dot{e}_k(\tau)d\tau$$

$$+ \int_0^t CAe^{A(t-\tau)}BK_2\ddot{e}_k(\tau)d\tau + CAe^{At}\ BK_2\dot{e}_k(0)].$$

But integration by parts indicates that

$$\int_0^t CAe^{A(t-\tau)}BK_2\ddot{e}_k(\tau)d\tau = [CABK_2\dot{e}_k(t) - CAe^{At}BK_2\dot{e}_k(0)]$$

$$+ \int_0^t CAe^{A(t-\tau)}ABK_2\dot{e}_k(\tau)d\tau$$

so that

$$\dot{e}_{k+1}(t) = (I_m - CBK_1 - CABK_2)\dot{e}_k(t) - \int_0^t CAe^{A(t-\tau)}(BK_1 + ABK_2)\dot{e}_k(\tau)d\tau \ .$$

Now, taking the norm of both sides of this equation, indicates that

$$\| \dot{e}_{k+1}(t) \|_\infty \leq \| I_m - CBK_1 - CABK_2 \|_\infty \cdot \| \dot{e}_k(t) \|_\infty$$

$$+ \sup_{0 \leq t \leq T_t} \int_0^t \| CAe^{A(t-\tau)}(BK_1 + ABK_2) \|_\infty \ \| \dot{e}_k(\tilde{\tau}) \|_\infty \, d\tau$$

$$\leq \rho \| \dot{e}_k(t) \|_\infty + \sigma \sup_{0 \leq t \leq T_t} \int_0^t \| \dot{e}_k(\tau) \|_\infty \, d\tau$$

where

$$\rho = \| I_m - CBK_1 - CABK_2 \|_\infty \quad , \qquad \text{...(3.6)}$$

$$\sigma = \sup_{0 \leq t \leq T_t} \| CAe^{At}(BK_1 + ABK_2) \|_\infty \quad , \qquad \text{...(3.7)}$$

and

$$\beta = \sup_{0 \leq t \leq T_t} \| \dot{e}_0(t) \|_\infty \quad .$$

Therefore,

$$\| \dot{e}_1(t) \|_\infty \leq \rho \| \dot{e}_0(t) \|_\infty + \sigma \int_0^t \| \dot{e}_0(\tau) \|_\infty d\tau$$

$$\leq \rho\beta + \sigma\beta t$$

$$\leq (\rho + \sigma t)\beta \quad ,$$

$$\| \dot{e}_2(t) \|_\infty \leq \rho \| \dot{e}_1(t) \|_\infty + \sigma \int_0^t \| \dot{e}_1(\tau) \|_\infty \, d\tau$$

$$\leq (\rho^2 + \sigma\rho t)\beta + \sigma \int_0^t (\rho + \sigma\tau)\beta \, d\tau$$

$$\leq (\rho^2 + \sigma\rho t)\beta + \sigma\rho\beta t + \frac{\sigma^2 t^2}{2!}\beta$$

$$\leq \left[\rho^2 + 2\sigma\rho t + \frac{\sigma^2 t^2}{2!}\right]\beta \quad ,$$

. . . . . .

$$\| \dot{e}_k(t) \|_\infty \leq (\rho^k + k\rho^{k-1}\sigma t + \frac{k(k-1)}{2!}\rho^{k-2}\frac{\sigma^2 t^2}{2!}$$

$$+ \frac{k(k-1)(k-2)}{3!}\rho^{k-3}\frac{\sigma^3 t^3}{3!}$$

$$+ \frac{k(k-1)(k-2)(k-3)}{4!}\rho^{k-4}\frac{\sigma^4 t^4}{4!} + \ldots$$

$$+ k\rho\frac{\sigma^{k-1} t^{k-1}}{(k-1)!} + \frac{\sigma^k t^k}{k!})\beta \quad ,$$

or, in closed form,

$$\| \dot{e}_k(t) \|_\infty \leq \beta \sum_{q=0}^{k} \frac{k!}{q!(k-q)!}\rho^{k-q}\frac{\sigma^q t^q}{q!} \quad . \qquad \ldots(3.8)$$

It is found that each term in the right-hand side of the inequality (3.8) is positive. Therefore, in order for $\| \dot{e}_k(t) \|_\infty$ to vanish as $k \to \infty$, each term must vanish as $k \to \infty$. Indeed, the only way to make these terms vanish is by satisfying condition (v) of Theorem 3.1 that $0 \leq \rho < 1$. This can be proved by noting that

$$\lim_{k\to\infty} k^s \rho^k \to 0$$

for any integer $s > 0$ provided that $|\rho| < 1$. This fact is best appreciated by considering the ratio of the kth term to the $(k\text{-}1)th$ term in the *series* $K^s\rho^k$. Thus,

$$\frac{\tau_k}{\tau_{k-1}} = \frac{(k)^s \rho^k}{(k-1)^s \rho^{k-1}}$$

$$= \left(\frac{k}{k-1}\right)^s \rho \quad .$$

Hence,

$$\lim_{k\to\infty} \frac{\tau_k}{\tau_{k-1}} = \rho \quad .$$

This means that

$$\lim_{k\to\infty} \tau_k = 0$$

provided that $|\rho| < 1$.

However, the last term of the inequality (3.8) will vanish in a different fashion, because the speed of the factorial function's progress is more rapid than the speed of the exponential function's progress. In other words, the denominator of $(\sigma^k t^k/k!)$ increases faster than the numerator so that this term vanishes as k increases. However, the speed at which this term disappears depends on the magnitude of the parameter, σ. The smaller the value of σ the faster the term will disappear.

It therefore follows from these considerations that $\|\dot{e}_k(t)\|_\infty \to 0$, as $k \to \infty$, which implies that $\dot{y}_k(t) \to \dot{v}(t)$ uniformly in $t \in [0,T_t]$ as $k \to \infty$. But

$$y_{k+1}(0) = Cx_{k+1}(0)$$

from which it follows, using (iv), that

$$y_{k+1}(0) = Cx_k(0) = y_k(0)$$

and therefore, using (iii), that

$$y_k(0) = v(0)$$

for all $k = 0,1,2,....$ It is therefore finally evident that

$$y_k(t) \to v(t)$$

uniformly in $t \in [0,T_t]$ as $k \to \infty$.

The difference between the method proposed in this chapter and that proposed in Chapter 2 is that the iterative learning controller using initial impulsive action does not require that the initial state be shifted directly. Indeed, examining the conditions of Theorem 3.1, it is clear that $x_{k+1}(0) = x_k(0)$ for all k. However, the initial state is shifted indirectly by the introduction of the initial impulsive action in the iterative learning controller so that the practical difficulties of implementing the iterative learning controllers with initial state shifting are thus circumvented. The effectiveness of this method can be seen clearly in the illustrative examples presented later in this chapter.

It is evident that, although the parameter σ defined in equation (3.7) is not involved in the sufficient conditions for learning enunciated in Theorem 3.1, the value of σ nevertheless affects the rate at which learning occurs. This parameter is accordingly called the learning parameter of the plant/controller combination and its effect is investigated in Section 3.4. Moreover, according to equation (3.7), the value of this parameter depends on the stability characteristics of the plant under control because of the presence of e^{At}.

Furthermore, as in Chapter 2, since CB has full-rank in the special case of regular plants, condition (ii) of Theorem 3.1 then indicates that $K_2 = 0$ so that the control-law and condition (v) reduce to the corresponding results of Arimoto et al (1984) for regular plants. However, it is clearly impossible to satisfy condition (v) of Theorem 3.1 in the case of plants with second or higher-order irregularities, i.e. plants with rank defective CB, CAB, CA^2B,...,$CA^{\ell-1}B$ Markov parameters and full-rank $CA^{\ell}B$ Markov parameter ($\ell \geq 2$). In such cases, the following generalised result can be proved by means of the same arguments as were used in the case of Theorem 3.1.

Theorem 3.2

In the case of the plant with state and output equations

$$\dot{x}_k(t) = Ax_k(t) + Bu_k(t)$$

and

$$y_k(t) = Cx_k(t)$$

under the action of the control law

$$u_{k+1}(t) = u_k(t) + \sum_{i=1}^{\ell+1} K_i e_k^{(i)}(t) + \sum_{j=2}^{\ell+1} \sum_{i=j}^{\ell+1} K_i \, e_k^{(i-j+1)}(0) \, \delta^{(i-2)}(t) \qquad ...(3.9)$$

where $K_i \in R^{m \times m}$ $(i = 1,2,...,\ell+1)$, $\delta(t)$ is the Dirac delta function, and

$$e_k(t) = v(t) - y_k(t)$$

assume that

(i) $u_0(t)$ is continuous on $[0,T_t]$ and $v(t)$, $\dot{v}(t)$ are continuously differentiable on $[0,T_t]$;

(ii) $\sum_{i=j}^{\ell+1} CA^{i-j}BK_i = 0 \quad (j = 2,3,...,\ell+1)$;

(iii) $x_0(0)$ is such that $y_0(0) = v(0)$;

(iv) $x_{k+1}(0) = x_k(0) \quad (k = 0,1,2,...)$;

(v) $\| I_m - \sum_{i=1}^{\ell+1} CA^{i-1}BK_i \|_\infty < 1.$

Then,

$$y_k(t) \rightarrow v(t)$$

uniformly in $t \in [0,T_t]$ as $k \rightarrow \infty$.

It transpires, in the course of the proof that,

$$\| \dot{e}_k(t) \|_\infty \leq \beta \sum_{q=0}^{k} \frac{k!}{q!(k-q)!} \rho^{(k-q)} \frac{\sigma^q t^q}{q!} \qquad ...(3.10)$$

where $k > 0$.

It is clear by comparing the inequality (3.10) with (3.8) that both inequalities are identical except that, in the inequality (3.10), the parameters ρ and σ are

$$\rho = \| I_m - \sum_{i=1}^{\ell+1} CA^{i-1} B K_i \|_\infty \qquad ...(3.11)$$

and

$$\sigma = \sup_{0 \le t \le T_t} \| CAe^{At} \sum_{i=1}^{\ell+1} A^{i-1} B K_i \|_\infty \qquad ...(3.12)$$

Thus, Theorem 3.2 establishes the conditions under which the iterative learning controller governed by equation (3.9) generates an input vector $u(t) \in R^m$ that produces an output vector $y(t) \in R^m$ which coincides with the command vector $v(t) \in R^m$ over the time interval $[0, T_t]$ for higher-order irregular plants.

It is clear by comparing the inequalities (3.8) and (3.10) with the inequalities (2.8) and (2.10), respectively, that these inequalities are pairwise identical. Thus, it follows that the quantity on the right hand side of the inequalities (3.8) and (3.10) is the upper bound of the rate of change of error. This bound, as shown in Chapter 2, can be used as a guide to show how the parameters ρ and σ affect learning rates in the case of iterative learning control with initial impulsive action.

3.3 Synthesis

It is clear that learning will occur, in the sense that $e_k \to 0$ as $k \to \infty$ in Theorems 3.1 and 3.2, provided that condition (v) is satisfied, i.e. $\rho < 1$. However, as shown in Chapter 2, the speed with which the plant learns is determined by the values of the

parameters ρ and σ. The smaller these parameters the faster the learning rate will be (see Section 3.4). The values of both parameters ρ and σ depend on the choice of the controller gain matrices; in addition, σ depends on the stability characteristics of the plant under control. Thus, the controller gain matrices must be designed so that both parameters are as small as possible. Therefore, in the case of first-order partially irregular plants, the controller gain matrices must be

$$K_1 = \lambda(CB + CABD)^{-1} \qquad ...(3.13)$$

and

$$K_2 = DK_1 \ , \qquad ...(3.14)$$

where $\lambda \in R^+$ and $D \in R^{m \times m}$. It is then clear from equation (3.6) that

$$\rho = |1-\lambda| \qquad ...(3.15)$$

which implies that the crucial condition (v) of Theorem 3.1 will be satisfied provided that $0 < \lambda < 2$. In addition, D must be chosen so that $CBD = 0$ (see Appendix A).

However, it is also clear from equation (3.7) that the choice of the controller gain matrices given by equations (3.13) and (3.14) implies that the corresponding value of the learning parameter, σ, is given by

$$\frac{\sigma}{\lambda} = \sup_{0 \le t \le T_t} \| CAe^{At}\,(B + ABD)(CB + CABD)^{-1} \|_\infty \ . \qquad ...(3.16)$$

It is thus evident from equation (3.16) that the value of the right-hand member of equation (3.16) depends upon the stability characteristics of the plant under control.

Indeed, it follows from equation (3.16) that

$$\frac{\sigma}{\lambda} \geq \| CA(B + ABD)(CB + CABD)^{-1} \|_{\infty} \qquad \ldots(3.17)$$

in the case of open-loop stable plants.

The effects of the parameters ρ and σ on the learning rate are investigated in Section 3.4 for various plants with different irregularity and stability characteristics. Similar synthesis considerations apply in the case of plants with higher-order irregularities when Theorem 3.2 is used with ρ and σ as defined in equations (3.11) and (3.12).

3.4 Illustrative Examples

The use of iterative learning controllers can be conveniently illustrated by designing iterative controllers with initial impulsive action for open-loop stable, neutrally stable, and unstable first-order irregular plants. In addition, the design of such controllers is extended so as to embrace an open-loop stable plant with second-order irregularity using the control law proposed in Theorem 3.2

In all these examples, in the iteration corresponding to $k = 0$ neither the inputs nor the outputs have been plotted since both are zero.

Example 3.1

The state and output equations of a linear time-invariant plant on the continuous-time set are

$$\begin{bmatrix} \dot{x}_1(t) \\ \dot{x}_2(t) \\ \dot{x}_3(t) \end{bmatrix} = \begin{bmatrix} -3 & , & 1 & , & 0 \\ -2 & , & -1 & , & 2 \\ 0 & , & 1 & , & -2 \end{bmatrix} \begin{bmatrix} x_1(t) \\ x_2(t) \\ x_3(t) \end{bmatrix} + \begin{bmatrix} 0 & , & 0 \\ 2 & , & 1 \\ 1 & , & 3 \end{bmatrix} \begin{bmatrix} u_1(t) \\ \\ u_2(t) \end{bmatrix}$$

...(3.18a)

and

$$\begin{bmatrix} y_1(t) \\ \\ y_2(t) \end{bmatrix} = \begin{bmatrix} 1 & , & 0 & , & -1 \\ & & & & \\ 1 & , & 0 & , & 0 \end{bmatrix} \begin{bmatrix} x_1(t) \\ x_2(t) \\ x_3(t) \end{bmatrix} \quad . \qquad \text{...(3.18b)}$$

In this case, the plant is asymptotically stable but first-order partially irregular since its first Markov parameter

$$CB = \begin{bmatrix} -1 & , & -3 \\ 0 & , & 0 \end{bmatrix} \qquad \text{...(3.19a)}$$

is rank defective whilst its second Markov parameter

$$CAB = \begin{bmatrix} 2 & , & 6 \\ 2 & , & 1 \end{bmatrix} \qquad \text{...(3.19b)}$$

evidently has full rank.

It is required that the output vector of this plant track the command vector

$$v(t) = \begin{bmatrix} 12t \\ \\ -12t \end{bmatrix} \quad (t \in [0, T_t]) \qquad \ldots(3.20)$$

on the time interval $[0, 1]$ *sec.*

In case

$$x_0(0) = \begin{bmatrix} 0 \\ 0 \\ 0 \end{bmatrix} \qquad \ldots(3.21)$$

and

$$u_0(t) = \begin{bmatrix} 0 \\ 0 \end{bmatrix} \quad , \qquad \ldots(3.22)$$

the learning characteristics of the iterative learning controller with different controller gain matrices given by equation (3.13) and (3.14) when

$$D = \begin{bmatrix} 0 & , & -3 \\ \\ 0 & , & 1 \end{bmatrix} \qquad \ldots(3.23)$$

so that $CBD = 0$ are shown in Figure 3.1. Indeed, the results in Figures 3.1(a,b) correspond to the choice $\lambda = 1$, $\rho = 0$, $\sigma = 5$; those in Figures 3.1(c,d) to the choice $\lambda = 0.8$, $\rho = 0.2$, $\sigma = 4$; and those in Figures 3.1(e,f) to the choice $\lambda = 0.5$, $\rho = 0.5$, $\sigma = 2.5$.

It is clear from these figures that learning is rapid as shown in Figures 3.1(a,b) when $\lambda = 1$, that learning is less rapid as shown in Figures 3.1(c,d) when $\lambda = 0.8$, and that

learning is even less rapid as shown in Figures 3.1(e,f) when $\lambda = 0.5$.

In all these cases, $v(t)$ is such that

$$\dot{e}_0(0) = \begin{bmatrix} 12 \\ -12 \end{bmatrix} \neq 0 \qquad \ldots(3.24)$$

and therefore initial state shifting is required in the iterative learning controller of Chapter 2. It is thus clear that the practical difficulties involved in such initial state shifting are circumvented by the introduction of initial impulsive action into iterative learning controllers.

Example 3.2

The state and output equations of a linear time-invariant plant on the continuous-time set are

$$\begin{bmatrix} \dot{x}_1(t) \\ \dot{x}_2(t) \\ \dot{x}_3(t) \\ \dot{x}_4(t) \end{bmatrix} = \begin{bmatrix} 0 & , & 0.5 & , & 0 & , & 0 \\ 0 & , & 0.1 & , & 0.75 & , & 0 \\ -1.5 & , & 0.5 & , & 1.25 & , & 0 \\ 2.5 & , & 0 & , & -2.5 & , & 0 \end{bmatrix} \begin{bmatrix} x_1(t) \\ x_2(t) \\ x_3(t) \\ x_4(t) \end{bmatrix}$$

$$+\begin{bmatrix} 0 & , & 0 \\ 1 & , & 2 \\ 3 & , & 1 \\ 0 & , & 0 \end{bmatrix}\begin{bmatrix} u_1(t) \\ \\ \\ u_2(t) \end{bmatrix} \qquad \ldots(3.25a)$$

and

$$\begin{bmatrix} y_1(t) \\ \\ y_2(t) \end{bmatrix} = \begin{bmatrix} 1 & , & 0 & , & 0 & , & 0 \\ & & & & & & \\ 0 & , & 0 & , & 0 & , & 1 \end{bmatrix}\begin{bmatrix} x_1(t) \\ x_2(t) \\ x_3(t) \\ x_4(t) \end{bmatrix} . \qquad \ldots(3.25b)$$

In this case, the plant is unstable and is first-order completely irregular since its first Markov parameter

$$CB = \begin{bmatrix} 0 & , & 0 \\ 0 & , & 0 \end{bmatrix} \qquad \ldots(3.26a)$$

is clearly null whilst its second Markov parameter

$$CAB = \begin{bmatrix} 0.5 & , & 1 \\ -7.5 & , & -2.5 \end{bmatrix} \qquad \ldots(3.26b)$$

evidently has full rank.

It is required that the output vector of this plant track the command vector

$$v(t) = \begin{bmatrix} 12t \\ \\ -12t \end{bmatrix} \quad (t \in [0, T_t]) \qquad \ldots(3.27)$$

on the time interval [0, 1] *sec.*

In case

$$x_0(0) = \begin{bmatrix} 0 \\ 0 \\ 0 \\ 0 \end{bmatrix} \qquad \ldots(3.28)$$

and

$$u_0(t) = \begin{bmatrix} 0 \\ 0 \end{bmatrix} , \qquad \ldots(3.29)$$

the learning characteristics of the iterative controller with different controller gain matrices given by equations (3.13) and (3.14) when $D = I_2$ are shown in Figure 3.2. In this case, the plant is unstable and equation (3.16) accordingly indicates that the large value of σ corresponds to the end of the task. The results in Figures 3.2(a,b) correspond to the choice $\lambda = 1$, $\rho = 0$, $\sigma = 9.58$; those in Figures 3.2(c,d) to the choice $\lambda = 0.5$, $\rho = 0.5$, $\sigma = 4.79$; and those in Figures 3.2(e,f) correspond to the choice $\lambda = 0.1$, $\rho = 0.9$, $\sigma = 0.958$. It is clear from these figures that, because of the instability of the plant under control, learning is slow and violent as shown in Figures 3.2(a,b) when $\lambda = 1$; that learning is slower but less violent as shown in Figures 3.2(c,d) when $\lambda = 0.5$; and that learning is even slower but even less violent as shown in Figures 3.2(e,f) when $\lambda = 0.1$. These results confirm that the instability of plants under control imposes unavoidable limits on the learning rates achievable in the iterative learning control. In all these cases, $v(t)$ is such that

$$\dot{e}_0(0) = \begin{bmatrix} 12 \\ \\ -12 \end{bmatrix} \neq 0 \qquad \text{...(3.30)}$$

so that initial state shifting is required in the iterative learning controller of Chapter 2.

Example 3.3

The state and output equations of a linear time-invariant plant on the continuous-time set are

$$\begin{bmatrix} \dot{x}_1(t) \\ \dot{x}_2(t) \\ \dot{x}_3(t) \\ \dot{x}_4(t) \end{bmatrix} = \begin{bmatrix} 0 & , & 0 & , & 1 & , & 3 \\ 0 & , & 0 & , & 0 & , & 1 \\ 0 & , & 0 & , & 0 & , & 0 \\ 0 & , & 0 & , & 0 & , & 0 \end{bmatrix} \begin{bmatrix} x_1(t) \\ x_2(t) \\ x_3(t) \\ (x_4(t)) \end{bmatrix}$$

$$+ \begin{bmatrix} 0 & , & 0 \\ 0 & , & 0 \\ 2 & , & 0 \\ 0 & , & -3 \end{bmatrix} \begin{bmatrix} u_1(t) \\ \\ \\ u_2(t) \end{bmatrix} \qquad \text{...(3.31a)}$$

and

$$\begin{bmatrix} y_1(t) \\ \\ y_2(t) \end{bmatrix} = \begin{bmatrix} 1 & , & 0 & , & 0 & , & 0 \\ \\ 0 & , & 1 & , & 0 & , & 0 \end{bmatrix} \begin{bmatrix} x_1(t) \\ x_2(t) \\ x_3(t) \\ x_4(t) \end{bmatrix} . \qquad \text{...(3.31b)}$$

In this case, the plant is clearly neutrally stable but first-order completely irregular since its first Markov parameter

$$CB = \begin{bmatrix} 0 & , & 0 \\ \\ 0 & , & 0 \end{bmatrix} \qquad \text{...(3.32a)}$$

is clearly null whilst its second Markov parameter

$$CAB = \begin{bmatrix} 2 & , & -9 \\ \\ 0 & , & -3 \end{bmatrix} \qquad \text{...(3.32b)}$$

evidently has full rank.

It is required that the output vector of this plant track the command vector

$$v(t) = \begin{bmatrix} 12t \\ \\ -12t \end{bmatrix}, (t \in [0, T_t]) \qquad \text{...(3.33)}$$

on the time interval [0, 1] *sec.*

In case

$$x_0(0) = \begin{bmatrix} 0 \\ 0 \\ 0 \\ 0 \end{bmatrix} \qquad \ldots(3.34)$$

and

$$u_0(t) = \begin{bmatrix} 0 \\ 0 \end{bmatrix} , \qquad \ldots(3.35)$$

the learning characteristics of the iterative controller with different controller gain matrices given by equations (3.13) and (3.14) when $D = I_2$ are shown in Figure 3.3. Figures 3.3(a,b),(c,d) and (e,f) show the learning controllers when $\lambda = (1, 0.5, 0.2)$, $\rho = (0, 0.5, 0.8)$ and $\sigma = (1, 0.5, 0.2)$ respectively. It is clear from these figures that, learning is fast but violent as shown in Figures 3.3(a,b) when $\lambda = 1$; that learning is slower but less violent as shown in Figures 3.3(c,d) when $\lambda = 0.5$; and that learning is even slower but even less violent as shown in Figures 3.3(e,f) when $\lambda = 0.2$. As explained in Chapter 2, neutrally stable plants are the best to be controlled using iterative learning control since they produce the smallest value of σ without affecting ρ. Thus, good learning performance and rapid convergence is achieved in controlling such plants. In all these cases, $v(t)$ is such that

$$\dot{e}_0(0) = \begin{bmatrix} 12 \\ \\ -12 \end{bmatrix} \neq 0 \qquad \ldots(3.36)$$

so that initial state shifting is required in the iterative learning controller of Chapter 2.

Example 3.4

In the previous examples, the effects of open-loop stability characteristics on the learning parameter and the learning rate were investigated. In this example, the effect of the design parameter D in the controller gain matrices on the learning parameter is investigated. This investigation is carried out in the hope of finding ways to reduce the parameter σ without affecting the parameter ρ in order to obtain better learning rates.

The state and output equations of a linear time-invariant plant on the continuous-time set are

$$\begin{bmatrix} \dot{x}_1(t) \\ \dot{x}_2(t) \\ \dot{x}_3(t) \\ \dot{x}_4(t) \end{bmatrix} = \begin{bmatrix} 0 & , & 5 & , & 0 & , & 0 \\ 0 & , & -8 & , & -6 & , & 0 \\ 3 & , & 2 & , & -3 & , & 0 \\ 5 & , & 0 & , & -5 & , & -6 \end{bmatrix} \begin{bmatrix} x_1(t) \\ x_2(t) \\ x_3(t) \\ x_4(t) \end{bmatrix}$$

$$+ \begin{bmatrix} 0 & , & 0 \\ 1 & , & 2 \\ 3 & , & 1 \\ 0 & , & 0 \end{bmatrix} \begin{bmatrix} u_1(t) \\ \\ \\ u_2(t) \end{bmatrix} \qquad \ldots(3.37a)$$

and

$$\begin{bmatrix} y_1(t) \\ \\ y_2(t) \end{bmatrix} = \begin{bmatrix} 1 & , & 0 & , & 0 & , & 0 \\ \\ 0 & , & 0 & , & 0 & , & 1 \end{bmatrix} \begin{bmatrix} x_1(t) \\ x_2(t) \\ x_3(t) \\ x_4(t) \end{bmatrix} . \qquad \text{...(3.37b)}$$

In this case, the plant is asymptotically stable but first-order completely irregular since its first Markov parameter

$$CB = \begin{bmatrix} 0 & , & 0 \\ \\ 0 & , & 0 \end{bmatrix} \qquad \text{...(3.38a)}$$

is clearly null whilst its second Markov parameter

$$CAB = \begin{bmatrix} 5 & , & 10 \\ \\ -15 & , & -5 \end{bmatrix} \qquad \text{...(3.38b)}$$

evidently has full rank.

It is required that the output vector of this plant track the command vector

$$v(t) = \begin{bmatrix} 12t \\ \\ -12t \end{bmatrix}, (t \in [0, T_t]) \qquad \text{...(3.39)}$$

on the time interval [0, 1] *sec.*

In case

$$x_0(0) = \begin{bmatrix} 0 \\ 0 \\ 0 \\ 0 \end{bmatrix} \qquad \ldots(3.40)$$

and

$$u_0(t) = \begin{bmatrix} 0 \\ 0 \end{bmatrix} \quad , \qquad \ldots(3.41)$$

the learning characteristics of the iterative controller with controller gain matrices given by equations (3.13) and (3.14) when $\lambda = 1$, $\rho = 0$ are shown in Figure 3.4. Indeed, the results presented in Figures 3.4(a,b) correspond to $D = I_2$, $\sigma = 15$; those in Figures 3.4(c,d) correspond to $D = 0.1I_2$, $\sigma = 8$; and those in Figures 3.4(e,f) correspond to $D = -(CA^2B)^{-1}(CAB)$, $\sigma = 4.92$. The last choice of D is made so that $\sigma = 0$ at $t = 0$, but the largest value of σ according to equation (3.7) corresponds to $t = 0.21$ *sec.* In addition, all these choices of D guarantee that $CBD = 0$, since CB is null. Thus it is clear from Figure 3.4 that the best learning performance and most rapid convergence is obtained when $D = -(CA^2B)^{-1}(CAB)$ (see Figures 3.4(e,f)). Finally, in all these cases, $v(t)$ is such that

$$\dot{e}_0(0) = \begin{bmatrix} 12 \\ -12 \end{bmatrix} \neq 0 \qquad \ldots(3.42)$$

and therefore initial state shifting is required in the iterative learning controller of Chapter 2.

Example 3.5

The state and output equations of a linear time-invariant plant on the continuous-time set are

$$\begin{bmatrix} \dot{x}_1(t) \\ \dot{x}_2(t) \\ \dot{x}_3(t) \\ \dot{x}_4(t) \\ \dot{x}_5(t) \\ \dot{x}_6(t) \end{bmatrix} = \begin{bmatrix} 0 & 0 & 1 & 0 & 0 & 0 \\ 0 & 0 & 0 & 1 & 0 & 0 \\ -4 & -1 & 1 & 2 & -4 & 2 \\ 1 & -2 & -3 & -2 & 1 & -3 \\ 0 & 0 & 0 & 0 & -3 & 0 \\ 0 & 0 & 0 & 0 & 0 & -2 \end{bmatrix} \begin{bmatrix} x_1(t) \\ x_2(t) \\ x_3(t) \\ x_4(t) \\ x_5(t) \\ x_6(t) \end{bmatrix}$$

$$+ \begin{bmatrix} 0 & 0 \\ 0 & 0 \\ 0 & 0 \\ 0 & 0 \\ 3 & 0 \\ 0 & 2 \end{bmatrix} \begin{bmatrix} u_1(t) \\ u_2(t) \end{bmatrix} \qquad \ldots(3.43a)$$

and

$$\begin{bmatrix} y_1(t) \\ \\ y_2(t) \end{bmatrix} = \begin{bmatrix} 1 , & -2 , & 0 , & 0 , & 0 , & 0 \\ \\ 1 , & 2 , & 0 , & 0 , & 0 , & 0 \end{bmatrix} \begin{bmatrix} x_1(t) \\ x_2(t) \\ x_3(t) \\ x_4(t) \\ x_5(t) \\ x_{6(t)} \end{bmatrix}. \qquad \text{...(3.43b)}$$

In this case, the plant is asymptotically stable but second-order completely irregular, since its first and second Markov parameters

$$CB = \begin{bmatrix} 0 & , & 0 \\ 0 & , & 0 \end{bmatrix} \qquad \text{...(3.44a)}$$

and

$$CAB = \begin{bmatrix} 0 & , & 0 \\ 0 & , & 0 \end{bmatrix} \qquad \text{...(3.44b)}$$

are clearly null whilst its third Markov parameter

$$CA^2B = \begin{bmatrix} -18 & , & 16 \\ -6 & , & -8 \end{bmatrix} \qquad \text{...(3.44c)}$$

evidently has full rank.

It follows therefore that such plants cannot be controlled using either the learning controller proposed by Arimoto et al (1984), or the controller proposed in Theorem 3.1. However, such plants can be controlled using the iterative learning controller proposed in Theorem 3.2.

It is required that the output vector of this plant track the command vector

$$v(t) = \begin{bmatrix} 12t \\ \\ -12t \end{bmatrix} \quad (t \in [0, T_t]) \qquad \ldots(3.45)$$

on the time interval [0, 1] *sec.*

In case

$$x(0) = \begin{bmatrix} 0 \\ 0 \\ 0 \\ 0 \\ 0 \\ 0 \end{bmatrix} \qquad \ldots(3.46)$$

and

$$u_0(t) = \begin{bmatrix} 0 \\ 0 \end{bmatrix} \quad , \qquad \ldots(3.47)$$

the learning characteristics of the iterative learning controller with the controller gain

matrices

$$K_1 = \lambda\,(CB + CABD_1 + CA^2BD_2)^{-1} \quad , \qquad \text{...(3.48a)}$$

$$K_2 = D_1K_1 \quad , \qquad \text{...(3.48b)}$$

and

$$K_3 = D_2K_1 \qquad \text{...(3.48c)}$$

are shown in Figure 3.5, where $\lambda \in R^+$ and $D_1, D_2 \in R^{m\times m}$. Since $CB = CAB = 0$, D_1 and D_2 can be arbitrary, but in this example $D_1 = D_2 = I_2$ are chosen.

The results presented in Figures 3.5(a,b),(c,d),(e,f) correspond to $\lambda = \{1, 0.5, 0.2\}$, $\rho = \{0, 0.5, 0.8\}$ and $\sigma = \{6.6, 3.3, 1.32\}$, respectively.

It is clear from these figures that learning is rapid as shown in Figures 3.5(a,b) when $\lambda = 1$; that learning is less rapid as shown in Figures 3.5(c,d) when $\lambda = 0.5$; and that learning is even less rapid as shown in Figures 3.5(e,f) when $\lambda = 0.2$.

Finally, in all these cases, $v(t)$ is such that

$$\dot{e}_0(0) = \begin{bmatrix} 12 \\ \\ -12 \end{bmatrix} \neq 0$$

and

$$\ddot{e}_0\ (0) = \begin{bmatrix} 0 \\ 0 \end{bmatrix}$$

so that initial state shifting is required in the iterative learning controller of Chapter 2. It is thus clear that the possible practical difficulties in such initial state shifting are circumvented by the introduction of initial impulsive action into iterative learning controllers.

3.5 Conclusion

It has been shown in this chapter that iterative learning controllers with initial impulsive action can be characterized for a class of first-order irregular linear time-invariant multivariable plants. In addition, these results have been extended so as to embrace plants with higher orders of irregularity. Thus, the possible practical difficulties involved in the shifting of the initial state required by the controllers of Chapter 2 have been circumvented. Furtnermore, it has been shown that these results can be used to obtain important information concerning the learning rates achievable by such controllers. Indeed, it has been found that the stability characteristics of the plants under control impose severe constraints on these achievable learning rates. Finally, these general results have been illustrated by the presentation of numerical results for the iterative learning control of different linear multivariable plants with various stability and irregularity characteristics.

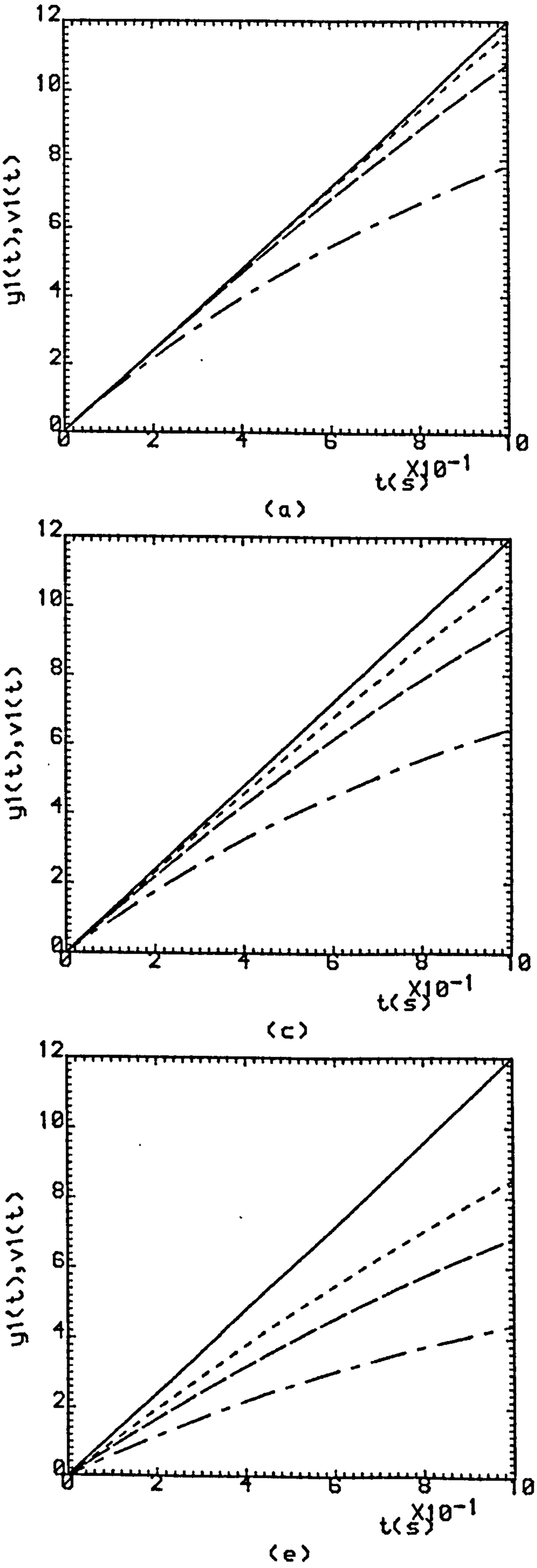

Fig.3.1(a,b) (rho=0.0,sigma=5.0).
(c,d) (rho=0.2,sigma=4.0).
(e,f) (rho=0.5,sigma=2.5).
-·-·- K=1 , ----- K=2 , ... K=3

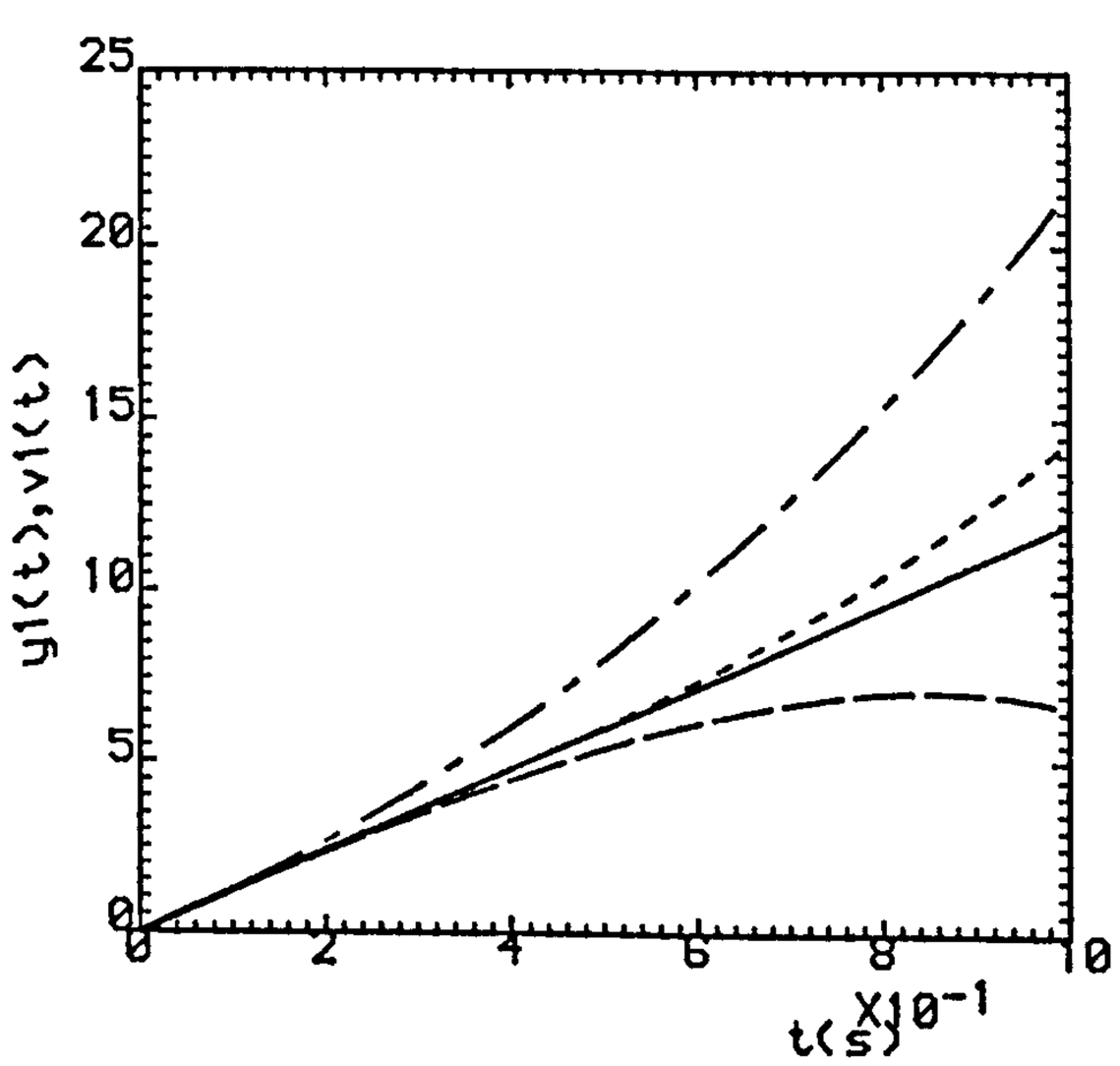

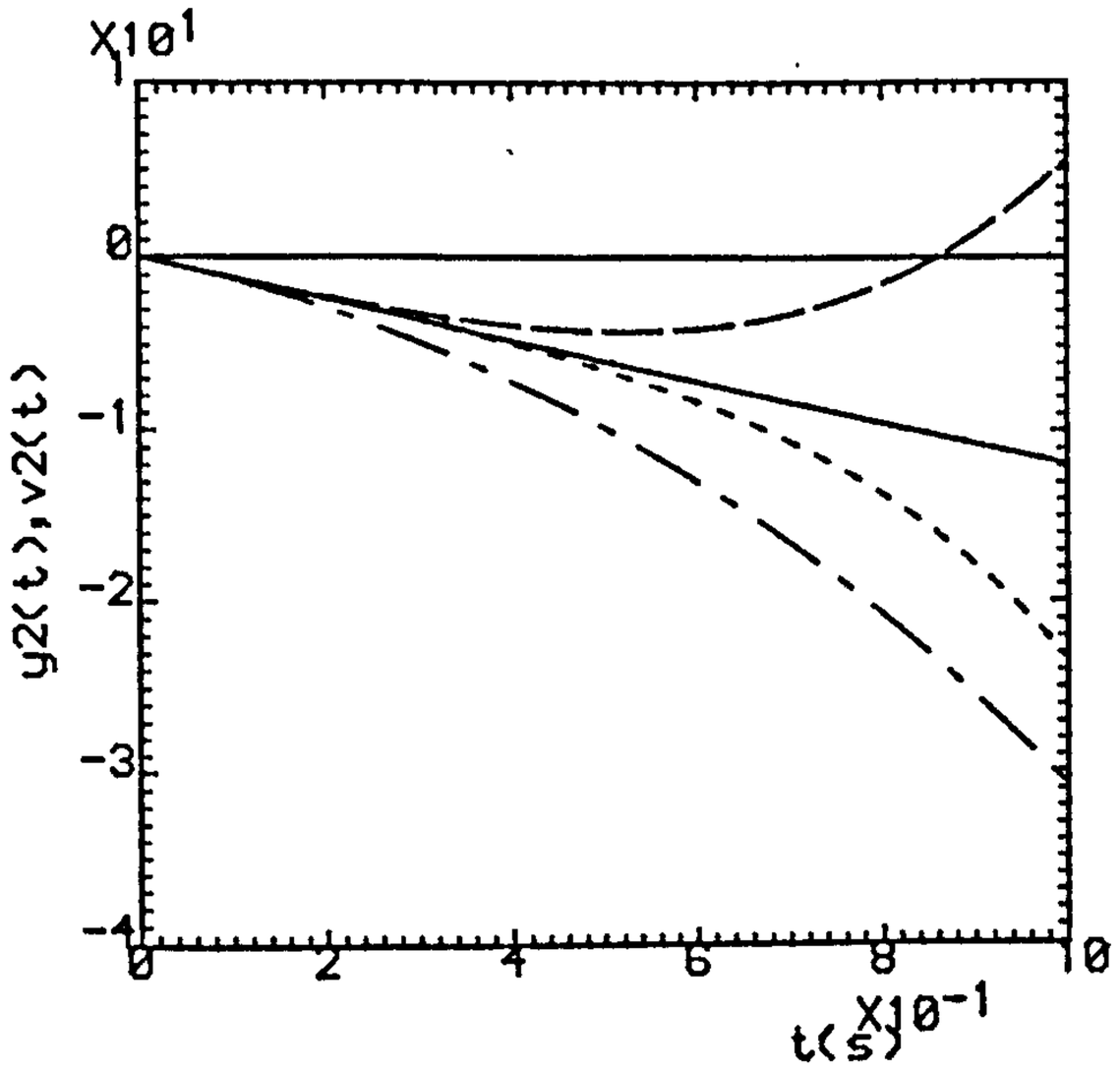

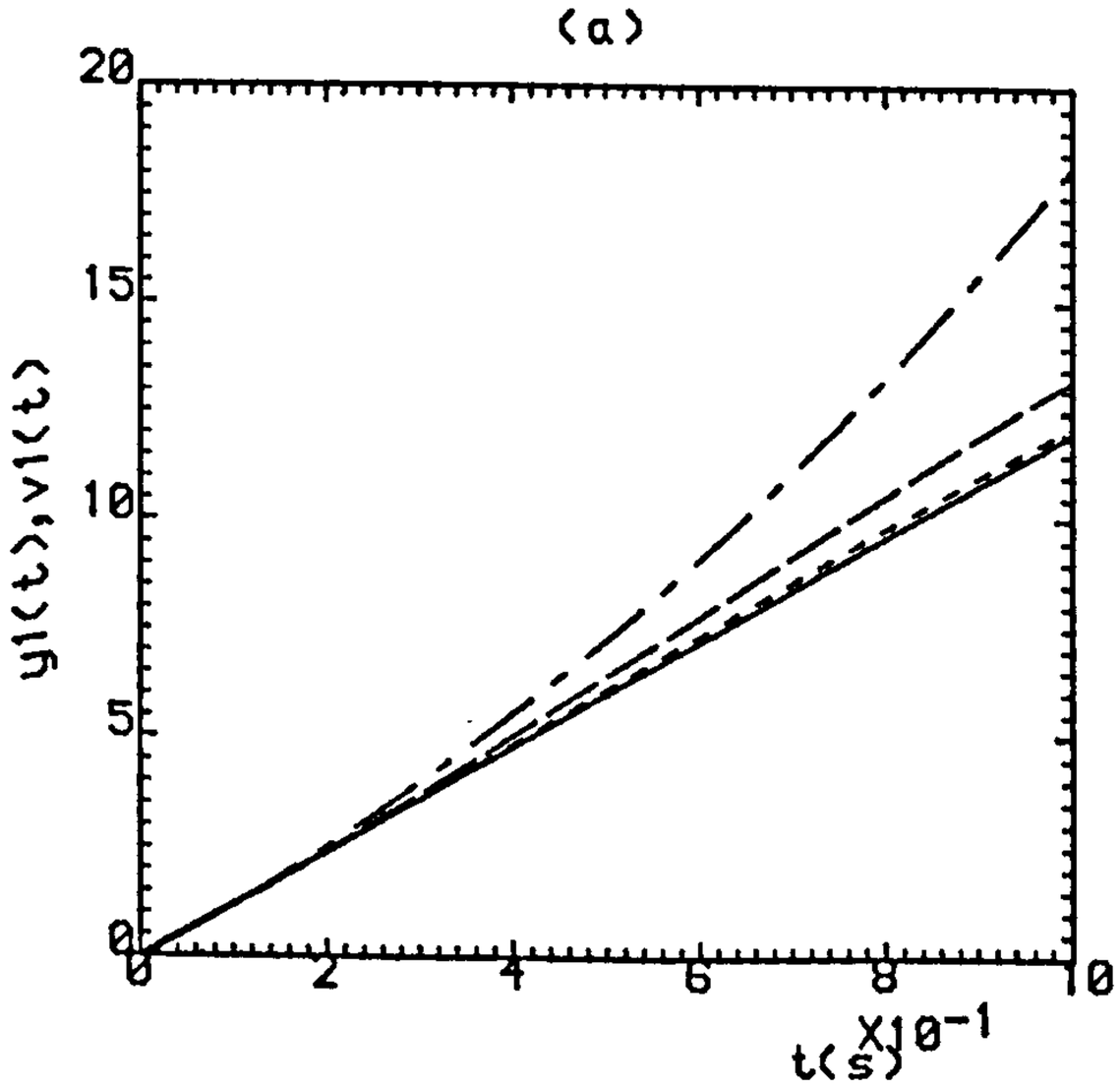

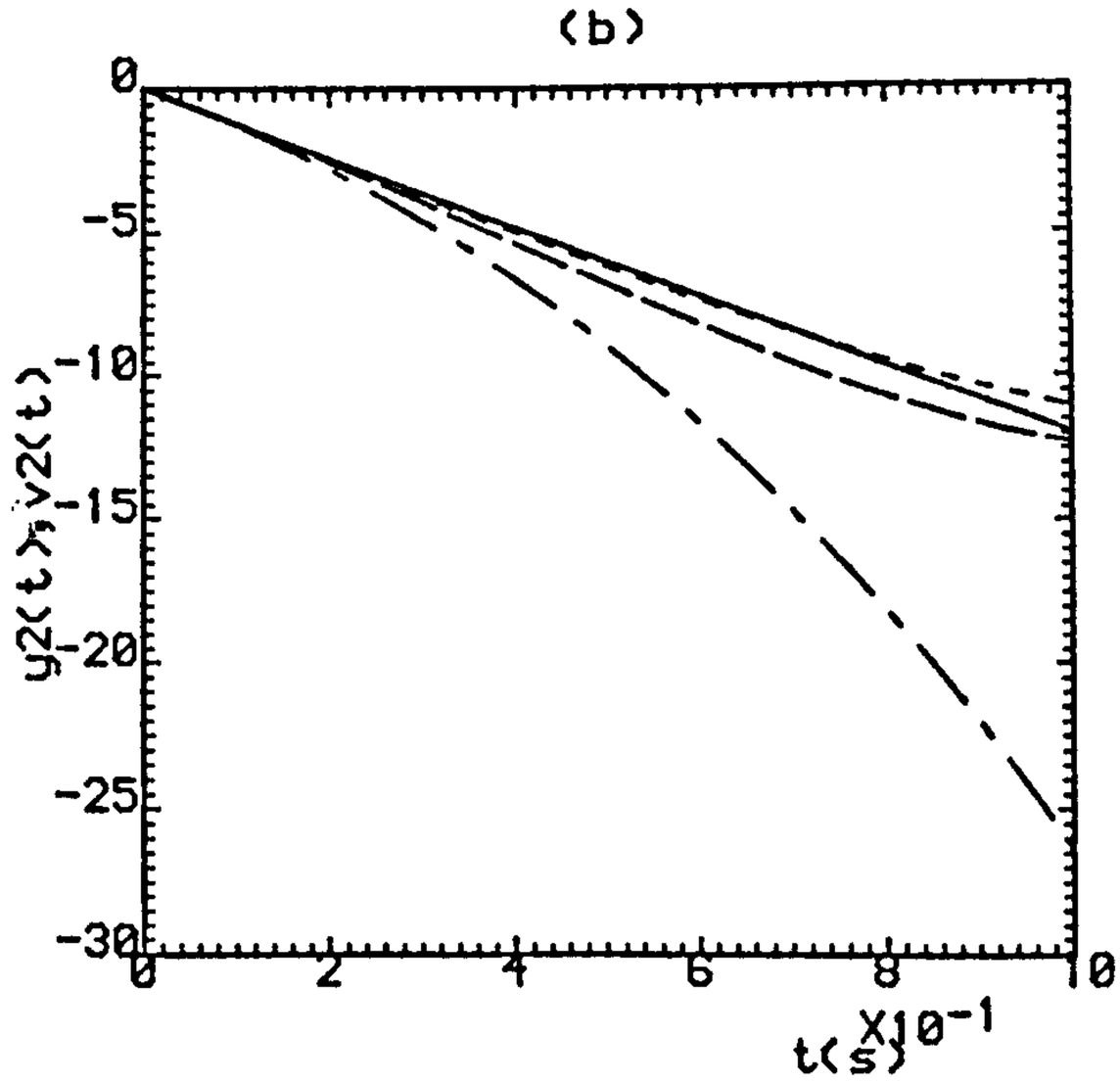

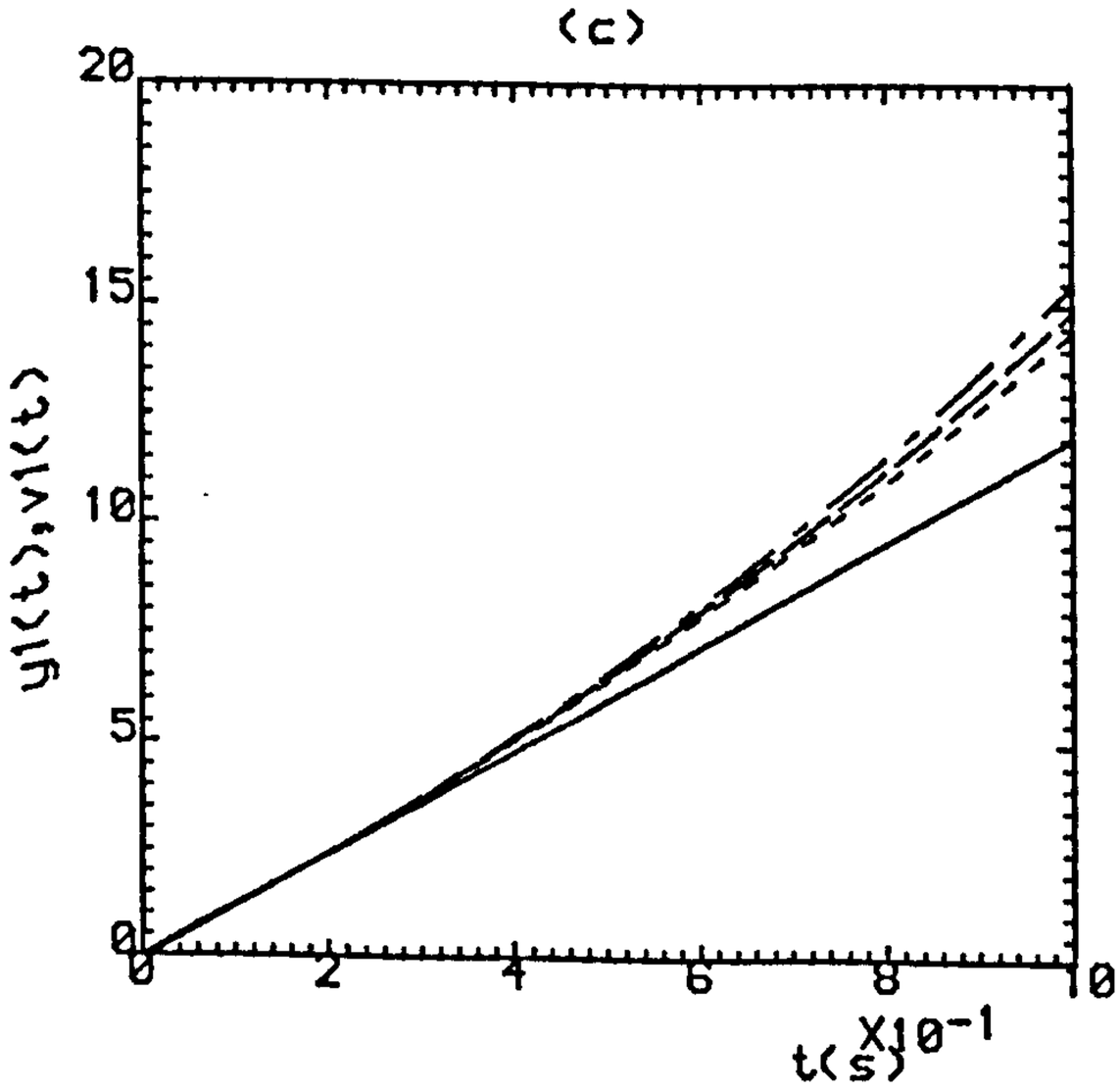

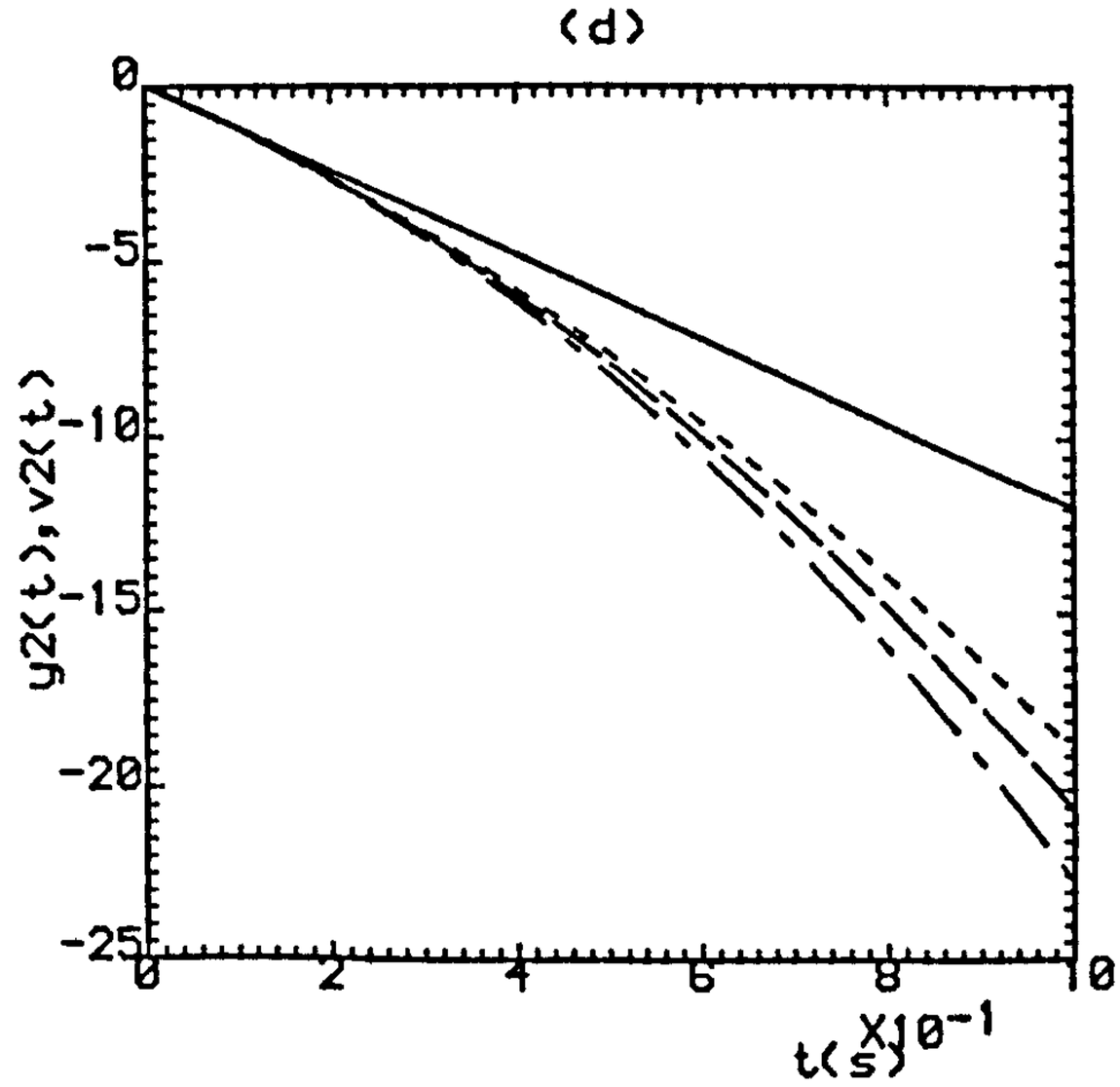

Fig.3.2(a,b) (rho=0.0,sigma=9.58).
(c,d) (rho=0.5,sigma=4.79).
(e,f) (rho=0.9,sigma=0.958).
-·-·- K=1 , ----- K=2 , ... K=3

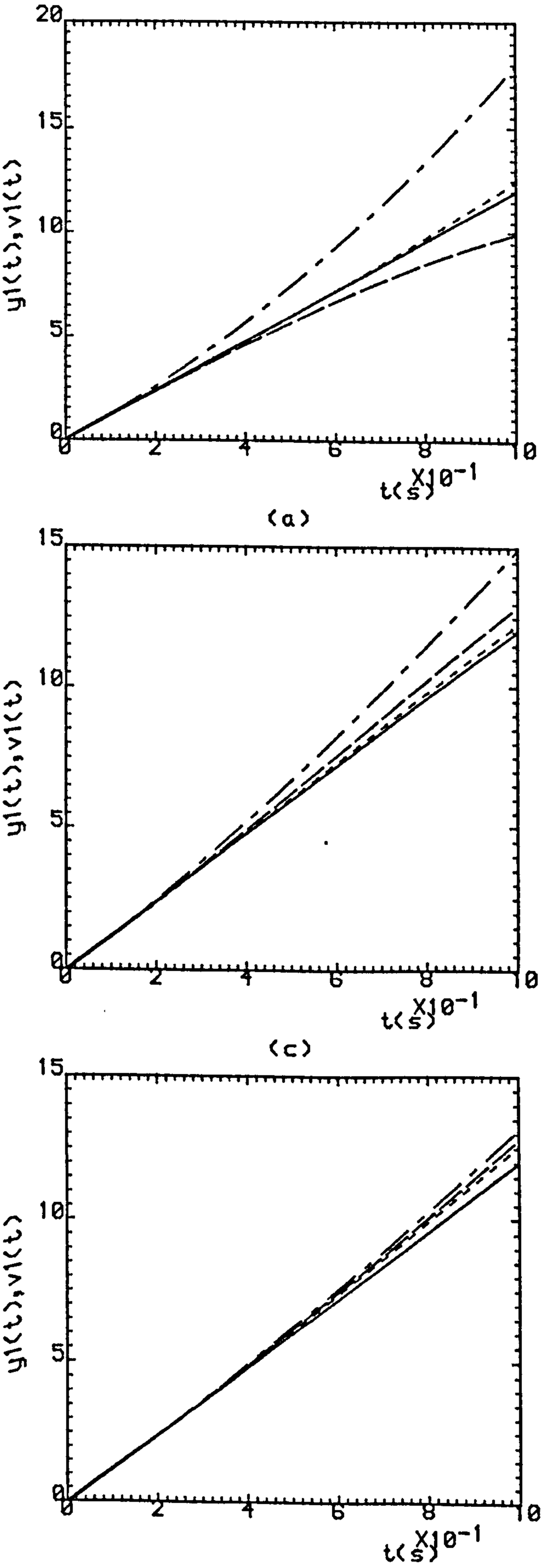

Fig.3.3(a,b) (rho=0.0,sigma=1.0).
(c,d) (rho=0.5,sigma=0.5).
(e,f) (rho=0.8,sigma=0.2).
-·-·- K=1 , ----- K=2 , ... K=3

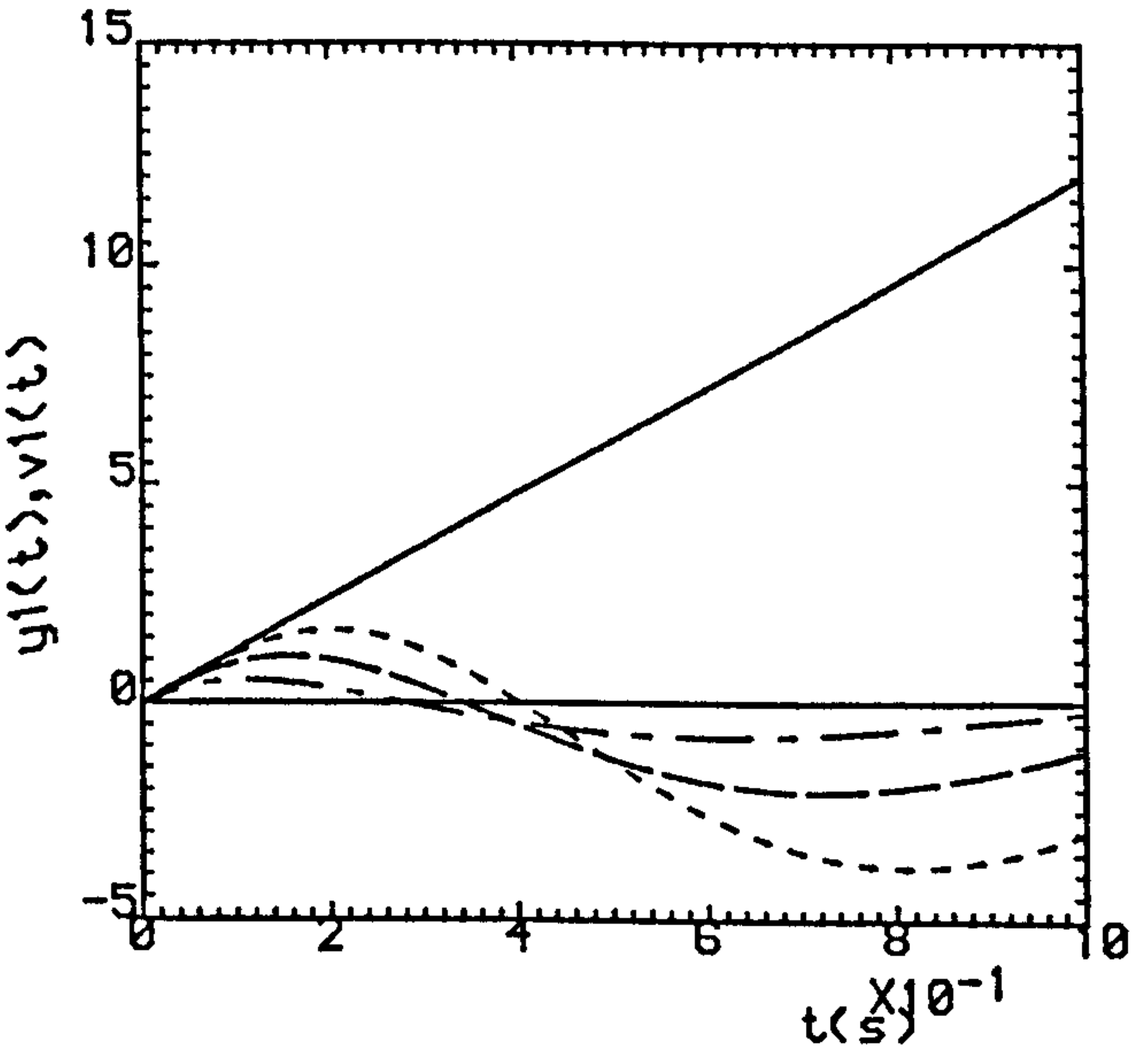

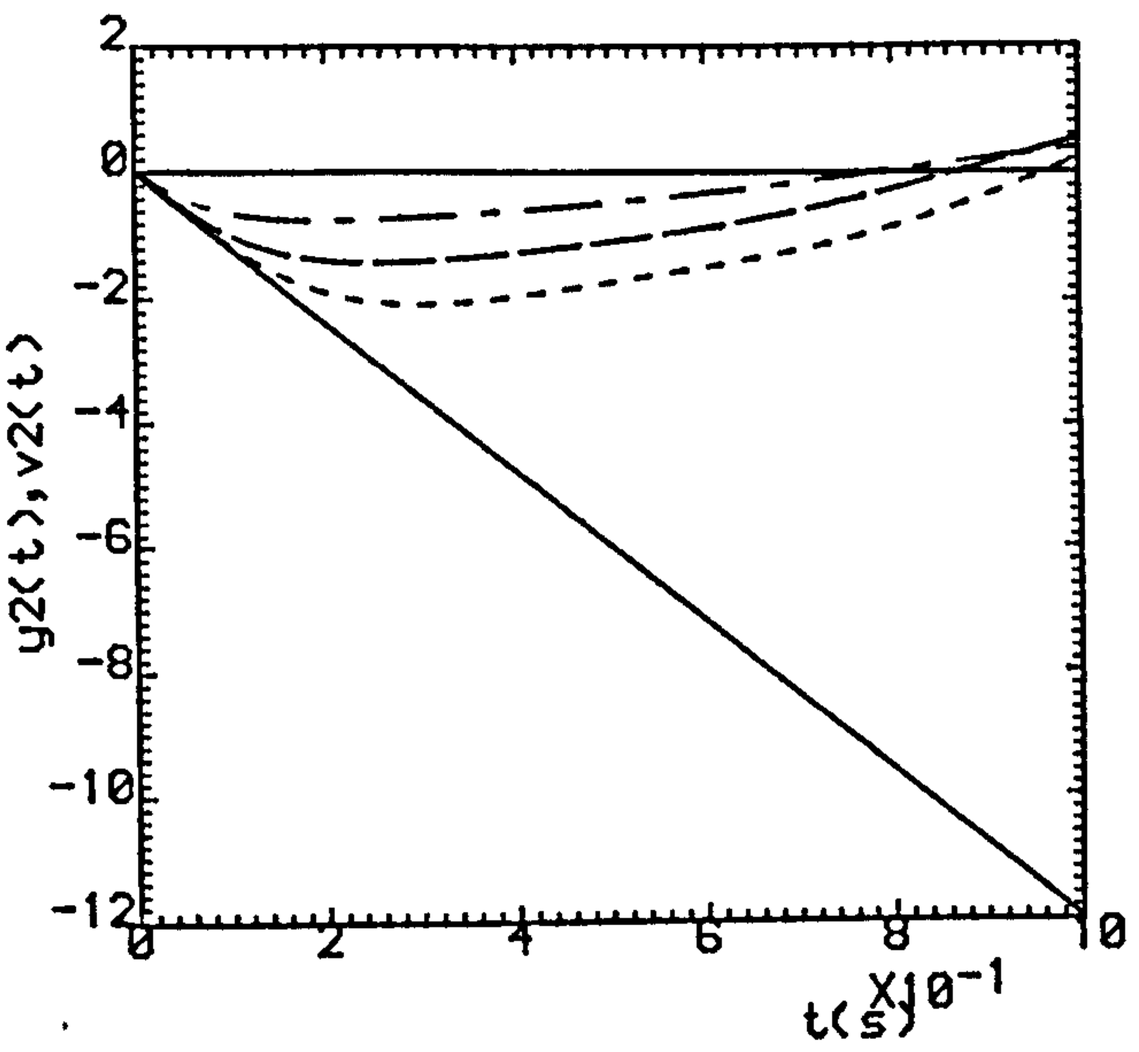

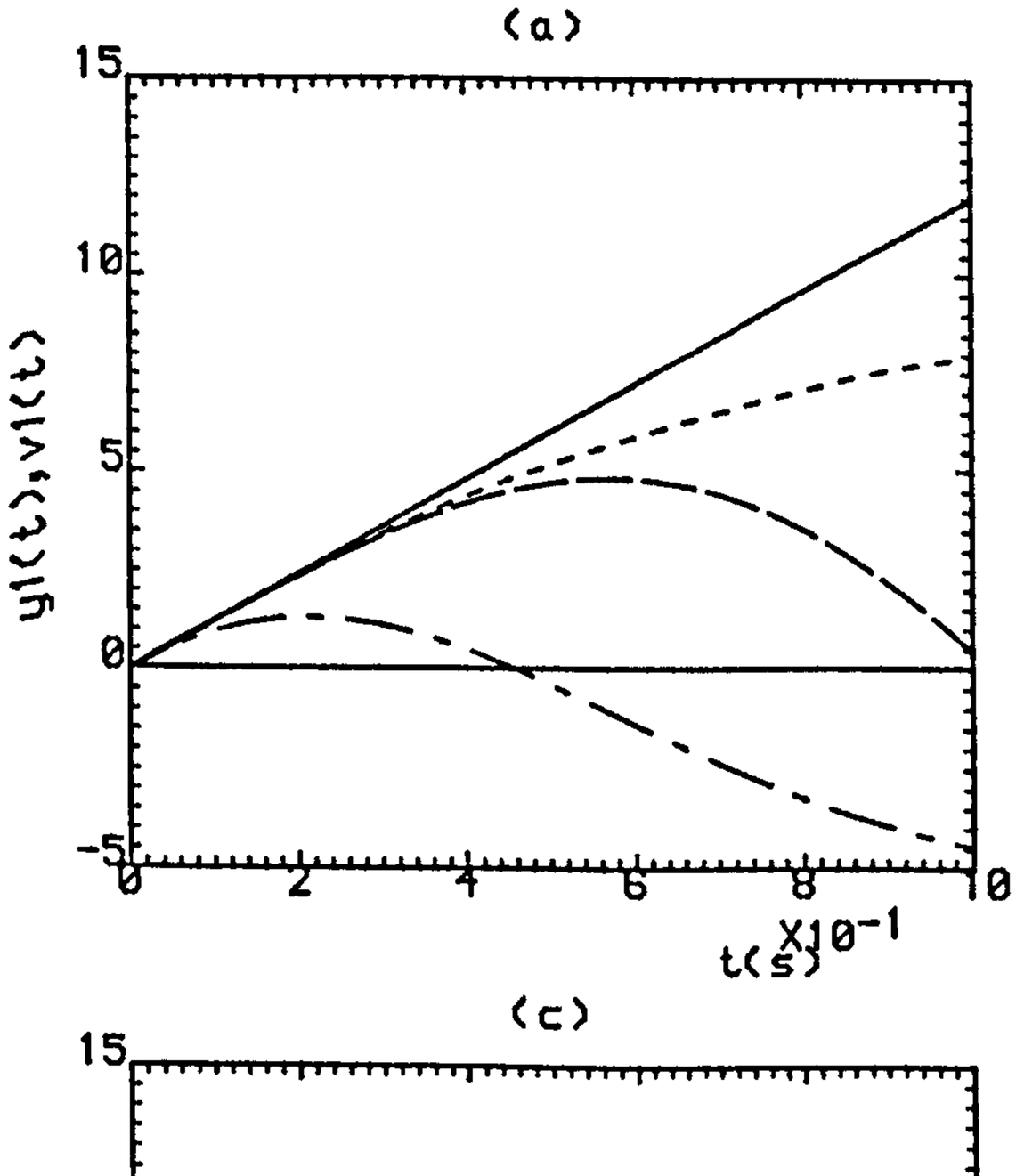

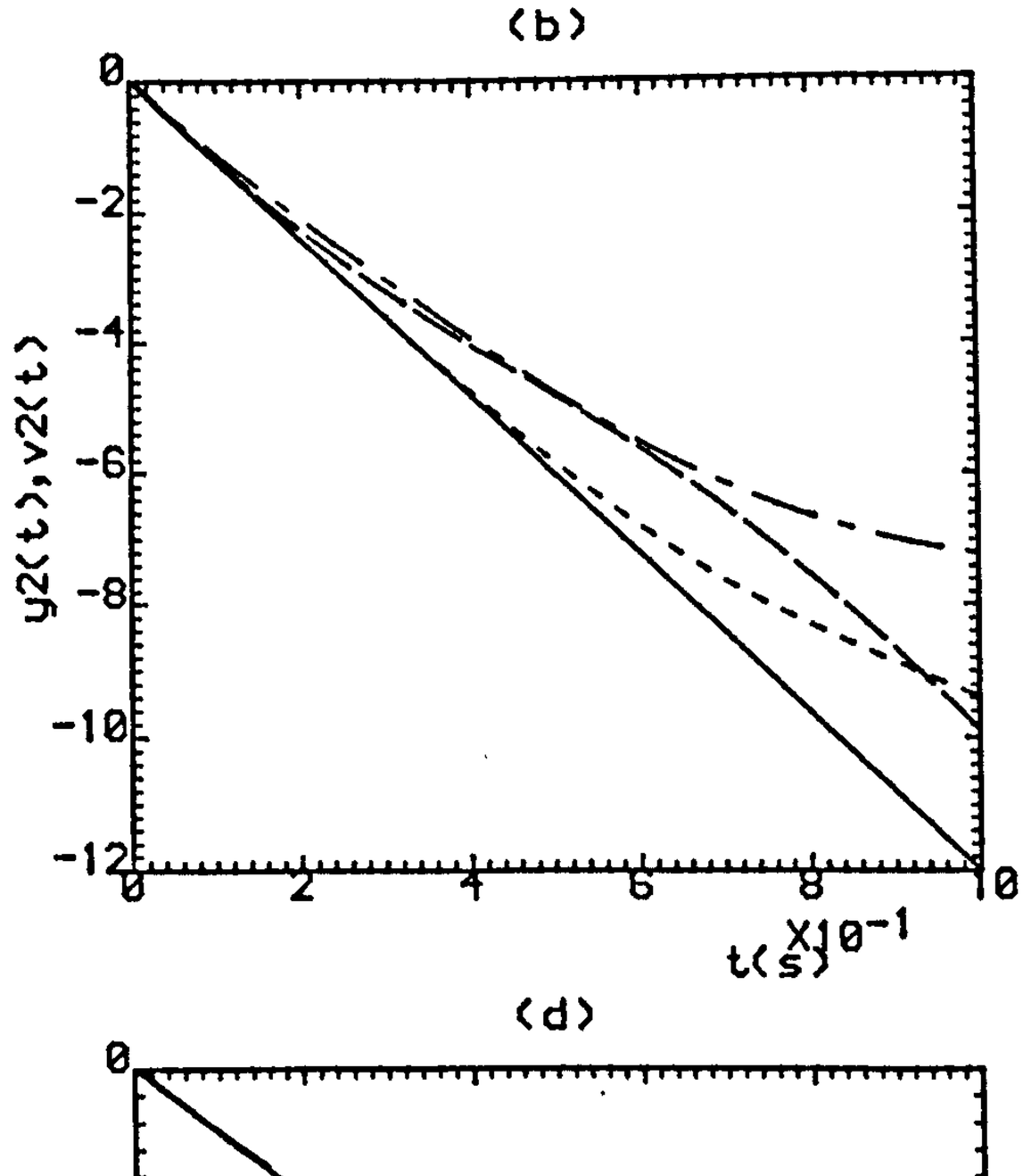

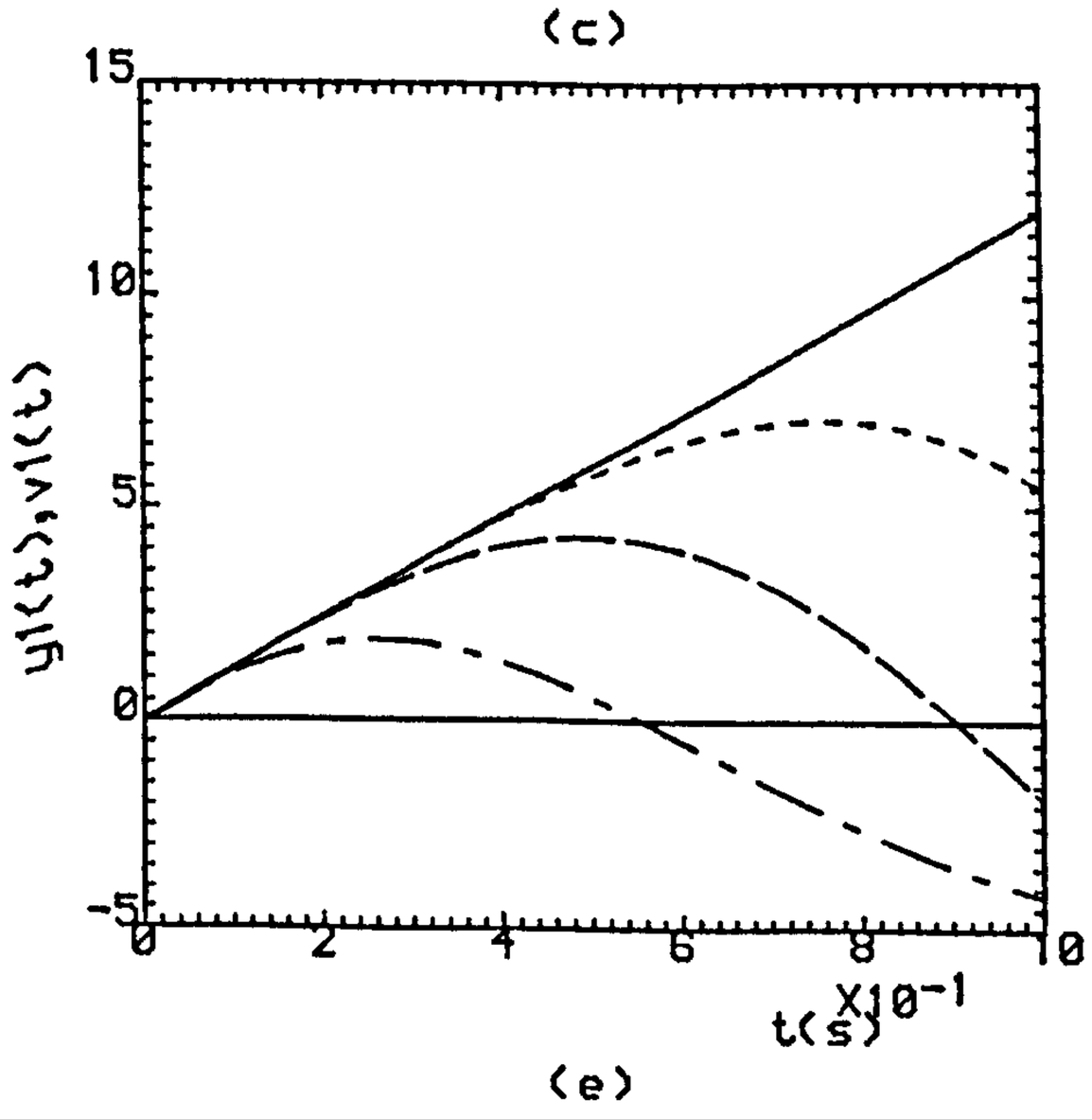

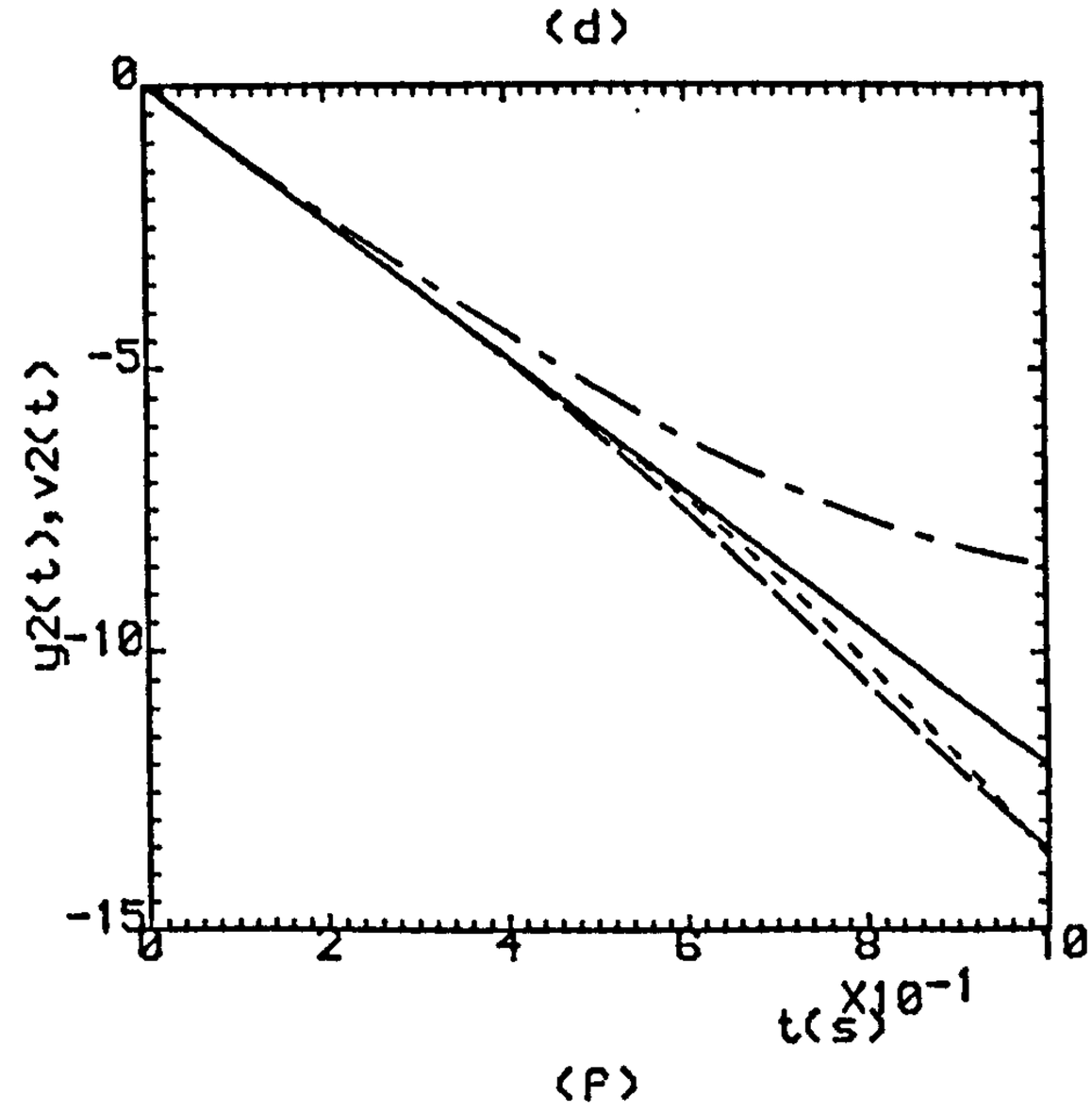

Fig.3.4(a,b) (rho=0.0,sigma=15.0).
(c,d) (rho=0.0,sigma=8.0).
(e,f) (rho=0.0,sigma=4.92).
-·-·- K=1 , ----- K=2 , ... K=3

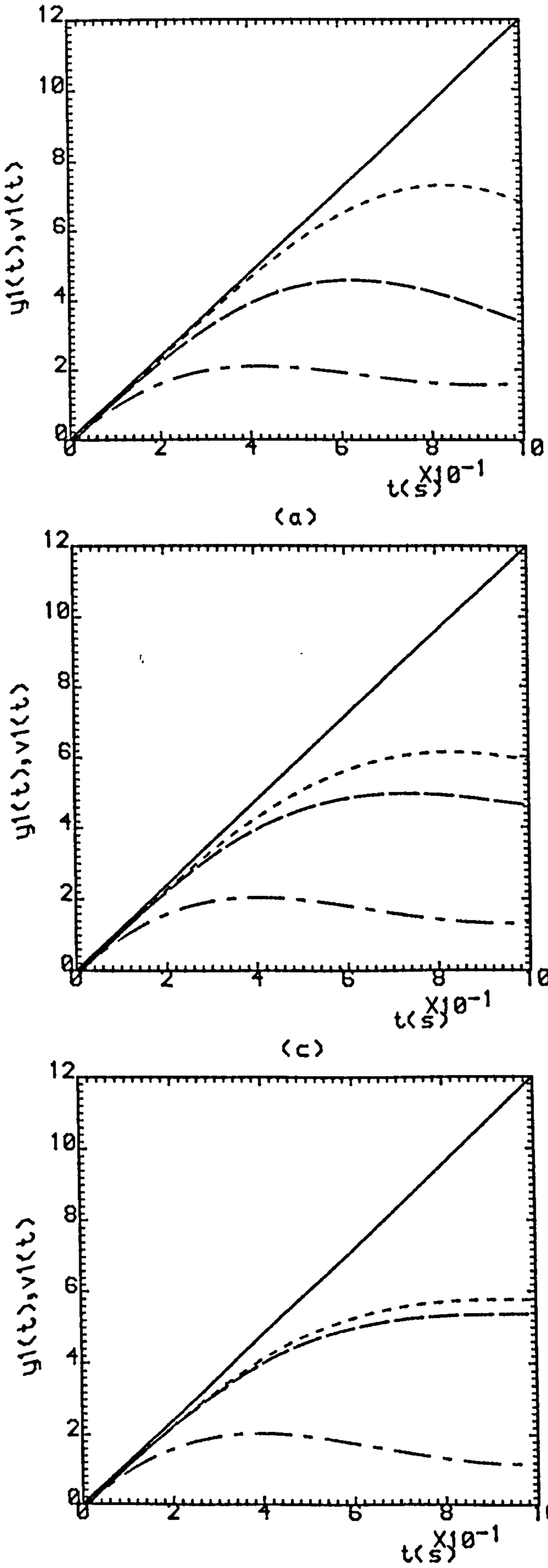

Fig.3.5(a,b) (rho=0.0,sigma=6.6).
(c,d) (rho=0.5,sigma=3.3).
(e,f) (rho=0.8,sigma=1.32).
-·-·- K=1 , ----- K=2 , ... K=3

PART III

DESIGN OF DIGITAL ITERATIVE LEARNING CONTROLLERS FOR LINEAR MULTIVARIABLE PLANTS

CHAPTER 4

DESIGN OF DIGITAL ITERATIVE LEARNING CONTROLLERS FOR LINEAR MULTIVARIATE PLANTS

4.1 INTRODUCTION

In Chapters 2 and 3, a complete theory of analogue iterative learning controllers was presented. This theory provides a generalisation of the seminal results of Arimoto et al (1984) so as to embrace plants with arbitrary irregularity characteristics as described by the Markov parameters of the plants under control.

However, all the existing theories of iterative learning control (Arimoto et al (1984) and, indeed, the theories of Chapters 2 and 3) are not entirely satisfactory in the context of practical application. This is because, in the implementation of all such analogue controllers, it is first necessary to digitalise these controllers. This indirect process of digitalisation is unsatisfactory since finite-difference approximations of derivative action can give rise to inaccuracies and instabilities. Furthermore, the state-space models of the plants must be known prior to the design of such controllers. Therefore, it is shown in this chapter that digital iterative learning controllers can be directly designed using only input/output representations of the multivariable plants under control. In particular, it is shown that digital iterative learning controllers can be designed using only the step-response matrices of such plants. Since such step-response matrices can be measured directly from input/output data, this result implies that digital iterative learning control can be applied to plants with unknown dynamics.

In this chapter, these results are stated in the form of the fundamental theorem presented by Porter and Mohamed (1991). In this theorem, the precise conditions under which learning occurs are fully established. In addition, the proof of this theorem leads to the introduction of an important new parameter which characterises the rate at which learning occurs in any plant/controller combination. Then, using this parameter, it is shown that the irregularity and stability characteristics of the plants under control impose severe constraints on the achievable learning rates. These results are not only significant in their own right but also strongly motivate the introduction of compensators to increase the learning rates achievable in irregular plants. These general results are illustrated in this chapter by the presentation of numerical results for the digital iterative learning control of both uncompensated and compensated plants with different orders of irregularity.

4.2 ANALYSIS

The dynamics of linear time-invariant plants governed on the continuous-time set $T = [0+\infty)$ by differential equations of the form

$$\dot{x}(t) = Ax(t) + Bu(t) \quad , \qquad \text{...(4.1a)}$$

and

$$y(t) = C\,x(t) \quad , \qquad \text{...(4.1b)}$$

are governed on the discrete-time set $T_T = \{0, T, ..., jT, ...\}$ by difference equations of the form

$$x(j+1) = \Phi x(j) + \Psi u(j) \qquad \text{...(4.2a)}$$

and

$$y(j) = \Gamma\, x(j) \quad . \qquad \text{...(4.2b)}$$

In equations (4.1), the state vector $x \in R^n$, the input vector $u \in R^m$, the output vector $y \in R^m$, the plant matrix $A \in R^{n \times n}$, the input matrix $B \in R^{n \times m}$, and the output matrix $C \in R^{m \times n}$; in equations (4.2), in addition

$$\Phi = e^{AT} \quad , \qquad \text{...(4.3a)}$$

$$\Psi = \int_0^T e^{At} B \, dt \quad , \qquad \text{...(4.3b)}$$

and

$$\Gamma = C \quad , \qquad \text{...(4.3c)}$$

where $T \in R^+$ is the sampling period.

The step-response matrices of such plants have the form

$$H(T) = \int_0^T Ce^{At} B \, dt \quad , \qquad \text{...(4.4)}$$

and describe the response of initially quiescent plants after one sampling period. Such step-response matrices can be measured directly from input/output data. Moreover, as the following theorem indicates, it is possible to design digital iterative learning controllers using only such step-response matrices to characterise the dynamics of linear multivariable plants:

Theorem 4.1

In the case of the plant with discrete-time governing equations

$$x_k(j+1) = \Phi x_k(j) + \Psi u_k(j) \qquad \ldots(4.5a)$$

and

$$y_k(j) = \Gamma x_k(j) \qquad \ldots(4.5b)$$

under the action of the digital iterative controller with control law

$$u_{k+1}(j) = u_k(j) + \Lambda\{e_k(j+1) - e_k(j)\} \qquad \ldots(4.6)$$

where

$$e_k(j) = v(j) - y_k(j) \qquad \ldots(4.7)$$

and $v(j)$ $(j \in [0,J])$ is the desired output trajectory, assume that

(i) $\| I_m - H(T)\Lambda \|_\infty < 1$;

(ii) $y_{k+1}(0) = y_k(0) = v(0)$ $(k = 0,1,2,\ldots)$;

(iii) $x_{k+1}(0) = x_k(0)$ $(k = 0,1,2,\ldots)$;

Then, when $j \in [0,J]$,

$$y_k(j) \to v(j)$$

as $k \to \infty$.

In this controller, the ultimate objective is to find an input $u(j)$ that produces a plant output $y(j)$ which coincides with the desired plant output $v(j)$ over a fixed time interval $[0,T_t]$ where $T_t = JT$. This objective is achieved by producing a sequence of outputs $\{y_0(j), y_1(j), y_2(j), \ldots, y_k(j), \ldots\}$ on $[0,T_t]$ corresponding to a sequence of inputs $\{u_0(j), u_1(j), u_2(j), \ldots, u_k(j), \ldots\}$ on $[0,T_t]$.

In order to establish the precise conditions under which learning occurs, it is first necessary to introduce the following vector and matrix norms:

$$\| \Delta e_k(j) \|_\infty = \max_{1 \le i \le m} |\Delta e_k^{(i)}(j)| \qquad \text{...(4.8a)}$$

and

$$\| G \|_\infty = \max_{1 \le i \le m} \{ \sum_{j=1}^{m} |g^{(i,j)}| \} \qquad \text{...(4.8b)}$$

In these norms, $\Delta e_k^{(i)}(j)$ is the ith element of $\Delta e_k(j) \in R^m$ and $g^{(i,j)}$ is the i,jth element of $G \in R^{m \times m}$. Then, in terms of these quantities, the proof of Theorem 4.1 can proceed.

Proof

The solution of equations (4.5) implies that

$$y_{k+1}(j) = \Gamma \Phi^j x_{k+1}(0) + \sum_{i=0}^{j-1} \Gamma \Phi^{j-1-i} \Psi u_{k+1}(i)$$

and therefore that

$$y_{k+1}(j+1) - y_{k+1}(j) = \Gamma \Phi^{j+1} x_{k+1}(0) - \Gamma \Phi^j x_{k+1}(0) + \Gamma \Psi u_{k+1}(j)$$

$$+ \sum_{i=0}^{j-1} \Gamma (\Phi^{j-i} - \Phi^{j-1-i}) \Psi u_{k+1}(i) \qquad .$$

Hence, using the condition (iii) and substituting for the control law, indicates that

$$y_{k+1}(j+1) - y_{k+1}(j) = y_k(j+1) - y_k(j) + \Gamma \Psi \Lambda \{e_k(j+1) - e_k(j)\}$$

$$+ \sum_{i=0}^{j-1} \Gamma (\Phi^{j-i} - \Phi^{j-1-i}) \Psi \Lambda \{e_k(i+1) - e_k(i)\} \quad .$$

Therefore, since

$$e_{k+1}(j+1) - e_{k+1}(j) = [v(j+1) - v(j)] - [y_{k+1}(j+1) - y_{k+1}(j)]$$

and

$$e_k(j+1) - e_k(j) = [v(j+1) - v(j)] - [y_k(j+1) - y_k(j)] \quad ,$$

it follows that

$$\Delta e_{k+1}(j) = (I_m - \Gamma \Psi \Lambda) \Delta e_k(j) - \sum_{i=0}^{j-1} \Gamma (\Phi^{j-i} - \Phi^{j-1-i}) \Psi \Lambda \Delta e_k(i)$$

where

$$\Delta e_{k+1}(j) = e_{k+1}(j+1) - e_{k+1}(j)$$

and

$$\Delta e_k(j) = e_k(j+1) - e_k(j) \quad .$$

Hence, since it follows from equations (4.3) and (4.4) that

$$\Gamma \Psi = H(T) \quad ,$$

it is evident that

$$\Delta e_{k+1}(j) = (I_m - H(T)\Lambda)\,\Delta e_k(j) - \sum_{i=0}^{j-1} \Gamma\,(\Phi^{j-i} - \Phi^{j-1-i})\,\Psi\,\Lambda\,\Delta e_k(i) \quad .$$

Now, taking the norm of both sides of this equation indicates that

$$\| \Delta e_{k+1}(j) \|_\infty \le \| I_m - H(T)\Lambda \|_\infty \cdot \| \Delta e_k(j) \|_\infty$$

$$+ \sup_{0 < j \le J} \sum_{i=0}^{j-1} \| \Gamma\,(\Phi^{j-i} - \Phi^{j-1-i})\,\Psi\,\Lambda \|_\infty \cdot \| \Delta e_k(i) \|_\infty$$

so that

$$\| \Delta e_{k+1}(j) \|_\infty \le \rho\ \| \Delta e_k(j) \|_\infty + \sigma \sup_{0 < j \le J} \sum_{i=0}^{j-1} \| \Delta e_k(i) \|_\infty \qquad ...(4.9)$$

where

$$\rho = \| I_m - H(T)\Lambda \|_\infty \quad , \qquad ...(4.10)$$

$$\sigma = \sup_{0 < j \le J} \| \Gamma\,(\Phi^{j} - \Phi^{j-1})\,\Psi\,\Lambda \|_\infty \quad , \qquad ...(4.11)$$

$$J = T_t / T \quad , \qquad ...(4.12)$$

and T_t is the duration of the fixed finite interval $[0, T_t]$ over which tracking of the command vector $v(j) \in R^m$ is to occur. Now,

$$\| \Delta e_1(j) \|_\infty \le \rho\ \| \Delta e_0(j) \|_\infty + \sigma \sum_{i=0}^{j-1} \| \Delta e_0(i) \|_\infty$$

$$\leq \rho\ \beta + \sigma\ j\ \beta$$

$$\leq (\rho + \sigma j)\beta$$

where

$$\beta = \sup_{0 \leq j \leq J} \| \Delta e_0(j) \|_\infty$$

Similarly,

$$\| \Delta e_2(j) \|_\infty \leq \rho\ \| \Delta e_1(j) \|_\infty + \sigma \sum_{i=0}^{j-1} \| \Delta e_1(i) \|_\infty$$

$$\leq \rho(\rho + \sigma j)\beta + \sigma \sum_{i=0}^{j-1} (\rho + \sigma i)\beta$$

$$\leq (\rho^2 + \rho\sigma j)\beta + \rho\sigma j\beta + \frac{\sigma^2\ \beta j(j-1)}{2!}$$

$$\leq \left[\rho^2 + 2\rho\sigma j + \frac{\sigma^2\ j(j-1)}{2!}\right]\beta$$

since

$$\sum_{i=0}^{j-1} i = \frac{j(j-1)}{2!}$$

In addition,

$$\| \Delta e_3(j) \|_\infty \leq \rho \| \Delta e_2(j) \|_\infty + \sigma \sum_{i=0}^{j-1} \| \Delta e_2(i) \|_\infty$$

$$\leq \rho \left[\rho^2 + 2\rho\sigma j + \frac{\sigma^2 \, j(j-1)}{2!} \right] \beta + \sigma \sum_{i=0}^{j-1} \left[\rho^2 + 2\rho\sigma i + \sigma^2 \, \frac{i(i-1)}{2!} \right] \beta$$

$$\leq \left[\rho^3 + 2\rho^2\sigma j + \rho \, \sigma^2 \, \frac{j(j-1)}{2!} \right] \beta + \rho^2 \sigma j \beta$$

$$+ 2\rho \, \sigma^2 \, \frac{j(j-1)}{2!} \beta + \sigma^3 \, \frac{j(j-1)(j-2)}{3!} \beta$$

since

$$\sum_{i=0}^{j-1} i(i-1) = \sum_{i=0}^{j-1} i^2 - \sum_{i=0}^{j-1} i$$

$$= \frac{j(j-1)(2j-1)}{6} - \frac{j(j-1)}{2}$$

$$= \frac{j(j-1)(j-2)}{3!} .$$

It therefore follows that

$$\| \Delta e_3(j) \|_\infty \leq \left[\rho^3 + 3\rho^2\sigma j + 3\rho \, \sigma^2 \, \frac{j(j-1)}{2!} + \sigma^3 \, \frac{j(j-1)(j-2)}{3!} \right] \beta .$$

Similarly, it follows in general that

$$\| \Delta e_k(j) \|_\infty \leq (\rho^k + k\rho^{k-1}\sigma j + \frac{k(k-1)}{2!} \rho^{k-2} \, \sigma^2 \, \frac{j(j-1)}{2!}$$

$$+ \frac{k(k-1)(k-2)}{3!} \rho^{k-3} \sigma^3 \frac{j(j-1)(j-2)}{3!}$$

$$+ \frac{k(k-1)(k-2)(k-3)}{4!} \rho^{k-4} \sigma^4 \frac{j(j-1)(j-2)(j-3)}{4!}$$

$$+ \ldots\ldots$$

$$+ k \rho \sigma^{k-1} \frac{j(j-1)(j-2)(j-3)\ldots(j-k+2)}{(k-1)!}$$

$$+ \sigma^k \frac{j(j-1)(j-2)\ldots(j-k+1)}{k!}) \beta$$

or, in closed form,

$$\| \Delta e_k(j) \|_\infty \leq \beta \sum_{q=0}^{k} \frac{k!}{q!(k-q)!} \rho^{k-q} \sigma^q \frac{j!}{q!(j-q)!} \quad . \qquad \ldots(4.13)$$

It is found, as for the inequalities of Chapters 2 and 3, that each term in the right-hand side of the inequality (4.13) is positive. Therefore, in order for $\| \Delta e_k(j) \|_\infty$ to vanish as $k \to \infty$, each term must vanish as $k \to \infty$. Indeed, the only way to make these terms vanish is by satisfying condition (i) of Theorem 4.1 that $0 \leq \rho < 1$.

This can be proved by noting

$$\lim_{k \to \infty} \quad k^s \rho^k \to 0$$

for any integer $s > 0$ provided that $|\rho| < 1$. This fact is best appreciated by considering the ratio of kth term to the $(k-1)th$ term in the *series* $K^s\rho^k$ Thus,

$$\frac{\tau_k}{\tau_{k-1}} = \frac{k^s \rho^k}{(k-1)^s \rho^{k-1}}$$

$$= \left(\frac{k}{k-1}\right)^s \rho$$

Hence,

$$\lim_{k \to \infty} \frac{\tau_k}{\tau_{k-1}} = \rho$$

for any integer $s > 0$. This means that

$$\lim_{k \to \infty} \tau_k = 0$$

provided that $|\rho| < 1$.

However, the last term of the inequality (4.13) will vanish in a different fashion because the speed of the factorial function's progress is higher than the speed of the exponential function's progres. Therefore, this term vanishes as k increases. However, the speed at which this term disappears depends on the size of the parameter σ. Indeed, the smaller the value of σ the faster that term will disappear. Hence,

$$\| \Delta e_k(j) \|_\infty \to 0$$

as $k \to \infty$ for all $j \in [0, J]$ for any value of σ and therefore

$$e_k(j+1) \to e_k(j)$$

Hence, in view of the condition (ii), it follows that

$$e_k(j) \rightarrow 0$$

and therefore finally that

$$y_k(j) \rightarrow y(j)$$

as $k \rightarrow \infty$ for all $j \in [0, J]$, as required.

It is evident that the parameter, σ, defined in equation (4.11) is not involved in the sufficient conditions for learning enunciated in Theorem 4.1. However, it is equally evident from the inequality (4.13) that the value of σ nevertheless affects the rate at which learning occurs. This parameter is accordingly called the learning parameter of the plant/controller combination represented by the particular choice of controller matrix $\Lambda \in R^{m \times m}$ in the control-law equation (4.6). In order to investigate systematically the learning rates achievable in the digital iterative learning control of linear multivariable plants, it is therefore convenient in equation (4.6) to choose

$$\Lambda = \lambda H^{-1}(T) \qquad \ldots(4.14)$$

where $\lambda \in R^+$. It is then clear from equation (4.10) that

$$\rho = |1-\lambda| \qquad \ldots(4.15)$$

which implies that the crucial condition (i) of Theorem 4.1 will be satisfied provided that $0 < \lambda < 2$. However, it is also clear from equation (4.11) that the choice of controller matrix given by equation (4.14) implies that the corresponding value of the learning parameter, σ, is given by

$$\frac{\sigma}{\lambda} = \sup_{0 < j \leq J} \left\| \Gamma \left(\Phi^{j} - \Phi^{j-1} \right) \Psi H^{-1}(T) \right\|_{\infty} \quad . \qquad \ldots(4.16)$$

It is thus evident from equations (4.3) and (4.4) that the value of the right-hand member of equation (4.16) depends upon the stability characteristics of the plant under control. Indeed, it follows from equation (4.16) that

$$\frac{\sigma}{\lambda} \geq \left\| \Gamma \left(\Phi - I \right) \Psi H^{-1}(T) \right\|_{\infty} \qquad \ldots(4.17)$$

where

$$\Phi - I = AT + \frac{1}{2} A^2 T^2 + \frac{1}{6} A^3 T^3 + \ldots \quad , \qquad \ldots(4.18a)$$

$$\Psi = BT + \frac{1}{2} AB T^2 + \frac{1}{6} A^2 BT^3 + \ldots \quad , \qquad \ldots(4.18b)$$

$$\Gamma = C \quad , \qquad \ldots(4.18c)$$

and

$$H(T) = CB T + \frac{1}{2} CAB T^2 + \frac{1}{6} CA^2 BT^3 + \ldots \quad . \qquad \ldots(4.18d)$$

Therefore, substituting from equations (4.18) into the inequality (4.17), yields as $T \rightarrow 0$ the following lower bounds for the learning parameters of plants with various irregularity characteristics:

(i) Regular plants (*CB* full rank)

$$\frac{\sigma}{\lambda} \geq 0 \quad ; \qquad \ldots(4.19a)$$

(ii) First-order completely irregular plants (*CB* null, *CAB* full-rank)

$$\frac{\sigma}{\lambda} \geq 2 \qquad ; \qquad \text{...(4.19b)}$$

(iii) Second-order completely irregular plants (CB null, CAB, null. CA^2B full rank)

$$\frac{\sigma}{\lambda} \geq 6 \qquad ; \qquad \text{...(4.19c)}$$

(iv) ℓth-order completely irregular plants (CB null,...., $CA^{\ell-1}B$ null, $CA^{\ell}B$ full rank)

$$\frac{\sigma}{\lambda} \geq \sum_{\substack{q+r=\ell+1 \\ q>0, r>0}} \frac{(q+r)!}{q!r!} \qquad . \qquad \text{...(4.19d)}$$

These results indicate that the lower bound on σ/λ increases rapidly with increases in the order of plant irregularity. Therefore, in order to obtain reasonably rapid learning rates in the case of irregular plants, it is evident from the inequality (4.13) that σ must be small by choosing $\lambda \in R^+$ to be small in equation (4.14). But it is then clear from equation (4.15) that ρ will increase towards unity and therefore, in view of the inequality (4.13), that the learning rate will be reduced. This shows that, even in the case of stable plants for which the lower bounds on σ/λ given by inequalities (4.19) are non-conservative, this trade-off between ρ and σ cannot produce rapid learning rates in the case of irregular plants, i.e. the irregularity characteristics of linear multivariable plants place unavoidable limits on the learning rates achievable in the digital iterative learning control of such plants. These results are illustrated in Section 4.4 of this chapter. It follows that an alternative must be found in order to reduce the learning parameter, σ, without effecting the value of ρ so as to achieve rapid learning in case of plants with high orders or irregularity. Thus in Chapters 2 and 3, it was shown that the results of Arimoto et al (1984) for regular linear multivariable plants can be generalised so as to embrace arbitrary irregular plants. This generalisation was effected by introducing compensators with transfer function

matrices of the form $(I_m + Ds)$, where $D \epsilon R^{m \times m}$, as pre-filters between the iterative learning controllers and the irregular linear multivariable plants under control (see Appendix A for more details).

This methodology for the introduction of analogue compensators in the context of analogue iterative learning control motivates the introduction of similar digital compensators in the present context of digital iterative learning control. The transfer function matrices of such digital compensators have the form $\left(I_m + \frac{2}{T} D \frac{z-1}{z+\alpha}\right)$, where $D \epsilon R^{m \times m}$ and α (-1,+1], and are governed by state and output equations of the form

$$r_k(j+1) = -\alpha I_p r_k(j) + [0_{m-p}, I_p] w_k(j) \qquad ...(4.20a)$$

and

$$u_k(j) = -\frac{2}{T}(1+\alpha) \begin{bmatrix} D_2 \\ {\scriptstyle m-p \times p} \\ \\ D_4 \\ {\scriptstyle p \times p} \end{bmatrix} r_k(j) + \left(I_m + \frac{2}{T} D\right) w_k(j) \qquad ...(4.20b)$$

where $p \epsilon [0, m]$.

These compensators can be introduced into digital iterative learning controllers in accordance with the following theorem in the case of first-order partially irregular linear multivariable plants:

Theorem 4.2

In the case of the plant with the discrete-time governing equations

$$x_k(j+1) = \Phi x_k(j) + \Psi u_k(j) \qquad ...(4.21a)$$

and

$$y_k(j) = \Gamma x_k(j) \qquad \text{...(4.21b)}$$

under the action of the digital iterative controller with control law

$$r_k(j+1) = -\alpha\, I_p\, r_k(j) + [0_{m-p}, I_p]\, w_k(j) \quad , \qquad (4.22a)$$

$$u_k(j) = -\frac{2}{T}(1+\alpha)\begin{bmatrix} D_2 \\ D_4 \end{bmatrix} r_k(j) + \left(I_m + \frac{2}{T} D\right) w_k(j) \quad , \qquad \text{...(4.22b)}$$

$$w_{k+1}(j) = w_k(j) + \Lambda\, \{e_k(j+1) - e_k(j)\} \quad , \qquad \text{...(4.22c)}$$

where

$$e_k(j) = v(j) - y_k(j) \quad ,$$

$v(j)$ $(j \in [0, J])$ is the desired output trajectory,

$$\text{rank} \quad CB = m\text{-}p \quad ,$$

$$p \in [0, m] \quad ,$$

$$\text{rank} \quad CAB = m \quad ,$$

$$\text{rank} \quad (CB + CABD) = m \quad ,$$

$$D = \begin{bmatrix} 0 & , & D_2 \\ 0 & , & D_4 \end{bmatrix} \epsilon\, R^{m \times m} \quad ,$$

$$D_2 \epsilon\, R^{m-p \times p}\ ,\ D_4 \epsilon\, R^{p \times p}\ ,\ \text{rank}\ D_4 = p \quad ,$$

and

$$\alpha \epsilon\, (-1,+1] \quad .$$

assume that:

(i) $\| I_m - H(T)\left[I_m + \frac{2}{T} D\right]\Lambda \|_\infty < 1;$

(ii) $y_{k+1}0 = y_k(0) = v(0) \quad (k = 0,1,2,...);$

(iii) $x_{k+1}(0) = x_k(0) \quad (k = 0,1,2,...);$

(iv) $r_{k+1}(0) = r_k(0) \quad (k = 0,1,2,...,);$

Then, when $j \epsilon\, [0, J]$,

$$y_k(j) \rightarrow \quad v(j)$$

as $k \rightarrow \infty$.

Proof

It follows from equations (4.21) and (4.22) that the overall plant shown in Figure 4.1 (i.e. the pre-filter in cascade with the irregular plant) is governed in discrete-time by state and output equations of the form

$$\hat{x}_k(j+1) = \hat{\Phi}\ \hat{x}_k(j) + \hat{\Psi}\ w_k(j) \qquad ...(4.23a)$$

and

$$y_k(j) = \hat{\Gamma}\hat{x}_k(j) \qquad \ldots(4.23b)$$

where

$$\hat{x}_k = \begin{bmatrix} x_k \\ r_k \end{bmatrix} , \qquad \ldots(4.24a)$$

$$\hat{\Phi} = \begin{bmatrix} \Phi & , & -\frac{2}{T}(1+\alpha)\,\Psi \begin{bmatrix} D_2 \\ D_4 \end{bmatrix} \\ \\ 0 & , & -\alpha\, I_p \end{bmatrix} , \qquad \ldots(4.24b)$$

$$\hat{\Psi} = \begin{bmatrix} \Psi\left(I_m + \frac{2}{T} D\right) \\ \\ [o, I_p] \end{bmatrix} , \qquad \ldots(4.24c)$$

and

$$\hat{\Gamma} = [\Gamma, 0] \; . \qquad \ldots(4.24d)$$

It therefore follows that Theorem 4.2 can be proved simply by applying the argument of Theorem 4.1 for uncompensated plants to the present case of compensated plants.

It thus follows that

$$\| \Delta e_k(j) \|_\infty \leq \beta \sum_{i=0}^{k} \frac{k!}{q!(k-q)!}\, \rho^{k-q}\, \sigma^q\, \frac{j!}{q!(j-q)!} \qquad \ldots(4.25)$$

where $k > 0$,

$$\Delta e_k(j) = e_k(j+1) - e_k(j) \quad , \tag{}$$

$$\beta = \sup_{0 \le j \le J} \| \Delta e_0(j) \|_\infty \quad , \tag{}$$

$$\rho = \| I_m - \hat{H}(T)\, \Lambda \|_\infty \quad , \tag{4.26}$$

$$\sigma = \sup_{0 < j \le J} \| \hat{\Gamma}(\hat{\Phi}^j - \hat{\Phi}^{j-1}) \hat{\Psi}\, \Lambda \|_\infty \quad , \tag{4.27}$$

$$J = T_t / T \quad , \tag{4.28}$$

and T_t is the duration of the fixed finite interval $[0, T_t]$ over which tracking of the command vector $v(j) \in R^m$ is to occur. In equation (4.26),

$$\hat{H}(T) = H(T) \left[I_m + \frac{2}{T} D \right] \tag{4.29}$$

is the step-response matrix of the compensated plant with uncompensated step-response matrix $H(T)$. Therefore, using condition (i) of Theorem 4.2, it follows from the inequality (4.25) that

$$\| \Delta e_k(j) \|_\infty \to 0$$

as $k \to \infty$ for all $j \in [0, J]$ for any value of σ and therefore that

$$e_k(j+1) \to e_k(j)$$

Hence, in view of the condition (ii) of Theorem 4.2, it follows that

$$e_k(j) \rightarrow 0$$

and therefore finally that

$$y_k(j) \rightarrow v(j)$$

as $k \rightarrow \infty$ for all $j \in [0, J]$, as required.

It is clear in the case of Theorem 4.2, that the parameter, σ, defined in equation (4.27) is not involved in the sufficient conditions for learning enunciated in Theorem 4.2. However, it is equally clear from the inequality (4.25) that the value of σ nevertheless affects the rate at which learning occurs. This parameter is accordingly called the learning parameter of the plant/compensator/controller combination represented by the particular choice of compensator and controller parameters $\alpha \in (-1,+1]$, $D \in R^{m \times m}$, and $\Lambda \in R^{m \times m}$ equation (4.22). In order to investigate systematically the learning rates achievable in the digital iterative learning control of compensated linear multivariable plants, it is therefore convenient in the last of equations (4.22) to choose

$$\Lambda = \lambda \hat{H}^{-1}(T) \qquad \ldots(4.30)$$

where $\lambda \in R^+$. It is then clear from equation (4.26) that

$$\rho = |1-\lambda| \qquad \ldots(4.31)$$

which implies that the crucial condition (i) of Theorem 4.2 will be satisfied provided that $0 < \lambda < 2$.

However, it is also clear from equation (4.27) that the choice of controller matrix given by equation (4.30) implies that the corresponding value of the learning parameter, σ, is given by

$$\frac{\sigma}{\lambda} = \sup_{0 < j \leq J} \| \hat{\Gamma}(\hat{\Phi}^j - \hat{\Phi}^{j-1})\hat{\Psi}\ \hat{H}^{-1}(T) \|_\infty \quad . \qquad ...(4.32)$$

Therefore, in view of equations (4.24), it is evident that

$$\frac{\sigma}{\lambda} \geq \| \left\{ (1-\alpha)CABDT + \left[CAB + \left(\frac{5}{3} - \frac{\alpha}{3} \right) CA^2BD \right] T^2 + 0(T^3) \right\}$$

$$\times \left\{ (CB + CABD)\, T + \left[\frac{1}{2} CAB + \frac{1}{3} CA^2BD \right] T^2 + \ldots \right\}^{-1} \|_\infty \quad . \qquad ...(4.33)$$

Thus, if no compensation is used so that $D = 0$, this indicates as $T \to 0$ that $\sigma/\lambda \geq 2$ in accordance with the results of equation (4.19b) for uncompensated plants. However, if compensation is used so that $D \neq 0$ and $\alpha = 1$, this inequality indicates at $T \to 0$ that $\sigma/\lambda \geq 0$. This dramatic reduction in the lower bound of σ/λ indicates the potential benefits obtainable by introducing compensation in order to increase the learning rates achievable in irregular linear multivariable plants. However, the choice $\alpha = 1$ would create in the compensated plant a marginally stable discrete-time pole at $z = -1$ which would cause 'ringing' to occur. This 'ringing' in the control effort is violent and impractical in the case of commands with initial discontinuities and constant first derivatives (e.g. $v(jT) = 12jT$). But it is tolerable and practically acceptable in the case of continuous compounds with initially zero first derivative (e.g $v(jT) = [4(jT)^3 - 3(jT)^4]$, (see Example 4.3 for illustration). However, for generality it is therefore necessary in practice to compromise by choosing $\alpha \in (-1,+1)$ in order to introduce only asymptotically stable discrete-time

poles from the compensator. Such choices of α nevertheless still lead to increased learning rates as compared with the learning rates achievable in the uncompensated case for the same value of $\lambda \epsilon R^+$ in equation (4.30). It is therefore evident from Theorem 4.2 that the provision of digital compensation in the case of first-order irregular linear multivariable plants facilitates the achievement of rapid learning rates by appropriate choice of $\alpha \epsilon (-1,+1)$ and $D \epsilon R^{m \times m}$ in addition to the choice of $\lambda \epsilon (0,2)$ available in the absence of compensation. In addition, the matrix D must be chosen so that $CBD = 0$ (see Appendix A). The effect of the compensator design parameters α and D on the learning rate is illustrated in Section 4.4.

It is important to note that Theorem 4.2 applies only to first-order partially irregular linear multivariable plants. However, it is possible to obtain similar results for plants with higher-order irregularities simply by introducing multi-stage compensators. Each stage of such compensators is governed by equations like that of equations (4.20) so that, in the general case of the ℓth-order irregular plants, there are parameters $\alpha_i \epsilon (-1,+1)$ and $D_i \epsilon R^{m \times m}$ $(i = 1,2,...,\ell)$ associated with the successive stages of the ℓth-stage compensator. Therefore, in the case of second-order irregular plants, two-stage pre-filters are required. These pre-filters have transfer function matrices of the form $\left[I_m + \frac{2}{T} D_1 \frac{z-1}{z+\alpha_1}\right]$ and $\left[I_m + \frac{2}{T} D_2 \frac{z-1}{z+\alpha_2}\right]$ and are governed by states and output equations of the form

$$r_{1k}(j+1) = -\alpha_1 I_p r_{1k}(j) + J_1 w_{1k}(j) \quad , \quad ...(4.34a)$$

$$w_{2k}(j) = F_1 r_{1k}(j) + G_1 w_{1k}(j) \quad , \quad ...(4.34b)$$

$$r_{2k}(j+1) = -\alpha_2 I_p r_{2k}(j) + J_2 w_{2k}(j) \quad , \quad ...(4.34c)$$

and

$$u_k(j) = F_2 r_{2k}(j) + G_2 w_{2k}(j) \quad , \quad ...(4.34d)$$

respectively. In equations (4.34) $J_1 = [0_{m-p}, I_p]$, $G_1 = \left[I_m + \frac{2}{T} D_1\right]$, $F_1 = -\frac{2}{T}(1+\alpha_1)\begin{bmatrix} D_{12} \\ D_{14} \end{bmatrix}$, $J_2 = [0_{m-p}, I_p]$, $G_2 = \left[I_m + \frac{2}{T} D_2\right]$ and $F_2 = -\frac{2}{T}(1+\alpha_2)\begin{bmatrix} D_{22} \\ D_{24} \end{bmatrix}$. It follows therefore from equations (4.21) and (4.34) that the compensated plant is governed on the discrete-time set by equations of the form

$$x_k(j+1) = \Phi\ x_k(j) + \Psi\ w_{1k}(j) \quad , \qquad \ldots(4.35a)$$

and

$$y_k(j) = \bar{\Gamma}\ \bar{x}_k(j) \quad , \qquad \ldots(4.35b)$$

where

$$\bar{x}_k = \begin{bmatrix} x_k \\ r_{1k} \\ r_{2k} \end{bmatrix} \quad , \qquad \ldots(4.36a)$$

$$\bar{\Phi} = \begin{bmatrix} \Phi & , & \Psi F_1 & , & \Psi G_1 F_2 \\ 0 & , & -\alpha_1 I_p & , & J_1 F_2 \\ 0 & , & 0 & , & -\alpha_2 I_p \end{bmatrix} \quad , \qquad \ldots(4.36b)$$

$$\bar{\Psi} = \begin{bmatrix} \Psi G_1 G_2 \\ J_1 G_2 \\ J_2 \end{bmatrix} \quad , \qquad \ldots(4.36c)$$

and

$$\bar{\Gamma} = [\Gamma, 0, 0] \quad , \qquad \ldots(4.36d)$$

with appropriate dimensions.

It is clear from equations (4.35) that the occurrence of learning can be investigated in this type of plant simply by applying the arguments of Theorem 4.1 to such equivalent plants. It follows therefore that

$$\| \Delta e_k(j) \|_\infty \leq \beta \sum_{q=0}^{k} \frac{k!}{q!(k-q)!} \rho^{k-q} \sigma^q \frac{j!}{q!(j-q)!} \qquad \ldots(4.37)$$

where $k > 0$, and $J = T_t/T$, T_t is the duration of the fixed finite interval $[0, T_t]$ over which the tracking of the command vector $v(j) \in R^m$ is to occur.

$$\Delta e_k(j) = e_k(j+1) - e_k(j) \quad ,$$

$$\beta = \sup_{0 \leq j \leq J} \| \Delta e_0(j) \|_\infty \quad ,$$

$$\rho = \| I_m - \bar{H}(T)\Lambda \|_\infty \quad , \qquad \ldots(4.38)$$

$$\sigma = \sup_{0 < j \leq J} \| \bar{\Gamma}(\bar{\Phi}^{\,j} - \bar{\Phi}^{\,j-1}) \bar{\Psi} \Lambda \|_\infty \quad , \qquad \ldots(4.39)$$

and

$$\bar{H}(T) = H(T) \left[I_m + \frac{2}{T} D_1 \right] \left[I_m + \frac{2}{T} D_2 \right] \quad . \qquad \ldots(4.40)$$

Therefore, by satisfying the condition of $0 < \rho < 1$ in equation (4.38) by choosing $\Lambda = \lambda \bar{H}^{-1}(T)$ where $\lambda \in (0,2)$, it follows from the inequality (4.37) that

$$y_k(j) \rightarrow r(j)$$

as $k \rightarrow \infty$ for all $j \in [0, J]$, as shown in Theorem 4.1. It is evident that, by using similar procedures, ℓth-order irregular plants together with ℓ-stage pre-filters can be represented by the discrete-time equations

$$\overline{x}_k(j+1) = \overline{\Phi}\,\overline{x}_k(j+1) + \overline{\Psi}\, w_{1k}(j) \quad , \qquad \text{...(4.41a)}$$

$$y_k(j) = \overline{\Gamma}\ \overline{x}_k(j) \quad , \qquad \text{...(4.41b)}$$

where

$$\overline{x}_k = \begin{bmatrix} x_k \\ r_{1k} \\ r_{2k} \\ r_{3k} \\ \cdot \\ \cdot \\ \cdot \\ r_{\ell k} \end{bmatrix} \quad , \qquad \text{...(4.42a)}$$

$$\overline{\Phi} = \begin{bmatrix} \Phi\,, & \Psi F_1\,, & \Psi G_1 F_2, & \Psi G_1 G_2 F_3\,, \ldots\ldots, & \Psi G_1 G_2 \ldots G_{k-1} F_\ell \\ 0\,, & -\alpha_1 I_p\,, & J_1 F_2\,, & J_1 G_2 F_3 \quad , \ldots\ldots, & J_1 G_2 G_3 \ldots G_{k-1} F_\ell \\ 0\,, & 0\ , & -\alpha_2 I_p, & J_2 F_3 \quad , \ldots\ldots, & J_2 G_3 G_4 \ldots G_{\ell-1} F_\ell \\ 0\,, & 0\ , & 0\ , & -\alpha_3 I_p \quad , \ldots\ldots, & J_3 G_4 G_5 \ldots G_{\ell-1} F_\ell \\ & & & & \\ 0\,, & 0\,, & 0\ , & 0, \quad , \ldots\ldots, & -\alpha_\ell I_p \end{bmatrix}, \qquad \text{...(4.42b)}$$

$$\overline{\Psi} = \begin{bmatrix} \Psi\, G_1 G_2 \ldots G_{\ell-1} \\ J_1 G_2 \ldots G_{\ell-1} \\ J_2 G_3 \ldots G_{\ell-1} \\ J_3 G_4 \ldots G_{\ell-1} \\ \vdots \\ J_\ell \end{bmatrix} \quad , \qquad \ldots(4.42c)$$

and

$$\overline{\Gamma} = [\Gamma, 0, 0, \ldots, 0_\ell] \quad . \qquad \ldots(4.42d)$$

It follows that

$$\rho = \| I_m - \overline{H}(T)\Lambda \|_\infty \qquad \ldots(4.43)$$

and

$$\sigma = \sup_{0 < j \leq J} \| \overline{\Gamma}(\overline{\Phi}^j - \overline{\Phi}^{j-1})\, \overline{\Psi}\, \Lambda \|_\infty \quad , \qquad \ldots(4.44)$$

where

$$\overline{H}(T) = H(T) \left[I_m + \frac{2}{T} D_1\right]\left[I_m + \frac{2}{T} D_2\right] \ldots + \left[I_m + \frac{2}{T} D_\ell\right] \qquad \ldots(4.45)$$

is the step-response matrix of the compensated plant with uncompensated step-response matrix $H(T)$. It is thus possible to use the arguments of Theorem 4.1 to prove the occurrence of learning for such compensated plants, providing that

$$\Lambda = \lambda\, \overline{H}^{-1}(T) \qquad \ldots(4.46)$$

Thus, the choice of the parameters α_i and D_i, in addition to the choice $\lambda \in (0,2)$ available in the absence of compensator, facilitates the achievement of rapid learning rates even in the case of high-order irregularities. Finally, it is important to mention that the quantity on the right-hand side of the inequalities (4.13), (4.25) and (4.37) represents an upper bound on the rate of change of error. This bound can be used as a guide to show how the parameters ρ and σ affect the learning rates in the case of digital iterative learning control. Thus, for example, it is evident when $\rho = 0$ that the inequality (4.13) becomes

$$\| \Delta e_k(j) \|_\infty \leq \beta \sigma^k \frac{j!}{k!(j-k)!} \qquad ...(4.47)$$

which shows that $y_k(j) = y(j)$ when $k > j$. This means that, when $\rho = 0$, the learning behaviour is propagated through the interval $[0,T_t]$ at least as rapidly as is implied by the sequence $e_k(0) = 0$, $e_k(T) = 0$, $e_k(2T) = 0,...,e_k((k-1)T) = 0$ $(k = 1,2,3,...)$, regardless of the value of σ. However, as indicated by the inequality (4.47), the learning behaviour when $\rho = 0$ is affected by the value of σ, as shown in Example 4.6.

4.3 SYNTHESIS

It is clear that learning will occur in the sense that $e_k \to 0$ as $k \to \infty$ in the controllers proposed in this chapter provided that the condition $0 \leq \rho < 1$ is satisfied. However, the speed with which the plant learns is determined by the values of the parameters ρ and σ. The values of both parameters depend on the choice of the controller gain matrix Λ; in addition, σ depends on the irregularity and stability characteristics of the open-loop plant as shown in Section 4.2. It is also shown in Section 4.2 that rapid convergence can be obtained provided that ρ and σ are very small. It follows, therefore, that the controller gain matrix, Λ, must be tuned so that

both ρ and σ are as small as possible. Thus, the controller gain matrix for ℓth-order irregular plants must be

$$\Lambda = \lambda\left[H(T)\left(I_m + \frac{2}{T} D_1\right)\left(I_m + \frac{2}{T} D_2\right)\cdots\left(I_m + \frac{2}{T} D_\ell\right)\right]^{-1} \quad \ldots(4.48)$$

so that good learning performance and rapid convergence can be guaranteed (see Section 4.4 for illustration).

4.4 Illustrative Examples

These general results can be conveniently illustrated by designing digital iterative learning controllers for different linear multivariable plants with different irregularity and stability characteristics. In addition, the upper bound of the rate of change of error is investigated for different stable SISO plants. In all these examples, in the iteration corresponding to $k = 0$ neither the inputs nor the outputs have been plotted since both are zero.

Example 4.1

The state and output equations of the linear time-invariant plant on the continuous-time set are

$$\begin{bmatrix} \dot{x}_1(t) \\ \dot{x}_2(t) \\ \dot{x}_3(t) \end{bmatrix} = \begin{bmatrix} -3 & , & 1 & , & 0 \\ -2 & , & -1 & , & 2 \\ 0 & , & 1 & , & -2 \end{bmatrix} \begin{bmatrix} x_1(t) \\ x_2(t) \\ x_3(t) \end{bmatrix} + \begin{bmatrix} 0 & , & 0 \\ 2 & , & 1 \\ 1 & , & 3 \end{bmatrix} \begin{bmatrix} u_1(t) \\ \\ u_2(t) \end{bmatrix} \qquad \ldots(4.49a)$$

and

$$\begin{bmatrix} y_1(t) \\ \\ y_2(t) \end{bmatrix} = \begin{bmatrix} 0 & , & 1 & , & -1 \\ & & & & \\ 1 & , & 0 & , & -1 \end{bmatrix} \begin{bmatrix} x_1(t) \\ x_2(t) \\ x_3(t) \end{bmatrix} \qquad \ldots(4.49b)$$

In this case, the plant is asymptotically stable and also regular since its first Markov parameter

$$CB = \begin{bmatrix} 1 & , & -2 \\ & & \\ -1 & , & -3 \end{bmatrix} \qquad \ldots(4.50)$$

evidently has full rank. In addition, for a sampling period $T = 0.1$ *sec*, the step-response matrix of this plant is

$$H(T) = \begin{bmatrix} 9.999\times10^{-3} & , & -19.505\times10^{-3} \\ & & \\ -9.901\times10^{-3} & , & -29.702\times10^{-3} \end{bmatrix} \qquad \ldots(4.51)$$

It is required that the output vector of this plant track the command vector

$$v(jT) = \begin{bmatrix} 12jT \\ -12jT \end{bmatrix} (j \in [0,100]) \qquad \ldots(4.52)$$

on the interval [0, 1].

In case

$$x_0(0) = \begin{bmatrix} 0 \\ 0 \\ 0 \end{bmatrix} \qquad \ldots(4.53)$$

and

$$u_0(jT) = \begin{bmatrix} 0 \\ 0 \end{bmatrix} (j \in [0,100]) \quad , \qquad \ldots(4.54)$$

the learning characteristics of the iterative learning controller with different controller gain matrices

$$\Lambda = \lambda H^{-1}(T) \qquad \ldots(4.55)$$

when

$$H^{-1}(T) = \begin{bmatrix} 6.040\times10^{1} & , & -3.979\times10^{1} \\ -2.030\times10^{1} & , & -2.040\times10^{1} \end{bmatrix} \qquad \ldots(4.56)$$

are shown in Figure 4.2. Indeed, the results in Figures 4.2(a,b) correspond to the choice $\lambda = 1$, $\rho = 0$ $\sigma = 0.00394$; those in Figures 4.2(c,d) to the choice $\lambda = 0.5$, $\rho =$

0.5, $\sigma = 0.0197$; and those in Figures 4.2(e,f) to the choice $\lambda = 0.1$, $\rho = 0.9$, $\sigma = 0.00039$. It is clear that excellent learning behaviour is obtained in all cases but that the rate of learning increases as the parameter ρ decreases. This trend is evident from Figure 4.2 even though, for this asymptotically stable and regular plant, the learning parameter, σ, increases as the parameter ρ decreases. However, the significance of the learning parameter is discussed in greater detail in the following examples, where the effects on this parameter of plant instability and irregularity are explicitly investigated. Figure 4.3 shows the corresponding control efforts.

Example 4.2

The state and output equations of a linear time-invariant plant on the continuous-time set are

$$\begin{bmatrix} \dot{x}_1(t) \\ \dot{x}_2(t) \\ \dot{x}_3(t) \end{bmatrix} = \begin{bmatrix} -3 & , & 1 & , & 0 \\ -2 & , & -1 & , & 2 \\ 0 & , & 1 & , & -2 \end{bmatrix} \begin{bmatrix} x_1(t) \\ x_2(t) \\ x_3(t) \end{bmatrix} + \begin{bmatrix} 0 & , & 0 \\ 2 & , & 1 \\ 1 & , & 3 \end{bmatrix} \begin{bmatrix} u_1(t) \\ \\ u_2(t) \end{bmatrix} \qquad \ldots(4.57a)$$

and

$$\begin{bmatrix} y_1(t) \\ \\ y_2(t) \end{bmatrix} = \begin{bmatrix} 1 & , & 0 & , & -1 \\ & & & & \\ 1 & , & 0 & , & 0 \end{bmatrix} \begin{bmatrix} x_1(t) \\ x_2(t) \\ x_3(t) \end{bmatrix} . \qquad \ldots(4.57b)$$

In this case, the plant is asymptotically stable but first-order partially irregular since

its first Markov parameter

$$CB = \begin{bmatrix} -1 & , & -3 \\ 0 & , & 0 \end{bmatrix} \qquad \text{...(2.58a)}$$

whilst its second Markov parameter

$$CAB = \begin{bmatrix} 2 & , & 6 \\ 2 & , & 1 \end{bmatrix} \qquad \text{...(2.58b)}$$

evidently has full rank. In addition, for a sampling period $T = 0.01$ *sec*, the step-response matrix of this plant is

$$H(T) = \begin{bmatrix} -9.901\times10^{-3} & , & -0.297\times10^{-1} \\ 0.990\times10^{-4} & , & 0.503\times10^{-4} \end{bmatrix} \qquad \text{...(4.59)}$$

It is required that the output vector of this plant track the command vector

$$v(jT) = \begin{bmatrix} 12jT \\ -12jT \end{bmatrix} \quad (j \in [0, 100]) \qquad \text{...(4.60)}$$

on the time interval [0, 1].

In case

$$x_0(0) = \begin{bmatrix} 0 \\ 0 \\ 0 \end{bmatrix} \qquad \ldots(4.61)$$

and

$$u_0(jT) = \begin{bmatrix} 0 \\ 0 \end{bmatrix} \ (j \in [0, 100]) \quad , \qquad \ldots(4.62)$$

the learning characteristics of the digital iterative learning controller with different controller gain matrices governed by equation (4.55) when

$$H^{-1}(T) = \begin{bmatrix} 0.205\times10^2 & , & 121.609\times10^2 \\ -0.405\times10^2 & , & -40.537\times10^2 \end{bmatrix} \qquad \ldots(4.63)$$

are shown in Figure 4.4. Indeed, the results in Figures 4.4(a,b) correspond to the choice $\lambda = 1$, $\rho = 0$ $\sigma = 2.0$; those in Figures 4.4(c,d) to the choice $\lambda = 0.1$, $\rho = 0.9$, $\sigma = 0.2$; and those in Figures 4.4(e,f) to the choice $\lambda = 0.01$, $\rho = 0.99$, $\sigma = 0.02$. It is clear from these figures that, because of the irregularity of the plant under control, learning is slow and violent as shown in Figures 4.4(a,b) when $\lambda = 1$; that learning is slower but less violent as shown in Figures 4.4(c,d) when $\lambda = 0.1$; and that learning is even slower but even less violent as shown in Figures 4.4(e,f) when $\lambda = 0.01$.

These results confirm that the irregularity characteristics of linear multivariable plants place unavoidable limits on the learning rates achievable in the digital iterative learning control of uncompensated plants, and thus motivate the introduction of compensators in order to increase these rates. Figure 4.5 shows the corresponding control efforts.

Indeed, if compensation is introduced (Theorem 4.2), rapid non-violent learning can be achieved without reducing the value of λ in order to de-tune the controller. This is demonstrated by the results presented in Figure 4.6 for digital iterative learning control in the presence of compensation with $\lambda = 1$,

$$D = \begin{bmatrix} 0 & , & -3 \\ 0 & , & 1 \end{bmatrix} \qquad \ldots(4.64)$$

so that $CBD = 0$, and different values of α. Indeed, the results in Figures 4.6(a,b) correspond to the choice of $\alpha = 1$, $\rho = 0$, $\sigma = 0.063$; those in Figures 4.6(c,d) to the choice $\alpha = 0.5$, $\rho = 0$, $\sigma = 0.461$; and those in Figures 4.6(e,f) to the choice $\alpha = 0$, $\rho = 0$, $\sigma = 0.962$. These results confirm the beneficial effects of compensation in achieving rapid learning rates, which nevertheless decrease slightly as α decreases from 1 to 0. This decrease in learning is, however, accompanied by reductions in controller oscillations (see Figure 4.7) which are frequently attractive in practice. Figure 4.8 shows the learning of the digital iterative controller when $\alpha = 0$ and $\lambda = 0.8, 0.5, 0.5$, respectively. These results indicate that the learning performance when $\alpha = 0$ can be improved by de-tuning the controller gain matrix, Λ. Figure 4.9 show the corresponding control efforts in all cases. However, in case $\alpha = 1$, it is still possible to obtain good learning performance and rapid convergemce with no oscillation in the control effort. This can be achieved by demanding that the output of the plant follows a continuous command with initially zero first derivative. This is demonstrated by the results presented in Figure 4.10, when it is required that the output follow a command vector of the form

$$v(jT) = \begin{bmatrix} (\,4(jT)^3 - 3(jT)^4) \\ -(4(jT)^3 - 3(jT)^4) \end{bmatrix} (j \in [0, 100]) \qquad \ldots(4.65)$$

on the time interval [0, 1].

In this case, $\lambda = 1$, $\rho = 0$, $\alpha = 1$ and $\sigma = 0.063$. It is clear from Figure 4.10 that rapid learning rates are achieved with no significant oscillation in the control effort.

Finally, it is important to mention that since the plant is first-order partially irregular, it is therefore possible to tune the controller matrix, Λ, using different values of λ for each channel. Indeed, it is possible to have $\lambda = 1$ for the regular channel and $\lambda < 1$ for the irregular channel.

Example 4.3

The state and output equations of the linear time-invariant plant on the continuous-time set are

$$\begin{bmatrix} \dot{x}_1(t) \\ \dot{x}_2(t) \\ \dot{x}_3(t) \\ \dot{x}_4(t) \end{bmatrix} = \begin{bmatrix} 0 & , & 0.5 & , & 0 & , & 0 \\ 0 & , & 0.1 & , & 0.75 & , & 0 \\ -1.5 & , & 0.5 & , & 1.25 & , & 0 \\ 2.5 & , & 0 & , & -2.5 & , & 0 \end{bmatrix} \begin{bmatrix} x_1(t) \\ x_2(t) \\ x_3(t) \\ x_4(t) \end{bmatrix}$$

$$+ \begin{bmatrix} 0 & , & 0 \\ 1 & , & 2 \\ 3 & , & 1 \\ 0 & , & 0 \end{bmatrix} \begin{bmatrix} u_1(t) \\ \\ \\ u_2(t) \end{bmatrix} \qquad \ldots(4.66a)$$

and

$$\begin{bmatrix} y_1(t) \\ \\ y_2(t) \end{bmatrix} = \begin{bmatrix} 1 & , & 0 & , & 0 & , & 0 \\ \\ 0 & , & 0 & , & 0 & , & 1 \end{bmatrix} \begin{bmatrix} x_1(t) \\ x_2(t) \\ x_3(t) \\ x_4(t) \end{bmatrix} . \qquad \text{...(4.66b)}$$

In this case, the plant is unstable and is first-order completely irregular since its first Markov parameter

$$CB = \begin{bmatrix} 0 & , & 0 \\ 0 & , & 0 \end{bmatrix} \qquad \text{...(4.67a)}$$

is clearly null whilst its second Markov parameter

$$CAB = \begin{bmatrix} 0.5 & , & 1 \\ -7.5 & , & -2.5 \end{bmatrix} \qquad \text{...(4.67b)}$$

evidently has full rank. In addition, for a sampling period $T = 0.01$ *sec*, the step-response matrix of this plant is

$$H(T) = \begin{bmatrix} 2.519\times10^{-5} & , & 5.008\times10^{-5} \\ -37.657\times10^{-5} & , & -12.552\times10^{-5} \end{bmatrix} . \qquad \text{...(4.68)}$$

Since this plant is first-order completely irregular, a pre-filter in addition to the digital iterative controller is required. Moreover, this pre-filter is designed so that no oscillation in the control effort is present and rapid convergence is achieved by

choosing $\alpha = 0$ and $D = I$ since CB is null. However, since the plant is unstable according to equation (4.39) the large value of σ corresponds to the end of the task. However, in this example the largest learning parameter is $\sigma = 1.021$ when $\lambda = 1$ at $j = 1$, since it is required that the output vector of this plant track the command vector

$$v(jT) = \begin{bmatrix} 12jT \\ -12jT \end{bmatrix} \quad (j \in [0, 100])$$

on the time interval [0, 1]. Therefore, de-tuning of the controller gain matrix, Λ, is required. In case

$$x_0(0) = \begin{bmatrix} 0 \\ 0 \\ 0 \\ 0 \end{bmatrix} \qquad \ldots(4.69)$$

and

$$u_0(jT) = \begin{bmatrix} 0 \\ 0 \end{bmatrix} (j \in [0, 100]) \quad , \qquad \ldots(4.70)$$

the learning of the digital iterative controller with different controller gain matrices governed by equation (4.48)

$$\left[H(T)\left(I_2 + \frac{2}{T} D\right)\right]^{-1} = \begin{bmatrix} -3.978\times10^1 & , & -1.587\times10^1 \\ 11.936\times10^1 & , & 0.798\times10^1 \end{bmatrix} \qquad \ldots(4.71)$$

are shown in Figure 4.11. It is clear from these figures that, because of the instability of the plant under control, learning is slow and violent as shown in Figures 4.11(a,b) when $\lambda = 1$; that learning is slower but less violent as shown in Figures 4.11(c,d) when $\lambda = 0.5$ and that learning is even slower but even less violent as shown in Figures 4.11(e,f) when $\lambda = 0.1$. These results confirm that the instability of linear multivariable plants places unavoidable limits on the learning rates achievable in the digital iterative learning control even of compensated plants. Figure 4.12 shows the corresponding control efforts.

Example 4.4

The state and output equations of a linear time-invariant plant on the continuous-time set are

$$\begin{bmatrix} \dot{x}_1(t) \\ \dot{x}_2(t) \\ \dot{x}_3(t) \\ \dot{x}_4(t) \end{bmatrix} = \begin{bmatrix} 0 & 0 & 1 & 3 \\ 0 & 0 & 0 & 1 \\ 0 & 0 & 0 & 0 \\ 0 & 0 & 0 & 0 \end{bmatrix} \begin{bmatrix} x_1(t) \\ x_2(t) \\ x_3(t) \\ x_4(t) \end{bmatrix} + \begin{bmatrix} 0 & 0 \\ 0 & 0 \\ 2 & 0 \\ 0 & -3 \end{bmatrix} \begin{bmatrix} u_1(t) \\ \\ \\ u_2(t) \end{bmatrix} \quad \ldots(4.72a)$$

and

$$\begin{bmatrix} y_1(t) \\ \\ y_2(t) \end{bmatrix} = \begin{bmatrix} 1 & , & 0 & , & 0 & , & 0 \\ \\ 0 & , & 1 & , & 0 & , & 0 \end{bmatrix} \begin{bmatrix} x_1(t) \\ x_2(t) \\ x_3(t) \\ x_4(t) \end{bmatrix} . \qquad \text{...(4.72b)}$$

In this case, the plant is clearly neutrally stable but first-order completely irregular since its first Markov parameter

$$CB = \begin{bmatrix} 0 & , & 0 \\ \\ 0 & , & 0 \end{bmatrix} \qquad \text{...(4.73a)}$$

is clearly null whilst its second Markov parameter

$$CAB = \begin{bmatrix} 2 & , & -9 \\ \\ 0 & , & -3 \end{bmatrix} \qquad \text{...(4.73b)}$$

evidently has full rank. In addition, for a sampling period $T = 0.01$ *sec*, the step-response matrix of this plant is

$$H(T) = \begin{bmatrix} 1.0\times10^{-4} & , & -4.5 \\ \\ 0.0 & , & -1.5\times10^{-4} \end{bmatrix} . \qquad \text{...(4.74)}$$

In this example, two issues are investigated; firstly, the effect of the compensator design parameter D and, secondly, the effect of open-loop poles on the value of the learning parameter, σ, and the learning rate.

It is required that the output vector of this plant track the command vector

$$v(jT) = \begin{bmatrix} 12jT \\ -12jT \end{bmatrix} \quad (j \in [0, 100])$$

on the time interval [0, 1].

In case

$$x_0(0) = \begin{bmatrix} 0 \\ 0 \\ 0 \\ 0 \end{bmatrix} \qquad \ldots(4.75)$$

and

$$u_0(jT) = \begin{bmatrix} 0 \\ 0 \end{bmatrix} (j \in [0, 100]]) \quad , \qquad \ldots(4.76)$$

the learning of the digital iterative learning controller with $\alpha = 0$, $D = 100\ I_2$, and different controller gain matrices governed by equation (4.48) corresponding to $\lambda =$ {1, 0.5, 0.2} when

$$\left[H(T)\left[I_2 + \frac{2}{T} D\right]\right]^{-1} = \begin{bmatrix} 4.999\times10^{-1} & , & -14.999\times10^{-1} \\ 0.0 & , & -3.333\times10^{-1} \end{bmatrix} \qquad \ldots(4.77)$$

are shown in Figure 4.13 and the corresponding control efforts are shown in Figure 4.14. These choices of λ and D made $\rho =$ {0, 0.5, 0.8} and $\sigma =$ {1, 0.5, 0.2} respectively. On the other hand the learning of the digital iterative learning controller with $D = I_2$, and different controller gain matrices governed by equation (4.48)

corresponding to $\lambda = (1, 0.5, 0.2)$ when

$$\left[H(T)\left(I_2 + \frac{2}{T} D\right)\right]^{-1} = \begin{bmatrix} 4.975\times10^{1} & , & -14.925\times10^{1} \\ 0.0 & , & -3.316\times10^{1} \end{bmatrix} \qquad \ldots(4.78)$$

are shown in Figure 4.15 and the corresponding control effort in Figure 4.16. These choices of λ and D made $\rho = (0, 0.5, 0.8)$ and $\sigma = (1.005, 0.5025, 0.201)$, respectively. It is clear by comparing the results presented in Figure 4.13 with those presented in Figure 4.15 that the learning performance and speed of convergence with $D = 100\ I_2$ are far better than those with $D = I_2$. This can be best appreciated by comparing the values of the learning parameter, σ, for both choices of D. However, unlike the parameter D in the analogue controllers of Chapters 2 and 3, it is clear that the effect of the parameter D in the digital iterative controller on the learning parameter σ is very limited. Therefore, the choice of D must be mainly concerned with the satisfaction of $CBD = 0$.

Finally, the second issue to be discussed is the location of the open-loop poles. Indeed, as in the analogue iterative learning controller of Chapters 2 and 3, it is interesting to investigate those plant characteristics that are most conducive to digital iterative learning control. Such plants characteristics can be recognised from the previous examples, which indicate that any plant/controller combination that produces a very small value of σ without affecting the value of ρ would be the optimal choice. Indeed, it has been shown in the previous examples that irregular and unstable plants produce very large values of σ. It has also been shown that regular stable plants produce very small values of σ. Thus, through thorough investigation, it has been found that regular plants with all eigenvalues on the boundary of the unit disc produce learning parameters $\sigma = 0$. In the current example, all the eigenvalues of the plant lie on this boundary but $\sigma = 2$ because of the irregularity problem for

the uncompensated plant when $\lambda = 1$. However, the compensated plant produces $\sigma \simeq 1$ when $\lambda = 1$ and $\alpha = 0$ (to prevent oscillation in the control effort). Indeed, if such oscillation is tolerated, $\sigma = 0$ can be achieved when $\alpha = 1$, $\lambda = 1$ and $\rho = 0$. This confirms that the best plants to be controlled using digital iterative controller are neutrally stable plants.

Example 4.5

In the previous examples, regular and first-order irregular plants were investigated. In this example, therefore, a second-order completely irregular plant is investigated to illustrate the effectiveness of digital iterative learning controller in controlling high-order irregular plants. The state and output equations of the linear time-invariant plant on the continuous-time set are

$$\begin{bmatrix} \dot{x}_1(t) \\ \dot{x}_2(t) \\ \dot{x}_3(t) \\ \dot{x}_4(t) \\ \dot{x}_5(t) \\ \dot{x}_6(t) \end{bmatrix} = \begin{bmatrix} 0 & 0 & 1 & 0 & 0 & 0 \\ 0 & 0 & 0 & 1 & 0 & 0 \\ -4 & -1 & 1 & 2 & -4 & 2 \\ 1 & -2 & -3 & -2 & 1 & -3 \\ 0 & 0 & 0 & 0 & -3 & 0 \\ 0 & 0 & 0 & 0 & 0 & -2 \end{bmatrix} \begin{bmatrix} x_1(t) \\ x_2(t) \\ x_3(t) \\ x_4(t) \\ x_5(t) \\ x_6(t) \end{bmatrix}$$

$$+\begin{bmatrix} 0 & , & 0 \\ 0 & , & 0 \\ 0 & , & 0 \\ 0 & , & 0 \\ 3 & , & 0 \\ 0 & , & 2 \end{bmatrix}\begin{bmatrix} u_1(t) \\ \\ \\ \\ u_2(t) \end{bmatrix} \qquad \ldots(4.79a)$$

and

$$\begin{bmatrix} y_1(t) \\ \\ \\ y_2(t) \end{bmatrix} = \begin{bmatrix} 1 & , & -2 & , & 0 & , & 0 & , & 0 & , & 0 \\ 1 & , & 2 & , & 0 & , & 0 & , & 0 & , & 0 \end{bmatrix}\begin{bmatrix} x_1(t) \\ x_2(t) \\ x_3(t) \\ x_4(t) \\ x_5(t) \\ x_6(t) \end{bmatrix}. \qquad \ldots(4.79b)$$

In this case, the plant is asymptotically stable but second-order completely irregular since its first and second Markov parameters

$$CB = \begin{bmatrix} 0 & , & 0 \\ 0 & , & 0 \end{bmatrix} \qquad \ldots(4.80a)$$

and

$$CAB = \begin{bmatrix} 0 & , & 0 \\ 0 & , & 0 \end{bmatrix} \qquad \ldots(4.80b)$$

are clearly null whilst its third Markov parameter

$$CA^2B = \begin{bmatrix} -18 & , & 16 \\ -6 & , & -8 \end{bmatrix} \qquad \ldots(4.80c)$$

evidently has full rank. It follows, therefore, that a two-stage pre-filter is required (see Section 4.2). Moreover, since $CB = CAB = 0$, D_1 and D_2 can be arbitrary. However, the choices $D_1 = D_2 = I_2$ are made together with $\alpha_1 = \alpha_2 = 0$. In addition, for a sampling period $T = 0.01$ *sec* the step-response matrix of the uncompensated plant is

$$H(T) = \begin{bmatrix} -3.0018\times10^{-6} & , & 2.6500\times10^{-6} \\ -0.9702\times10^{-6} & , & -1.3300\times10^{-6} \end{bmatrix} . \qquad \ldots(4.81)$$

It is required that the output vector of this plant track the command vector

$$v(jT) = \begin{bmatrix} 12jT \\ -12jT \end{bmatrix} \quad (j \in [0, 100])$$

on the time interval [0, 1].

In case

$$x(0) = \begin{bmatrix} 0 \\ 0 \\ 0 \\ 0 \\ 0 \\ 0 \end{bmatrix} \qquad \ldots(4.82)$$

and

$$u_0(jT) = \begin{bmatrix} 0 \\ 0 \end{bmatrix} (j \in [0, 100]) \quad , \qquad \ldots(4.83)$$

the learning of the digital iterative learning controller with different controller gain matrices governed by equation (4.48) when

$$\left[H(T)\left(I_2 + \frac{2}{T} D\right)\left(I_2 + \frac{2}{T} D\right)\right]^{-1} = \begin{bmatrix} -5.0126 & , & -9.9877 \\ 3.6567 & , & -11.3256 \end{bmatrix} \qquad \ldots(4.84)$$

are shown in Figure 4.17 and the corresponding control efforts are shown in Figure 4.18. Thus, according to the analysis of Section 4.2, the uncompensated plant with second-order irregularity produces a learning parameter $\sigma = 6$ when $\rho = 0$. However, the introduction of compensators makes $\sigma = 4$ when $\alpha_1 = \alpha_2 = 0$ and $\rho = 0$. It is clear that this value of σ is still high. Indeed, even if $\alpha_1 = \alpha_2 = 1$ are chosen, the minimum value of the learning parameter achieved is $\sigma = 2$ which is still large. Thus, the controller gain matrix must be de-tuned with different values of λ in order to obtain good learning performance without violence Indeed, the results presented in Figures 4.17(a,b) correspond to $\lambda = 0.25$ and hence $\rho = 0.75$, $\sigma = 1$;

those in Figures 4.17 (c,d) correspond to $\lambda = 0.2$ and hence $\rho = 0.8$, $\sigma = 0.8$; and those in Figures 4.17(e,f) correspond to $\lambda = 0.1$ and hence $\rho = 0.9$, $\sigma = 0.4$. It is very clear, therefore, that considerable improvement in the learning performance (by eliminating violence) can be achieved using de-tuning.

Example 4.6

This example is given so as to illustrate the conservativeness (or otherwise) of the bound on the rate of change of error given by the inequality (4.13). This illustration is affected by considering two SISO plants governed by state and output equations of the respective forms

$$\dot{x}(t) = a\, x(t) + b\, u(t) \qquad \text{...(4.85a)}$$

$$y(t) = c\, x(t) \qquad \text{...(4.85b)}$$

for which

$a = -1$

$b = 1$

$c = 1$

and

$a = -10$

$b = 1$

$c = 1$

respectively. The step-response functions of these two plants when the sampling period $T = 0.01$ *sec* are $h(T) = 9.9502 \times 10^{-3}$ and $h(T) = 9.5163 \times 10^{-3}$, respectively. Thus, using Theorem 4.1, it is evident that $\sigma = 9.95 \times 10^{-3}$ and $\sigma = 95.16 \times 10^{-3}$, respectively, for these plants in case the digital iterative learning controller is designed such that $\rho = 0$. Now, it is required to investigate the relation between the inequality (4.47) and $\frac{\| \Delta e_k(j) \|_\infty}{\beta}$ of the actual process for ($j \in [0,200]$). It is clear from Figures 4.19(a,b) that the bound is non-conservative when σ is small. On the other hand, the results represented in Figures 4.19(c,d) confirm that the bound is loose and conservative when σ is large. In addition, it is clear by comparing Figures 4.19(a,d) that learning is slow when σ is large. This is confirmed in Figures 4.19(a,c).

4.5 CONCLUSION

In this chapter, it has been shown that digital iterative learning controllers can be designed for linear multivariable plants using only the step-response matrices of such plants. This demonstration has been effected by proving a fundamental theorem which establishes precise sufficient conditions under which iterative learning control is achieved by such digital controllers. In addition, it has been shown that these results can be used to obtain important information concerning the learning rates achievable by such controllers. Indeed, it has been found that the irregularity and stability characteristics of the plants under control impose severe constraints on these achievable learning rates. However, it has been shown that these severe constraints can be removed by designing digital iterative learning controllers with appropriate digital compensators for irregular linear multivariable plants. This demonstration has been effected by proving a fundamental theorem which establishes precise sufficient conditions under which iterative learning control is achieved by such digital controllers and compensators in the case of first-order irregular plants. The extension

of such results to higher-order irregular plants has been presented. In addition, the effect of the open-loop eigenvalues of plants on the learning rate has been investigated. Furthermore, the upper bound of the rate of change of error has been investigated. Finally, these general results have been illustrated by the presentation of numerical results for the digital iterative learning control of plants with different irregularity and stability characteristics.

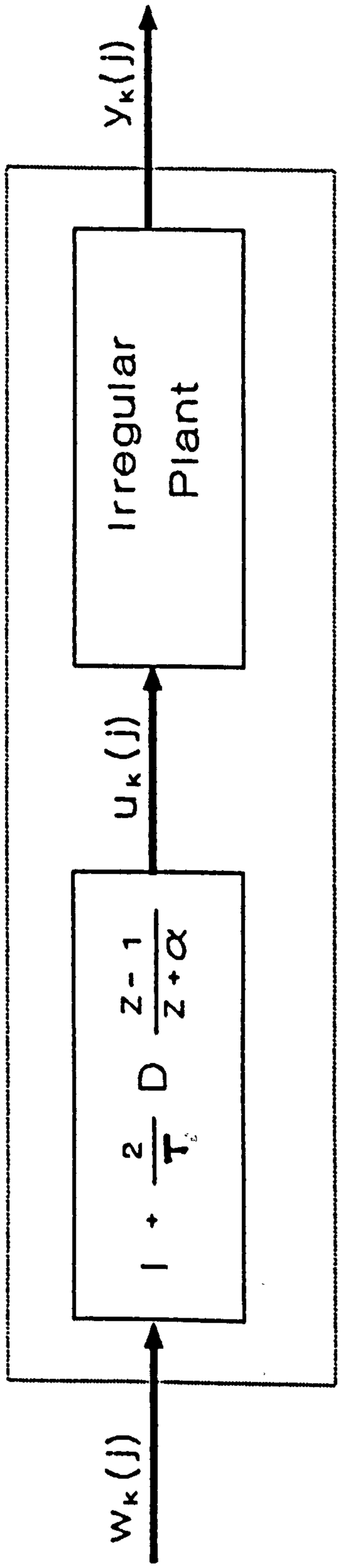

Overall Plant

Fig.4.1 Pre_filter in Cascade with First_Order Irregular Plant.

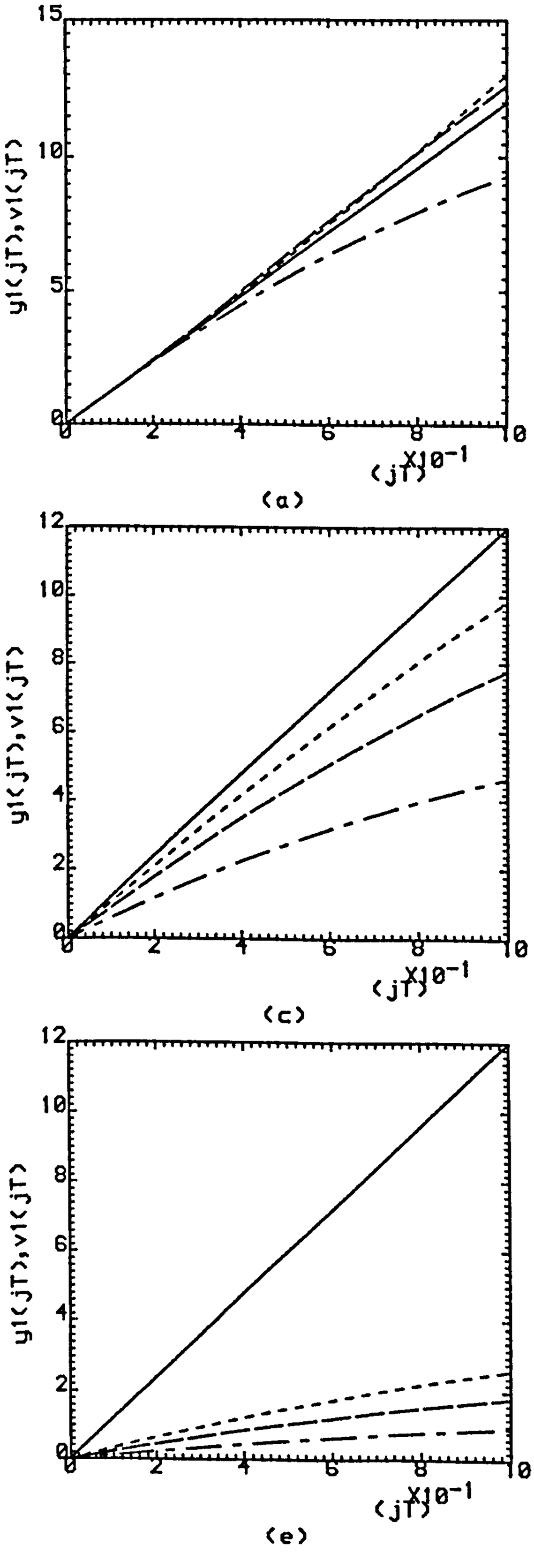

Fig.4.2(a,b) (rho=0.0,sigma=0.0394).
(c,d) (rho=0.5,sigma=0.0197).
(e,f) (rho=0.9,sigma=0.00394).
-·-·- K=1 , ----- K=2 , ... K=3

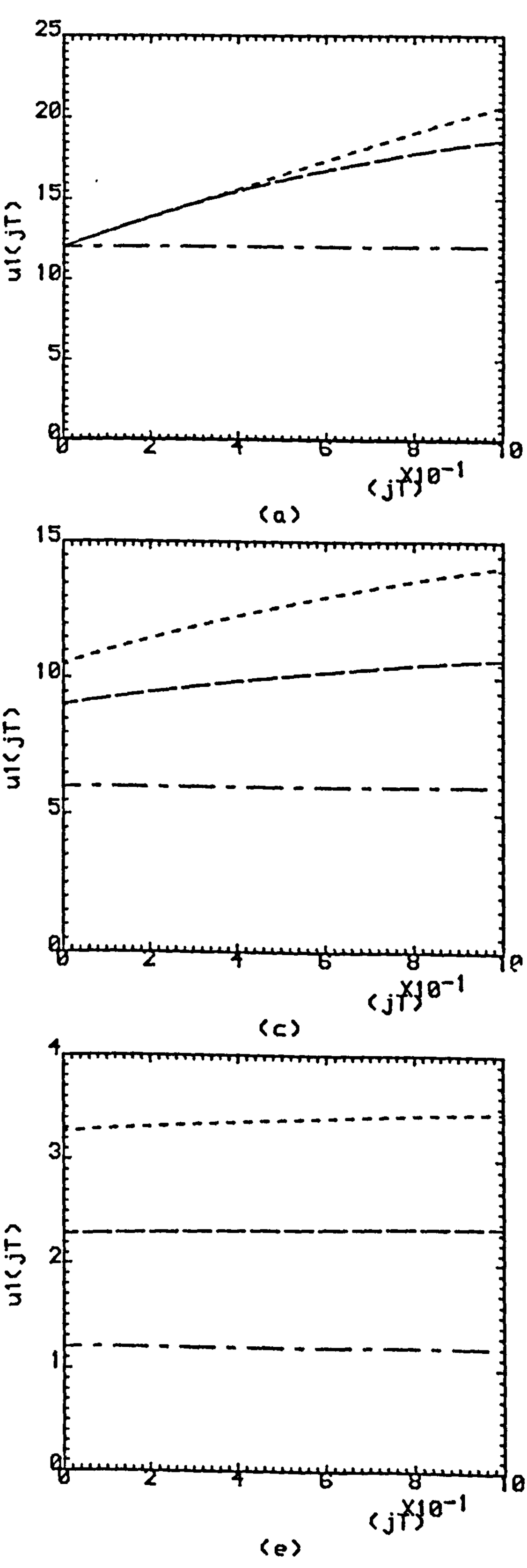

Fig.4.3(a,b) (rho=0.0,sigma=0.0394).
(c,d) (rho=0.5,sigma=0.0197).
(e,f) (rho=0.9,sigma=0.00394).
-·-·- K=1 , ----- K=2 , ... K=3

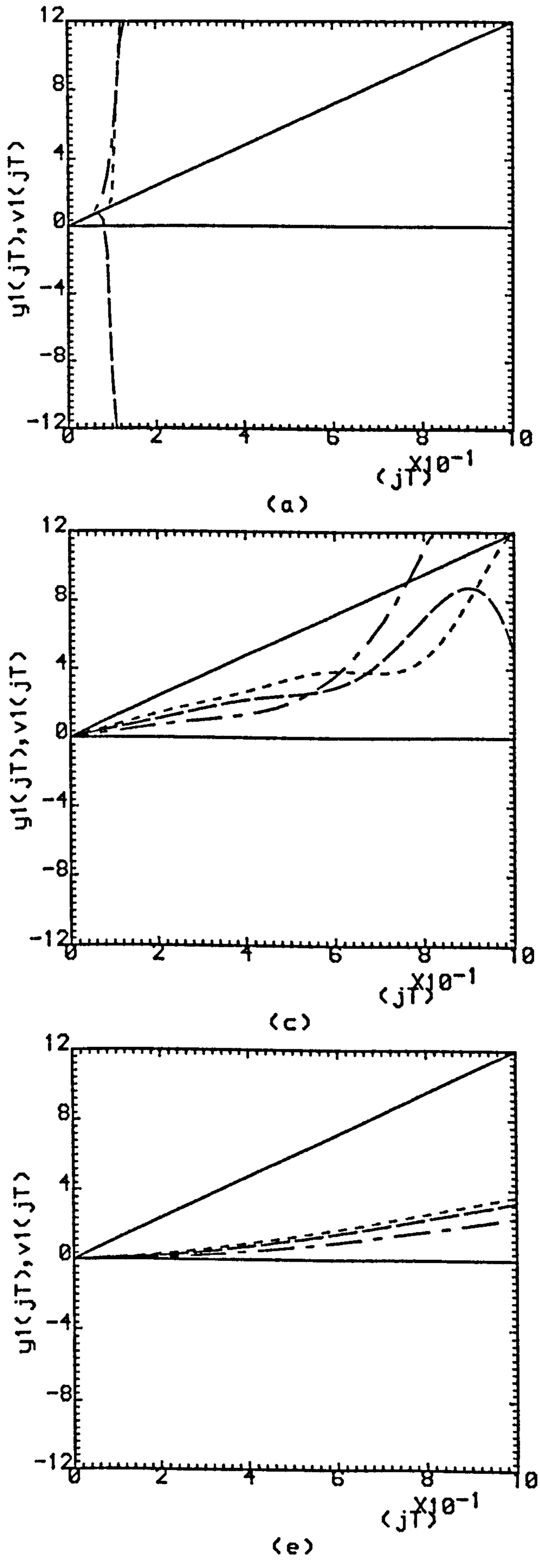

Fig.4.4(a,b) (rho=0.0,sigma=2.0).
(c,d) (rho=0.9,sigma=0.2).
(e,f) (rho=0.99,sigma=0.02).
-·-·- K=1 , ----- K=2 , ... K=3

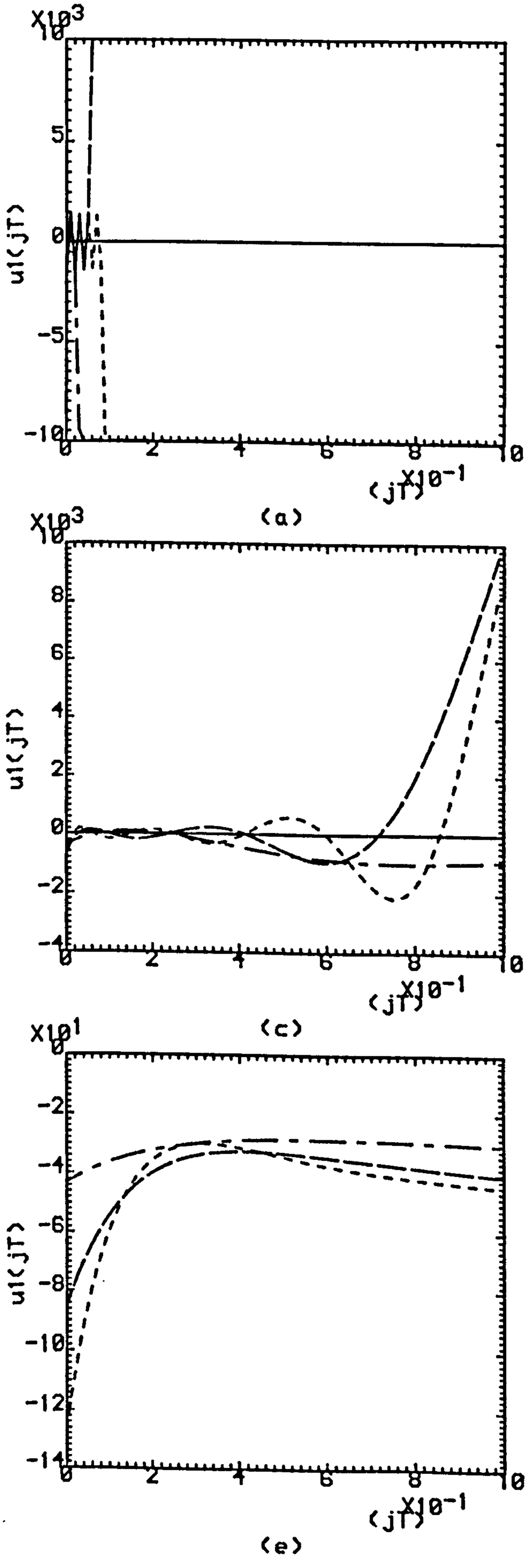

Fig.4.5(a,b) (rho=0.0,sigma=2.0).
(c,d) (rho=0.9,sigma=0.2).
(e,f) (rho=0.99,sigma=0.02).
-·-·- K=3 , ----- K=6 , ... K=9

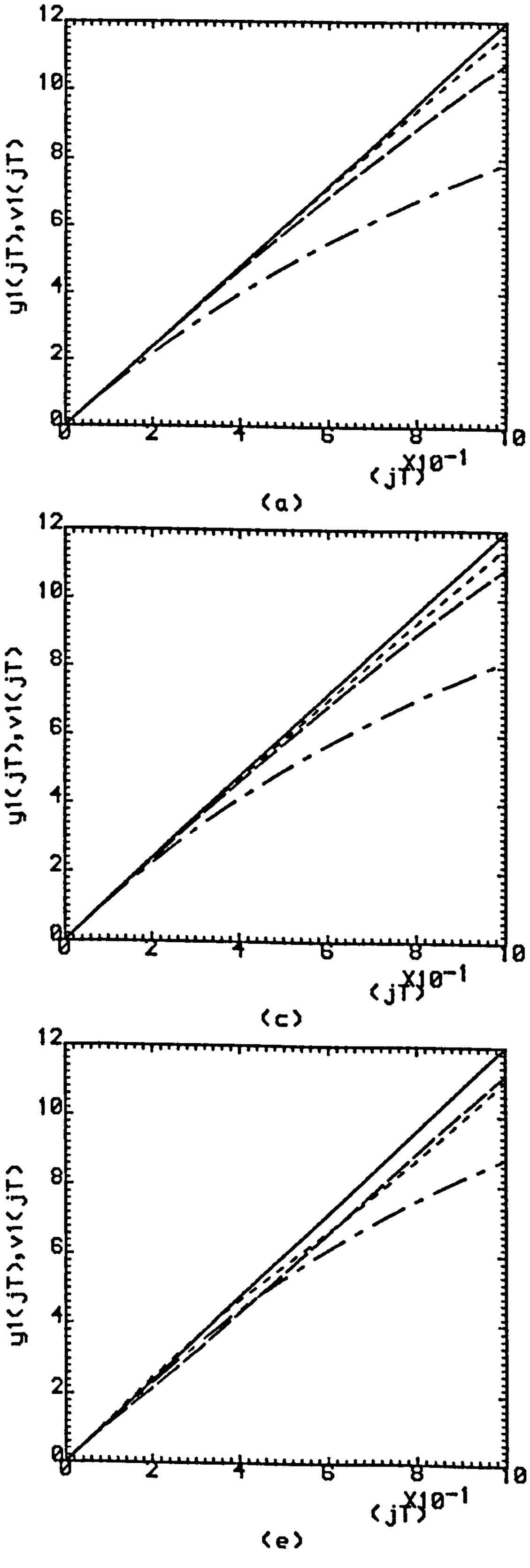

Fig.4.6(a,b) (rho=0.0,sigma=0.063).
(c,d) (rho=0.0,sigma=0.461).
(e,f) (rho=0.0,sigma=0.962).
-·-·- K=1 , ----- K=2 , ... K=3

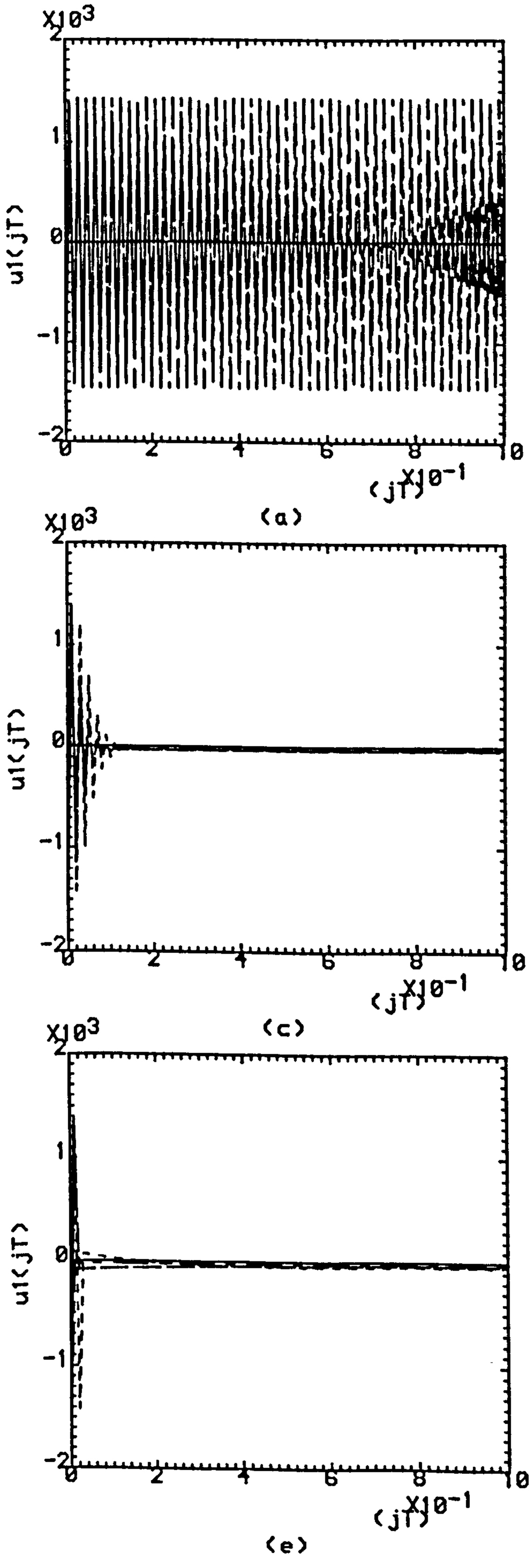

Fig.4.7(a,b) (rho=0.0,sigma=0.063).
(c,d) (rho=0.0,sigma=0.461).
(e,f) (rho=0.0,sigma=0.962).
-·-·- K=1 , ----- K=2 , ... K=3

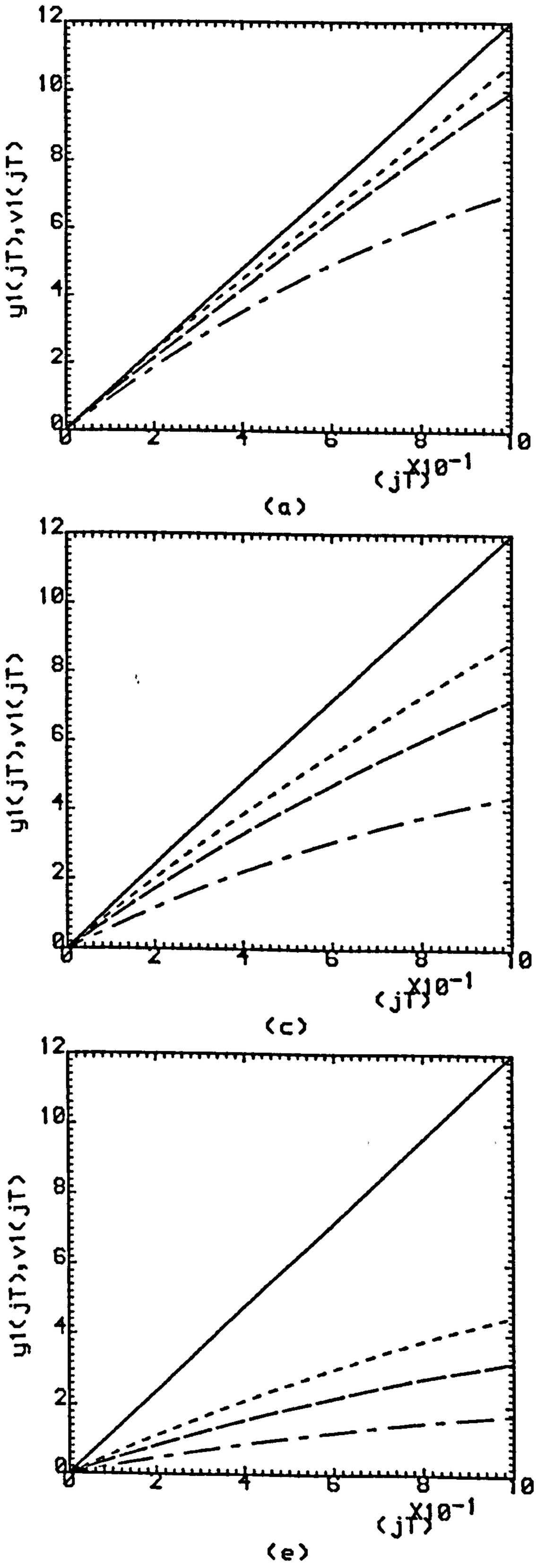

Fig.4.8(a,b) (rho=0.2,sigma=0.769).
(c,d) (rho=0.5,sigma=0.481).
(e,f) (rho=0.8,sigma=0.192).
-·-·- K=1 , ----- K=2 , ... K=3

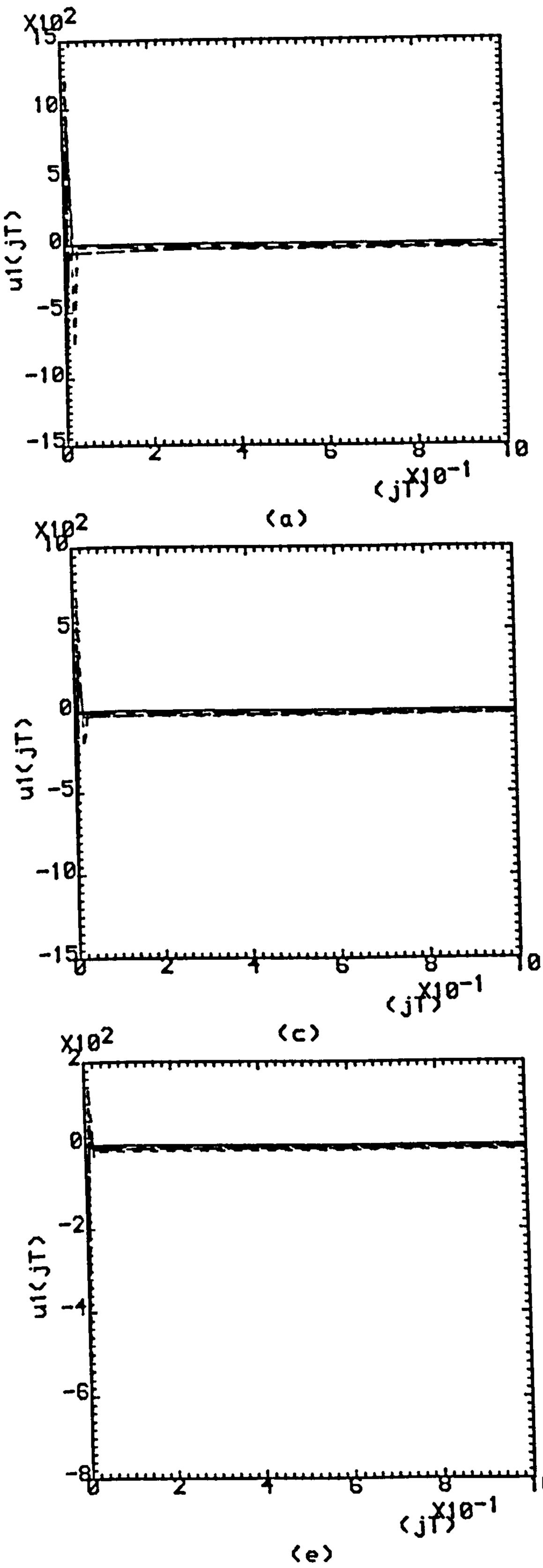

Fig.4.9(a,b) (rho=0.2,sigma=0.769).
(c,d) (rho=0.5,sigma=0.481).
(e,f) (rho=0.8,sigma=0.192).
-·-·- K=1 , ----- K=2 , ... K=3

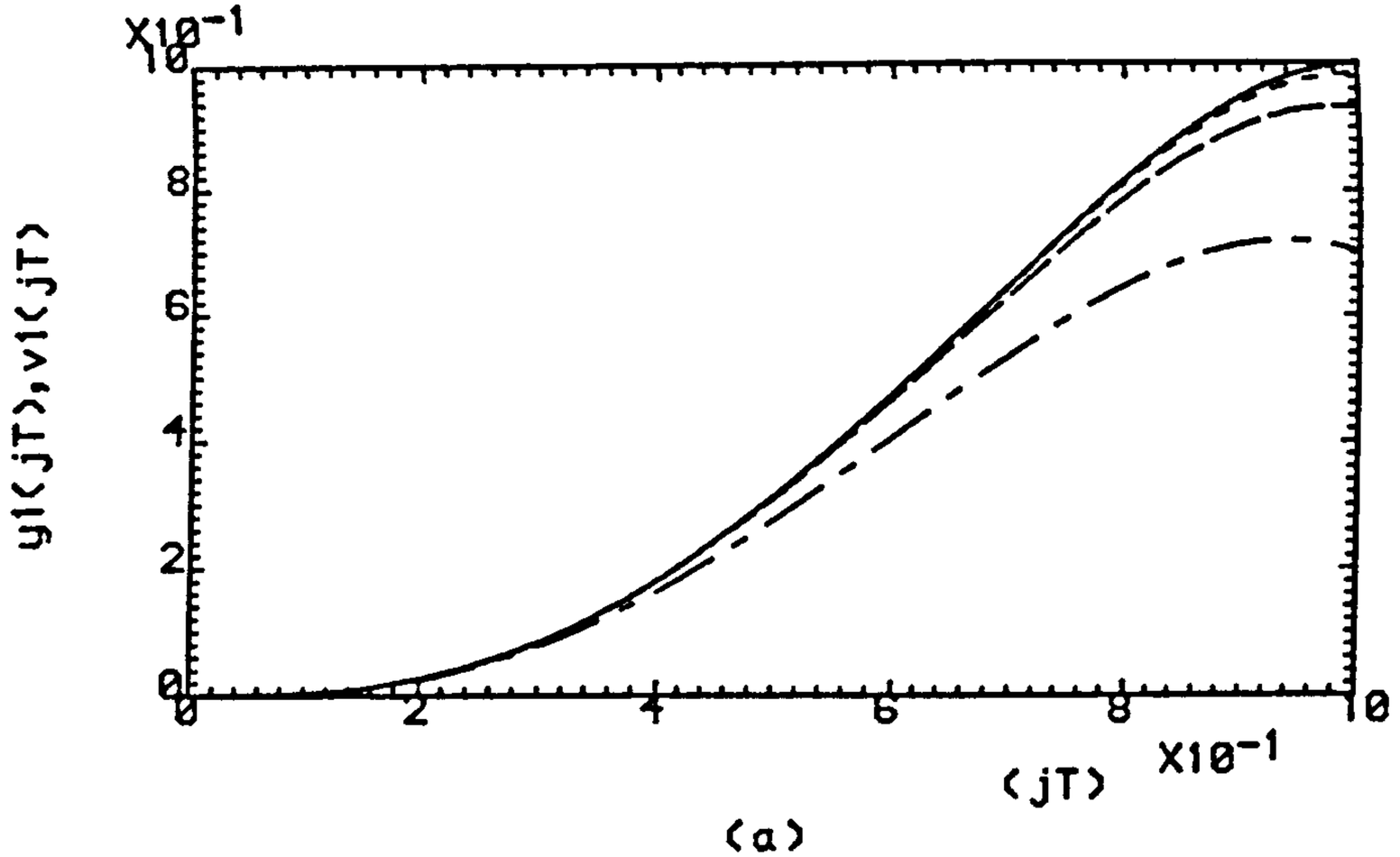

(a)

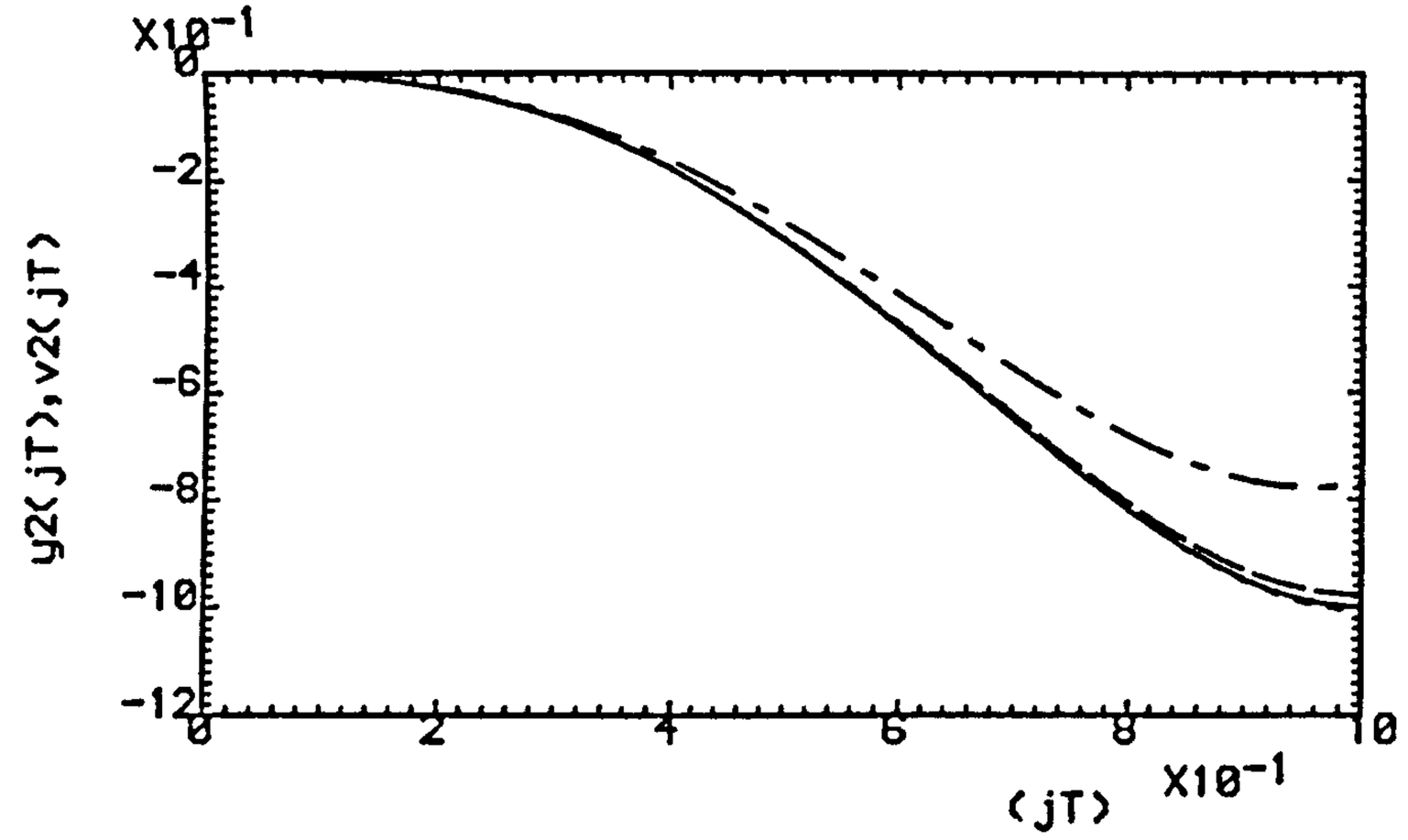

(b)

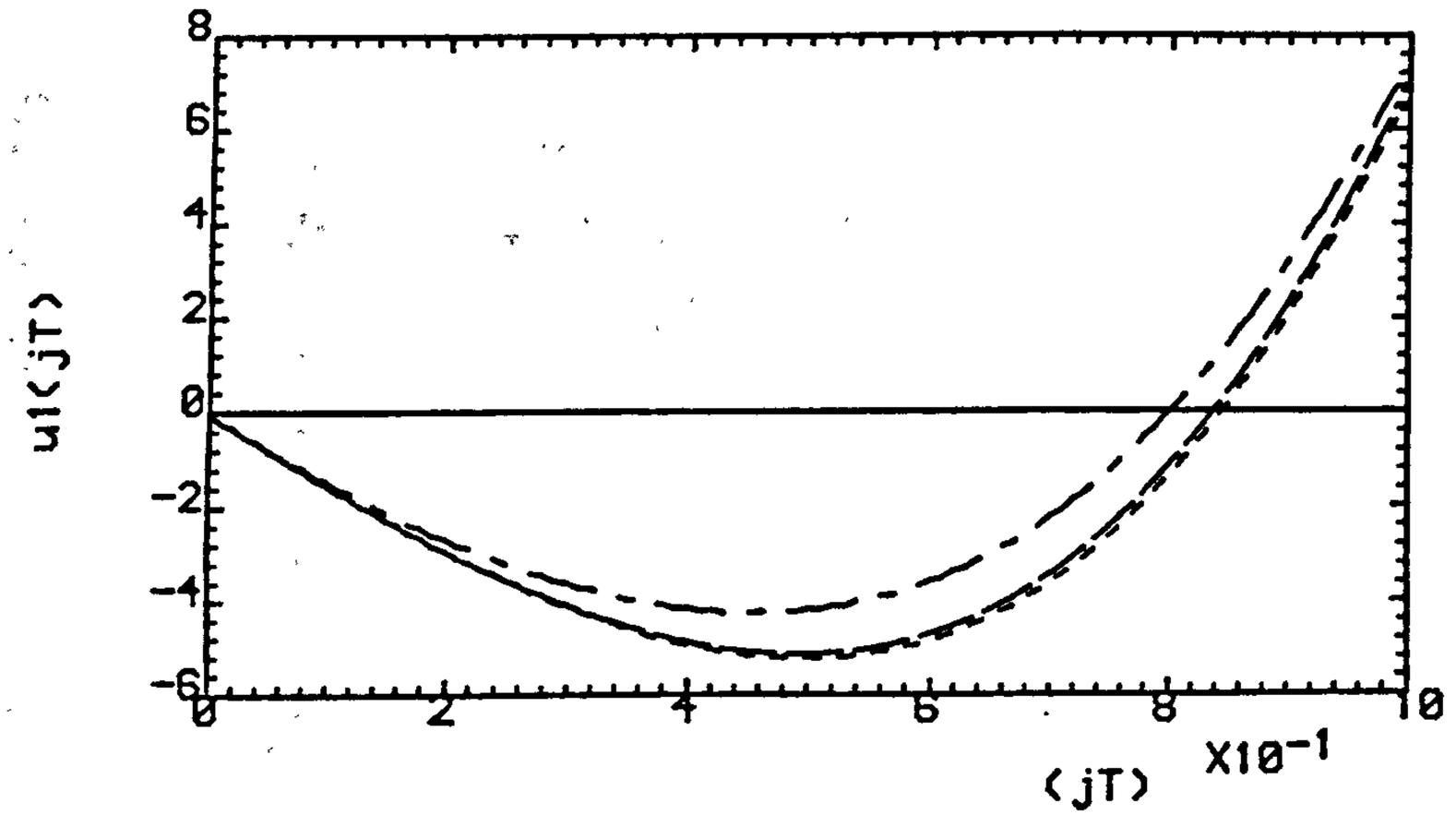

(c)

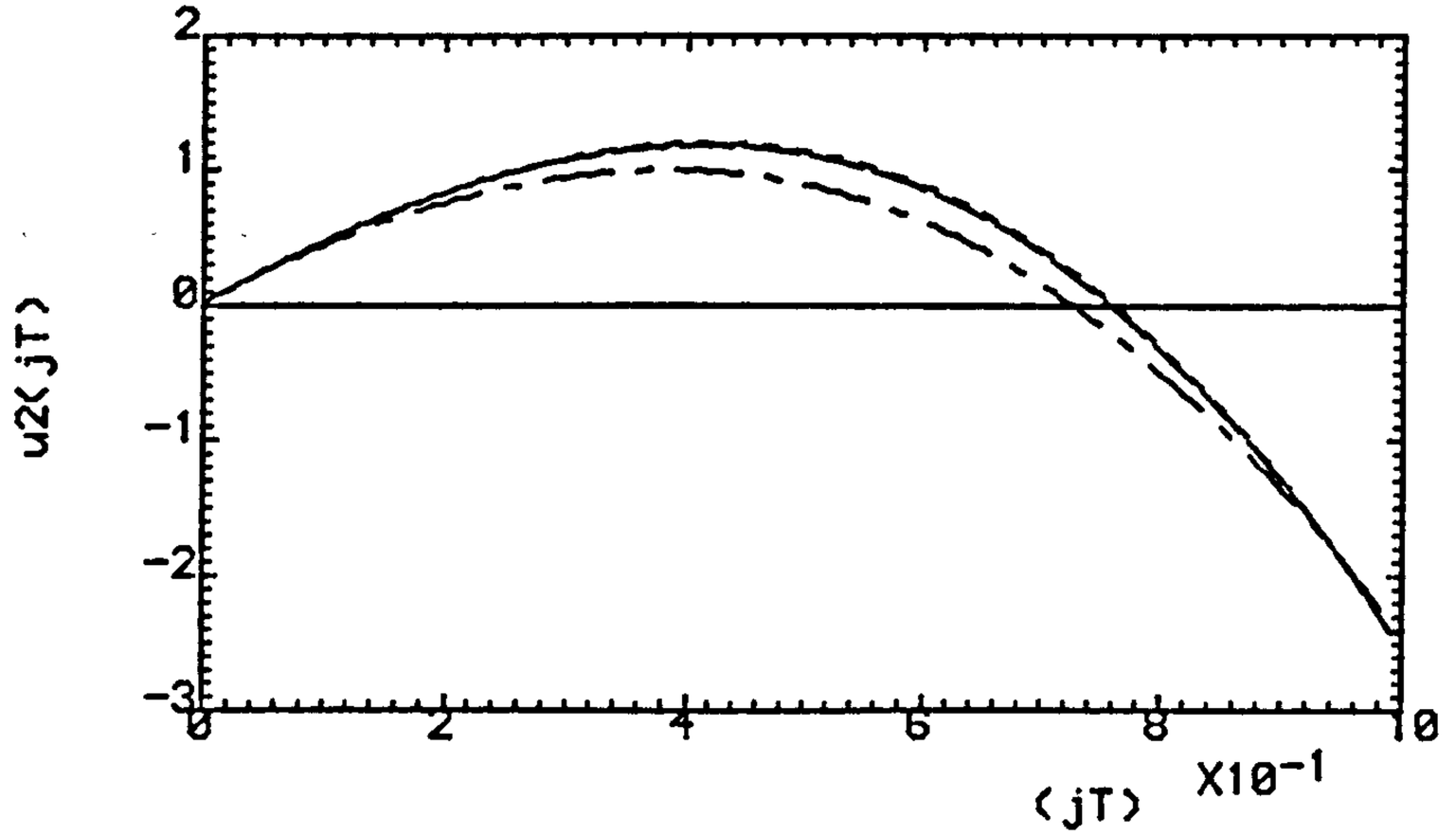

(d)

Fig.4.10 (rho=0.0,sigma=0.063).
(a,b) Plant Outputs.
(c,d) Control Efforts.
-·-·- K=1 , ----- K=2 , ... K=3

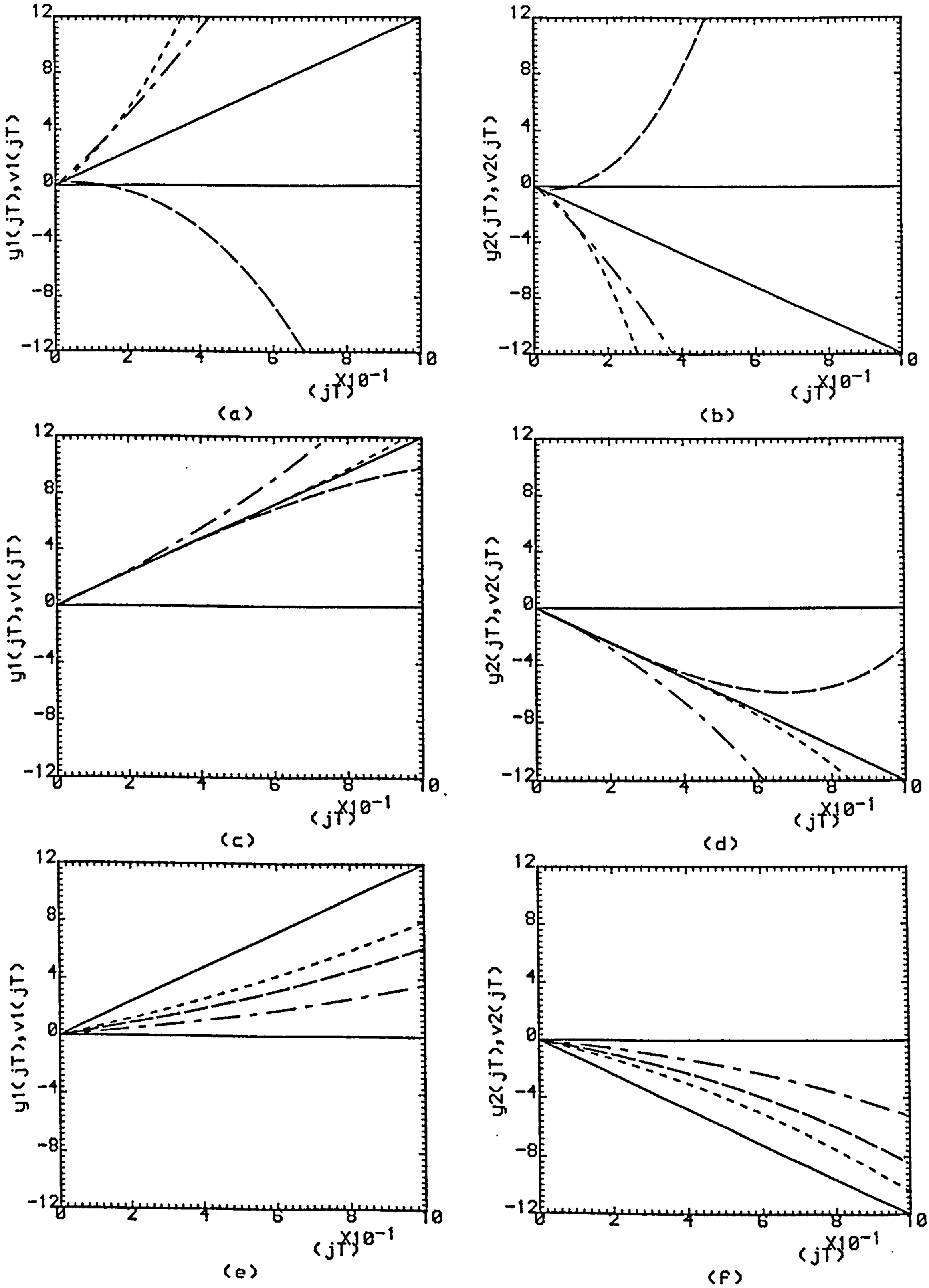

Fig.4.11(a,b) (rho=0.0,sigma=1.021).
(c,d) (rho=0.5,sigma=0.510).
(e,f) (rho=0.9,sigma=0.1021).
-·-·- K=1 , ----- K=2 , ... K=3

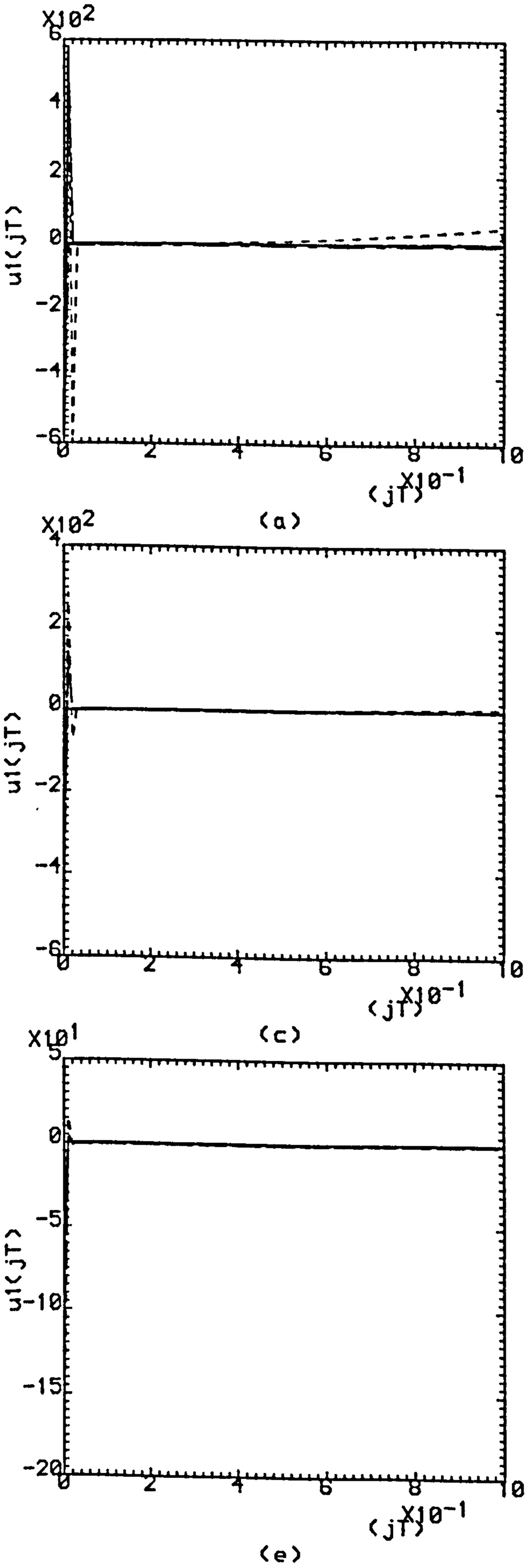

Fig.4.12(a,b) (rho=0.0,sigma=1.021).
(c,d) (rho=0.5,sigma=0.510).
(e,F) (rho=0.9,sigma=0.1021).
-·-·- K=1 , ----- K=2 , ... K=3

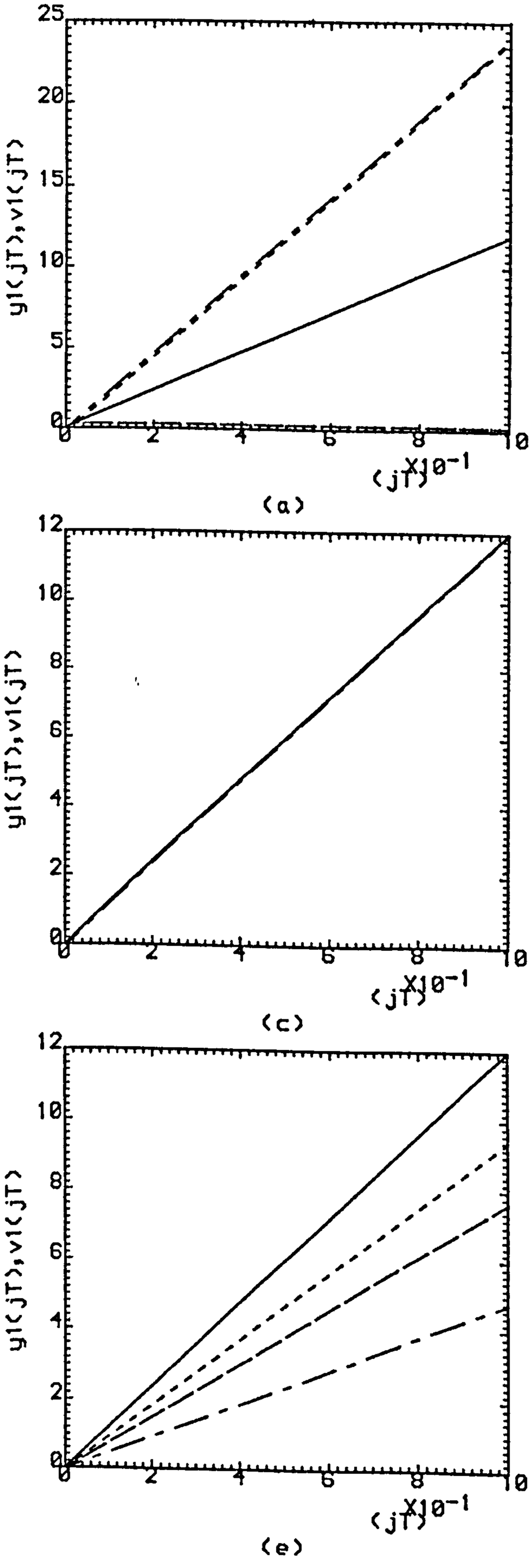

Fig.4.13(a,b) (rho=0.0,sigma=1.0).
(c,d) (rho=0.5,sigma=0.5).
(e,f) (rho=0.8,sigma=0.2).
-·-·- K=1 , ----- K=2 , ... K=3

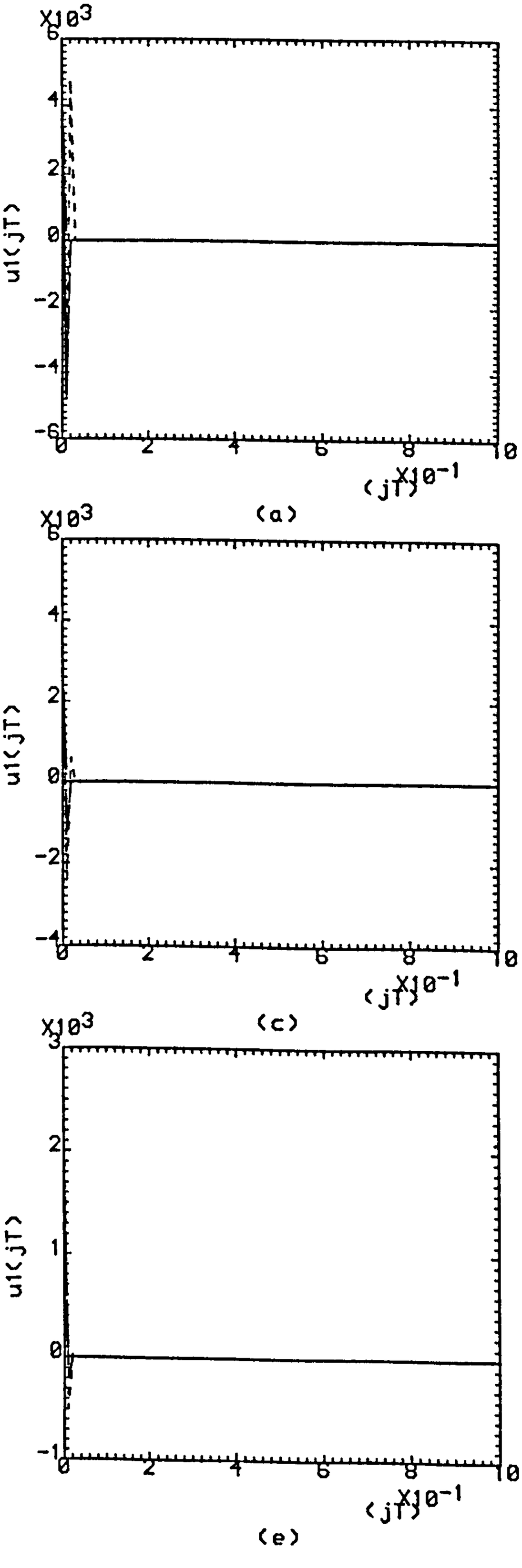

Fig.4.14(a,b) (rho=0.0,sigma=1.0).
(c,d) (rho=0.5,sigma=0.5).
(e,F) (rho=0.8,sigma=0.2).
-·-·- K=1 , ----- K=2 , ... K=3

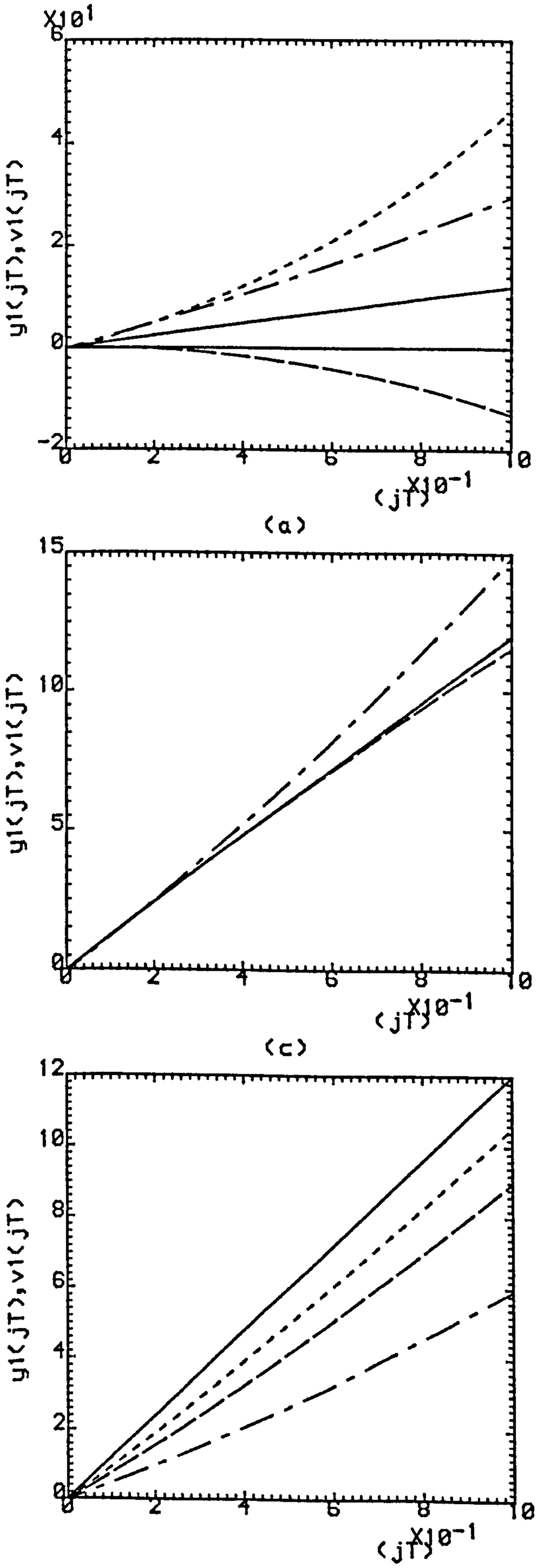

Fig.4.15(a,b) (rho=0.0,sigma=1.005).
(c,d) (rho=0.5,sigma=0.5025).
(e,F) (rho=0.8,sigma=0.201).
-·-·- K=1 , ----- K=2 , ... K=3

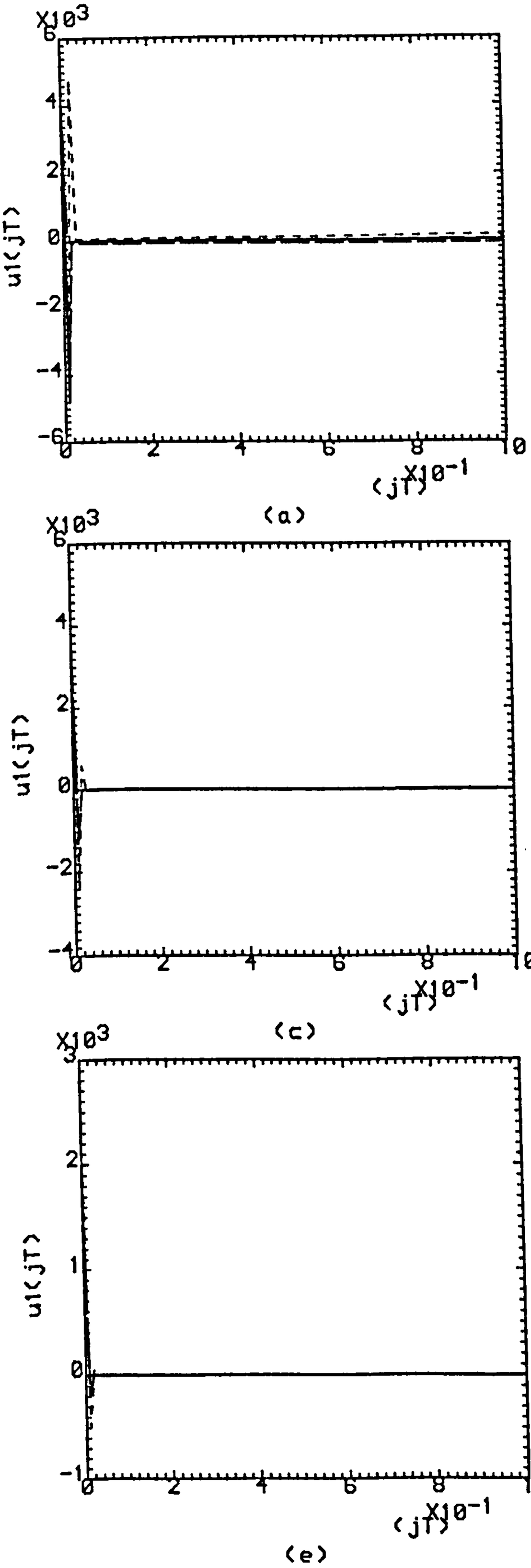

Fig.4.16(a,b) (rho=0.0,sigma=1.005).
(c,d) (rho=0.5,sigma=0.5025).
(e,f) (rho=0.8,sigma=0.201).
-·-·- K=1 , ----- K=2 , ... K=3

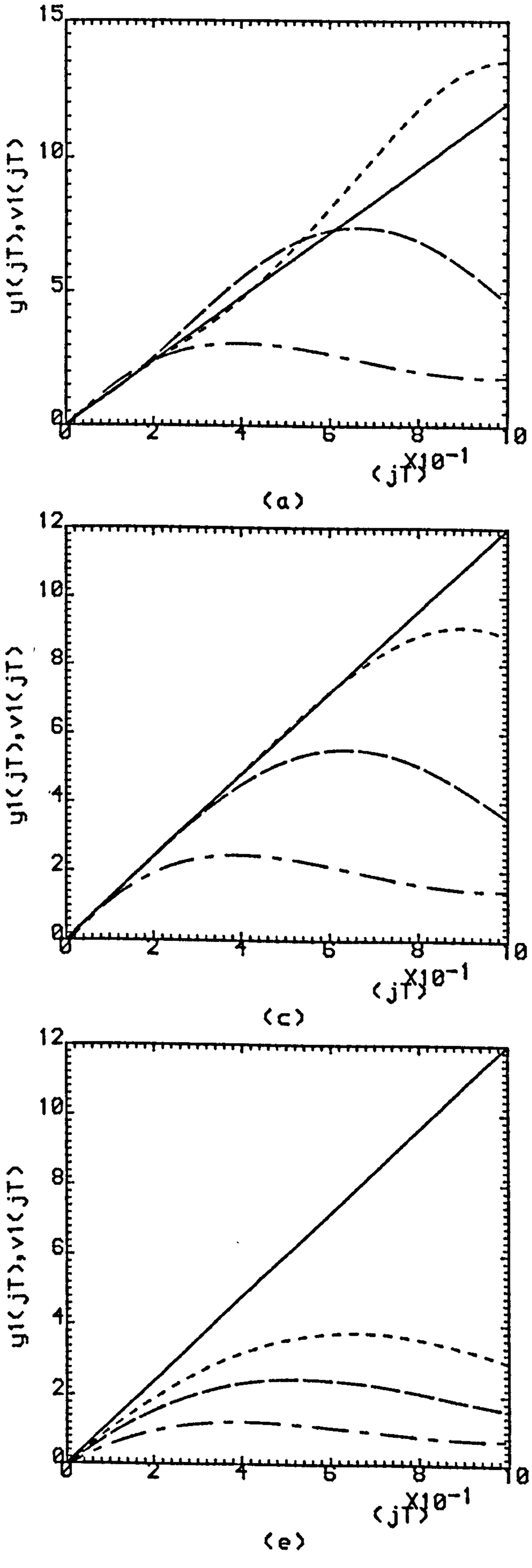

Fig.4.17(a,b) (rho=0.75,sigma=1.0).
(c,d) (rho=0.8,sigma=0.8).
(e,f) (rho=0.9,sigma=0.4).
-·-·- K=1 , ----- K=2 , ... K=3

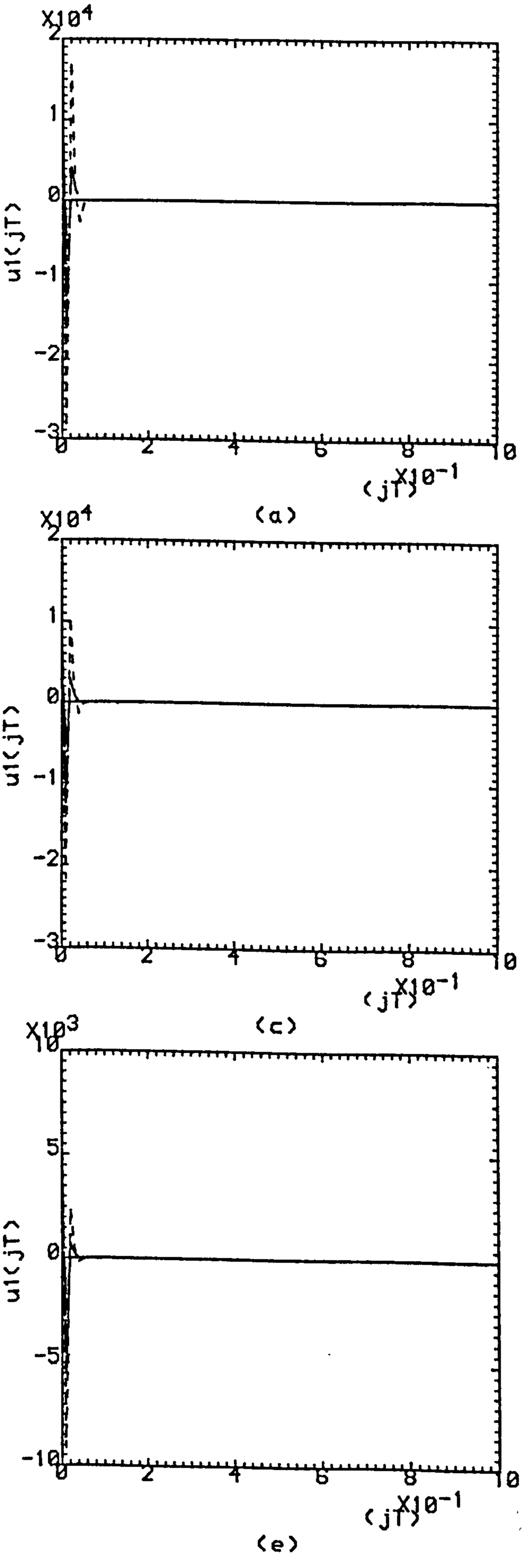

Fig.4.18(a,b) (rho=0.75,sigma=1.0).
(c,d) (rho=0.8,sigma=0.8).
(e,f) (rho=0.9,sigma=0.4).
-·-·- K=1 , ----- K=2 , ... K=3

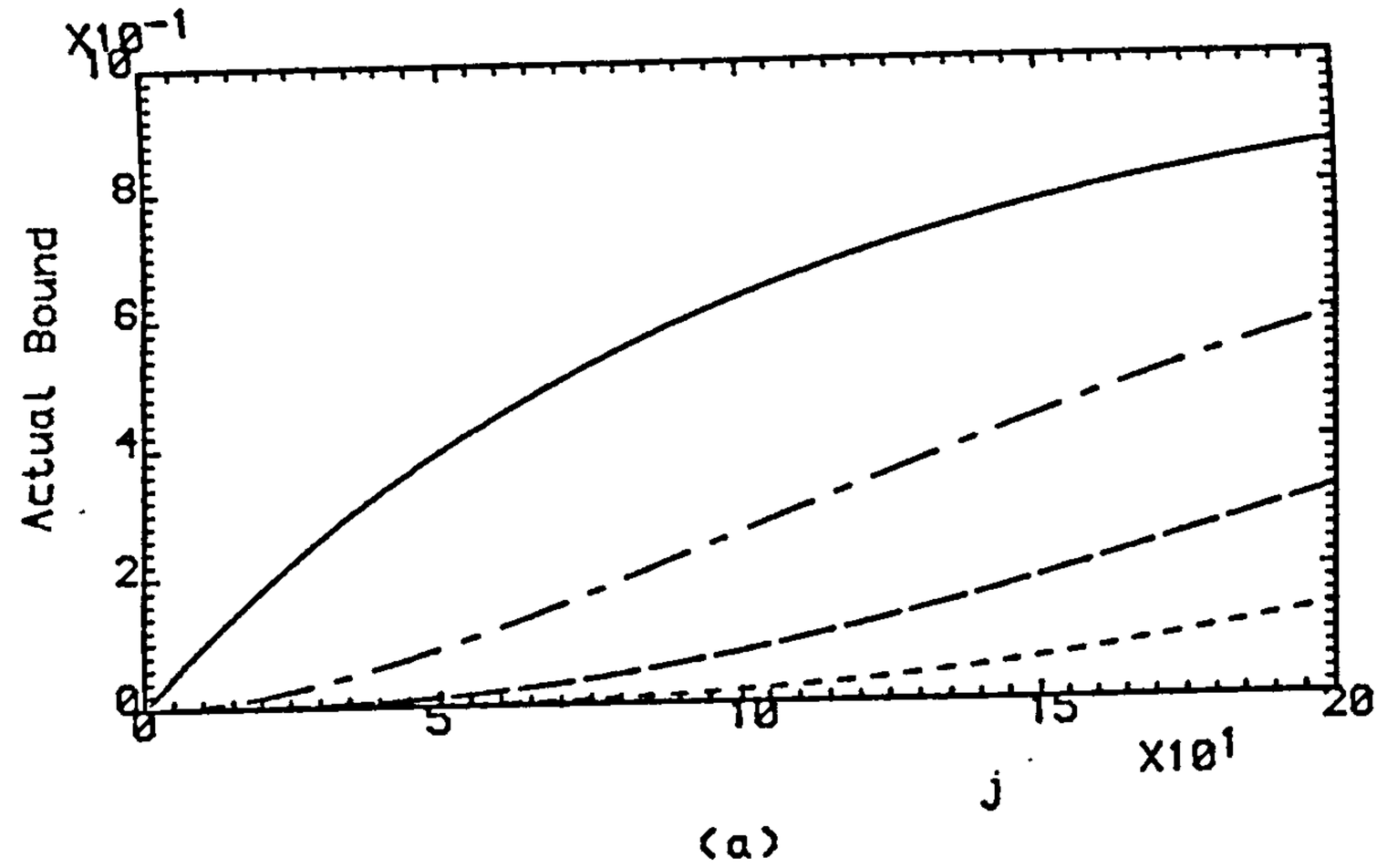

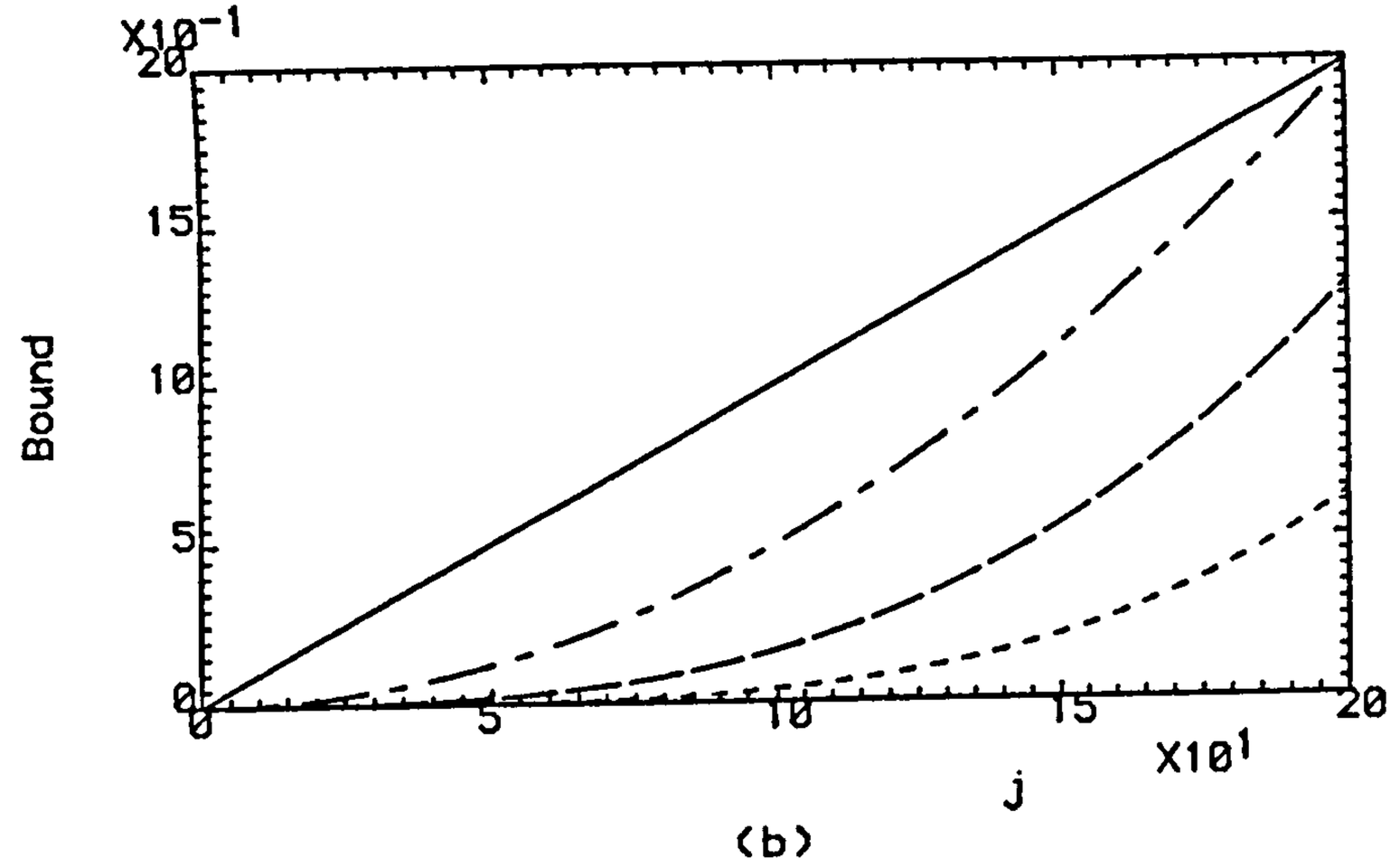

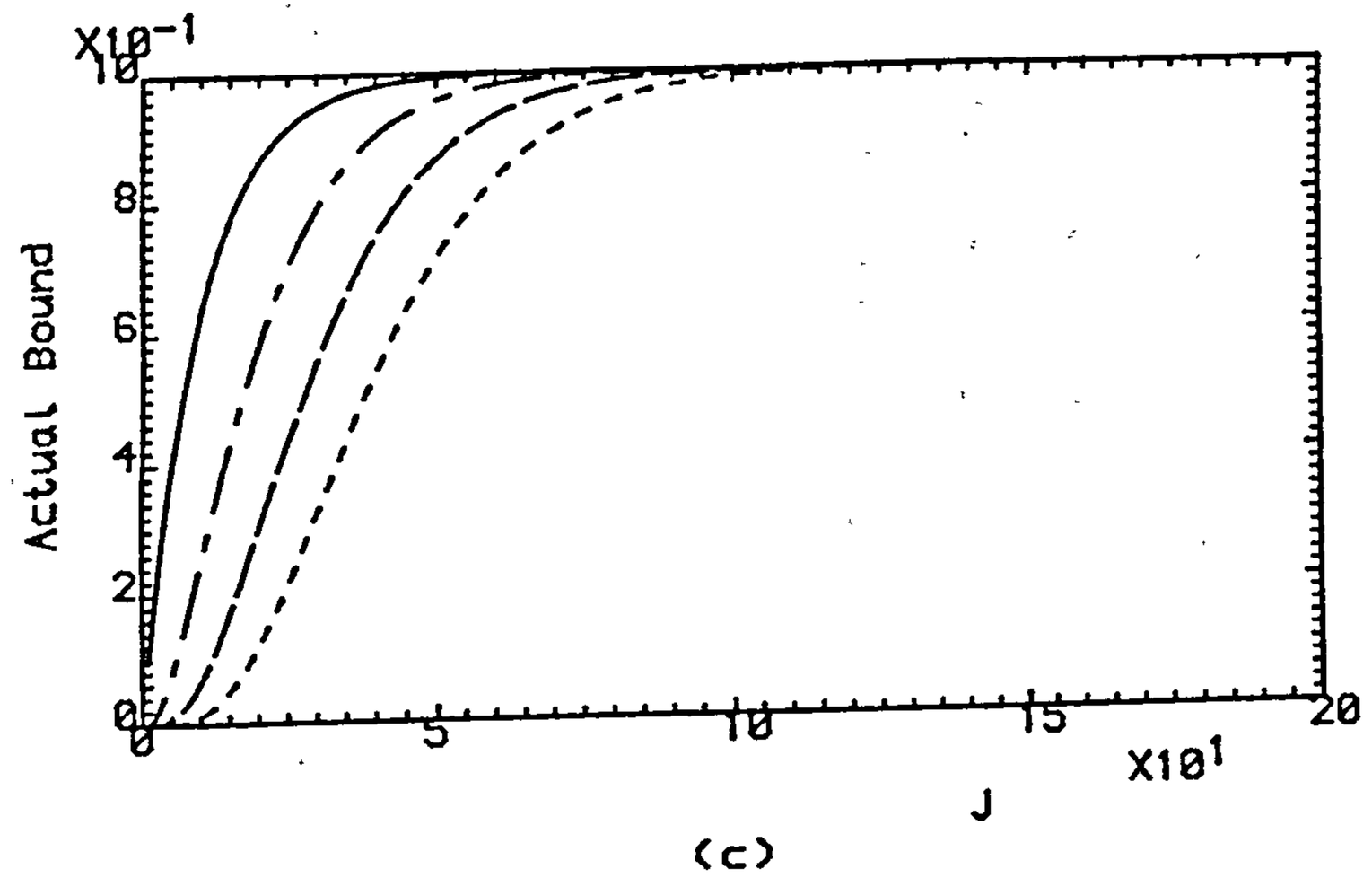

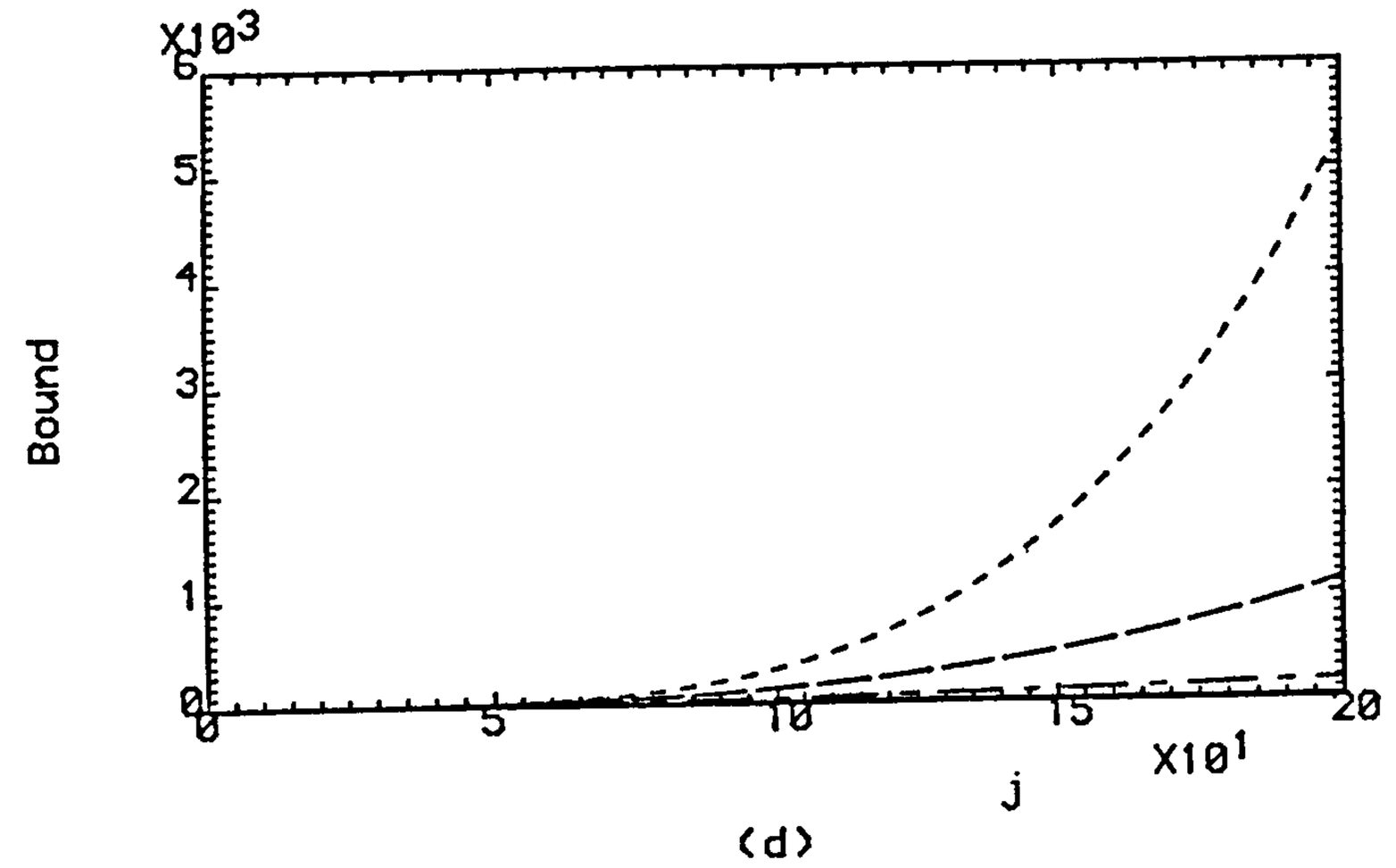

Fig.4.19 (a,b) (rho=0.0,sigma=9.95e-3).
(c,d) (rho=0.0,sigma=95.16e-3).

—— K=1 , -·-·- K=2 , ----- K=3 , ... K=4

CHAPTER 5

DESIGN OF ADAPTIVE DIGITAL ITERATIVE LEARNING CONTROLLERS FOR MULTIVARIABLE PLANTS

5.1 INTRODUCTION

The design of digital iterative learning controllers for linear multivariable plants was discussed in Chapter 4. However, although such controllers are intrinsically robust in the face of plant-parameter variations, some degradation in their performance will inevitably occur in the case of large plant-parameter variations. It is therefore the purpose of this chapter to design controllers that avoid such degradation by the inclusion of recursive estimators in digital iterative learning controllers. These estimators provide on-line updated step-response matrices for inclusion in the digital iterative learning control law in order to achieve the desired learning performance and rapid convergence. It is accordingly shown in this chapter that digital iterative learning controllers can indeed be readily rendered adaptive. The effectiveness of such adaptive digital iterative learning controllers is illustrated in this chapter by designing adaptive digital iterative learning controllers for various types of plant with various degrees of irregularity.

5.2 ANALYSIS

The dynamics of linear time-invariant plants governed on the continuous-time set $T = [0,+\infty)$ by differential equations of the form

$$\dot{x}(t) = Ax(t) + Bu(t) \quad , \qquad \text{...(5.1a)}$$

$$y(t) = Cx(t) \quad , \qquad \text{...(5.1b)}$$

are governed on the discrete-time set $\mathbf{T}_T = \{0, T, ..., jT, ..\}$ by difference equations of the form

$$x(j+1) = \Phi x(j) + \Psi u(j) \quad , \qquad \text{...(5.2a)}$$

$$y(j) = \Gamma x(j) \quad , \qquad \text{...(5.2b)}$$

where

$$\Phi = e^{AT} \quad , \qquad \text{...(5.3a)}$$

$$\Psi = \int_0^T e^{At} B dt \quad , \qquad \text{...(5.3b)}$$

$$\Gamma = C \quad , \qquad \text{...(5.3c)}$$

and T is the sampling period. In addition, $x(j) \epsilon R^n$ is the state vector, $u(j) \epsilon R^m$ is the input vector, $y(j) \epsilon R^m$ is the output vector, $\Phi \epsilon R^{n \times n}$ is the discrete-time plant matrix, $\Psi \epsilon R^{n \times m}$ is the discrete-time input matrix, and $\Gamma \epsilon R^{m \times n}$ is the output matrix.

The step-response matrices of such plants have the form

$$H(T) = \int_0^T Ce^{At} B dt \qquad \text{...(5.4)}$$

and characterise the response of initially quiescent plants after one sampling period. Such step-response matrices can be measured directly from input/output test data. Therefore, and according to Theorems 4.1 and 4.2 of Chapter 4, such plants are amenable to the design of digital iterative learning controllers using only such step-response matrices to characterise the dynamics of linear time-invariant plants. Moreover, Theorems 4.1 and 4.2 can be readily deployed in the design of iterative learning controllers for multivariable plants.

In the case of such plants whose dynamics are initially unknown or time-variant, it is necessary to provide updated step-response matrices for inclusion in the control-law design equation

$$\Lambda = H^{-1}(T) \quad . \qquad ...(5.5)$$

Such step-response matrices can be obtained on-line by estimating the parameters of the autoregressive moving average (ARMA) model which is given by an *Nth*-order difference equation of the form

$$y_k(j) + A_1 y_k(j-1) + A_2 y_k(j-2) +...+ A_N y_k(j-N)$$

$$= B_1 u_k(j-1) + B_2 u_k(j-2) +...+ B_N u_k(j-N) \quad . \qquad ...(5.6)$$

In order to estimate the parameters of this ARMA model, a Recursive Least Squares (RLS) algorithm is utilised. This can be expressed by the equations (Borison (1979))

$$\hat{\Theta}(jT) = \hat{\Theta}[(j-1)T] + K(jT)\left[y_k^T(jT) - \Phi^T(jT)\hat{\Theta}[(j-1)T]\right] , \qquad ...(5.7)$$

$$K(jT) = P[(j-1)T]\Phi(jT)[\gamma+\Phi^{T}(jT)P[(j-1)T]\,\Phi(jT)]^{-1} \quad , \qquad ...(5.8)$$

and

$$P(jT) = \frac{1}{\gamma}\,[I_{N(2m)} - K(jT)\Phi^{T}(jT)]\,P[(j-1)T] \qquad . \qquad ...(5.9)$$

In equations (5.7), (5.8) and (5.9),

$$\Phi(jT) = [-y_k^{T}[(j-1)T],\ -y_k^{T}[j-2)T],....,-y_k^{T}[(j-N)],$$

$$u_k^{T}[(j-1)T],\ u_k^{T}[j-2)T],...,u_k^{T}[(j-N)T]^{T} \in R^{N(2m)} \qquad ...(5.10)$$

is the vector of outputs and inputs for N previous sampling periods, $\hat{\Theta}(jT)$ is the estimated value of the parametric matrix

$$\Theta = [A_1, A_2,...., A_N, B_1, B_2,...., B_N]^{T} \in R^{N(2m)\times m} \qquad , \qquad ...(5.11)$$

$P(jT) \in R^{N(2m)\times N(2m)}$ is the symmetric covariance matrix, $K(jT) \in R^{N(2m)}$ is the Kalman gain vector, and $\gamma \in (0,1]$ is the forgetting factor.

Thus, at each sampling instant the estimated parameters of the ARMA model can be used to compute updated step-response matrices for implementation in the design equation (5.5). Indeed, it is clear from equation (5.10) that

$$H(T) = B_1 \qquad . \qquad ...(5.12)$$

It is therefore evident that the control law described by Theorems 4.1 and 4.2 can be readily made adaptive by using in the iterative learning controller the current estimate of the step-response matrix, $H(T)$, from the parameter-estimation algorithm.

In order to achieve good learning performance and fast convergence from the adaptive digital iterative learning controller, it is required to have rapid and accurate estimation of the ARMA model from the RLS algorithm. It is clear from equations (5.7), (5.8), and (5.9) that, in order to evaluate the estimated parameter vector, $\hat{\Theta}(jT)$, the RLS algorithm should be provided with prior estimates of $\hat{\Theta}[(j-1)T]$ and $P[(j-1)T]$. Hence, a choice of $\hat{\Theta}(0)$ and $P(0)$ should be made to start the RLS. Indeed, the choice of $\hat{\Theta}(0)$ is dependent on prior information about the plant and in the absence of such information the choice is usually (Clarke (1981))

$$\hat{\Theta}(0) = 0 \quad . \qquad ...(5.13)$$

Similarly, the initial choice of the covariance matrix is usually (Clarke (1981))

$$P(0) = P_0 I_{N(m+m)} \quad , \qquad ...(5.14)$$

where the value of P_0 is chosen to be sufficiently large to cause rapid discarding of the old estimated data so as to speed up convergence to the true parameters. Moreover, the identified parameters $\hat{\Theta}(jT)$ will converge to the actual parameters Θ only if the input to the RLS algorithm is sufficiently 'rich' or persistently exciting and if Θ is constant (Goodwin and Sin (1984)).

5.3 ILLUSTRATIVE EXAMPLES

The use of adaptive digital iterative learning controllers can be conveniently illustrated by designing such controllers for typical multivariable regular, first-order partially irregular, and second-order completely irregular plants whose dynamical characteristics are initially unknown to these controllers.

Example 5.1

The regular plant under consideration is governed by equations of the form (5.1a) and (5.1b) with

$$A = \begin{bmatrix} -3, & 1, & 0 \\ -2, & -1, & 2 \\ 0, & 1, & -2 \end{bmatrix} \quad , \qquad \text{...(5.15a)}$$

$$B = \begin{bmatrix} 0, & 0 \\ 2, & 1 \\ 1, & 3 \end{bmatrix} \quad , \qquad \text{...(5.15b)}$$

and

$$C = \begin{bmatrix} 0, & 1, & -1 \\ 1, & 0, & -1 \end{bmatrix} \quad . \qquad \text{...(5.15c)}$$

In this case, the step-response matrix is

$$H(T) = \begin{bmatrix} 9.999\times10^{-3}, & -19.505\times10^{-3} \\ -9.900\times10^{-3}, & -29.702\times10^{-3} \end{bmatrix} \qquad \text{...(5.16)}$$

when the sampling period $T = 0.01$ *sec.* Furthermore, the control law of Theorem 4.1 is used in this case.

However, the digital iterative learning controller is designed initially for a different plant governed by equations of the form (5.1a) and (5.1b) with

$$A = \begin{bmatrix} -3, & 1, & 0 \\ 0, & 0, & 1 \\ -6, & -11, & -6 \end{bmatrix} \quad , \qquad \text{...(5.17a)}$$

$$B = \begin{bmatrix} 0, & 0 \\ 2, & 1 \\ 1, & 3 \end{bmatrix} \quad , \qquad \text{...(5.17b)}$$

and

$$C = \begin{bmatrix} 0, & 10, & -10 \\ 10, & 0, & -10 \end{bmatrix} \quad , \qquad \text{...(5.17c)}$$

for which the step-response matrix is

$$H(T) = \begin{bmatrix} 1.1421\times10^{-1}, & -1.8427\times10^{-1} \\ -0.8525\times10^{-1}, & -2.8522\times10^{-1} \end{bmatrix} \qquad \text{...(5.18)}$$

when the sampling period $T = 0.01$ *sec*.

In addition, the RLS algorithm uses the initial condition $P_0 = 10^8$ and the forgetting factor $\gamma = 1$, and $\hat{\Theta}(0)$ contains the information for the plant with matrices A, B, and C described by equation (5.17). The numerical results shown in Figures 5.1 and 5.2 for non-adaptive iterative learning control indicate that, when $v(jT) = [12jT, -12jT]^T$ and the task time $T_t = 1$ *sec*, the step-response matrix used in the controller remains fixed at the 'incorrect' value given by equation (5.18) and that the iterative controller learns rather slowly as a consequence. However, the numerical results shown in Figures 5.3 and 5.4 for adaptive iterative learning control indicate that, when $v(jT) = [12jT, -12jT]^T$ and $T_t = 1$ *sec*, the step-response matrix

changes very rapidly from the 'incorrect' value given by equation (5.18) to the 'correct' value given by equation (5.16) and that the iterative controller learns very rapidly as a consequence. These results thus demonstrate the improvements in learning performance and convergence achievable by the introduction of adaptive action. It must be emphasised that when $k = 0$ the output is zero since the assumed value of the input is zero initially using both non-adaptive and adaptive iterative learning control. In addition, the elements of the step-response matrix are fixed at the 'incorrect' values in both non-adaptive and adaptive iterative learning control when $k = 0$ as shown in Figures 5.2 and 5.4.

Since the values of the parameters ρ and σ determine the learning performance and the convergence speed of iterative learning controllers, it is only natural to refer to the definitions of these parameters (page 94) in Chapter 4 at this stage. These definitions indicate that using the 'incorrect' step-response matrix decelerates learning whilst using the 'correct' step-response matrix accelerates it. Indeed, according to Chapter 4, both parameters must be as small as possible in order to achieve good learning performance and rapid convergence. However, using the 'incorrect' step-response matrix makes $\rho = 0.9445$ and $\sigma = 4\times10^{-3}$, whilst using the 'correct' step-response matrix makes $\rho = 0$ and $\sigma = 39.4\times10^{-3}$. Thus, it is clear by using the 'correct' step-response matrix from the recursive identifier that the two parameters become very small and accordingly that the learning performance improves and the convergence speed increases.

Example 5.2

The first-order partially irregular plant under consideration is governed by equations of the form (5.1a) and (5.1b) with

$$A = \begin{bmatrix} -3 & , & 1 & , & 0 \\ -2 & , & -1 & , & 2 \\ 0 & , & 1 & , & -2 \end{bmatrix} \quad , \qquad \text{...(5.19a)}$$

$$B = \begin{bmatrix} 0 & , & 0 \\ 2 & , & 1 \\ 1 & , & 3 \end{bmatrix} \quad , \qquad \text{...(5.19b)}$$

and

$$C = \begin{bmatrix} 1 & , & 0 & , & -1 \\ 1 & , & 0 & , & 0 \end{bmatrix} \quad . \qquad \text{...(5.19c)}$$

In this case, the step-response matrix is

$$H(T) = \begin{bmatrix} -0.990099\times10^{-2} & , & -0.297021\times10^{-1} \\ 0.990058\times10^{-4} & , & 0.503238\times10^{-4} \end{bmatrix} \qquad \text{...(5.20)}$$

when the sampling period $T = 0.01$ *sec.*

Since the plant is first-order partially irregular, a pre-filter with discrete-time transfer function

$$\left(I_m + \frac{2}{T} D \frac{z-1}{z+\alpha}\right)$$

must be used in cascade with the plant in order to remove this irregularity, as shown in Chapter 4. In other words, the control law of Theorem 4.2 must be used in this case. The choice of D and α must be made so that $CBD = 0$ and so that no

switching is present in the control action. Hence,

$$D = \begin{bmatrix} 0 & , & -3 \\ 0 & , & 1 \end{bmatrix}$$

and $\alpha = 0$. Therefore, the step-response matrix of the overall plant is

$$\hat{H}(T) = H(T)\left[I_m + \frac{2}{T} D\right] = \begin{bmatrix} -0.990099\times10^{-2} & , & -2.95379\times10^{-2} \\ 0.990058\times10^{-4} & , & -4.92883\times10^{-2} \end{bmatrix} . \quad ...(5.21)$$

However, the digital iterative learning controller is initially designed for a different plant governed by equations of the form (5.1a) and (5.1b) with

$$A = \begin{bmatrix} -30 & , & 10 & , & 0 \\ -20 & , & -10 & , & 20 \\ 0 & , & 10 & , & -20 \end{bmatrix} , \quad ...(5.22a)$$

$$B = \begin{bmatrix} 0 & , & 0 \\ 2 & , & 1 \\ 1 & , & 3 \end{bmatrix} , \quad ...(5.22b)$$

and

$$C = \begin{bmatrix} 1 & , & 0 & , & -1 \\ 1 & , & 0 & , & 0 \end{bmatrix} , \quad ...(5.22c)$$

for which the step-response matrix is

$$H(T) = \begin{bmatrix} -0.90929\times10^{-2} & , & -0.27207\times10^{-1} \\ 0.90562\times10^{-3} & , & 0.52463\times10^{-3} \end{bmatrix} \qquad ...(5.23)$$

when the sampling period $T = 0.01$ *sec.*

This plant is also first-order partially irregular and therefore a pre-filter must be used to remove this irregularity. The tuning parameters D and α of this filter have been chosen as before, ie,

$$D = \begin{bmatrix} 0 & , & -3 \\ 0 & , & 1 \end{bmatrix}$$

and $\alpha = 0$. Therefore, the step-response matrix of the overall plant is

$$\hat{H}(T) = H(T)\left[I_m + \frac{2}{T}D\right] = \begin{bmatrix} -0.90929\times10^{-2} & , & -0.12844\times10^{-1} \\ 0.90562\times10^{-3} & , & -0.43792 \end{bmatrix}. \qquad ...(5.24)$$

In addition, the RLS algorithm uses the initial condition $P_0 = 10^8$, the forgetting factor $\gamma = 1$, and $\hat{\Theta}(0)$ contains the information for the plant with the matrices A, B, and C described by equation (5.22).

The numerical results shown in Figures 5.5 and 5.6 for non-adaptive iterative learning control indicate that, when $v(jT) = [12jT, -12jT]^T$ and the task time $T_t = 1$ *sec*, the step-response matrix used in the controller remains fixed at the 'incorrect' value given by equation (5.23) and that the iterative controller learns rather slowly as a consequence. However, the numerical results shown in Figures 5.7 and 5.8 for adaptive iterative learning control indicate that, when $v(jT) = [12jT, -12jT]^T$ and $T_t = 1$ *sec*, the step-response matrix changes very rapidly from the 'incorrect' value

given by equation (5.23) and that the iterative controllers learn very rapidly as a consequence. These results thus demonstrate the improvements in learning performance and convergence achievable by the introduction of adaptive action.

It must be emphasised that when $k = 0$ the output is zero since the assumed value of the input is zero initially, using both non-adaptive and adaptive iterative learning control. In addition, the elements of the step-response matrix are fixed at the 'incorrect' values in both non-adaptive and adaptive iterative learning control when $k = 0$, as shown in Figures 5.6 and 5.8.

The reason for the slow learning rate using the 'incorrect' step-response matrix is the same as in Example 5.1, since using the 'incorrect' step-response matrix makes $\rho = 0.8877$ and $\sigma = 0.1175$ whilst using the 'correct' step-response matrix makes $\rho = 0$ and $\sigma = 0.9623$. Therefore, the learning performance has improved and the convergence speed has increased as a result of using the 'correct' step-response matrix obtained from the recursive identifier.

Example 5.3

The second-order completely irregular plant under consideration is governed by equations of the form (5.1a) and (5.1b) with

$$A = \begin{bmatrix} 0 & 0 & 1 & 0 & 0 & 0 \\ 0 & 0 & 0 & 1 & 0 & 0 \\ -4 & -1 & 1 & 2 & -4 & 2 \\ 1 & -2 & -3 & -2 & 1 & -3 \\ 0 & 0 & 0 & 0 & -3 & 0 \\ 0 & 0 & 0 & 0 & 0 & -2 \end{bmatrix}, \quad \text{...(5.25a)}$$

$$B = \begin{bmatrix} 0 & , & 0 \\ 0 & , & 0 \\ 0 & , & 0 \\ 0 & , & 0 \\ 3 & , & 0 \\ 0 & , & 2 \end{bmatrix} \quad , \qquad \text{...(5.25b)}$$

and

$$C = \begin{bmatrix} 1 , & -2 , & 0 , & 0 , & 0 , & 0 \\ 1 , & 2 , & 0 , & 0 , & 0 , & 0 \end{bmatrix} \quad . \qquad \text{...(5.25c)}$$

In this case, the step-response matrix is

$$H(T) = \begin{bmatrix} -3.004788\times10^{-6} & , & 2.649985\times10^{-6} \\ -9.701972\times10^{-7} & , & -1.329962\times10^{-6} \end{bmatrix} \qquad \text{...(5.26)}$$

when the sampling period $T = 0.01$ *sec.*

Since the plant is second-order completely irregular, a two-stage pre-filter with discrete-time transfer functions

$$\left(I_m + \frac{2}{T} D_1 \frac{z-1}{z+\alpha_1}\right)$$

and

$$\left(I_m + \frac{2}{T} D_2 \frac{z-1}{z+\alpha_2}\right)$$

must be used in cascade with the plant in order to remove this irregularity, as shown

in Chapter 4. Since $CB = CAB = 0$, the choice $D_1 = D_2 = I_m$ and the choice $\alpha_1 = \alpha_2 = 0$ is made in order to prevent switching in the control actions. Therefore, the step-response matrix of the overall plant is

$$\tilde{H}(T) = H(T)\left[I_m + \frac{2}{T} D_1\right]^2 = \begin{bmatrix} -0.1214, & 0.1071 \\ -0.0392, & -0.0537 \end{bmatrix} \quad . \qquad ...(5.27)$$

However, initially the digital iterative learning controller is designed for a different plant governed by equations of the form (5.1a) and (5.1b) with

$$A = \begin{bmatrix} 0, & 0, & 2, & 0, & 0, & 0 \\ 0, & 0, & 0, & 2, & 0, & 0 \\ -8, & -2, & 2, & 4, & -8, & 4 \\ 2, & -4, & -6, & -4, & 2, & -6 \\ 0, & 0, & 0, & 0, & -6, & 0 \\ 0, & 0, & 0, & 0, & 0, & -4 \end{bmatrix}, \qquad ...(5.28a)$$

$$B = \begin{bmatrix} 0, & 0 \\ 0, & 0 \\ 0, & 0 \\ 0, & 0 \\ 3, & 0 \\ 0, & 2 \end{bmatrix} \qquad , \qquad ...(5.28b)$$

and

$$C = \begin{bmatrix} 1, & -2, & 0, & 0, & 0, & 0 \\ 1, & 2, & 0, & 0, & 0, & 0 \end{bmatrix} \qquad , \qquad ...(5.28c)$$

for which the step-response matrix is

$$H(T) = \begin{bmatrix} -0.12040\times10^{-4} & , & 0.10530\times10^{-4} \\ -0.37630\times10^{-5} & , & -0.53060\times10^{-5} \end{bmatrix} \quad . \qquad ...(5.29)$$

when the sampling period $T = 0.01$ *sec.*

This plant is also second-order completely irregular so that a two-stage pre-filter is required to remove this irregularity. The tuning parameters of these pre-filters are chosen as before so that $D_1 = D_2 = I_m$ and $\alpha_1 = \alpha_2 = 0$. Therefore, the step-response matrix of the overall plant is

$$\tilde{H}(T) = H(T)\left[I_m + \frac{2}{T} D_1\right]^2 = \begin{bmatrix} -4.8629\times10^{-1} & , & 4.2555\times10^{-1} \\ -1.5204\times10^{-1} & , & -2.1437 \end{bmatrix} . \qquad ...(5.30)$$

In this example, the control gain matrix Λ is chosen in the case of both non-adaptive and adaptive iterative learning control with the tuning parameter $\lambda = 0.25$ so that

$$\Lambda = 0.25\ \tilde{H}^{-1}(T)$$

This choice is made in order to achieve a balance between the two most important parameters in learning control (ie, ρ and σ).

In addition, the RLS algorithm uses the initial condition $P_0 = 10^8$, the forgetting factor $\gamma = 1$, and $\hat{\Theta}(0)$ contains the information for the plant with the matrices A, B, and C described by equation (5.28).

The numerical results shown in Figures 5.9 and 5.10 for non-adaptive iterative learning control indicate that, when $v(jT) = [12jT, -12jT]^T$ and the task time $T_t = 1$ *sec*, the step-response matrix used in the controller remains fixed at the 'incorrect'

value given by equation (5.29) and that the iterative controller learns rather slowly as a consequence. However, the numerical results shown in Figures 5.11 and 5.12 for adaptive iterative learning control indicate that, when $v(jT) = [12jT, -12jT]^T$ and $T_t = 1$ *sec*, the step-response matrix changes very rapidly from the 'incorrect' value given by equation (5.29) to the 'correct' value given by equation (5.26) and that the iterative controllers learn very rapidly as a consequence. These results thus demonstrate the improvements in learning performance and convergence achievable by the introduction of adaptive action.

It must be emphasised that when $k = 0$ the output is zero since the assumed value of the input is zero initially, using both non-adaptive and adaptive iterative learning control. In addition, the elements of the step-response matrix are fixed at the 'incorrect' values in the case of both non-adaptive and adaptive iterative learning control when $k = 0$, as shown in Figures 5.10 and 5.12.

The reason for the slow learning rate using the 'incorrect' step-response matrix is the same as in Example 5.1, since using the 'incorrect' step-response matrix makes $\rho = 0.938$ and $\sigma = 0.2526$ whilst using the 'correct' step-response matrix makes $\rho = 0.75$ and $\sigma = 1.0$. Therefore, the learning performance has improved and the convergence speed has increased as a result of using the 'correct' step-response matrix obtained from the recursive identifier.

5.4 CONCLUSION

In Chapter 4, it was shown that digital iterative learning controllers can be directly designed using only input/output models of plants in the form of step-response matrices. Therefore, since the step-response matrices of plants can be readily identified in real time, it has been shown in this chapter that performance degradation

in digital iterative learning control due to initially unknown dynamical characteristics can be avoided by deploying on-line recursive identifiers. Such identifiers, which employ the recursive least squares (RLS) method of identification, provide updated step-response matrices for inclusion in the digital iterative learning controllers introduced in Chapter 4. Moreover, it has been shown that these identifiers are rapid and accurate, so that learning performance and convergence rates are greatly improved. These theoretical results have been illustrated by the presentation of numerical results for the adaptive iterative learning control of regular, first-order partially irregular, and second-order completely irregular plants whose dynamical characteristics are initially unknown to the controllers.

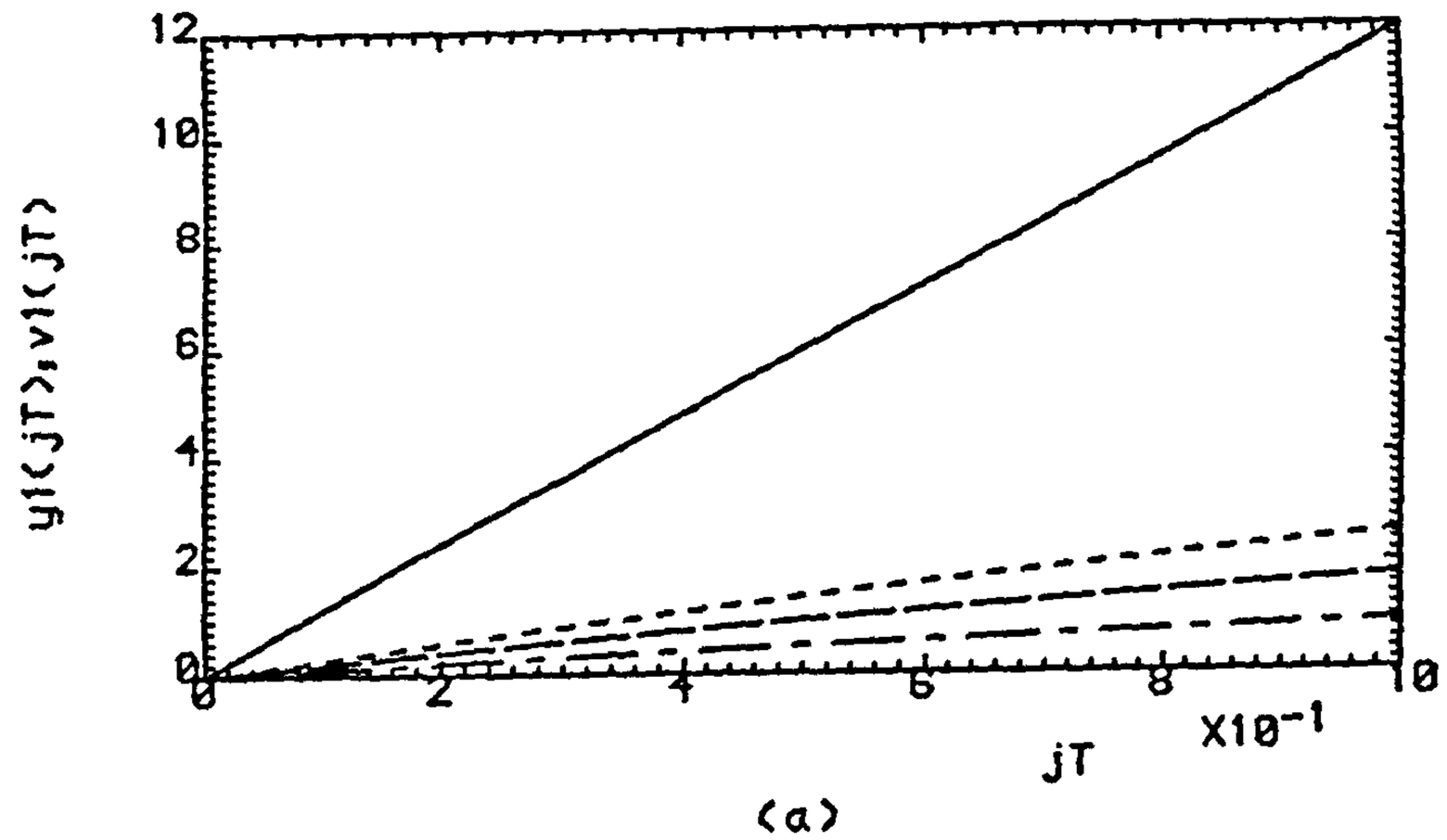

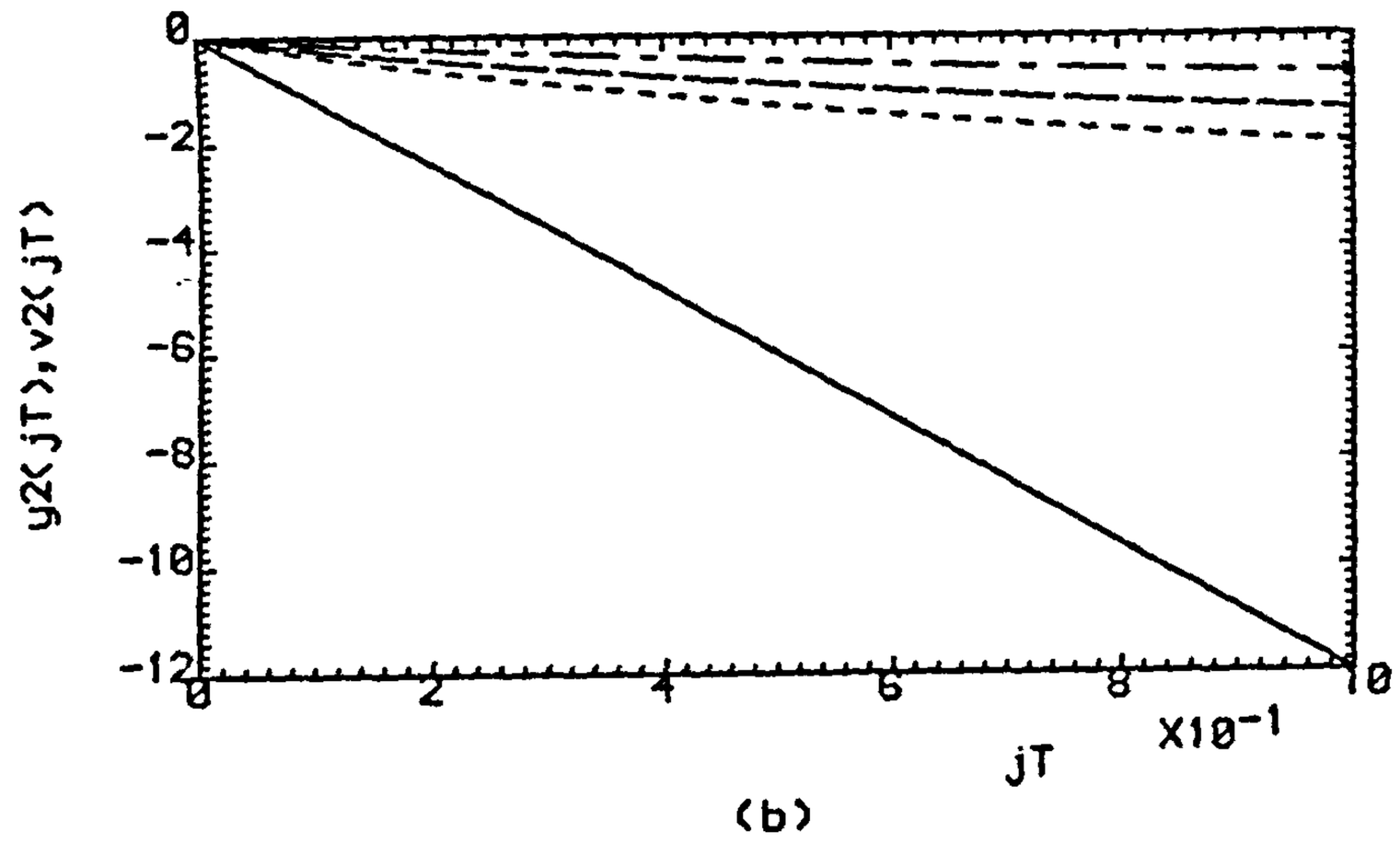

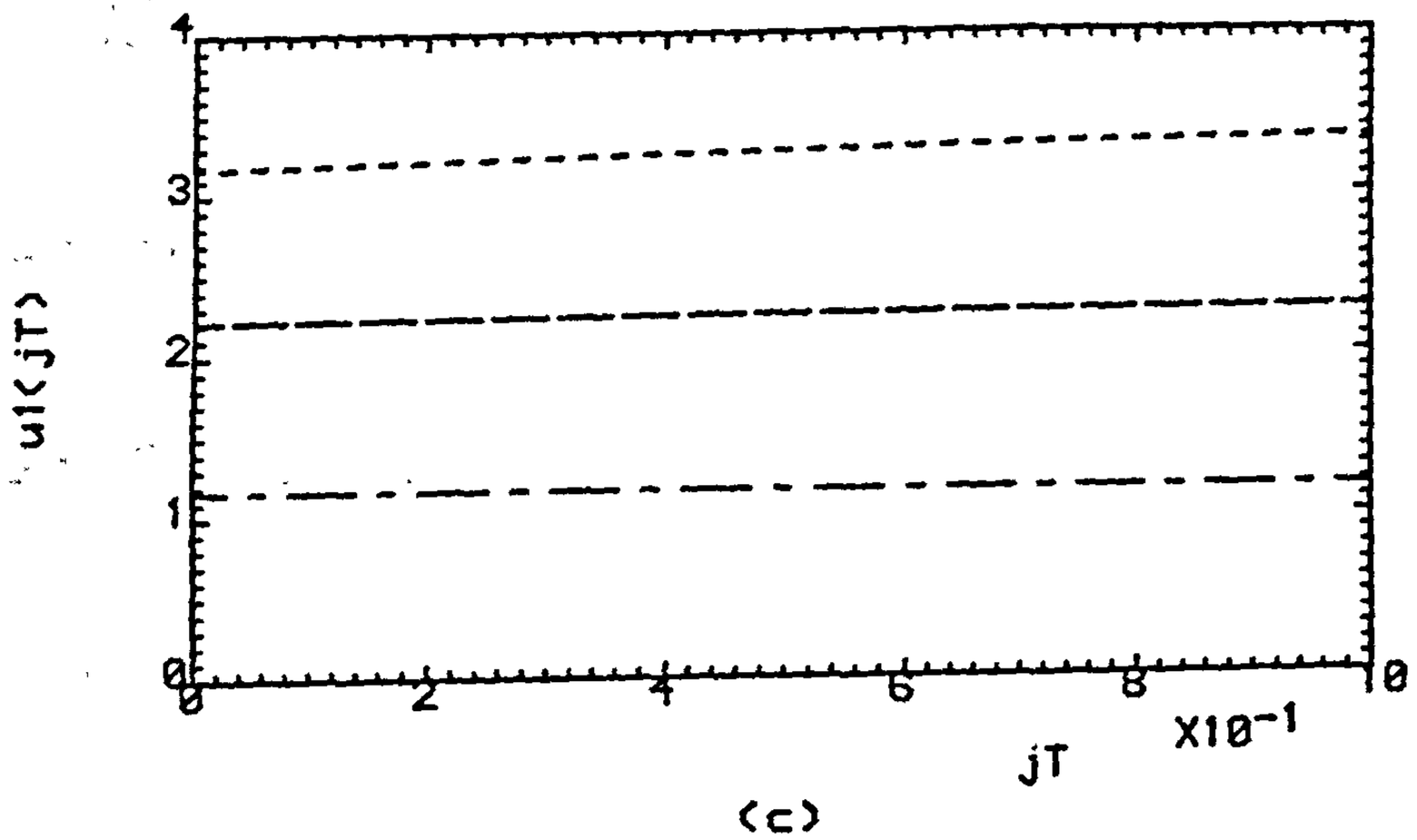

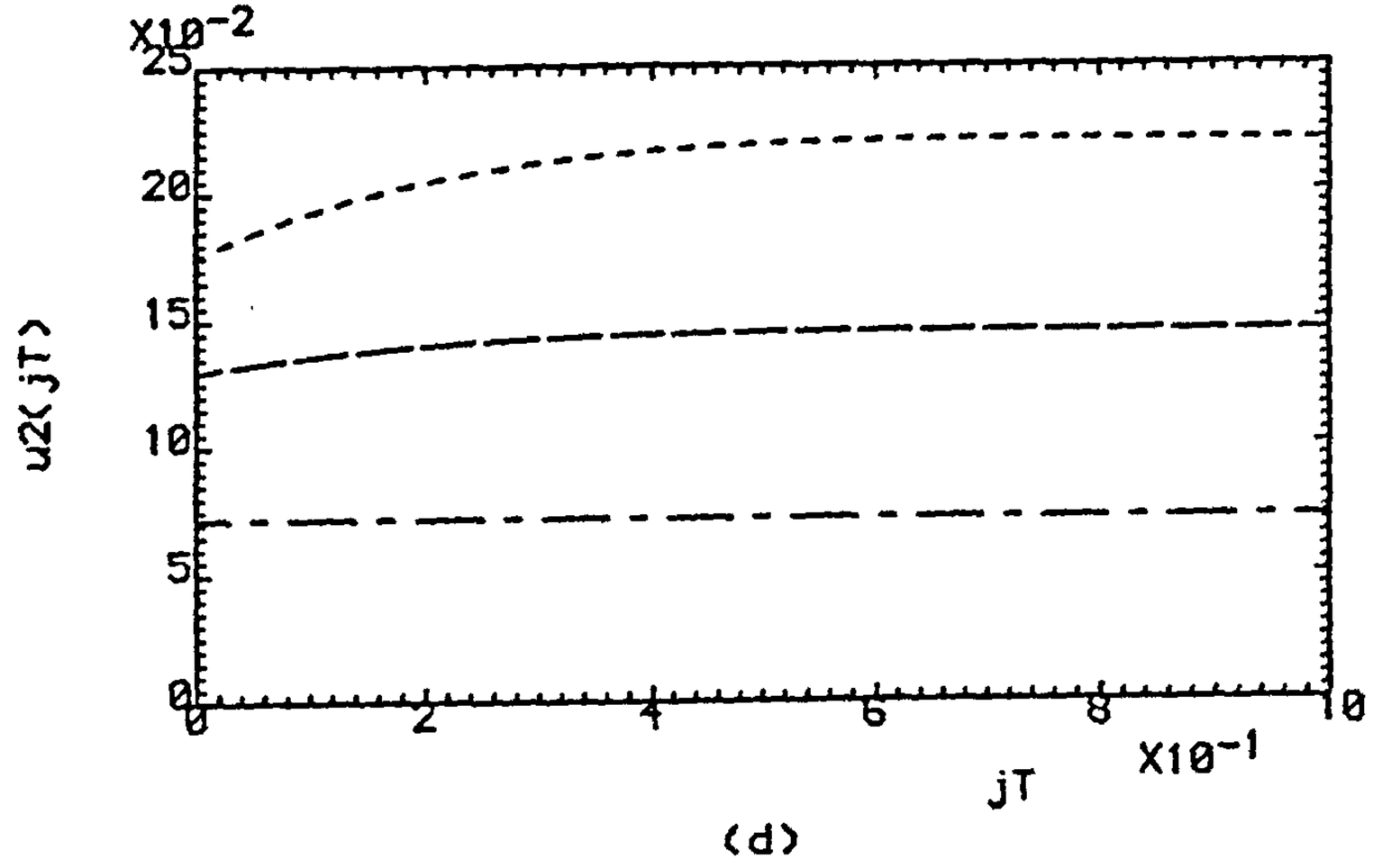

Fig.5.1(a,b) Succesive Outputs OF The Plant.
(c,d) Succesive Control Efforts.
Under Non-Adaptive Control.
-.-.- K=1 , ----- K=2 , ... K=3

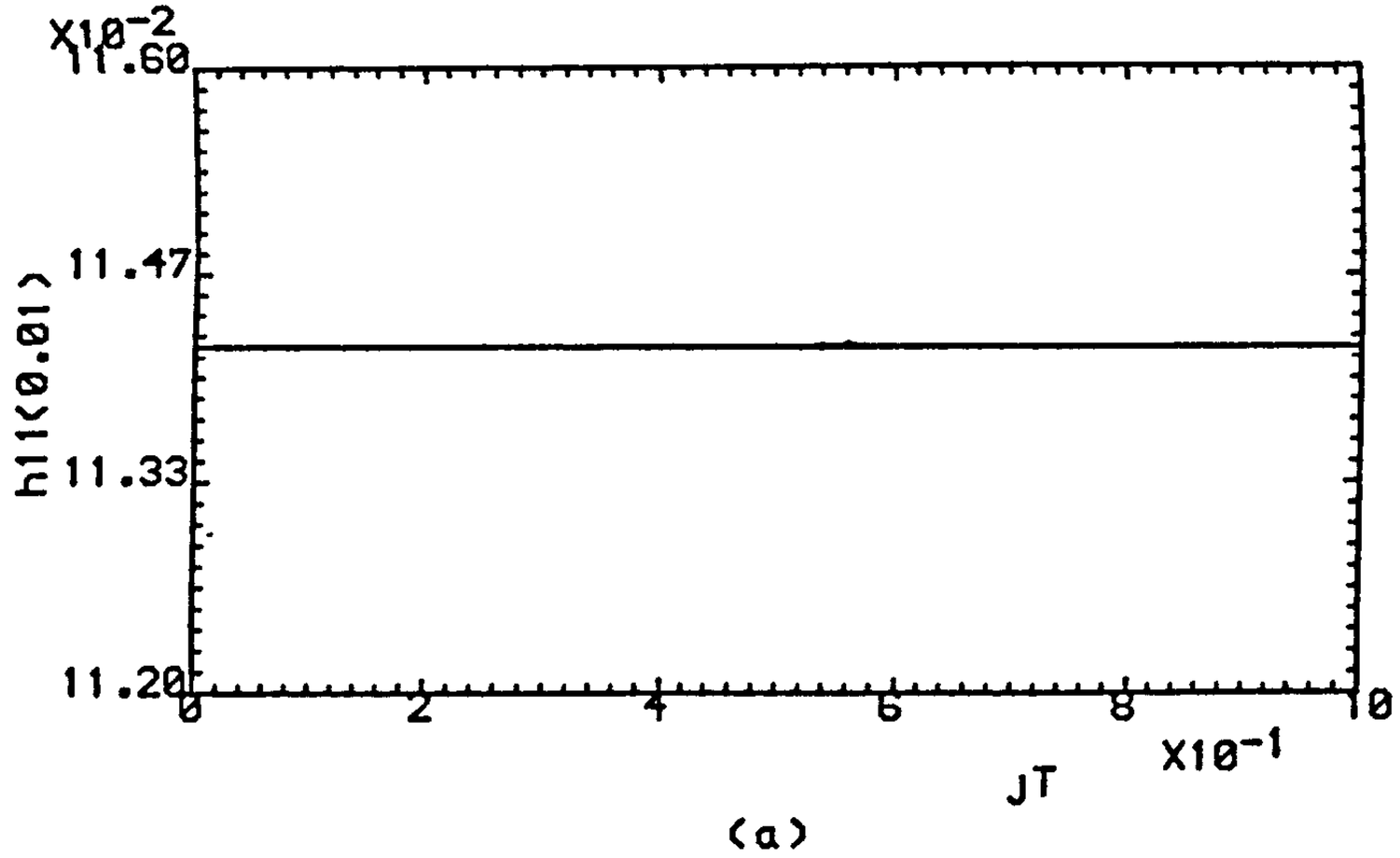

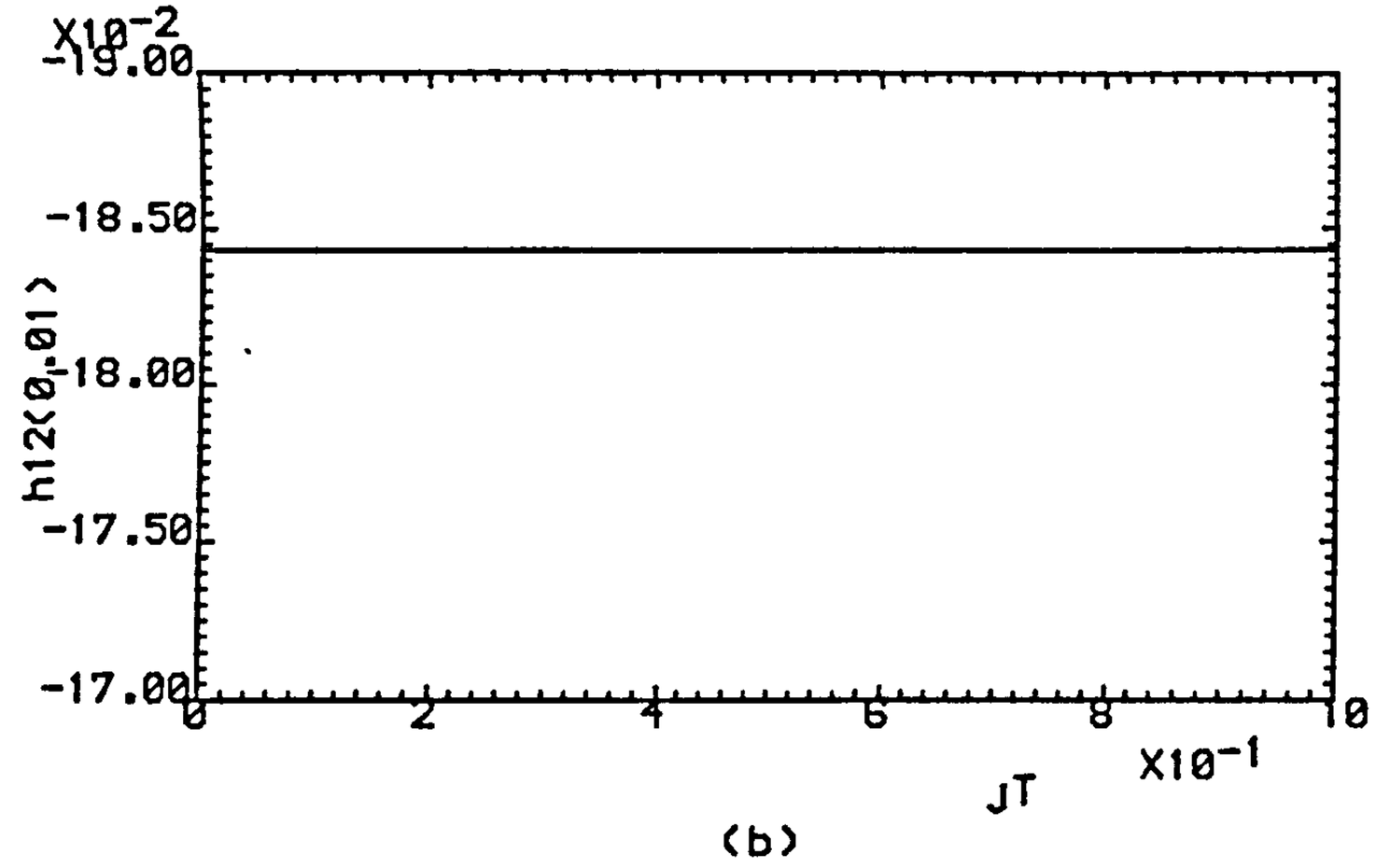

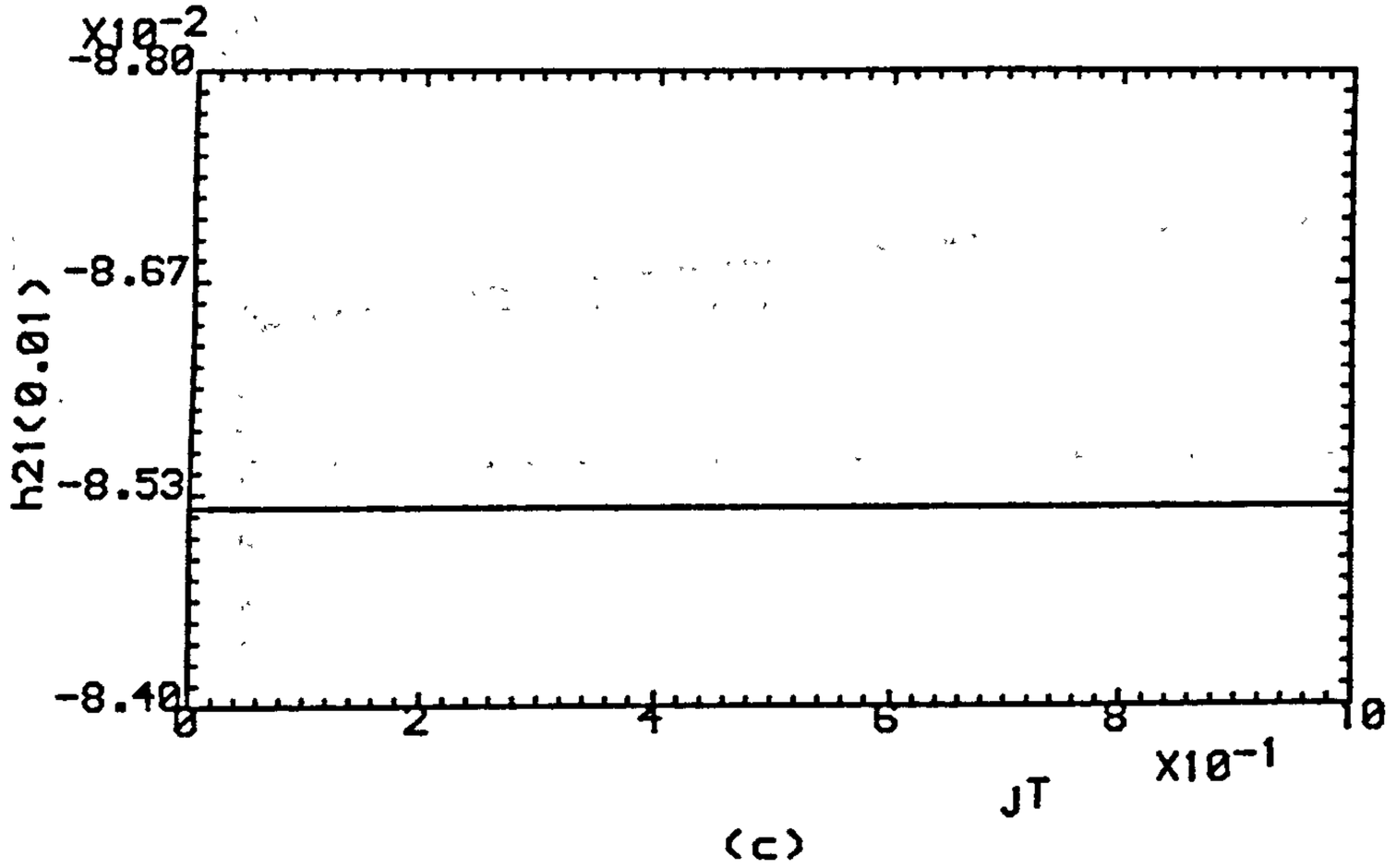

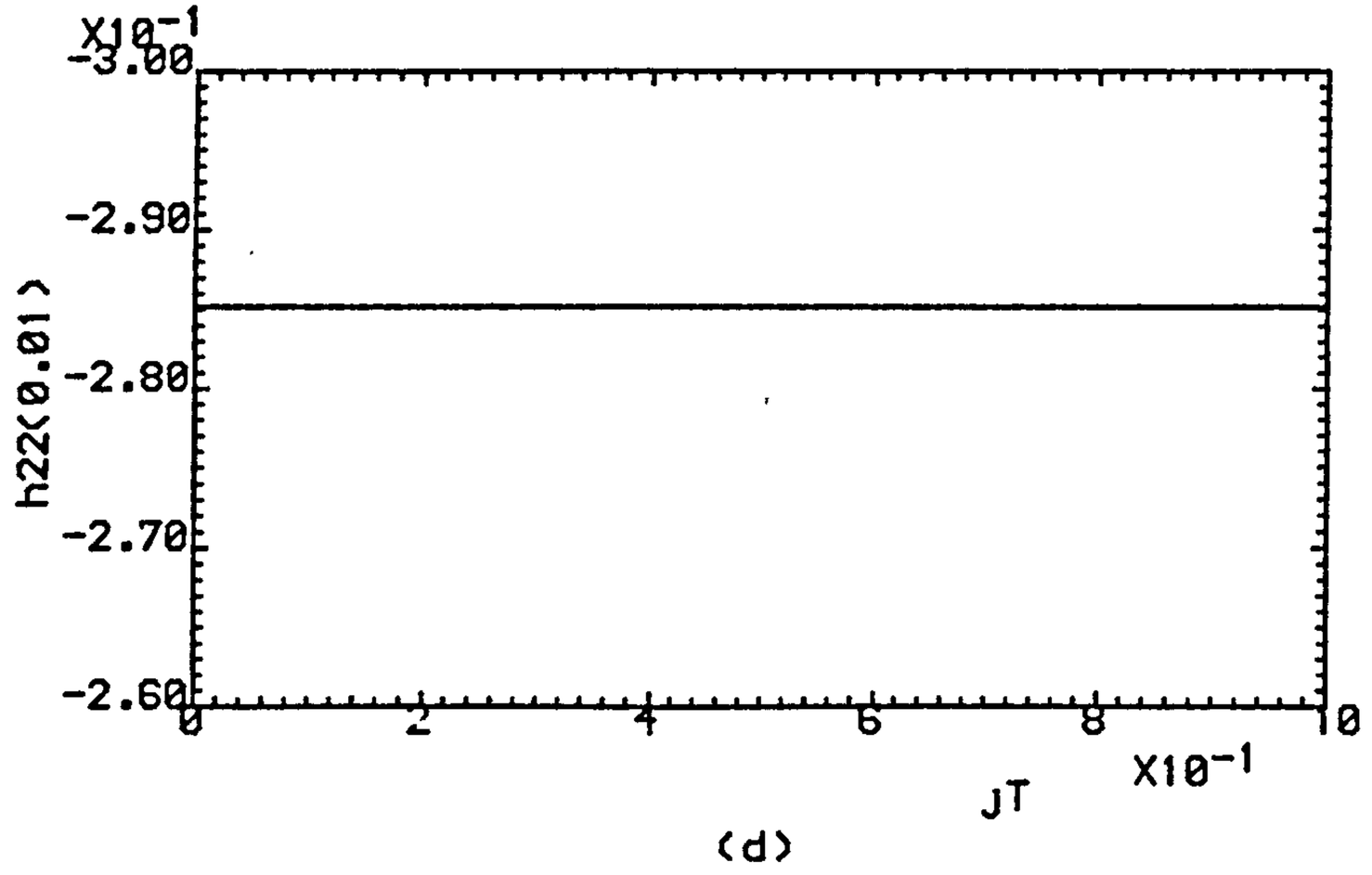

Fig.5.2Succesive Estimates Of Step-Response Matrix
Of Plant Under Non-Adaptive Control.
-·-·- K=1 , ----- K=2 , ... K=3

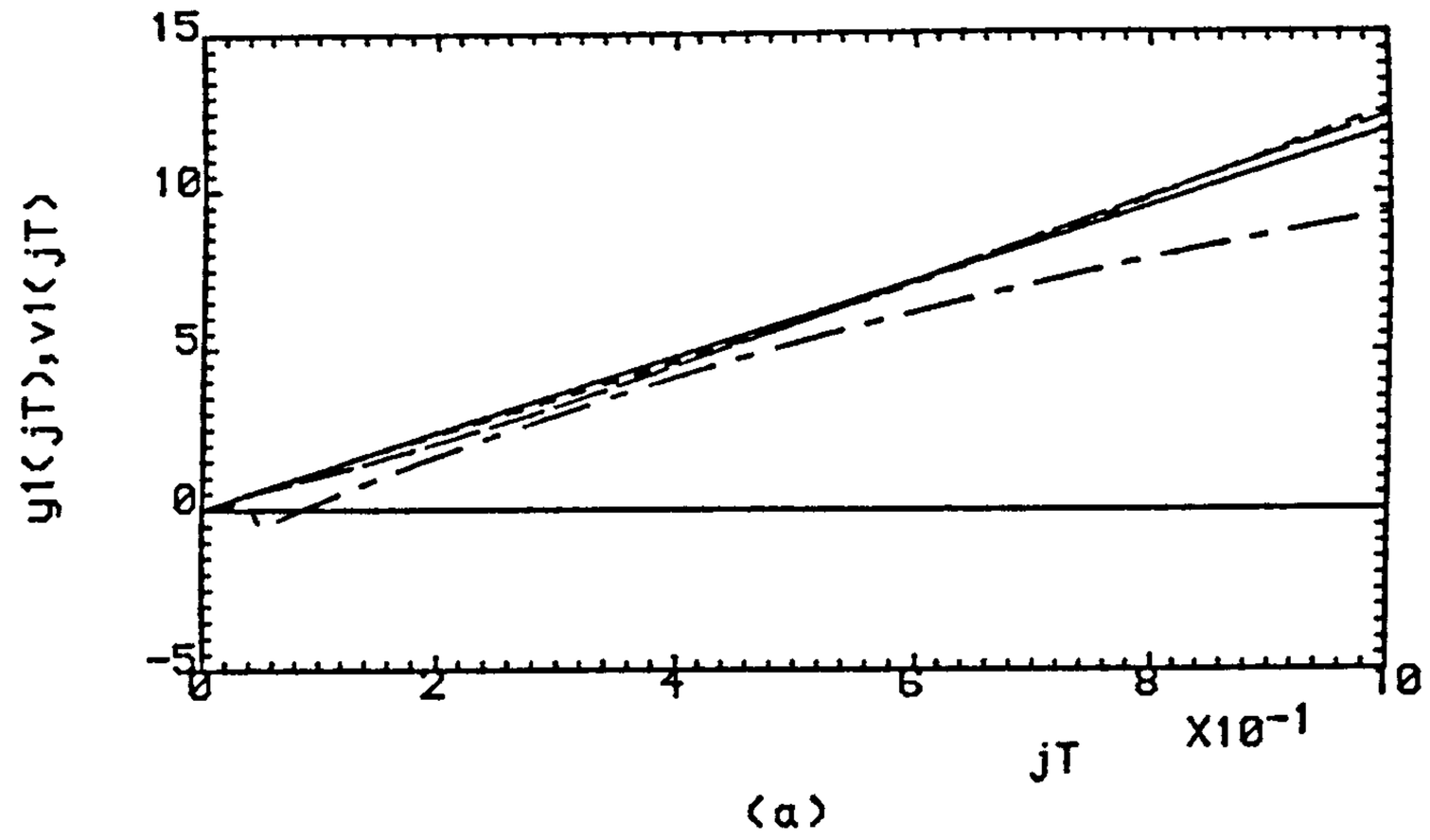

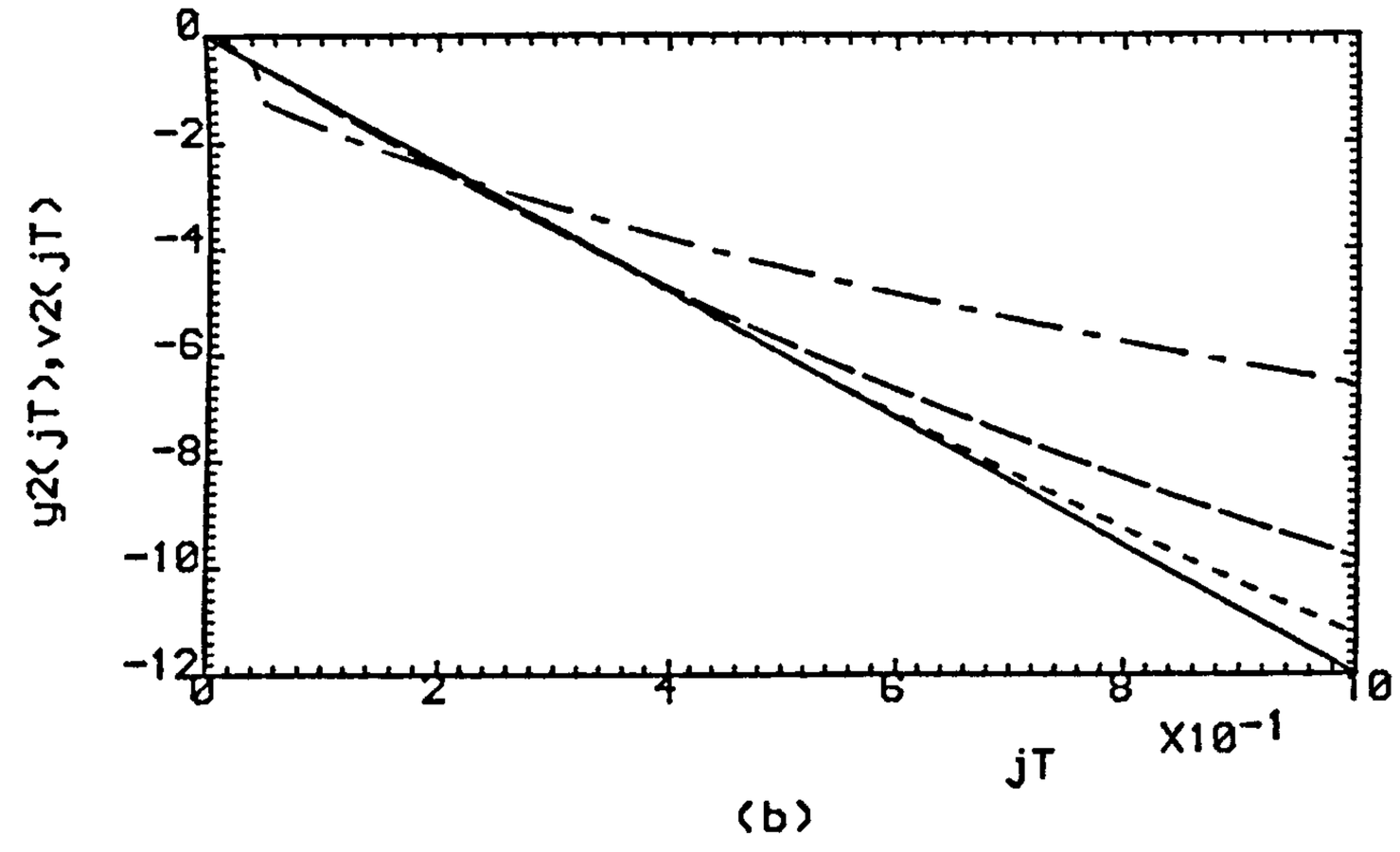

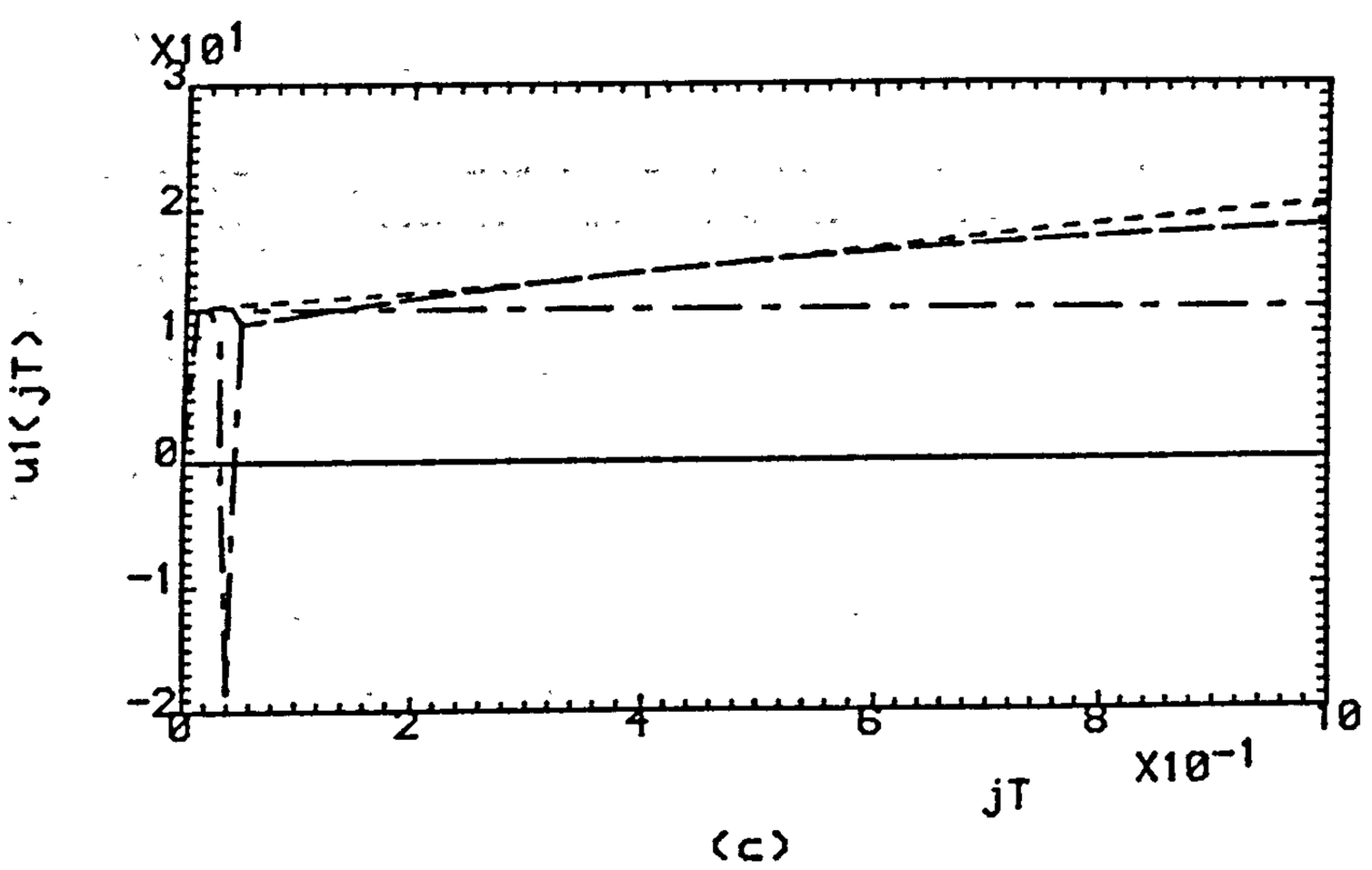

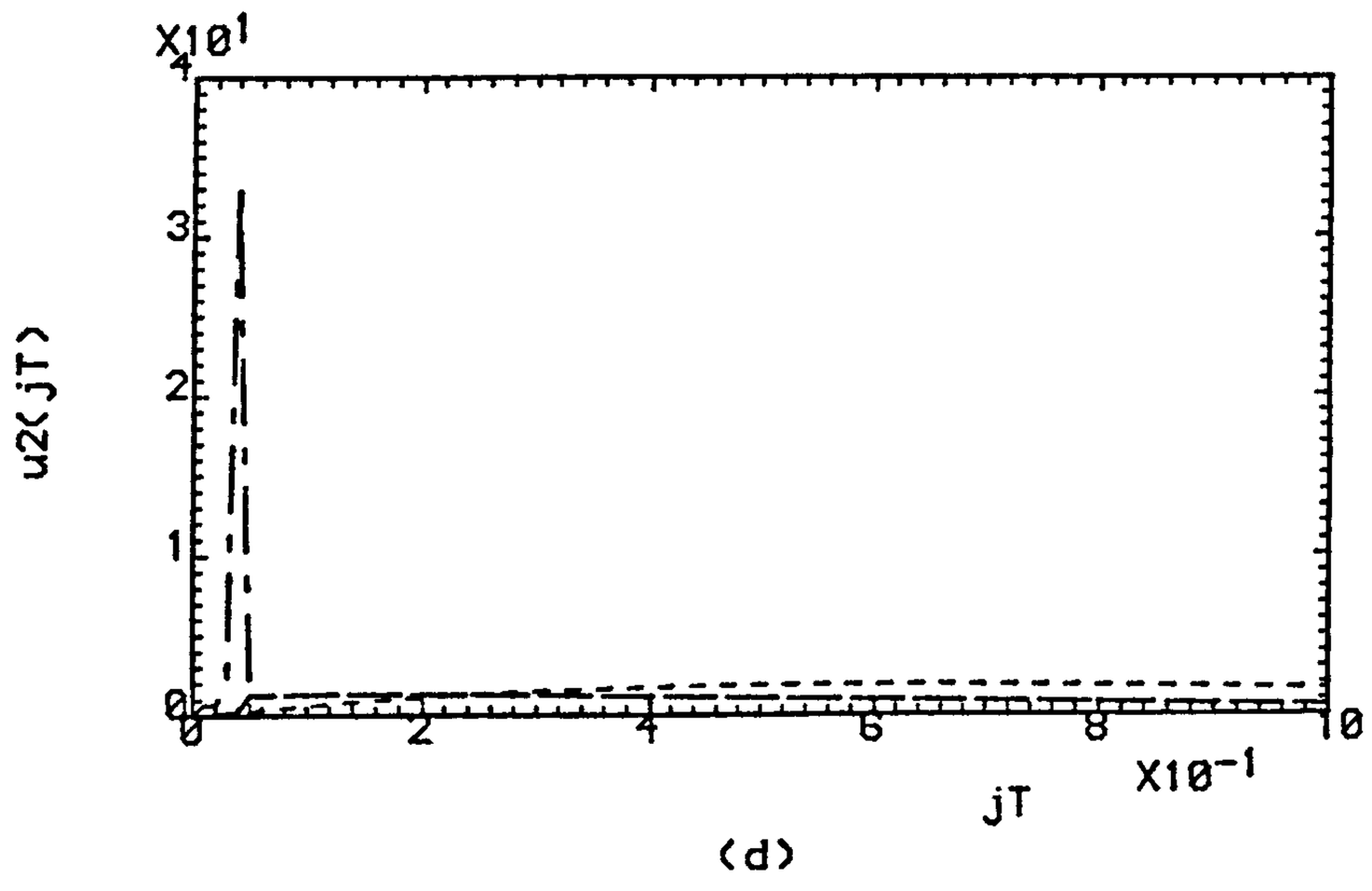

Fig.5.3(a,b) Succesive Outputs OF The Plant.
(c,d) Succesive Control EFforts.
Under Adaptive Control.
-·-·- K=1 , ----- K=2 , ... K=3

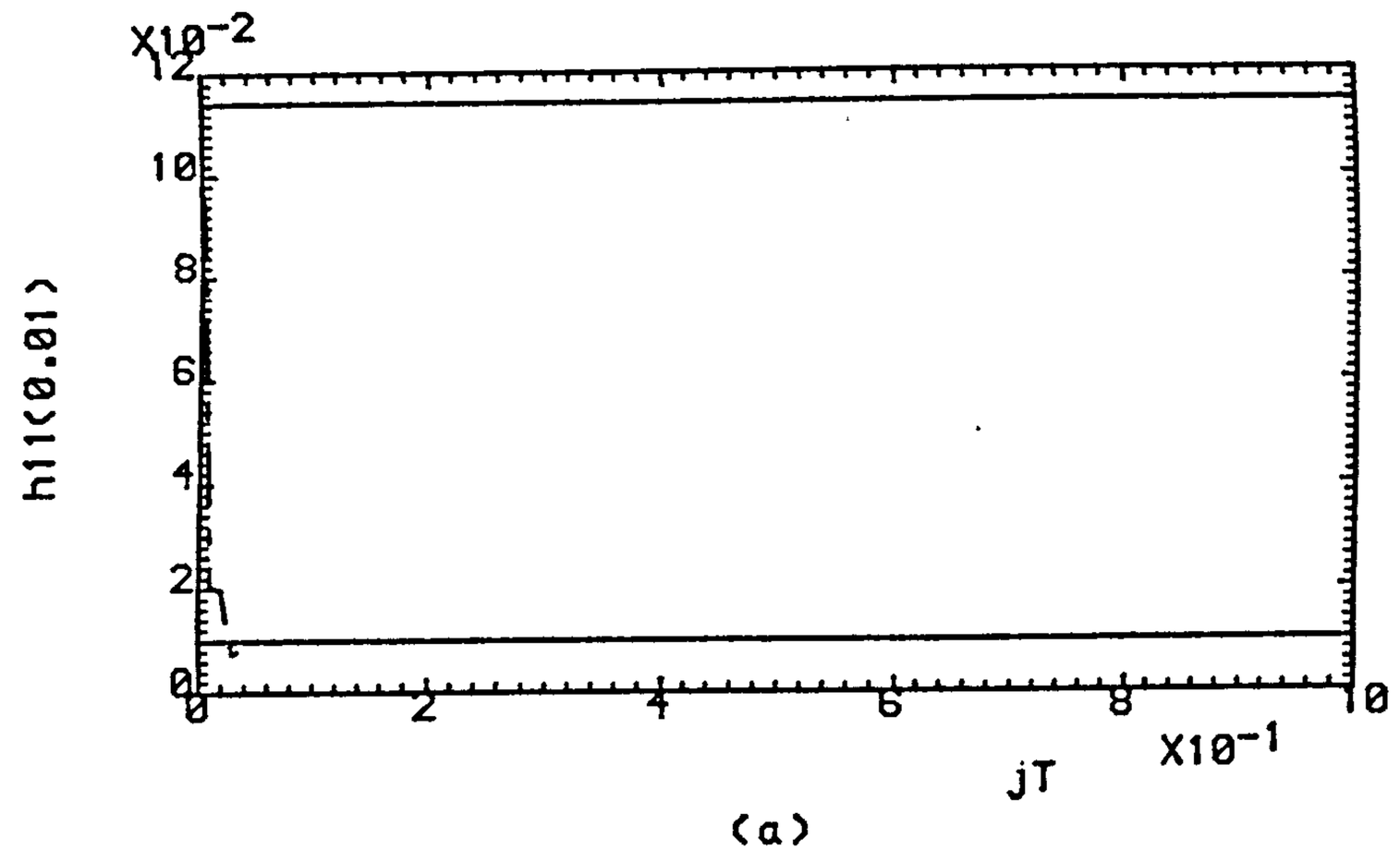

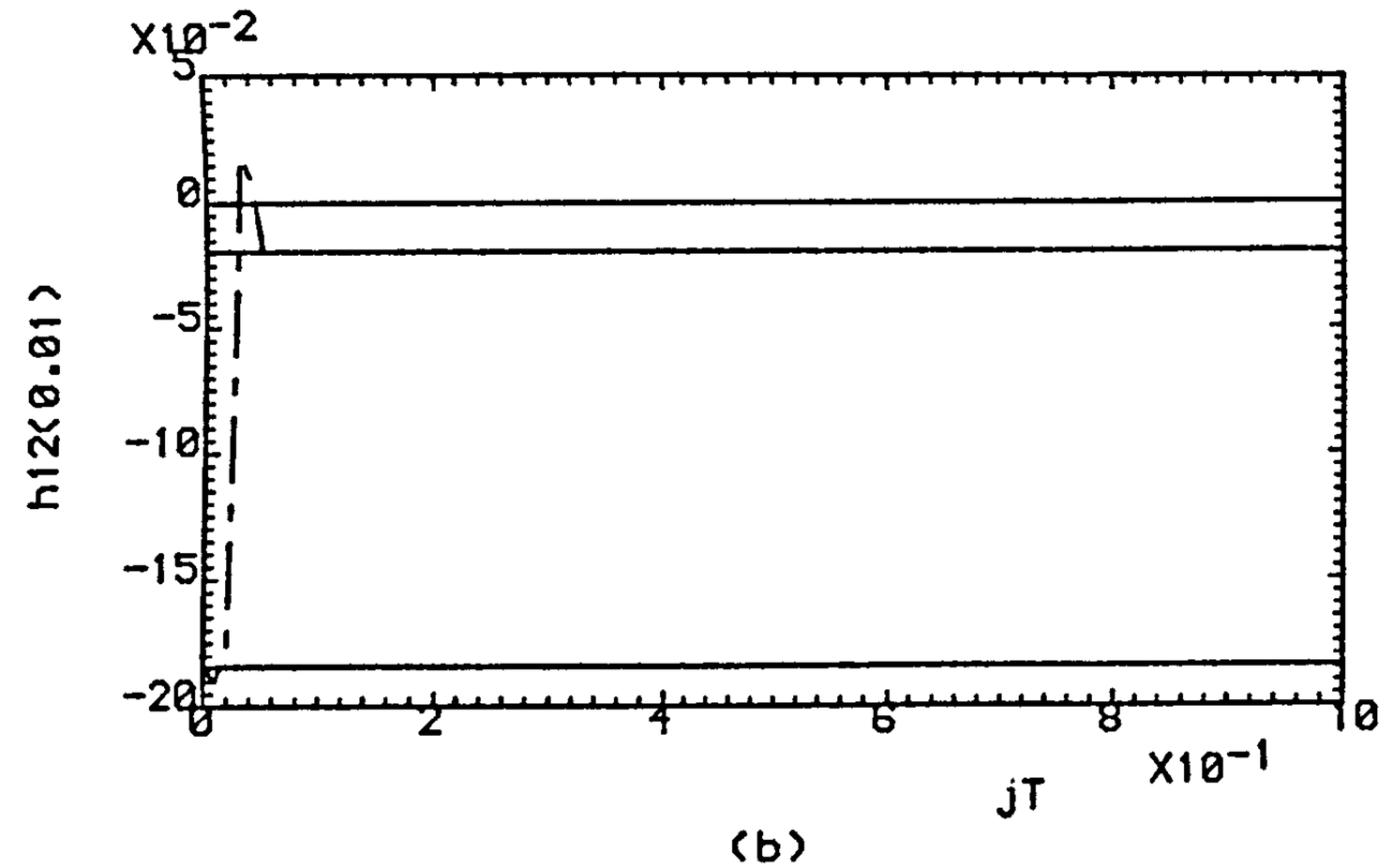

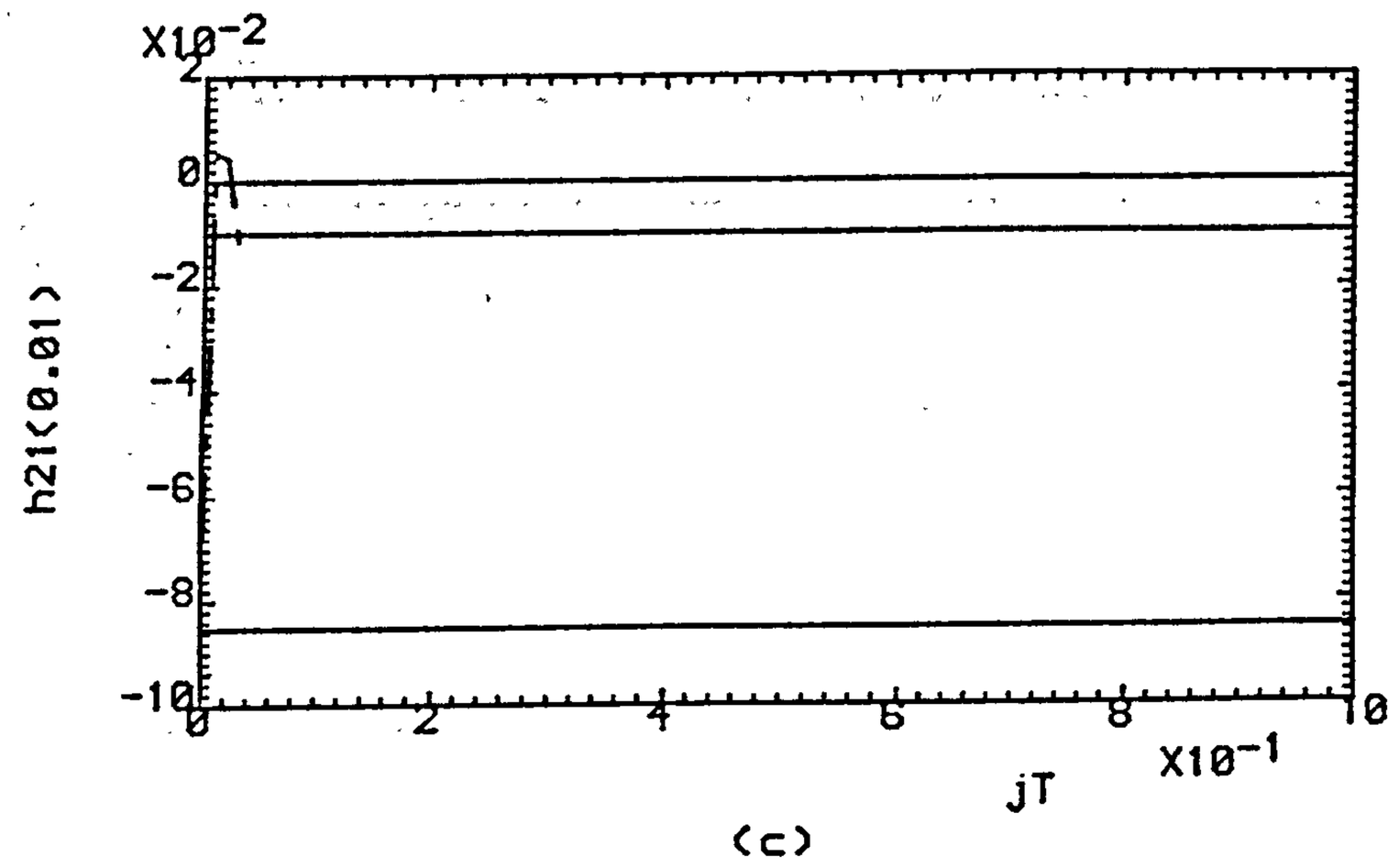

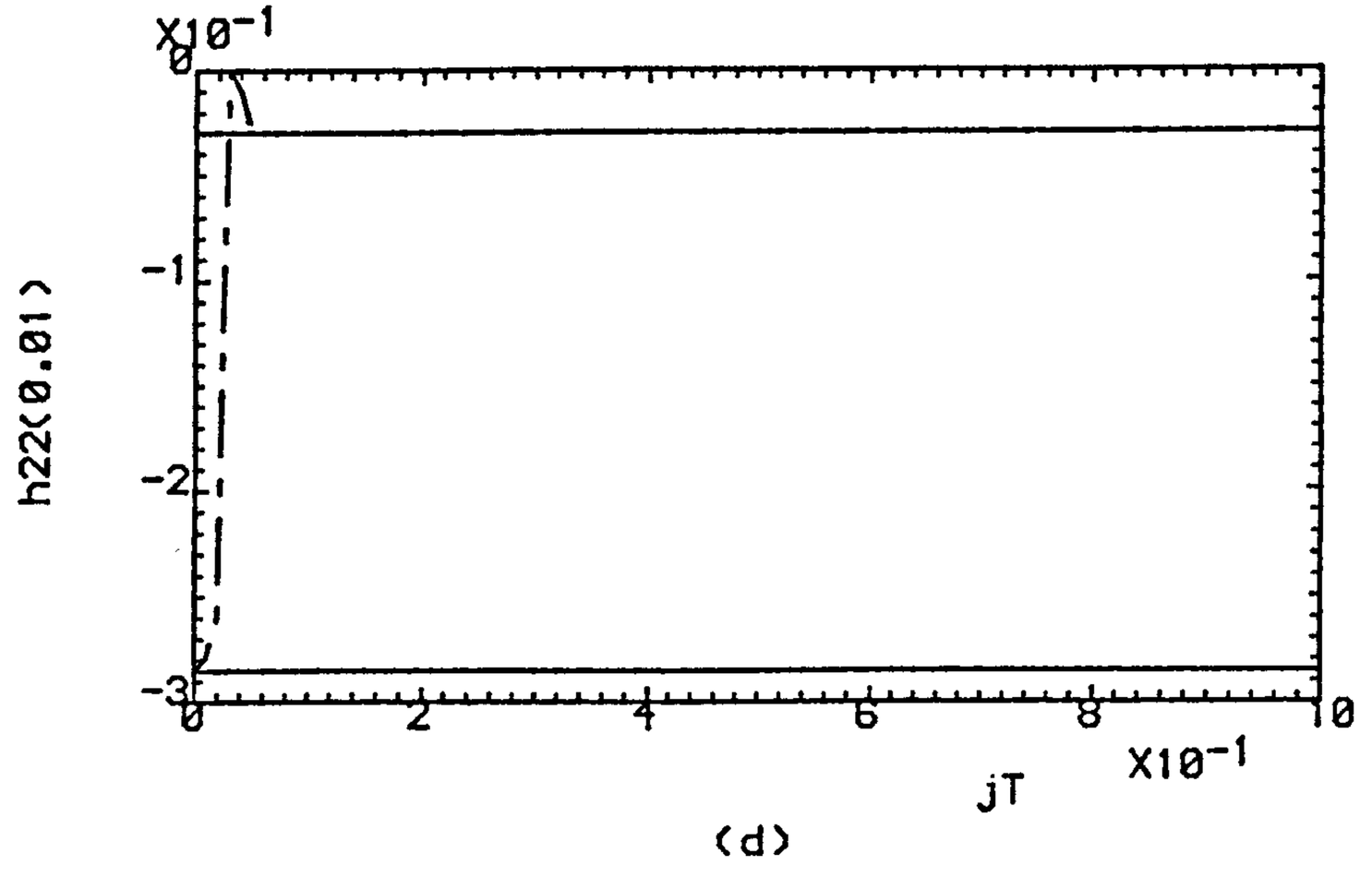

Fig.5.4Succesive Estimates OF Step-Response Matrix
OF Plant Under Adaptive Control.
-·-·- K=1 , ----- K=2 , ... K=3

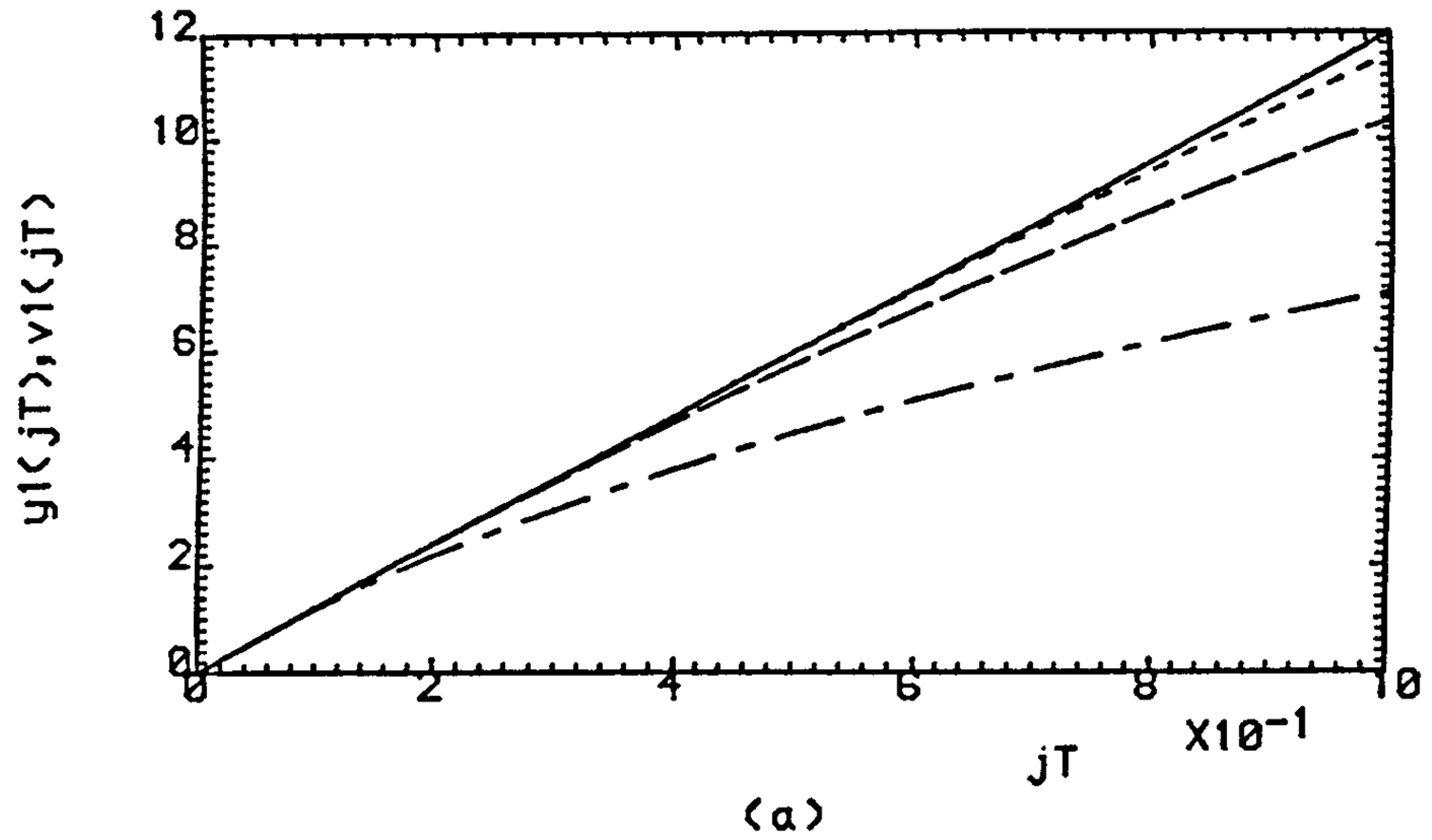

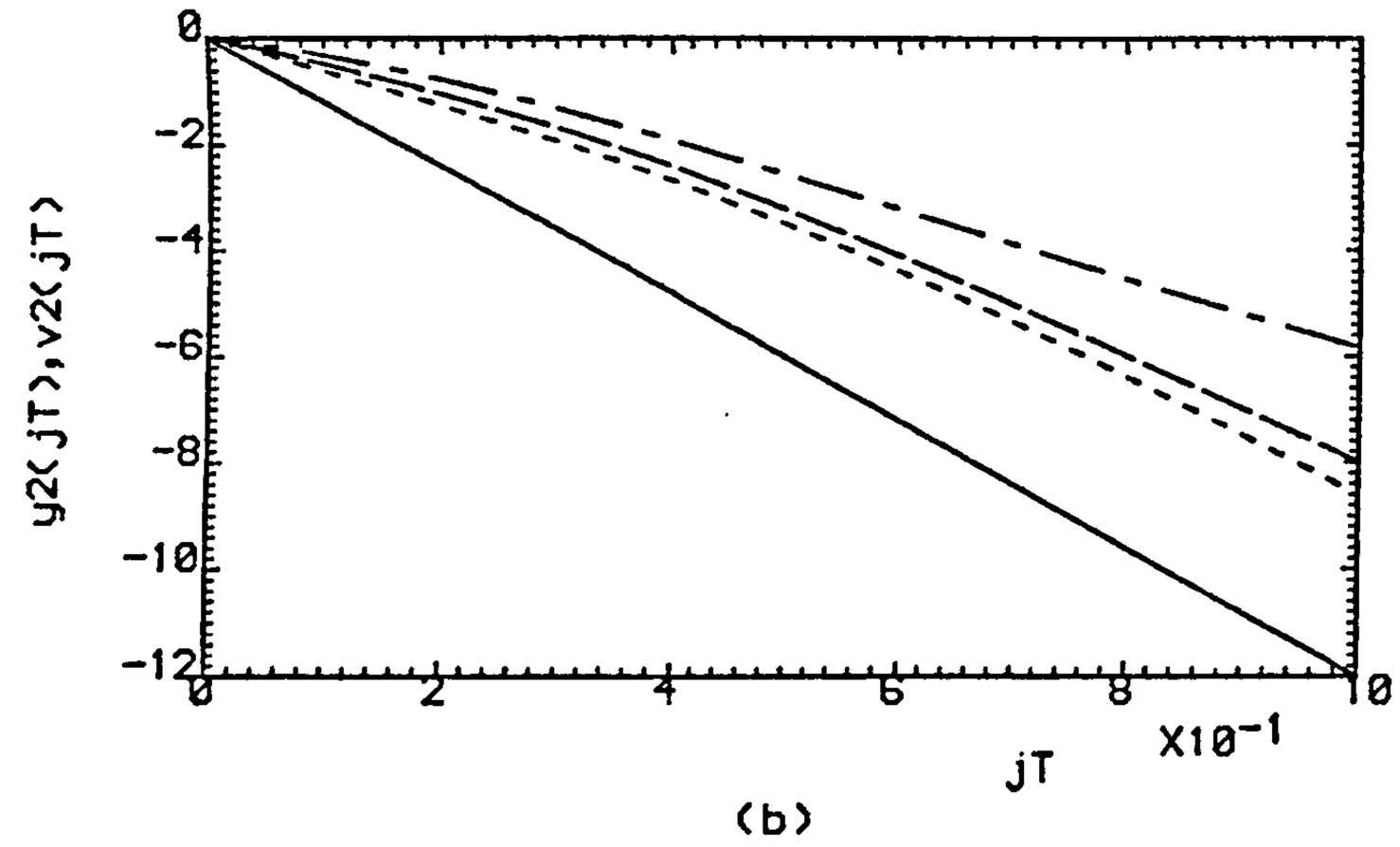

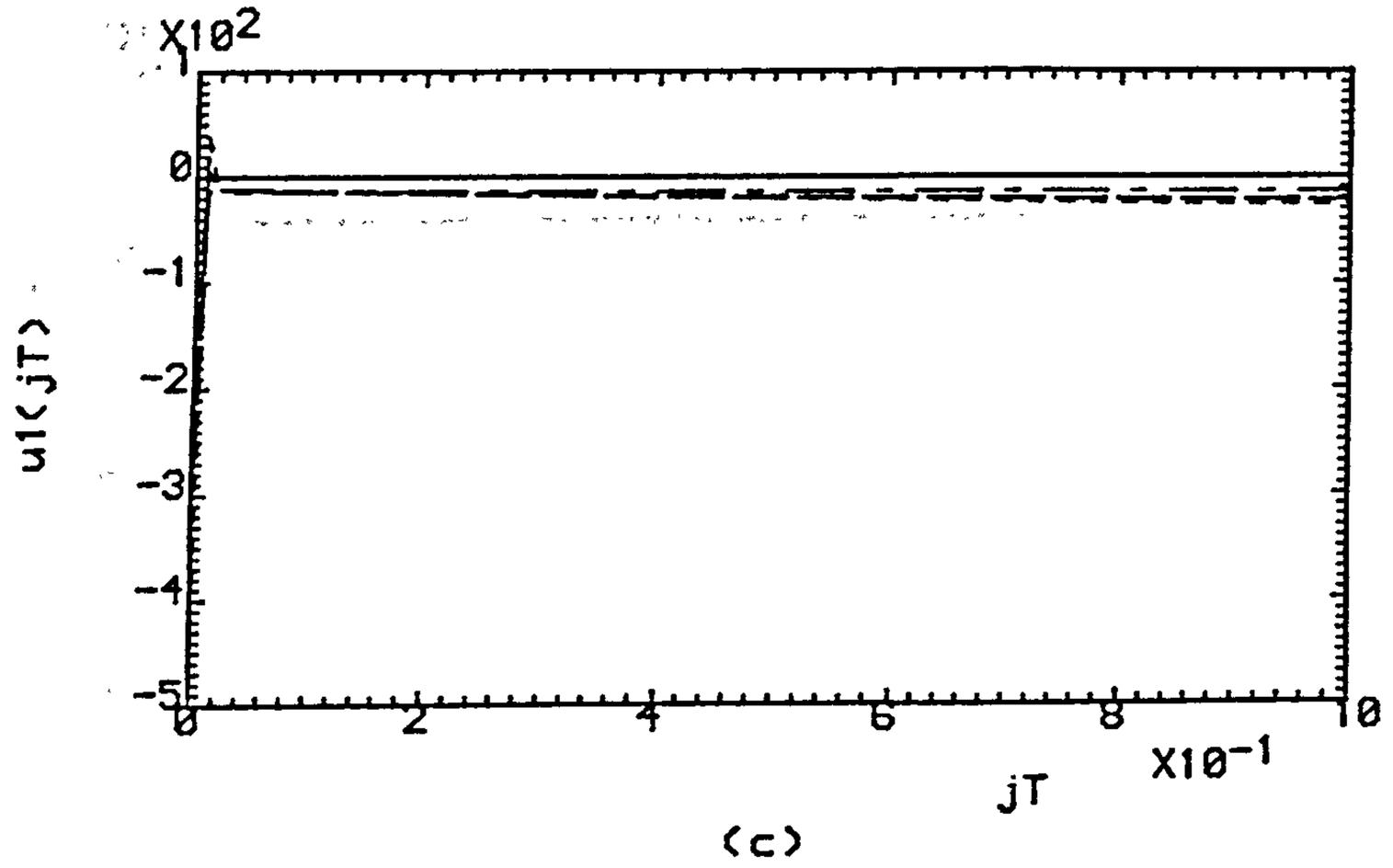

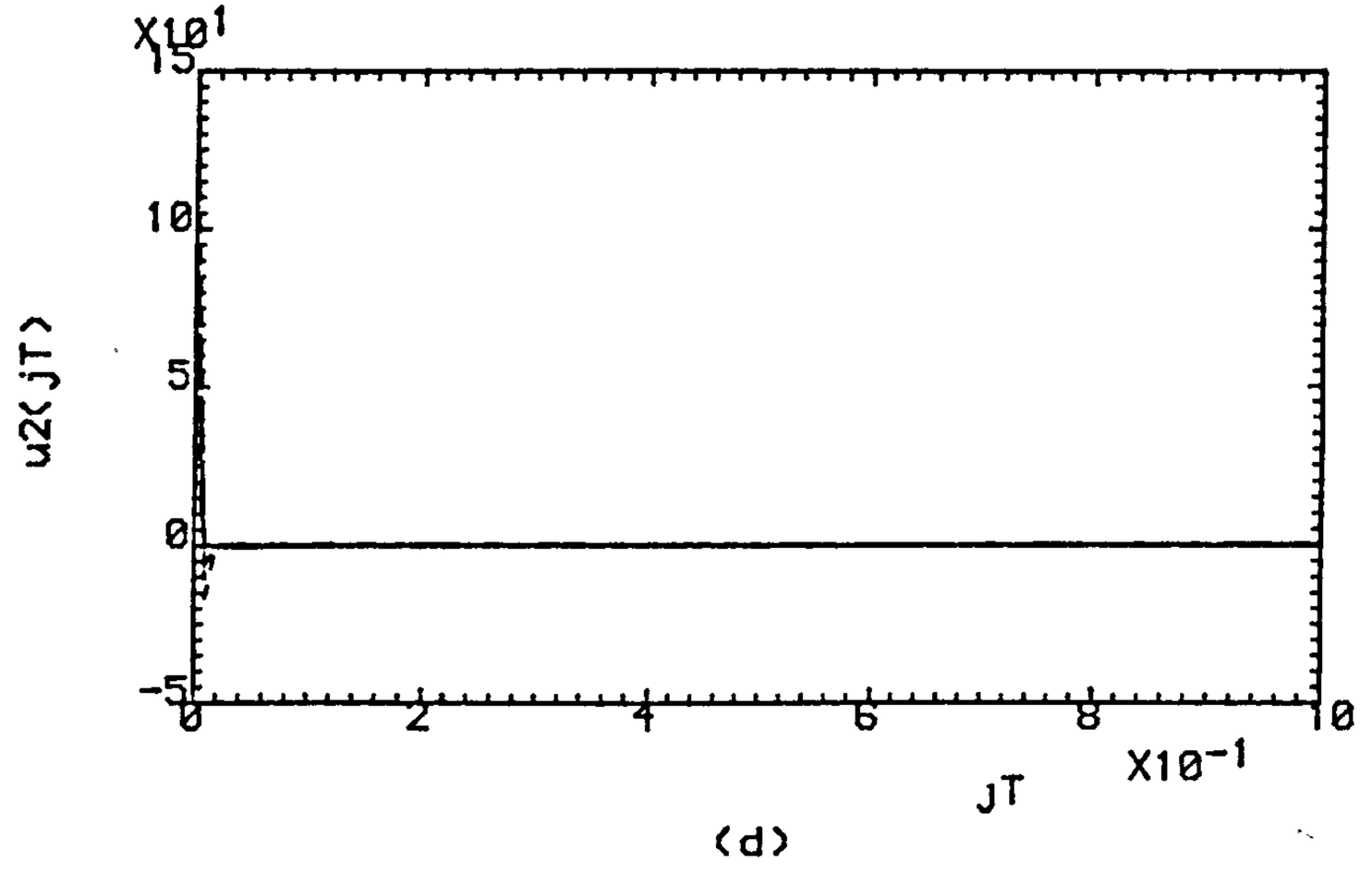

Fig.5.5(a,b) Succesive Outputs OF The Plant.
(c,d) Succesive Control EFforts.
Under Non-Adaptive Control.
-·-·- K=1 , ----- K=2 , ... K=3

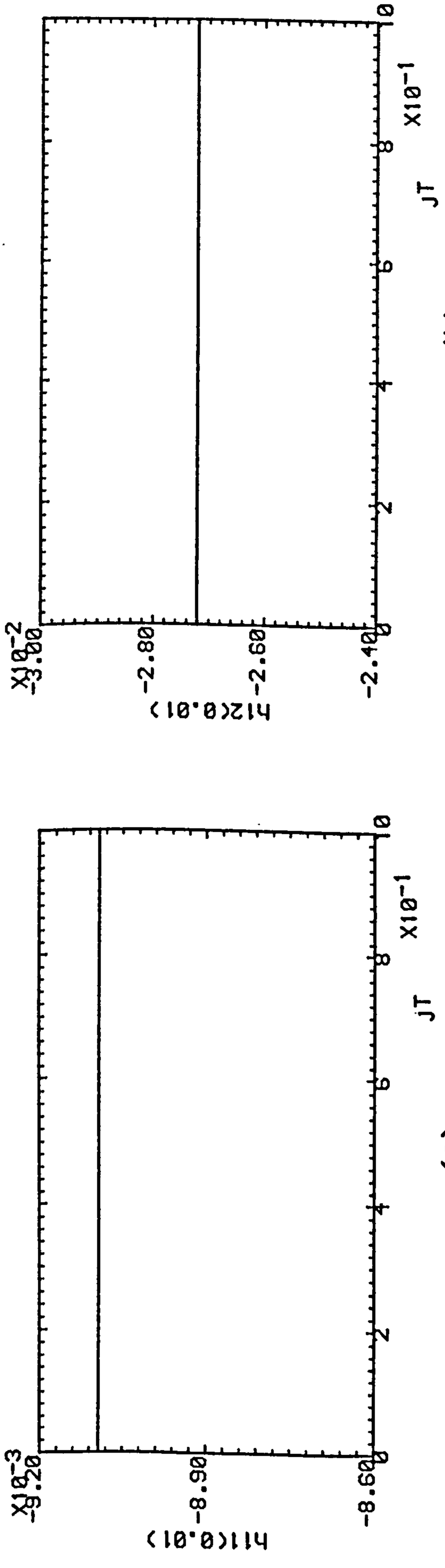

Fig.5.6Succesive Estimates Of Step-Response Matrix Of Plant Under Non-Adaptive Control.
-·-·- K=1 , ----- K=2 , ... K=3

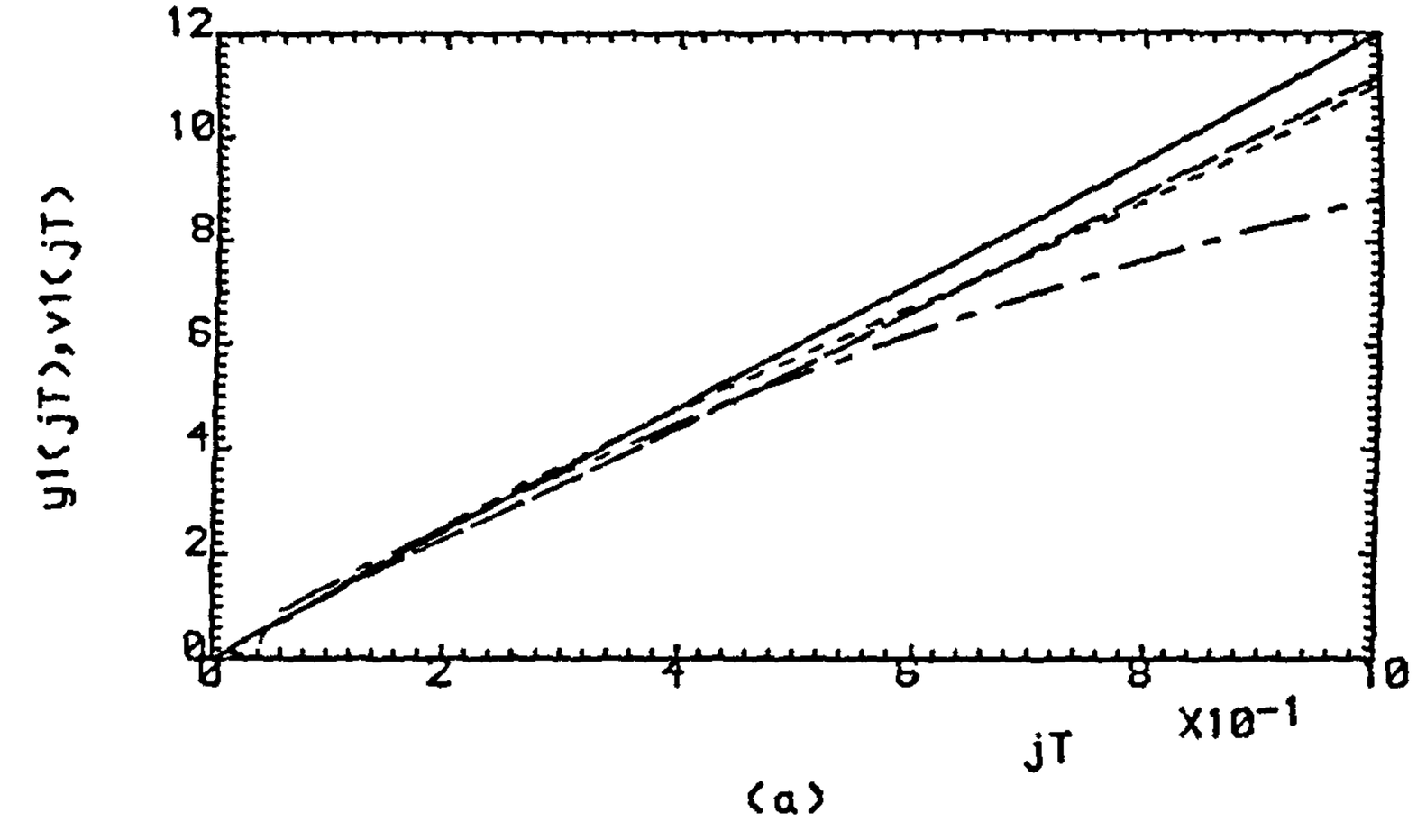

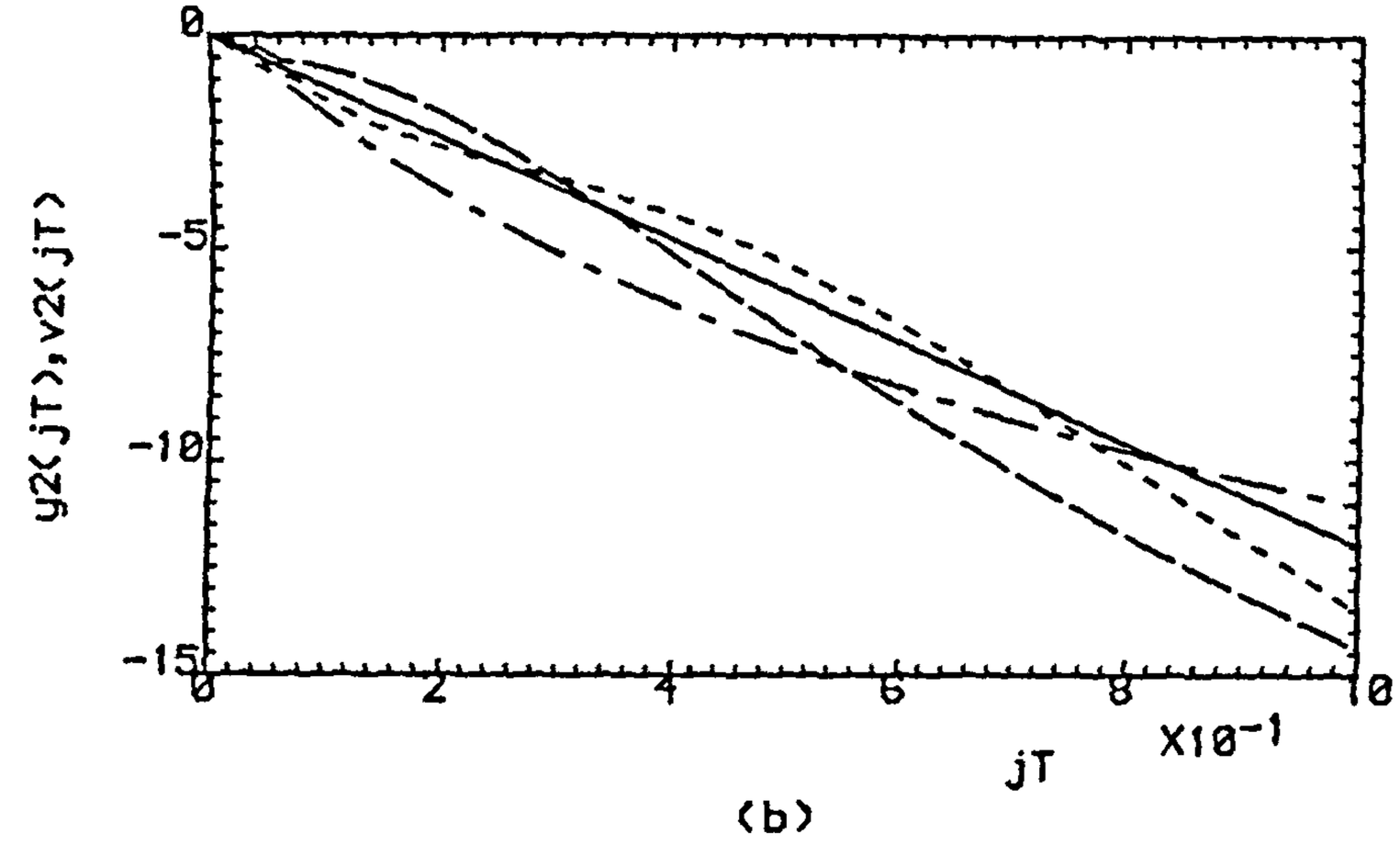

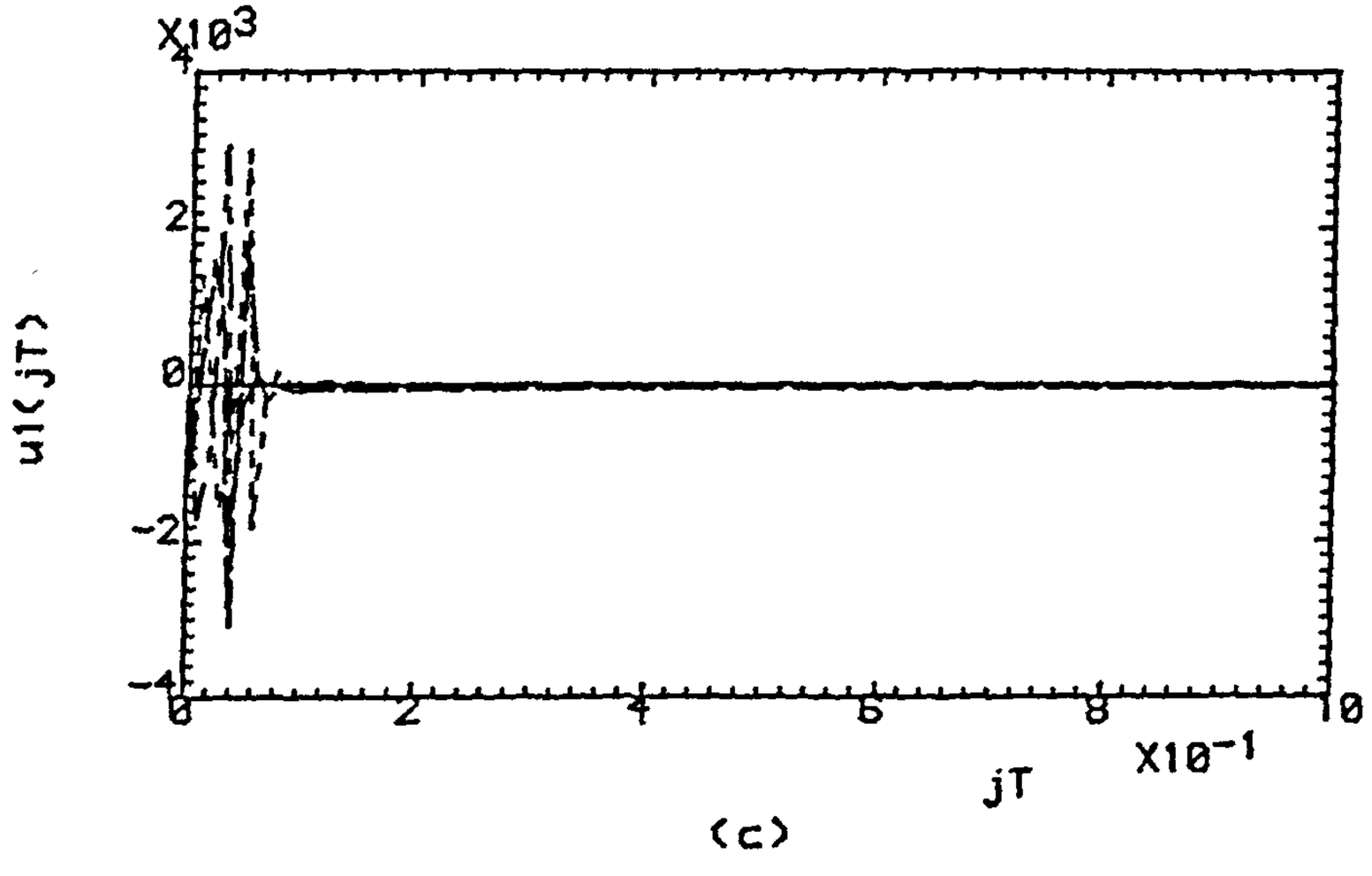

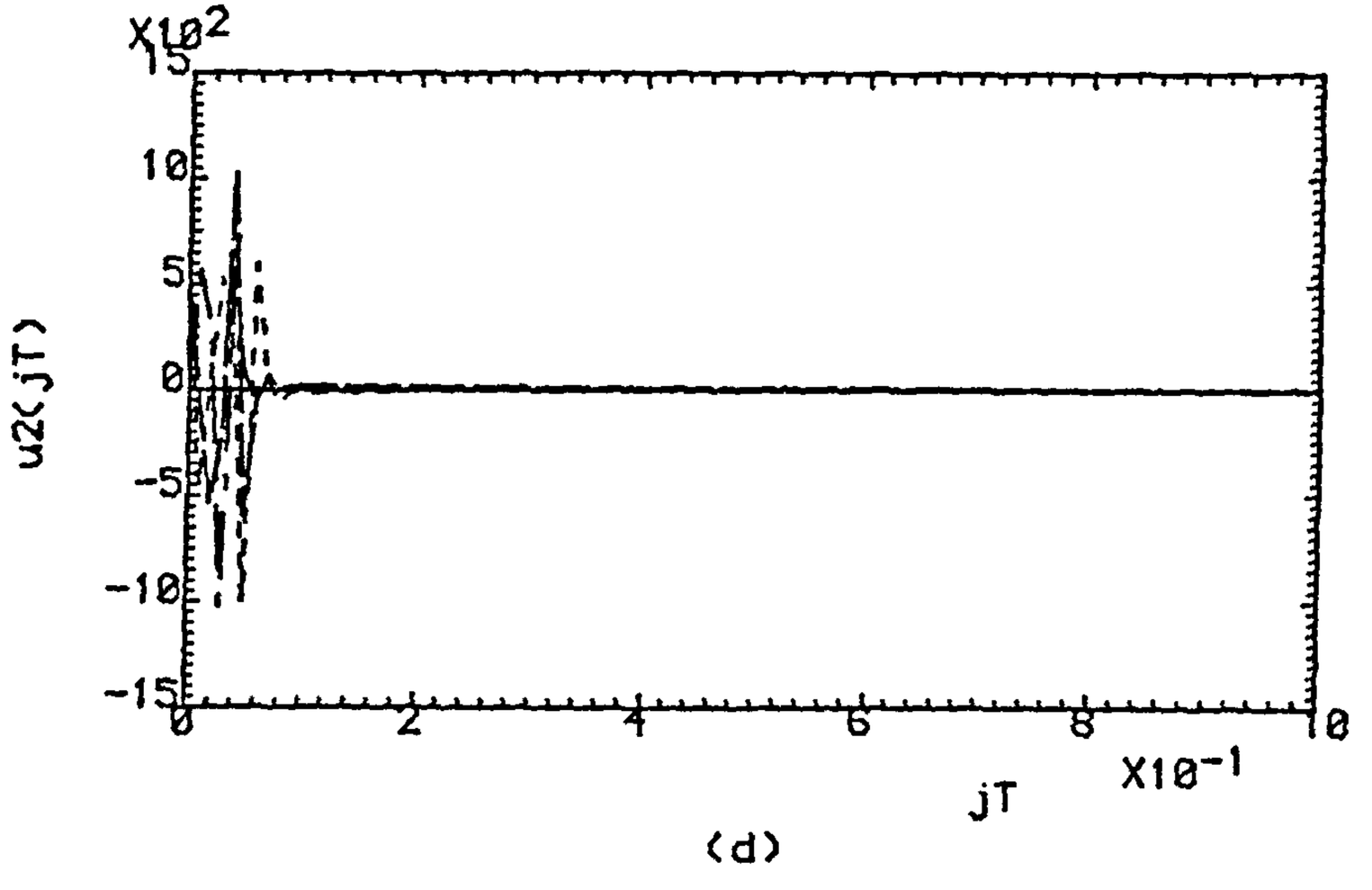

Fig.5.7(a,b) Succesive Outputs Of The Plant.
(c,d) Succesive Control Efforts.
Under Adaptive Control.
-.-.- K=1 , ----- K=2 , ... K=3

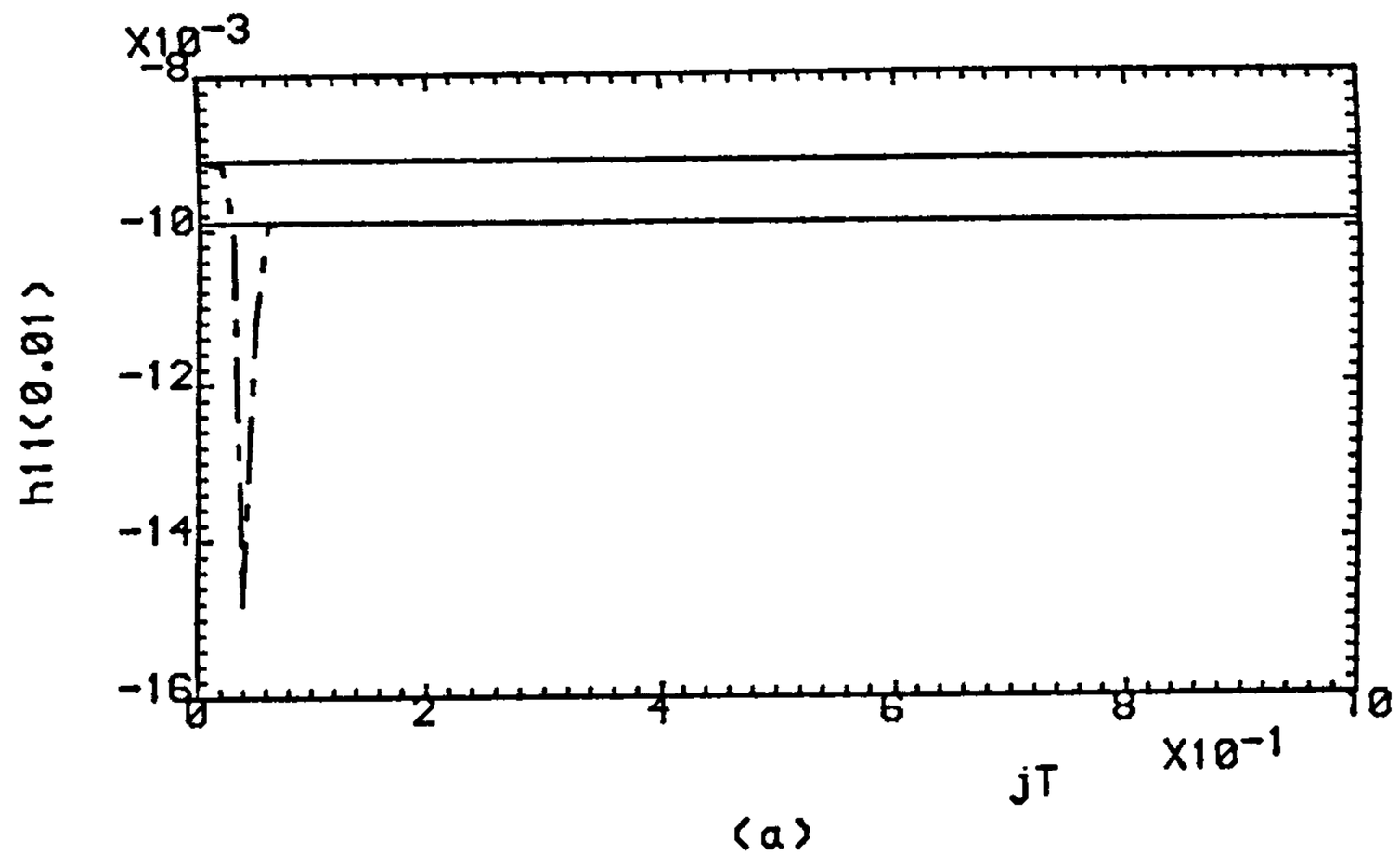

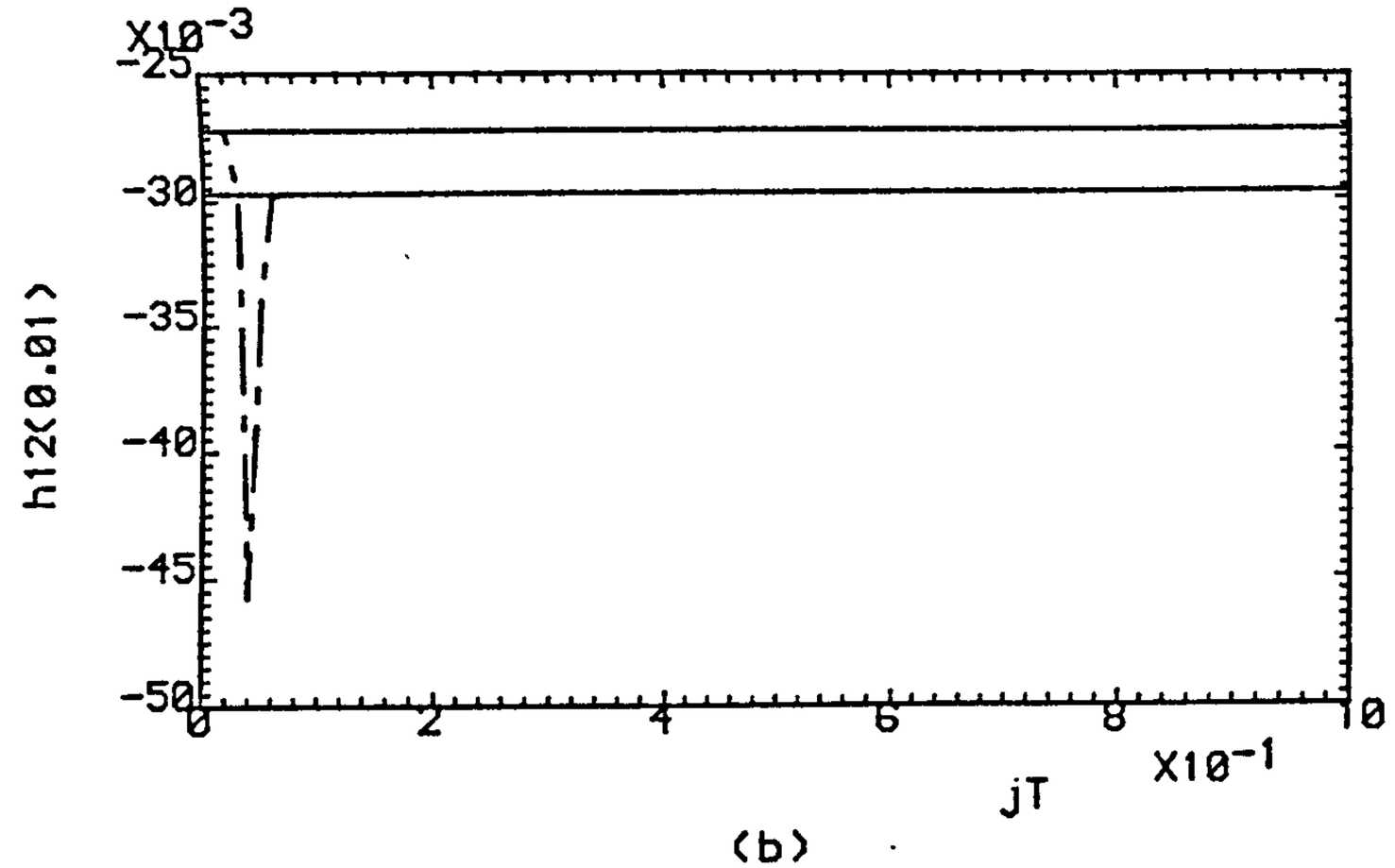

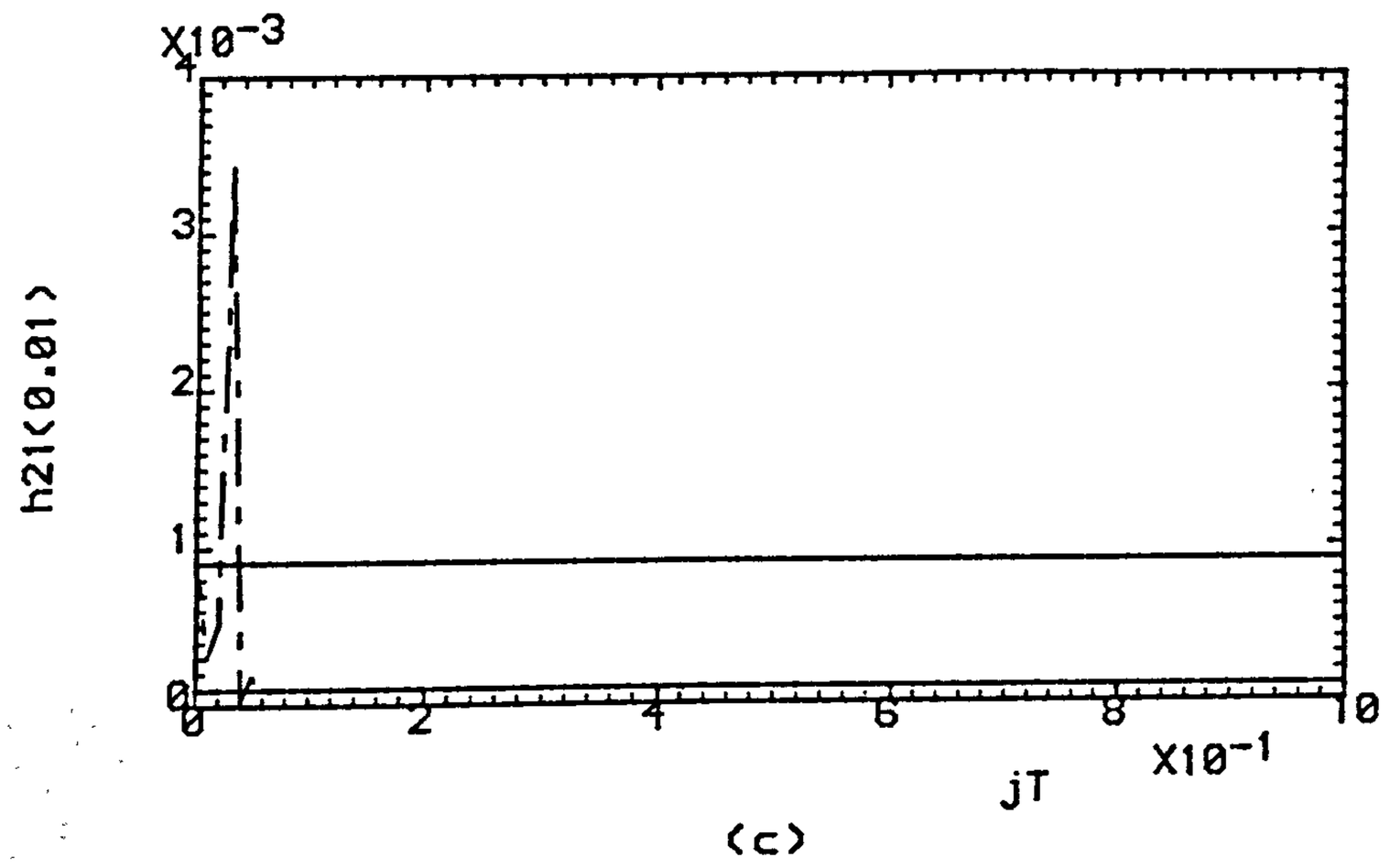

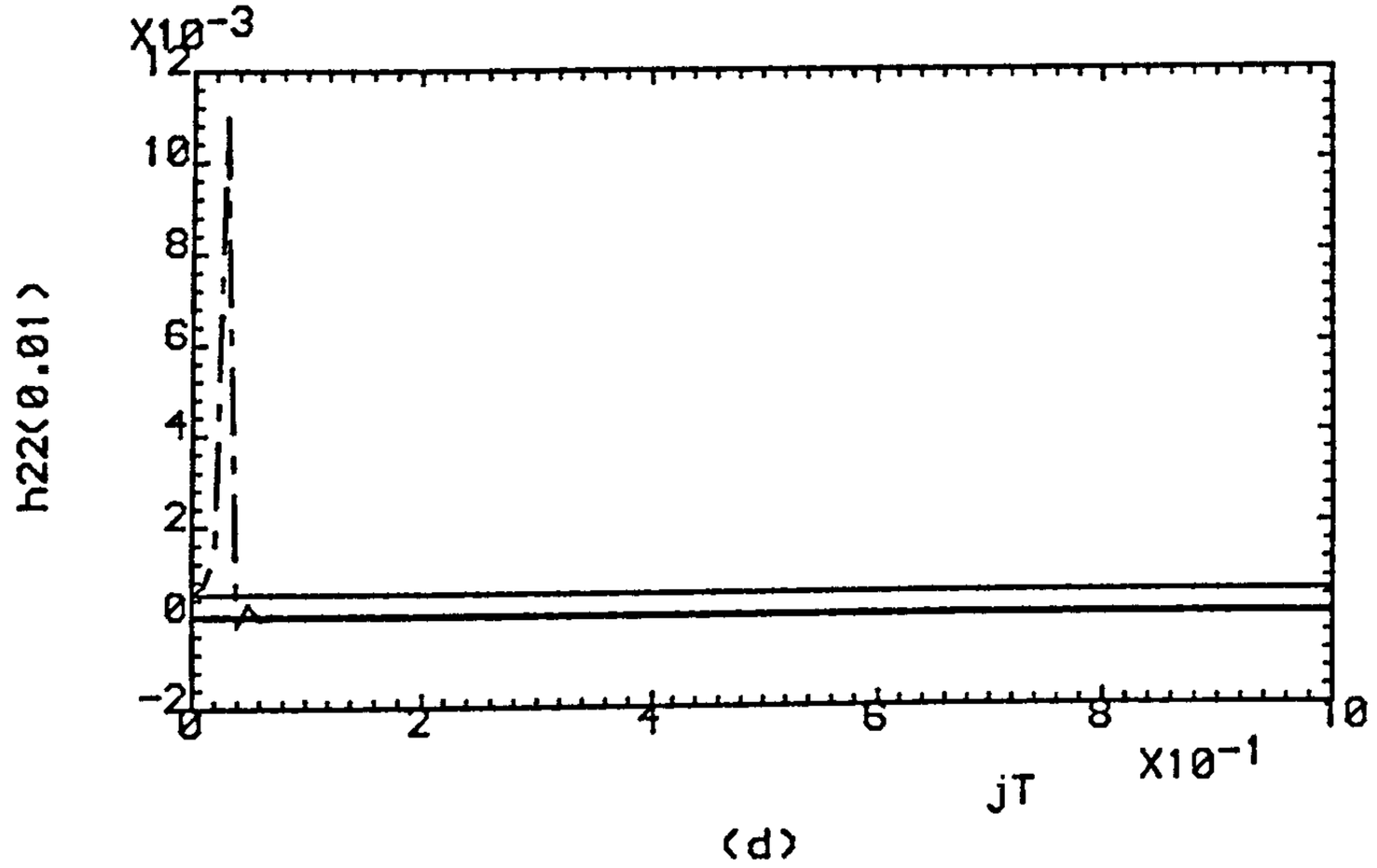

Fig.5.8Succesive Estimates OF Step-Response Matrix
OF Plant Under Adaptive Control.

-·-·- K=1 , ----- K=2 , ... K=3

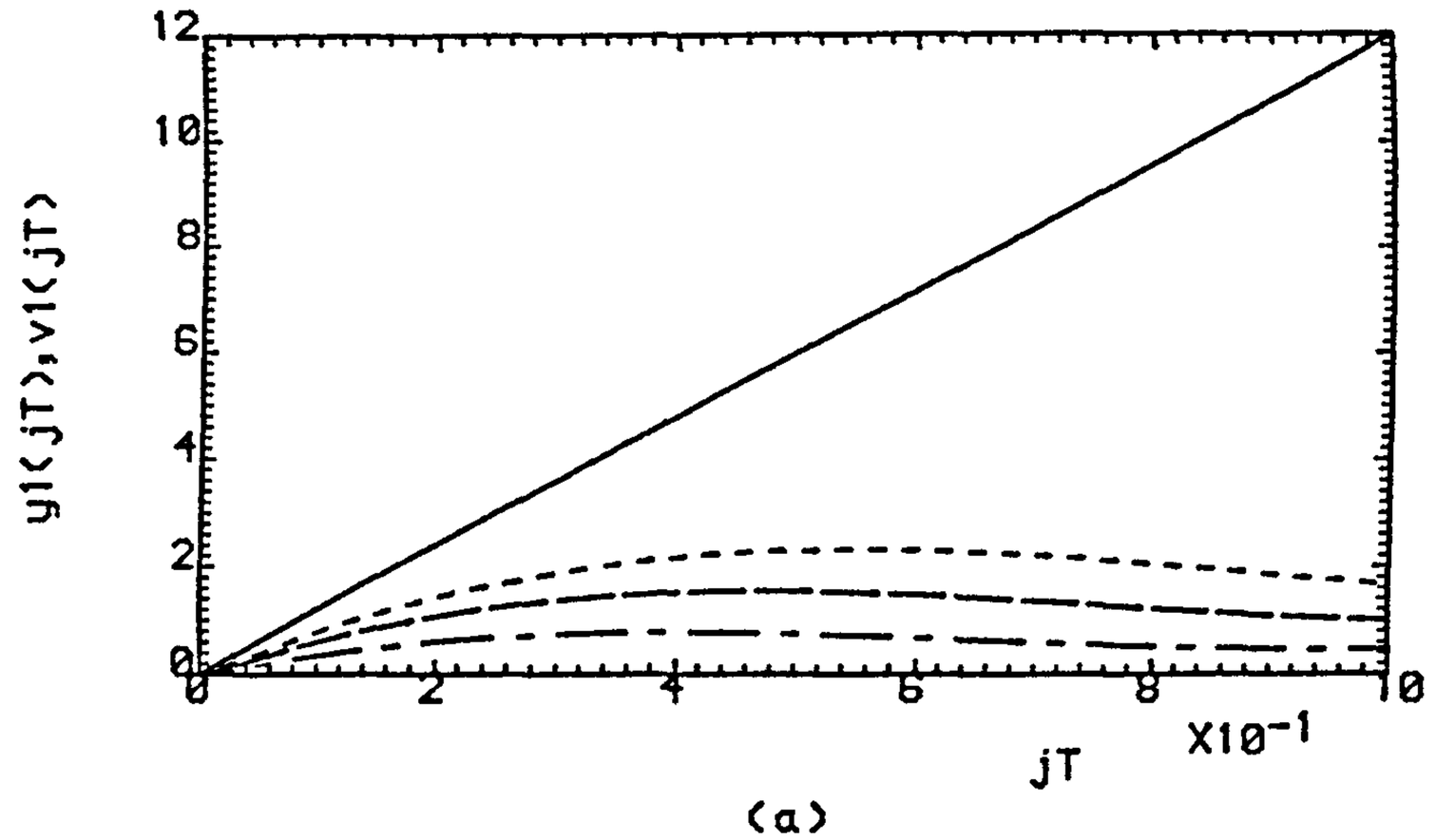

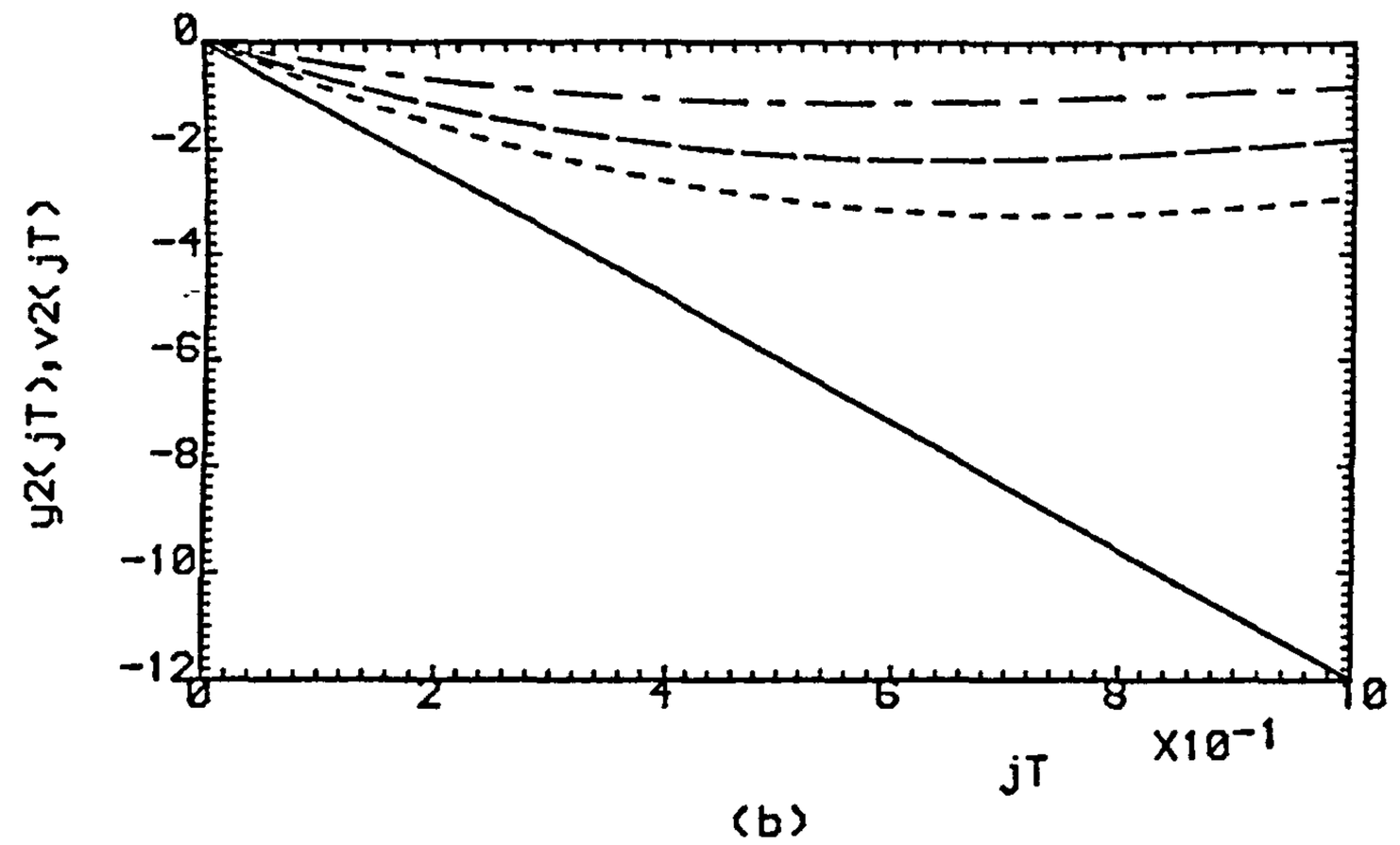

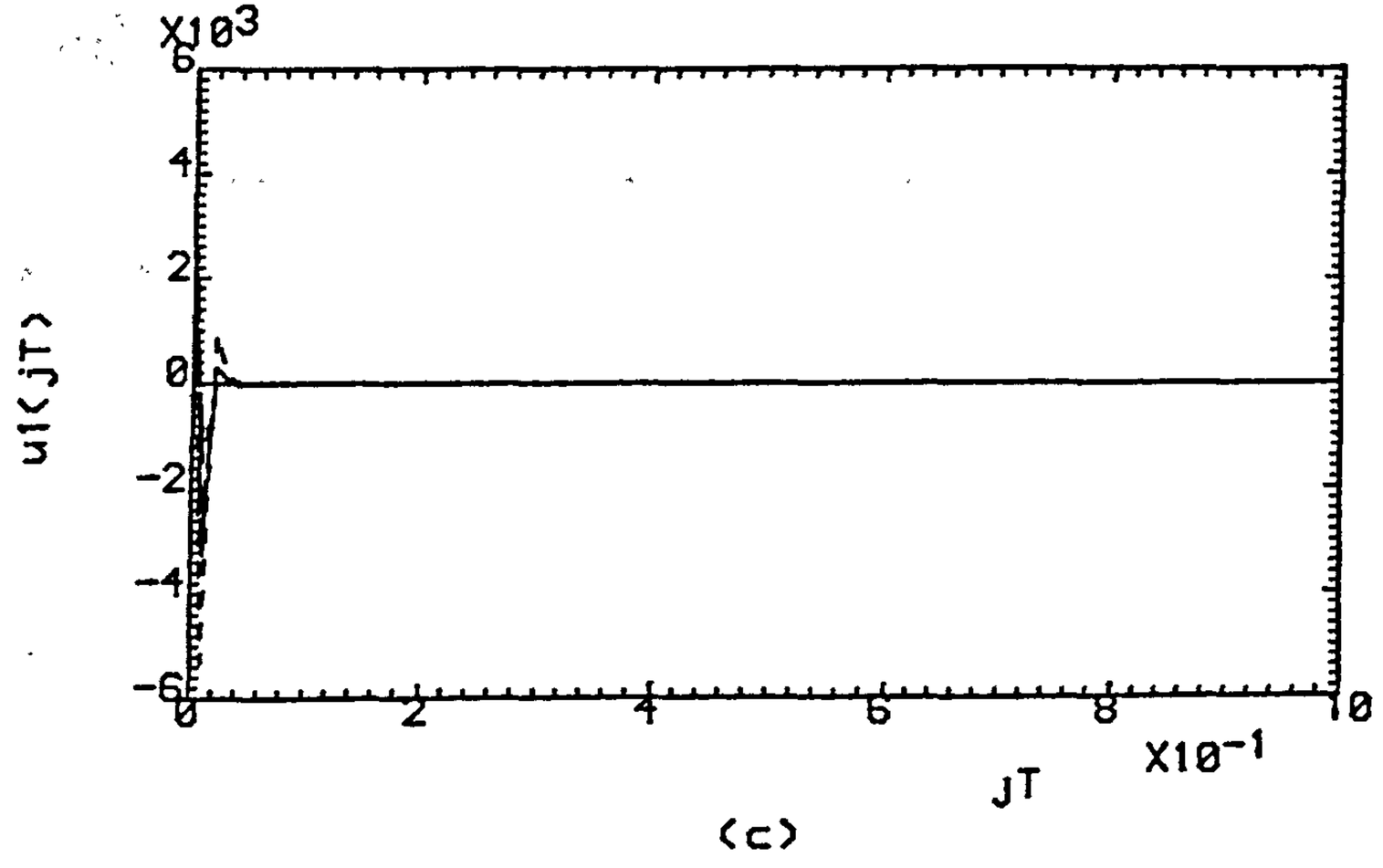

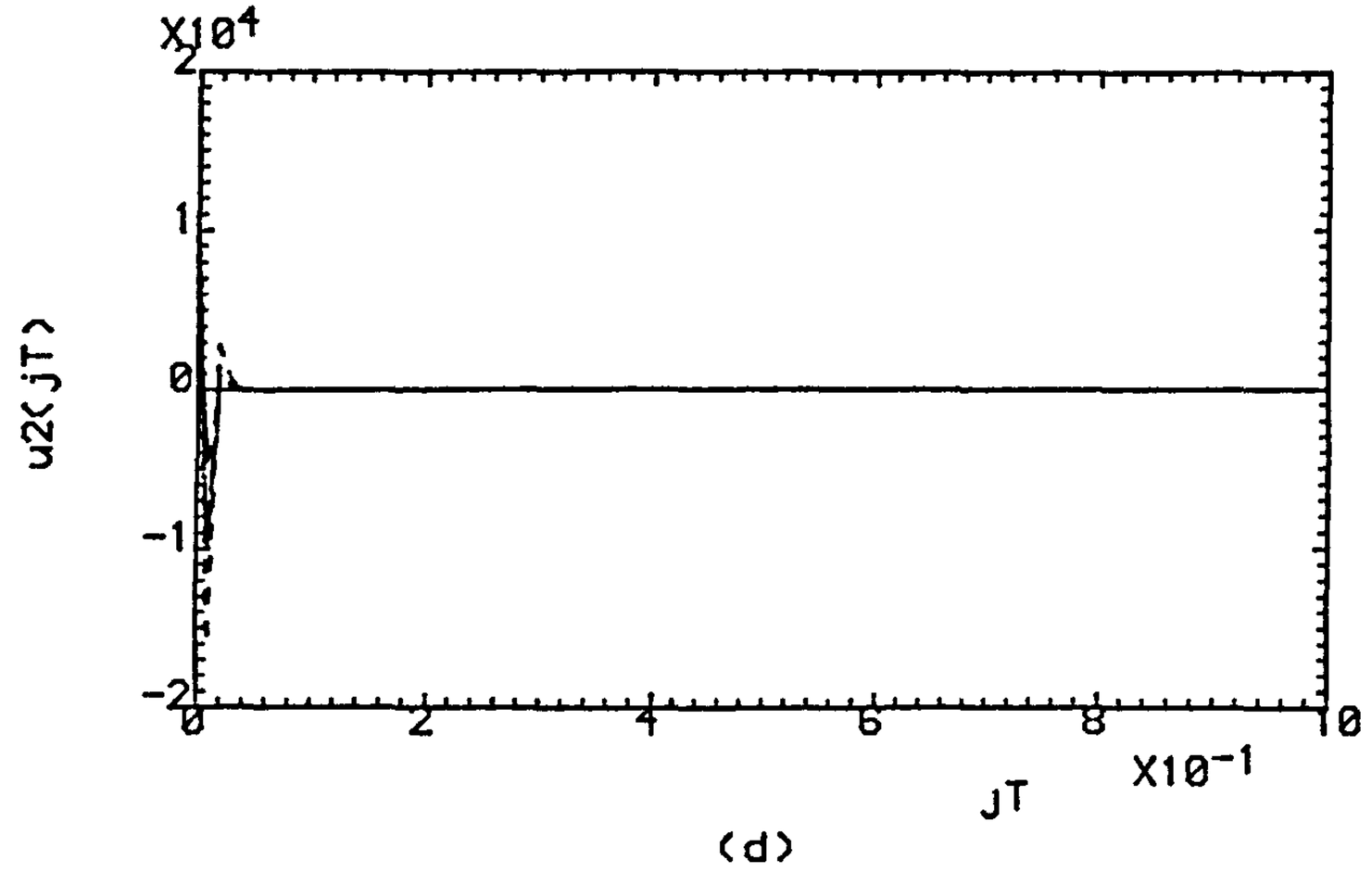

Fig.5.9(a,b) Succesive Outputs OF The Plant.
(c,d) Succesive Control EFforts.
Under Non-Adaptive Control.
-·-·- K=1 , ----- K=2 , ... K=3

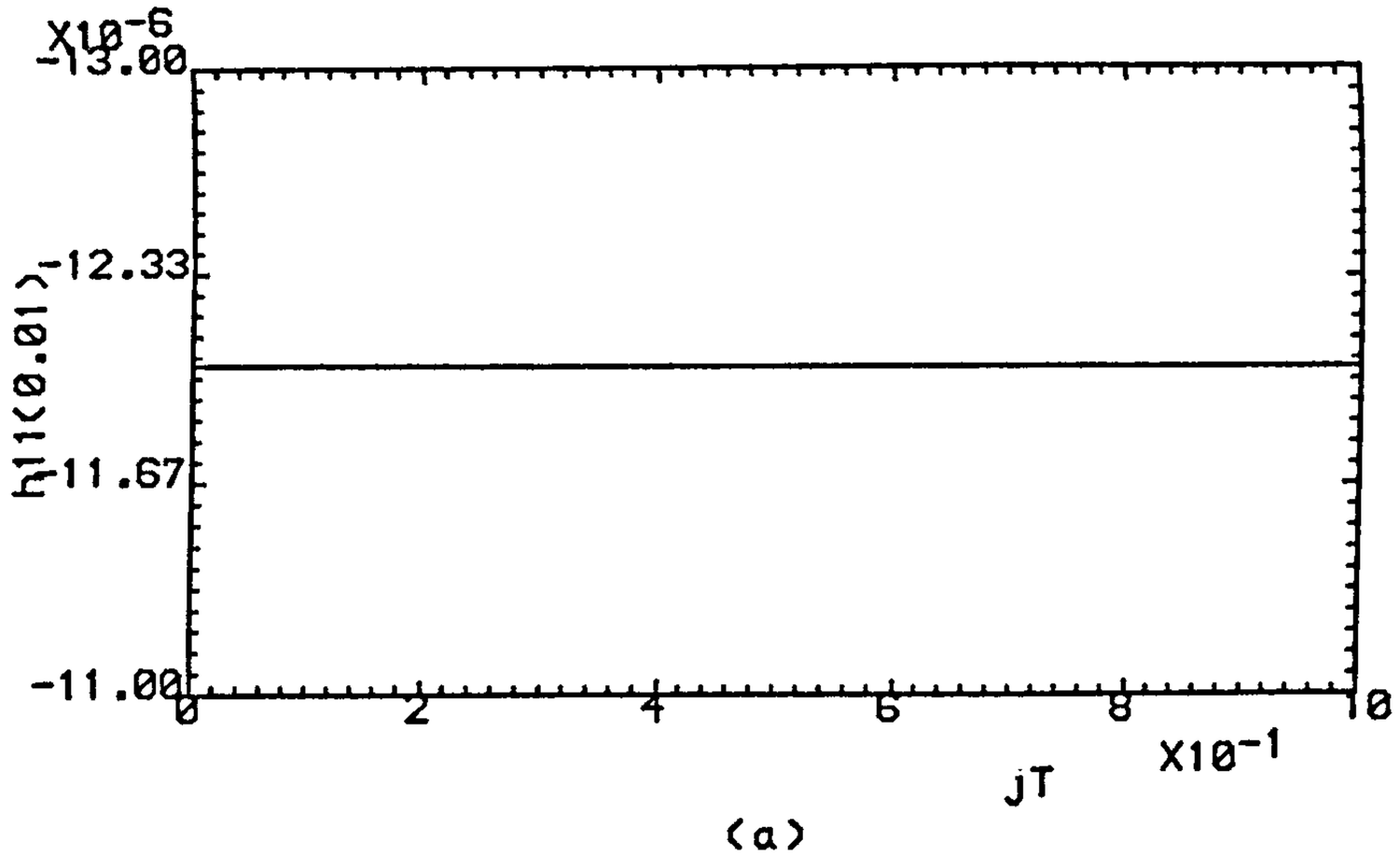

(a)

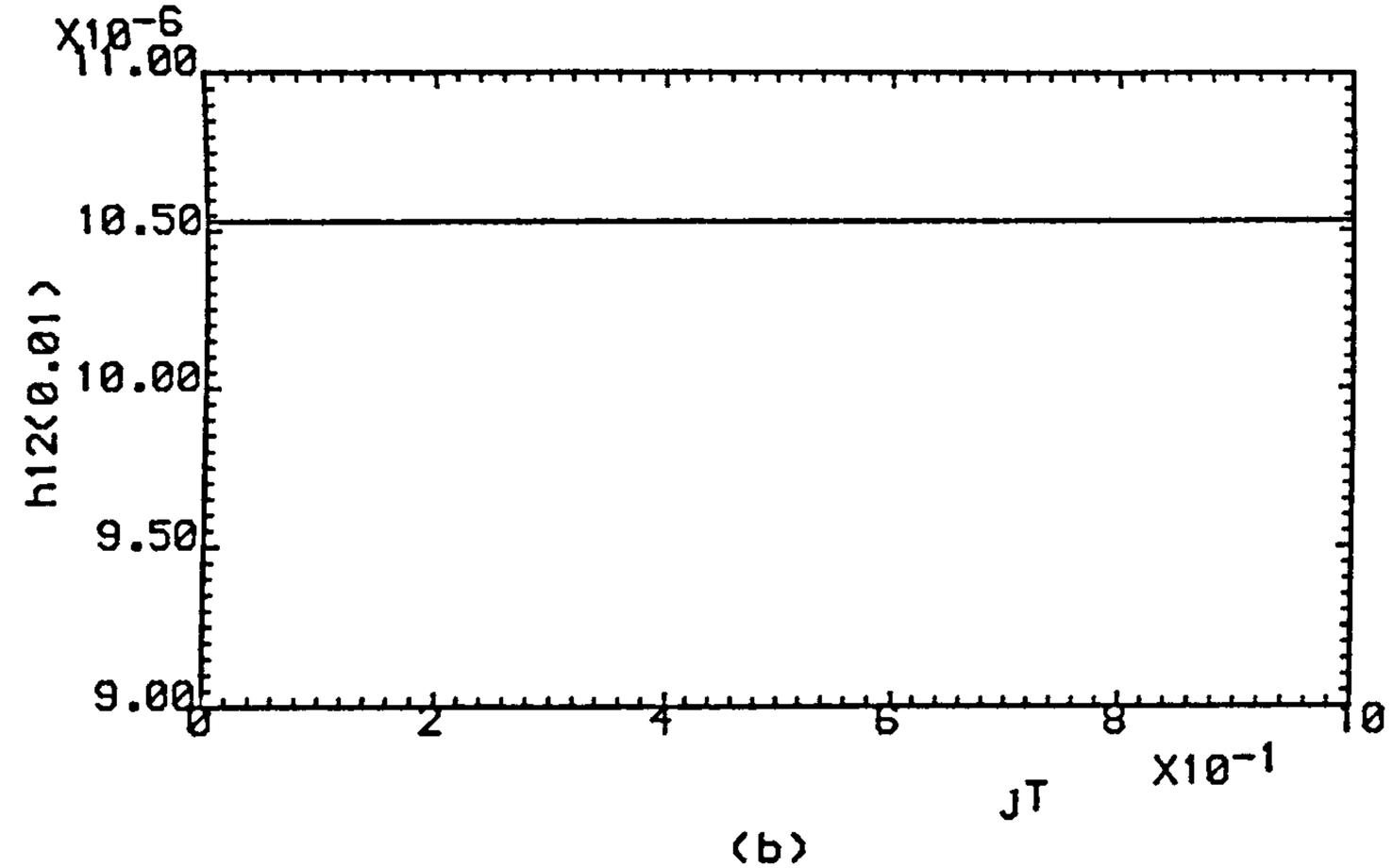

(b)

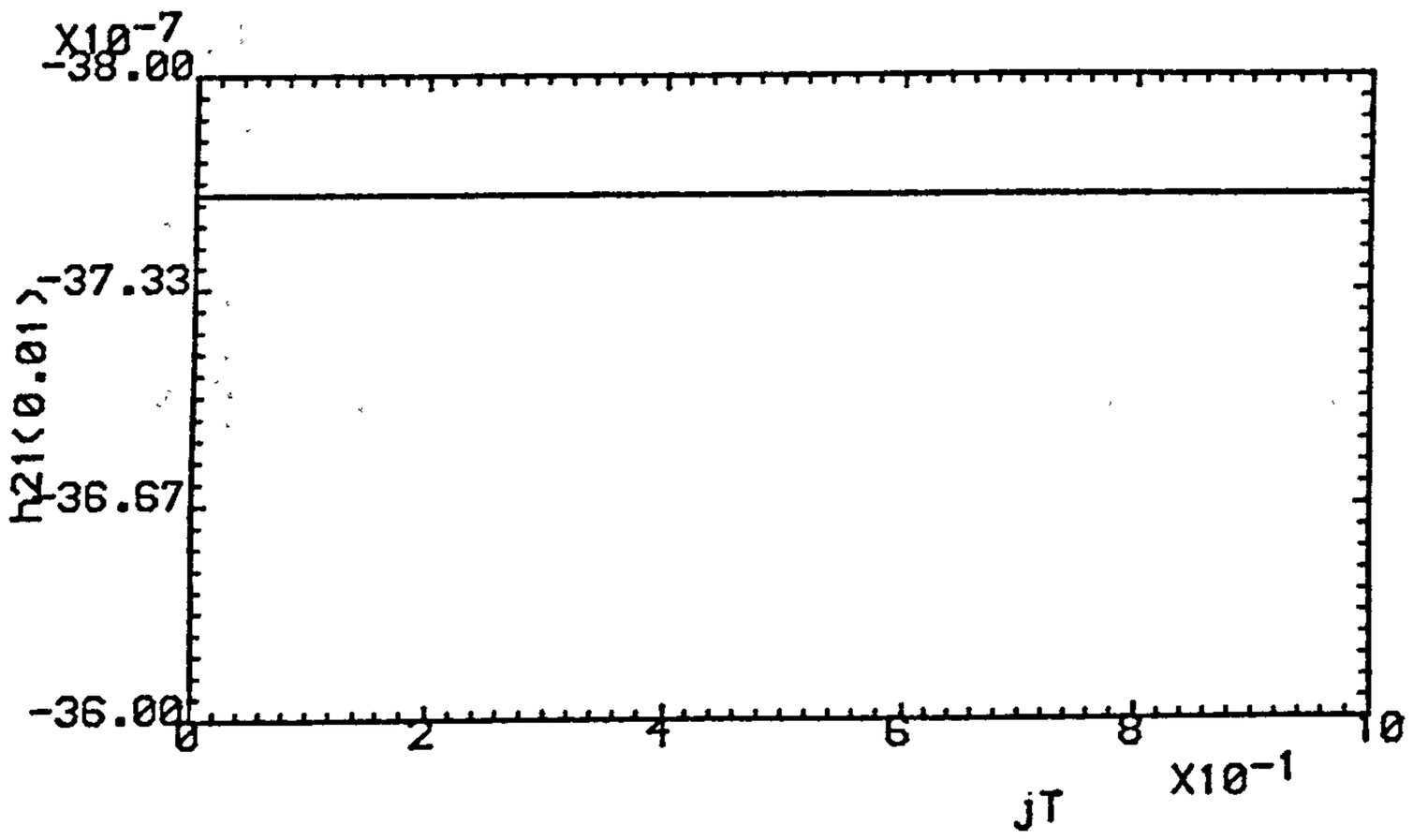

(c)

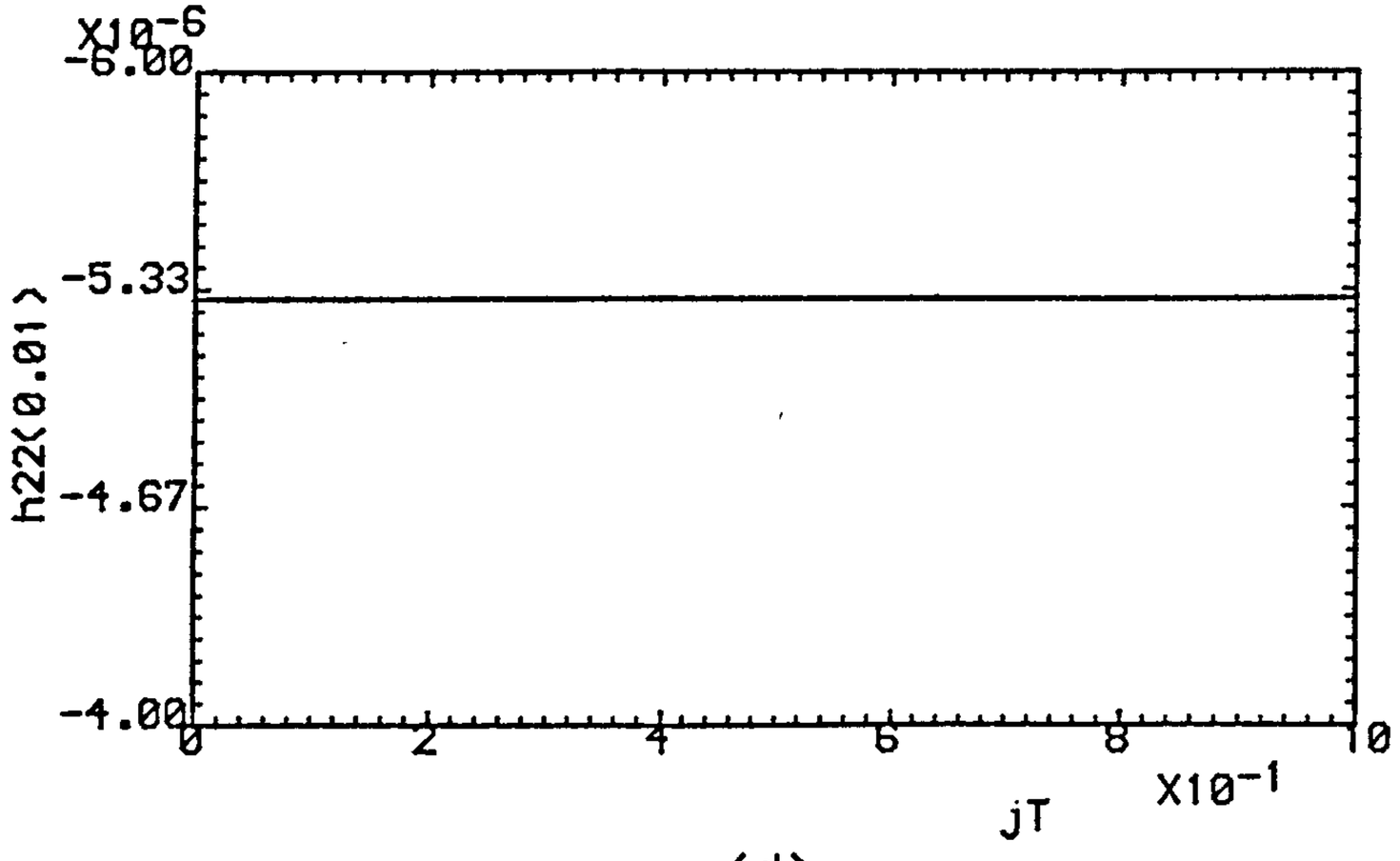

(d)

Fig.5.10 Succesive Estimates Of Step-Response Matrix Of Plant Under Non-Adaptive Control.
-·-·- K=1 , ----- K=2 , ... K=3

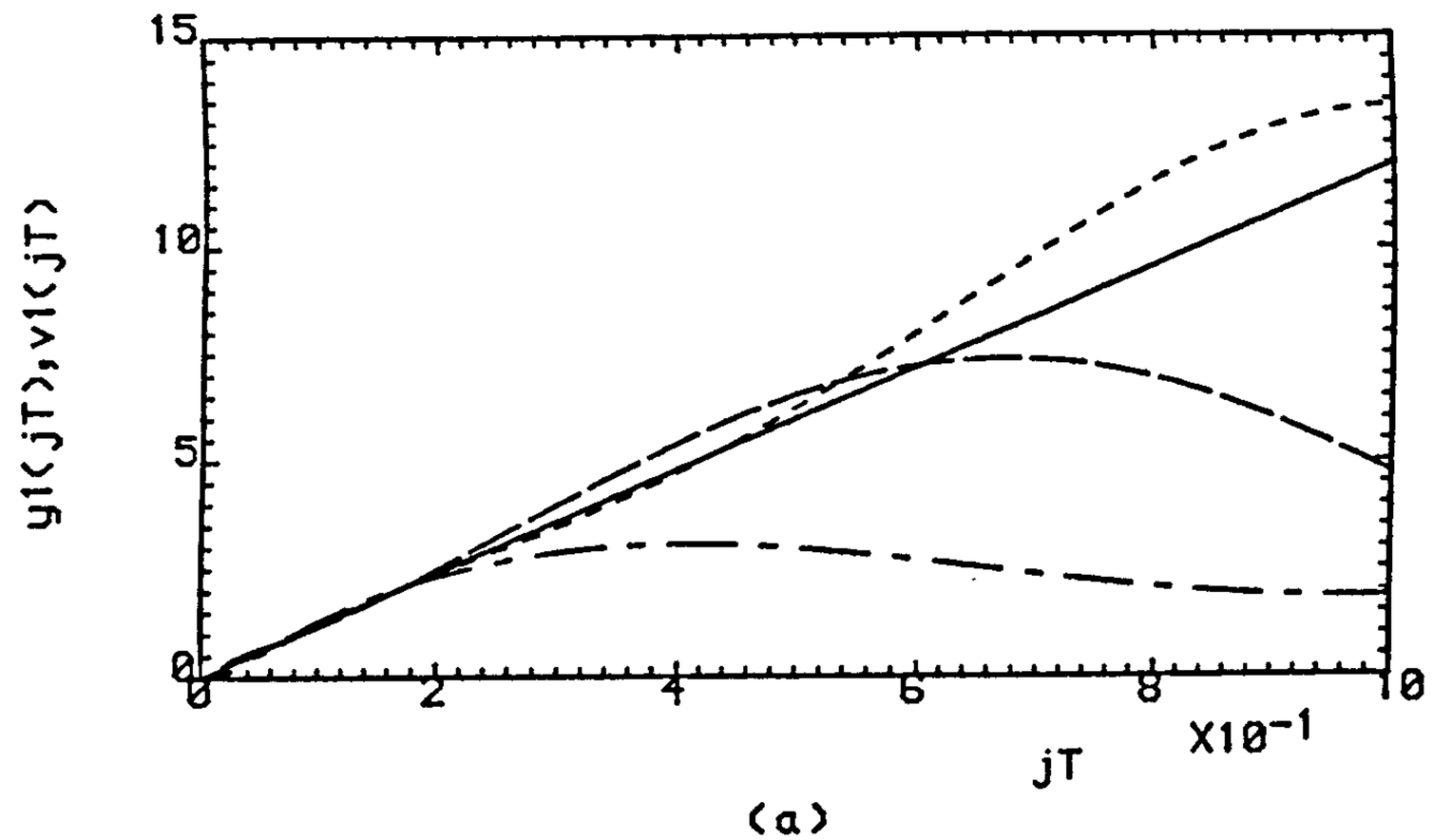

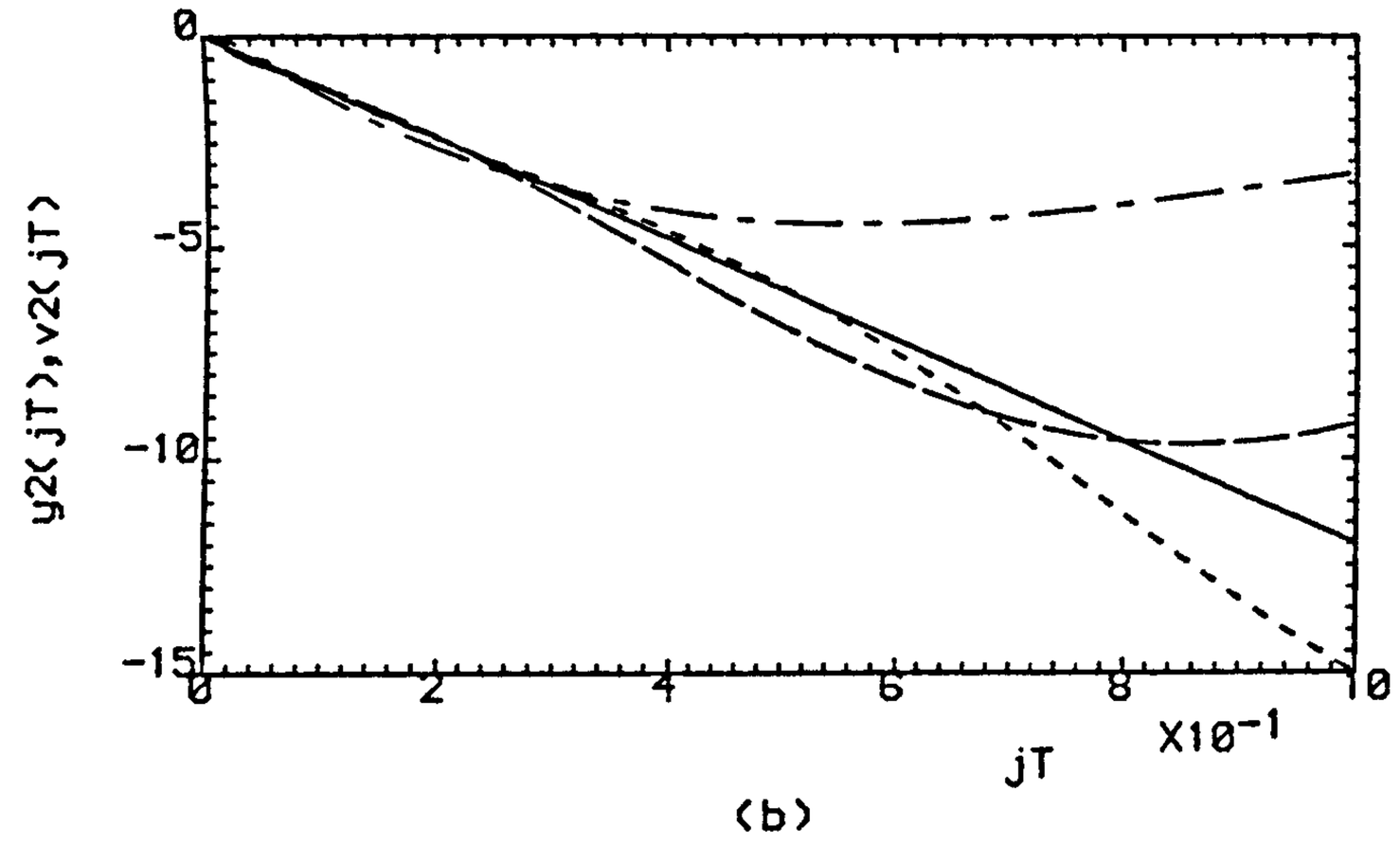

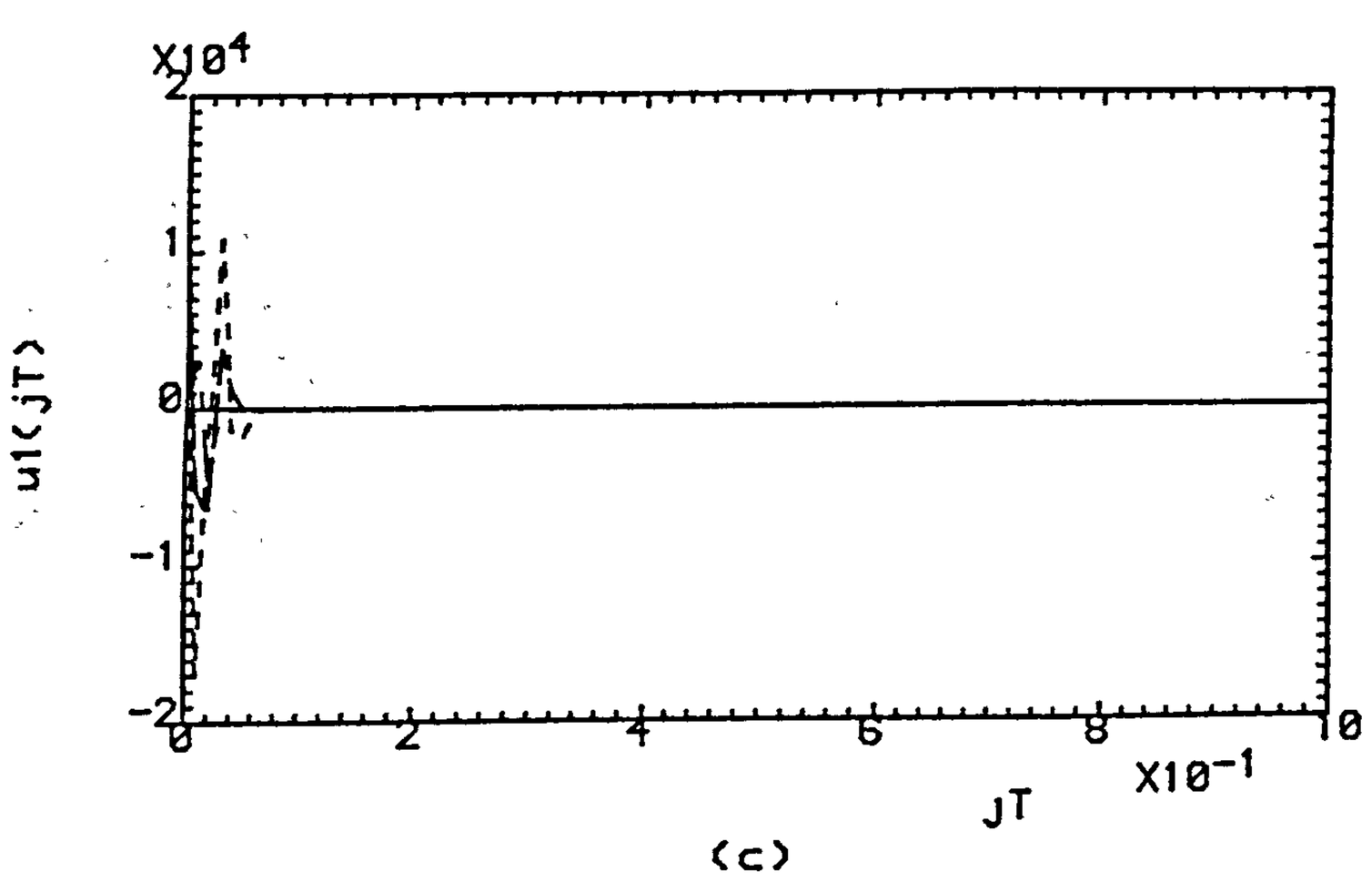

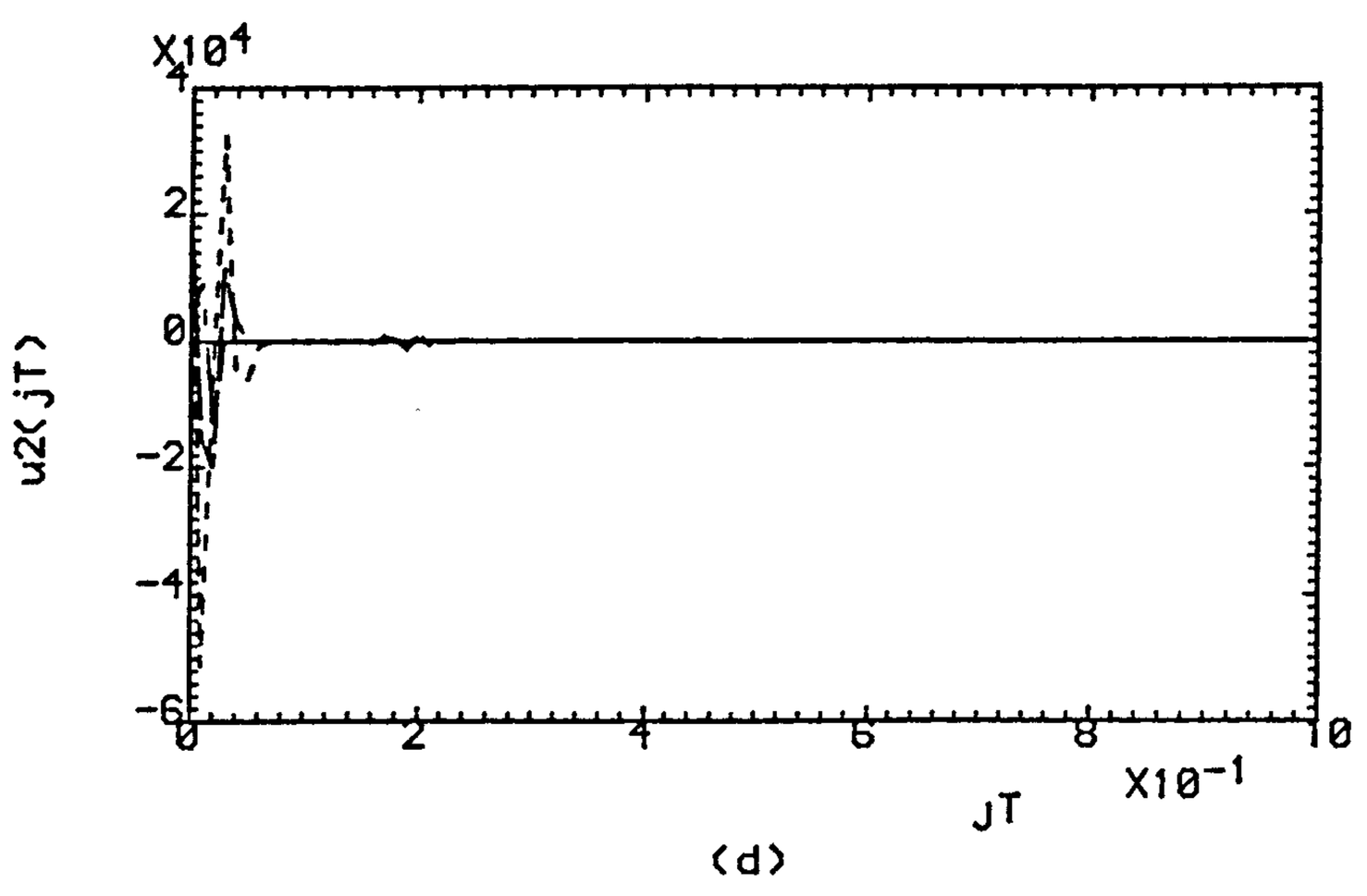

Fig.5.11(a,b) Succesive Outputs Of The Plant.
(c,d) Succesive Control Efforts.
Under Adaptive Control.
-·-·- K=1 , ----- K=2 , ... K=3

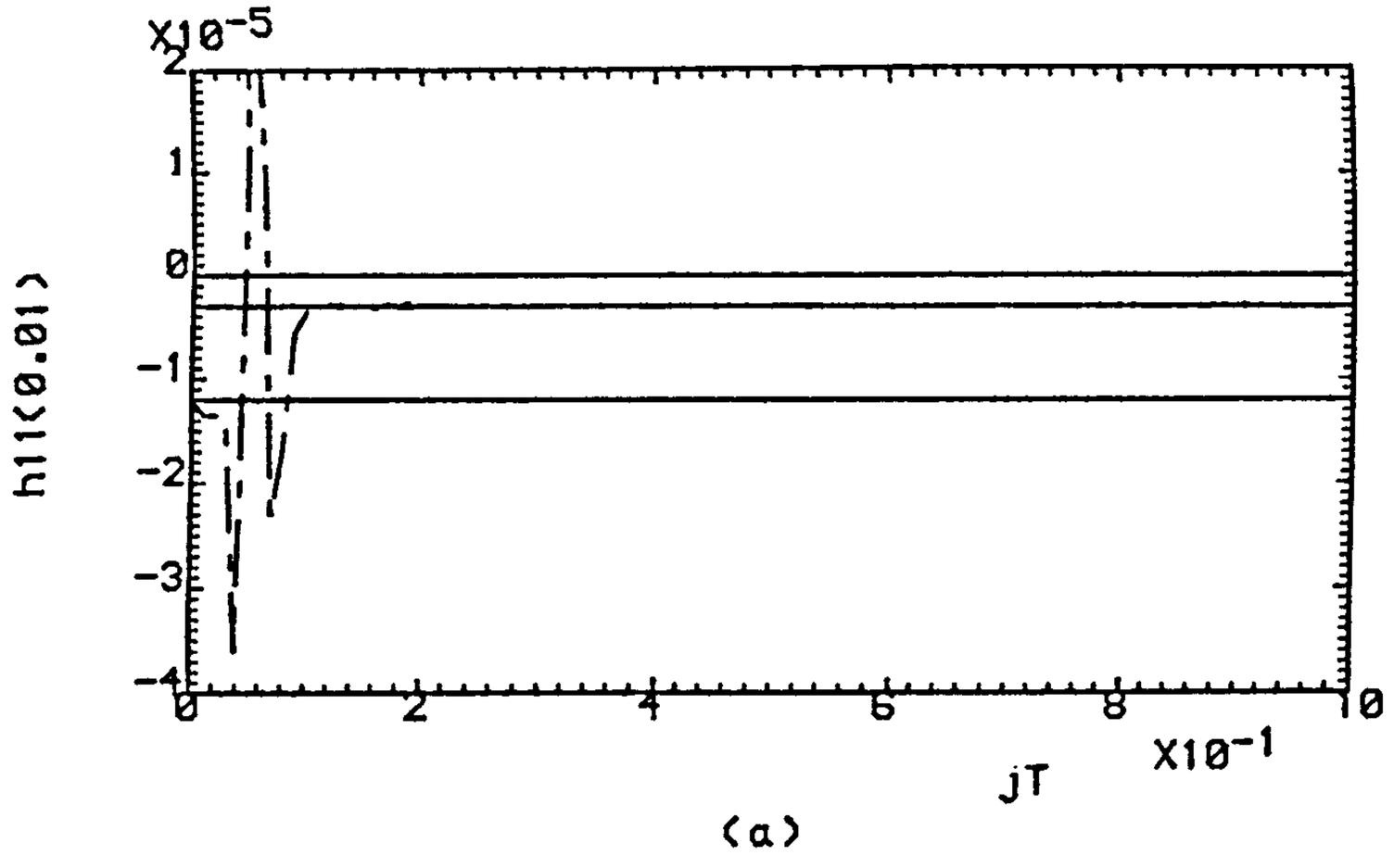

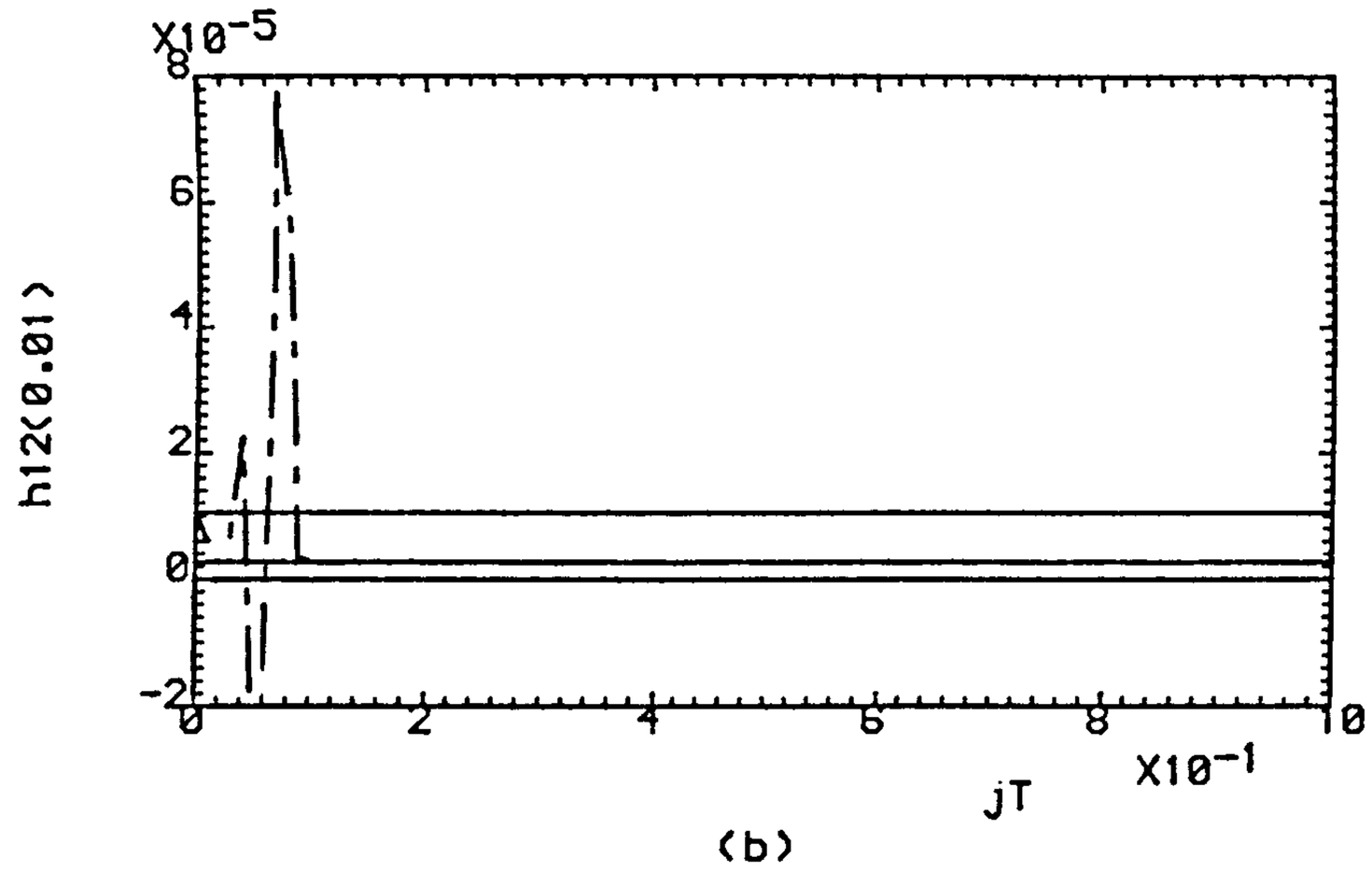

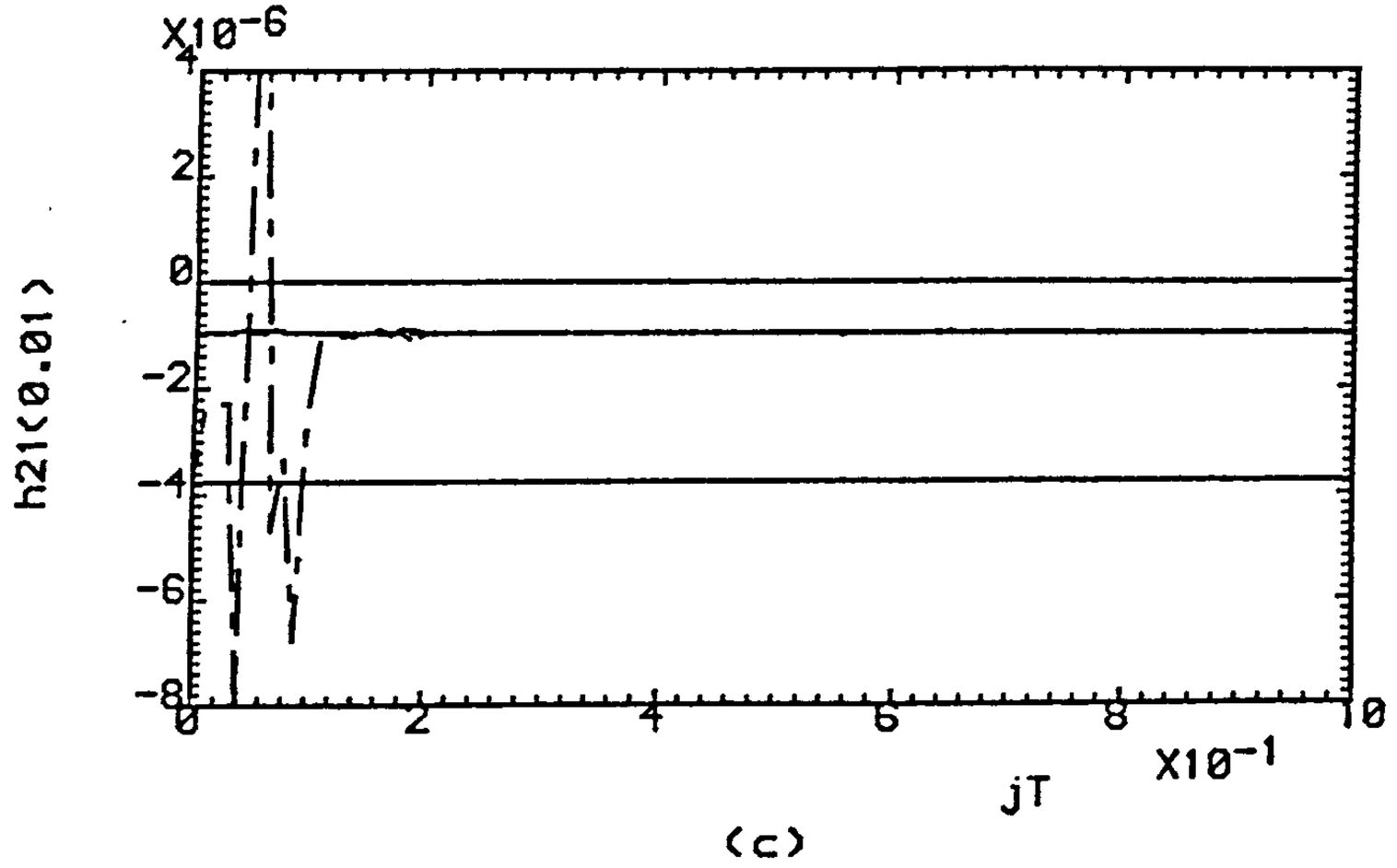

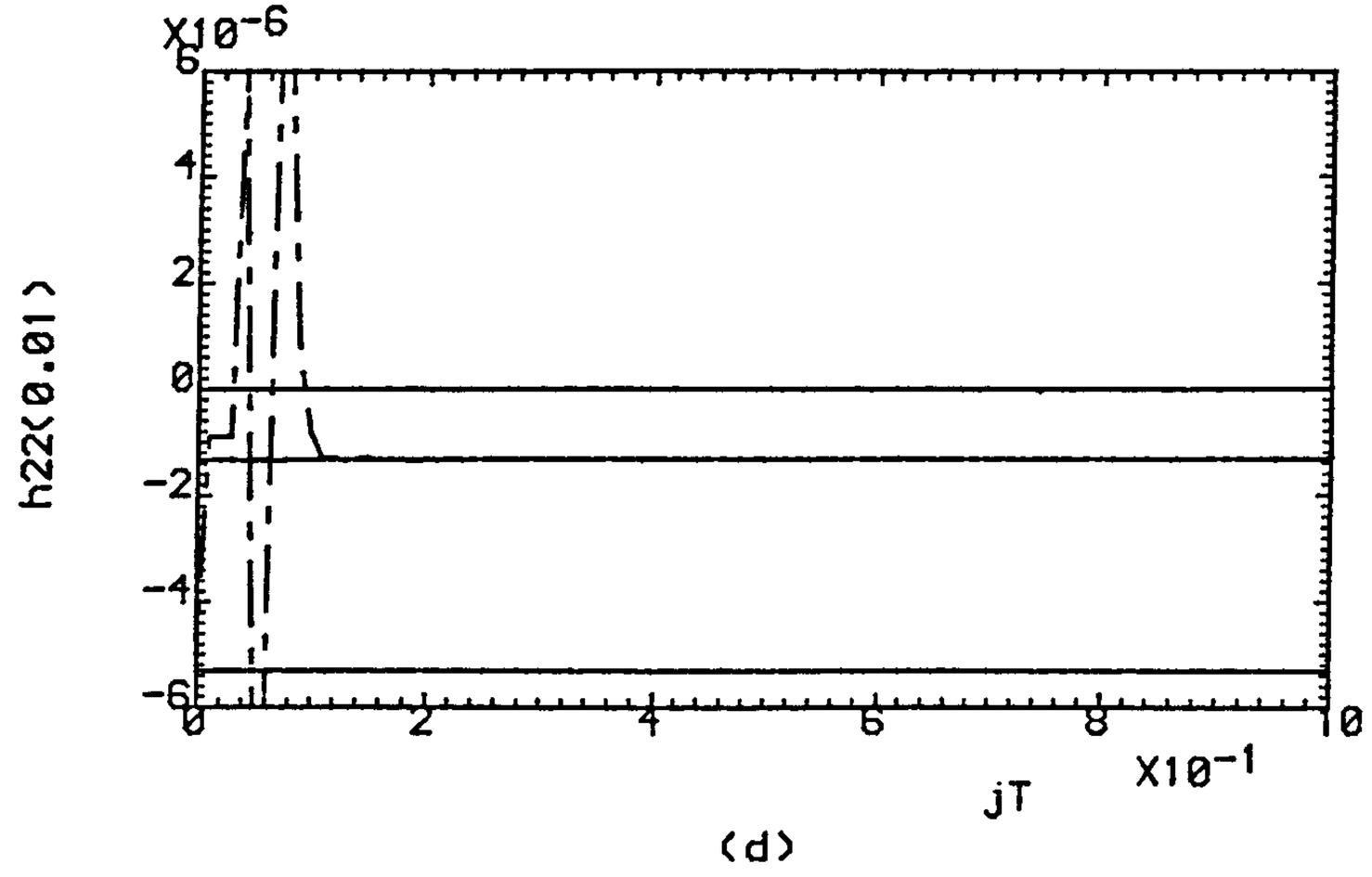

Fig.5.12 Succesive Estimates OF Step-Response Matrix OF Plant Under Adaptive Control.
-·-·- K=1 , ----- K=2 , ... K=3

PART IV

DESIGN STUDIES

CHAPTER 6

DESIGN OF ANALOGUE MODEL-BASED ITERATIVE LEARNING CONTROLLERS FOR ROBOTIC MANIPULATORS

6.1 INTRODUCTION

In Chapters 2, 3, and 4, analogue and digital iterative learning control design methodologies were proposed for linear time-invariant multivariable plants of arbitrary orders of irregularity. These methodologies proved to be effective in designing iterative learning controllers for such plants in the case of repetitive tasks. The most common example of plants with repetitive tasks is the industrial robotic manipulator. Indeed, the vast majority of such manipulators at work in factories repeat their motions over and over in cycles. Unfortunately, whatever errors that may exist in following a trajectory are also repeated from cycle to cycle in the absence of learning control. Therefore, it is important to attempt to design a control scheme that will improve the performance of such manipulators as their actions are repeated. However, these robotic manipulators are highly coupled non-linear devices and therefore the controllers referred to in Chapters 2, 3, and 4 are not directly applicable.

Therefore, in order to apply these controllers to robotic manipulators, the influence of the non-linearities associated with these manipulators must be removed first. It is shown in this chapter that non-linear robotic manipulators can be reduced to linear time-invariant plants under the action of computed-torque control. Moreover, it is shown that such robotic manpulators give rise to completely irregular plants under the action of computed-torque control in both joint and task space co-ordinates. It is therefore evident that the results of Arimoto et al (1984) for the iterative learning control of regular plants are inapplicable in such cases. Indeed, Arimoto et al (1984)

stated that, "*it is impossible to choose the positional variables as outputs in robotic applications and the velocity variables must be chosen instead*". This is because choosing the position variables as output in robotic systems will render the resulting linear plants irregular. However, the results of Chapters 2, 3, and 4 are immediately applicable to the design of iterative learning controllers for irregular linear time-invariant plants. In this chapter, because of the practical difficulties possibly involved in implementing the controllers of Chapter 2 (in which the initial states must be shifted at the beginning of each iteration for learning to occur), the controllers of Chapter 3 are chosen for use. In such controllers, the practical difficulties possibly involved in shifting initial states are circumvented by the introduction of initial impulsive action into the iterative learning process.

The practical relevance of these theoretical results is illustrated in this chapter by designing a model-based iterative learning controller with initial impulsive action for a two-degree-of-freedom robotic manipulator with gravity compensation in both joint and task space co-ordinates. It is also shown that such model-based iterative learning controllers are robust in the sense that rapid learning behaviour is obtained even when crude dynamical models are used. In particular, it is shown that fixed model-based iterative controllers exhibit excellent learning characteristics which emulate those of more complex exact model-based iterative controllers as reduction gear ratios increase.

6.2 ANALYSIS

The dynamics of n-link non-redundant robotic manipulators, driven by armature-controlled DC motors through reduction gearing, are governed by non-linear vector differential equations of the form (Arimoto and Miyazaki (1985))

$$[J_0 + H(q)]\,\ddot{q} + [B_0 + \dot{H}(q)]\,\dot{q} - \frac{\partial T}{\partial q} + g(q) = K_0 r\,. \qquad \ldots(6.1)$$

In this equation, $q \in R^n$ is the vector of joint angles, $H(q) \in R^{n\times n}$ is the inertia matrix of the manipulator, $T = \frac{1}{2}\,\dot{q}^T H(q)\,\dot{q} \in R^n$ is the kinetic energy, $g(q) \in R^n$ is the vector of gravitational torques, $r \in R^n$ is the vector of voltage inputs to the armature circuits. In addition, $B_0 = K^2/\nu^2 R \in R^{n\times n}$, $J_0 = J_m/\nu^2 \in R^{n\times n}$, and $K_0 = K/\nu R \in R^{n\times n}$ are diagonal matrices associated with actuators, where J_m is the motor inertia, R is the motor resistance, K is the torque constant of the motor, and ν is the gear ratio. In order to control such manipulators when their dynamical models are well known, it is possible to implement computed-torque (or inverse dynamics) control laws (Spong and Vidyasagar (1989)) of the form

$$K_0 r = [J_0 + H(q)]\,u + [B_0 + \dot{H}(q)]\,\dot{q} - \frac{\partial T}{\partial q} + g(q) \qquad \ldots(6.2)$$

where $u \in R^n$ is the vector of new inputs. Then, since the inertia matrix is invertible, it follows from equations (6.1) and (6.2) that

$$\ddot{q} = u \qquad \ldots(6.3)$$

This equation indicates that non-linear robotic manipulators become linear time-invariant systems under the action of computed-torque control. Indeed, equation (6.3) is obviously a double-integrator system in joint space.

Similarly, a double-integrator system can also be obtained in task space. Thus, equation (6.1) can be written directly in terms of the end-effector co-ordinates by introducing the relationship between the vector of the end-effector co-ordinates, Ω, and the vector of joint co-ordinates, q, in the form

$$\Omega = \Pi(q) \qquad \ldots(6.4)$$

where the function $\Pi(q)$ represents the forward kinematic equations. In general, this function can only be determined uniquely in a region free from kinematic singularities. Then, taking the first and second derivatives of (6.4) yields

$$\dot{\Omega} = J(q)\,\dot{q} \qquad \ldots(6.5)$$

and

$$\ddot{\Omega} = J(q)\,\ddot{q} + \dot{J}\,\dot{q} \qquad \ldots(6.6)$$

where $J(q)$ is the manipulator Jacobian . But it follows from equation (6.1) that

$$\ddot{q} = (J_0 + H(q))^{-1}\left[K_0 r - (B_0 + \dot{H}(q))\dot{q} + \frac{\partial T}{\partial q} - g(q)\right] \qquad \ldots(6.7)$$

and therefore from equation (6.6) that

$$\ddot{\Omega} = J(q)\,(J_0 + H(q))^{-1}\left[K_0 r - (B_0 + \dot{H}(q))\,\dot{q} + \frac{\partial T}{\partial q} - g(q)\right] + \dot{J}(q)\,\dot{q}\ . \qquad \ldots(6.8)$$

Equation (6.8) can now be re-written concisely as

$$M(\Omega)\,\ddot{\Omega} + h\,(\Omega,\dot{\Omega}) = F \qquad \ldots(6.9)$$

where

$$F = (J^{T}(q))^{-1}\,K_0 r \quad , \qquad \ldots(6.10a)$$

$$M(\Omega) = (J^{T}(q))^{-1}\,[J_0 + H(q)]\,(J(q))^{-1} \quad , \qquad \ldots(6.10b)$$

and

$$h(\Omega,\dot{\Omega}) = (J^T(q))^{-1}\left[(B_0 + \dot{H}(q))\dot{q} - \frac{\partial T}{\partial q} + g(q)\right] -$$

$$(J^T(q))^{-1}\,[J_0 + H(q)]\,(J(q))^{-1}\,\dot{J}(q)\,(J(q))^{-1}\,\dot{\Omega} \quad . \quad \text{...(6.10c)}$$

Now, to obtain the double-integrator system in task space, F may be written as

$$F = M(\Omega)u + h(\Omega,\dot{\Omega}) \quad . \quad \text{...(6.11)}$$

Substituting (6.11) in (6.9) then yields

$$\ddot{\Omega} = u \quad \text{...(6.12)}$$

where $u \in R^n$ is the vector of new inputs. Equation (6.12) is obviously a double-integrator system in task space.

It is thus evident that any technique for the design of controllers for linear time-invariant plants can be applied to 'equivalent' systems governed by equations of the form (6.3) or (6.12) in both joint and task space co-ordinates, respectively. In particular, the theory of iterative learning control for linear time-invariant plants can be used. Indeed, equations (6.3) and (6.12) can obviously be expressed in the state-space form

$$\begin{bmatrix} \dot{q}(t) \\ \ddot{q}(t) \end{bmatrix} = \begin{bmatrix} 0 & , & I_n \\ 0 & , & 0 \end{bmatrix}\begin{bmatrix} q(t) \\ \dot{q}(t) \end{bmatrix} + \begin{bmatrix} 0 \\ I_n \end{bmatrix} u(t) \quad , \quad \text{...(6.13a)}$$

$$y(t) = [I_n, 0]\begin{bmatrix} q(t) \\ \dot{q}(t) \end{bmatrix} \quad , \quad \text{...(6.13b)}$$

and

$$\begin{bmatrix} \dot{\Omega}(t) \\ \ddot{\Omega}(t) \end{bmatrix} = \begin{bmatrix} 0 , & I_n \\ 0 , & 0 \end{bmatrix} \begin{bmatrix} \Omega(t) \\ \dot{\Omega}(t) \end{bmatrix} + \begin{bmatrix} 0 \\ I_n \end{bmatrix} u(t) \quad , \qquad \text{...(6.14a)}$$

$$y(t) = [I_n, 0] \begin{bmatrix} \Omega(t) \\ \dot{\Omega}(t) \end{bmatrix} \quad , \qquad \text{...(6.14b)}$$

respectively. It is therefore evident from equations (6.13) and (6.14) that the first and second Markov parameters of both systems are, respectively,

$$M_1 = [I_n, 0] \begin{bmatrix} 0 \\ I_n \end{bmatrix} = 0 \qquad \text{...(6.15a)}$$

and

$$M_2 = [I_n, 0] \begin{bmatrix} 0 , & I_n \\ 0 , & 0 \end{bmatrix} \begin{bmatrix} 0 \\ I_n \end{bmatrix} = I_n \quad . \qquad \text{...(6.15b)}$$

These results indicate that robotic manipulators give rise to completely irregular linear time-invariant plants under the action of computed-torque control in both joint and task spaces. This implies immediately that the results of Arimoto et al (1984) for the iterative learning control of regular plants are inapplicable in such cases.

However, the results of Chapter 3 are directly applicable to the design of iterative learning controllers for irregular linear time-invariant plants. The precise conditions under which learning occurs in such iterative controllers are established in Chapter 3, Theorem 3.1, which is re-stated here for convenience. In the following T_t is the duration of the task:

Theorem

In the case of the plant with state and output equations

$$\dot{x}_k(t) = Ax_k(t) + B\,u_k(t) \qquad \text{...(6.16a)}$$

and

$$y_k(t) = C\,x_k(t) \qquad \text{...(6.16b)}$$

under the action of the control law

$$u_{k+1}(t) = u_k(t) + K_1\dot{e}_k(t) + K_2\tilde{e}_k(t) + K_2\dot{e}_k(0)\,\delta(t) \qquad \text{...(6.17)}$$

where $\delta(t)$ is the Dirac delta function and

$$e_k(t) = v(t) - y_k(t)$$

assume that

(i) $u_0(t)$ is continuous on $[0,T_t]$ and $v(t)$, $\dot{v}(t)$ are continuously differentiable on $[0,T_t]$;

(ii) $CBK_2 = 0$;

(iii) $x_0(0)$ is such that $y_0(0) = v(0)$;

(iv) $x_{k+1}(0) = x_k(0)$ $(k = 0,1,2,...)$;

(v) $\| I_n - CBK_1 - CABK_2 \|_\infty < 1$.

Then,

$$y_k(t) \to v(t)$$

uniformly in $t \in [0, T_t]$ as $k \to \infty$.

Hence, it follows from this analysis that the control law for robotic manipulators consists of two parts. The first part is the model-based controller which is governed by equations (6.2) and (6.11) in joint and task spaces, respectively; and the second part is the iterative learning controller which is governed by equation (6.17). Thus, in the case of robotic manipulators under the action of computed-torque control, it is immediately evident from equations (6.13) and (6.14) for both joint and task spaces, respectively, that iterative learning controllers with any $K_1 \in R^{n \times n}$ and $K_2 = I_n$ satisfy this theorem in the sense that $CBK_2 = 0$ and $\| I_n - CBK_1 - CABK_2 \|_\infty = 0$. Therefore, if these values of K_1 and K_2 are used in equation (6.17) to determine u_k, it follows from equation (6.12) that iterative learning control of robotic manipulators occurs in joint space when the vector of voltage inputs are given by

$$K_0 r_k = (J_0 + H(q)) u_k + (B_0 + \dot{H}(q)) \dot{q} - \frac{\partial T}{\partial q} + g(q) \qquad \ldots(6.18)$$

in the kth iteration.

This equation governs the behaviour of <u>exact</u> model-based controllers which are clearly devices with complex time-varying non-linear characteristics. However, the introduction of reduction gearing makes it possible to implement <u>approximate</u> model-based controllers with simpler time-invariant linear characteristics governed by equations of the form

$$K_0 r_k = J_0 u_k + B_0 \dot{q}_k \qquad \ldots(6.19)$$

These approximate model-based controllers emerge as a result of increasing the reduction gear ratio which makes J_0 and B_0 more dominant than $H(q)$ and $\dot{H}(q)$,

respectively. Moreover, it is clear from equation (6.19) that the torques due to gravity and kinetic energy are neglected in this case. The robustness of these approximate controllers governed by equation (6.19) when the reduction gear ratio increases is investigated in detail in Section 6.3.

Similarly, with the same choice of K_1 and K_2, it follows from equation (6.11) that iterative learning control occurs in task space when the inputs are governed by

$$F_k = M(\Omega_k)\, u_k + h(\Omega_k, \dot{\Omega}_k) \qquad ...(6.20)$$

in the kth iteration. This equation, as in joint space, governs the behaviour of exact model-based controllers. However, as the reduction gear ratio increases, it is possible to implement approximate model-based controllers which are much simpler than those governed by equation (6.20) in order to control robotic manipulators in task space. Such approximate model-based controllers are governed by equations of the form

$$F_k = (J^T(q))^{-1} [J_0(J(q))^{-1}\, u_k + B_0\, \dot{q} + J_0(J(q))^{-1}\, \dot{J}(q)\dot{q}] \ . \qquad (6.21)$$

These approximate model-based controllers emerge as a result of the domination of J_0 and B_0 over $H(q)$ and $\dot{H}(q)$ in equations (6.10b) and (6.10c), respectively, as the reduction gear ratio increases. Moreover, it is clear from equation (6.21) that the torques due to gravity and kinetic energy are neglected in this case.

The robustness of these approximate controllers governed by equation (6.21) when the reduction gear ratio increases is investigated in detail in Section 6.3. However, when robotic manipulators are direct-drive devices with no reduction gearing, their full dynamics in joint or task space must be used in exact model-based controllers (ie, control-law equation of the form (6.18) or (6.20) must be used).

6.3 ILLUSTRATIVE EXAMPLES

These theoretical results can be conveniently illustrated by considering the iterative learning control of the planar motions of a two-link manipulator in both joint and task space. In addition, armature-controlled dc motors with reduction gearing and direct-drive servo motors are used to drive the robot arm. The dc motor in use for both joints is such that $J_m = 6.204\times10^{-4}\ Kg.m^2$ is the motor inertia, R = 2.7 *ohm* is the motor resistance, and K = 0.23033 *N.m/amp* is the torque constant of the motor. Moreover, the inductance of the motor is ignored and the gear ratio for both joints is $\nu = n_1/n_2 = \omega_{output}/\omega_{input}$. These dc motors with gearing are used in order to make the task of the iterative learning controller as easy as possible by attenuating the effect of the manipulator's non-linearities as the reduction gear ratio increases. On the other hand, direct-drive servo motors are used in order to make the task of the iterative learning controller as difficult as possible by not attenuating the effects of the manipulator's non-linearities by the introduction of reduction gearing. In addition, the two-link manipulator under investigation has $\ell_1 = \ell_2 = 0.432\ m$, $m_1 = 15.91\ Kg$ and $m_2 = 11.36\ Kg$ where (ℓ_1,ℓ_2) are the lengths and (m_1,m_2) are the masses of links 1 and 2, respectively. These values correspond to links 2 and 3 of the Unimation PUMA 560 manipulator (Seraji (1986)).

The behaviour of the manipulator is governed by the non-linear vector differential equation

$$H(q)\,\ddot{q} + \dot{H}(q)\,\dot{q} - \frac{\partial T}{\partial q} + g(q) = \tau \quad , \qquad \ldots(6.22)$$

where

$$H(q) = \begin{bmatrix} J_1+J_2\,(1+3\,\eta^2) + 3\,J_2\eta\,Cosq_2, & J_2\left[1 + \frac{3}{2}\,\eta\,\mathrm{Cos}\,q_2\right], \\ J_2\left[1 + \frac{3}{2}\,\eta\,\mathrm{Cos}\,q_2\right] & , \qquad J_2 \end{bmatrix}, \qquad \ldots(6.23)$$

$$g(q) = \begin{bmatrix} \frac{1}{2}\,m_2\,\ell_2\,g\,\cos\,(q_1+q_2) + \left[\frac{1}{2}\,m_1 + m_2\right]\ell_1 g\,\cos\,q_1 \\ \frac{1}{2}\,m_2\,\ell_2\,g\,\cos\,(q_1+q_2) \end{bmatrix}, \qquad \ldots(6.24)$$

and

$$\dot{H}(q)\dot{q} - \frac{\partial T}{\partial q} = \begin{bmatrix} -3\,J_2\,\eta\left[\dot{q}_1 + \frac{1}{2}\,\dot{q}_2\right]\dot{q}_2 \sin\,q_2 \\ \frac{3}{2}\,J_2\,\eta\,\dot{q}_1\,\sin\,q_2 \end{bmatrix}, \qquad \ldots(6.25)$$

in which $J_1 = (1/3)\,m_1\,\ell_1^2$, $J_2 = (1/3)\,m_2\,\ell_2^2$, $\eta = \ell_1/\ell_2$, and $g = 9.8$. In Examples 6.1 and 6.2, the application of a model-based iterative controller to a robotic manipulator in joint space is considered. Similarly, in Examples 6.3 and 6.4 the application of such a controller to a robotic manipulator in task space is considered.

Example 6.1

In this example, direct-drive servo motors are used. It follows therefore that the model-based controller in the kth iteration is

$$\tau_k = H(q)\,u_k + \dot{H}(q)\,\dot{q} - \frac{\partial T}{\partial q} + g(q) \qquad . \qquad \ldots(6.26)$$

In this case, it is desired that the joint angles perform the motions

$$v(t) = \begin{bmatrix} -\frac{\pi}{4} - 4(t^3 - t^4) \\ \\ \frac{\pi}{4} + 4\,(t^3 - t^4) \end{bmatrix} \qquad \ldots(6.27)$$

in 1.0 sec. In addition, the initial input vector is

$$u_0(t) = \begin{bmatrix} 0 \\ 0 \end{bmatrix} \quad , \qquad \ldots(6.28)$$

and the matrices used in the iterative learning controller are

$$K_1 = \begin{bmatrix} 1 & , & 0 \\ 0 & , & 1 \end{bmatrix} \qquad \ldots(6.29)$$

and

$$K_2 = \begin{bmatrix} 1 & , & 0 \\ 0 & , & 1 \end{bmatrix} \quad . \qquad \ldots(6.30)$$

The rapid learning of the iterative learning controller is shown in Figures 6.1(a,b). It is clear that the actual motions of the two arms of the robotic manipulator are indistinguishable from the desired motions specified in equation (6.27) after three iterations. Figures 6.1(c,d) show the corresponding control efforts.

Example 6.2

In this example, dc motors with reduction gearing are used. It follows therefore that the model-based controller can be either the exact or the approximate controller governed by equation (6.18) or (6.19), respectively. In addition, in equations (6.18)

and (6.19), $J_0 = J_m/\nu^2$, $K_0 = K/\nu R$, and $B_0 = K^2/\nu^2 R$ are all constant diagonal matrices.

In this case, it is desired that the joint angles perform the motions

$$v(t) = \begin{bmatrix} -\frac{\pi}{4} - 4(t^3 - t^4) \\ \\ \frac{\pi}{4} + 4\,(t^3 - t^4) \end{bmatrix} \qquad \ldots(6.31)$$

in 1.0 sec. In addition, the initial input vector is

$$u_0(t) = \begin{bmatrix} 0 \\ 0 \end{bmatrix} \quad , \qquad \ldots(6.32)$$

and the matrices used in the iterative learning controller are

$$K_1 = \begin{bmatrix} 1 & , & 0 \\ 0 & , & 1 \end{bmatrix} \qquad \ldots(6.33)$$

and

$$K_2 = \begin{bmatrix} 1 & , & 0 \\ 0 & , & 1 \end{bmatrix} \qquad \ldots(6.34)$$

The rapid learning of the exact model-based iterative learning controller is shown for each of the two joint angles in Figures 6.2(a,b), from which it is clear that the actual motions are indistinguishable from the desired motions after three iterations. However, it is also evident from Figures 6.2(c,d), (e,f) and (g,h) that similarly rapid learning is obtained when approximate model-based iterative learning controllers are used. Furthermore, it is evident that the characteristics of these approximate model-

based controllers rapidly approach those of the exact model-based controller as the reduction gear ratio (assumed identical for each joint) increases. Figure 6.3 shows the corresponding control efforts in all cases.

Example 6.3

In this example, direct-drive servomotors are used. It follows therefore that the model-based controller in the kth iteration is

$$f_k = (J^T(q))^{-1} \left[H(q)J^{-1}(q)\, u_k + \dot{H}(q)\dot{q} - \frac{\partial T}{\partial q} + g(q) - H(q)\, J^{-1}(q)\, \dot{J}(q)\, \dot{q} \right] \quad ...(6.35)$$

where

$$J(q) = \begin{bmatrix} -\ell_1 \sin q_1 - \ell_2 \sin(q_1+q_2) & , & -\ell_2 \sin(q_1+q_2) \\ \ell_1 \cos q_1 + \ell_2 \cos(q_1+q_2) & , & \ell_2 \cos(q_1+q_2) \end{bmatrix} . \quad ...(6.36)$$

In this case, it is desired that the end-effector perform the following rectilinear motions in the plane of cartesian co-ordinates :

(i) moves between $R(0.7375, -0.3055)\ m$ and $Q\ (0.7, -0.25)\ m$ in 0.15 sec with equal periods of acceleration, cruise, and deceleration from rest to $669.398 \times 10^{-3}\ m/s$ and back to rest ;

(ii) then moves immediately between $Q(0.7, -0.25)\ m$ and $R(0.7375, -0.3055)\ m$ in 0.15 sec with equal periods of acceleration, cruise, and deceleration from rest to $669.398 \times 10^{-3}\ m/s$ and back to rest.

The initial input vector is

$$u_0(t) = \begin{bmatrix} 0 \\ 0 \end{bmatrix} \quad , \qquad \text{...(6.37)}$$

and the matrices used in the iterative learning controller are

$$K_1 = \begin{bmatrix} 1 & , & 0 \\ 0 & , & 1 \end{bmatrix} \qquad \text{...(6.38)}$$

and

$$K_2 = \begin{bmatrix} 1 & , & 0 \\ 0 & , & 1 \end{bmatrix} \quad . \qquad \text{...(6.39)}$$

The rapid learning of the iterative learning controller is shown in Figures 6.4(a,b). It is clear that the actual motions of the two arms of the robotic manipulator are indistinguishable from the desired motions specified in step (i) and (ii) after three iterations. Figures 6.4(c,d) show the corresponding control effects.

Example 6.4

In this example, dc motors with reduction gearing are used. It follows therefore that the model-based controller can either be the exact or the approximate controller governed by equation (6.20) or (6.21), respectively. In addition, in equations (6.20) and (6.21), $J_0 = J_m/\nu^2$, $K_0 = K/\nu R$, and $B_0 = K^2/\nu^2 R$ are all constant diagonal matrices.

In this case, it is desired that the end-effector perform the motions of Example 6.3 in the plane of cartesian co-ordinates. The initial input vector is

$$u_0(t) = \begin{bmatrix} 0 \\ 0 \end{bmatrix} \quad , \qquad \ldots(6.40)$$

and the matrices used in the iterative learning controller are

$$K_1 = \begin{bmatrix} 1 & , & 0 \\ 0 & , & 1 \end{bmatrix} \qquad \ldots(6.41)$$

and

$$K_2 = \begin{bmatrix} 1 & , & 0 \\ 0 & , & 1 \end{bmatrix} \quad . \qquad \ldots(6.42)$$

The rapid learning of the exact model-based iterative learning controller is shown in Figures 6.5(a,b), from which it is clear that the actual motions are indistinguishable from the desired motions after three iterations. However, it is also evident from Figures 6.5(c,d), (e,f) and (g,h) that similarly rapid learning is obtained when approximate model-based iterative learning controllers are used. Furthermore, it is evident that the characteristics of these approximate model-based controllers rapidly approach those of the exact model-based controller as the reduction gear ratio (assumed identical for both joints) increases. Figure 6.6 shows the corresponding control efforts in all cases.

6.4 CONCLUSION

It has been shown in this chapter that robotic manipulators give rise to completely irregular linear time-invariant plants under the action of computed-torque control in both joint and task spaces. It follows, therefore, that the results of Arimoto et al (1984) for the iterative learning control of regular plants are inapplicable in such cases. However, it has also been shown that the results of Chapters 2 and 3 for the

iterative learning control of irregular plants are directly applicable to the design of model-based learning controllers for robotic manipulators. The practical relevance of these theoretical results to the design of model-based iterative controllers for robotic manipulators has been illustrated by the presentation of numerical results for the iterative learning control of a typical two-degree-of-freedom robotic manipulator in both joint and task spaces using power transmission with either direct-drive or reduction gearing characteristics. These results have indicated that such model-based iterative learning controllers are robust in the sense that rapid learning behaviour is obtained even when crude dynamical models are used.

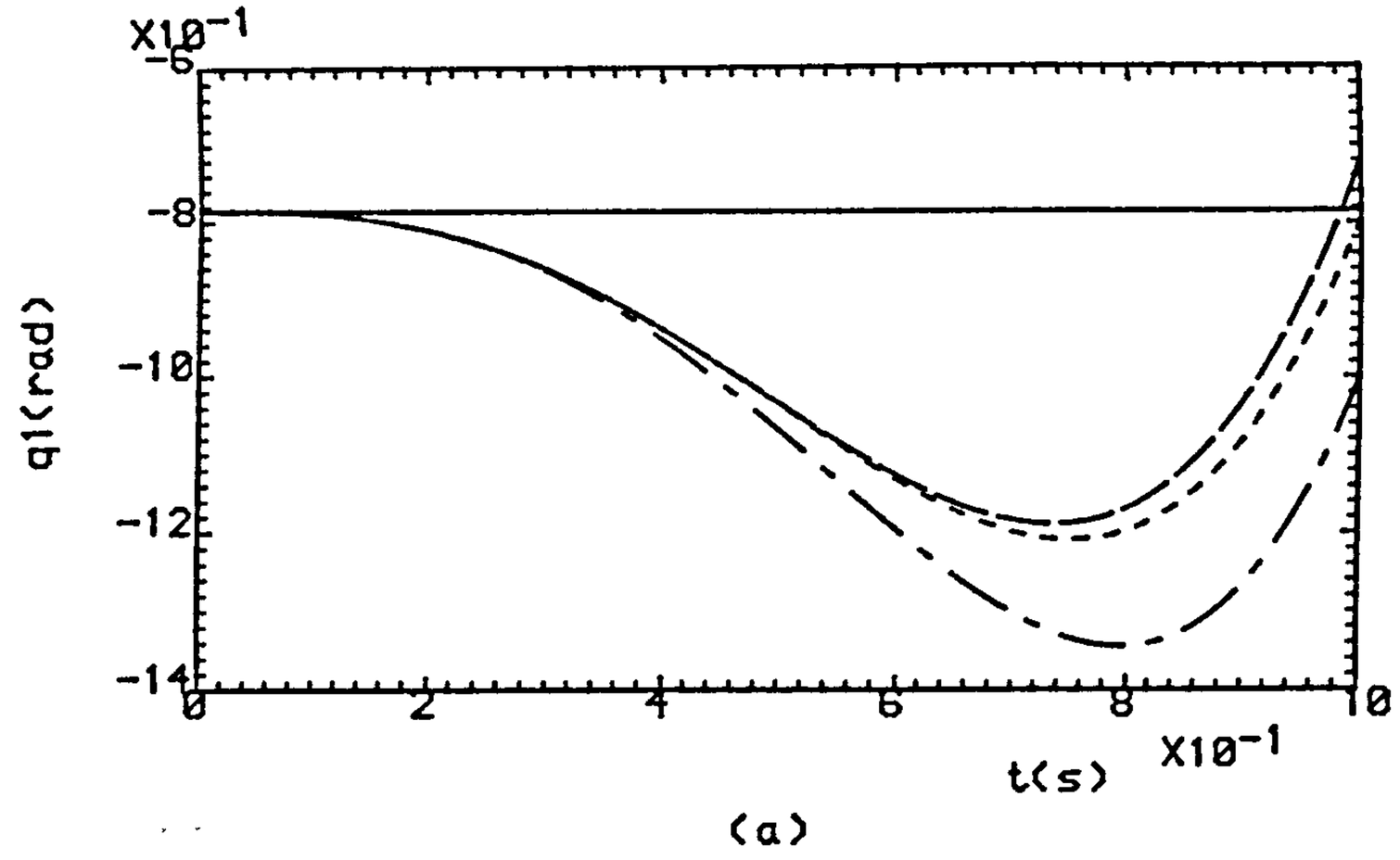

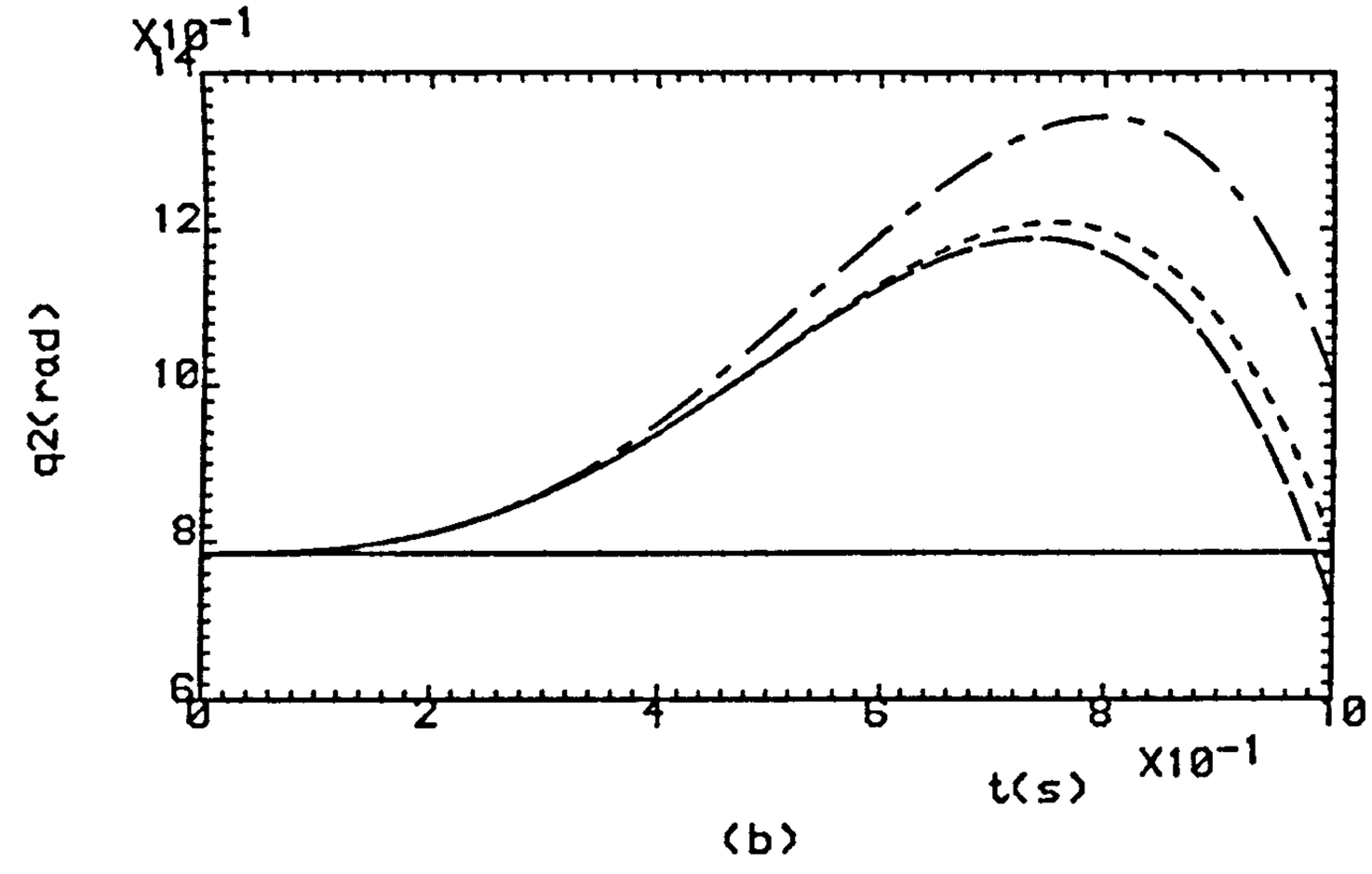

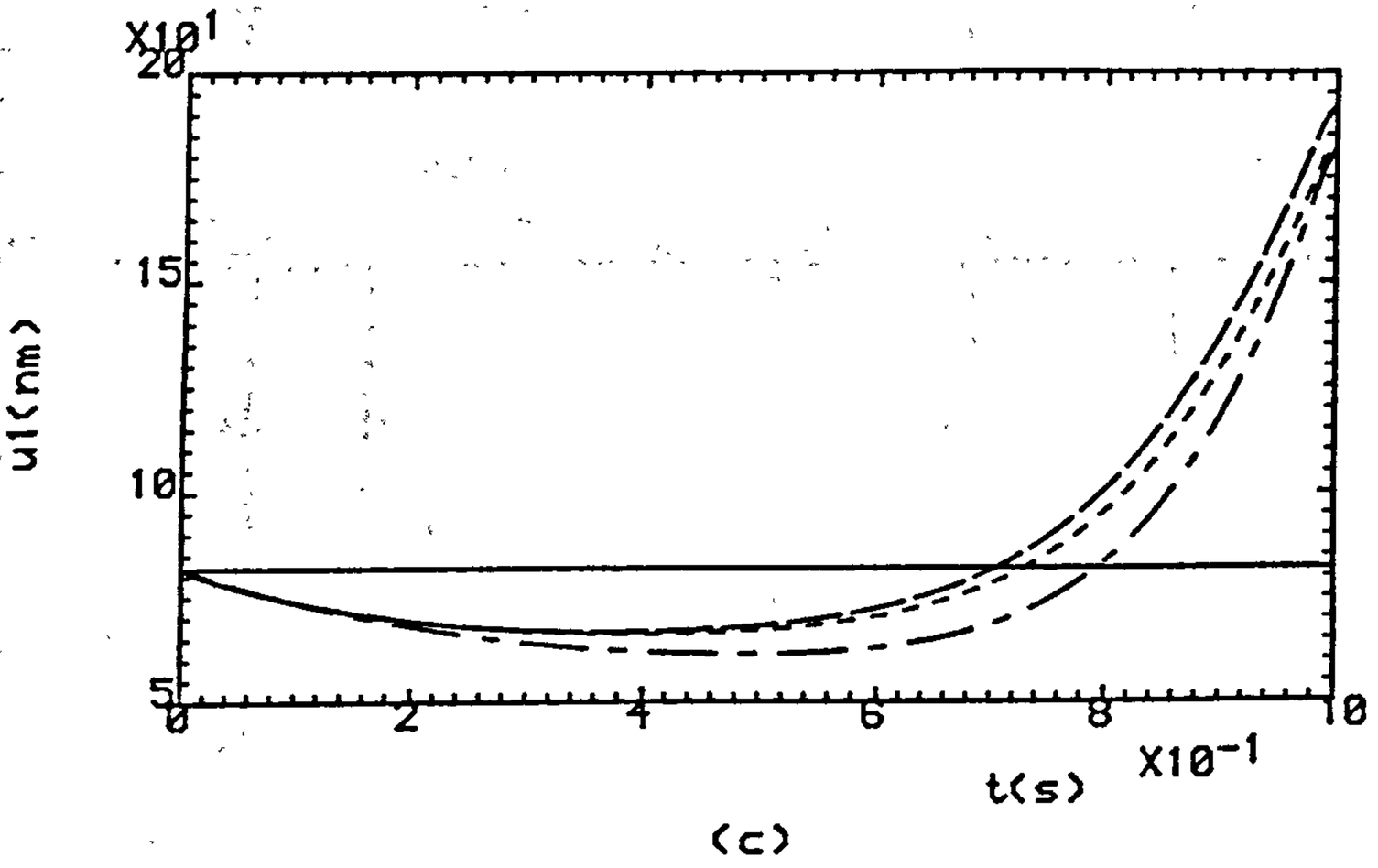

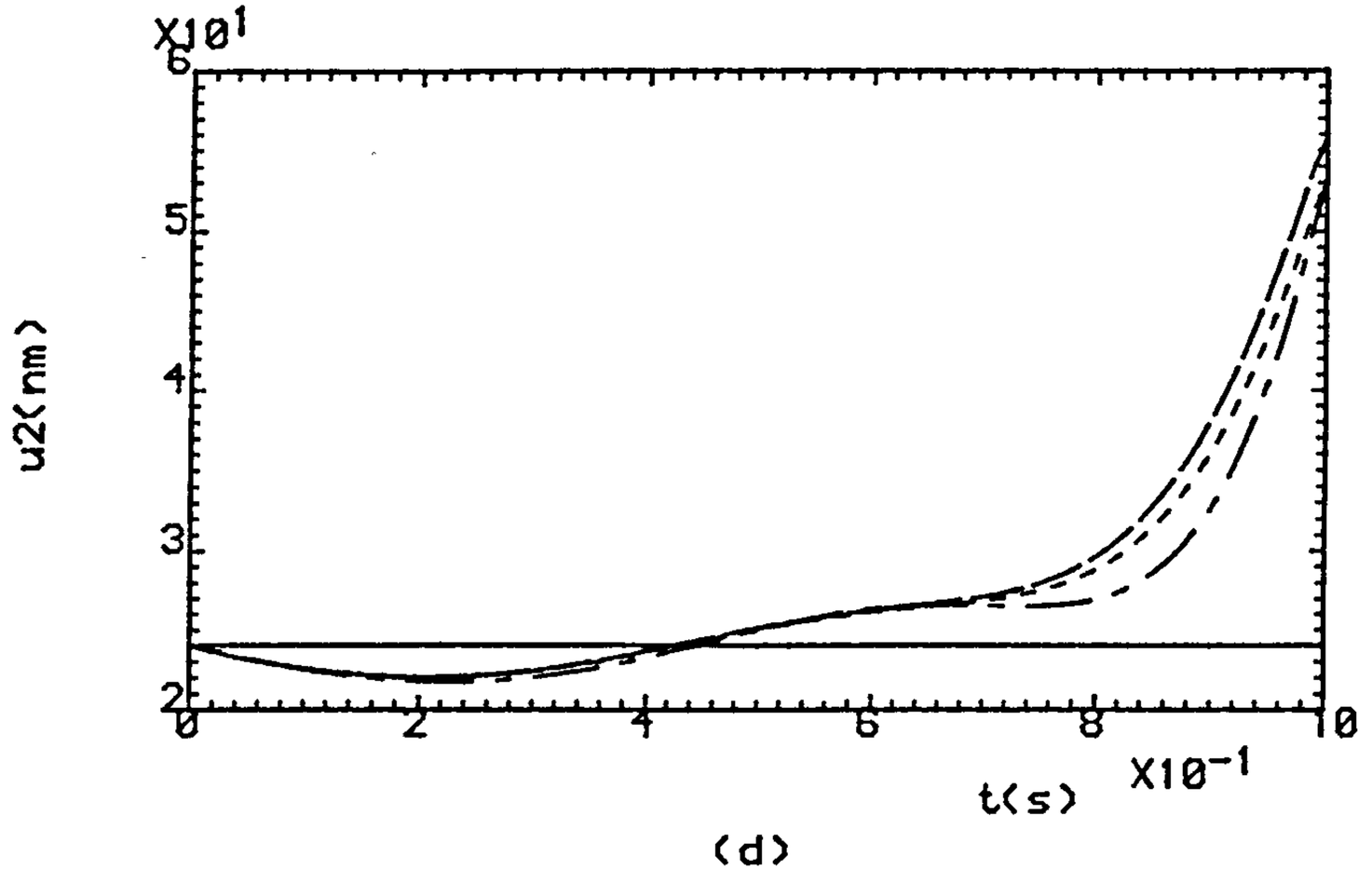

Fig.6.1(a,b) Successive Outputs OF Two-Link Manipulator.
(c,d) Successive Torques Acting On The Joints.
——— K=0 , -·-·- K=1 , ----- K=2 , ... K=3

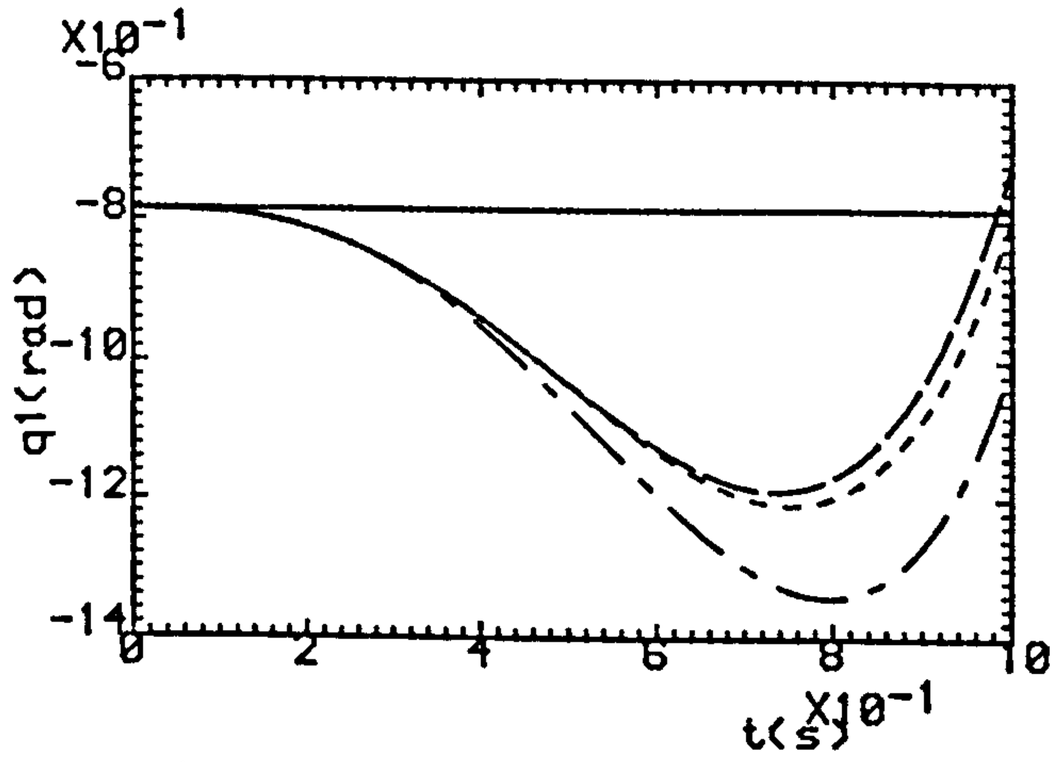

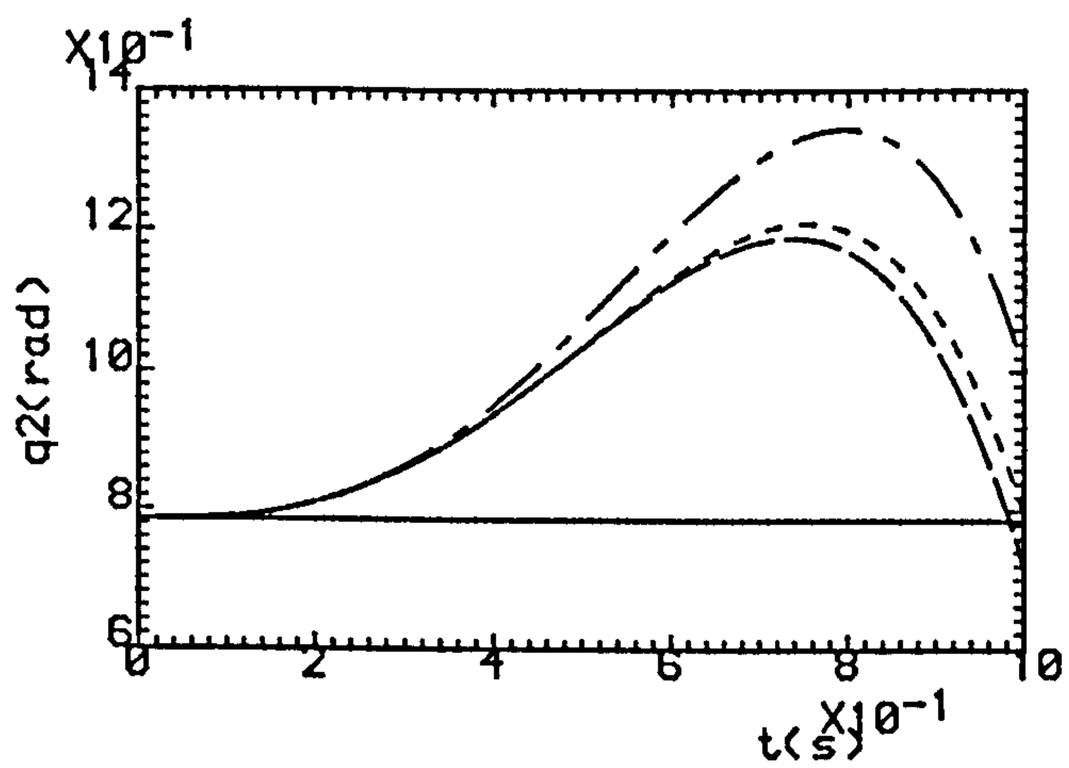

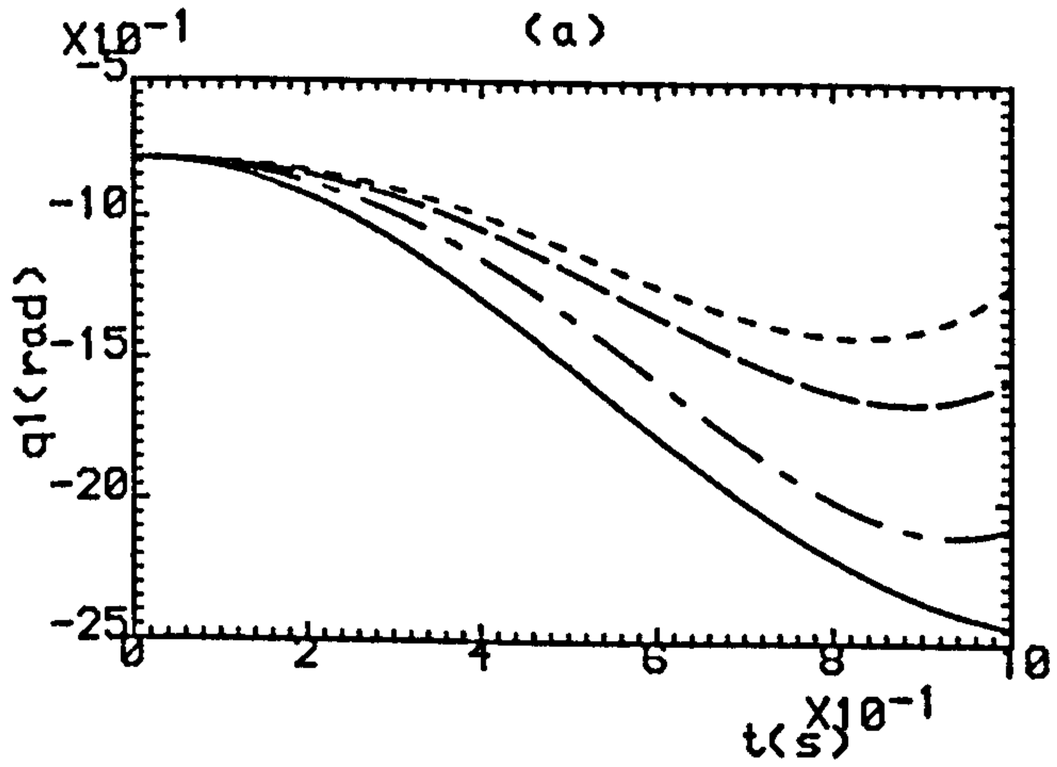

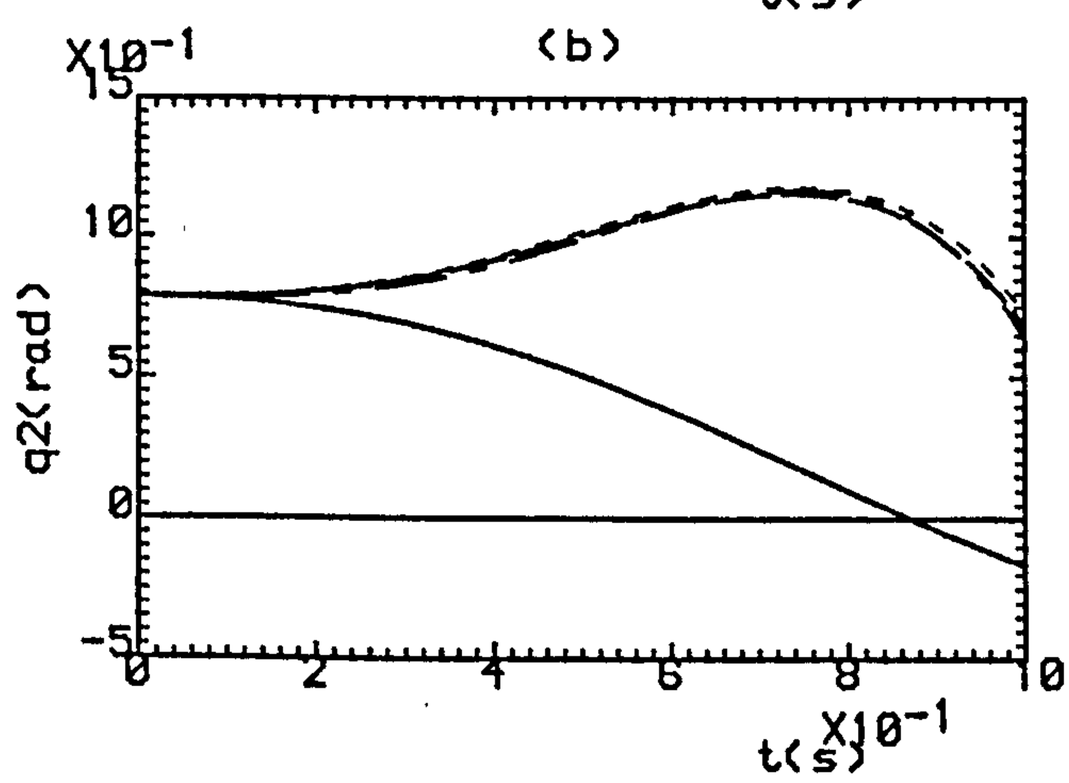

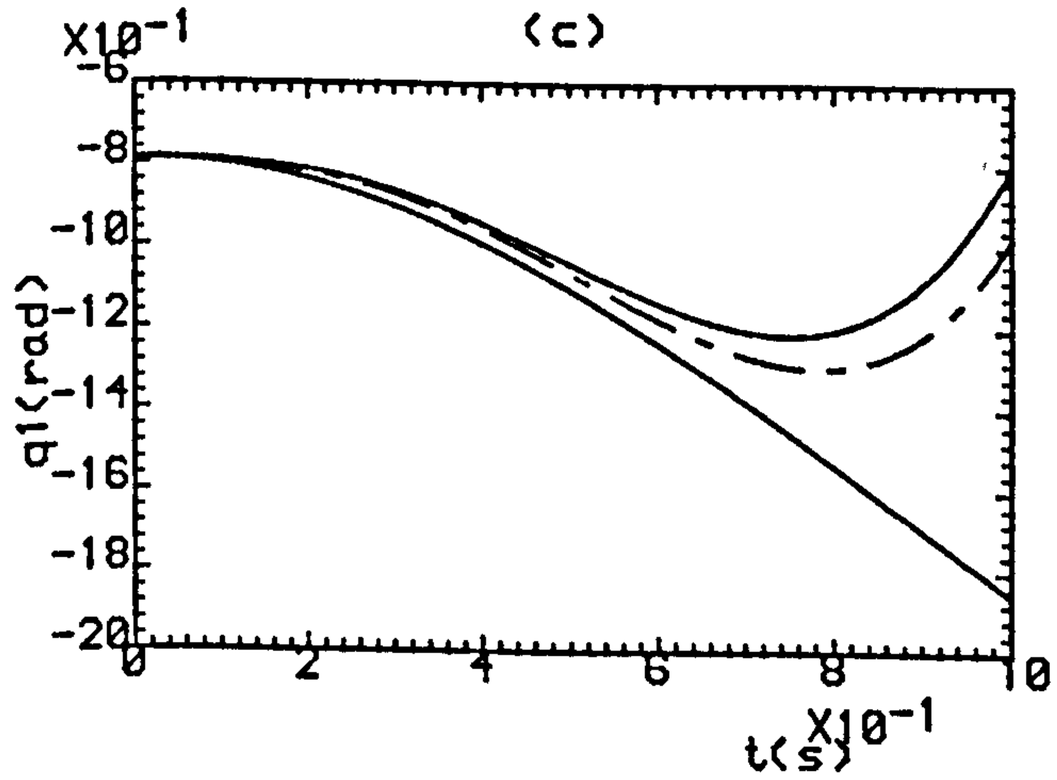

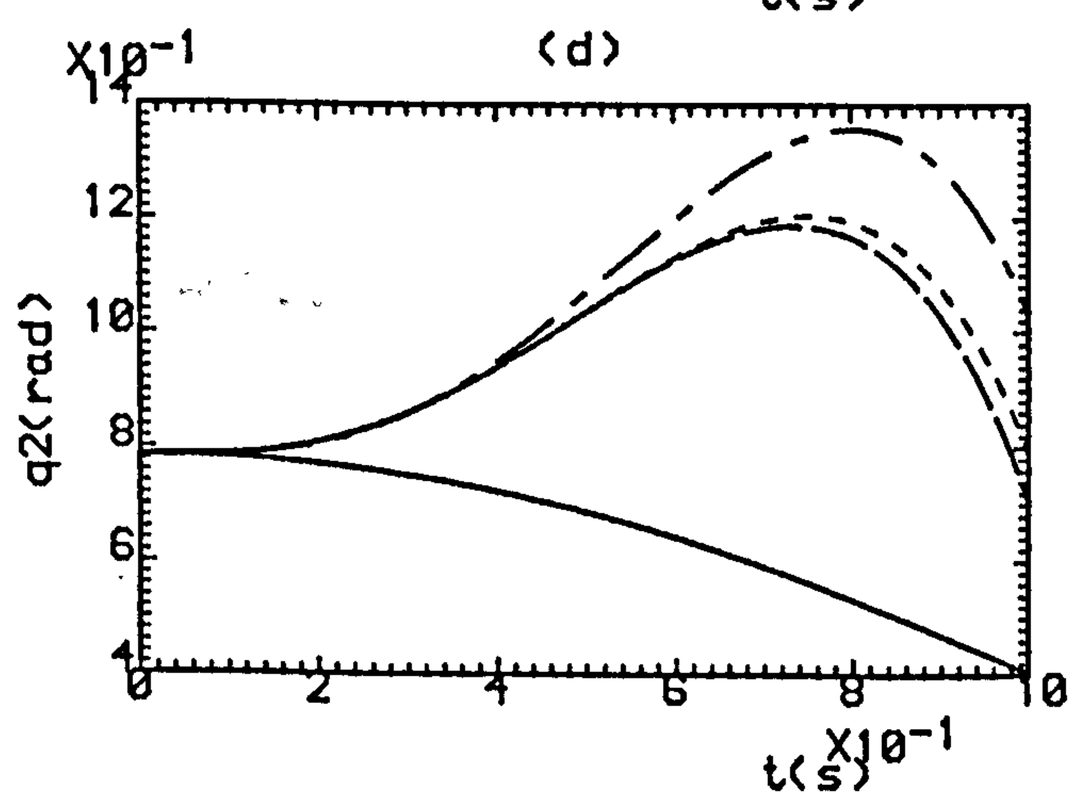

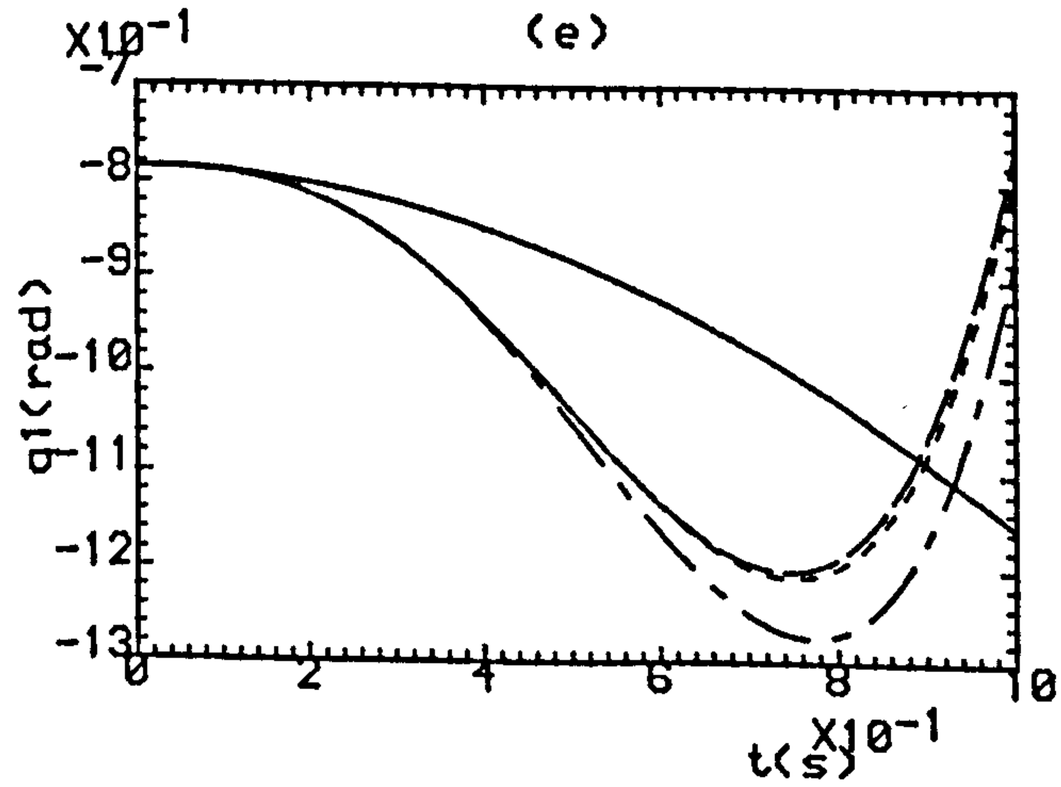

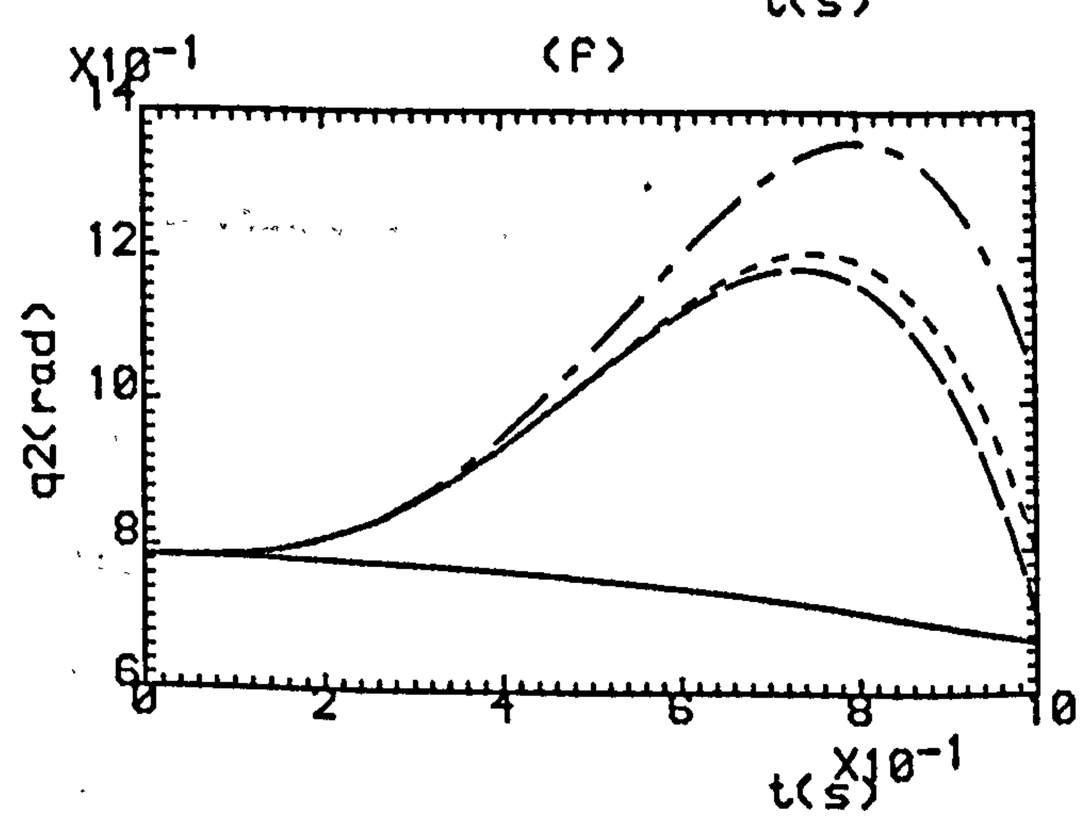

Fig.6.20utputs Under:(a,b)Exact Model-Based.
Fixed Controller With reduction gear ratio
(c,d) 100:1 , (e,F) 200:1 , (g,h) 400:1 .
——— K=0 , -·-·- K=1 , ----- K=2 , ... K=3

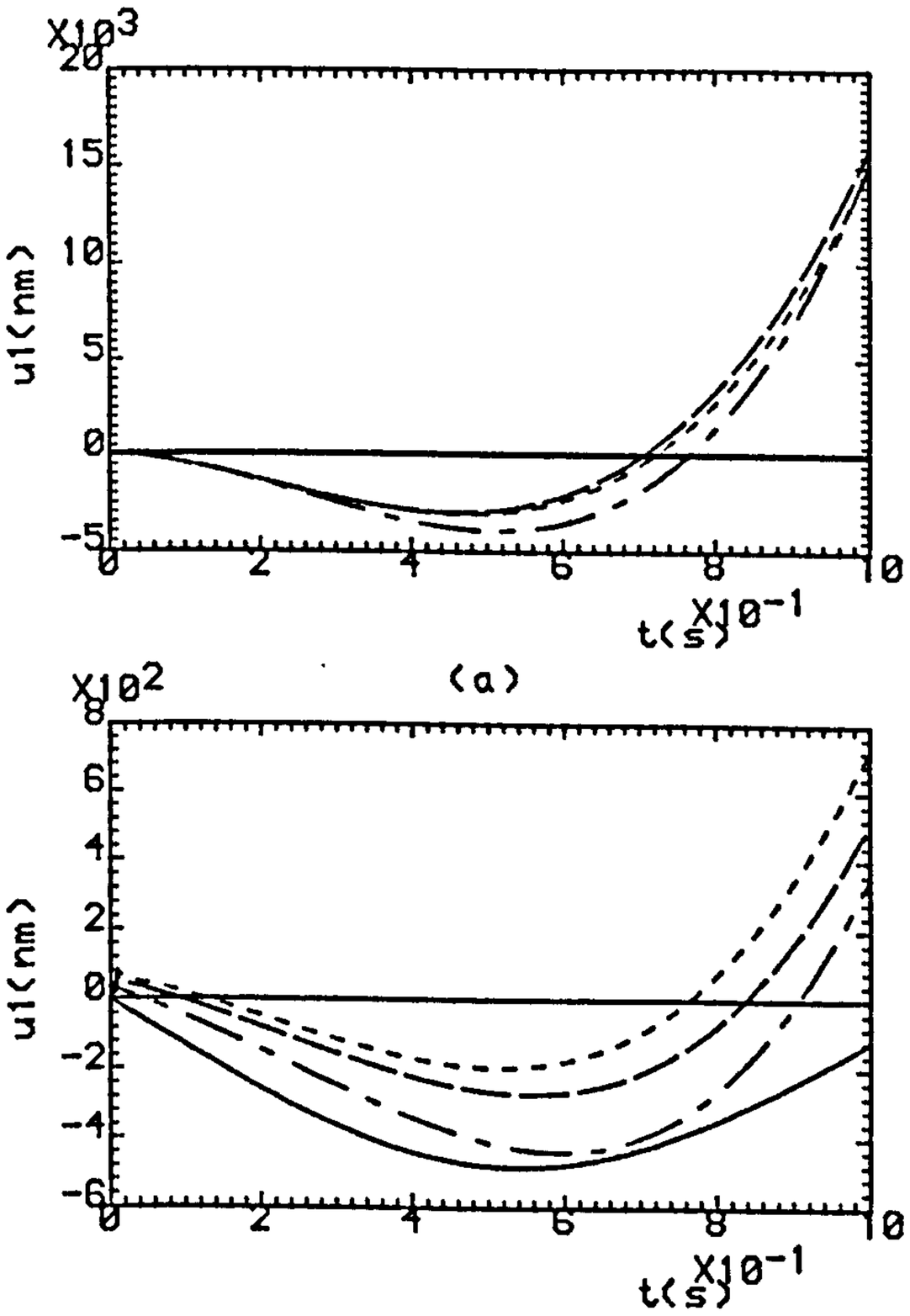

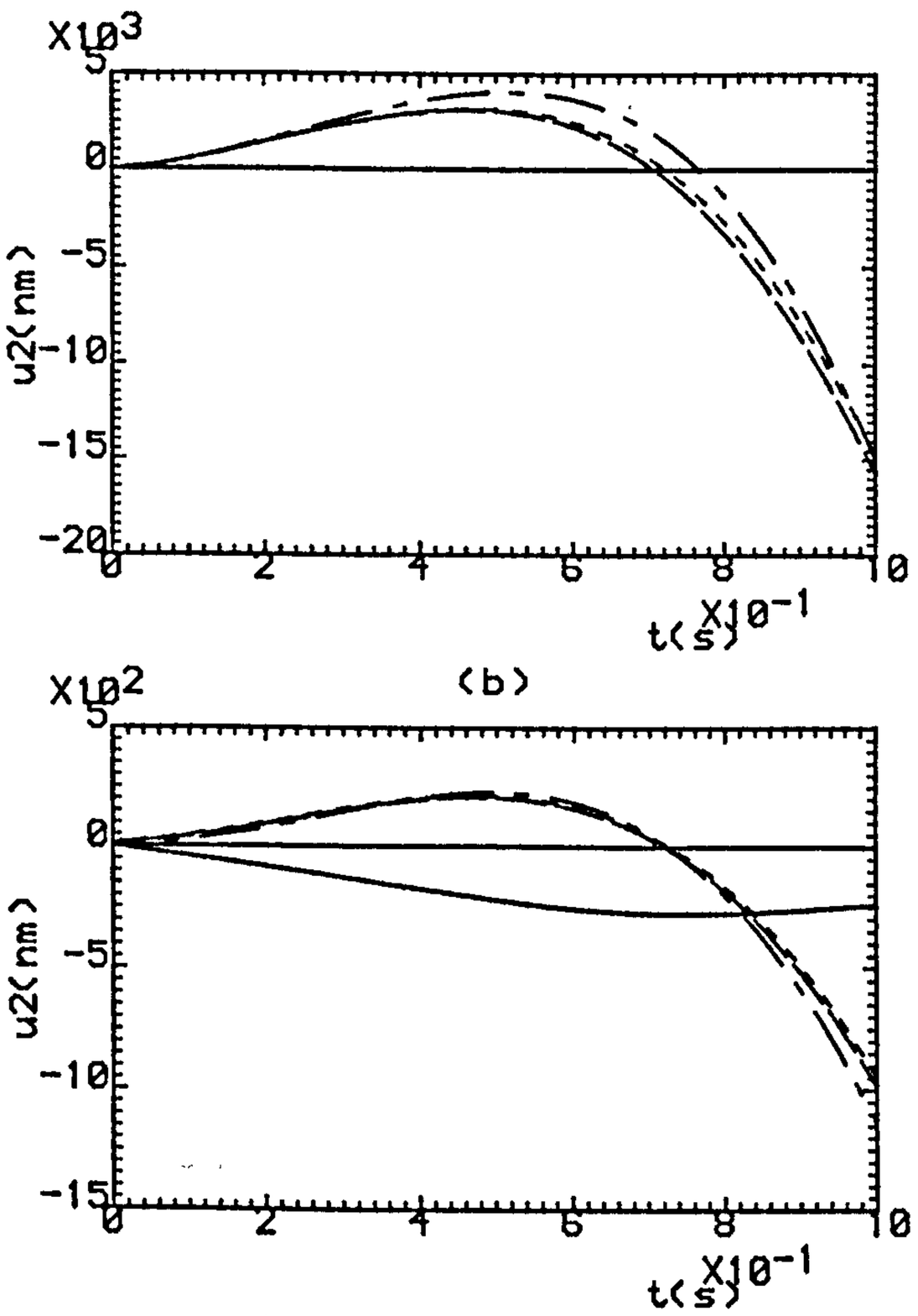

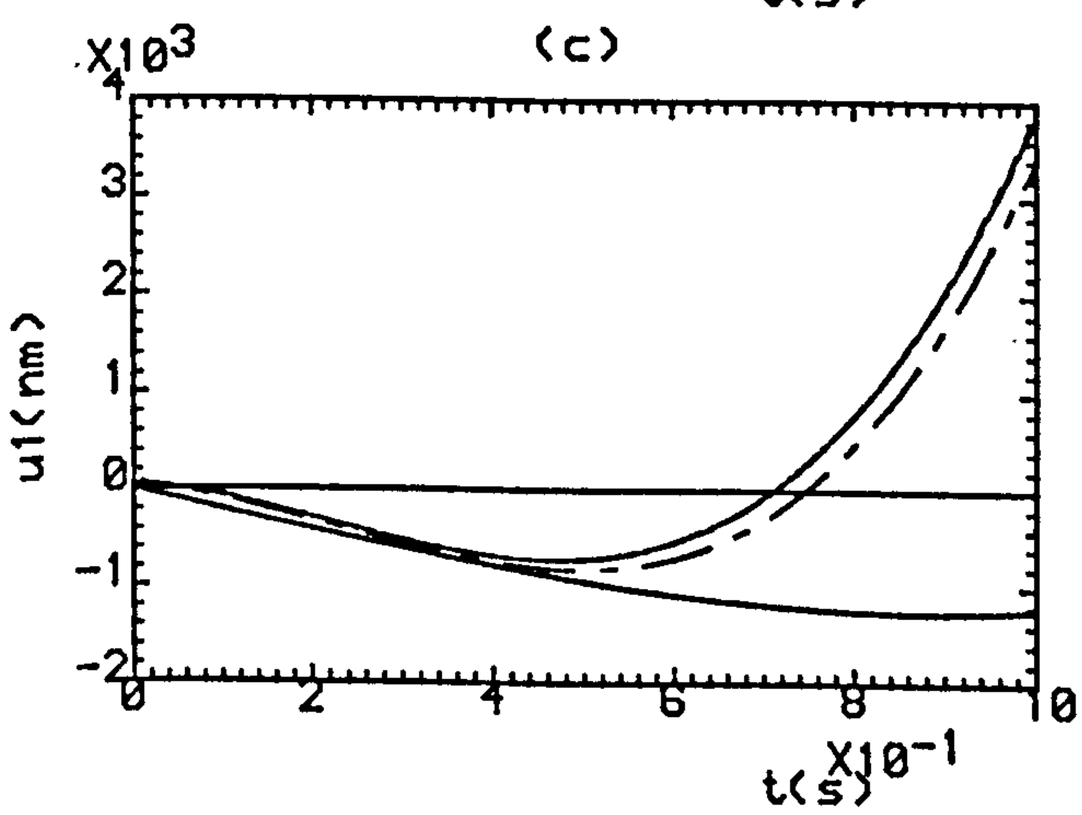

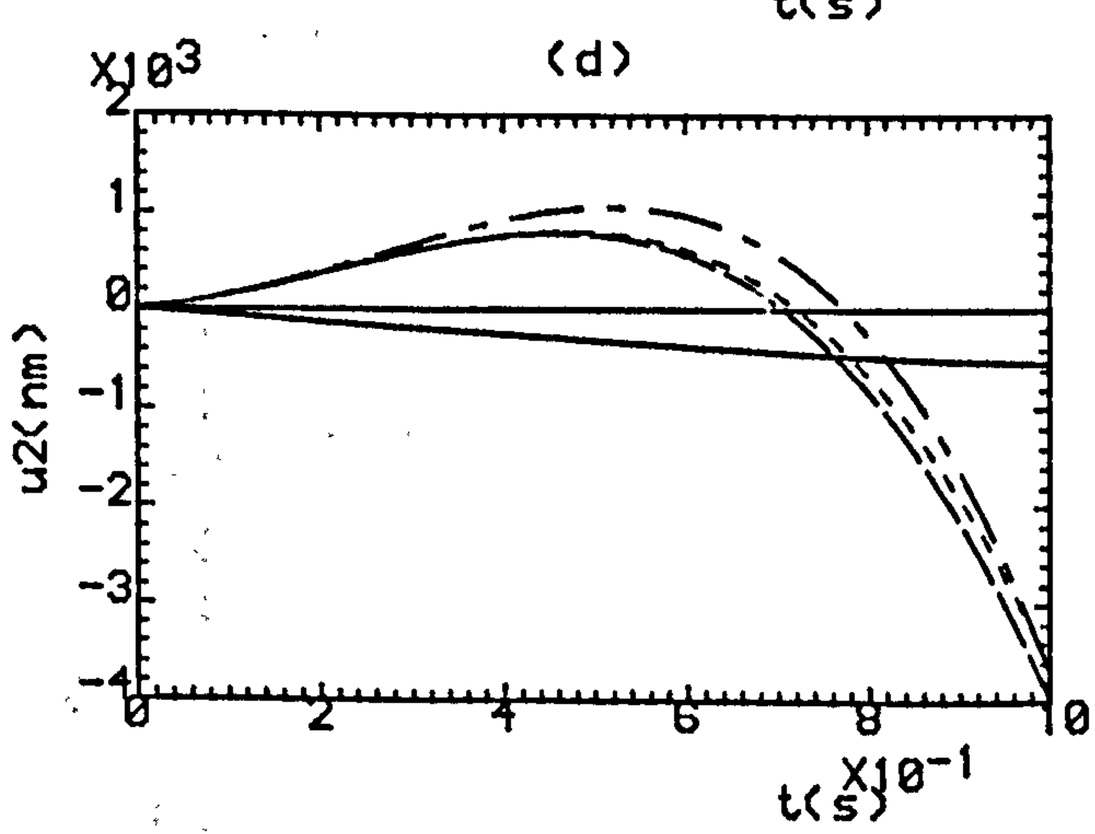

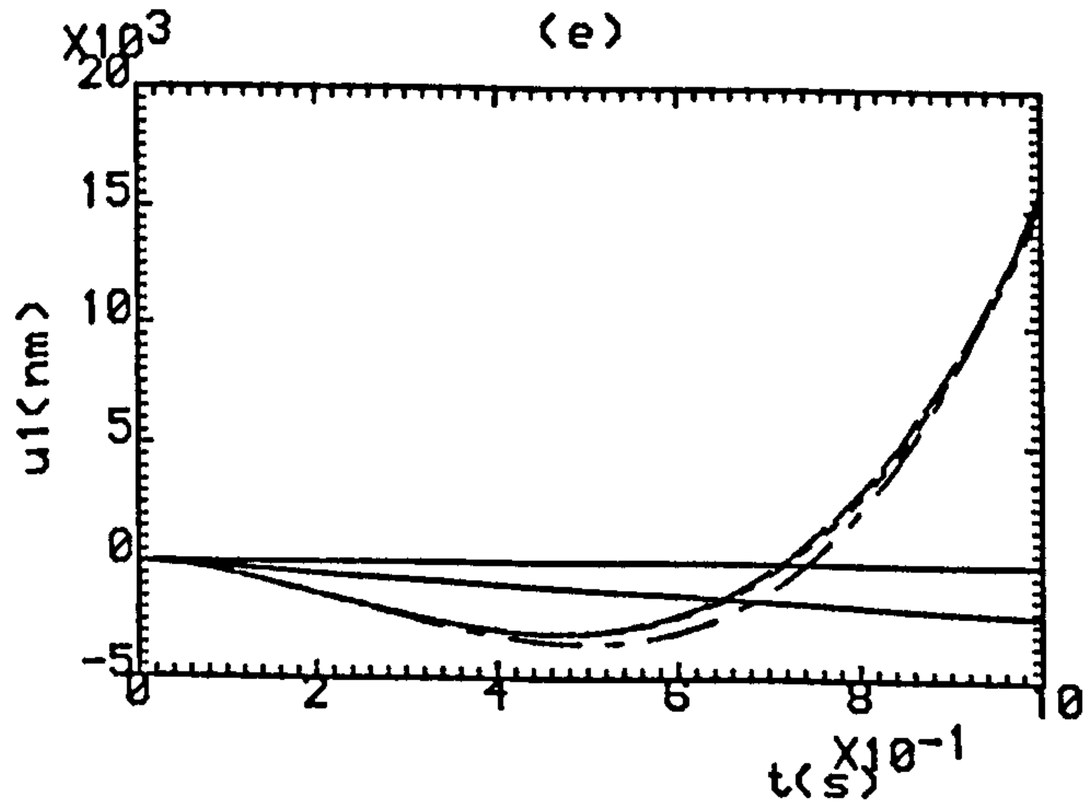

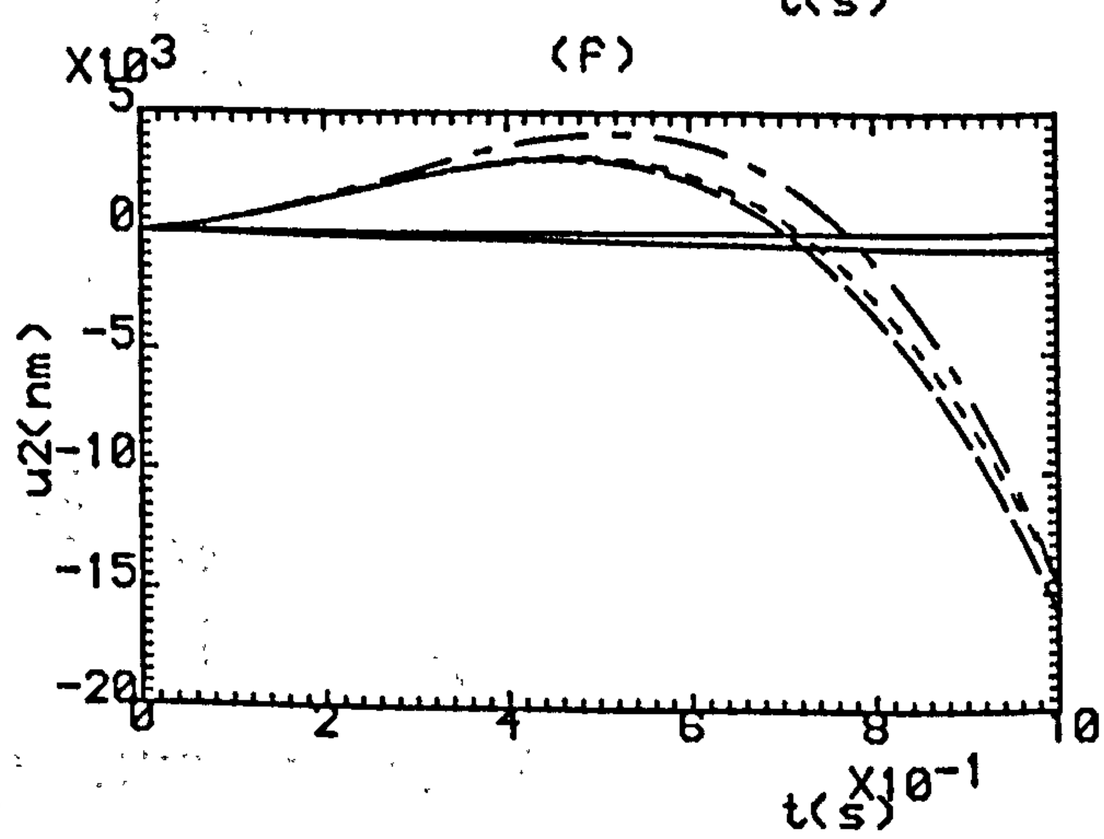

Fig.6.3Control Efforts:(a,b)Exact Model-Based,
(c,d)gear ratio 100:1,(e,f)gear ratio 200:1,
(g,h)gear ratio 400:1 .
——— K=0 , -·-·- K=1 , ----- K=2 , ... K=3

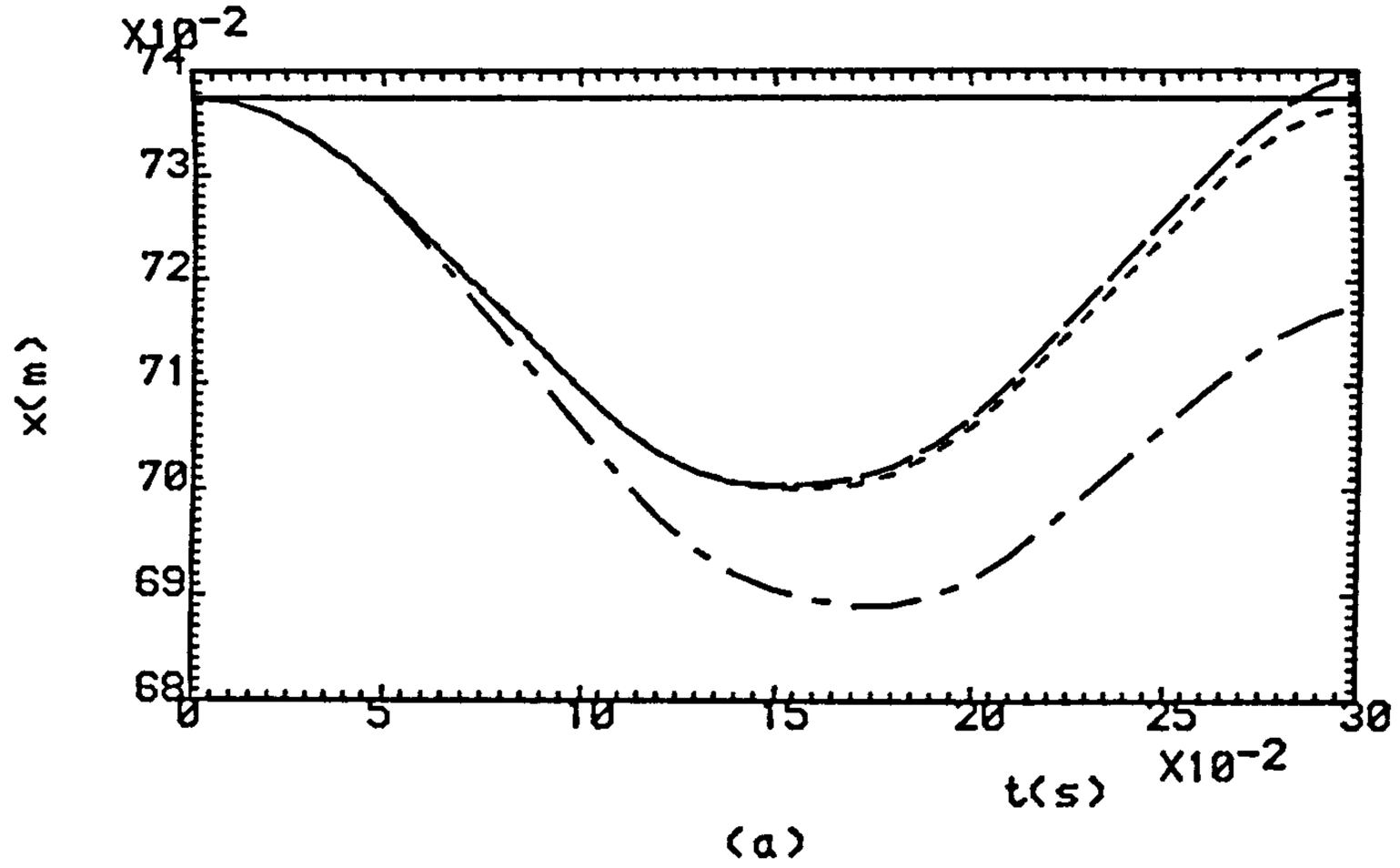

(a)

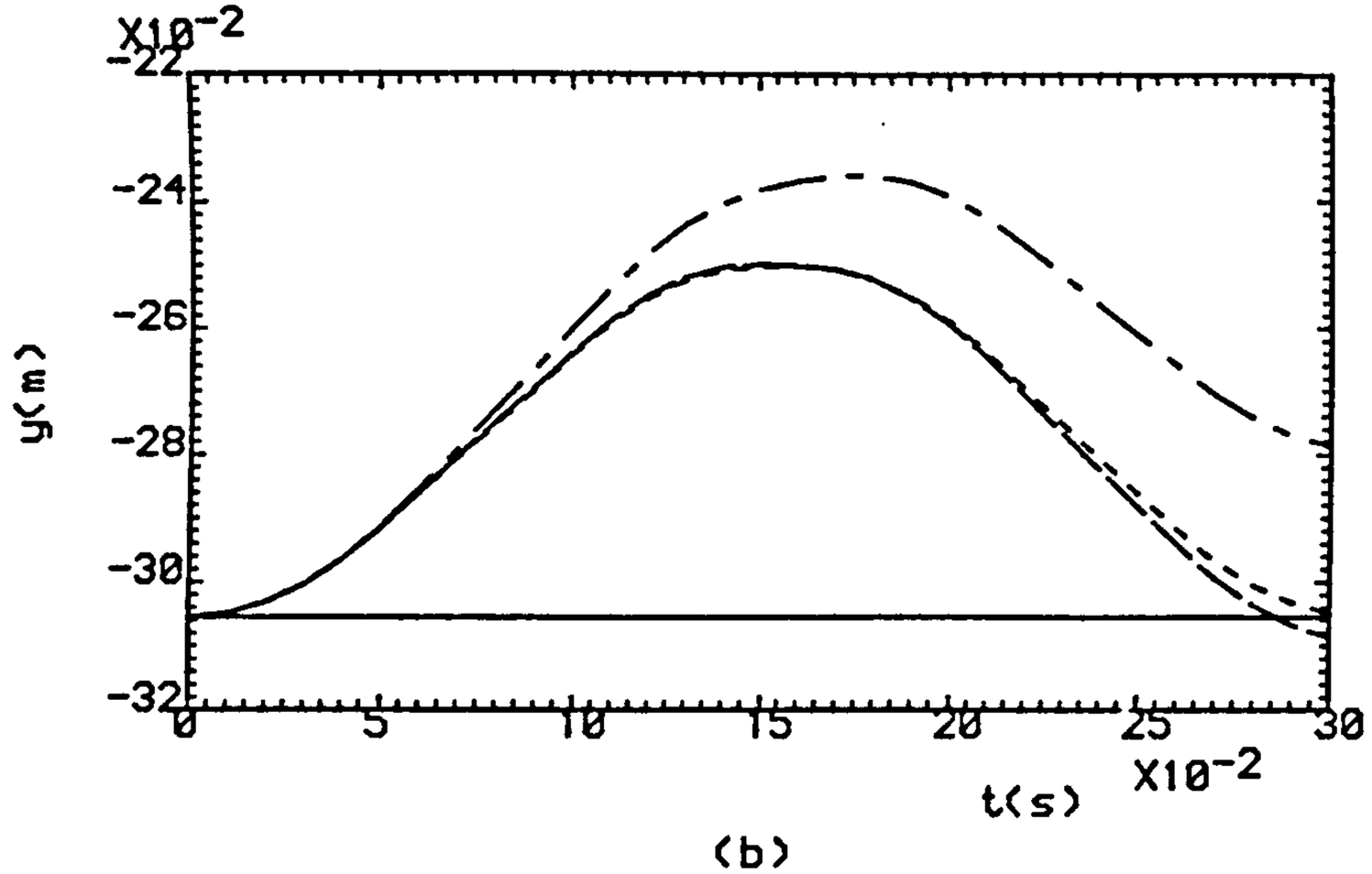

(b)

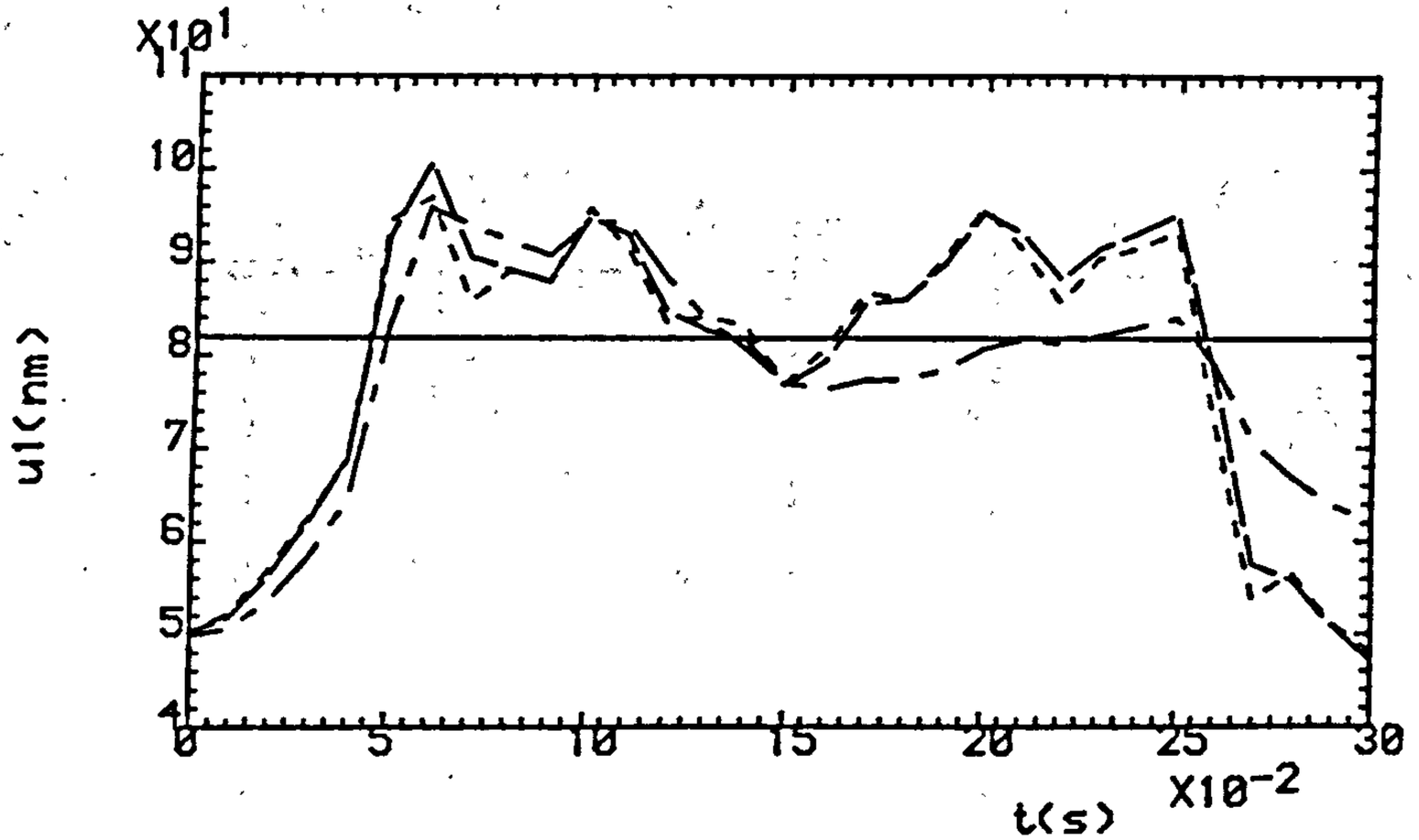

(c)

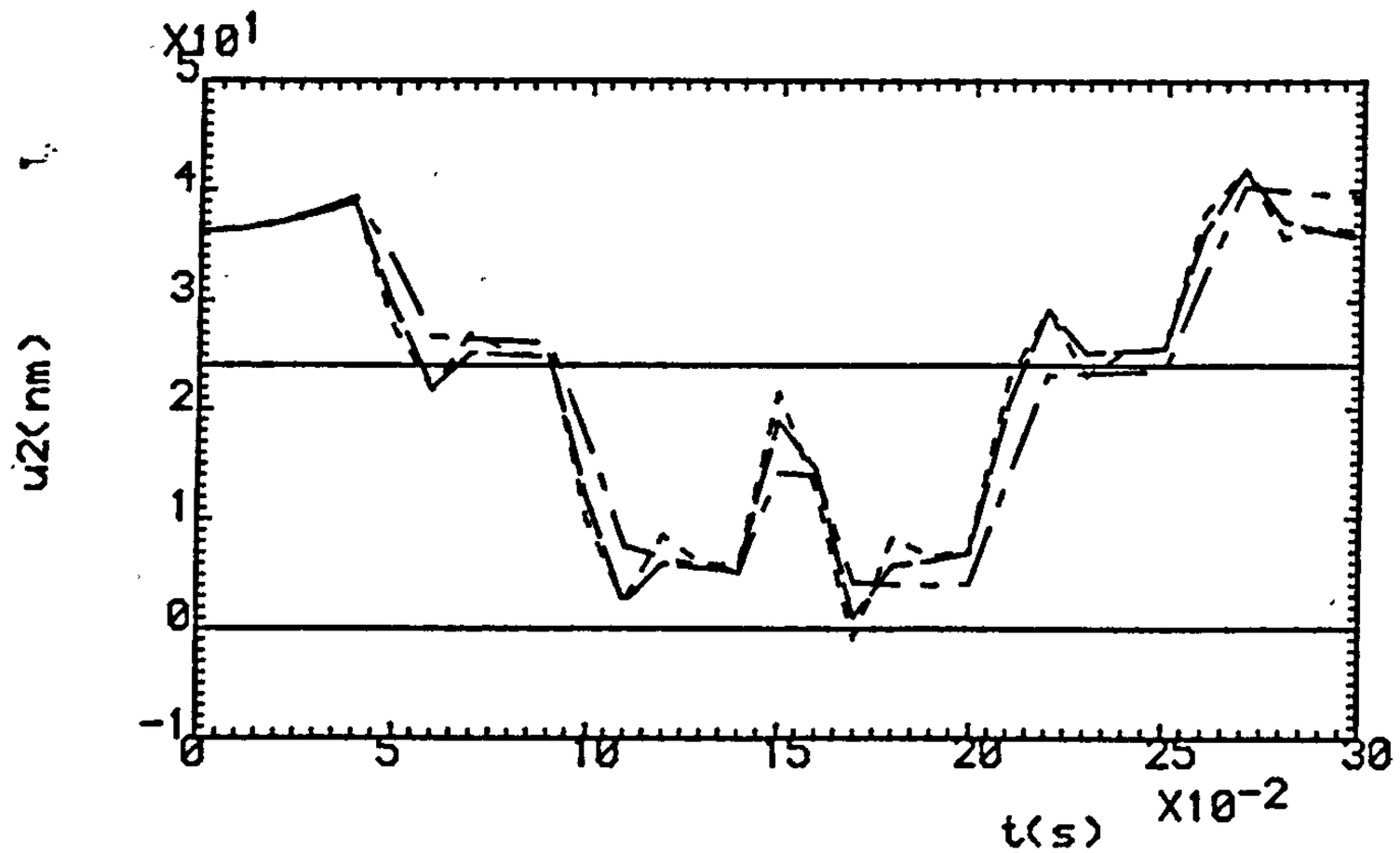

(d)

Fig.6.4(a,b) Successive Outputs Of Two-Link Manipulator.
(c,d) Successive Torques Acting On The Joints.
——— K=0, -·-·- K=1,----- K=2, ...K=3

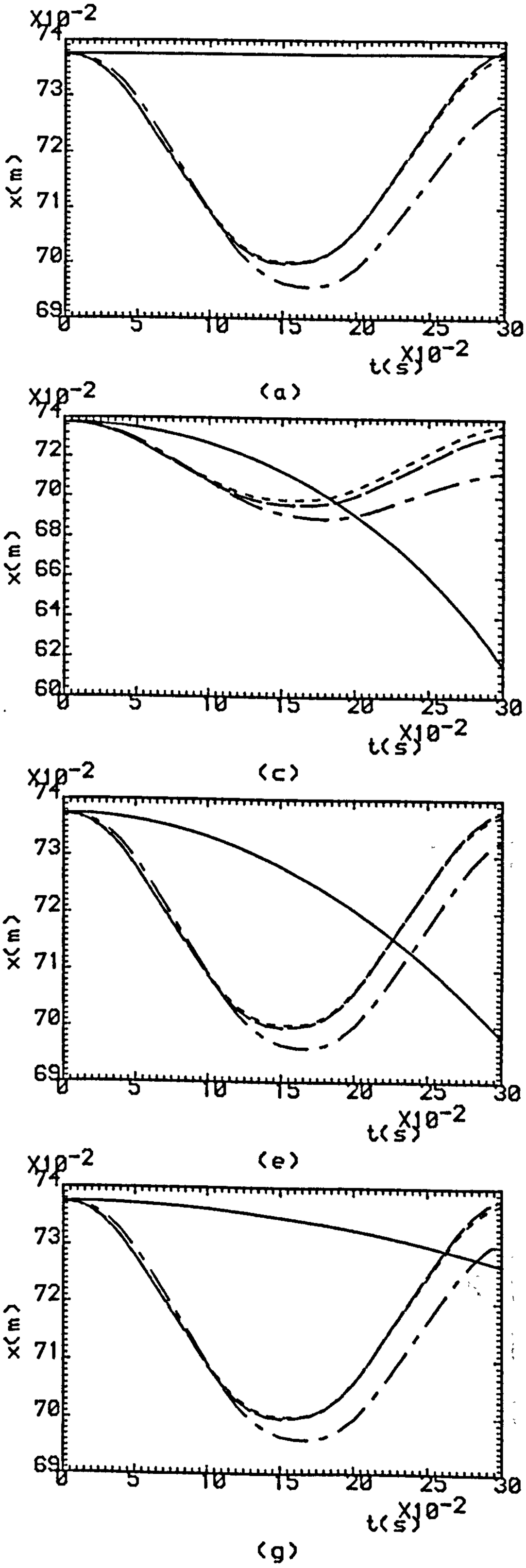

Fig.6.5Outputs Under:(a,b)Exact Model-Based,
Fixed Controller With reduction gear ratio
(c,d) 100:1 , (e,F) 200:1 , (g,h) 400:1 .
——— K=0 , -·-·- K=1 , ----- K=2 , ... K=3

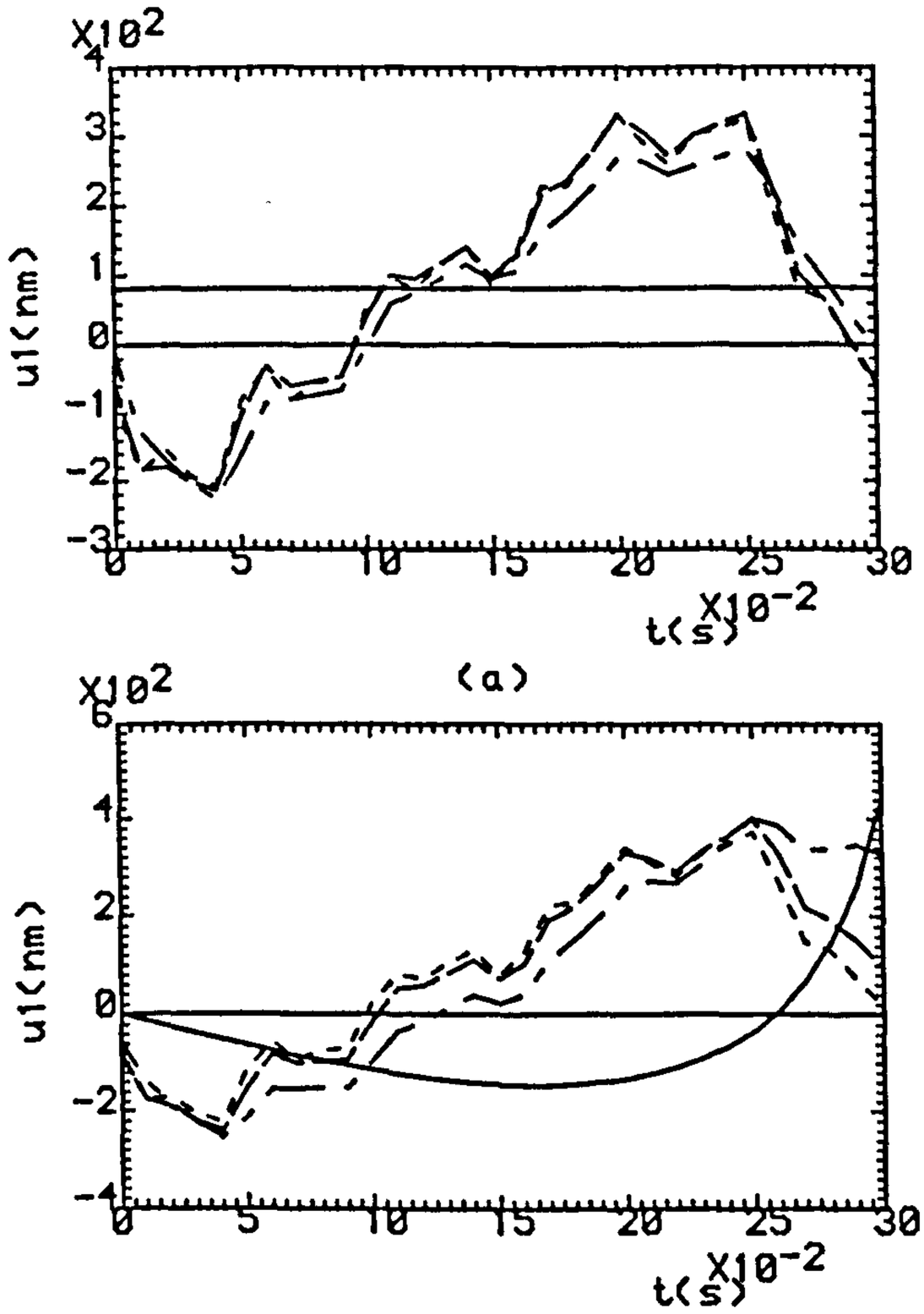

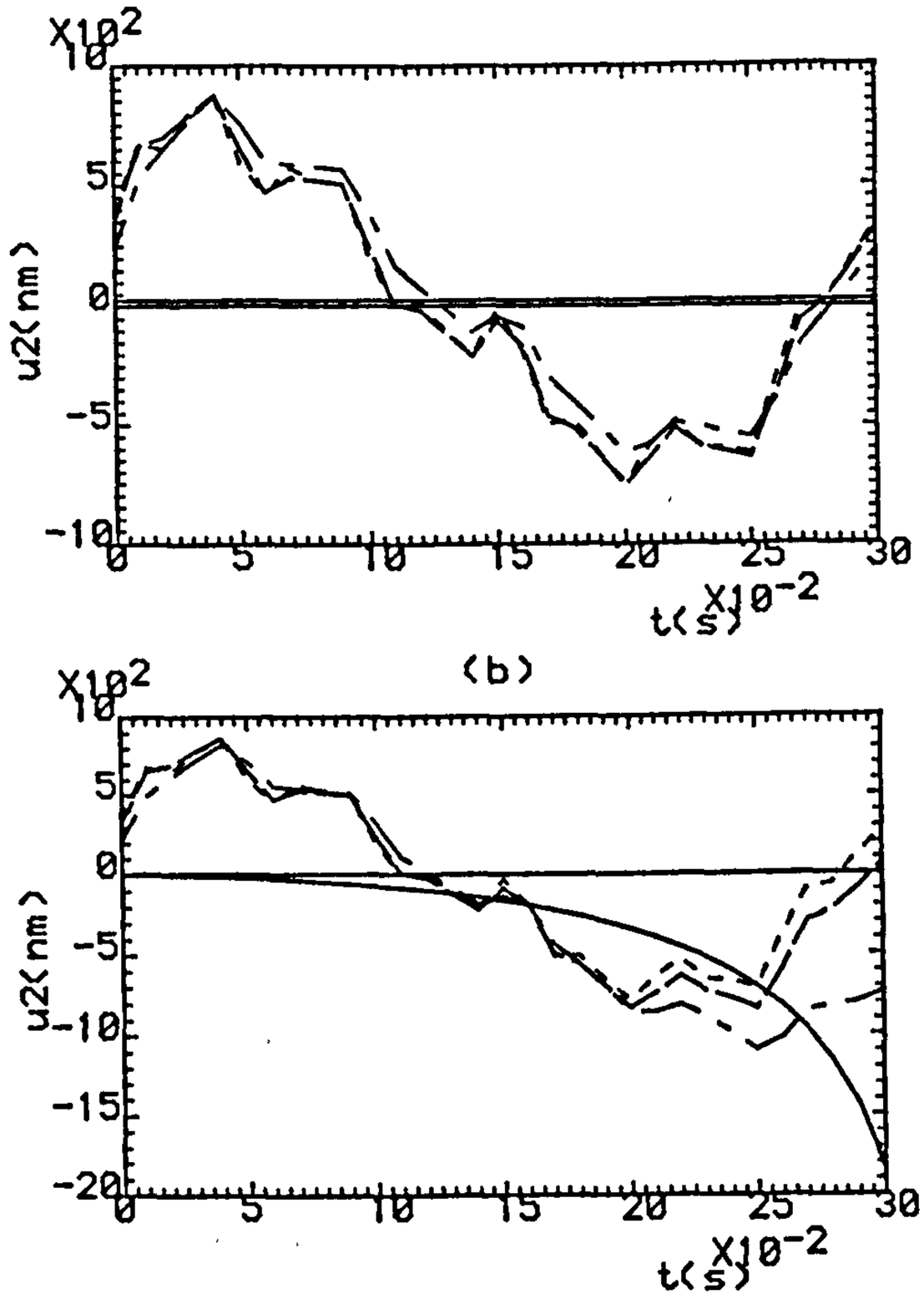

(a)

(b)

(c)

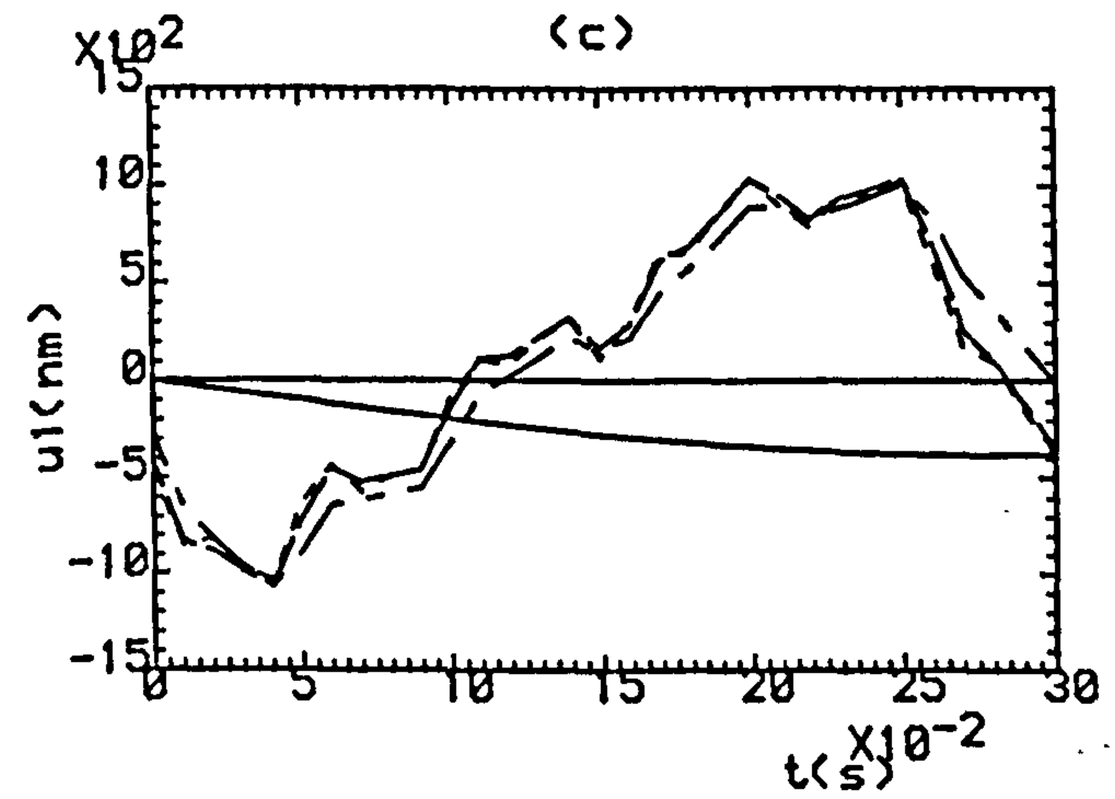

(d)

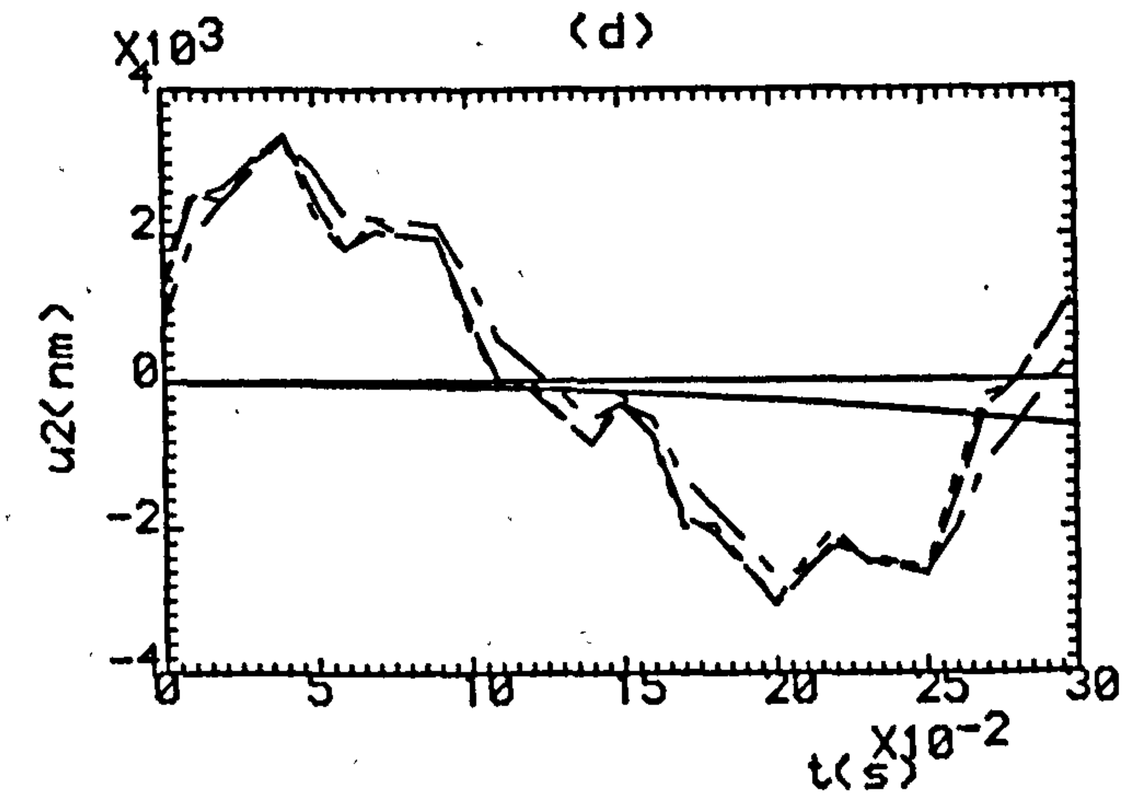

(e)

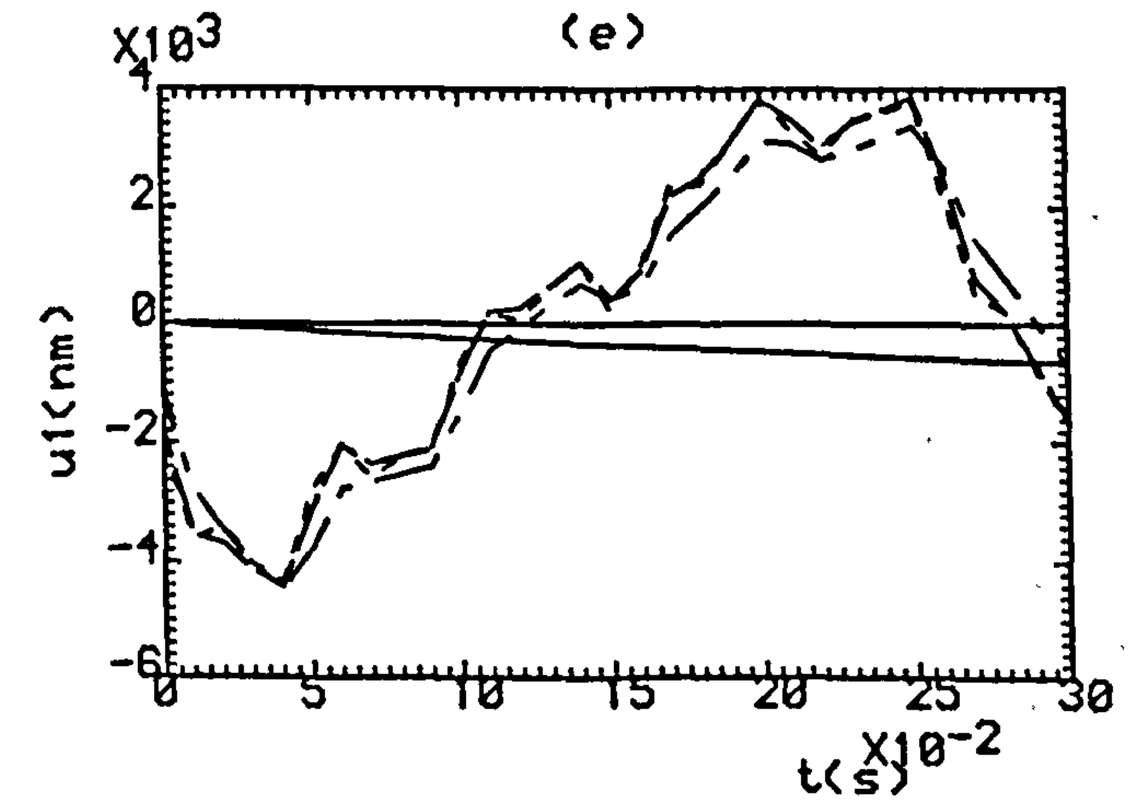

(f)

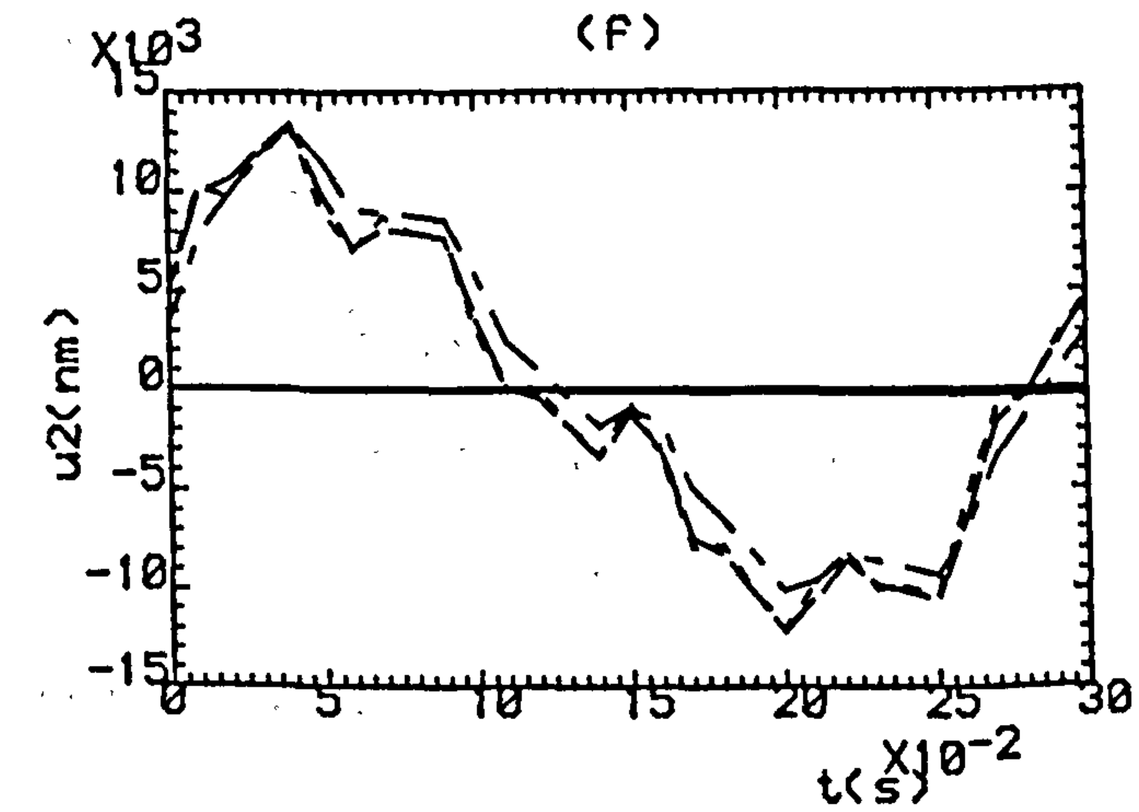

(g)

(h)

Fig.6.6Control Efforts:(a,b)Exact Model-Based,
(c,d)gear ratio 100:1,(e,F)gear ratio 200:1,
(g,h)gear ratio 400:1 .
——— K=0 , -·-·- K=1 , ----- K=2 , ... K=3

CHAPTER 7

DESIGN OF DIGITAL MODEL-BASED ITERATIVE LEARNING CONTROLLERS FOR ROBOTIC MANIPULATORS

7.1 INTRODUCTION

The design and application of analogue model-based iterative learning controllers with initial impulsive action were considered in Chapter 6. Such controllers proved to be robust and effective in controlling robotic manipulators in both joint and task space co-ordinates. However, these controllers were analogue and were digitalised for purposes of implementation. This indirect process of digitalisation is unsatisfactory since finite-difference approximations of derivative action can give rise to inaccuracies and instabilities. Moreover, these controllers use impulsive action when the desired trajectory has initial discontinuities and this use of impulsive action is undesirable practically. Therefore, digital iterative learning controllers are required in order to remove these limitations in connection with the control of robotic manipulators. Indeed, it was shown in Chapter 4 that such digital iterative learning controllers can be designed for linear time-invariant multivariables plants of any orders of irregularity, using only input/output models of the plants in the form of step-response matrices. Moreover, it was also shown in Chapter 6 that non-linear robotic manipulators can be reduced to linear time-invariant plants under the action of computed-torque control. Therefore, such robotic manipulators under the action of computed-torque control are amenable to digital iterative learning control.

It is accordingly shown in this chapter that digital model-based iterative learning controllers can be readily designed and implemented for robotic manipulators.

Furthermore, the effectiveness of such controllers is illustrated by designing a digital iterative learning controller for a two-degree-of-freedom robotic manipulator with gravity compensation in both joint and task space co-ordinates. It is also shown that such digital model-based iterative learning controllers are robust in the sense that rapid learning behaviour is obtained even when crude dynamical models are used. In particular, it is shown that simple fixed digital model-based iterative learning controllers exhibit excellent learning characteristics which emulate those of more complex exact model-based controllers as reduction gear ratios increase.

7.2 ANALYSIS

The dynamics of n-link non-redundant robotic manipulators, driven by armature-controlled dc motors through reduction gearing, are as in Chapter 6 governed by non-linear vector differential equations of the form Arimoto and Miyazaki (1989)

$$[J_0 + H(q)]\,\ddot{q} + [B_0 + \dot{H}(q)]\,\dot{q} - \frac{\partial T}{\partial q} + g(q) = K_0 r \quad . \qquad ...(7.1)$$

In this equation, $q \in R^n$ is the vector of joint angles, $H(q) \in R^{n\times n}$ is the inertia matrix of the manipulator, $T = \frac{1}{2}\,\dot{q}^T\,H(q)\,\dot{q} \in R^n$ is the kinetic energy, $g(q) \in R^n$ is the vector of gravitational torques, $r \in R^n$ is the vector of voltage inputs to the armature circuits, and $B_0 \in R^{n\times n}$, $J_0 \in R^{n\times n}$ and $K_0 \in R^{n\times n}$ are diagonal matrices associated with the actuators when gearing is used. However, according to the analysis in section 6.2 of Chapter 6, such non-linear robotic manipulators become linear time-invariant plants under the action of computed-torque control. Such linear time-invariant plants are governed by the equations

$$\ddot{q}(t) = u(t) \qquad ...(7.2)$$

and

$$\ddot{\Omega}(t) = u(t) \qquad \text{...(7.3)}$$

in joint and task space co-ordinates, respectively. In these equations, $u \in R^n$ is the vector of new inputs in joint and task space co-ordinates, respectively, and $\Omega \in R^n$ is the vector of end-effector co-ordinates. Equations (7.2) and (7.3) are known as double-integrator equations as they obviously represent n uncoupled double integrators.

Furthermore, in Chapter 6 these equations were expressed in the standard state-space form

$$\dot{x}(t) = Ax(t) + B\,u(t) \qquad \text{...(7.4a)}$$

and

$$y(t) = Cx(t) \quad , \qquad \text{...(7.4b)}$$

with

$$x(t) = \begin{bmatrix} q \\ \dot{q} \end{bmatrix} \text{ or } \begin{bmatrix} \Omega \\ \dot{\Omega} \end{bmatrix} \in R^{2n} \quad , \qquad \text{...(7.5a)}$$

$$A = \begin{bmatrix} 0 & , & I_n \\ 0 & , & 0 \end{bmatrix} \in R^{2n \times 2n} \quad , \qquad \text{...(7.5b)}$$

$$B = \begin{bmatrix} 0 \\ I_n \end{bmatrix} \in R^{2n \times n} \quad , \qquad \text{...(7.5c)}$$

and $$C = [I_n \, , \, 0] \in R^{n \times 2n} \quad , \qquad \text{...(7.5d)}$$

where y can either be the vector of joint angles or end-effector co-ordinates depending on which co-ordinates are being used.

But the dynamics of linear plants governed on the continuous-time set by differential equations of the form (7.4) are governed on the discrete-time set by difference equations of the form

$$x(j+1) = \Phi x(j) + \Psi u(j) \quad , \qquad \text{...(7.6a)}$$

and

$$y(j) = \Gamma x(j) \quad , \qquad \text{...(7.6b)}$$

where

$$\Phi = e^{AT} \quad , \qquad \text{...(7.7a)}$$

$$\Psi = \int_0^T e^{At} B \, dt \quad , \qquad \text{...(7.7b)}$$

$$\Gamma = C \quad , \qquad \text{...(7.7c)}$$

and T is the sampling period.

The step-response matrices of such plants have the form

$$H(T) = \int_0^T C \, e^{At} B \, dt \qquad \text{...(7.8)}$$

and characterise the responses of initially quiescent plants after one sampling period. Such step-response matrices can evidently be measured directly from input/output data.

It is clear from equations (7.5b), (7.5c) and (7.5d) that robotic manipulators give rise to completely irregular linear time-invariant plants under the action of computed-

torque control in both joint and task spaces. This implies, as shown in Chapter 6, that the results of Arimoto et al (1984) for the iterative learning control of regular plants are inapplicable in such cases. However, the results of Chapter 4 and in particular of Theorem 4.2 are directly applicable to the design of digital iterative learning controllers for irregular linear time-invariant plants. This theorem is accordingly re-stated here for convenience.

Theorem

In the case of the completely irregular plant with discrete-time governing equations

$$x_k(j+1) = \Phi x_k(j) + \Psi u_k(j)$$

and

$$y_k(j) = \Gamma x_k(j) \quad ,$$

under the action of the control law

$$u_k(j) = -\frac{2}{T}(1+\alpha) D z_k(j) + \left[I_n + \frac{2}{T} D\right] s_k(j) \quad , \qquad (7.9a)$$

$$z_k(j+1) = -\alpha z_k(j) + s_k(j) \quad , \qquad ...(7.9b)$$

$$s_{k+1}(j) = s_k(j) + \Lambda \{e_k(j+1) - e_k(j)\} \quad , \qquad ...(7.9c)$$

where $\alpha(-1,+1]$, $D \in R^{n \times n}$, and $e_k(j) = v(j) - y_k(j)$, assume that

(i) $$\Lambda = \left[H(T)\left(I_n + \frac{2}{T} D\right)\right]^{-1} ;$$

(ii) $y_{k+1}(0) = y_k(0) = v(0) \quad (k = 0, 1, 2, \ldots)$.

Then, when $j \in [0, J]$,

$$y_k(j) \rightarrow v(j)$$

as $k \rightarrow \infty$.

It follows, therefore, that the control law consists of two parts. The first part is the model-based controller which is governed by equations (6.2) and (6.11) in joint and task spaces, respectively, (see Chapter 6); and the second part is the iterative learning controller which is governed by equations (7.9).

7.3 ILLUSTRATIVE EXAMPLES

These theoretical results can be conveniently illustrated by considering the digital iterative learning control of the planar motions of a two-link manipulator in both joint and task space co-ordinates. In addition, armature-controlled dc motors with gearing or direct drive servo motors are used to drive the robot arm. These dc motors have the same specifications as those of Chapter 6. Furthermore, $J_0 = J_m/\nu^2$, $K_0 = K/\nu R$, $B_0 = K^2/\nu^2 R$, and ν is the gear ratio as described in Chapter 6. In addition, the two-link manipulator under investigation has the same specifications as that of Chapter 6. Moreover, the non-linear dynamics of the two-link manipulator are governed by equation (6.23) together with equations (6.24), (6.25) and (6.26).

Examples 7.1 and 7.2 consider the application of model-based iterative learning controllers for a robotic manipulator in joint space; Examples 7.3 and 7.4 consider the application of such controllers in task space.

In all of these examples, the step response matrix $H(T)$ of the linear multivariable plants governed by equation (7.6) when the sampling time $T = 0.01$ *sec* is

$$H(T) = \begin{bmatrix} 0.5\times10^{-4} & , & 0 \\ 0 & , & 0.5\times10^{-4} \end{bmatrix} \quad . \qquad ...(7.10)$$

This step-response matrix is used to obtain the controller gain matrix, Λ. In addition, since CB is null, D can be arbitrary (since $CBD = 0$). Therefore, $D = I_n$ is chosen. It follows from condition (i) of Theorem 4.2 that

$$\Lambda = \begin{bmatrix} 99.5025 & , & 0 \\ 0 & , & 99.5025 \end{bmatrix} \qquad ...(7.11)$$

in all the Examples.

Example 7.1

In this example, direct-drive servomotors are used. It follows therefore that the torque developed by the model-based controller in the kth iteration is that given by equation (6.26).

In this case, it is desired that the joint angles perform the motions

$$v(j) = \begin{bmatrix} -\frac{\pi}{4} - 4\,[(jT)^3 - (jT)^4] \\ \frac{\pi}{4} + 4\,[(jT)^3 - (jT)^4] \end{bmatrix} \qquad ...(7.12)$$

in 1.0 *sec*. In addition, the initial input vector is

$$s_0(jT) = \begin{bmatrix} 0 \\ 0 \end{bmatrix} \quad , \qquad \text{...(7.13)}$$

the parameter $\alpha = 1$ is chosen so that rapid convergence is obtained, and the controller gain matrix A is as specified in equation (7.11). In this case, as in Example 6.1 of Chapter 6, the rapid learning of the digital iterative learning controller is shown in Figures 7.1(a,b). It is also clear that the actual motions of the two arms of the robotic manipulator are indistinguishable from the desired motions after three iterations. Figures 7.1(c,d) show the corresponding control efforts.

Example 7.2

In this example, dc motors with reduction gearing are used. It follows therefore that the model-based controller can be either the <u>exact</u> or the <u>approximate</u> controller governed by equation (6.18) or (6.19), respectively. Such an approximate controller is obtained when the reduction gear ratio is increased as explained in Chapter 6.

In this case, it is desired that the joint angles perform the motions

$$v(j) = \begin{bmatrix} -\frac{\pi}{4} - 4\left[(jT)^3 - (jT)^4\right] \\ \\ \frac{\pi}{4} + 4\left[(jT)^3 - (jT)^4\right] \end{bmatrix} \qquad \text{...(7.14)}$$

in 1.0 *sec.* In addition, the initial input vector is

$$s_0\,(jT) = \begin{bmatrix} 0 \\ 0 \end{bmatrix} \quad , \qquad \text{...(7.15)}$$

the parameter $\alpha = 1$ is chosen so that rapid convergence is obtained, and the controller gain matrix A is that of equation (7.11). In this case, as in Example 6.2 of Chapter 6, the rapid learning of the exact model-based iterative controller is shown for each of the two joint angles in Figures 7.2(a,b), from which it is clear that the actual motions are indistinguishable from the desired motions after three iterations. Similarly rapid learning is achieved when approximate model-based iterative controllers are used (see Figures 7.2(c,d), (e,f) and (g,h)). It is evident that the characteristics of these approximate model-based controllers rapidly approach those of the exact model-based controllers as the reduction gear ratio increases. Figure 7.3 shows the corresponding control efforts in all cases.

Example 7.3

In this example, direct-drive servomotors are used. It follows therefore that the force developed by the model-based controller in the kth iteration is that given by equation (6.35)

In this case, it is required that the end-effector perform the following rectilinear motions in the plane of cartesian co-ordinates:

(i) moves between $R(0.7375, -0.3055)m$ and $Q(0.7,-0.25)m$ in 0.15 *sec* with equal periods of acceleration, cruise, and deceleration from rest to $669.398 \times 10^{-3} m/s$ and back to rest;

(ii) then moves immediately between $Q(0.7,-0.25)m$ and $R(0.7375,-0.3055)m$ in 0.15 *sec* with equal periods of acceleration, cruise and deceleration from rest to 669.398×10^{-3} m/s and back to rest.

The initial input vector is

$$s_0(jT) = \begin{bmatrix} 0 \\ 0 \end{bmatrix}, \qquad \ldots(7.16)$$

the parameter $\alpha = 1$ is chosen so that rapid convergence is obtained, and the controller gain matrix $\mathbf{A}$ is as specified in equation (7.11).

The rapid learning of the digital iterative learning controller is shown in Figures 7.4(a,b), and the corresponding control effort is shown in Figures 7.4(c,d).

Example 7.4

In this example, dc motors with reduction gearing are used. It follows therefore that the model-based controller can be either the exact or the approximate controller governed by equation (6.20) or (6.21) in Chapter 6, respectively. Such an approximate controller is obtained when the reduction gear ratio increases as explained in Chapter 6. In addition, in equations (6.20) and (6.21), $J_0 = J_m/\nu^2$, $K_0 = k/\nu R$, and $B_0 = K^2/\nu^2 R$ are all constant diagonal matrices.

In this case, it is desired that the end-effector perform the motions of Example 7.3 in the plane of cartesian co-ordinates.

The initial input vector is

$$s_0(jT) = \begin{bmatrix} 0 \\ 0 \end{bmatrix}, \qquad \ldots(7.17)$$

the parameter $\alpha = 1$ is chosen so that rapid convergence is obtained, and the controller gain matrix A is as specified in equation (7.11).

The rapid learning of the exact model-based iterative controller is shown in Figures 7.5(a,b). It is also clear from Figures 7.5(c,d), (e,f) and (g,h) that, by using the approximate model-based iterative controller, rapid learning can be obtained as the reduction gear ratios increase. Figure 7.6 shows the corresponding control efforts in all cases.

7.4 CONCLUSION

It has been shown that the results of Chapter 4 for the digital iterative learning control of irregular plants are directly applicable to the design of iterative learning controllers for robotic manipulators, since such manipulators become irregular linear time-invariant plants under the action of computed-torque control in both joint and task spaces as shown in Chapter 6. The practical relevance of these theoretical results to the design of model-based iterative controllers for robotic manipulators has been illustrated by the presentation of numerical results for the iterative learning control of a typical two-degree-of-freedom robotic manipulator in both joint and task spaces using dc motors with reduction gearing or direct-drive servomotors. These results have indicated that such model-based iterative controllers are robust in the sense that rapid learning is obtained even when crude dynamical models are used following the introduction of reduction gearing. The digital controllers proposed in this chapter circumvent the need for the approximations involved in digitalising the analogue controllers discussed in Chapter 6.

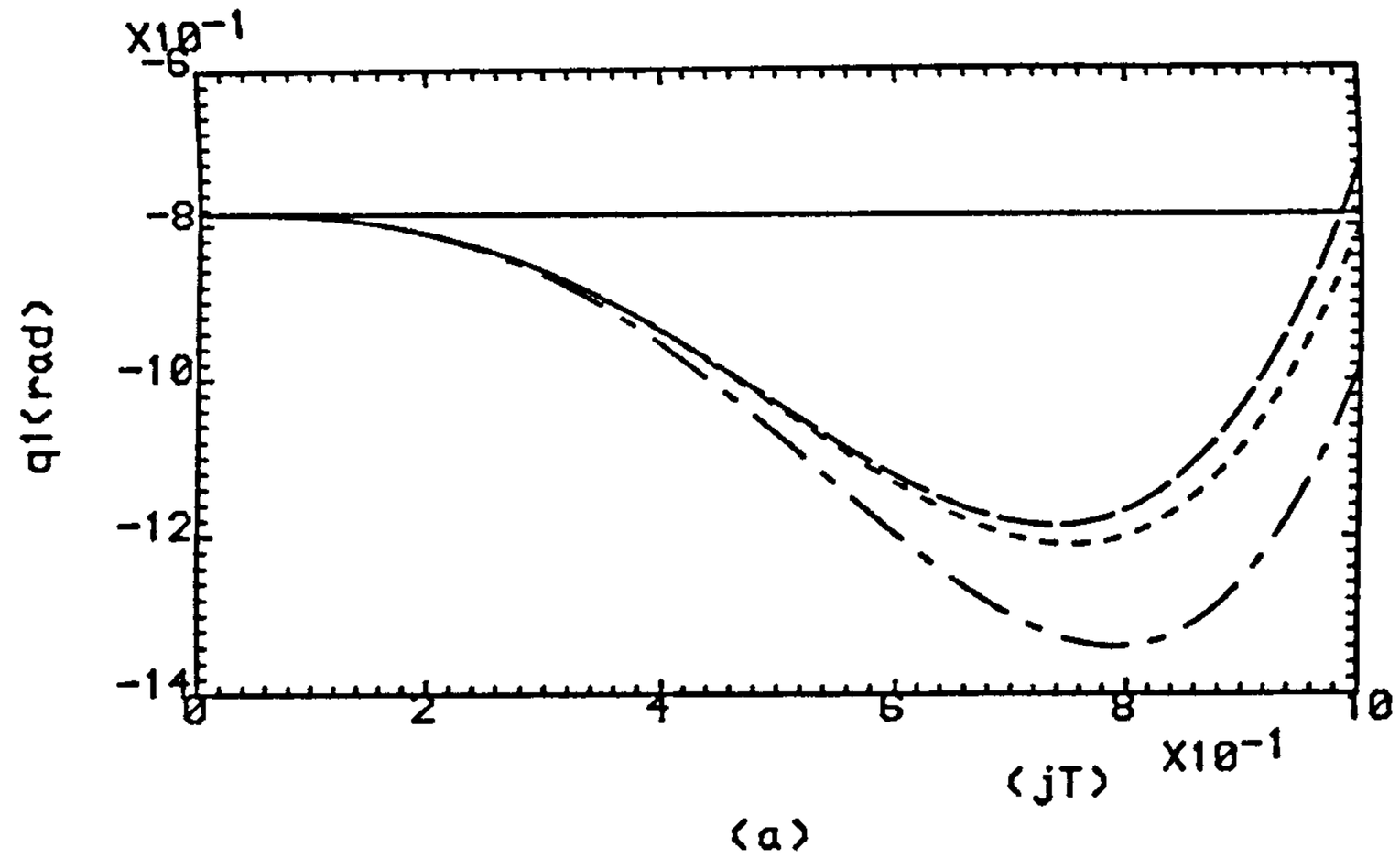

(a)

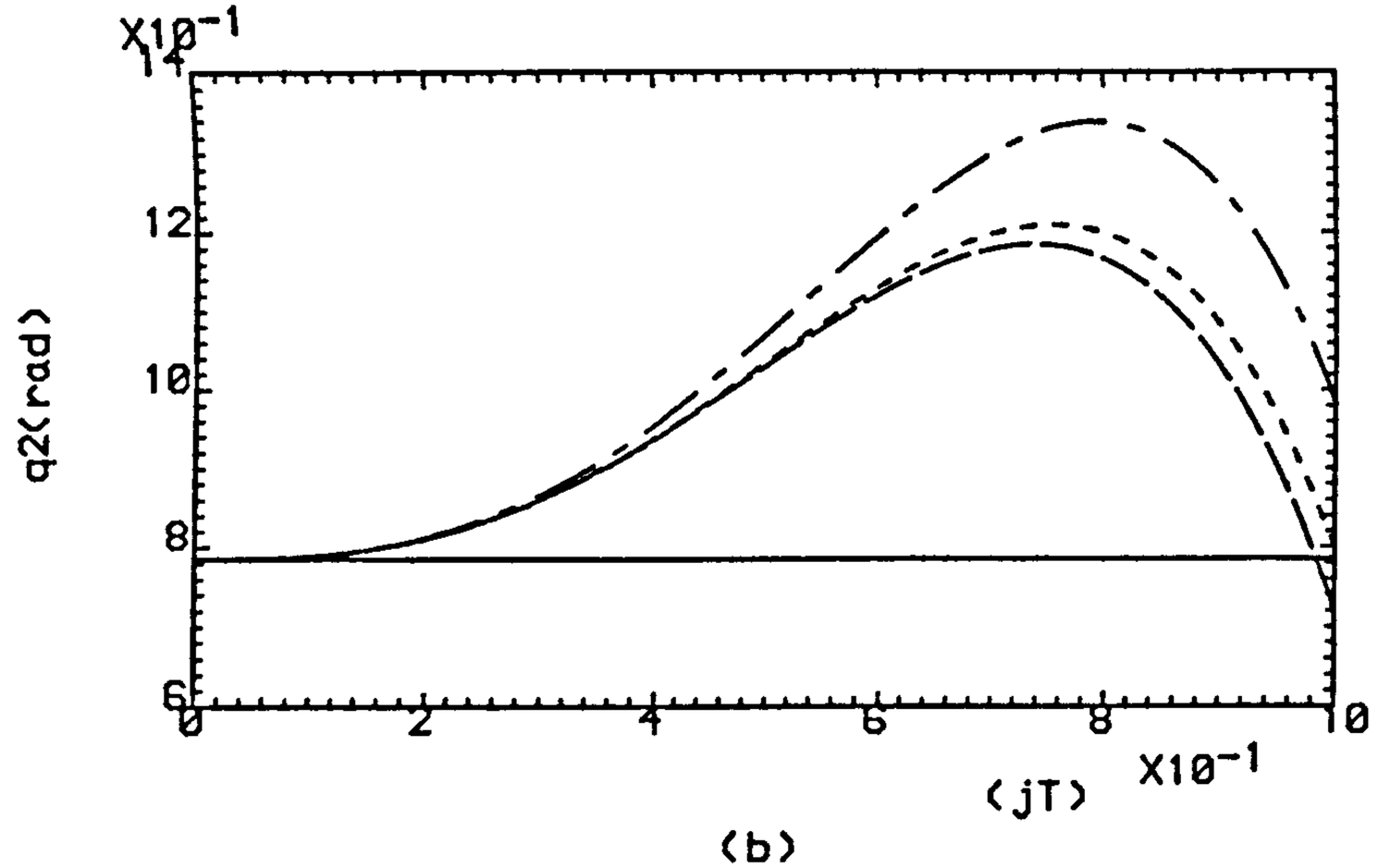

(b)

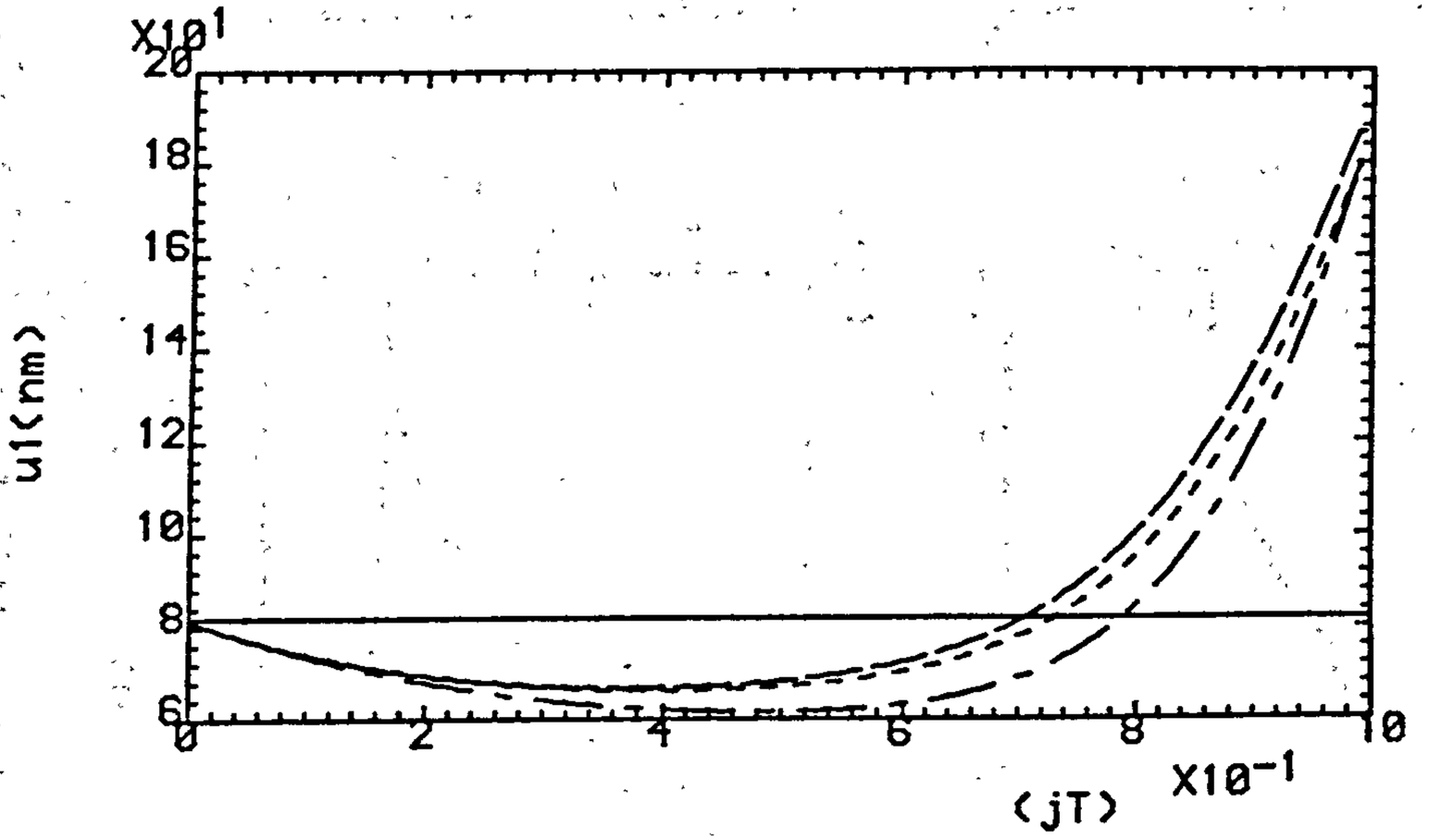

(c)

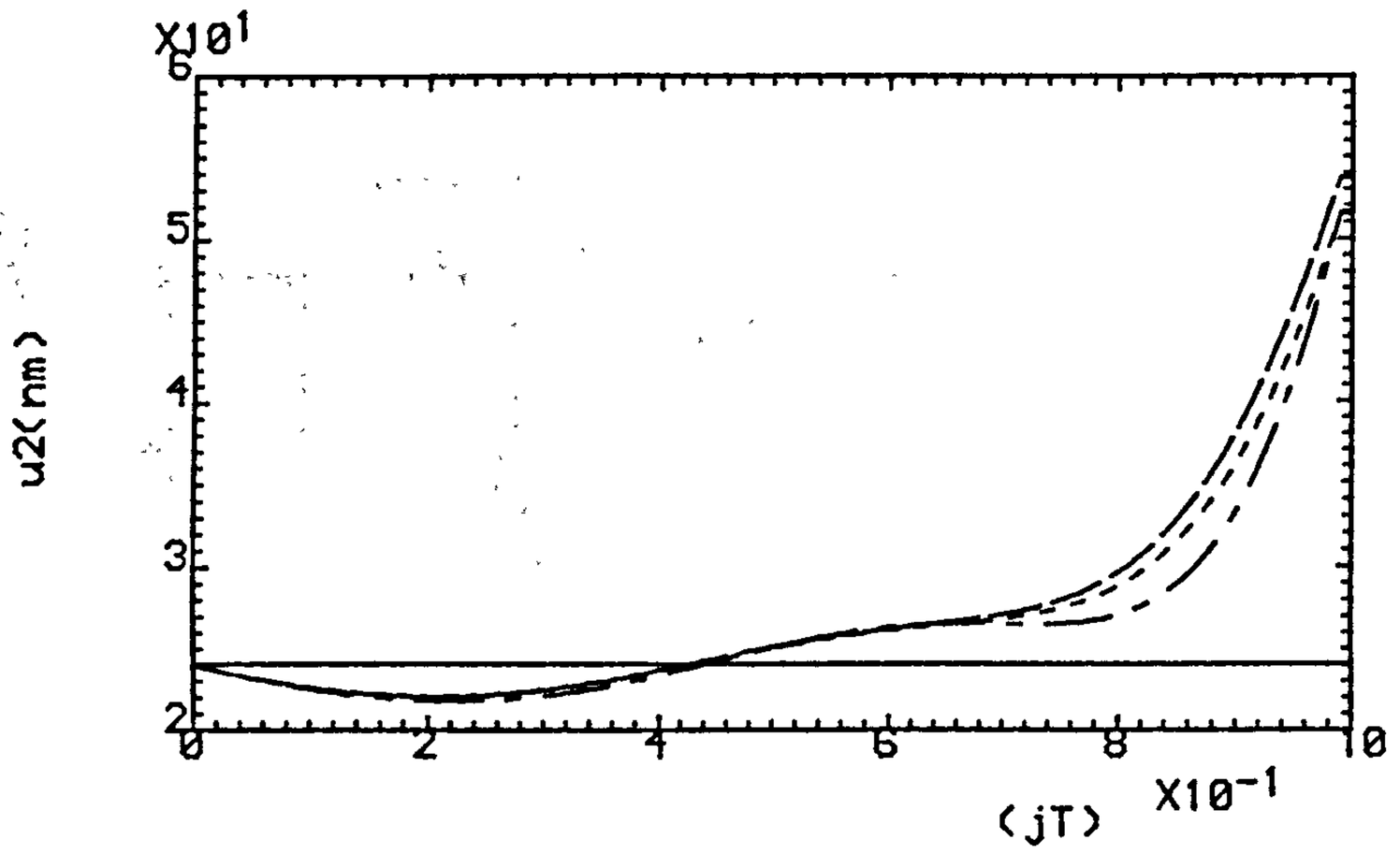

(d)

Fig.7.1(a,b) Successive Outputs OF Two-Link Manipulator.
(c,d) Successive Torques Acting On The Joints.
——— K=0 , -·-·- K=1 , ----- K=2 , ... K=3

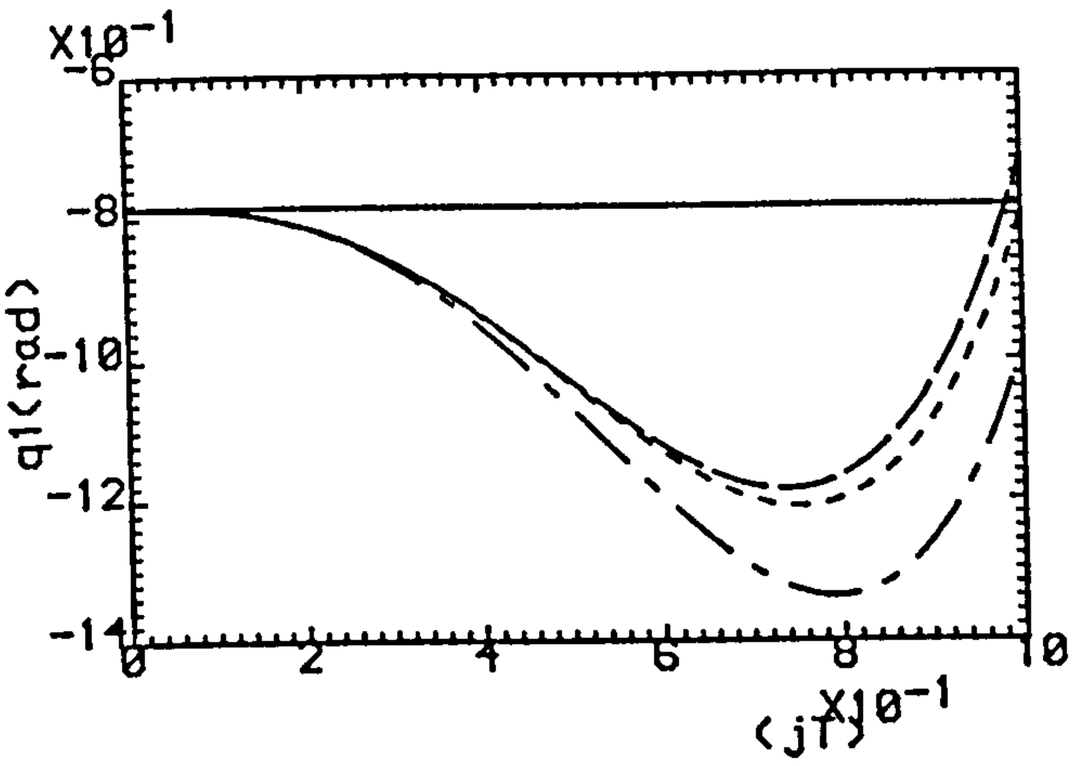

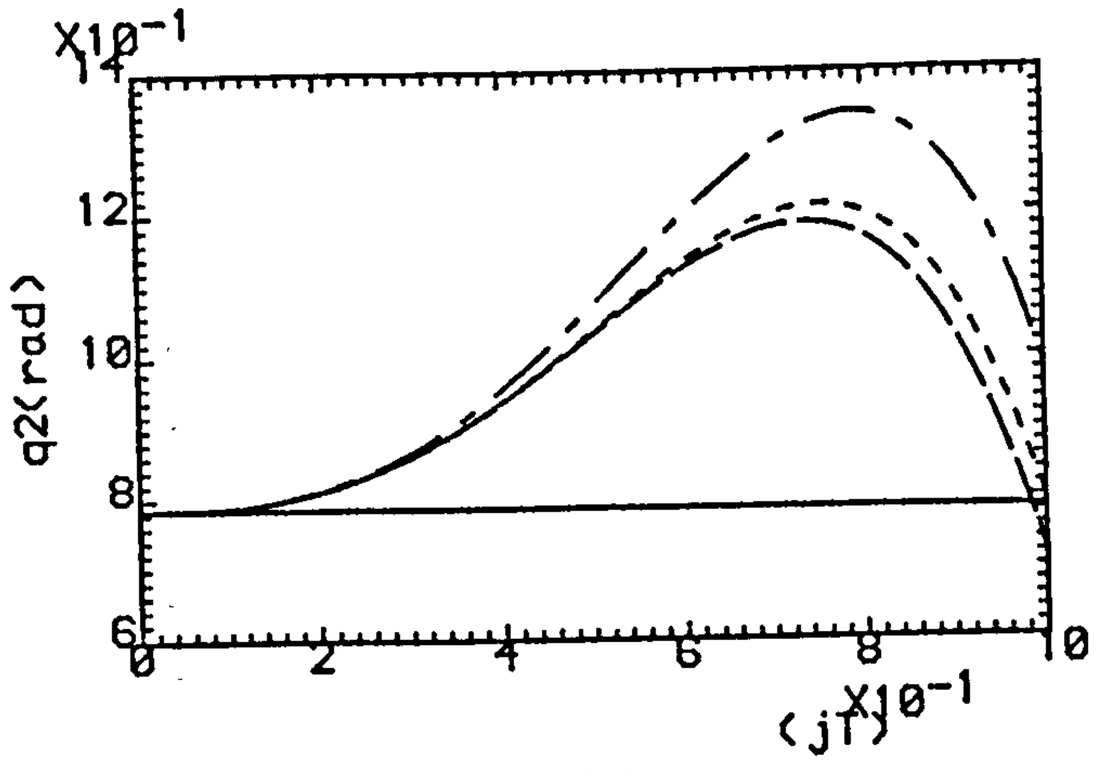

(a)

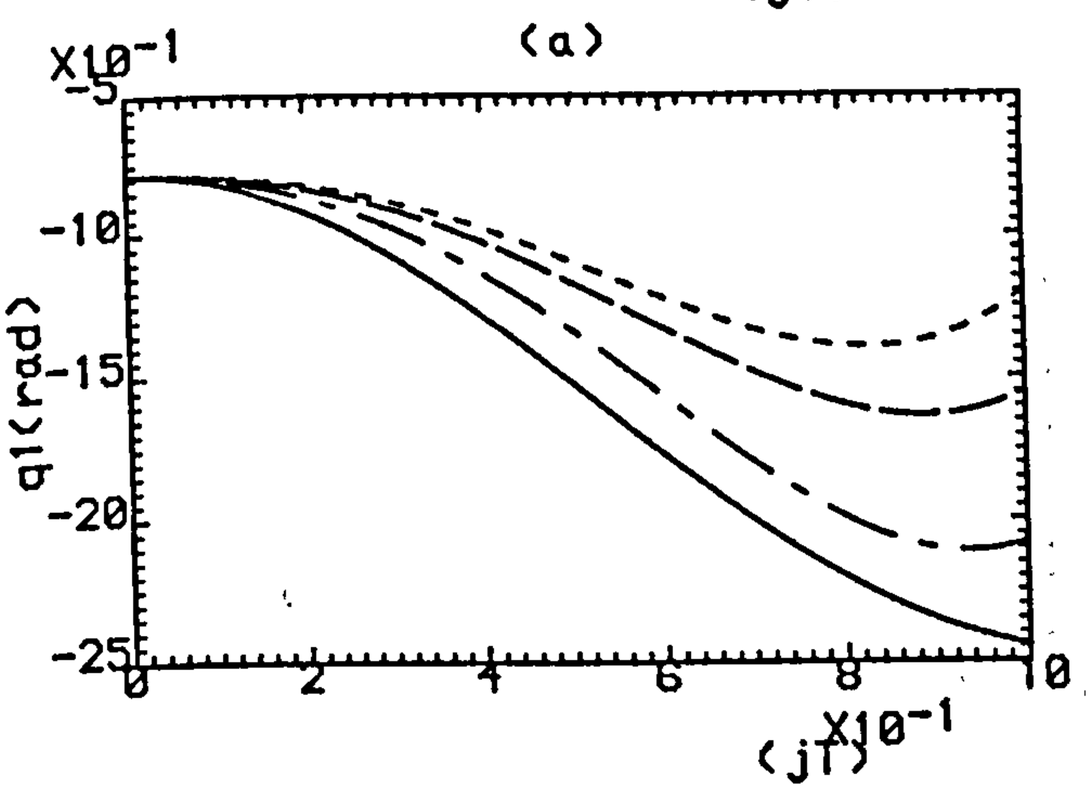

(b)

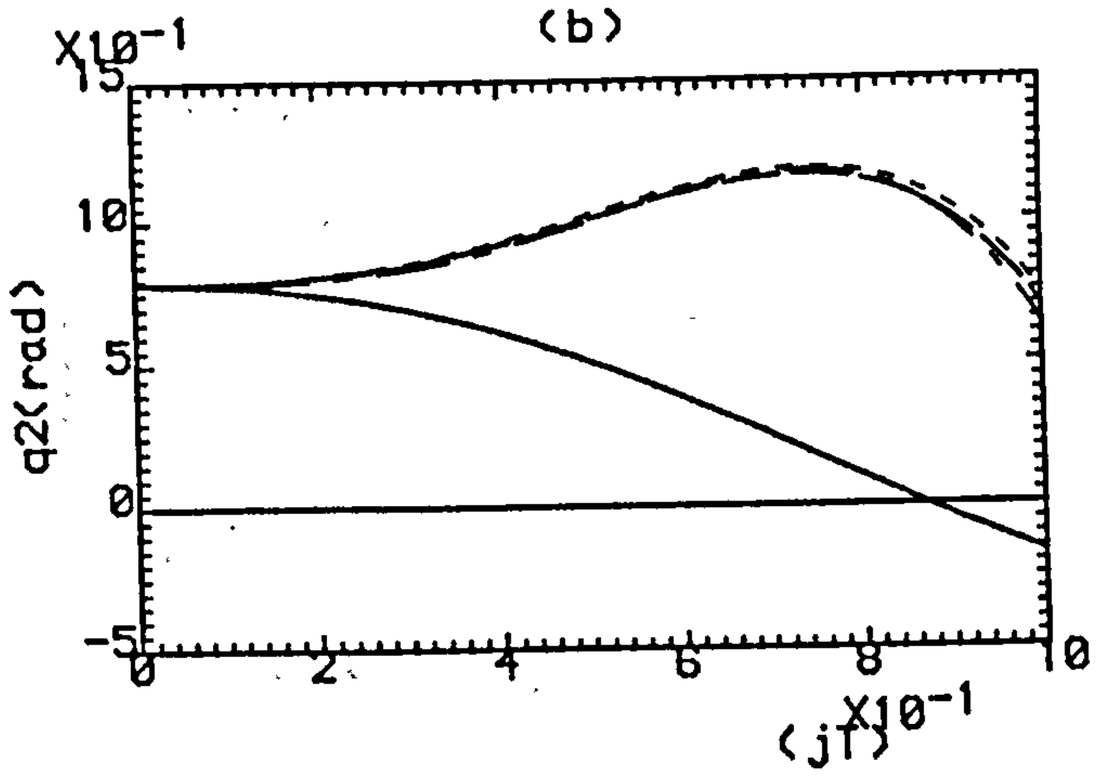

(c)

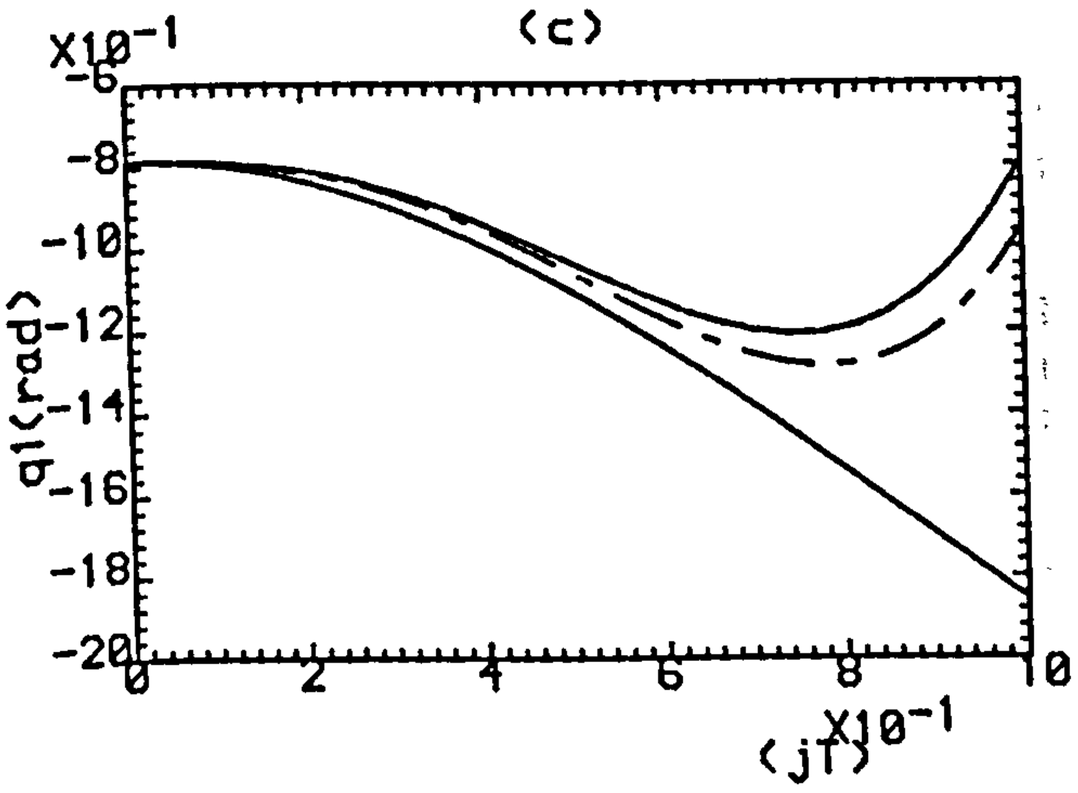

(d)

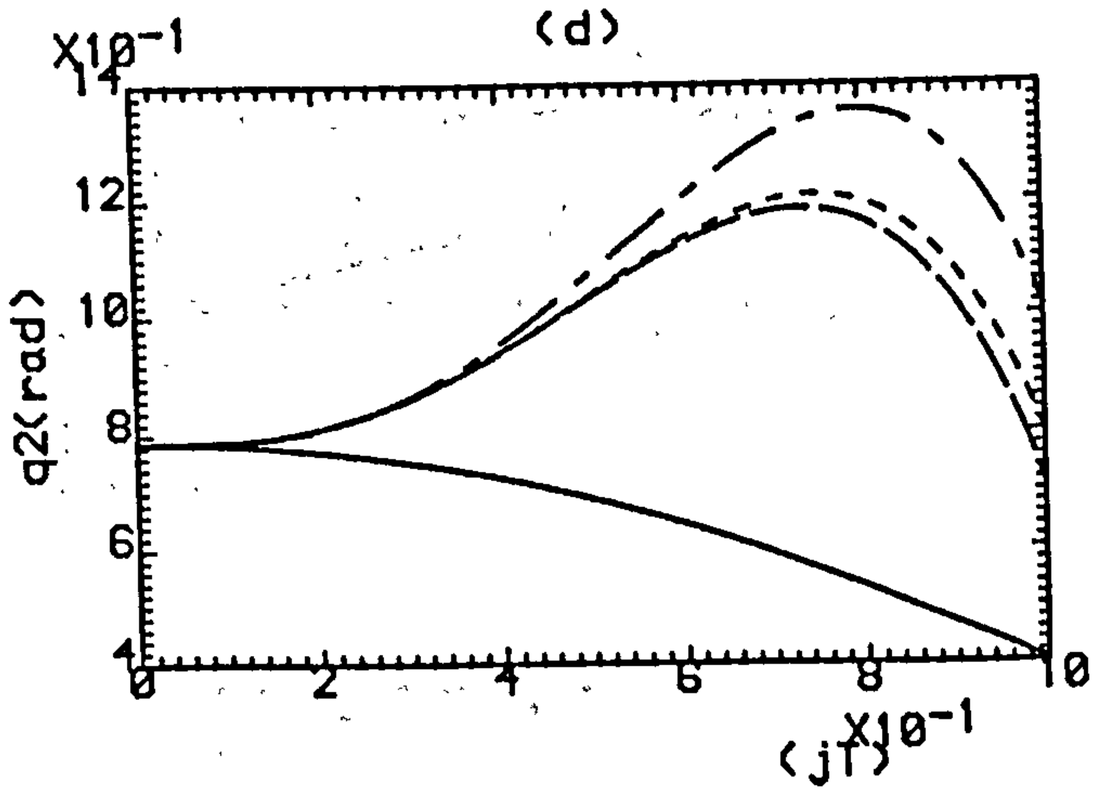

(e)

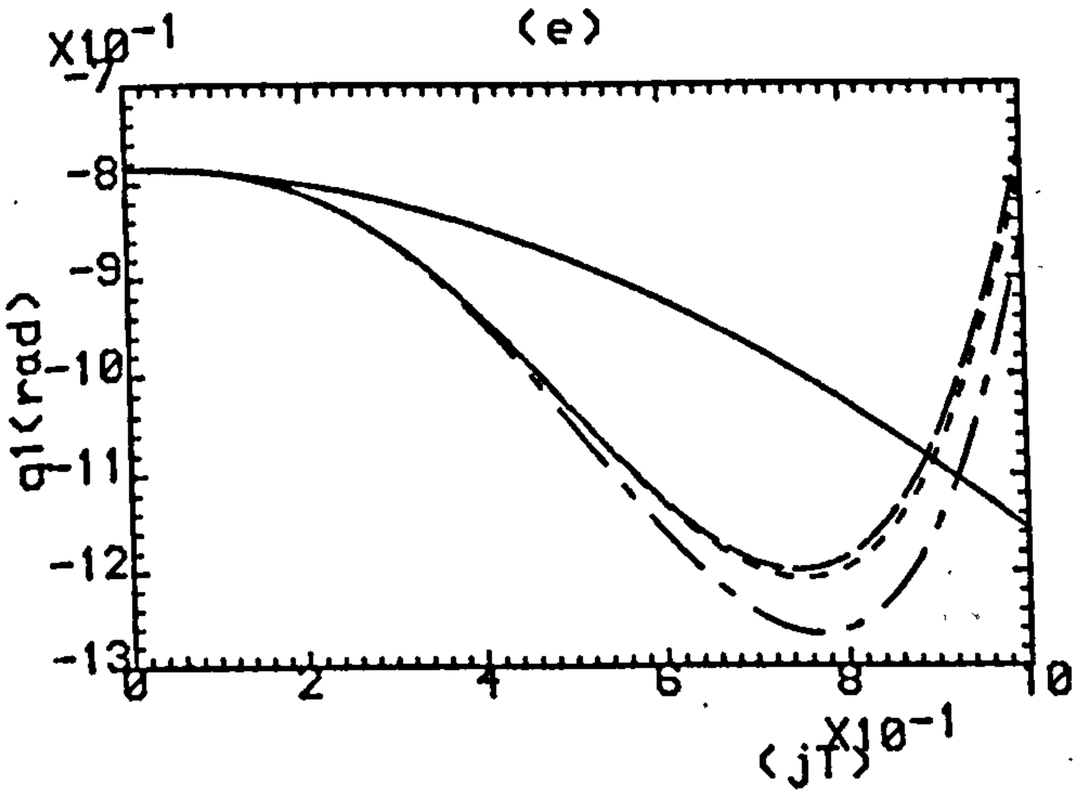

(F)

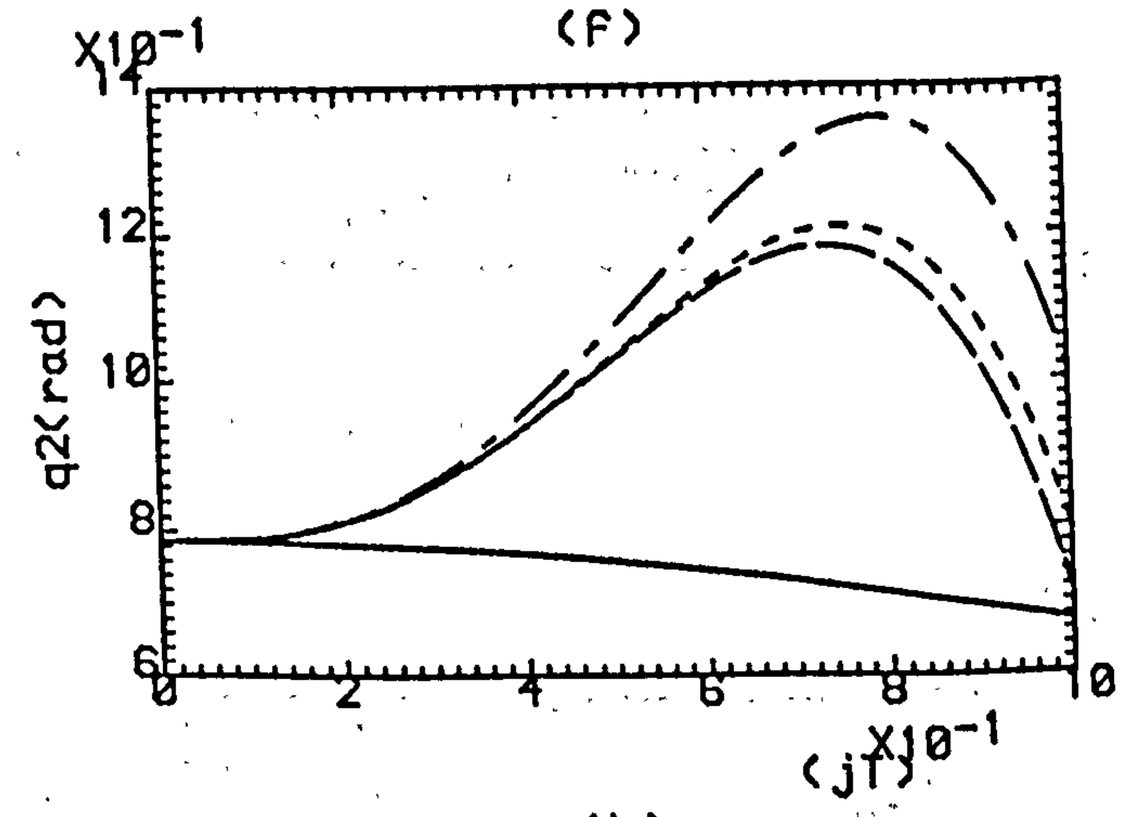

(g) (h)

Fig.7.20utputs Under:(a,b)Exact Model-Based.
Fixed Controller With reduction gear ratio
(c,d) 100:1 , (e,F) 200:1 , (g,h) 400:1 .
——— K=0 , -·-·- K=1 , ----- K=2 , ... K=3

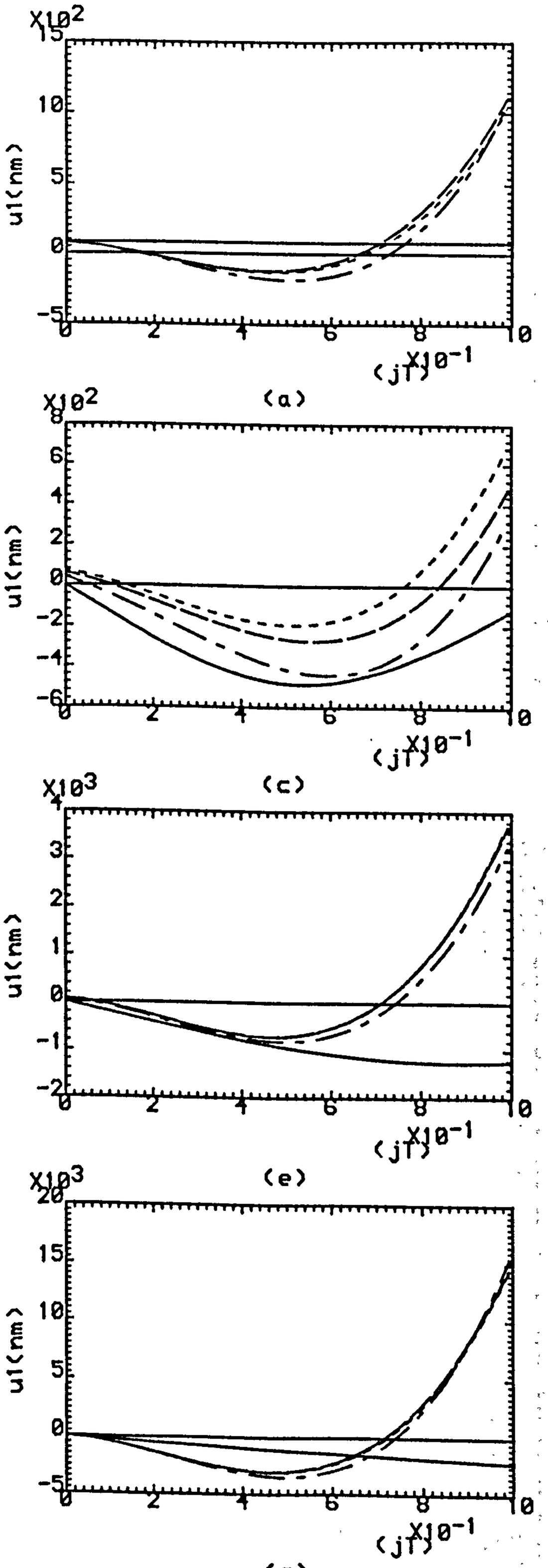

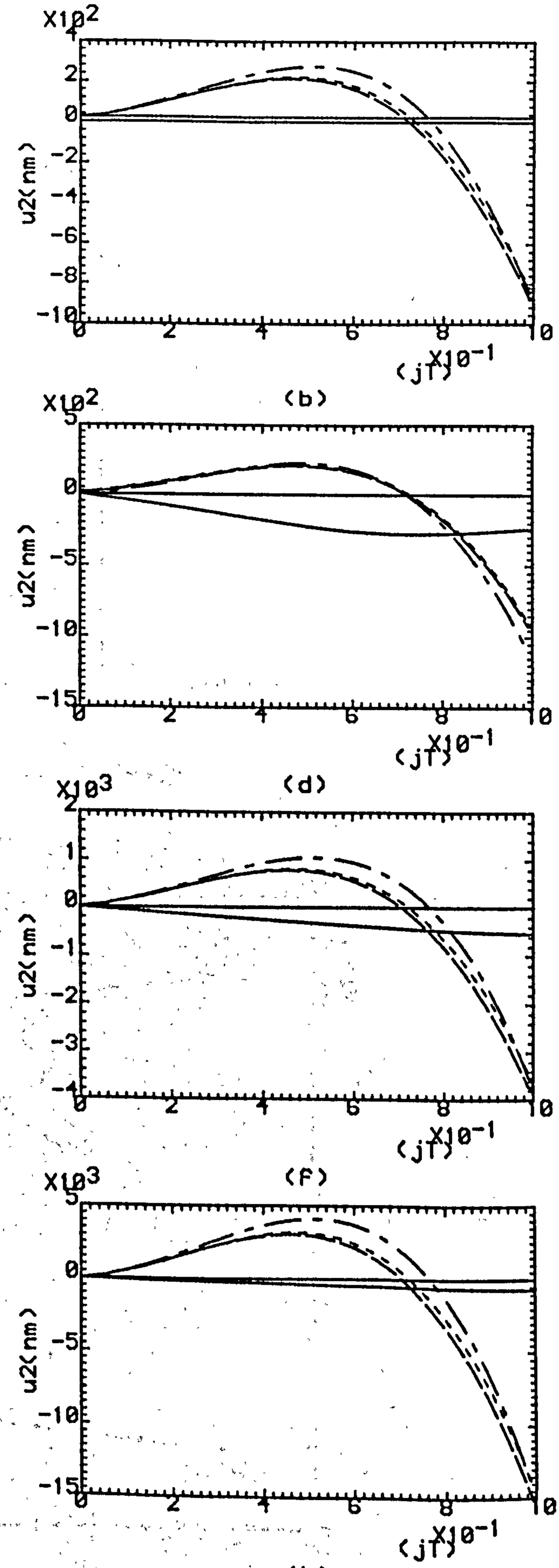

Fig.7.3Control EFForts:(a,b)Exact Model-Based,
(c,d)gear ratio 100:1,(e,F)gear ratio 200:1,
(g,h)gear ratio 400:1 .
——— K=0 , -·-·- K=1 , ----- K=2 , ... K=3

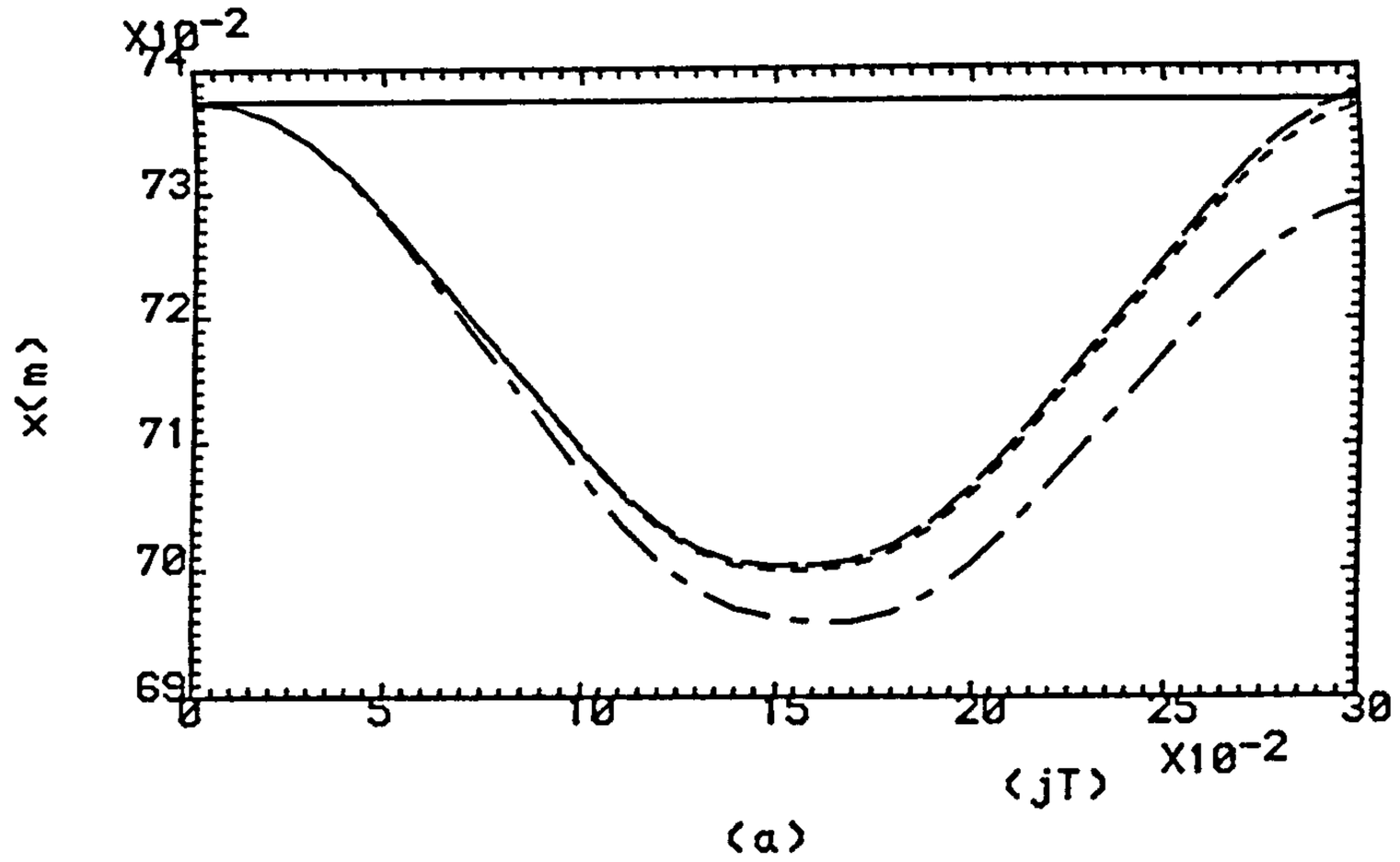

(a)

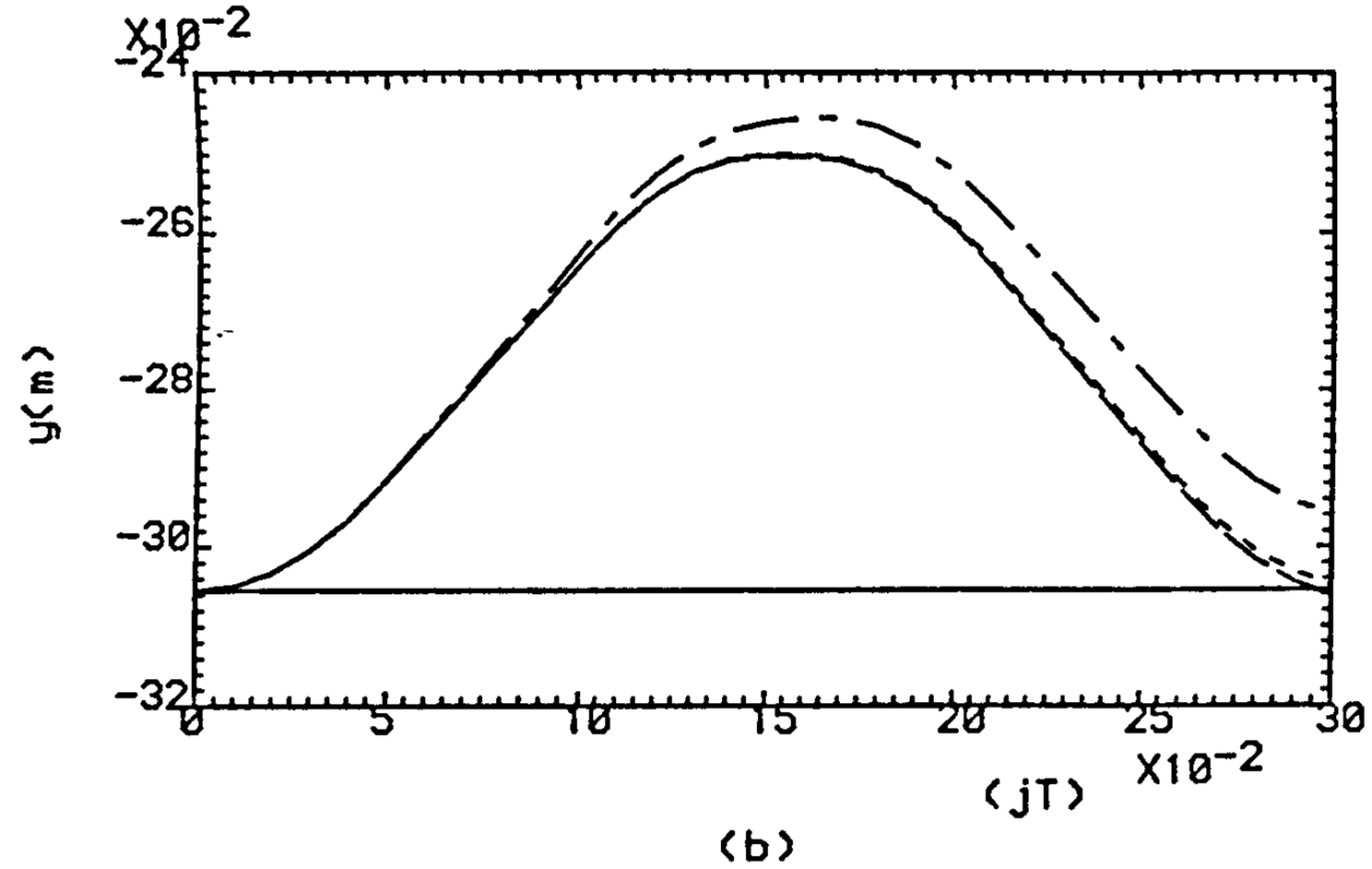

(b)

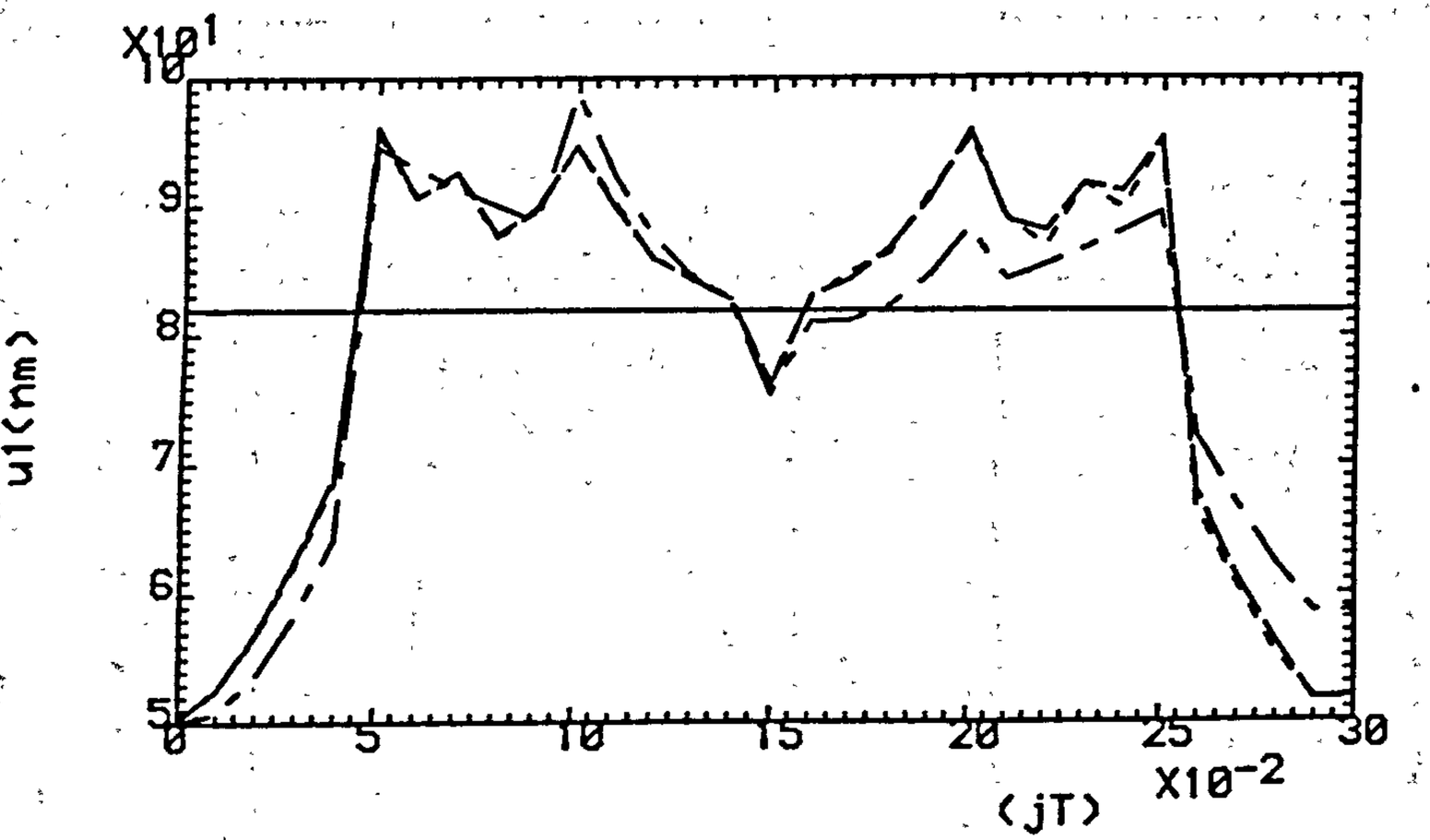

(c)

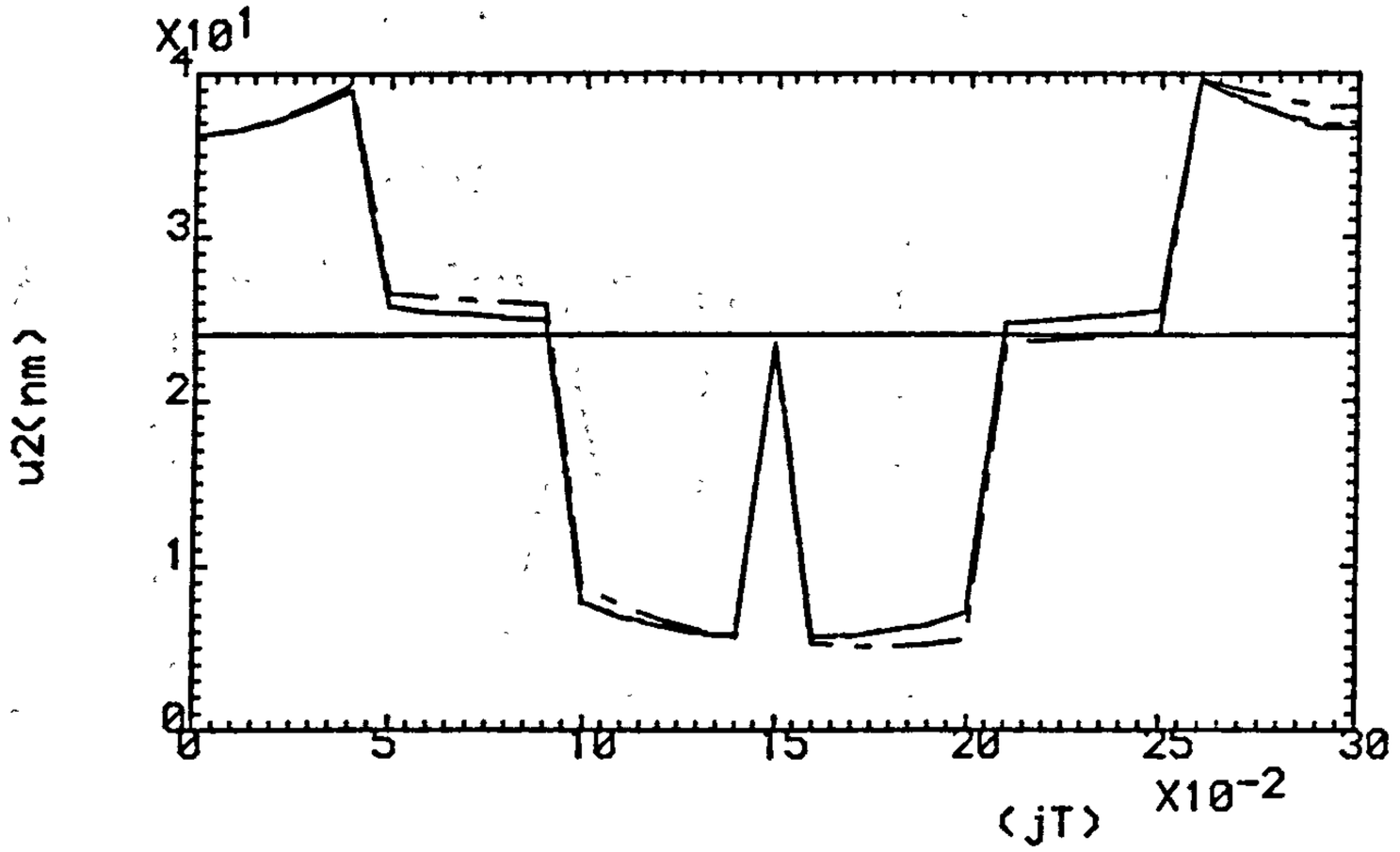

(d)

Fig.7.4(a,b) Successive Outputs OF Two-Link Manipulator.
(c,d) Successive Torques Acting On The Joints.
——— K=0 , -·-·- K=1 , ----- K=2 , ... K=3

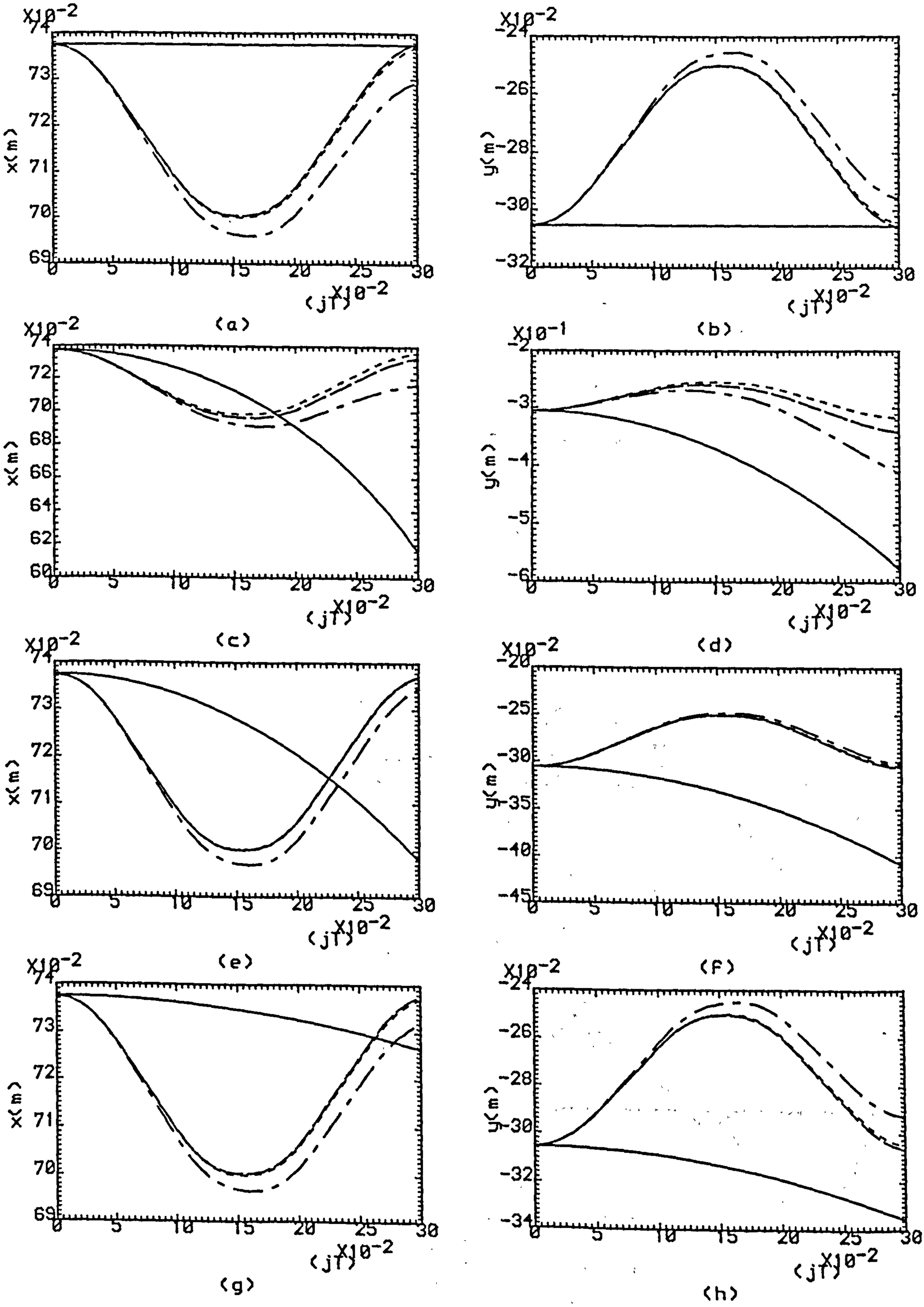

Fig.7.5Outputs Under:(a,b)Exact Model-Based, Fixed Controller With reduction gear ratio (c,d) 100:1 , (e,F) 200:1 , (g,h) 400:1 .
——— K=0 , -·-·- K=1 , ----- K=2 , ... K=3

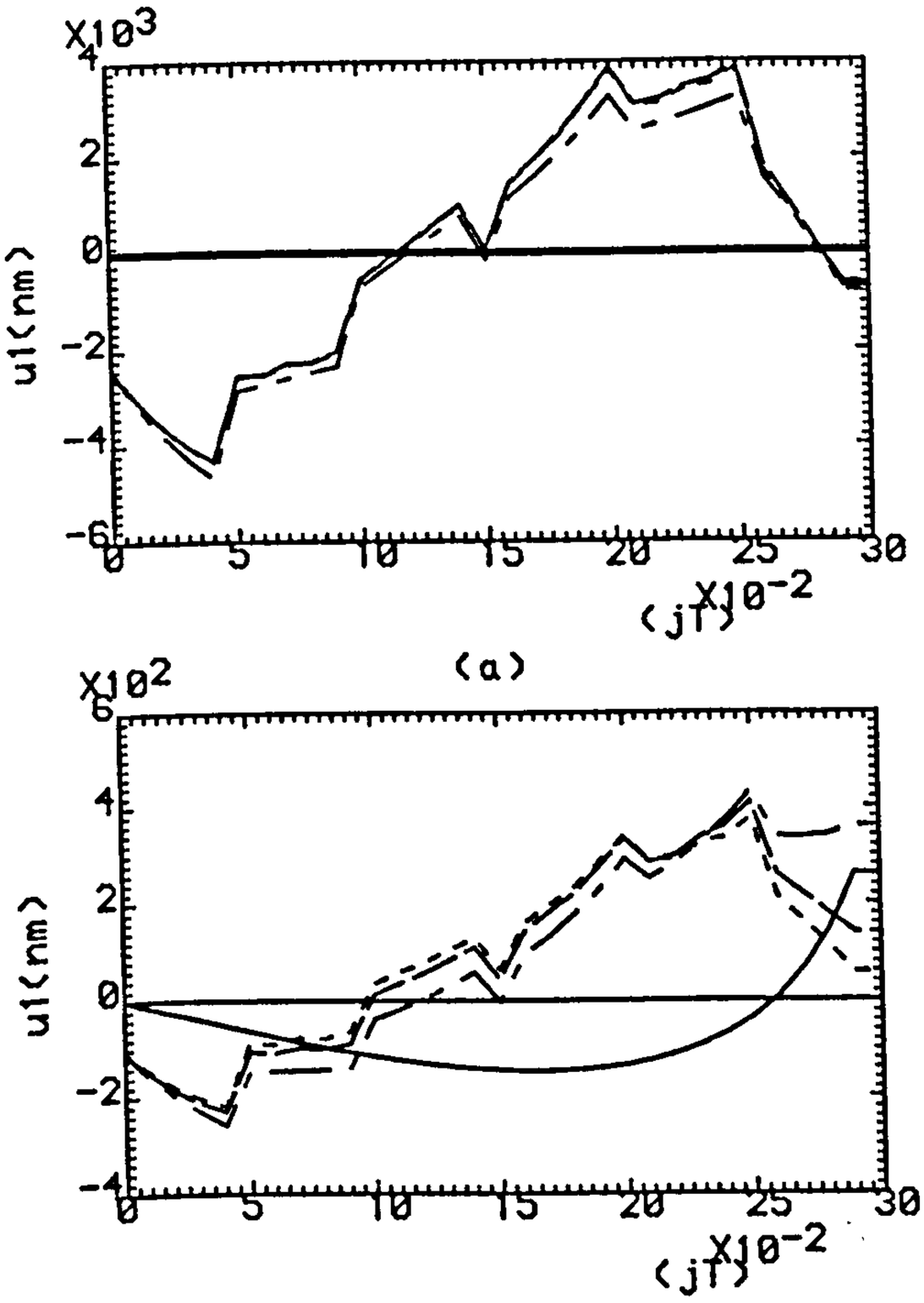

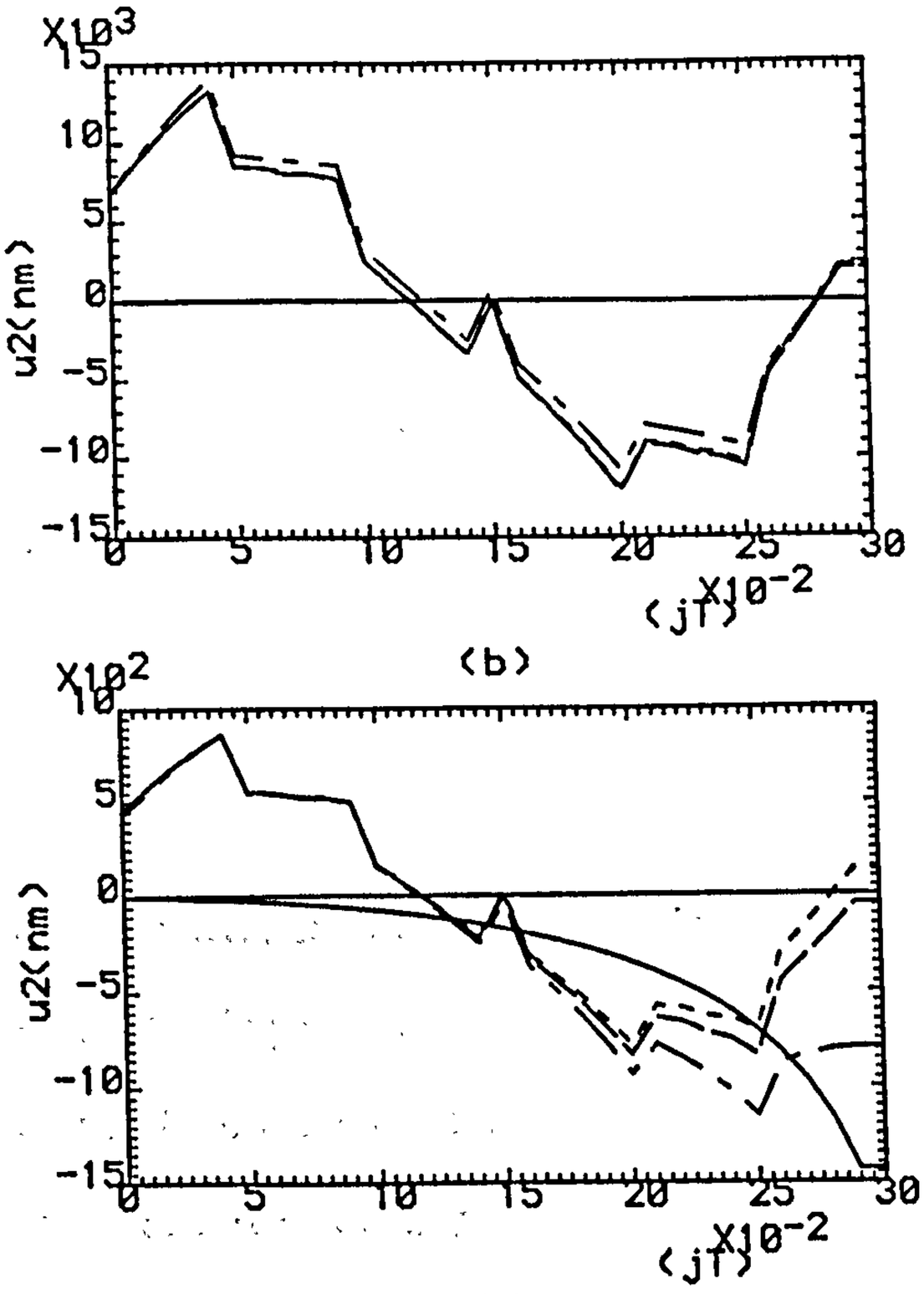

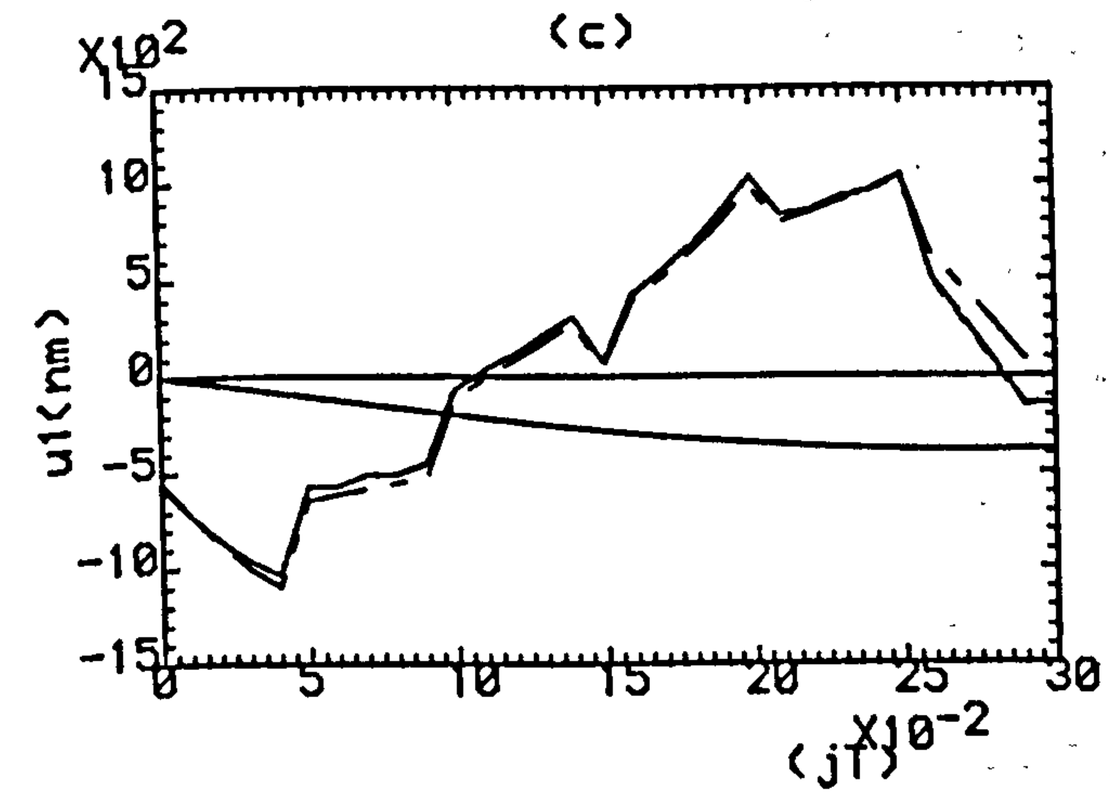

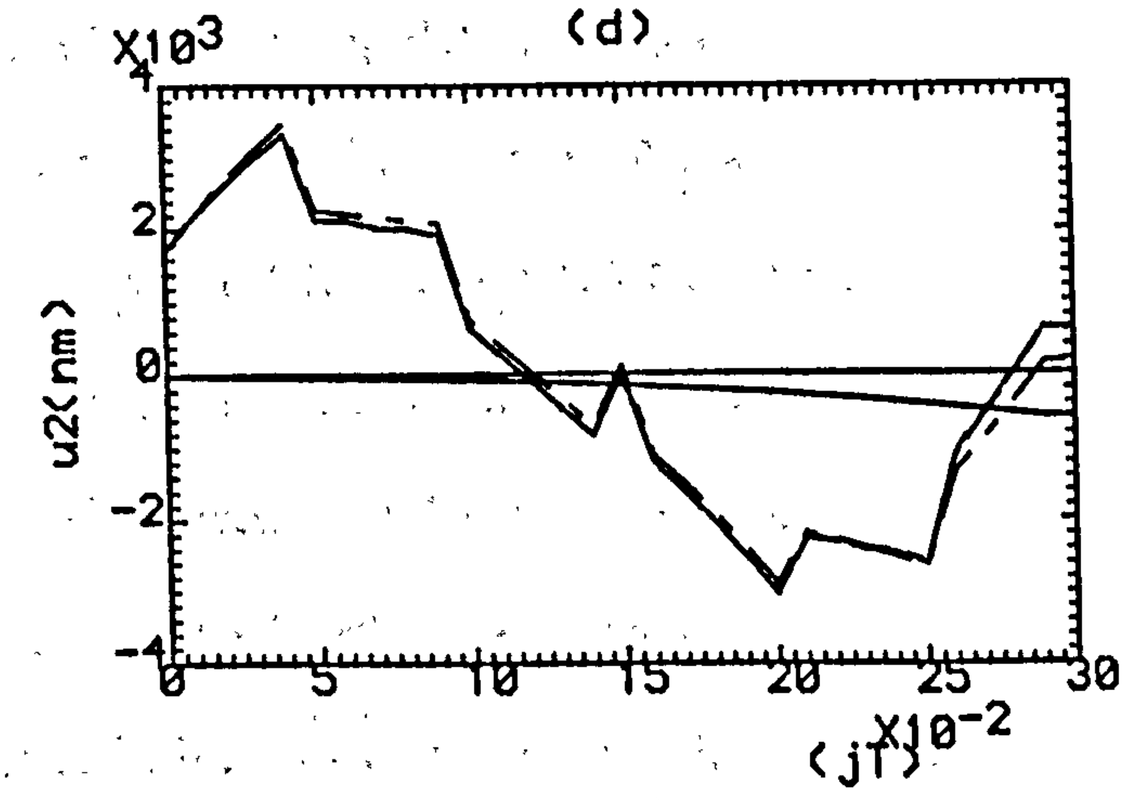

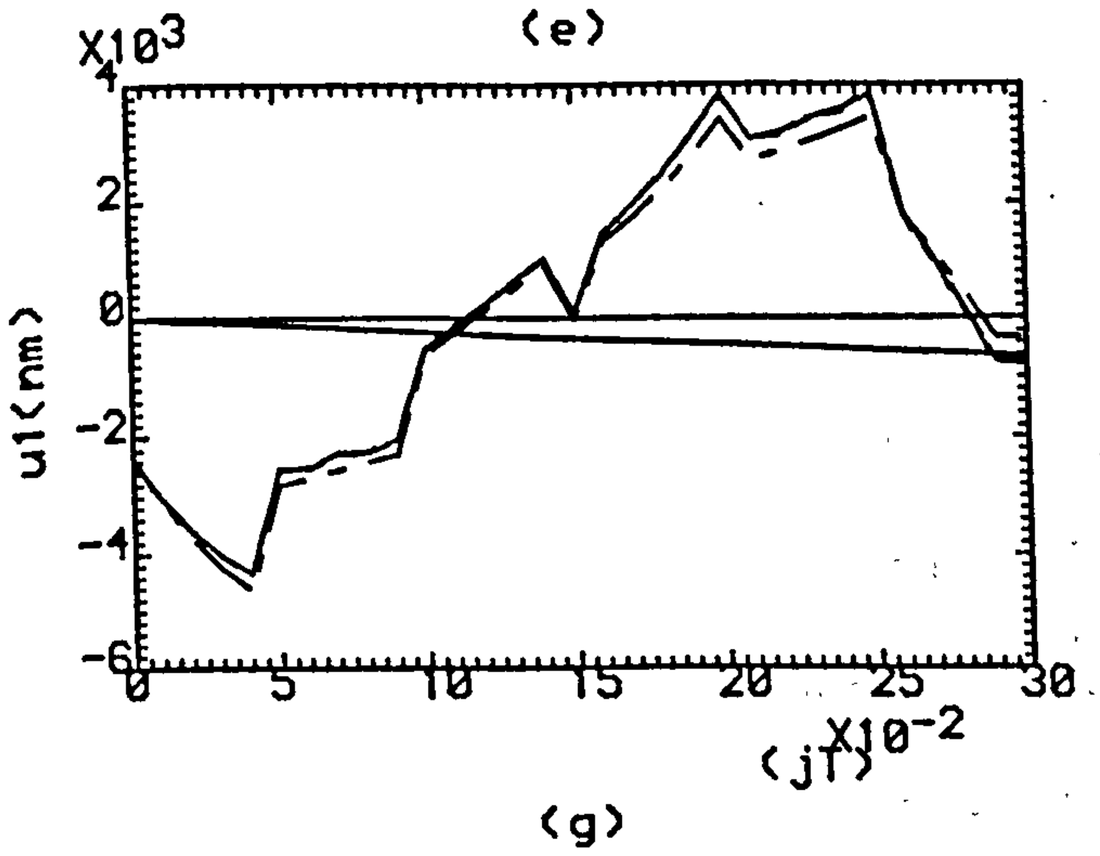

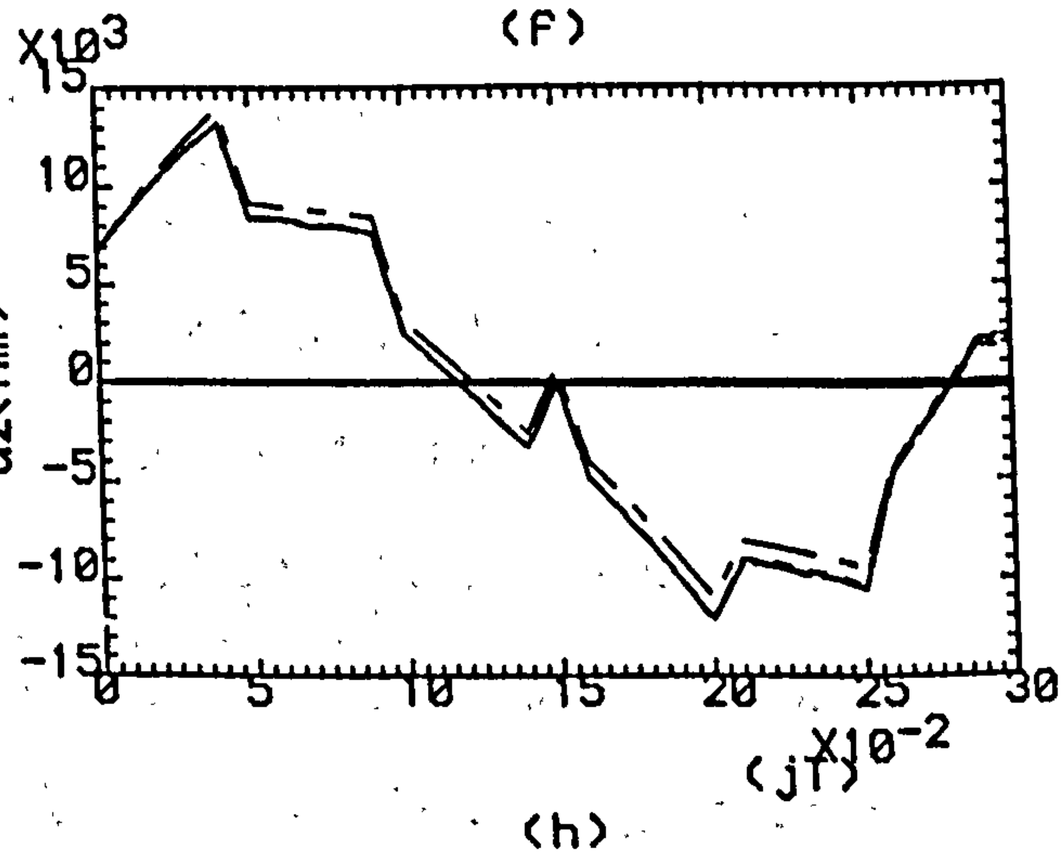

Fig.7.6Control Efforts:(a,b)Exact Model-Based,
(c,d)gear ratio 100:1,(e,f)gear ratio 200:1,
(g,h)gear ratio 400:1 .
——— K=0 , -·-·- K=1 , ----- K=2 , ... K=3

CHAPTER 8

DESIGN OF ADAPTIVE DIGITAL ITERATIVE LEARNING CONTROLLERS FOR ROBOTIC MANIPULATORS

8.1 INTRODUCTION

The model-based computed-torque method together with iterative learning control was introduced in Chapter 6 and 7 as a method of using the dynamic model of a manipulator explicitly in control law formulations in both joint and task spaces. Such an approach yields a controller that supresses disturbances and tracks desired trajectories uniformly in all configurations of the manipulator. However, any mismatch between the values of the plant parameters used in the control law and the actual plant parameters could lead to a degradation in the learning performance and to a reduction in the convergence speed. It was therefore shown in Chapters 6 and 7 that this problem can be overcome by the use of an actuator with gearing to drive the robotic manipulator. In this case, it was found that the inertia of the motor dominates that of the manipulator as the reduction gear ratio increases and as a result that good learning performance and rapid convergence were achieved. However, it was also found that the reduction gear ratio cannot be increased too much, because that will increase the size of the gear box so that it becomes impractical. Therefore, an alternative must be found whereby no prior knowledge of the robotic dynamics is required in order to design a controller. This alternative lies in the use of adaptive digital iterative learning controllers. It was shown in Chapter 5 that such adaptive digital iterative learning controllers can be designed by introducing recursive estimators to provide the updated step-response matrices which are required for designing such controllers. Furthermore, it was shown that this estimation technique

is capable of providing these identified matrices accurately in a few sampling periods.

It is shown in this chapter that robotic manipulators are amenable to adaptive digital iterative learning control, by identifying the step-response matrices of such manipulators along their trajectories. In this way, the need for dynamical models of robotic manipulators is diminished. These general results are illustrated in this chapter by the presentation of numerical results for the adaptive digital iterative learning control of a two-link robotic manipulator in both joint- and task-space co-ordinates.

8.2 ANALYSIS

The dynamics of n-link non-redundant manipulators are governed on the continuous-time set by a non-linear differential equation of the form

$$M(q)\,\ddot{q} + N(q,\dot{q}) + g(q) = \Xi \quad , \qquad \ldots(8.1)$$

where $q \in R^n$ is the vector of joint angles, $M(q) \in R^{n\times n}$ is the inertia matrix, $N(q,\dot{q}) \in R^n$ is the vector of coriolis torques, $g(q)$ is the vector of gravitational torques, and $\Xi \in R^n$ is the vector of joint torques. It is well known that the linearised dynamics of such manipulators in the neighbourhood of an operating point $P = (\hat{q}, \hat{\Xi})$ are governed on the continuous-time set by linear differential equations of the form

$$L_2\,\ddot{q} + L_1\,\dot{q} + L_0\,q = \xi \qquad \ldots(8.2)$$

where $q = \hat{q} + q$, $\Xi = \hat{\Xi} + \xi$, and

$$L_2 = M(\hat{q}) \epsilon R^{n \times n} \quad , \qquad \text{...(8.3a)}$$

$$L_1 = \frac{\partial N}{\partial \dot{q}} \epsilon R^{n \times n} \quad , \qquad \text{...(8.3b)}$$

and

$$L_0 = \frac{\partial N}{\partial q} + \frac{\partial G}{\partial q} \epsilon R^{n \times n} \quad . \qquad \text{...(8.3c)}$$

In all cases, these equations are evaluated at the operating point $P = (\hat{q}, \hat{\Xi})$.

The output equation in task space is

$$\Omega = \Pi(q) \quad , \qquad \text{...(8.4)}$$

where $\Pi(q) \epsilon R^n$ is the vector of forward kinematic relationships and $\Omega \epsilon R^n$ is the vector of end-effector co-ordinates. Thus, after linearisation around the operating point P, the output equation becomes

$$\omega = \hat{J}\, q \quad , \qquad \text{...(8.5)}$$

where $\Omega = \hat{\Omega} + \omega$ and $\hat{J} \epsilon R^{n \times n}$ is the Jacobian matrix evaluated at the operating point.

Now the end-effector force $F \epsilon R^n$ is related to the joint torque $\Xi \epsilon R^n$ by the equation

$$\Xi = J^T (q)\, F \qquad \text{...(8.6)}$$

so that

$$\xi = \hat{J}^T \quad \mathrm{f} \quad , \qquad \text{...(8.7)}$$

where $F = \hat{F} + f$ and $\hat{F}$ is the end-effector force at the operating point P. It therefore follows from equations (8.2), (8.5) and (8.7) that the linearised dynamics of robotic manipulators in task space are governed on the continuous-time set by linear differential equations of the form

$$(\hat{J}^T)^{-1} L_2 \hat{J}^{-1} \ddot{\omega} + (\hat{J}^T)^{-1} L_1 \hat{J}^{-1} \dot{\omega} + (\hat{J}^T)^{-1} L_0 \hat{J}^{-1} \omega = f \quad . \qquad ...(8.8)$$

Such equations can obviously be expressed in the standard state space form

$$\dot{x}(t) = Ax(t) + Bf(t) \qquad ...(8.9a)$$

and

$$\omega(t) = Cx(t) \quad , \qquad ...(8.9b)$$

with

$$x = \begin{bmatrix} \omega \\ \dot{\omega} \end{bmatrix} \epsilon R^{2n} \quad , \qquad ...(8.10a)$$

$$A = \begin{bmatrix} 0 & , & I_n \\ -\hat{J}\ L_2^{-1} L_0 \hat{J}^{-1} & , & -\hat{J}\ L_2^{-1} L_1 \hat{J}^{-1} \end{bmatrix} \epsilon R^{2n \times 2n} \quad , \qquad ...(8.10b)$$

$$B = \begin{bmatrix} 0 \\ \hat{J}\ L_2^{-1} \hat{J}^T \end{bmatrix} \epsilon R^{2n \times n} \quad , \qquad ...(8.10c)$$

and

$$C = [I_n , 0] \epsilon R^{n \times 2n} \quad . \qquad ...(8.10d)$$

Similarly, equation (8.2) representing the linearised dynamics of robotic manipulators in joint space can be expressed in the standard state-space form

$$\dot{x}(t) = Ax(t) + B\xi(t) \qquad \text{...(8.11a)}$$

and

$$q(t) = Cx(t) \quad , \qquad \text{...(8.11b)}$$

where

$$x(t) = \begin{bmatrix} q \\ \dot{q} \end{bmatrix} \epsilon\, R^{2n} \quad , \qquad \text{...(8.12a)}$$

$$A = \begin{bmatrix} 0 & , & I_n \\ -L_2^{-1} L_0 & , & -L_2^{-1} L_1 \end{bmatrix} \epsilon\, R^{2n \times 2n} \quad , \qquad \text{...(8.12b)}$$

$$B = \begin{bmatrix} 0 \\ L_2^{-1} \end{bmatrix} \epsilon\, R^{2n \times n} \quad , \qquad \text{...(8.12c)}$$

and

$$C = [I_n \ , \ 0] \epsilon\, R^{n \times 2n} \quad . \qquad \text{...(8.12d)}$$

But the dynamics of linear plants governed on the continuous-time set by differential equations of the form (8.9) or (8.11) are governed on the discrete-time set by difference equations of the form

$$x(j+1) = \Phi\, x(j) + \Psi\, u(j) \qquad \text{...(8.13a)}$$

and

$$y(j) = \Gamma\, x(j) \quad , \qquad \text{...(8.13b)}$$

where

$$\Phi = e^{AT} \quad , \qquad \text{...(8.14a)}$$

$$\Psi = \int_0^T e^{At}\, B\, dt \quad , \qquad \text{...(8.14b)}$$

and

$$\Gamma = C \quad . \qquad \text{...(8.14c)}$$

The step response matrices of such plants have the form

$$H(T) = \int_0^T C\, e^{At}\, B\, dt \qquad \text{...(8.15)}$$

and characterise the response of initially quiescent plants after one sampling period. Such step-response matrices can evidently be measured directly from input/output data.

It is clear from equations (8.10b), (8.10c) and (8.10d) and equations (8.12b), (8.12c) and (8.12d) in both task and joint spaces, respectively, that robotic manipulators give rise in the neighbourhood of an operating point to linearised plants with null first Markov parameters but full-rank second Markov parameters. Such plants are therefore completely irregular and it is accordingly immediately possible to use Theorem 4.2 of Chapter 4 to design digital iterative learning controllers for small motions of robotic manipulators in the neighbourhood of an operating point.

However, in order to design iterative learning controllers for large motions of robotic manipulators it is necessary to render such controllers adaptive by identifying the step-response matrices of such manipulators along the appropriate trajectories emanating from an operating point. Such step-response matrices can be obtained on-line by estimating the parameters of an appropriate autoregressive moving average ARMA model using the RLS algorithm which is given by equations (5.7), (5.8), (5.9) and (5.10) in Chapter 5. Thus, at each sampling interval, the estimated parameters of the ARMA model can be used to compute updated step-response matrices for implmentation in the design equation

$$\Lambda = \left[H(T)\left(I_m + \frac{2}{T}D\right)\right]^{-1}$$

Indeed, it was shown in Chapter 5 (in particular, in equation (5.12)) that $H(T) = B_1$, and therefore that the control-law of Theorem 4.2 in Chapter 4 can be readily made adaptive. It was also shown in Chapter 5 that, in order to start the identification process, the RLS algorithm must be initialized; in particular, initial values must be given to $\hat{\Theta}(0)$ and $P(0)$. Moreover, the initial values of the elements of the covariance matrix $P(0)$ must be large enough to cause rapid discarding of the old estimated data so as to speed up the convergence process to the true parameters.

However, as time increases, the covariance matrix will 'wind down' to a very small value and the norm of the Kalman gain vector will tend to zero. Therefore, if a change occurs, the identifier will lose its ability to detect this unexpected change as it will be limited by the small size of the elements of the covariance matrix. Many techniques have accordingly been proposed to enhance the response of the RLS to any plant-parameter changes. These techniques are focussed on ways to increase the covariance matrix and to prevent the 'winding down' phenomenon occurring, either

by resetting the covariance matrix to a pre-specified value (Goodwin and Sin (1984)) or by changing the forgetting factor γ (Aström et al (1977)), Fortesque et al (1981) and (Sailed and Foss (1983)). It must also be emphasized that, due to the non-linearities of robotic manipulators, the RLS performance will be degraded and as a result the learning performance of the digital iterative learning controller will be degraded too. Therefore, a method eliminating such an undesirable phenomenon is required and was found by Petropoulakis (1986). In this solution of Petropoulakis (1986), the non-linearities of the robot dynamics were considered as disturbances and accordingly the RLS algorithm was modified to accommodate these non-linearities. This modification entailed expressing the governing equations of new process models in the form

$$y_k(j) + A_1 y_k(j\text{-}1) + A_2 y_k(j\text{-}2) +\ldots+ A_N y_k(j\text{-}N) =$$

$$B_1 u_k(j\text{-}1) + B_2 u_k(j\text{-}2) +\ldots+ B_N u_k(j\text{-}N) + h, \qquad \ldots(8.16)$$

where $h \in R^m$ is a vector incorporating unknown and varying non-linearities. Therefore, in such circumstances equations (5.10) and (5.11) of Chapter 5 are modified so as to assume the respective forms

$$\Phi(jT) = [-y_k^T[(j\text{-}1)T], -y_k^T[(j\text{-}2)T],\ldots, -y_k^T[(j\text{-}N)T];$$

$$u_k^T[(j\text{-}1)T], u_k^T[(j\text{-}2)T],\ldots,u_k^T[(j\text{-}N)T]\,;\,1]^T \in R^{N(2m)+1} \qquad \ldots(8.17)$$

and

$$\Theta = [A_1, A_2,\ldots, A_N; B_1, B_2,\ldots, B_N\,;\,h]^T \in R^{N(2m)+1\times m} \qquad \ldots(8.18)$$

This modification also involves an increase in the dimensions of the covariance matrix, P, and the Kalman gain, K to $[N(2m+1)] \times [N(2m+1)]$ and $[N(2m)+1]\times 1$,

respectively. More details of this approach are given by Petropoulakis (1986).

It is finally important to note from equations (8.6) and (8.7) that the actual vector of joint torques applied to the robotic manipulator in the kth iteration is

$$\Xi_k(j) = \hat{\Xi} + u_k(j) \qquad \ldots(8.19)$$

where, according to equation (8.11), $u_k(j) = \xi_k(j) = J^T(q)\, f_k(j)$. Therefore, this new input $u_k(j)$ is provided by the iterative learning controller proposed in Theorem 4.2 of Chapter 4, where $j \in [0, J]$, $J = T_t/T$ and T_t is the total task time.

8.3 ILLUSTRATIVE EXAMPLES

These general results can be conveniently illustrated by considering the adaptive iterative learning control of a two-link robotic manipulator in both task and joint space co-ordinates. The dynamics of this manipulator operating in a gravity-free environment are governed on the continuous-time set by the non-linear differential equations

$$\begin{bmatrix} J_1+J_2\,(1+3\,\eta^2) + 3\,J_2\eta\cos q_2, & J_2\left(1+\frac{3}{2}\,\eta\cos q_2\right) \\ J_2\left(1+\frac{3}{2}\,\eta\cos q_2\right), & J_2 \end{bmatrix} \begin{bmatrix} \ddot{q}_1 \\ \ddot{q}_2 \end{bmatrix}$$

$$+ \begin{bmatrix} -3\,J_2\,\eta\left(\dot{q}_1+\frac{1}{2}\,\dot{q}_2\right)\dot{q}_2\sin q_2 \\ \frac{3}{2}\,J_2\,\eta\,\dot{q}_1^2\sin q_2 \end{bmatrix} = \begin{bmatrix} \Xi_1 \\ \Xi_2 \end{bmatrix} \qquad \ldots(8.20)$$

where ℓ_1 and ℓ_2 are the lengths of the links, m_1 and m_2 are the masses of the links, $J_1 = (1/3)\, m_1\, \ell_1^2$, $J_2 = (1/3)\, m_2\, \ell_2^2$, and $\eta = \ell_1/\ell_2$. In case this manipulator corresponds to the second and third links of the Unimation PUMA 560 robot, $\ell_1 = \ell_2 = 0.432m$, $m_1 = 15.91\ Kg$ and $m_2 = 11.36\ Kg$.

Example 8.1

In this example, the adaptive iterative learning control of the two-link manipulator in task space is considered where the outputs are governed by forward kinematic equations of the form

$$\begin{bmatrix} \Omega_1 \\ \Omega_2 \end{bmatrix} = \begin{bmatrix} x \\ y \end{bmatrix} = \begin{bmatrix} \ell_1 \cos q_1 + \ell_2 \cos (q_1+q_2) \\ \ell_1 \sin q_1 + \ell_2 \sin (q_1+q_2) \end{bmatrix} \qquad \ldots(8.21)$$

It is desired that the end-effector perform the following rectilinear motions in the plane of Cartesian co-ordinates :

(i) moves between $R(0.7375,-0.3055)m$ and $Q(0.7,-0.25)m$ in 1.5 *sec* with equal periods of acceleration, cruise and deceleration from rest to $66.939 \times 10^{-3}\ m/s$ and back to rest;

(ii) then moves immediately between $Q(0.7,-0.25)m$ and $R(0.7375,-0.3055)m$ in 1.5 *sec* with equal periods of acceleration, cruise and deceleration from rest to $66.939 \times 10^{-3}\ m/s$ and back to rest.

The RLS algorithm is initialized with $\Theta(0)$ having the correct information about the robot dynamics at the starting point R, the forgetting factor $\gamma = 1$, and $P_0 = 100$. This initialization process is repeated at the beginning of each successive iteration. In order to improve the performance of the identifier, the covariance resetting technique

is used. Thus, whenever the value of its trace goes below a specified threshold, the covariance matrix will be set to its initial value. In addition, a random noise signal of zero mean and 0.01 standard deviation is added to the control effort in order to improve the identification of the system parameters using the RLS algorithm. However, the amount of noise added to the control effort must not be excessive, because otherwise the identification will be improved at the cost of degrading the performance of the learning controller.

The control-law of Theorem 4.2 is used. In addition, the choice of the parameters D and α is made so that $CBD = 0$ and fast convergence is achieved. Indeed, since CB is null, according to equations (8.10c,d) D can be arbitrary. Thus,

$$D = \begin{bmatrix} 1 & , & 0 \\ 0 & , & 1 \end{bmatrix}$$

is chosen, and $\alpha = 1$, with a sampling time of $T = 0.01$ *sec.*

In Figure 8.1, the desired trajectories of the end effector are shown together with the torques acting on the joints and also with the corresponding variations of the elements of the step-response matrix.

The rapid learning of the adaptive iterative controller is indicated in Figures 8.2-8.5. These figures show the actual trajectories of the end-effector under adaptive iterative learning control, together with the identified elements of the step-response matrix of the manipulator after 0, 1, 5 and 9 iterations. It can be seen by comparing Figures 8.1-8.5(a,b) that the adaptive iterative learning controller rapidly generates the desired trajectories of the end-effector in task space and, by comparing Figures 8.1-8.5(e-h), that the recursive-least-squares identifier obtains reasonably accurate estimates of the

step-response matrix of the manipulator.

However, by comparing Figures 8.1-8.5(c,d) it is also clear that the actual torque acting on the joints suffers from high-frequency oscillation. Thus, although the learning performance is excellent, this high-frequency oscillation is undesirable from a practical view point. It has been found that this is not due to the controller or the choice of its design parameters but to the identification process as Figure 8.1(c,d) suggest. However, this issue is open to further investigation. The results plotted in Figure 8.6 show the switching in the trace due to the resetting of the covariance matrix for $k = 0, 1, 5$ and 9.

Example 8.2

In this example, the adaptive iterative learning control of the two-link manipulator in joint space is considered, where the outputs are the joint angles q_1 and q_2, respectively. It is desired that the joint angles perform the motions

$$v(jT) = \begin{bmatrix} v_1(jT) \\ v_2(jT) \end{bmatrix} = \begin{bmatrix} 0.1125\ (1 - \cos 2\pi\ jT) \\ -0.1125\ (1 - \cos 2\pi\ jT) \end{bmatrix} \qquad \ldots(8.22)$$

in 1.0 *sec.*

The RLS algorithm is initialized with $\Theta(0)$ having the correct information about the robot dynamics at the starting point when $q_1 = q_2 = 0$ and $P_0 = 10^{11}$. This initialization process is repeated at the beginning of each successive iteration. In the previous example, covariance resetting was used to improve the performance of the identifier. However, in the present example a different technique is used to improve the identification of the system parameters by keeping the forgetting factor $\gamma = 0.7$

all the time during the task time. It is found thst this technique is better than the previous one in identifying manipulator parameters in joint-space co-ordinates. However, as in the previous example, a random noise signal of zero mean and 0.1 standard deviation is added to the control effort in order to improve the identification of the system parameters using the RLS algorithm. Again, the amount of noise added to the control effort must not be excessive, because otherwise the identification will be improved at the cost of degrading the performance of the learning controller. The control-law of Theorem 4.2 is used. In addition, the choice of the parameters D and α is made so that $CBD = 0$ and fast convergence is achieved. Indeed, since CB is null, according to equations (8.10c,d) D can be arbitrary. Thus,

$$D = \begin{bmatrix} 1 & , & 0 \\ 0 & , & 1 \end{bmatrix}$$

is chosen, and $\alpha = 0.8$, with a sampling time of $T = 0.01$ *sec.*

In Figure 8.7, the desired trajectories of the joint angles are shown together with the torques acting on the joints and also with corresponding variations of the elements of the step-response matrix. The rapid learning of the adaptive iterative controller is indicated in Figures 8.8-8.11. These figures show the actual trajectories of the joint angles under adaptive iterative learning control, together with the identified elements of the step-response matrix of the manipulator after 0, 1, 5 and 9 iterations. It can be seen by comparing Figures 8.7-8.11(a,b) that the adaptive iterative learning controller rapidly generates the desired trajectories of the joint angles in joint space and, by comparing Figures 8.7-8.11(e-h), that the recursive-least-squares identifier obtains reasonably accurate estimates of the step-response matrix of the manipulator.

However, as in the previous example, it is also clear by comparing Figures 8.7-8.11(c,d) that the actual torque acting on the joints suffers from high-frequency oscillation. However, the oscillation in the present example is not as impractical as that in the previous example. The reason for this high-frequency oscillation is, as stated earlier, the identification process as Figures 8.7(c,d) suggest.

Figure 8.12 shows the changes in the trace of the covariance matrix that occur through keeping the forgetting factor $\gamma = 0.7$ at all times for $k = 0, 1, 5,$ and 9.

However, since Figure 8.12 does not give a clear picture of the behaviour of the trace, the logarithmic value of the trace is plotted against time in Figure 8.13.

8.4 CONCLUSION

It has been shown in this chapter that linearized models of robot dynamics give rise to completely irregular plants in both task and joint space co-ordinates. Therefore, the results of Chapter 4 (and in particular of Theorem 4.2) are readily applicable to the design of controllers that are suitable for the control of such plants. It was shown in Chapter 5 that the control law of Theorem 4.2 can be made adaptive by identifying in real time the step-response matrices of such plants. In similar fashion, it has been shown in this chapter that the results of Chapter 5 can be used to identify the step-response matrices of robotic manipulators along their trajectories in both task and joint spaces, thus indicating that such manipulators are amenable to iterative learning control.

In this chapter, a modification of the identification algorithm has been used to ensure good estimating features in the presence of disturbances in the form of non-linearities. Different techniques have been tried to make sure that the 'wind down'

phenomenon of the covariance matrix will not occur and as a result that the identification of the plant parameters will be good. Also, noise signals have been introduced to ensure that the inputs to the RLS algorithm are always rich and sufficiently exciting in order to help the RLS deliver good identification. These general results have been illustrated by the presentation of numerical results for the adaptive iterative learning control in both task and joint spaces of a two-link manipulator operating in a gravity-free environment.

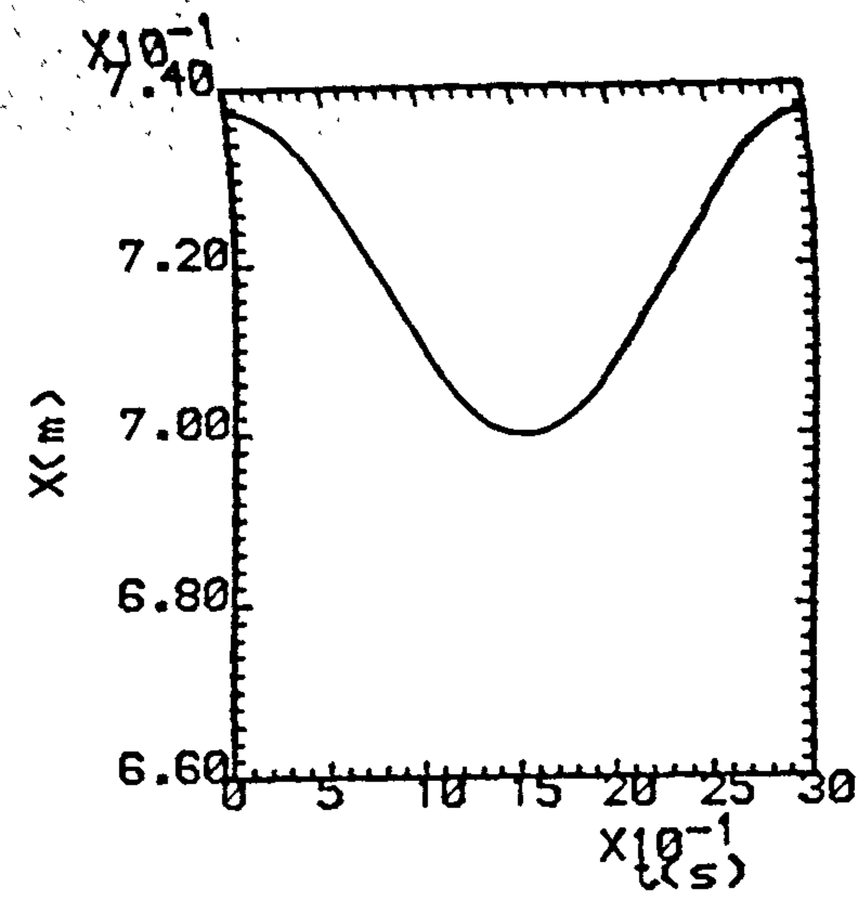

(a)

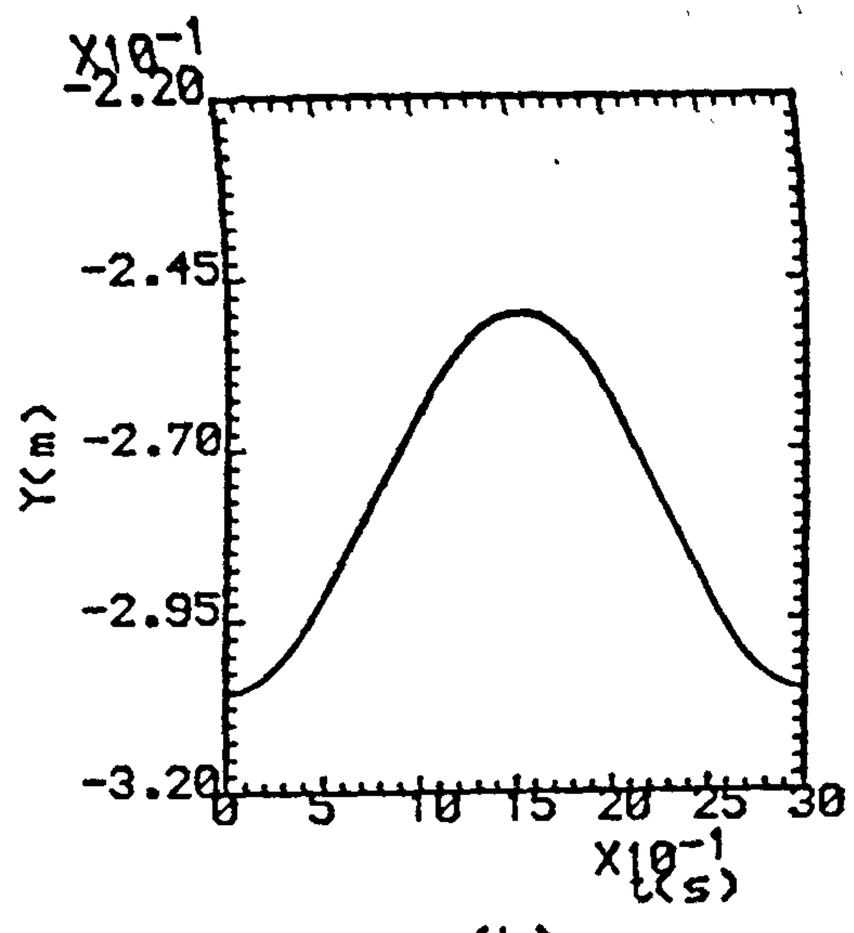

(b)

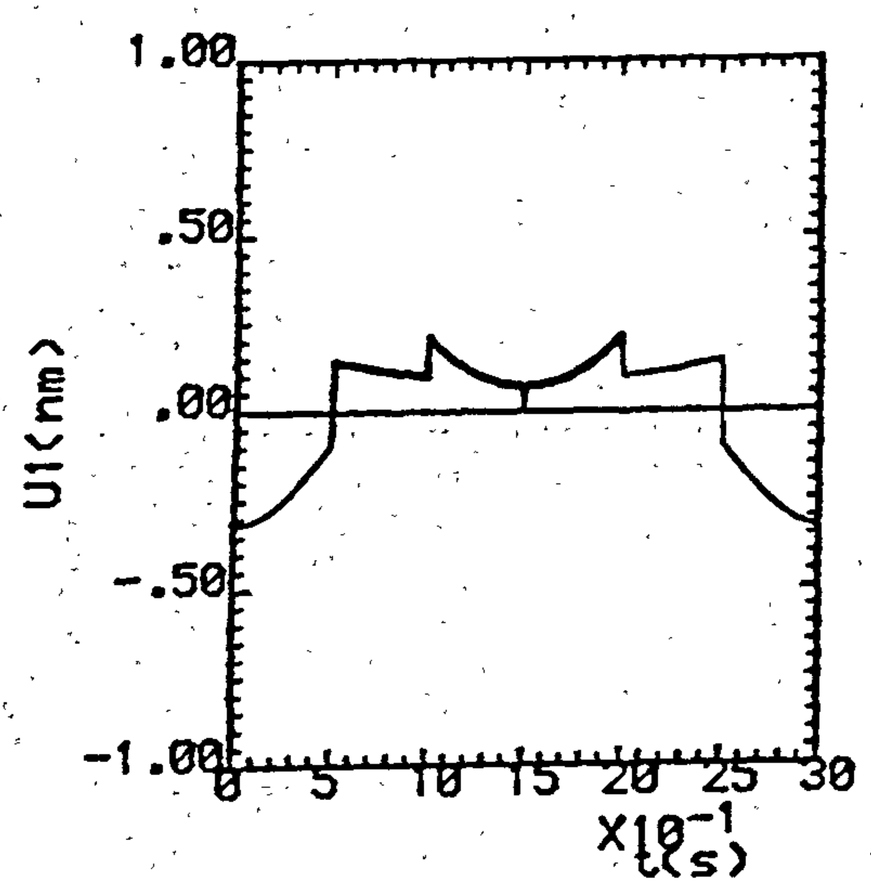

(c)

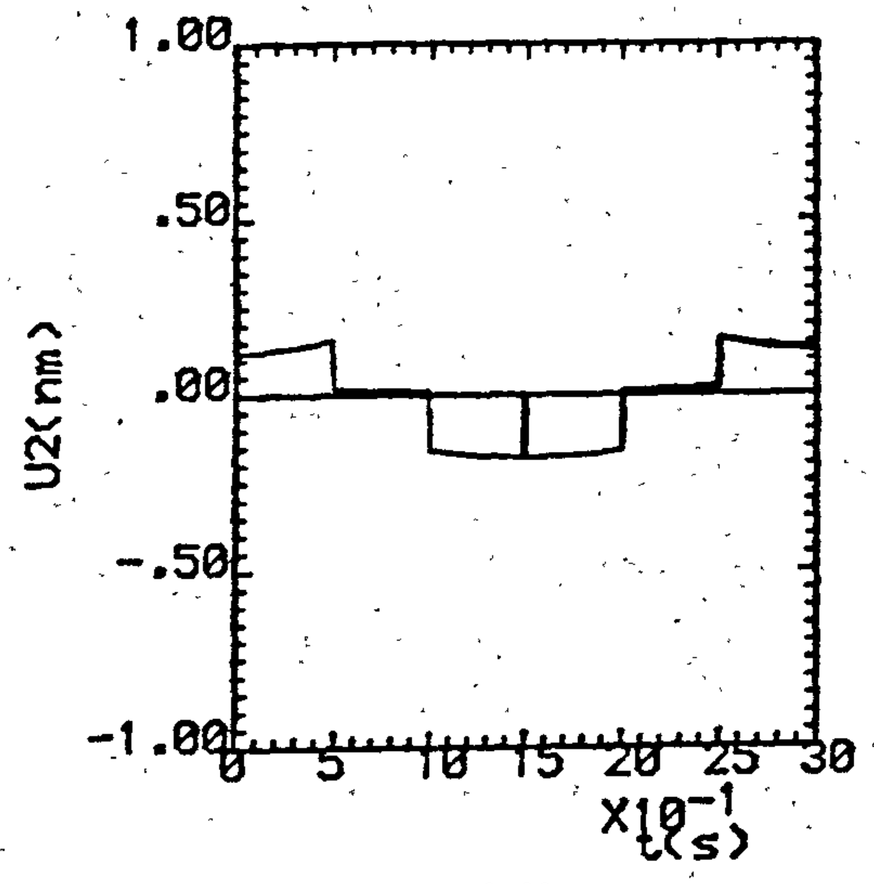

(d)

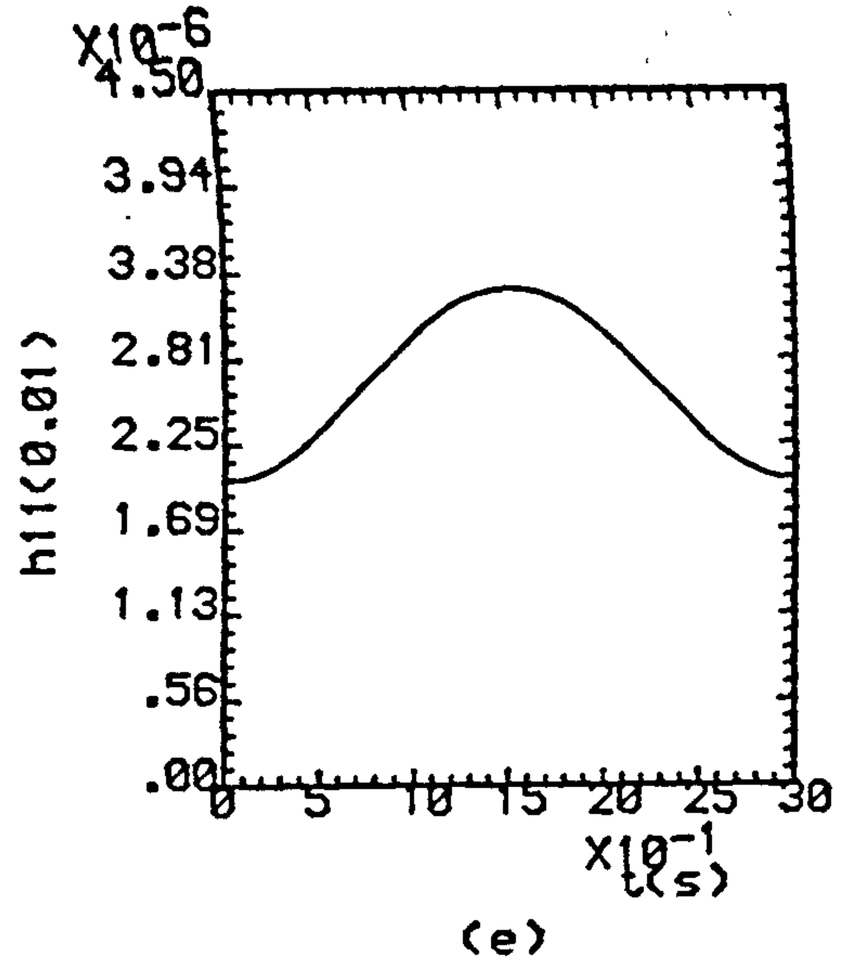

(e)

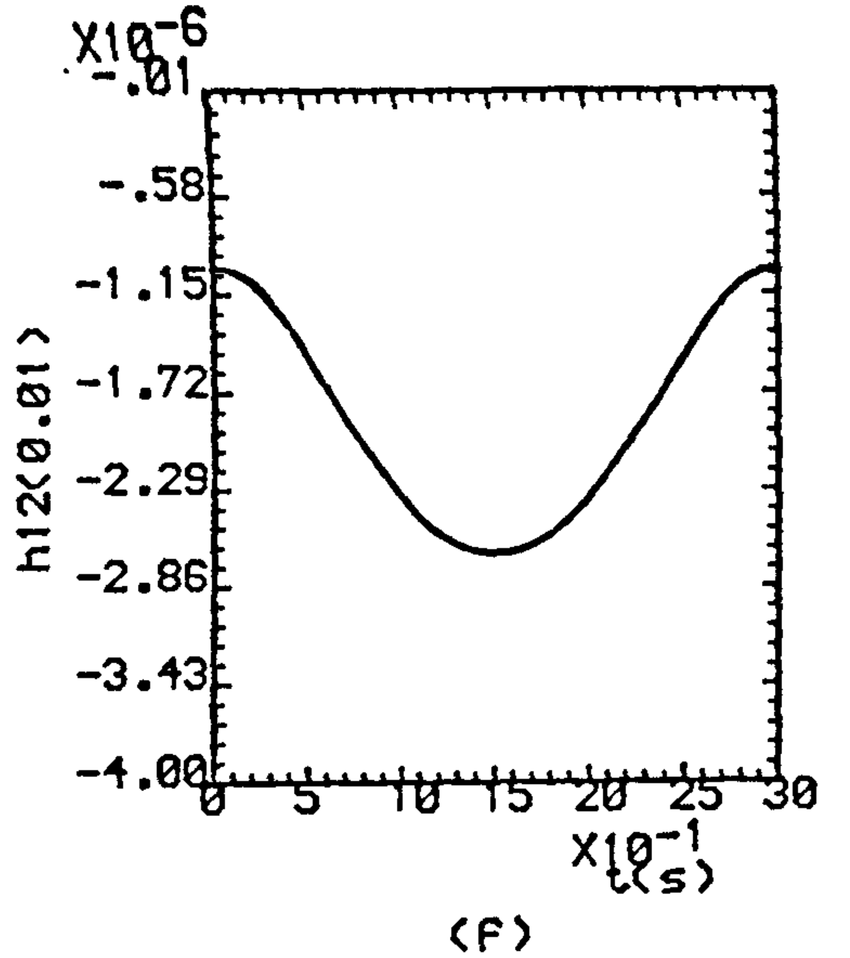

(F)

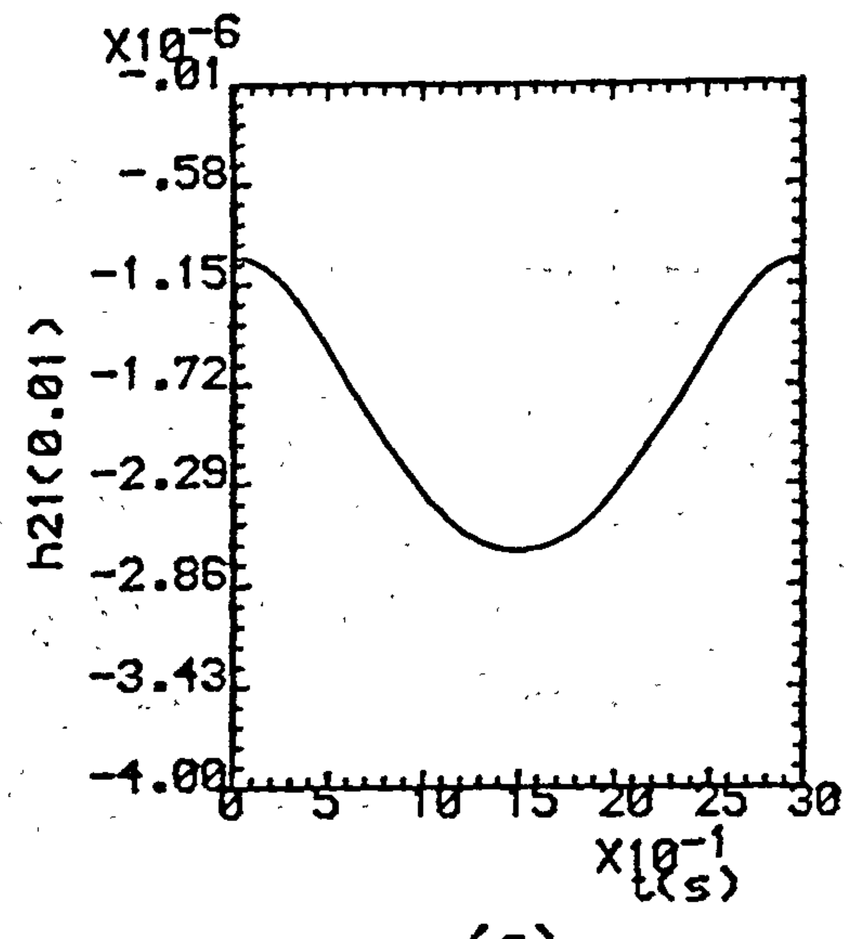

(g)

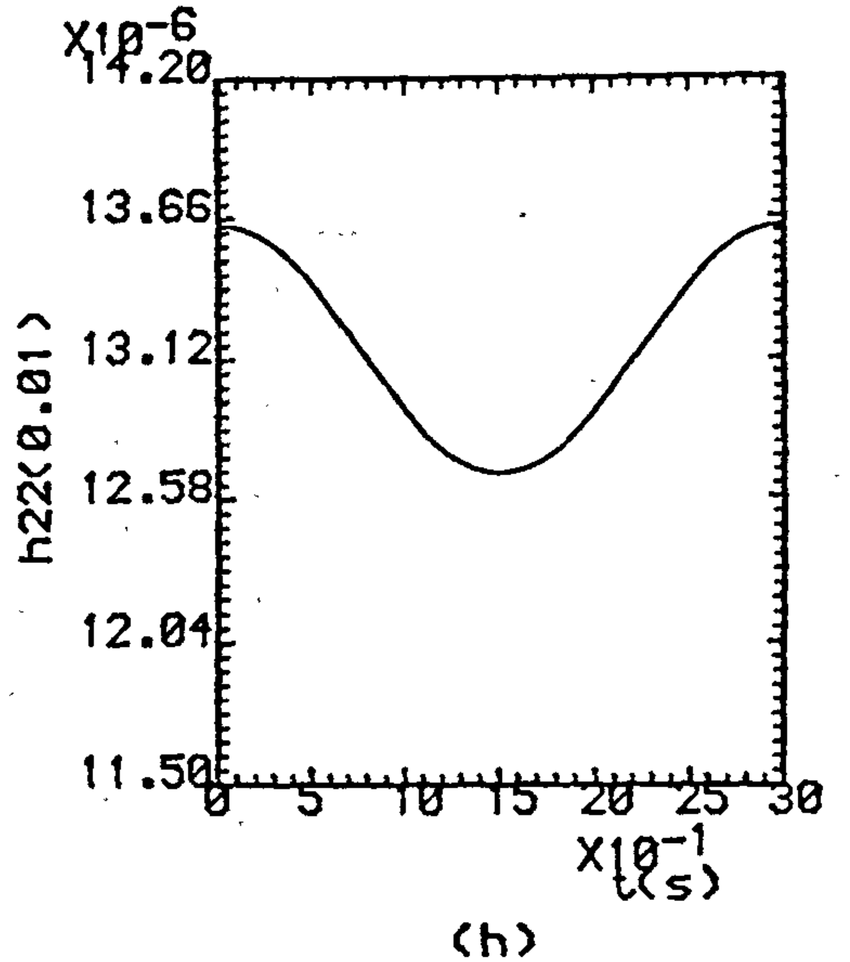

(h)

Fig.8.1(a,b)Desired Trajectories OF End Effector.
(c,d) Desired Torques Acting On The Joints.
(e,f,g,h) Actual Elements OF Step-Response Matrix.

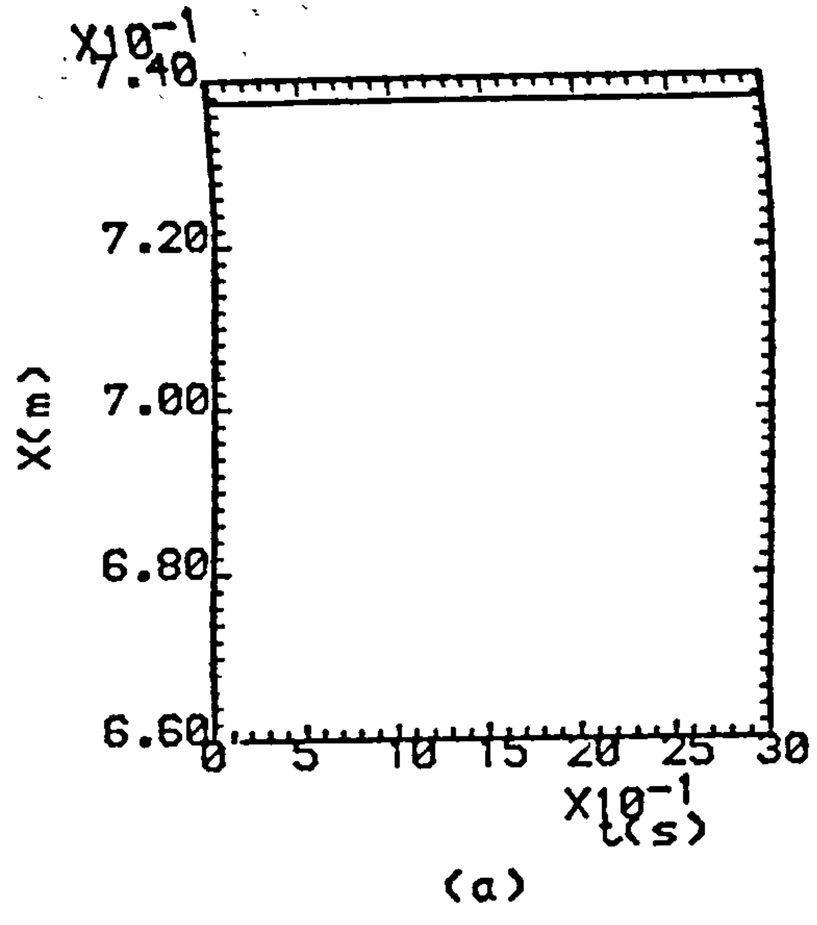

(a)

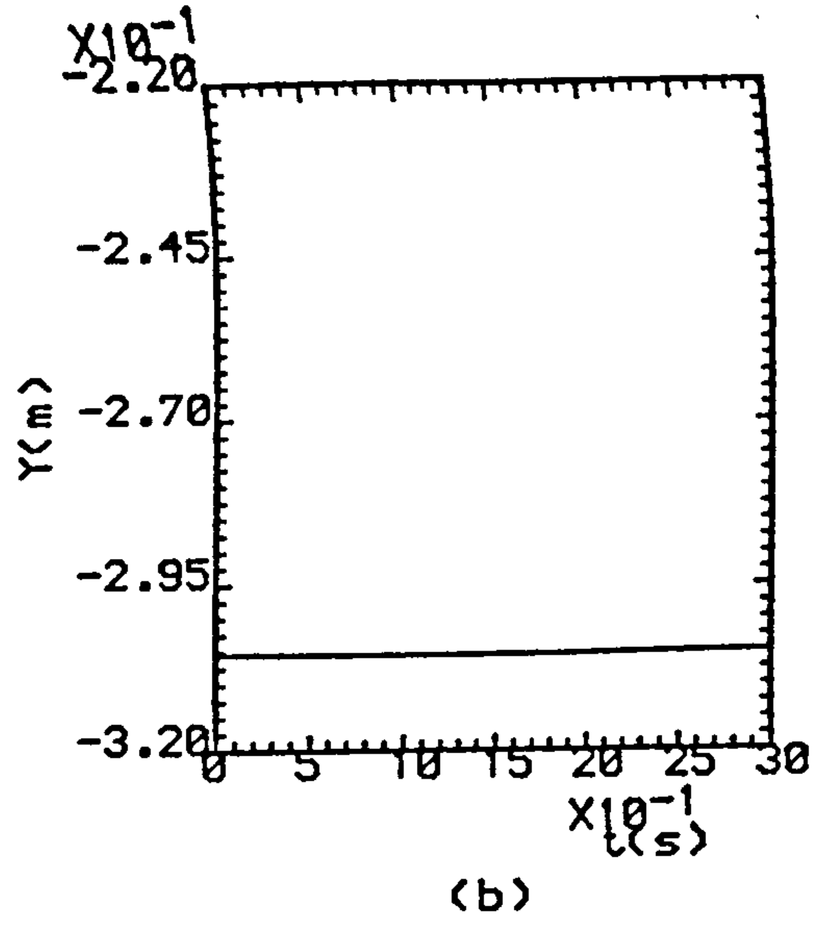

(b)

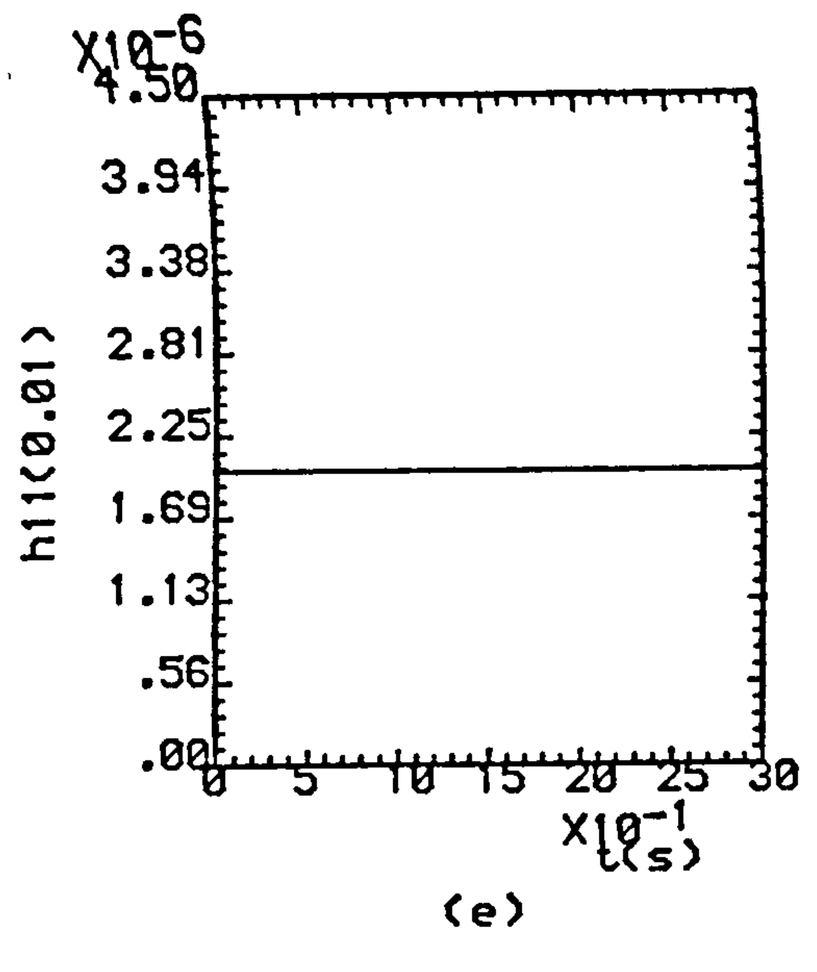

(e)

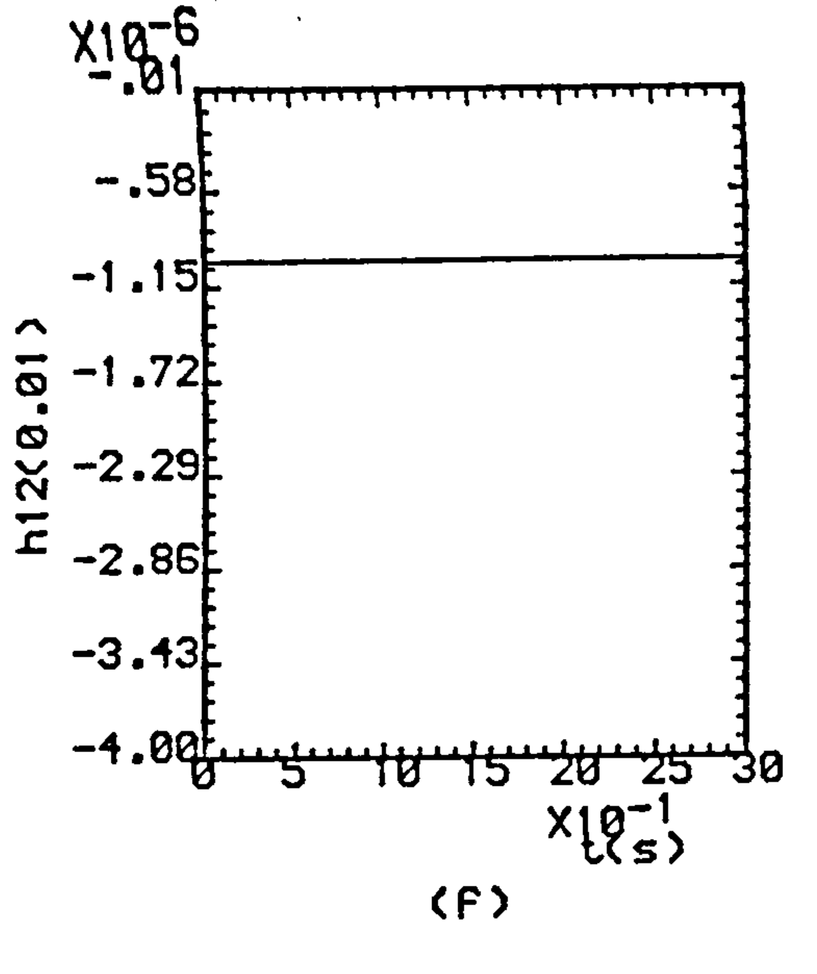

(f)

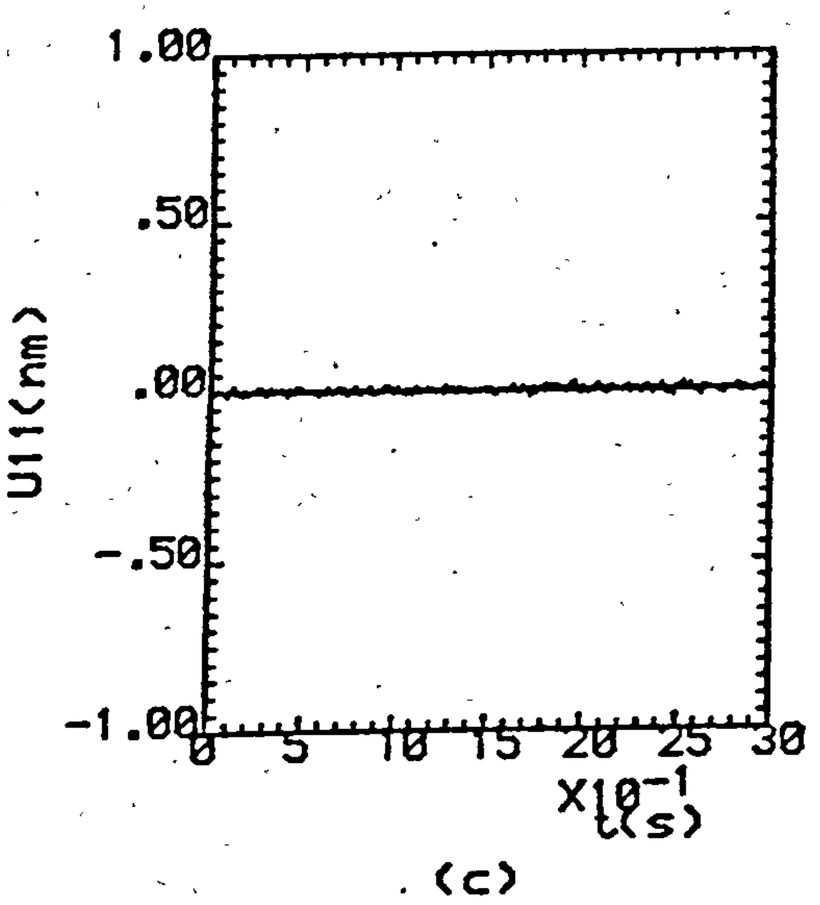

(c)

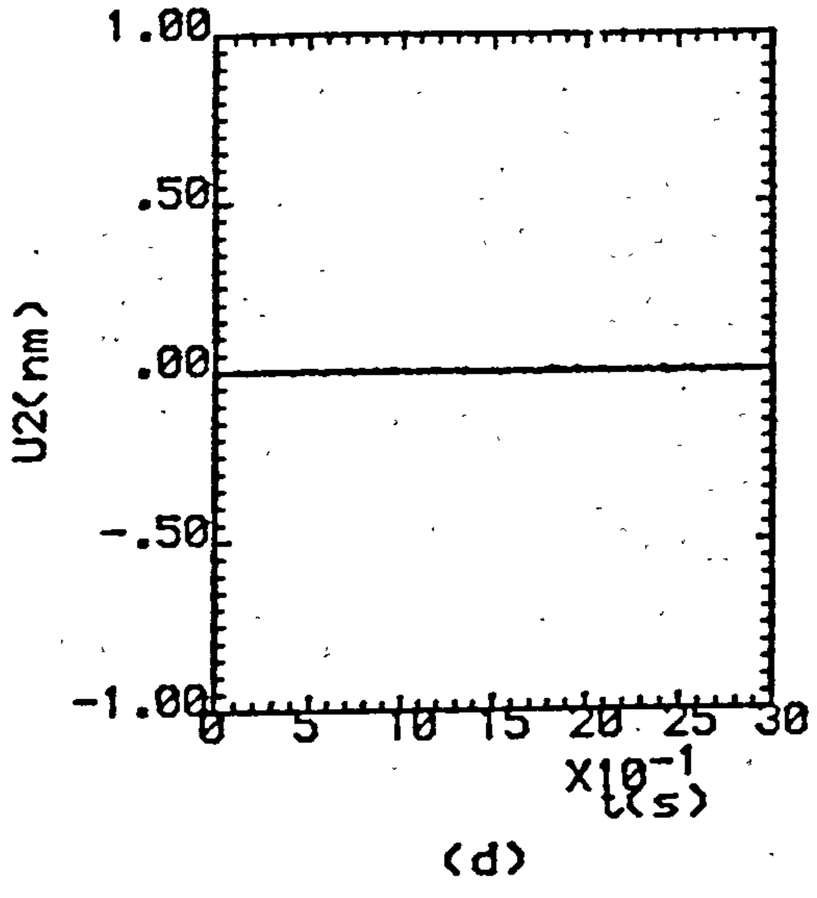

(d)

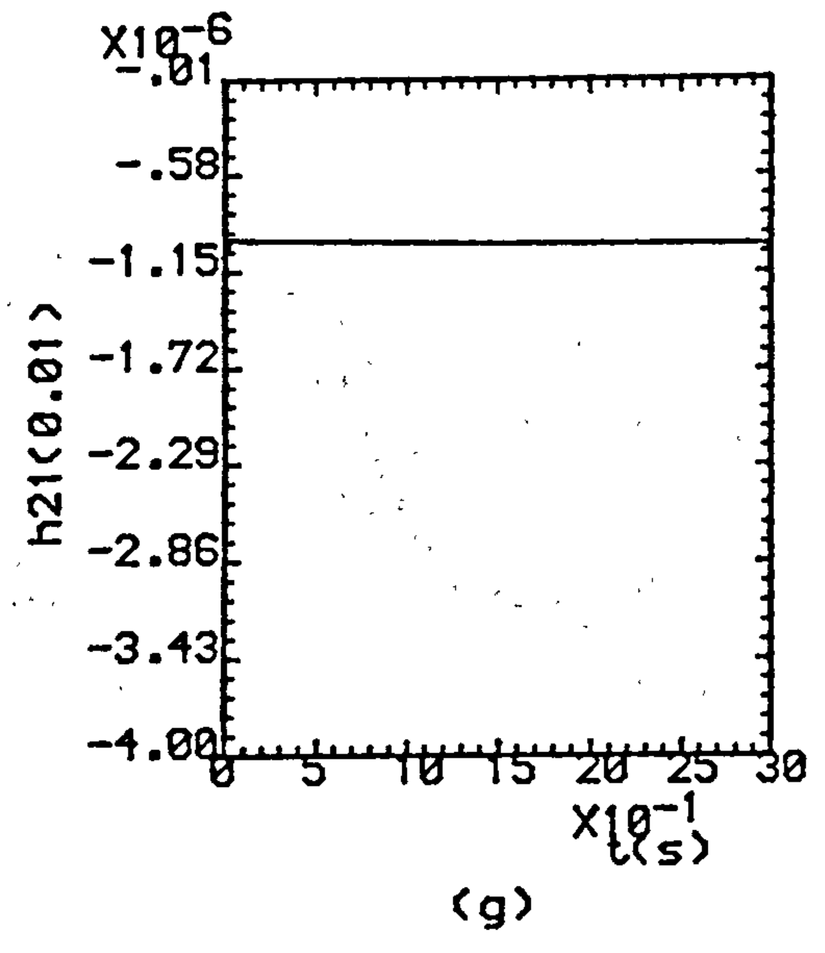

(g)

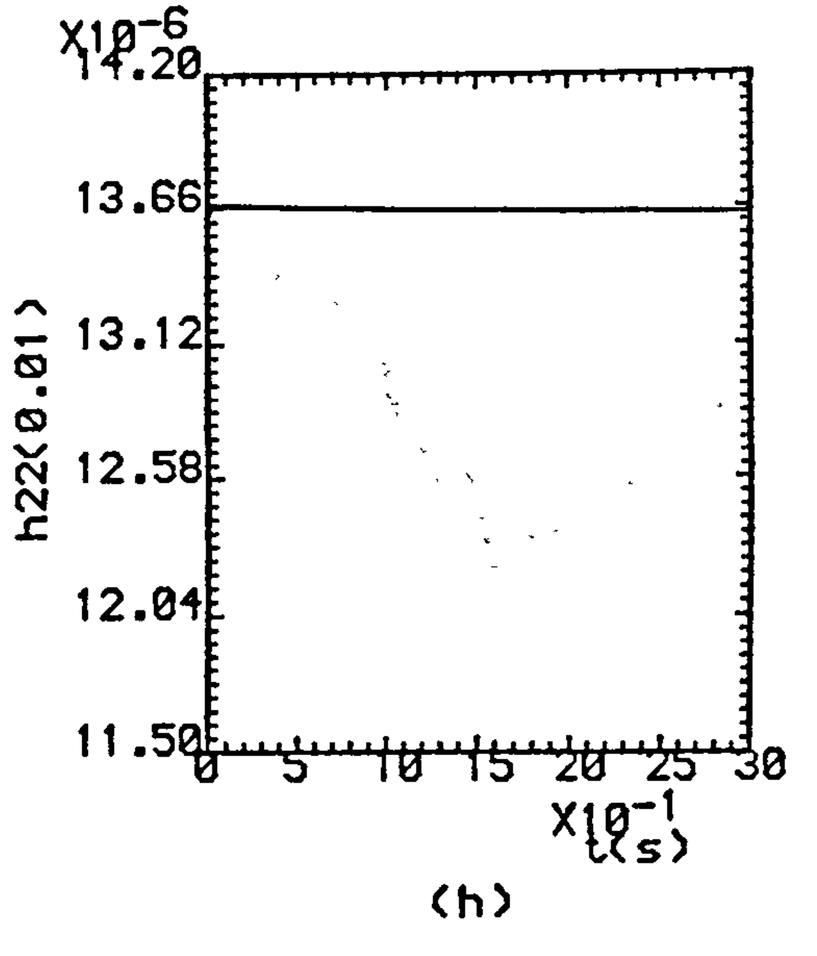

(h)

Fig.8.2(a,b)Actual Trajectories Of End Effector.
(c,d) Actual Torques Acting On The Joints.
(e-h) Identified Elements Of Step-Response Matrix.
K=0

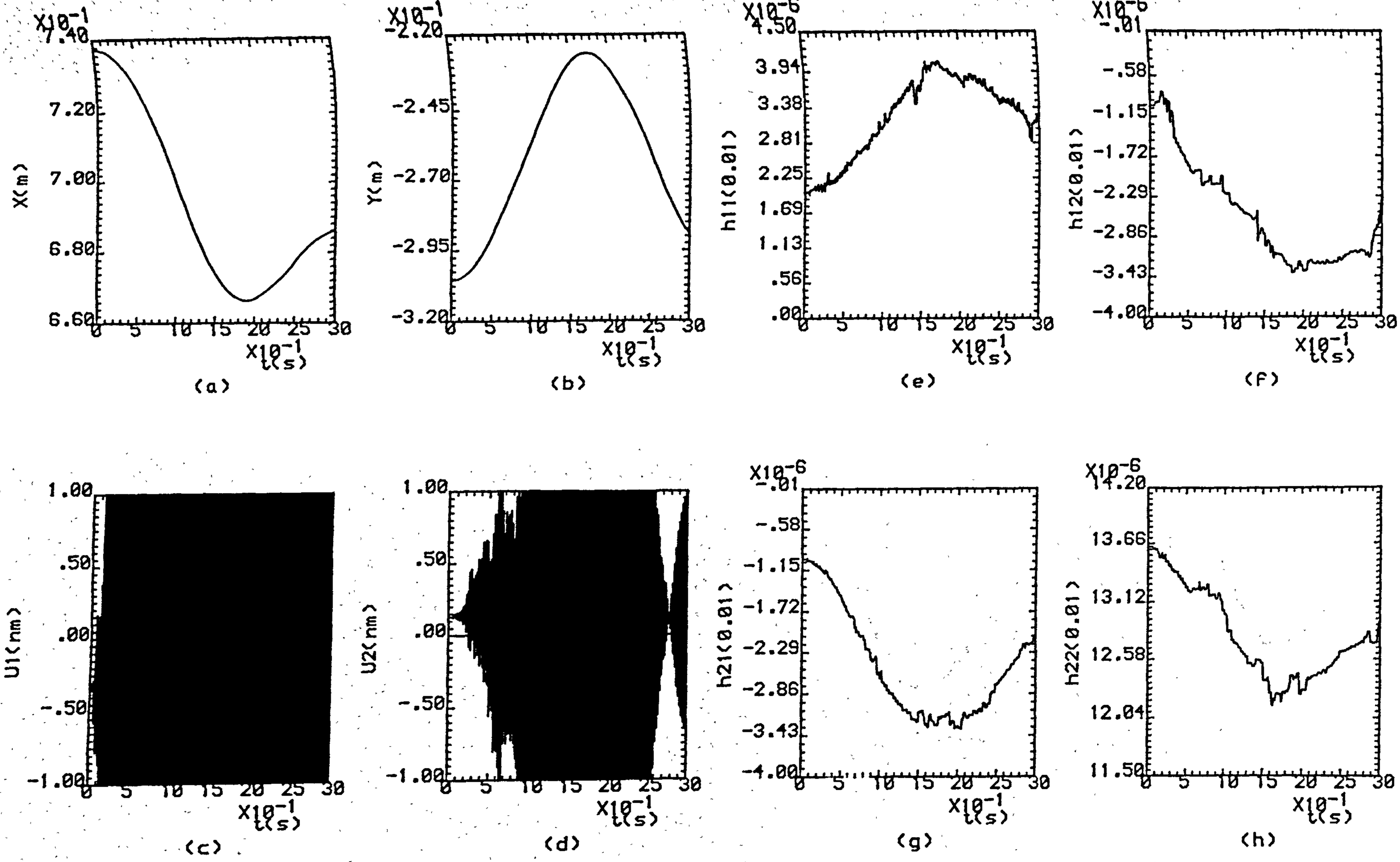

Fig.8.3(a,b)Actual Trajectories Of End Effector.
(c,d) Actual Torques Acting On The Joints.
(e-h) Identified Elements Of Step-Response Matrix.
K=1

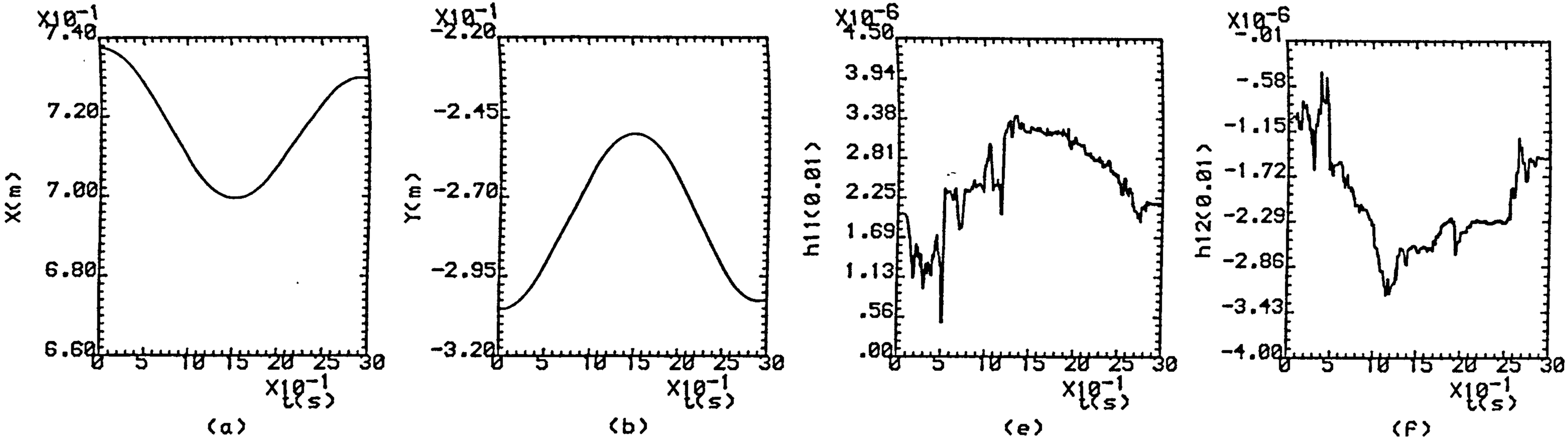

Fig.8.4(a,b)Actual Trajectories Of End Effector.
(c,d) Actual Torques Acting On The Joints.
(e-h) Identified Elements Of Step-Response Matrix.
K=5

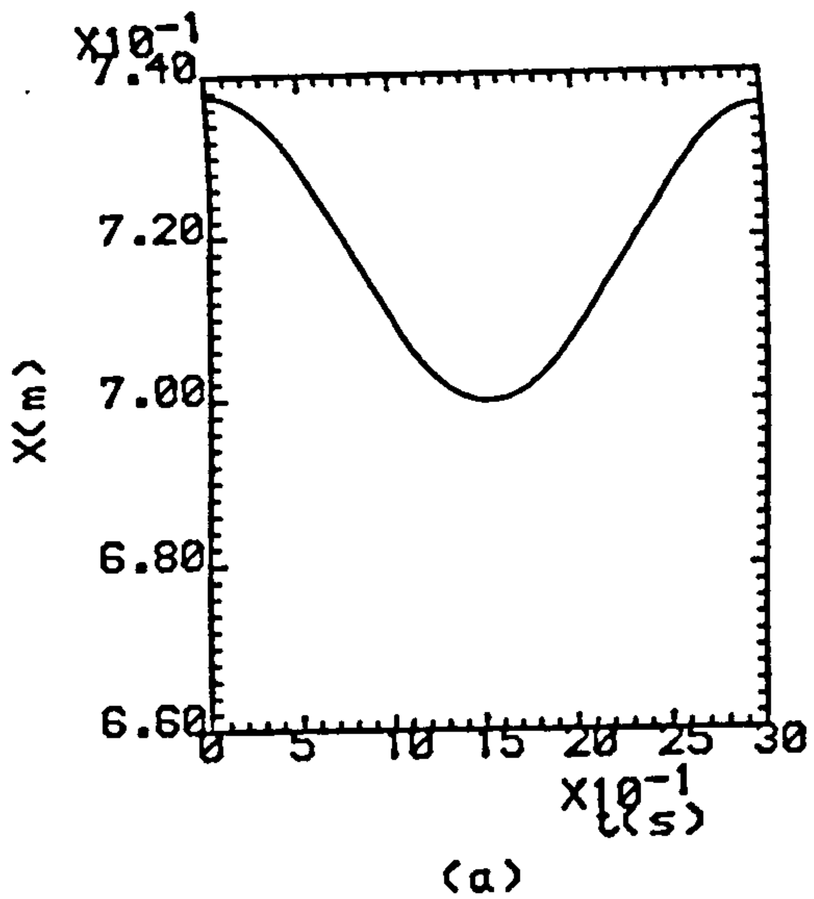

(a)

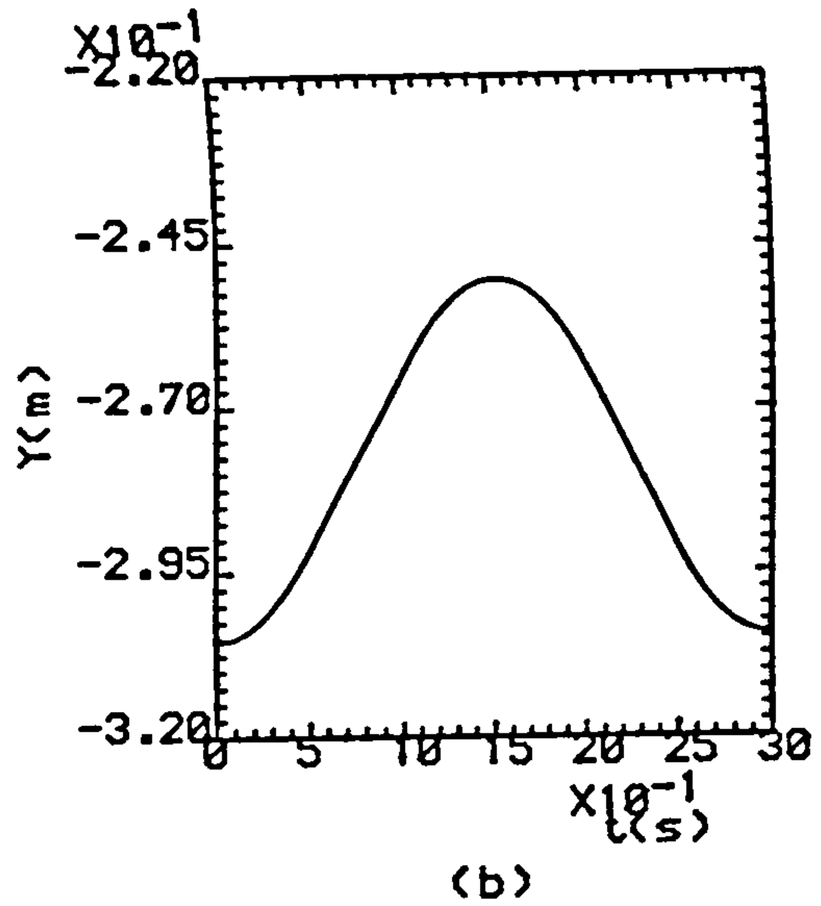

(b)

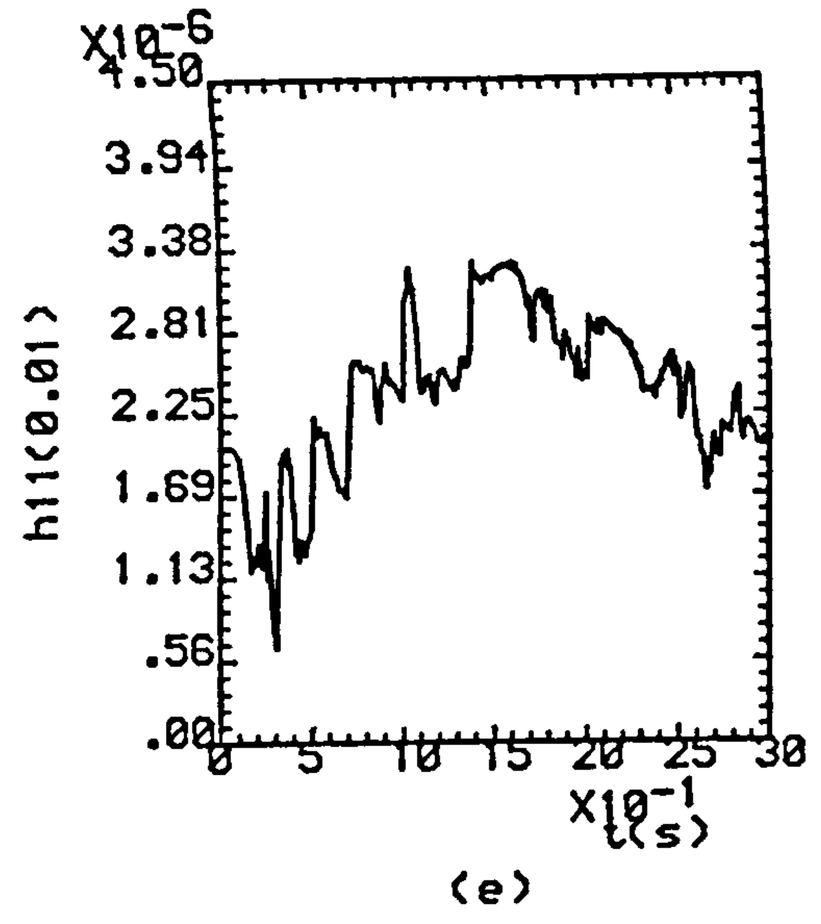

(e)

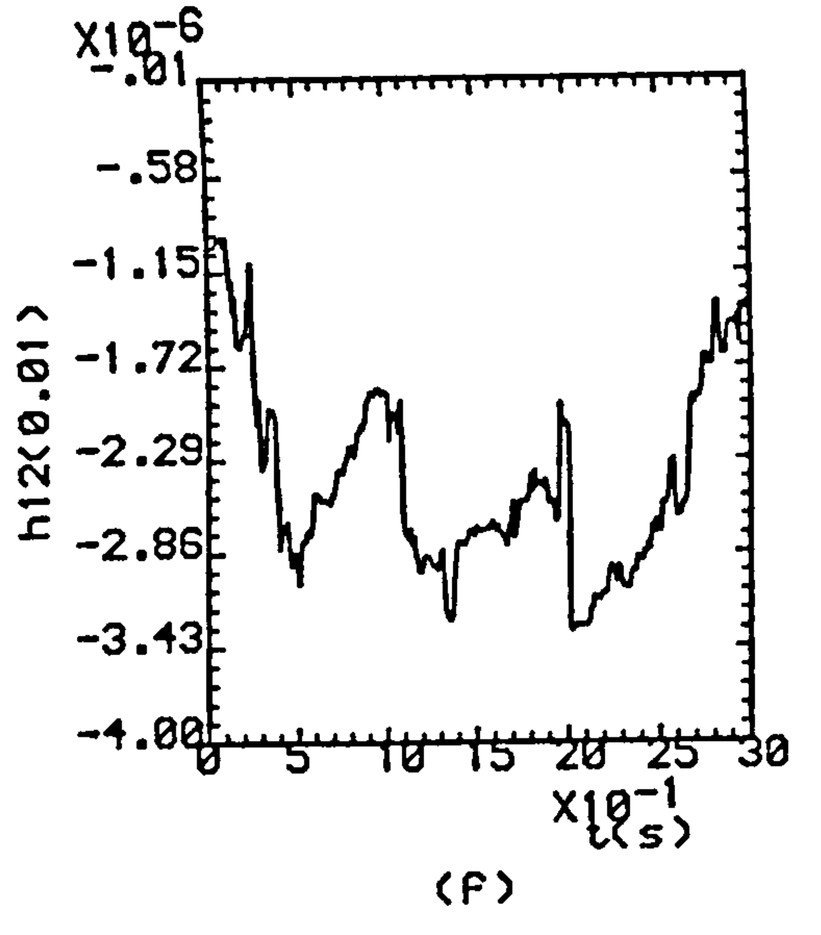

(f)

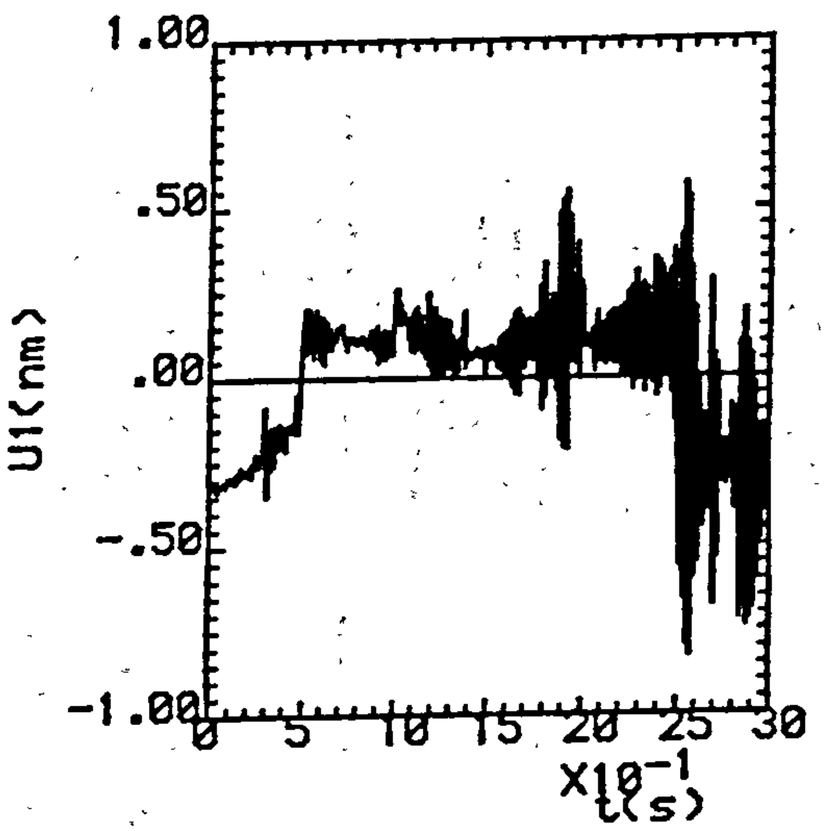

(c)

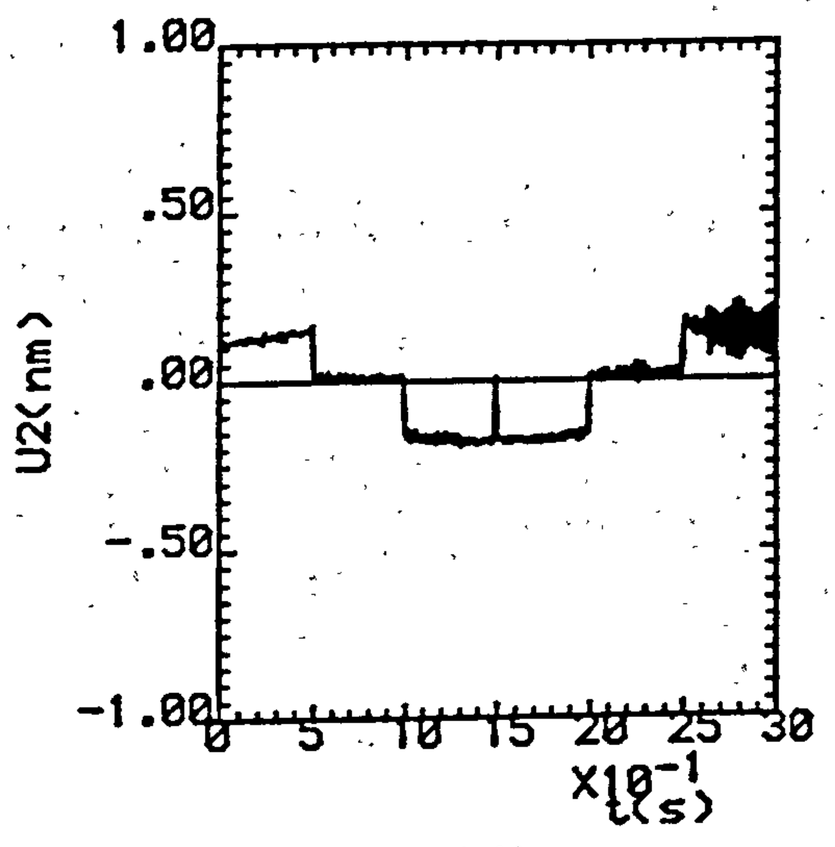

(d)

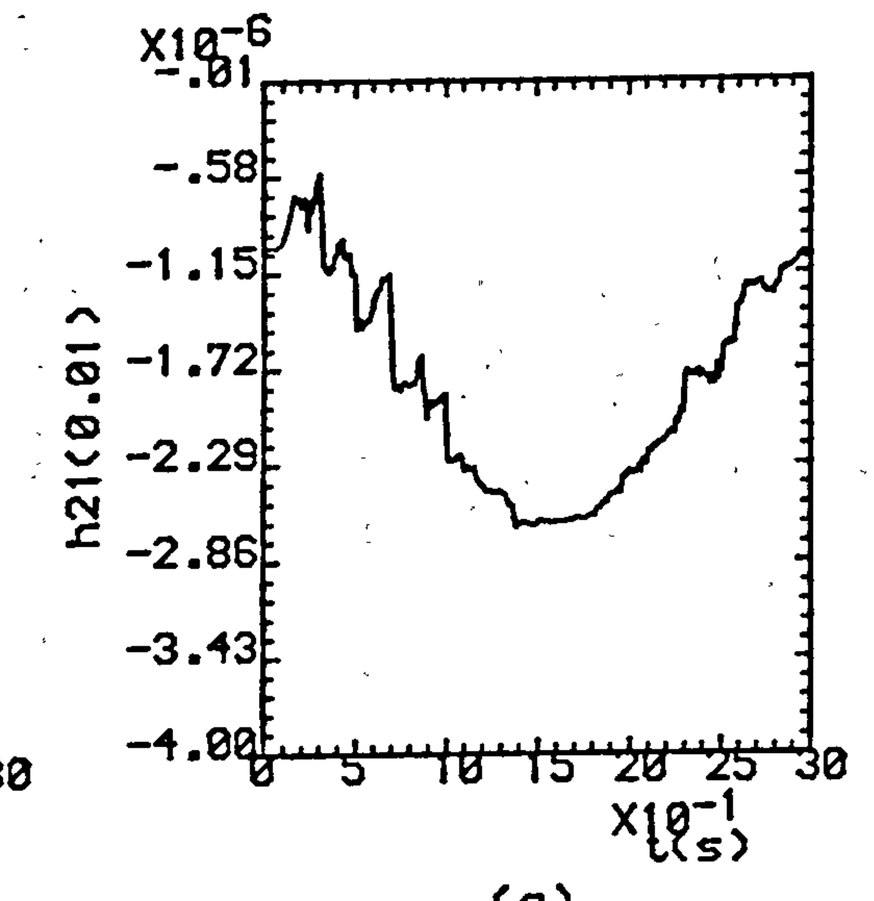

(g)

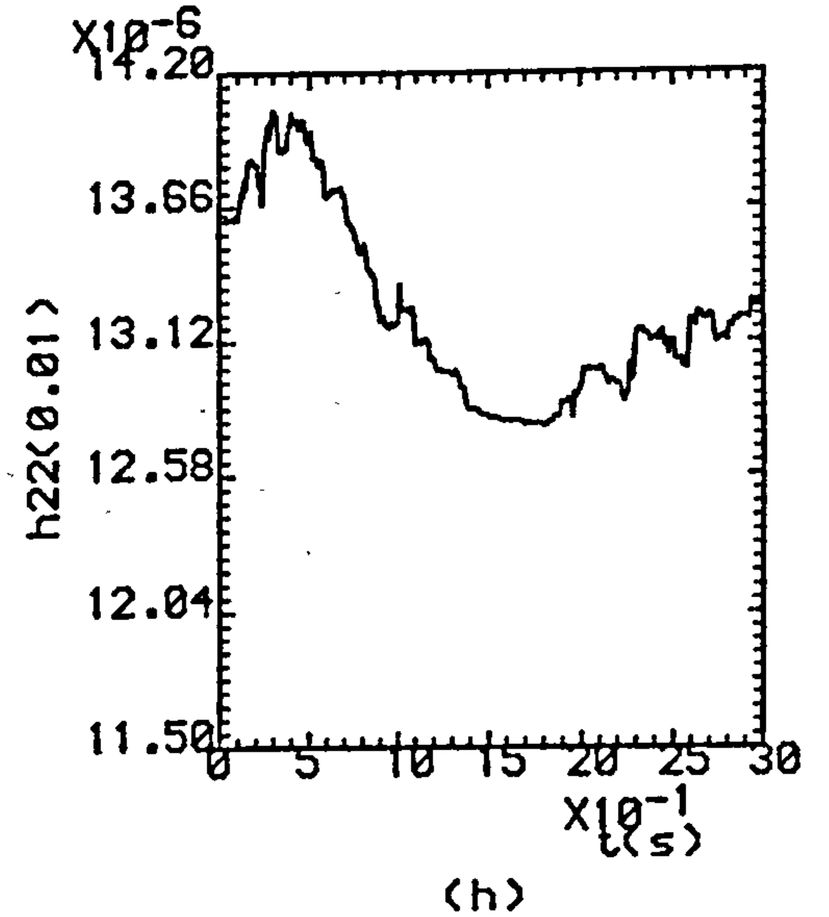

(h)

Fig.8.5(a,b)Actual Trajectories Of End Effector.
(c,d) Actual Torques Acting On The Joints.
(e-h) Identified Elements Of Step-Response Matrix.
K=9

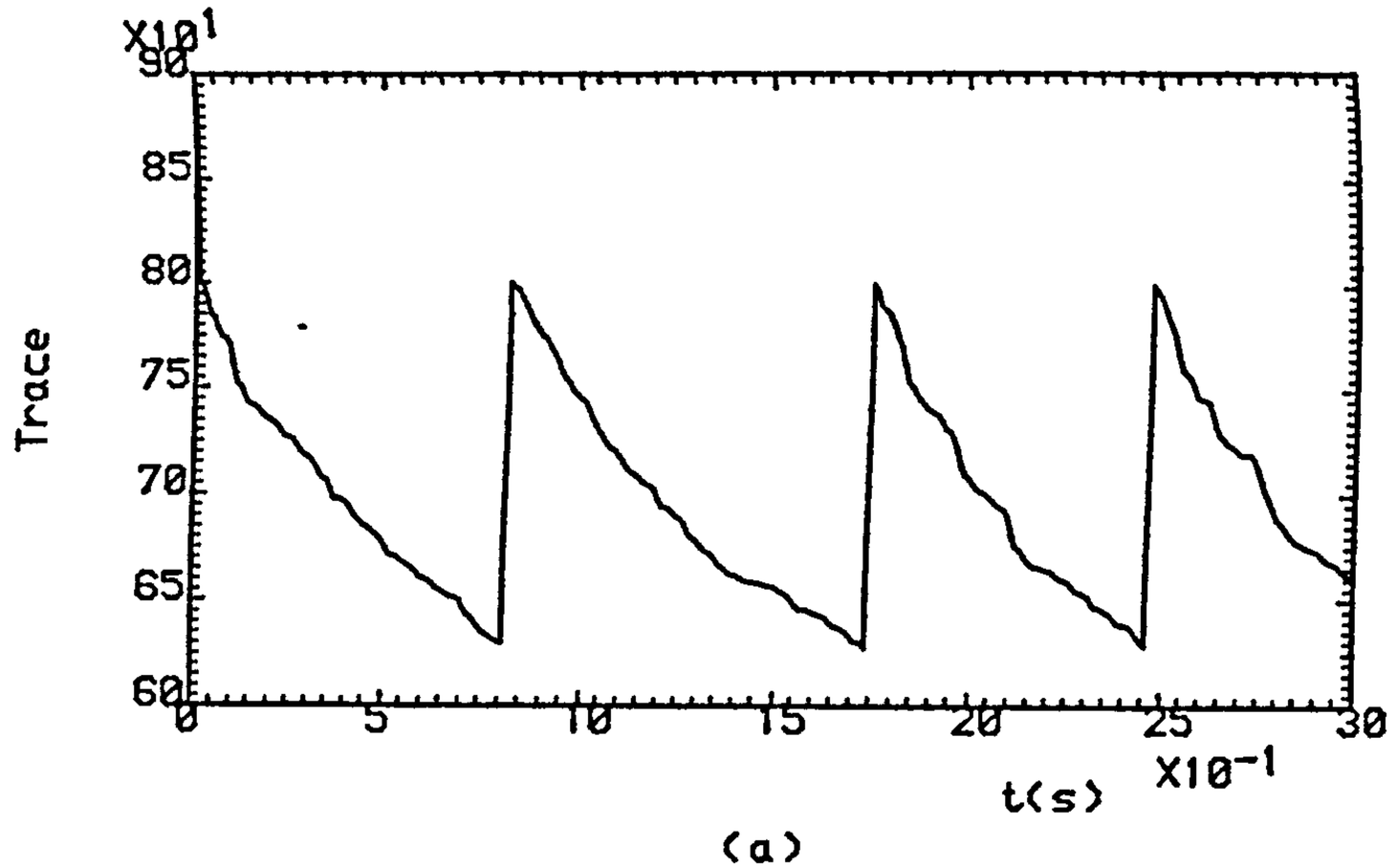

(a)

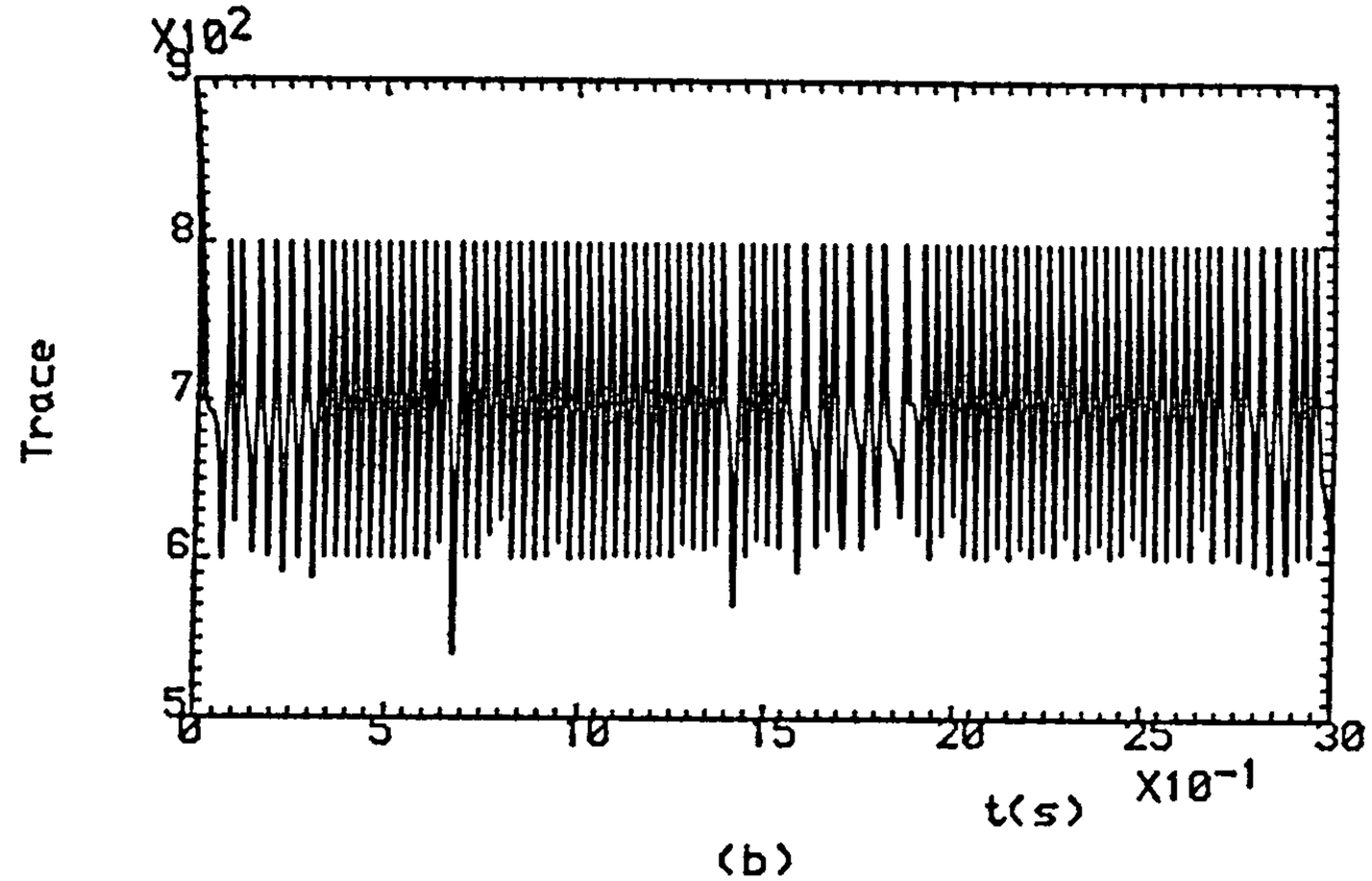

(b)

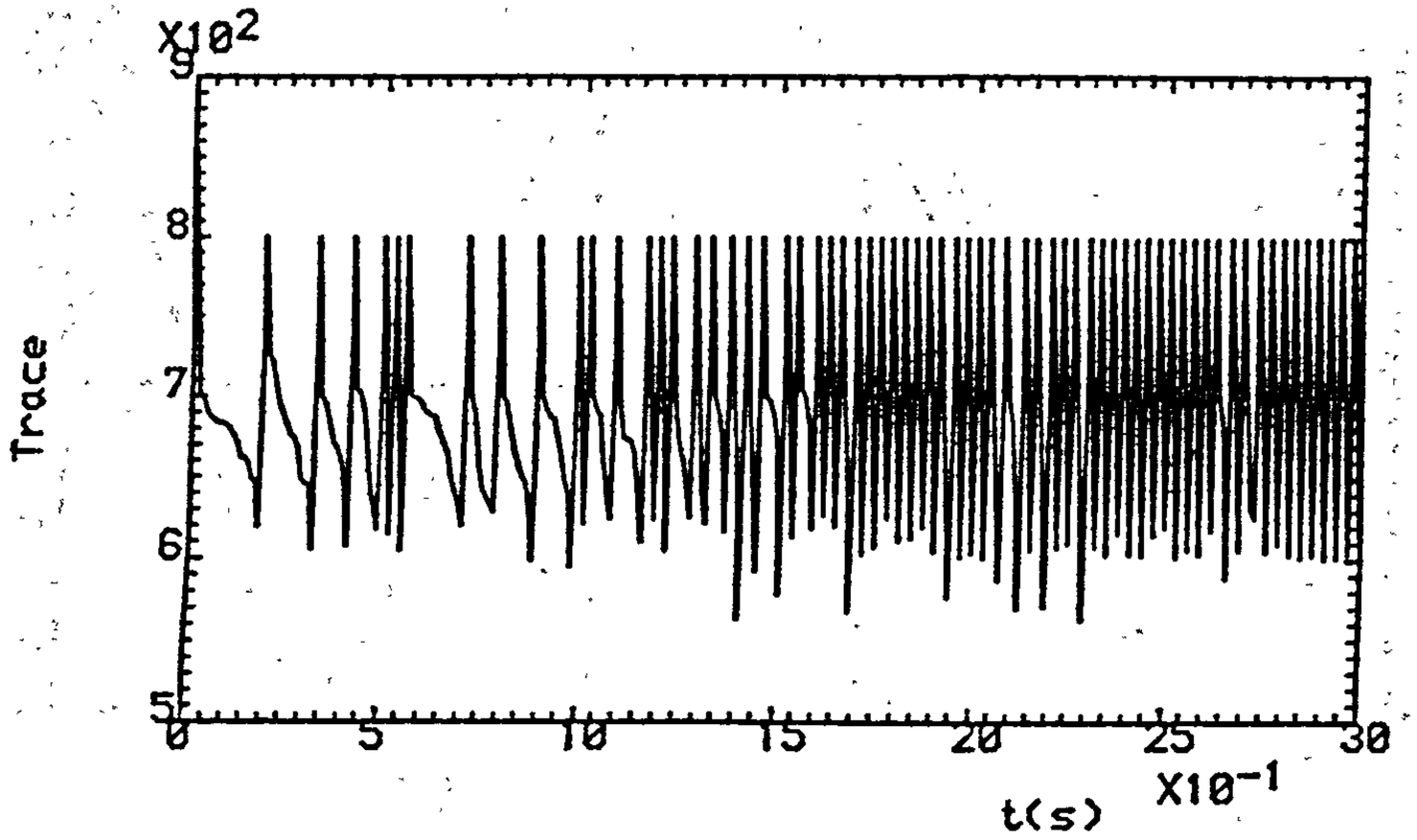

(c)

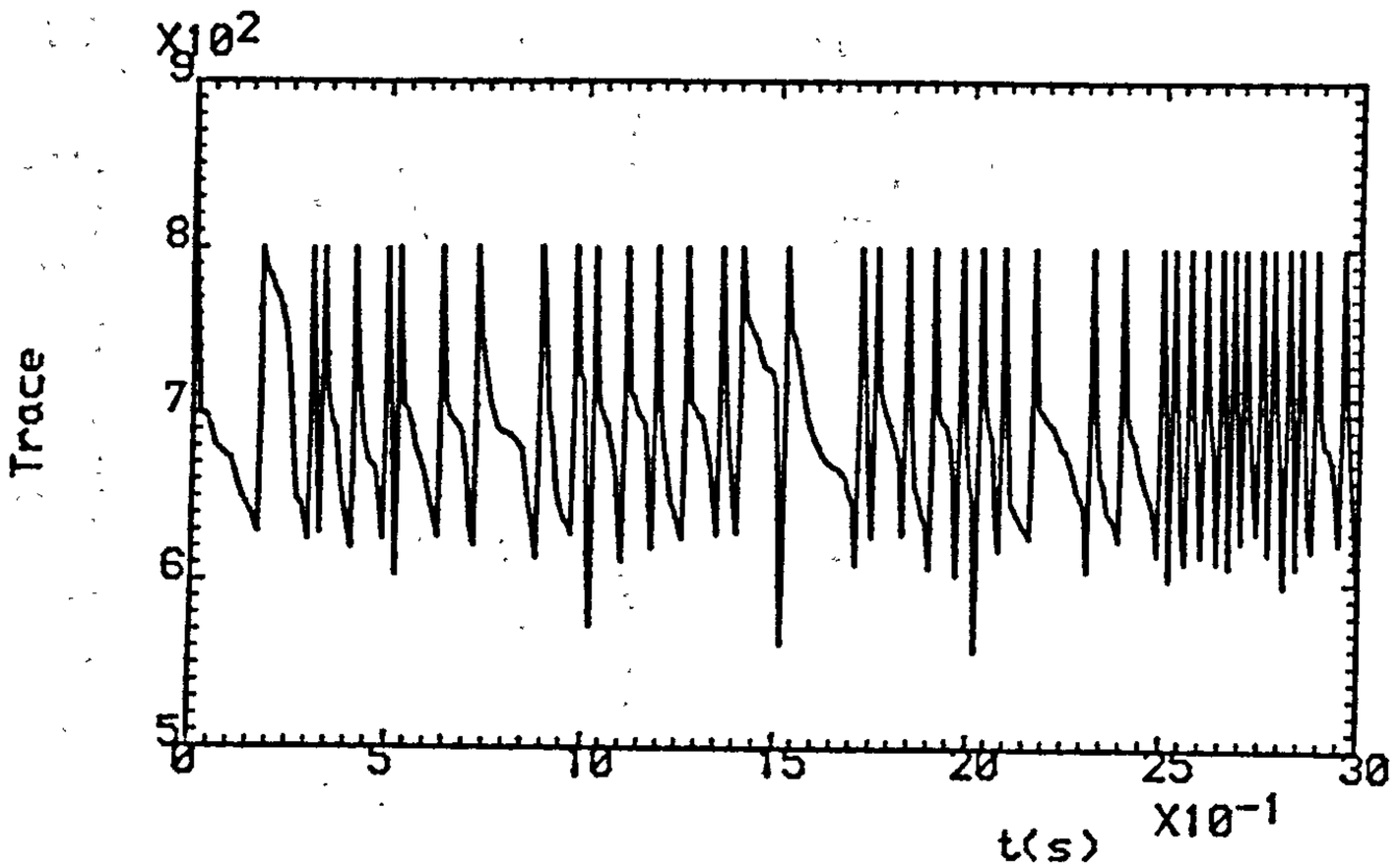

(d)

Fig.8.6(a-d) Trace Changes Due To Resetting Of The Covariance Matrix For K=0,K=1,K=5,K=9 Respectively.

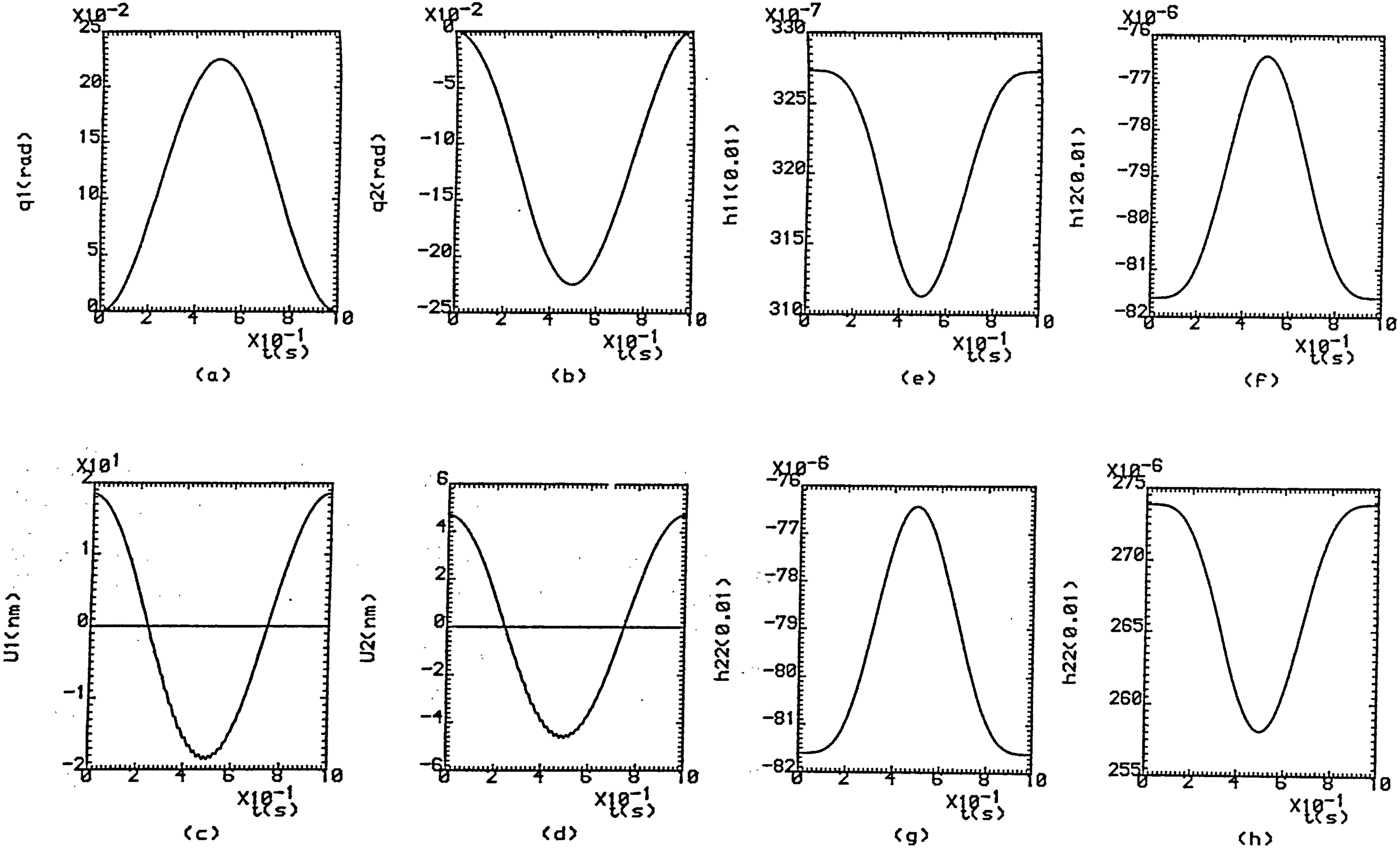

Fig.8.7(a,b)Desired Trajectories OF Joint Angles.
(c,d) Desired Torques Acting On The Joints.
(e-h) Actual Elements OF Step-Response Matrix.

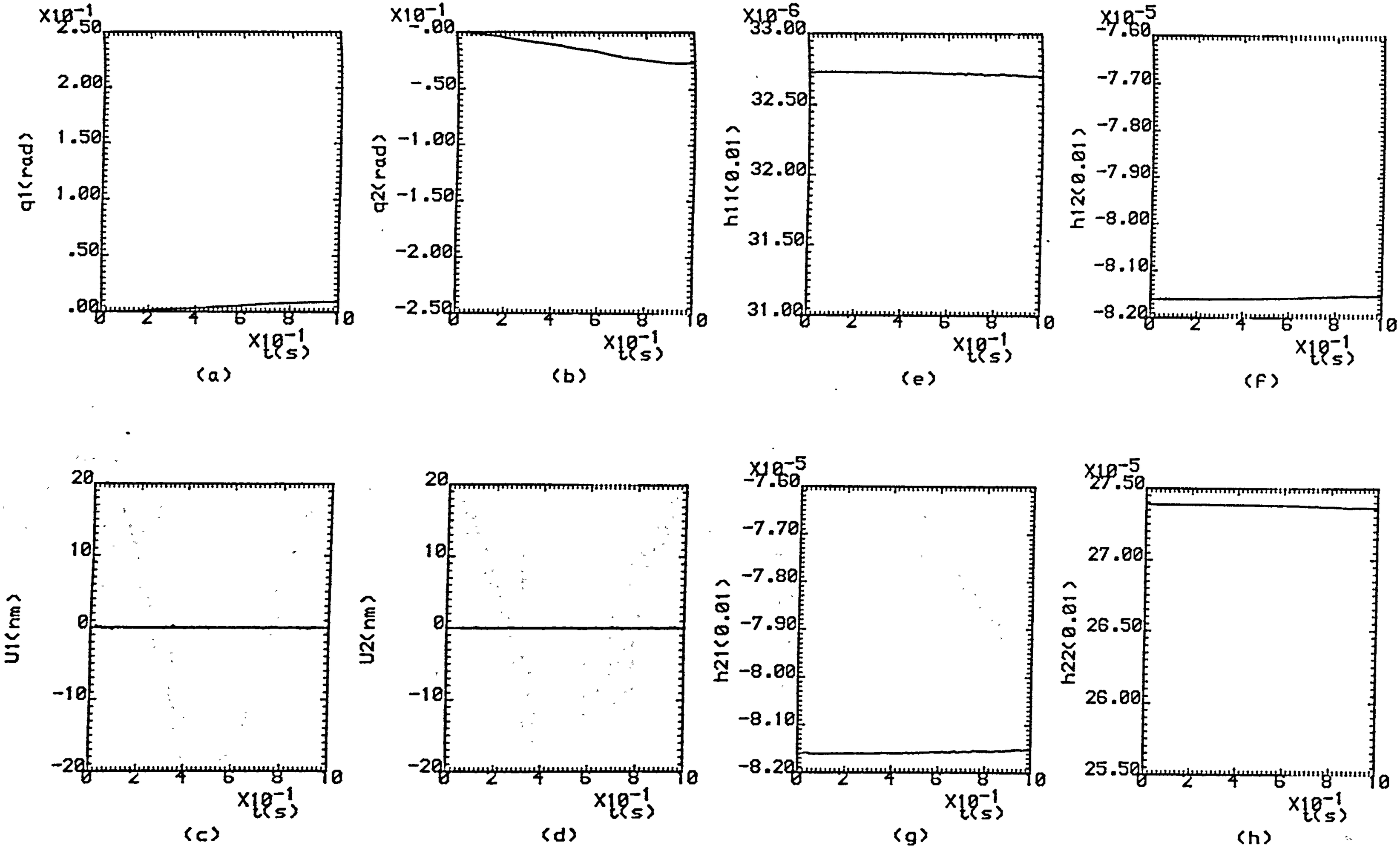

Fig.8.8(a,b)Actual Trajectories Of Joint Angles.
(c,d) Actual Torques Acting On The Joints.
(e-h) Identified Elements Of Step-Response Matrix.
K=0

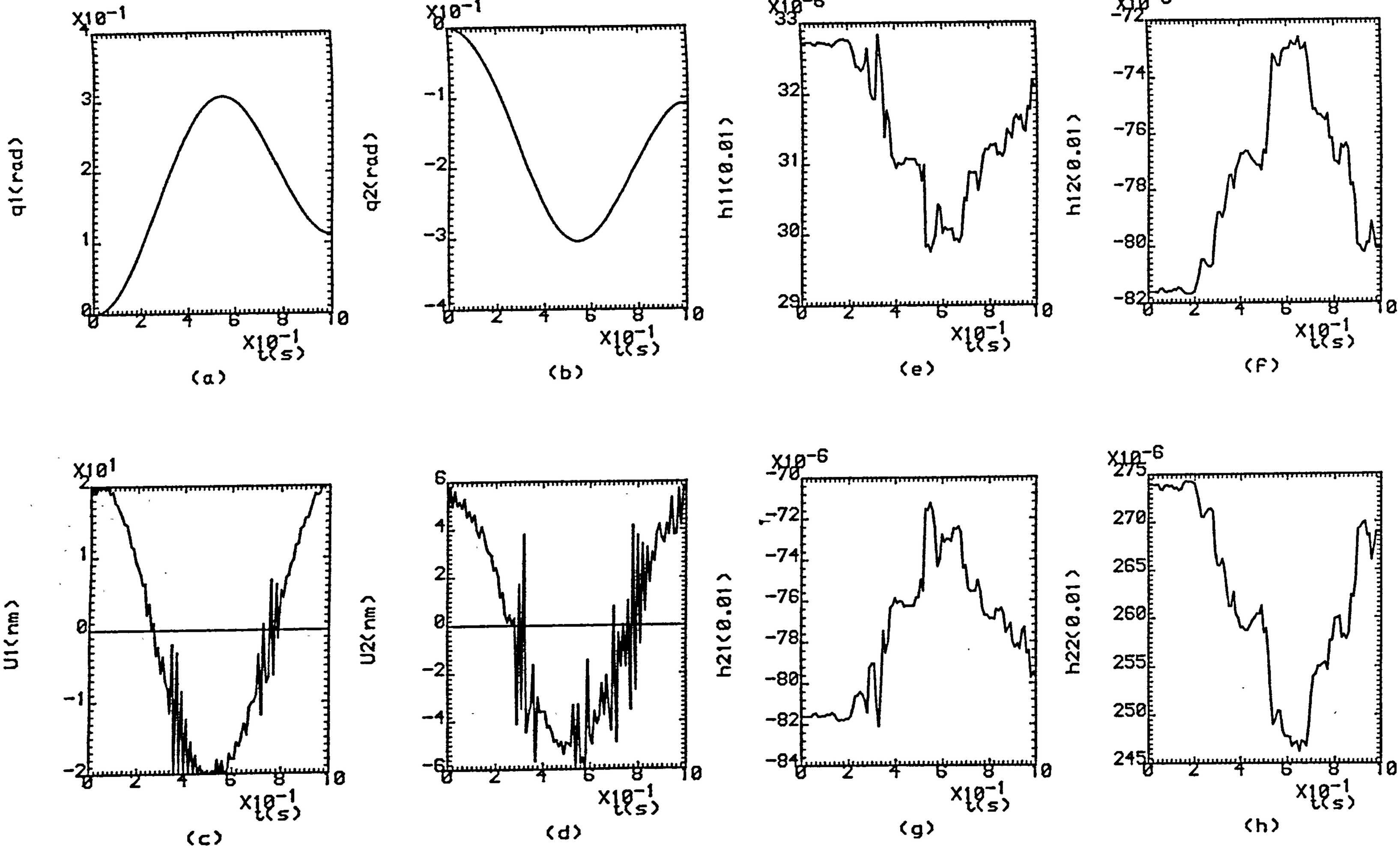

Fig.8.9(a,b)Actual Trajectories Of Joint Angles.
(c,d) Actual Torques Acting On The Joints.
(e-h) Identified Elements Of Step-Response Matrix.
K=1

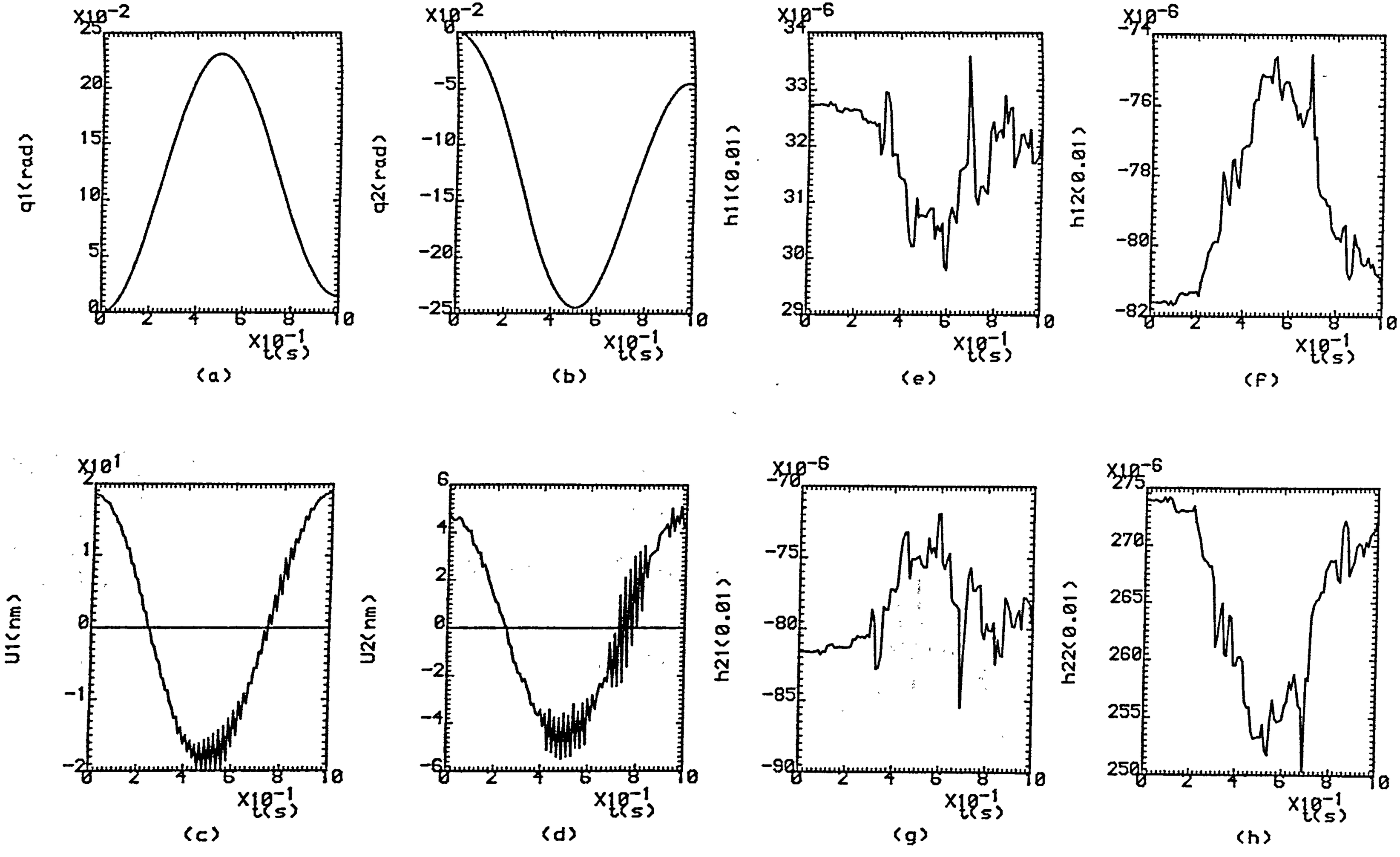

Fig.8.10(a,b)Actual Trajectories Of Joint Angles.
(c,d) Actual Torques Acting On The Joints.
(e-h) Identified Elements Of Step-Response Matrix.
K=5

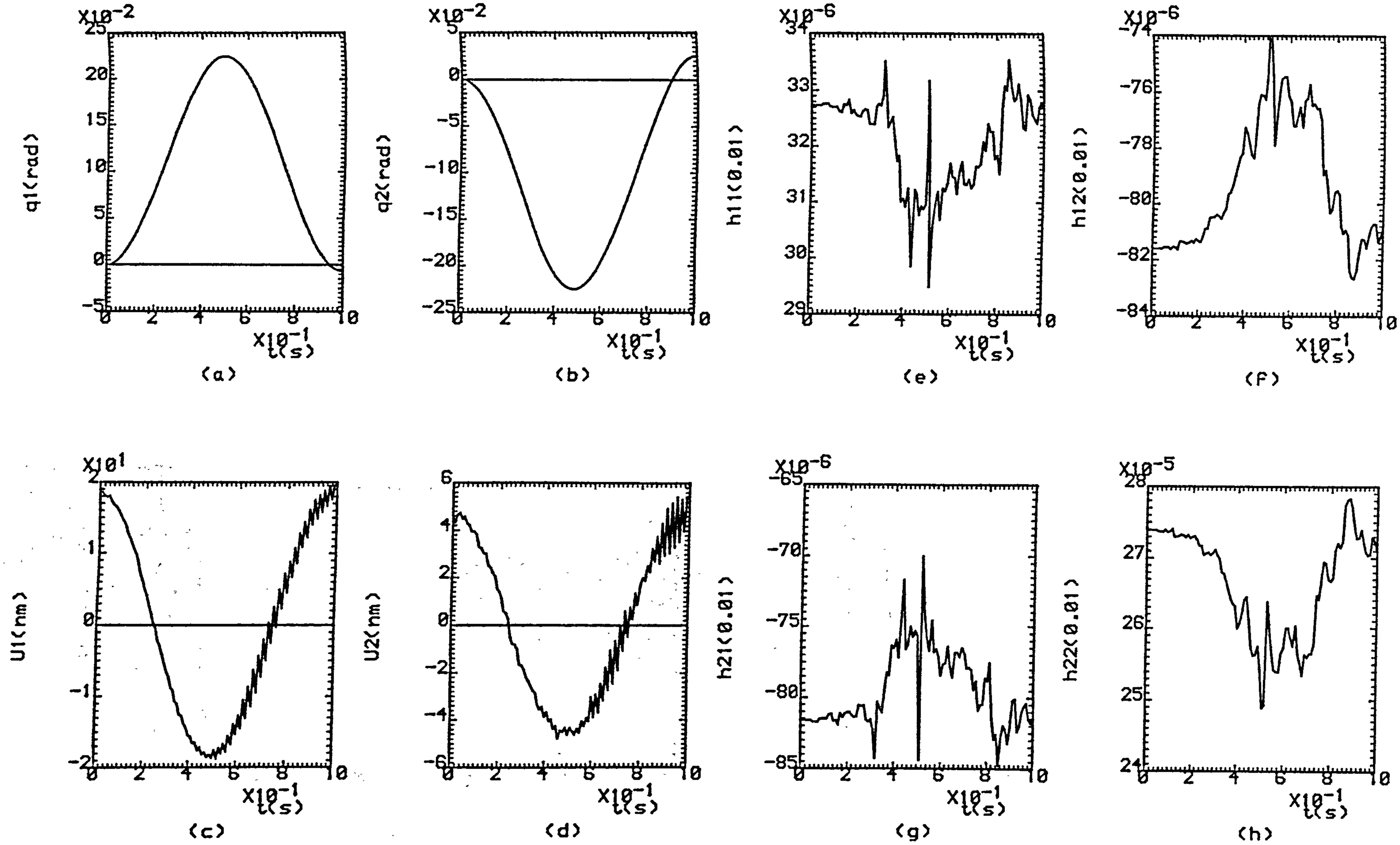

Fig.8.11(a,b)Actual Trajectories Of Joint Angles.
(c,d) Actual Torques Acting On The Joints.
(e-h) Identified Elements Of Step-Response Matrix.
K=9

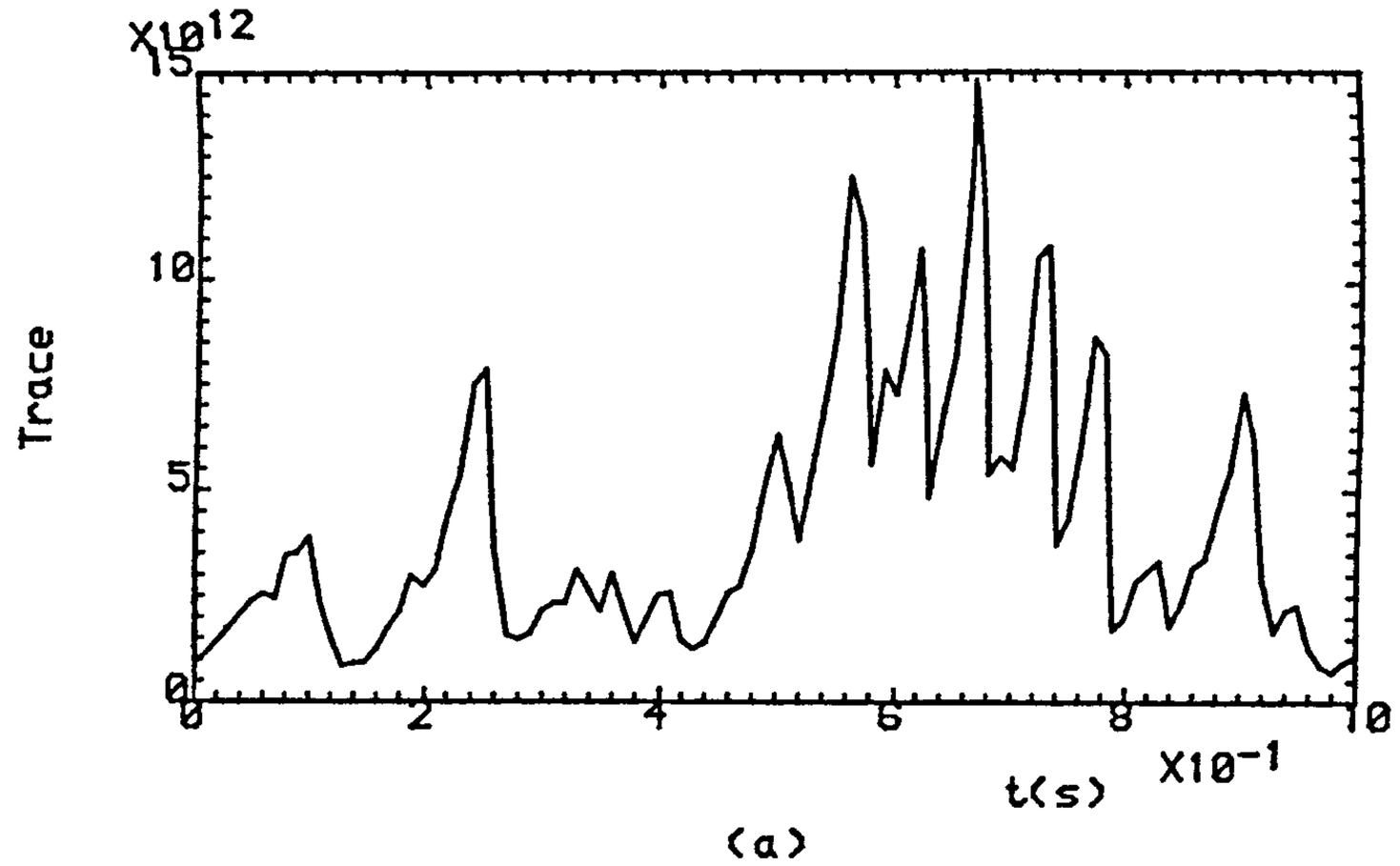

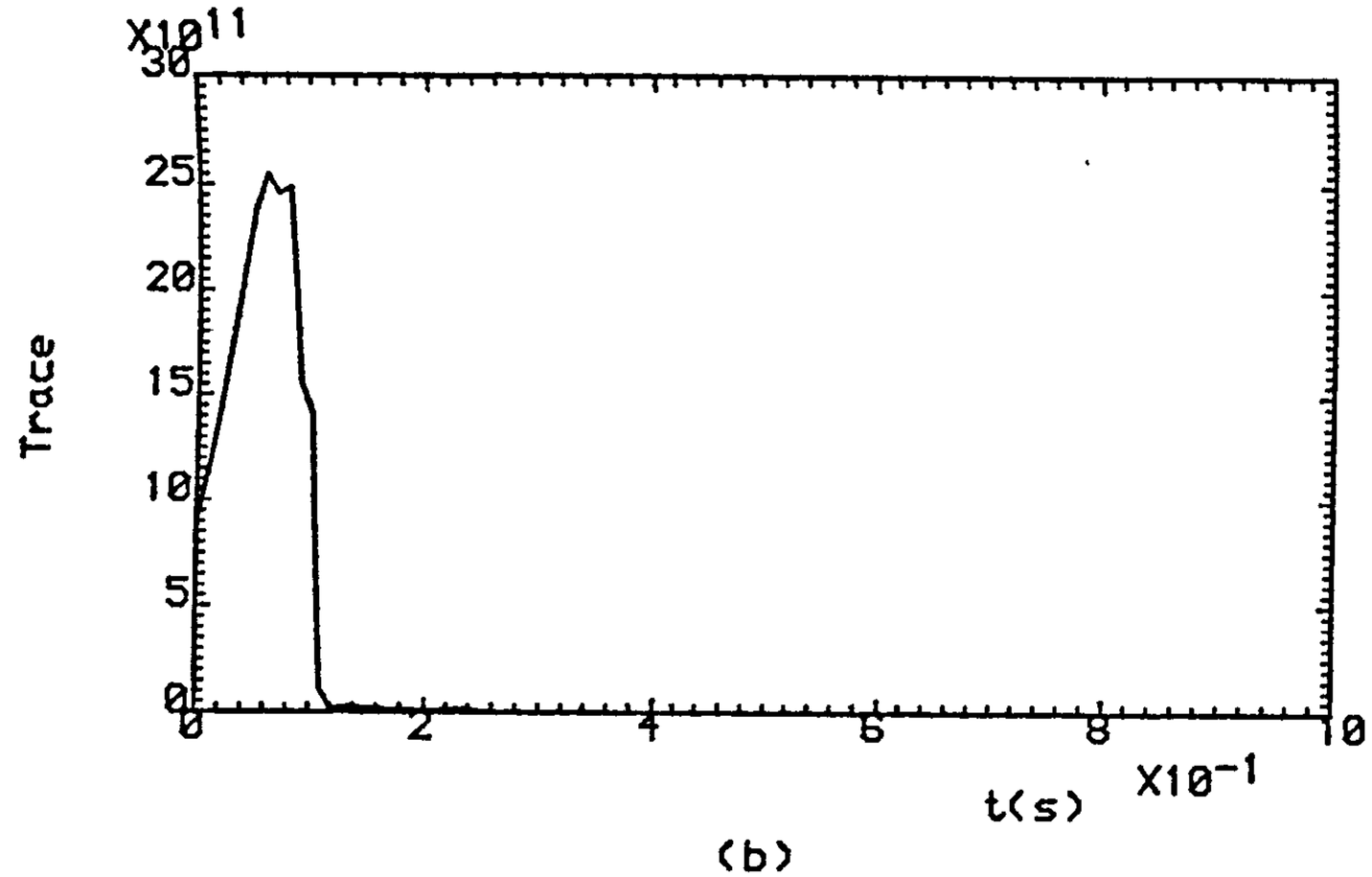

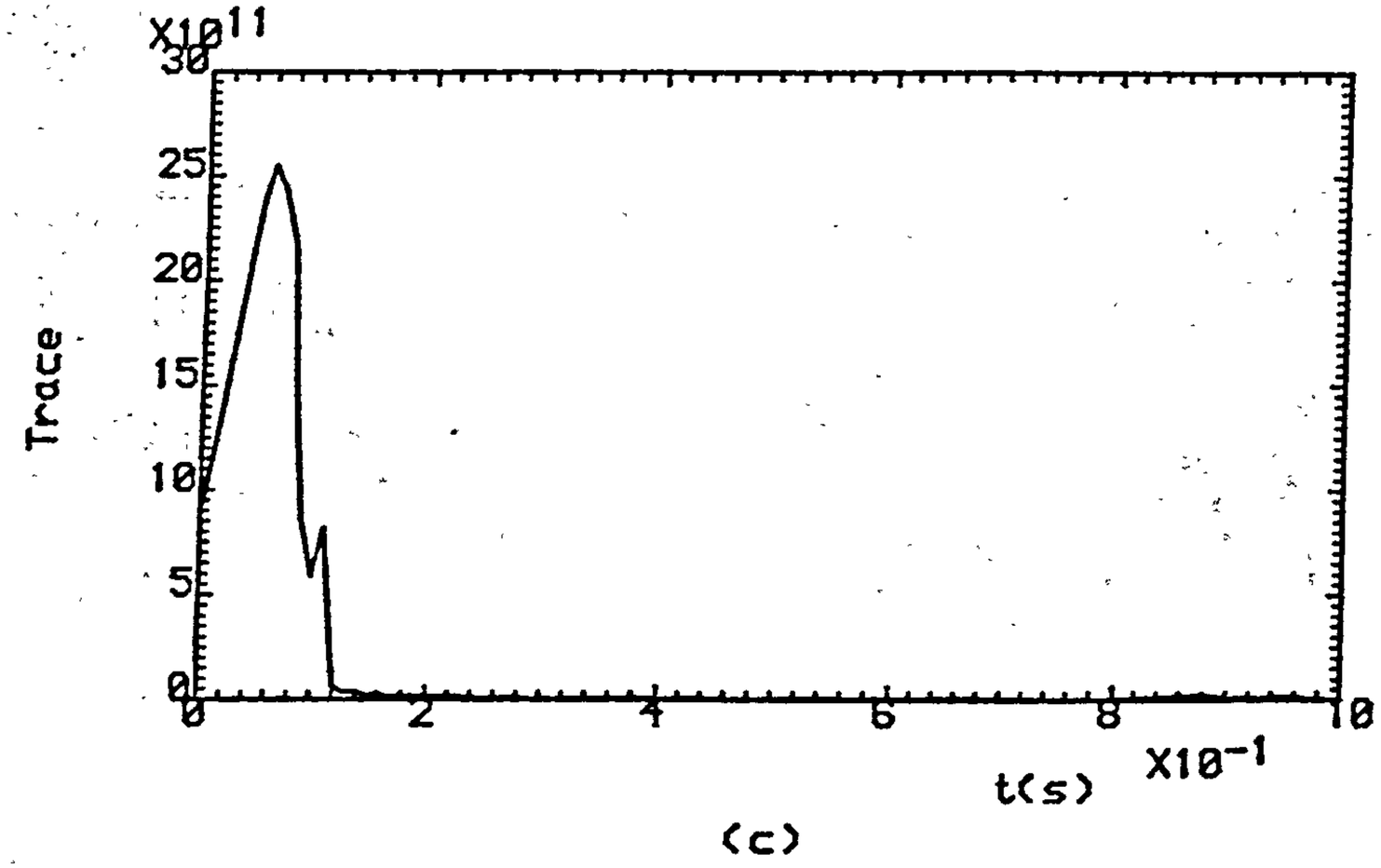

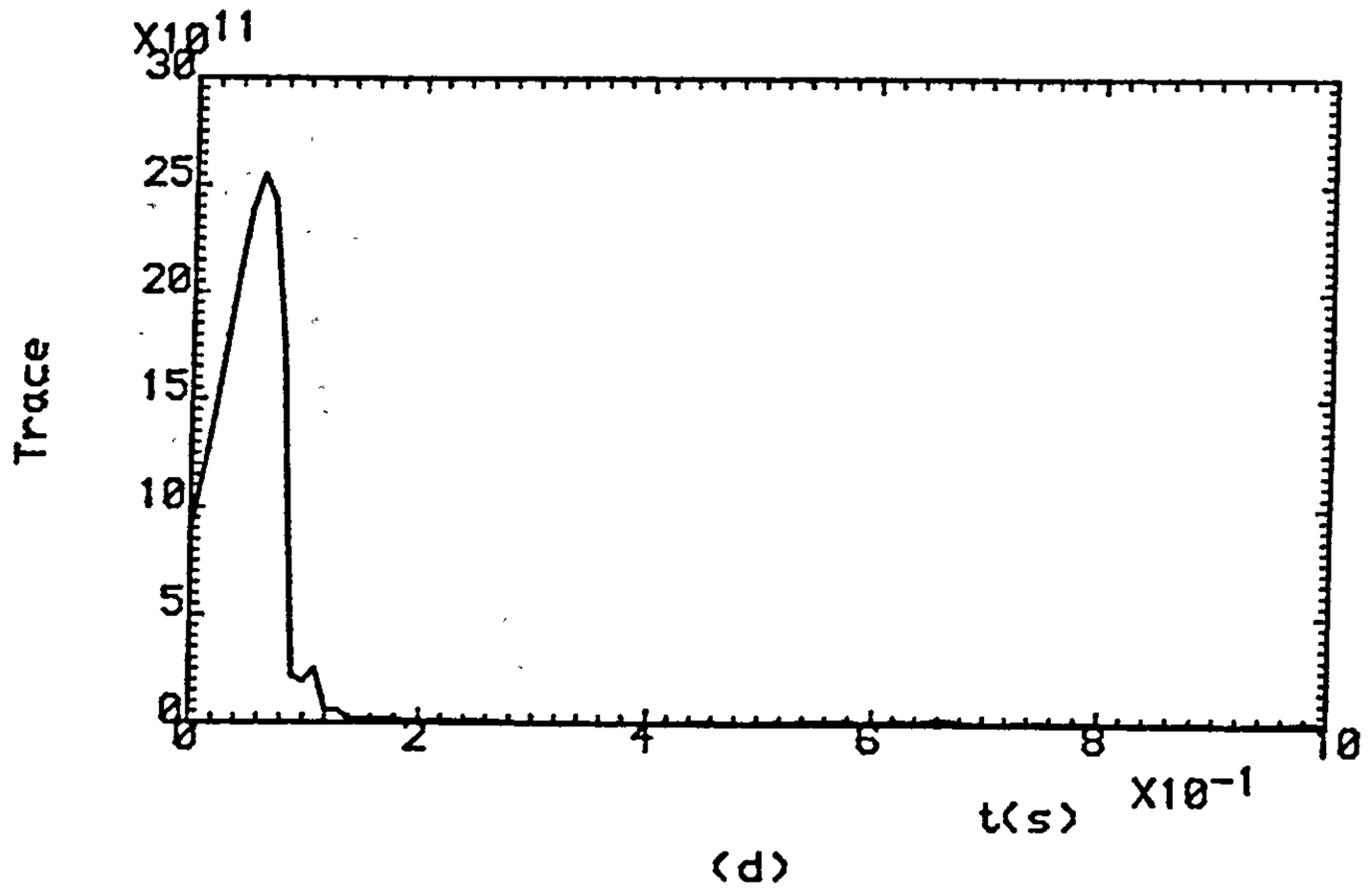

Fig.8.12(a-d) Trace Changes With Forgetting Factor
OF 0.7 For K=0,K=1,K=5,K=9 Respectively.

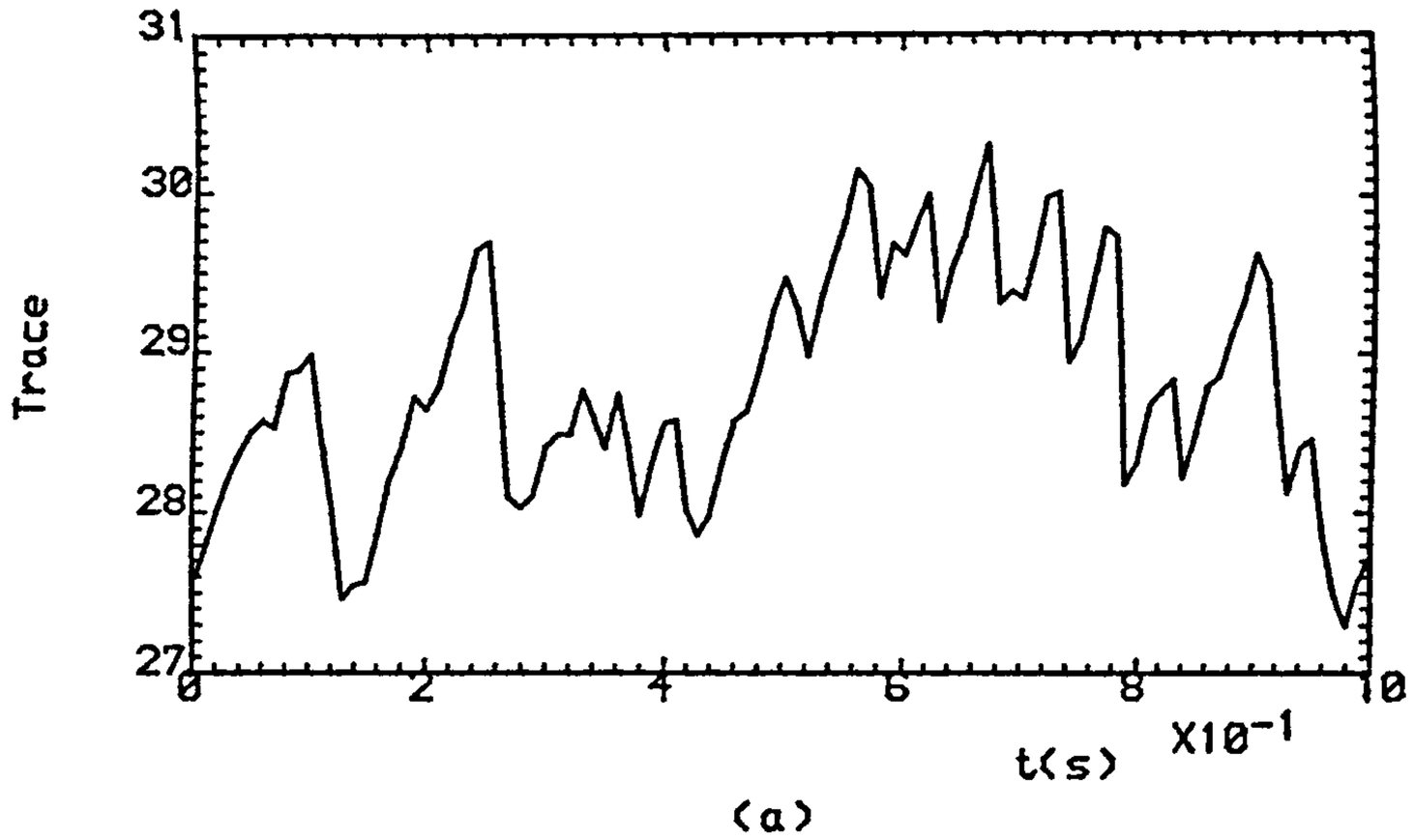

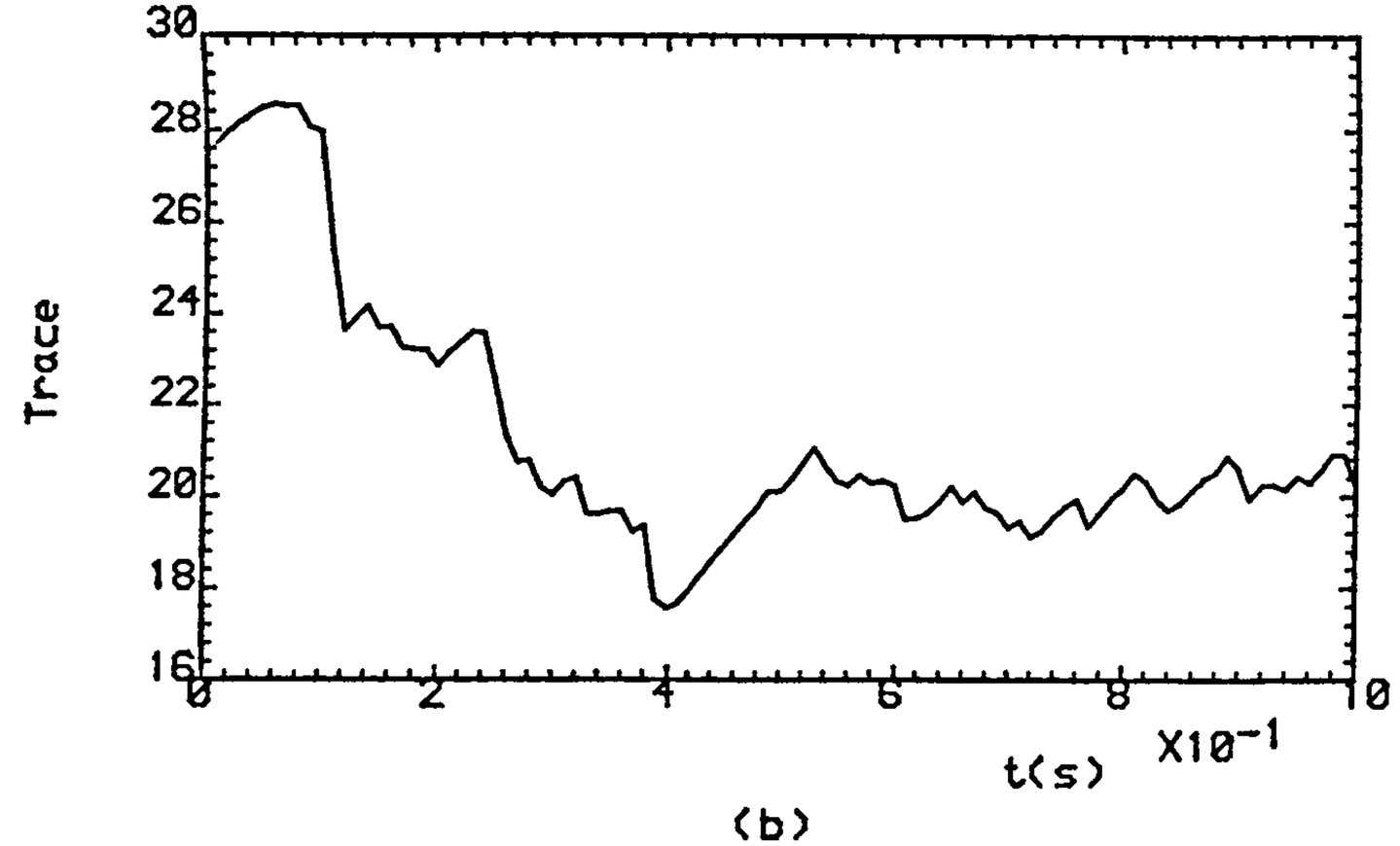

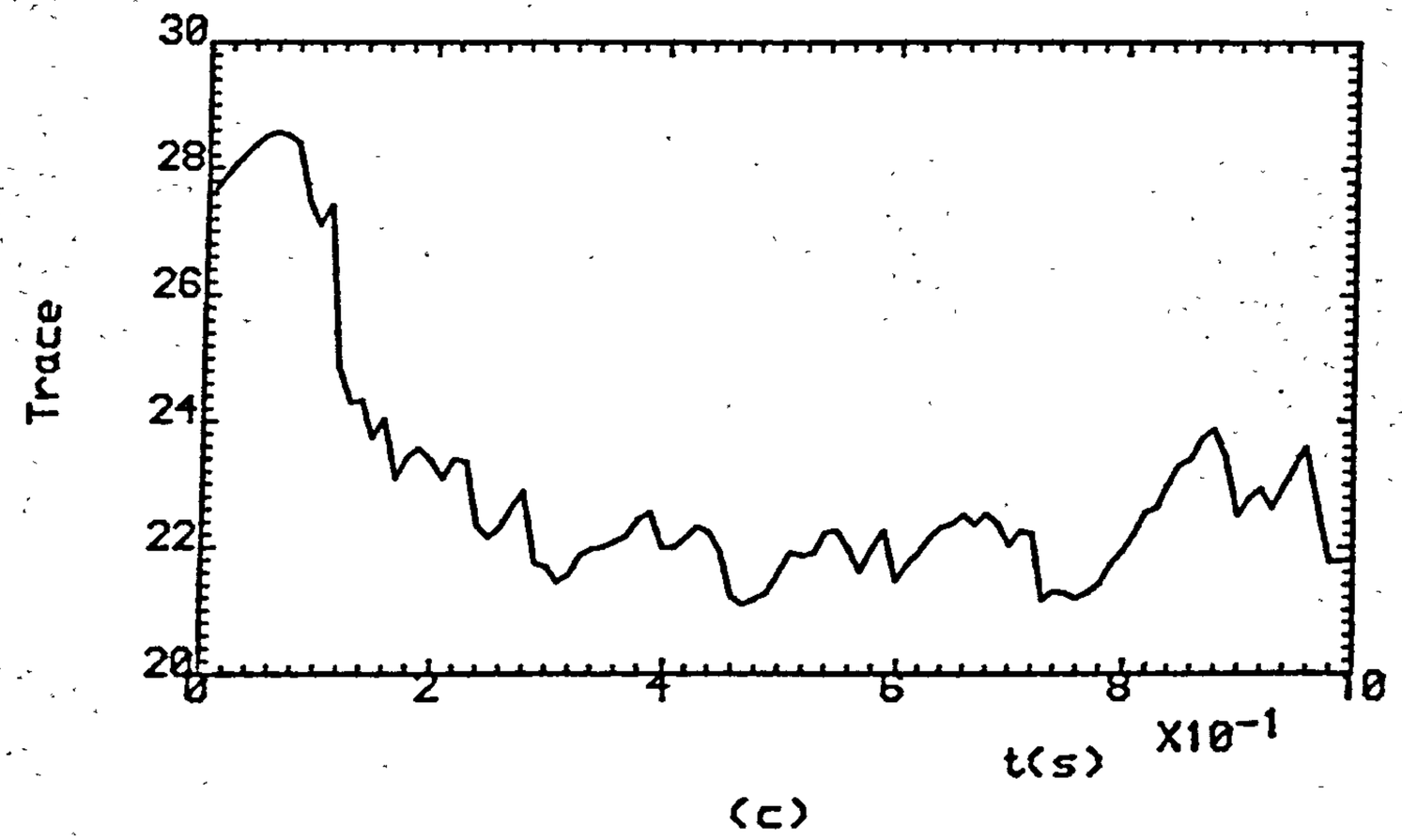

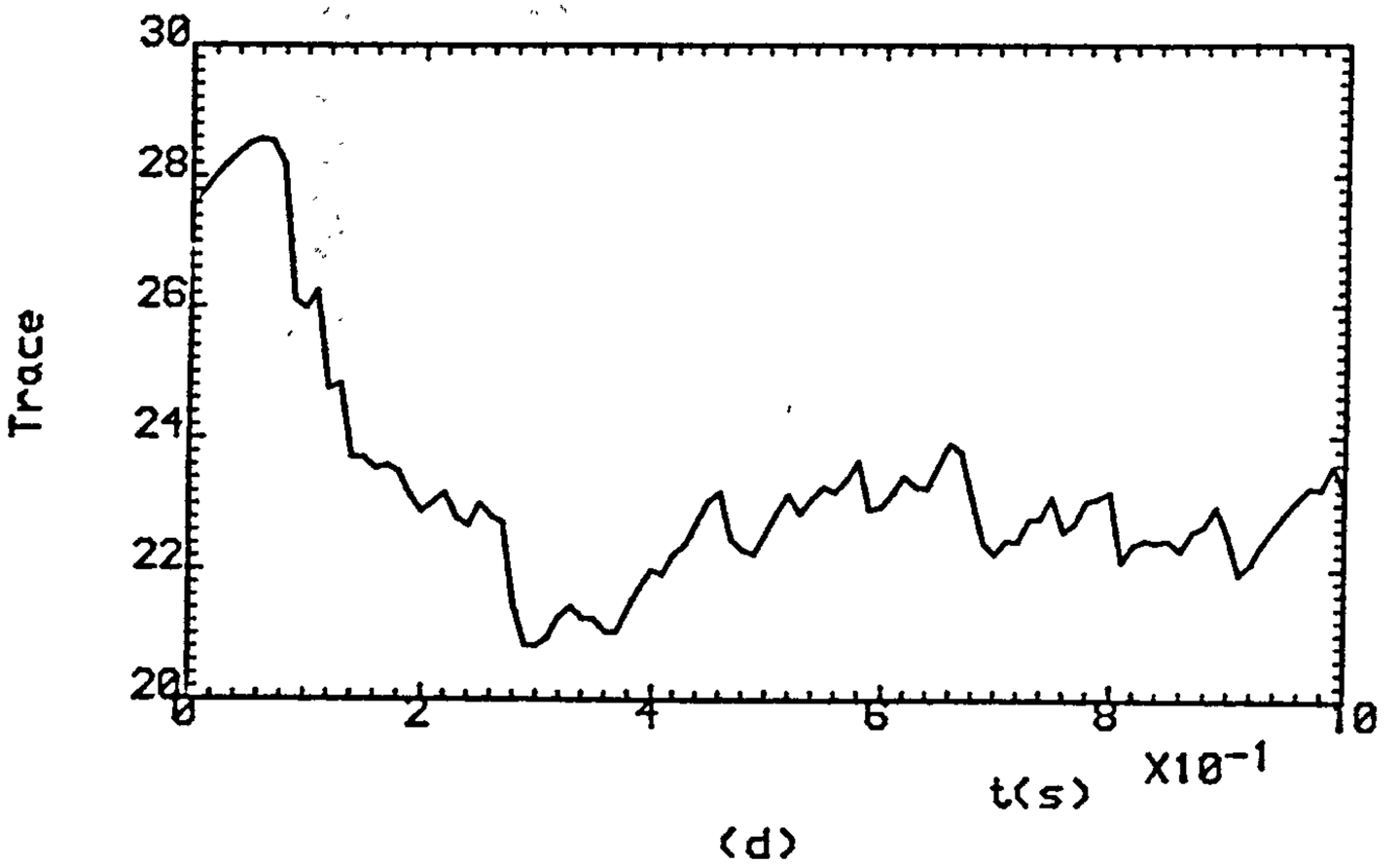

Fig.8.13(a-d)Logarithmic Values OF The Trace With Forgetting Factor OF 0.7 For K=0,K=1,K=5,K=9 Respectively.

PART V

EXPERIMENTAL STUDIES

CHAPTER 9

DIGITAL ITERATIVE LEARNING CONTROL OF A DC SERVO-ACTUATOR

9.1 INTRODUCTION

In previous chapters, theories and numerical examples were given in order to demonstrate the effectiveness of analogue and digital iterative learning controllers. In this chapter, the real-time positional control of a laboratory dc servo-actuator, using digital iterative learning control, is investigated experimentally in order to provide a more practical emphasis.

This dc servo-actuator comprises an inertia and a viscous load driven, via a gear box, by a dc motor. The motor velocity is sensed by a tachogenerator and the angular position of the output is derived from a potentiometer, as illustrated in Figure 9.1. The unit incorporates an eddy-current damper which can be adjusted to provide varying levels of damping. Figure 9.2 represents the mimic panel where the configuration of the motor, gear box, tacho, and output potentiometer and the points at which the output velocity and displacement signals appear. In addition, this mimic panel provides the power to drive the motor.

In this work, a linear time-invariant model of the dc servo actuator is first obtained in order to provide the necessary step-response fuction which is used in the design of the digital iterative learning controller. In addition, the conditions under which learning occurs and the procedure to implement such controllers are investigated in this chapter. Finally, the effectiveness of implementing such digital iterative learning controllers in the case of the dc servo-actuator is illustrated in Section 9.3 of this chapter.

9.2 DESCRIPTION OF EXPERIMENTAL SYSTEM

9.2.1 Analysis

In order to obtain an accurate and reliable model of the dc servo-actuator, it is first necessary to identify the components and the stages that comprise the forward path of Figure 9.2. Indeed, by investigating Figure 9.2, it is clear that the forward path - as far as the position $q(t)$ is concerned - consists of a control amplifier, power amplifier, loaded motor, gear box, and finally an integrator. This can be illustrated in Figure 9.3, where K_P and K_A are the proportional gain constants of the control amplifier and the power amplifier, respectively, $G_m(s)$ is the transfer function of the motor $1/\nu$:1, is the reduction gear ratio, and finally $1/s$ is the integrator transfer function.

The transfer function $G_m(s)$ of the motor can be obtained following a standard procedure (for details see the manufacturer's manual "Introduction To Analogue Control Of ES151"). In this way, it is found that

$$\frac{\dot{q}(s)}{V_m(s)} = G_m(s) = \frac{K_m}{(1+\tau s)} \quad , \qquad ...(9.1)$$

where $K_m = \frac{K_T}{R_a F + K_T K_v}$, $\tau = \frac{R_a J_m}{R_a F + K_T K_v}$, R_a is the armature resistance, J_m is moment of inertia, K_v is the motor emf constant, K_T is the torque constant, and F is the viscous friction coefficient.

Finally, the overall transfer function of the forward path is

$$\frac{q(s)}{V_a(s)} = G(s) = \frac{K_p K_A K_m}{\nu(1+\tau s)s} . \qquad \text{...(9.2)}$$

Then, in a more simplified form,

$$\frac{q(s)}{V_a(s)} = \frac{K}{s(1+\tau s)} \qquad \text{...(9.3)}$$

where

$$K = \frac{K_p K_A K_m}{\nu} .$$

The two paramaters K and τ of the transfer function $G(s)$ were estimated by carrying out open-loop response tests on the dc servo actuator (for details see manufacturer's manual). These values were thus found to be $K = 480$ *deg/sec/volt* and $\tau = 0.25$ *sec* for a value of $K_p = 1$.

The governing equations of the system represented by equation (9.3) can obviously be expressed in the standard state-space form

$$\dot{x}(t) = Ax(t) + B\,u(t) \qquad \text{...(9.4a)}$$

and

$$y(t) = C\,x\,(t) \qquad \text{...(9.4b)}$$

with

$$x = \begin{bmatrix} q \\ \dot{q} \end{bmatrix} \epsilon\, R^{2\times 1} \quad , \qquad \text{...(9.5a)}$$

$$A = \begin{bmatrix} 0 & , & 1 \\ 0 & , & -\frac{1}{\tau} \end{bmatrix} = \begin{bmatrix} 0 & , & 1 \\ 0 & , & -4 \end{bmatrix} \epsilon\, R^{2\times 2} \quad , \qquad \text{....(9.5b)}$$

$$B = \begin{bmatrix} 0 \\ \frac{K}{\tau} \end{bmatrix} = \begin{bmatrix} 0 \\ 1920 \end{bmatrix} \epsilon\, R^{2\times 1} \quad , \qquad \text{...(9.5c)}$$

and

$$C = [1,0] \in R^{1\times 2} \quad . \qquad (9.5d)$$

But the dynamics of linear plants governed on the continuous-time set by differential equations of the form (9.4) are governed on the discrete-time set by difference equations of the form

$$x(j+1) = \Phi\, x(j) + \Psi\, u(j) \qquad ...(9.6a)$$

and

$$y(j) = \Gamma\, x(j) \qquad ...(9.6b)$$

where

$$\Phi = e^{AT} \quad , \qquad ...(9.7a)$$

$$\Psi = \int_0^T e^{At}\, B\, dt \quad , \qquad ...(9.7b)$$

$$\Gamma = C \quad , \qquad ...(9.7c)$$

and T is the sampling period. The step-response matrices of such plants have the form

$$H(T) = \int_0^T C\, e^{At}\, B\, dt \qquad ...(9.8)$$

and characterise the responses of initially quiescent plants to unit step inputs after one sampling period. Such step-response matrices can evidently be measured directly from input/output data.

It is clear from equations (9.5b),(9.5c), and (9.5d) that the linearised model of the dc servo-actuator gives rise to a linear time-invariant plant with a null first Markov parameter but a full-rank second Markov parameter. Such a plant is therefore completely irregular and it is accordingly immediately possible to use the results of Chapter 4. These imply the following result for such plants:

Theorem

In the case of the completely irregular plant with discrete-time governing equations

$$x_k(j+1) = \Phi\, x_k(j) + \Psi\, u_k(j)$$

and

$$y_k(j) = \Gamma\, x_k(j) \quad ,$$

under the action of the control law

$$u_k(j) = -\frac{2}{T}(1+\alpha)\, D\, r_k(j) + \left[I_m + \frac{2}{T} D\right] s_k(j)$$

$$r_k(j+1) = -\alpha\, r_k(j) + s_k(j)$$

$$s_{k+1}(j) = s_k(j) + \Lambda\, \{e_k(j+1) - e_k(j)\}$$

where $\alpha \in (-1,+1]$, $D \in R^{m \times m}$ and $e_k(j) = v(j) - y_k(j)$, assume that

(i) $$\Lambda = \lambda \left[H(T)\left[I_m + \frac{2}{T} D\right]\right]^{-1} ;$$

(ii) $x_{k+1}(0) = x_k(0)$ $(k = 0, 1, 2, \ldots)$;

(iii) $y_k(0) = v(0)$ $(k = 0, 1, 2, \ldots)$.

Then, when $j \in [0, J]$,

$$y_k(j) \rightarrow v(j)$$

as $k \rightarrow \infty$.

9.2.2 Implementation Procedure

In the implementation of the digital iterative learning controller, the following items of hardware were required:

(i) an IBM pc or any compatible system;

(ii) a 12-bit A/D and D/A interface card for high-performance data conversion;

(iii) a user-friendly computer program;

(iv) an electronic scaling circuit, so that the voltages of the overall system are compatible;

(v) a dc power supply, supplying a bias voltage between ±15 *volt* to the scaling circuit;

(vi) a digital voltmeter to ensure that the initial position and velocity are the same at the beginning of each successive iteration;

(vii) a dc servo-actuator unit plus the drive power unit (see Figures 9.1 and 9.2).

The A/D and D/A conversion was done using a high-performance data conversion card operating at a 12-bit resolution for an IBM pc or any compatible system. The

card operates with one channel for 12-bit data transfer from digital to analogue form in either unipolar or bipolar operation, and sixteen unipolar channels for 12-bit analogue to digital data conversion. The computer used was an Elonex 286 machine with VGA colour screen.

The program was written in PASCAL . It gives the user a coloured graphics representation of the output signal on the screen, and allows the output signal to be stored in a file for further manipulation if required. Finally, this program was written so that the user could complete as many iterations as desired. Moreover, at the end of each iteration, the program execution halts, so that the user has time to return the output rotor at rest to its initial position. This was done in order to satisfy condition (ii) of the theorem for learning to occur.

In this apparatus, the electronic scaling circuit was used so that the overall system voltages were compatible. This circuit is necessary because the A/D and D/A card accepts an input between 0-9 *volt* and produces an output between 0-9 *volt*, while the dc servo-actuator produces a range of voltages between ∓15 *volt* depending on the direction of rotation.

The ∓15 *volt* output from the dc servo-actuator comes from the potentiometer. This potentiometer has a constant of 0.1 *volt/deg*. This value was found by carrying out a simple test on the dc servo-actuator (for details see the manufacturer's manual). It was also found that this potentiometer has linear characteristics between ∓150 *degree*.

Therefore, the scaling was done for the A/D convertor as follows:

(i) voltages between (0-15) *volt* scaled to (4.5-9) *volt*;

(ii) voltages between (0- -15) *volt* scaled to (4.5-0) *volt*.

The output of the D/A converter was scaled in a reverse manner, namely:

(iii) voltages between (4.5-9) *volt* scaled to (0-15) *volt*;

(iv) voltages between (4.5-0) *volt* scaled to (0- -15) *volt*.

The procedure for carrying out the experiment was as follows:

(i) turn on all the devices;

(ii) position the brake clear of the output disc;

(iii) use the digital voltmeter to ensure that the position at the beginning of each successive iteration is the same;

(iv) run the computer program to start the iterative learning process.

A block diagram of the overall system is shown in Figure 9.4. Figure 9.5 shows the dc servo-actuator on its own. Figure 9.6 shows the power drive unit with its front panel mimicking the actuator, together with the actual dc servo-actuator. Finally, Figure 9.7 shows the layout of all the devices used in this experiment.

9.3 EXPERIMENTAL RESULTS

In order to illustrate the effectiveness of digital iterative learning controllers, three experiments were performed. The experimental results thus obtained were interpreted in the light of the theoretical results obtained earlier in this thesis.

In all three experiments, it is desired that the output disc follow the trajectory

$$v(j) = 28.41\ (1 - \cos jT\ (21.486)) \qquad \ldots(9.9)$$

in 6.48 *sec* (or $J = 540$, since $T = 12$ *msec*). This sampling time was determined according to the time required to perform one cycle of calculation. In addition, the step-response function is

$$H(T) = \Gamma \Psi = 136.05 \times 10^{-3} \qquad \ldots(9.10)$$

in view of equations (9.7b) and (9.7c).

Experiment 9.1

In this experiment, the controller parameter D, α and λ were chosen to be 0, 0, and 1, respectively, i.e, no compensator was used and the controller was not de-tuned. It therefore follows that $\rho = 0$ and $\sigma = 1.937$ using their definitions in Chapter 4.

Indeed,

$$\rho = \| I_m - \hat{H}(T)\, \Lambda \|_\infty \qquad \ldots(9.11)$$

$$= \left| 1 - H(T)\left(1 + \frac{2}{T} D\right) . \lambda \left[H(T)\left(1 + \frac{2}{T} D\right)\right]^{-1} \right|$$

$$= |1 - \lambda| = 0$$

and

$$\sigma = \sup_{0 < J \leq J} \| \hat{\Gamma}(\hat{\Phi}^J - \hat{\Phi}^{J-1})\, \hat{\Psi}\, \Lambda \|_\infty \qquad \ldots(9.12)$$

$$= 1.937 \ .$$

The experimental results obtained in this case are plotted in Figure 9.8. It is evident

from this figure that, as expected from the theoretical results of Chapter 4, the learning is slow and violent because ρ is small and σ is relatively large.

Experiment 9.2

In this experiment, the controller parameters D, α and λ were chosen to be 0, 0, and 0.1 respectively, i.e no compensator was used but the controller was strongly de-tuned. It therefore follows that $\rho = 0.9$ and $\sigma = 0.1937$ using equation (9.13) and (9.14), respectively. The experimental results obtained in this case are plotted in Figure 9.9. It is evident from this figure that, as expected from the theoretical results of Chapter 4, the learning is slower than in experiment 9.1 but non-violent because ρ is large and σ is relatively small.

Experiment 9.3

In this experiment, the controller parameters D, α and λ were chosen to be 0.01,0.01 and 0.3, respectively, i.e a compensator was used but the controller was moderately de-tuned. It therefore follows that $\rho = 0.7$ and $\sigma = 0.3918$ using equation (9.13) and (9.14), respectively. The experimental results obtained in this case are plotted in Figure 9.10. It is evident from this figure that, as expected from the theoretical results of Chapter 4, the learning is faster than in experiment 9.2 but still non-violent because ρ is small and σ is still relatively small.

9.4 CONCLUSION

It has been shown in this chapter that digital iterative learning controllers for irregular plants can be designed and implemented practically. Their effectiveness has been illustrated by implementing such controllers in the real-time positional control of a dc

servo-actuator. The experimental results thus obtained confirm the theoretical predictions of Chapter 4 regarding the effects of compensation and controller tuning on the speed and smoothness of the learning behaviour.

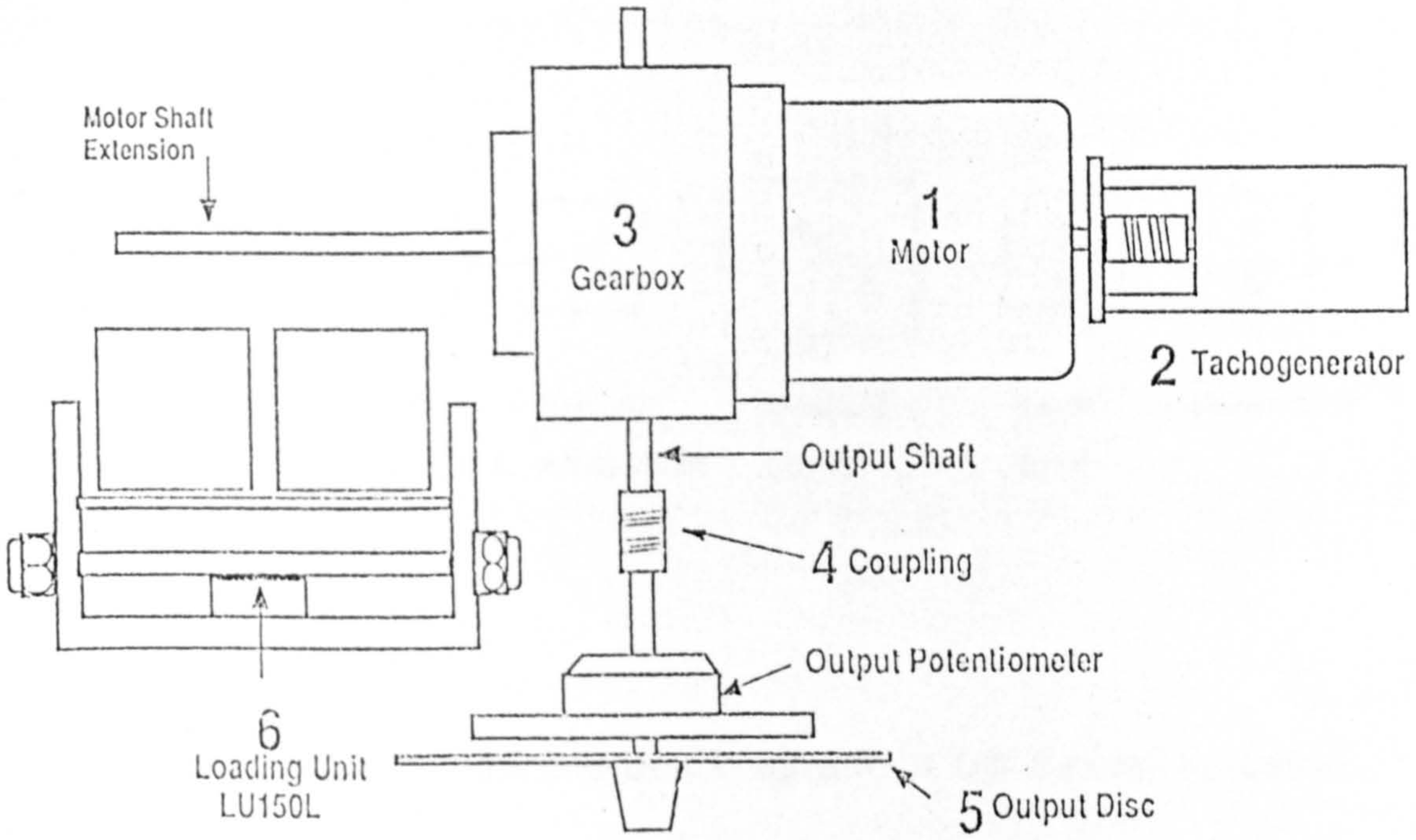

Fig.9.1: Schematic Diagram Of DC Servo-Actuator.

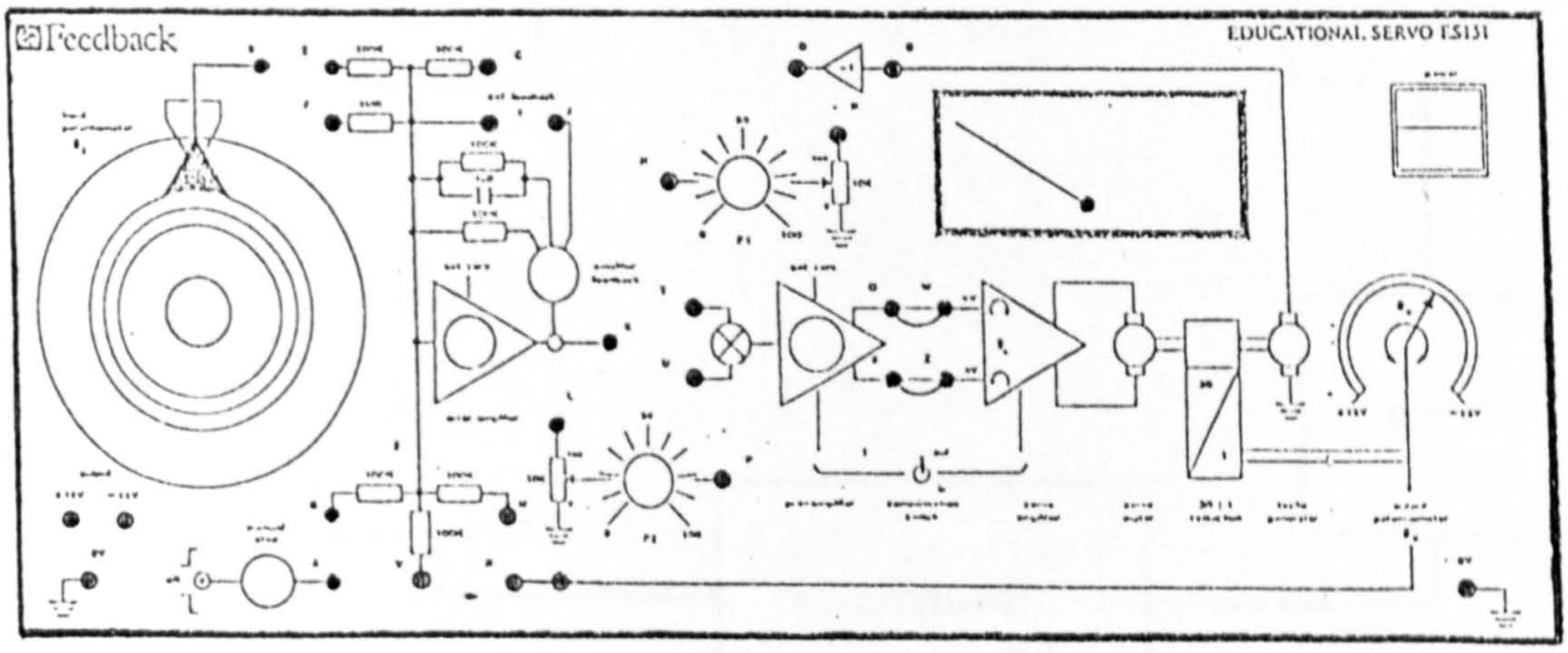

Fig.9.2: Front Panel Of Power Unit Of DC Servo-Actuator.

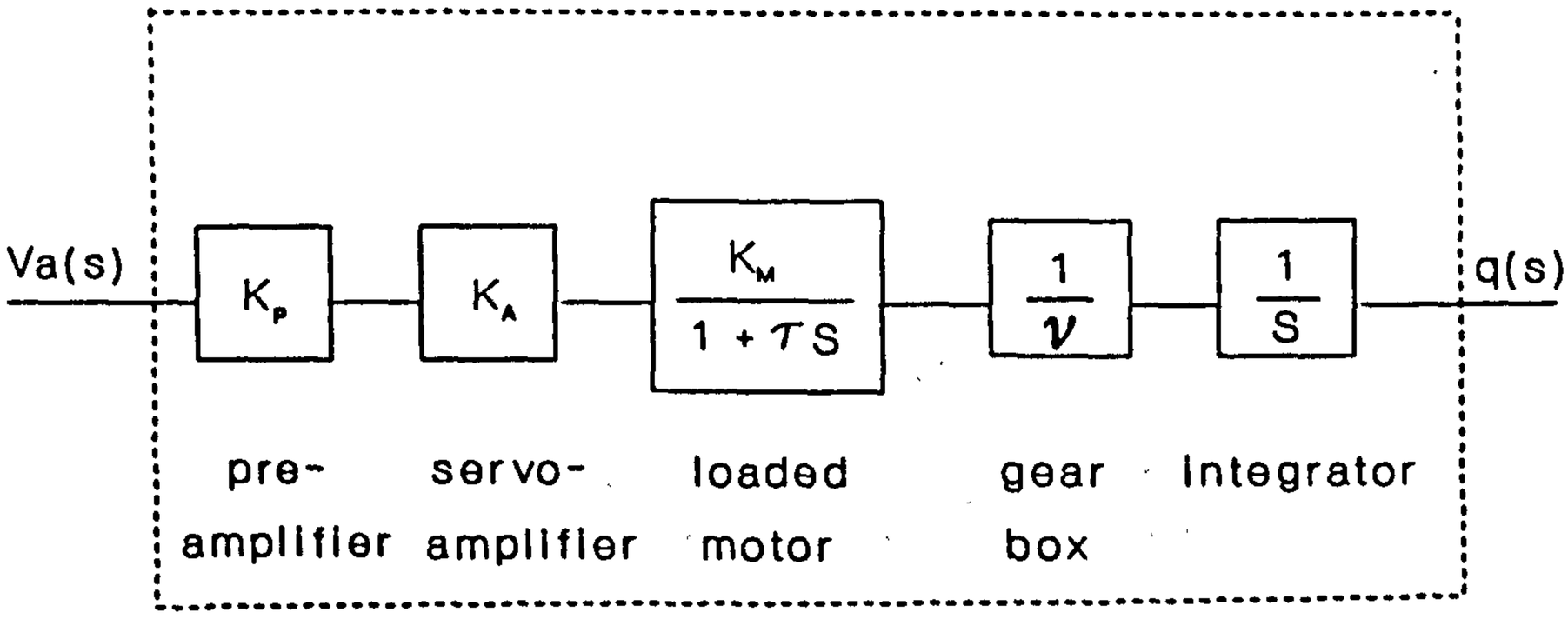

Fig.9.3:Block Diagram Of DC Servo-Actuator.

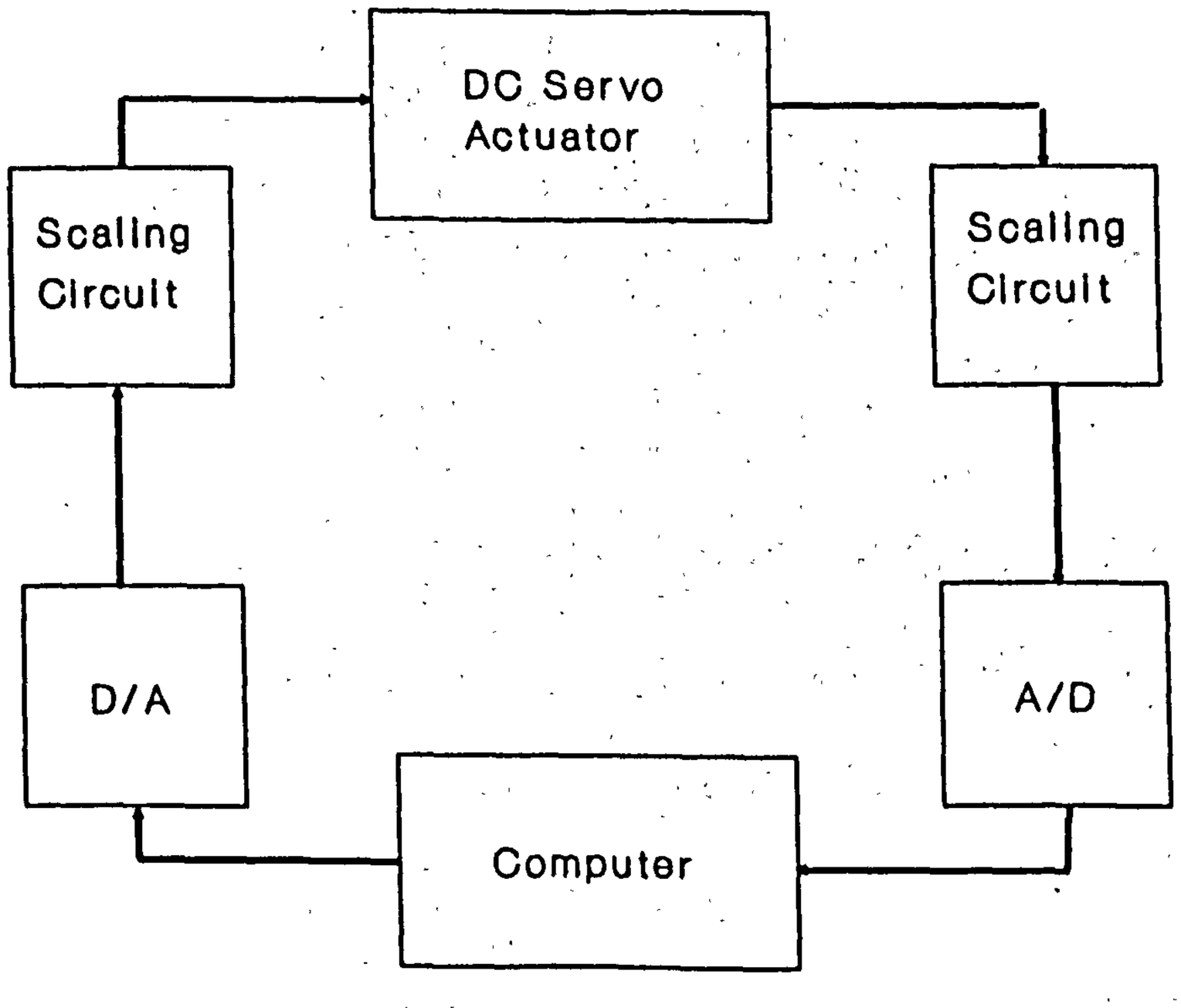

Fig.9.4:Block Diagram Of Experimental System.

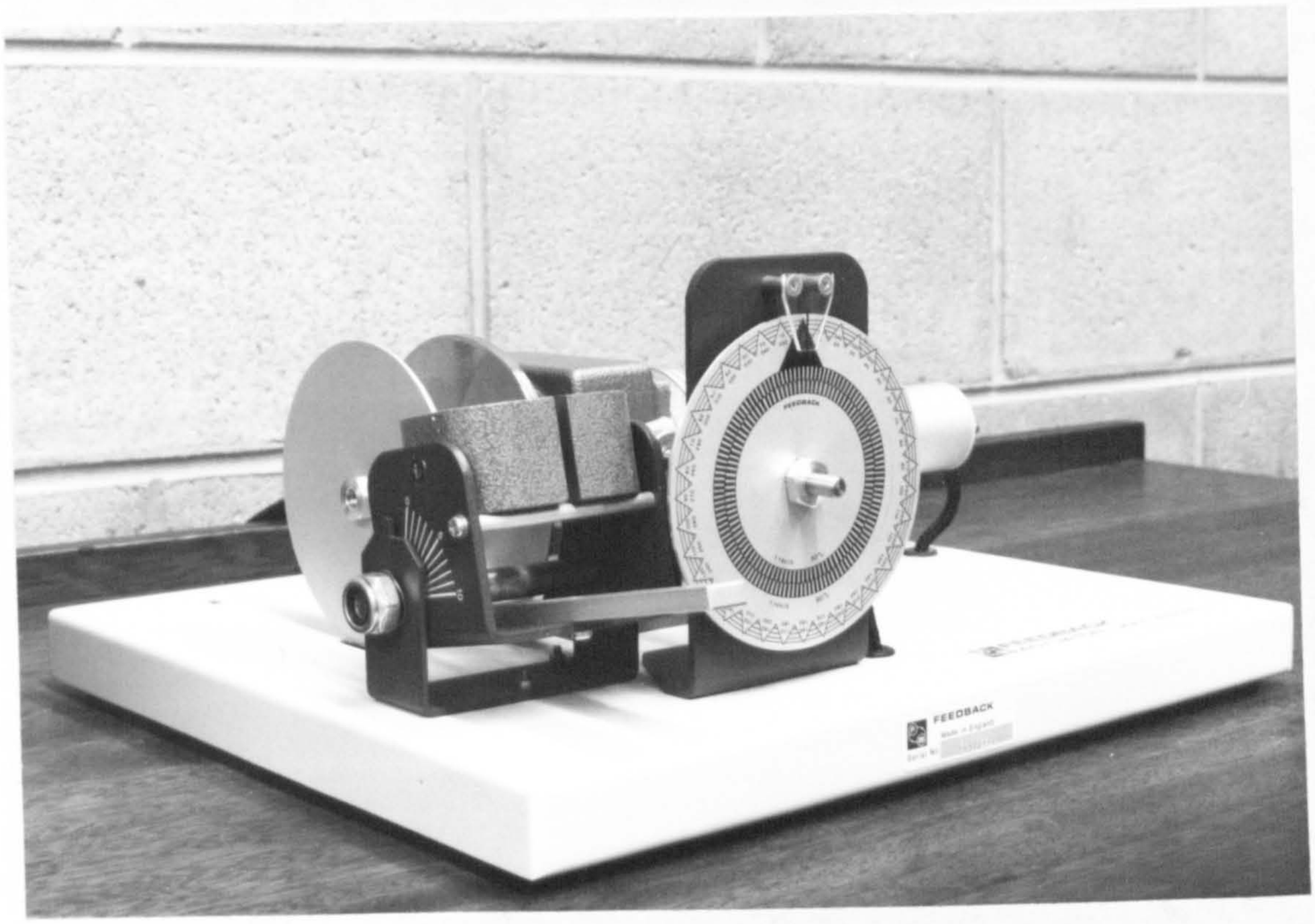

Fig.9.5: DC Servo-Actuator.

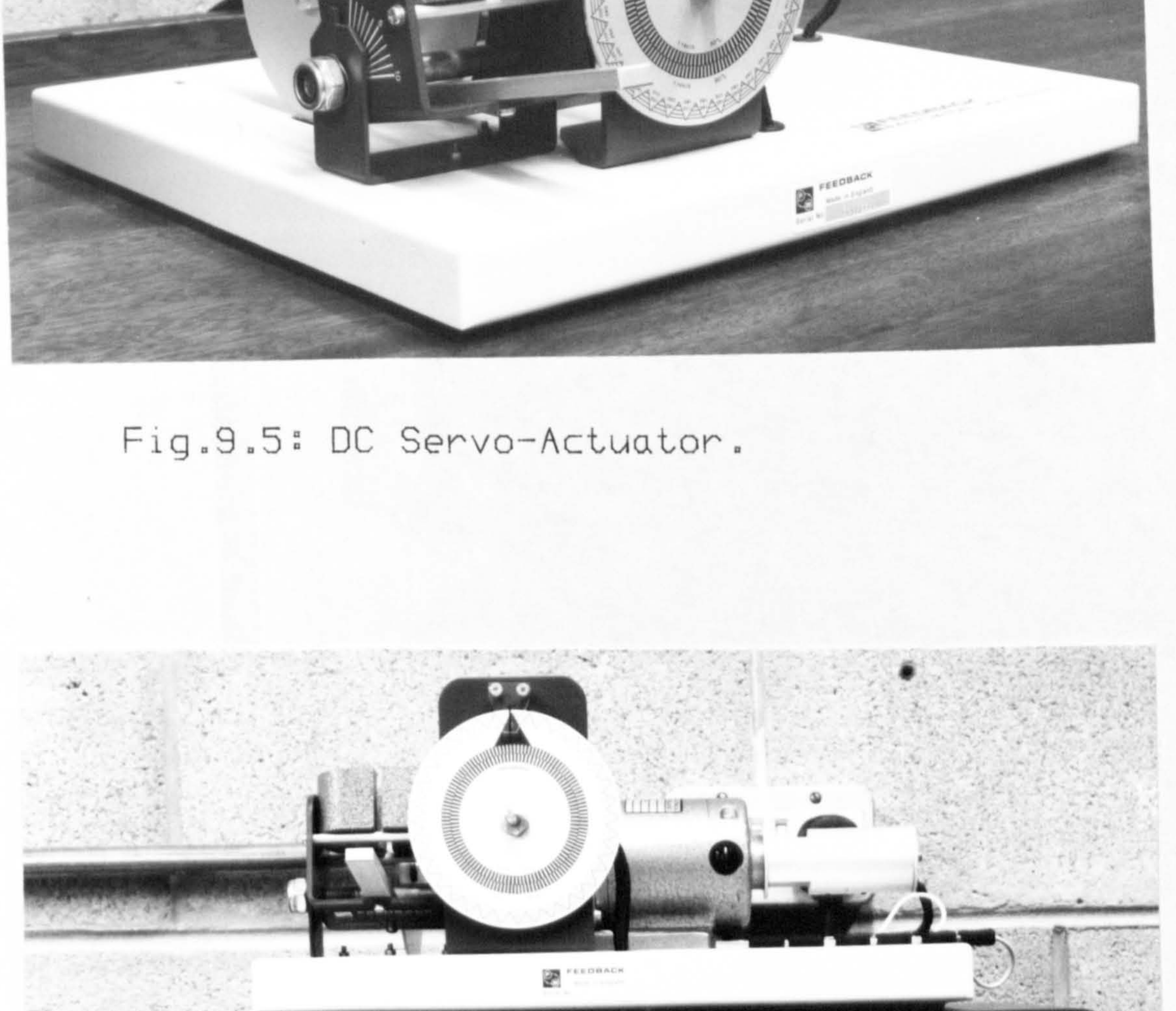

Fig.9.6: DC Servo-Actuator With Power Drive Unit.

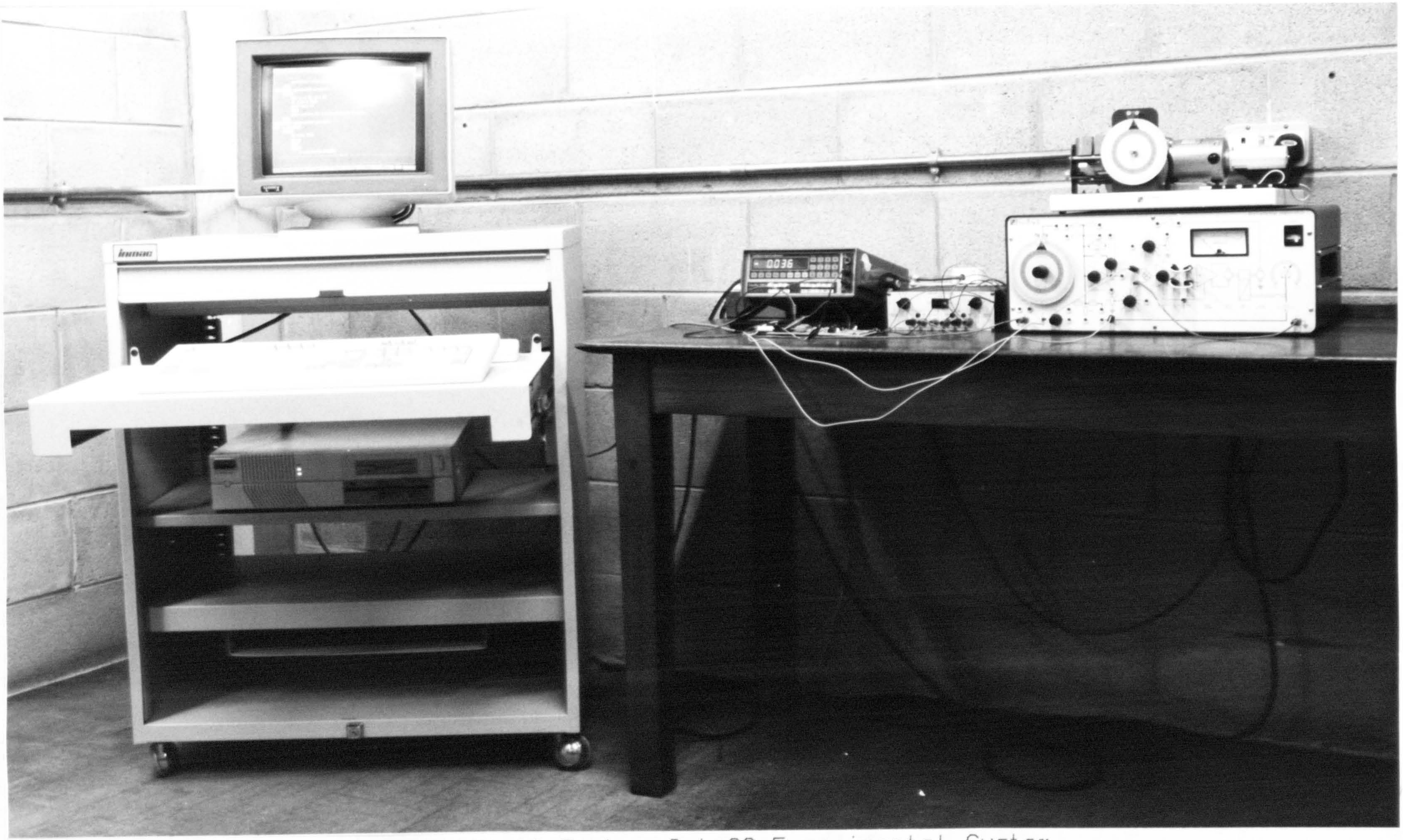

Fig.9.7: Lay-Out Of Experimental System.

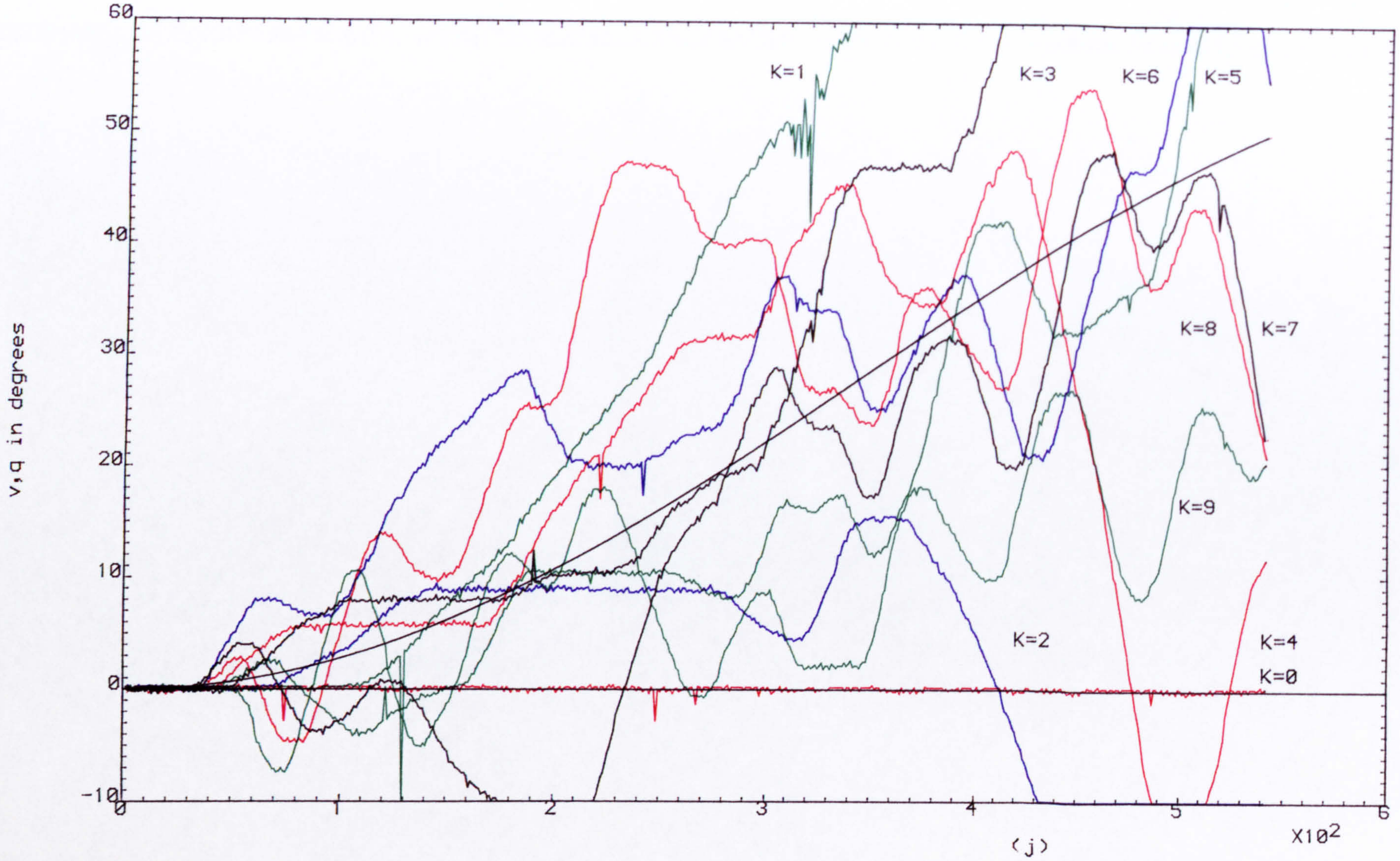

Fig.9.8:Successive Outputs Of DC Servo-Actuator
Under Digital Iterative Learning Control With
(dee=0.0,alfa=0.0,lambda=1.0).

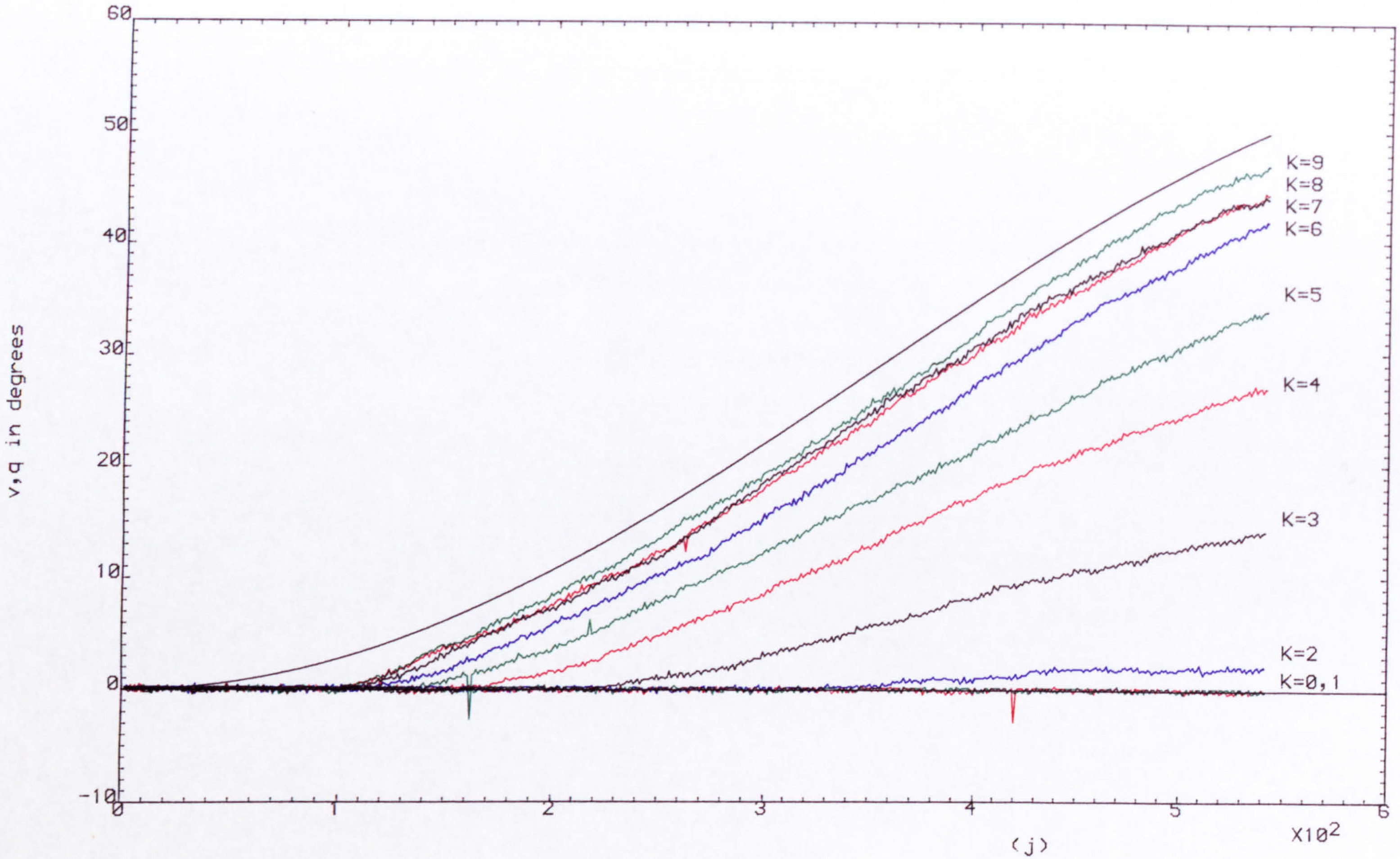

Fig.9.9:Successive Outputs Of DC Servo-Actuator
Under Digital Iterative Learning Control With
(dee=0.0,alfa=0.0,lambda=0.1).

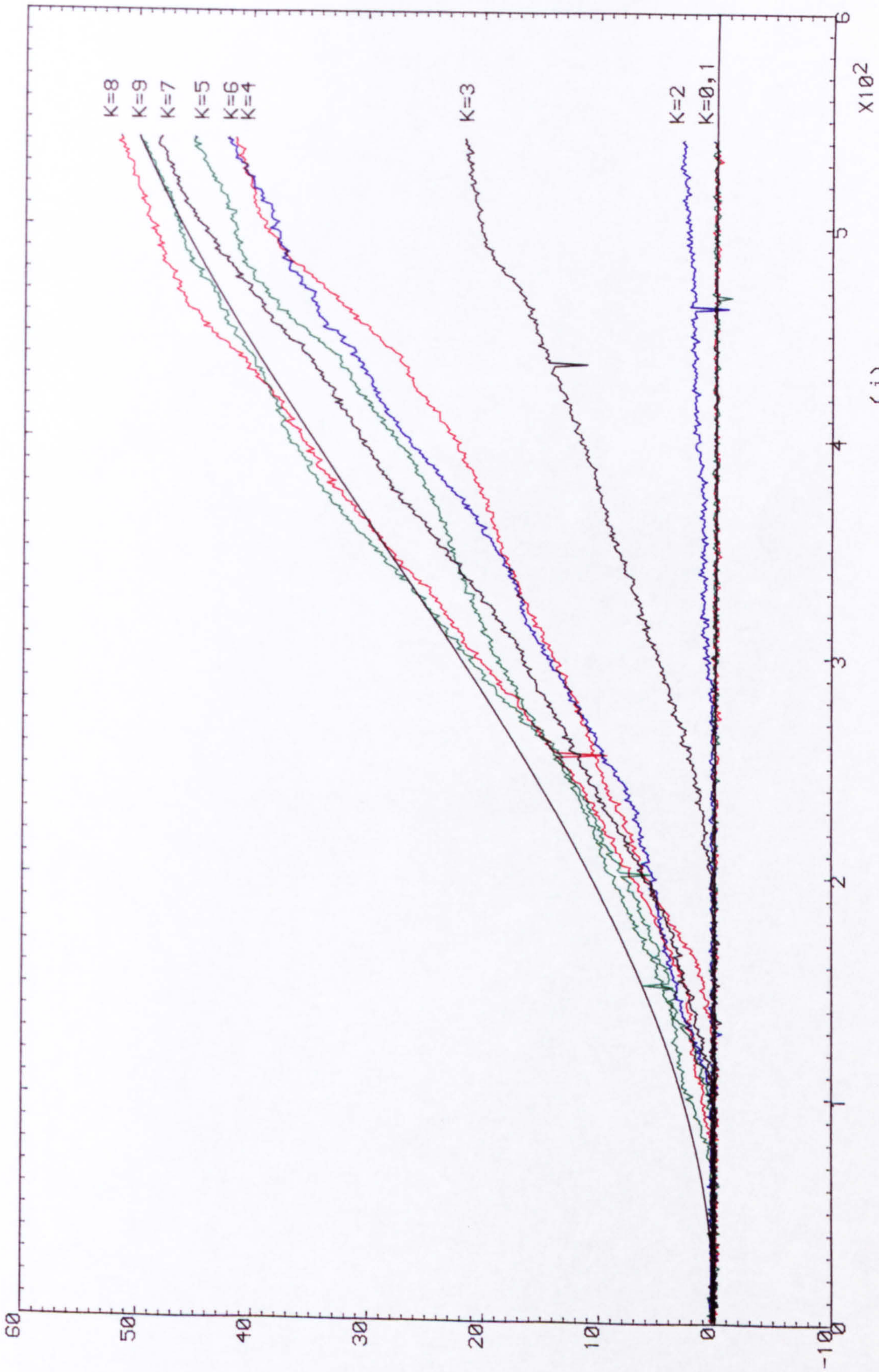

Fig.9.10:Successive Outputs OF DC Servo-Actuator Under Digital Iterative Learning Control With (dee=0.01,alFa=0.01,lambda=0.3).

PART VI

CONCLUSIONS AND RECOMMENDATIONS

CHAPTER 10

CONCLUSIONS AND RECOMMENDATIONS

10.1 CONCLUSIONS

In the last decade, much attention has been devoted to controllers that improve their performance progressively in tracking pre-specified trajectories, have simple structure, and involve simple algorithms. These controllers are so-called iterative learning controllers. The pioneer in designing and applying such controllers was Arimoto (1984,1985) who gave, for the first time, details of a controller that improves its performance progressively thus causing machines to learn without the help of human operators.

Unfortunately, this controller like many others has many limitations and, in particular, requires that the plant under control be regular. This means that linear time-invariant plants must have full-rank first Markov parameters and therefore that velocity variables must be chosen as output rather than positional variables in robotic applications. In addition, the plants under control must have known time-invariant state-space models. Finally, the methodology of Arimoto (1984,1985) yields analogue controllers which must then be digitalised for purpose of implementation. Therefore, the objective of this research was to eliminate all these limitations.

In order to achieve this objective, this research has proposed different new design methodologies. The methodologies proposed in Chapters 2 and 3 illustrate clearly the fact that analogue iterative learning controllers can be designed for plants with any order of irregularity, using initial state shifting or initial impulsive action. These proposed methodologies rely only on the Markov parameters of the state-space model

in the synthesis of their control laws. However, although the irregularity problem was solved using such controllers, two other problems remained. These are the need for the explicit state-space model of the plants under control in the synthesis of the control law, and also the need for the digitalisation of such controllers for the purpose of implementation.

In Chapter 4, a new design methodology has accordingly been proposed for the design of digital iterative learning controllers that circumvents the need for detailed mathematical models in state-space form. The proposed methodology relies only on input/output data in the synthesis of the control law. It has thus been shown that digital iterative learning controllers can be readily designed for multivariable plants of any order of irregularity using such input/output data in the form of step-response matrices.

In these studies of analogue and digital iterative learning controllers, two very important parameters have emerged, namely, ρ and σ. Thus, it has been found that the parameter ρ dictates whether learning occurs or not, whilst both parameters ρ and σ dictate the quality of the learning performance and the speed of convergence. Indeed, it has been shown that keeping both parameters at very small values achieves good learning performance and rapid convergence. However, the relation between these two parameters is unfortunately inversely proportional. Therefore, if one parameter is increased the other must be decreased and as a result the learning performance and convergence are affected positively or negatively depending on the values of these two parameters. It has been found, in the case of irregular plants, that the value of σ is high compared with that for regular plants and that this value increases as the order of irregularity increases. This discovery has led to the introduction of compensators in the design of digital iterative learning controllers for irregular plants. These compensators help to reduce the value of the learning

parameter, σ, without having to increase the value of ρ and so both the learning performance and convergence of irregular plants are improved. In addition, it has been found that the required number of compensators increases as the order of irregularity increases.

Since digital iterative learning controllers use step-response matrices in the synthesis of their control laws and since the step-response characteristics of plants can be identified in real time, it has been shown in this thesis that iterative learning controllers can readily be rendered adaptive. In these adaptive controllers, recursive least square (RLS) parameter estimators have been used to estimate the elements of the step-response matrices for inclusion in the digital control laws. It has been shown that such identifiers are rapid and accurate, and that the resulting adaptive digital iterative learning controllers are highly effective in preventing performance degradation due to unknown dynamical charactersitics of the model.

The effectiveness of all these analogue and digital iterative learning controllers in providing high-quality performance has been demonstrated through comprehensive simulation studies. Furthermore, design studies have been presented in order to demonstrate the applicability to robotics of the design methodologies described in this thesis. This demonstration has been effected by designing both analogue and digital model-based iterative learning controllers for a typical two-link manipulator in both Cartesian and joint spaces. These studies have indicated that such model-based iterative learning controllers are robust in the sense that rapid learning behaviour is obtained even when crude models are used, as a result of large reduction gear ratios. Moreover, these design studies include designing adaptive digital iterative learning controllers for the two-link manipulator in both Cartesian and joint spaces. By identifying the step-response matrices of such robotic manipulators along their trajectories in both Cartesian and joint spaces respectively, it has been shown that

such manipulators are amenable to adaptive iterative learning control.

Finally, it has been shown in this thesis that digital iterative learning controllers can be implemented practically. Their effectiveness has been illustrated by implementing such controllers in the real-time positional control of a dc servo-actuator, which is a typical completely irregular plant. Therefore, it can be concluded that the research objectives set out at the beginning of this thesis have been achieved.

10.2 RECOMMENDATIONS FOR FURTHER WORK

The strength and power of the proposed iterative learning controllers presented in this thesis can be considered as a step forward in achieving highly effective and sophisticated intelligent machinery. However, the proposed iterative learning controllers still need to be investigated further.

Thus, the issue of robustness of such iterative learning controllers with respect to the existence of initialisation errors should be investigated. At the moment, the algorithms assume that the initial states are regulated precisely at the beginning of each successive iteration. Moreover, the robustness of such controllers with respect to the existence of measurement noise and disturbances needs to be investigated. In particular, the solution to this problem suggested by Arimoto (1991a,1991b) (by introducing a forgetting factor in the iterative learning algorithm) warrants close scrutiny.

The introduction of compensators in the case of high-order irregularity plants did not significantly reduce the parameter σ, and the trade-off technique therefore had to be used to achieve such reductions. This has been proven to be undesirable, since the learning rate will be adversely affected. Therefore, a solution to this problem must be

found. In addition, there is a need to investigate whether a compensator can be found so that the learning parameter, σ, can be reduced without producing 'ringing phenomena' in the control signal.

In addition, it has been shown that the smallest values of σ can be achieved if all the eigenvalues of the open-loop plant are located at the origin of the s-domain. So, if a mechanism could be found to shift all the open-loop eigenvalues of plants to the origin prior to the implementation of iterative learning controllers, very good learning performance and rapid convergence would then be expected. Furthermore, the proposed digital and analogue are restricted to operate in a finite time interval $(0,T_f)$ and it is not clear how such controllers will operate over $(0,\infty)$. Therefore, it is important to determine whether this information obtained over $(0,T_f)$ for a specific trajectory can be used to learn the other trajectories over larger periods. There is also a need to investigate whether the bounds of the rate of change of error obtained in this thesis can be made less conservative, so that qualitative and quantitative information can be obtained more easily from such bounds. Finally, the practical implementation of such controllers in the real-time positional and velocity control of robotic manipulators would be a real step forward towards making such machines more intelligent.

APPENDICES

APPENDIX A

In this appendix, three issues are explained in connection with the analogue iterative learning controllers of Chapters 2 and 3. This explanation can conveniently be given by answering the following three questions:

(i) how do such analogue iterative learning controllers emerge?

(ii) why is initial state shifting necessary for learning to occur?

(iii) why is the choice of the design parameter D so specific?

In order to answer question (i), it is worth recalling that Arimoto et al in (1984) proposed iterative learning controllers with control laws of the form

$$w_{k+1}(t) = w_k(t) + \Gamma\, \dot{e}_k(t) \qquad \text{...(A.1)}$$

in connection with plants governed by state and output equations of the respective forms

$$\dot{x}(t) = Ax(t) + Bu(t) \qquad \text{...(A.2a)}$$

and

$$y(t) = Cx(t) \qquad \text{...(A.2b)}$$

In such cases, Arimoto et al (1984) stated that "it is impossible to choose the positional variable as an output" if the plant governed by equation (A.2) is irregular, i.e. the plant has a rank defective first Markov parameter CB. This limitation was removed in the present thesis by introducing compensators with transfer function matrices of the form $(I_m + Ds)$, where $D \in R^{m \times m}$, as pre-filters between the iterative learning

controller of equation (A.1) and the plant under control. Figure A.1 shows how such pre-filters can be introduced in cascade with the plant when the plant under control is first-order irregular.

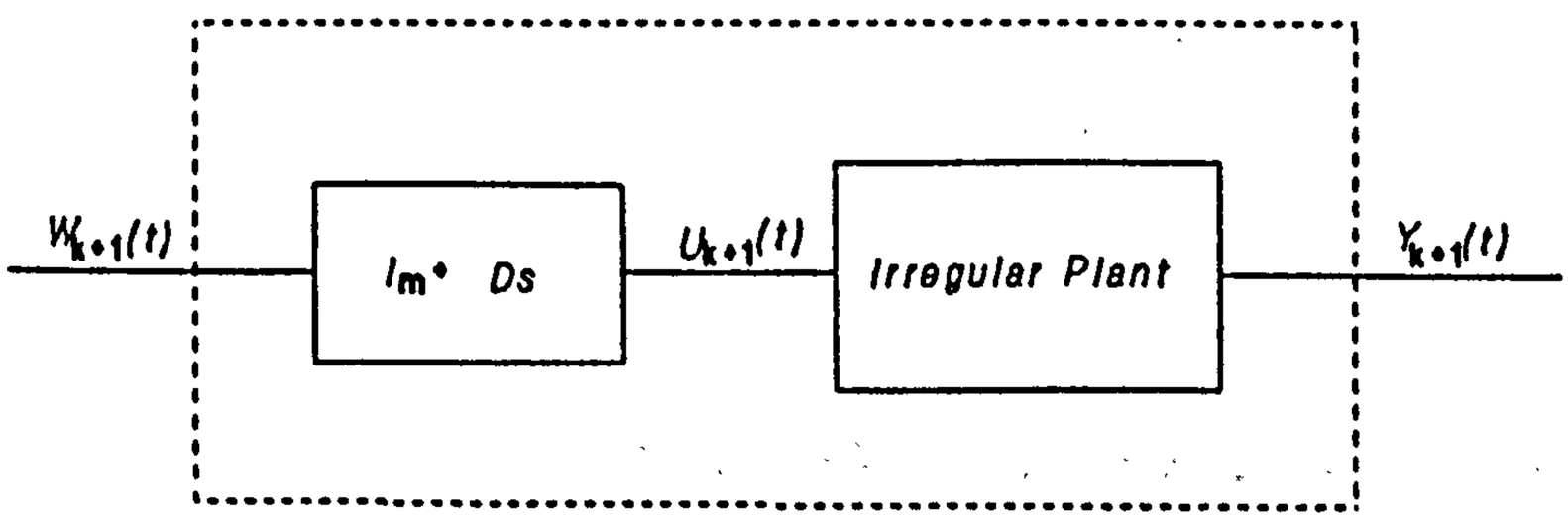

Figure A.1 Irregular plant in cascade with a pre-filter.

Thus,

$$u_{k+1}(t) = (I_m + Ds)\, w_{k+1}(t) \qquad \text{...(A.3)}$$

where $u_{k+1}(t)$ is the new input to the plant and $w_{k+1}(t)$ is given by equation (A.1). It is therefore evident from equation (A.3) that

$$u_{k+1}(t) = w_{k+1}(t) + D\, \dot{w}_{k+1}(t) \qquad \text{...(A.4)}$$

Now, substituting equation (A.1) in (A.4) gives

$$u_{k+1}(t) = w_{k+1}(t) + \Gamma\, \dot{e}_k(t) + D\, \dot{w}_k(t) + D\, \Gamma\, \ddot{e}_k(t) \qquad \text{...(A.5)}$$

But, according to equation (A.4), it follows that

$$u_{k+1}(t) = u_k(t) + \Gamma\, \dot{e}_k(t) + D\, \Gamma\, \ddot{e}_k(t) \qquad \text{...(A.6)}$$

or

$$u_{k+1}(t) = u_k(t) + K_1\,\dot{e}_k(t) + K_2\,\ddot{e}_k(t) \qquad \text{...(A.7)}$$

where

$$K_1 = \Gamma \qquad \text{...(A.8a)}$$

and

$$K_2 = D\,\Gamma \qquad \text{...(A.8b)}$$

Thus, the iterative learning controller of Chapter 2 has emerged. Similar procedures must be followed in case the plant under control has higher-order irregularity. In such cases, the pre-filter must have a transfer function matrix of the form

$$\left[I_m + \frac{2}{T} D_1\right]\left[I_m + \frac{2}{T} D_2\right].....\left[I_m + \frac{2}{T} D_\ell\right]$$

where ℓ is the order of the irregularity and $D_i \in R^{m\times m}$ $(i = 1,2,....,\ell)$.

In order to answer question (ii) regarding the introduction of initial state shifting in the controller of Chapter 2, it is necessary to re-examine Figure A.1. This indicates that the overall time-invariant linear multivariable plant is governed by a state equation of the form

$$\dot{x}(t) = Ax(t) + Bw(t) + BD\,\dot{w}(t) \qquad \text{...(A.9)}$$

which is clearly not in the standard state-space form. However, the state equation of such a plant can be represented in the standard state-space form according to Porter and Bradshaw (1972a, 1972b, 1972c). Thus, introducing in equation (A.9) the state

$$\chi(t) = x(t) - BD\ w(t) \qquad \ldots(A.10)$$

of the equivalent plant, it follows immediately that

$$\dot{\chi}(t) = A\ \chi(t) + (B + ABD)\ w(t) \qquad \ldots(A.11)$$

This is the differential equation of the overall plant in the standard state-space form.

Now, for learning to occur in the $(k+1)th$ iteration in such plants, it follows from the results of Chapter 2 that

$$\chi_{k+1}(0) = \chi_k(0) \ , \ (k = 0, 1, 2, \ldots) \qquad \ldots(A.12)$$

But equation (A.10) at the kth and $(k+1)th$ iterations indicates that

$$\chi_{k+1}(t) = x_{k+1}(t) - BD\ w_{k+1}(t) \qquad \ldots(A.13)$$

and

$$\chi_k(t) = x_k(t) - BD\ w_k(t) \qquad \ldots(A.14)$$

It therefore follows from equations (A.12), (A.13) and (A.14) that

$$x_{k+1}(0) - BD\ w_{k+1}(0) = x_k(0) - BD\ w_k(0) \qquad \ldots(A.15)$$

so that

$$x_{k+1}(0) = x_k(0) + BD\ (w_{k+1}(0) - w_k(0)) \qquad \ldots(A.16)$$

Therefore, according to equation (A.1), it is evident that

$$x_{k+1}(0) = x_k(0) + B\,K_2\,\dot{e}_k(0) \qquad \text{...(A.17)}$$

since, according to equation (A.8),

$$K_2 = D\,\Gamma$$

Thus, equation (A.17) indicates that the initial state of the irregular plant must be shifted at the beginning of each successive iteration by the amount $B\,K_2\,\dot{e}_k(0)$ for learning to occur. Similar procedures must be followed to determine by how much the initial state must be shifted in the case of plants with higher-order irregularity characteristics for learning to occur.

Finally, in order to answer question (iii) regarding the choice of the design parameter D, it is worth noting that the transfer function matrix of the overall plant shown in Figure A.1 is

$$(C(sI - A)^{-1}B)\,(I + Ds)$$

$$= \left(\frac{CB}{s} + \frac{CAB}{s^2} + \frac{CA^2B}{s^3} + \ldots\right)(I + Ds)$$

$$= \frac{CB}{s} + \frac{CAB}{s^2} + \frac{CA^2B}{s^3} + \ldots.$$

$$+ CBD + \frac{CABD}{s} + \frac{CA^2BD}{s^2} + \ldots.$$

$$= CBD + \frac{(CB+CABD)}{s} + \frac{(CAB+CA^2BD)}{s^2} + \ldots. \qquad \text{...(A.18)}$$

Therefore, the design parameter D must be chosen so that $CBD = 0$ in order to make the compensated plant proper. Then, according to equation (A.18), the matrix

($CB+CABD$) is the first Markov parameter of the equivalent plant which can be made full-rank if the plant is first-order irregular. Similar procedures must be followed if the plant under control has higher-order irregularity characteristics. Thus, for example, if the plant is second-order irregular, a two-stage pre-filter is required to cure this irregularity problem. Then, the transfer function matrix of the overall plant is

$$(C(sI-A)^{-1}B)\,(I + D_1 s)\,(I + D_2 s)$$

$$\left[\frac{CB}{s} + \frac{CAB}{s^2} + \frac{CA^2B}{s^3} + \frac{CA^3B}{s^4} + \ldots\right][I + (D_1+D_2)s + D_1D_2\,s^2]$$

$$= CB\,(D_1 + D_2) + CAB\,D_1D_2 + CB\,D_1D_2\,s$$

$$+ \frac{[CB + CAB(D_1 + D_2) + (CA^2BD_1D_2)]}{s} + \frac{[CAB + CA^2B(D_1+D_2) + CA^3\,BD_1D_2]}{s^2}$$

$$+ \ldots\ldots \qquad \ldots(A.19)$$

Thus, it is clear that D_1 and D_2 must be chosen so that $CBD_1D_2 = 0$ and $CB(D_1+D_2) + CABD_1D_2 = 0$ in order to make the compensated plant proper. Then, according to equation (A.19), the matrix $[CB+CAB(D_1+D_2)+(CA^2BD_1D_2)]$ is the first Markov parameter of the equivalent plant which can be made full-rank if the plant is second-order irregular.

REFERENCES

REFERENCES

Ahn, H.S. and Choi, C.H.: "Iterative learning controllers for linear systems with disturbances", Electronics Letters, Vol. 26, pp.1542-1544, 1990.

An, C.H., Atkeson, C.G. and Hollerbach, J.M.: "Model-Based Control of a Robot Manipulator", The MIT Press, 1988.

Arimoto, S., Kawamura, S. and Miyazaki, F.: "Bettering operation of robots by learning" J. of Robotic Systems, pp.123-140, 1984.

Arimoto, S., Kawamura, S. and Miyazaki, F.: "Can mechanical robots learn by themselves?" Proc. 2nd International Symposium Robotics Res., Kyoto, Japan, pp.127-134, 1984.

Arimoto, S., Kawamura, S. and Miyazaki, F.: "Bettering operation of dynamics systems by learning; A new control theory of servo-mechanisms or mechatronics systems", Proc. of 23rd IEEE Conference on Decision and Control, Las Vegas, NV, pp.1064-1069, 1984.

Arimoto, S., Kawamura, S. and Miyazaki, F. and Tamakis, S.: "Learning control theory for dynamical systems", Proc. of 24th IEEE Conference on Decision and Control, Ft. Lauderdale, FL, pp.1375-1380, 1985.

Arimoto, S.: "Mathematical theory of learning controls", Proc. 4th Yale Workshop on Applications of Adaptive Systems Theory, New Haven, CT, 1985.

Arimoto, S., Kawamura, S. and Miyazaki, F.: "Convergence, stability and robustness of learning control schemes for robot manipulators", Recent Trends in Robotics: Modelling, Control and Education, eds. Jamshidi, M. Luh, L. and Shahinpoor, M. pp.307-316, Elsevier Publishing Co., Inc. 1986.

Arimoto, S., Miyazaki, F. and Kawamura, S.: "Motion control of robotic manipulator based on motor program learning", Proc. of the Symposium on Robot Control, IFAC, 1988.

Arimoto, S.: "Learning control theory for robotic motion", International J. of Adaptive Control and Signal Processing, Vol. 4, pp.543-564, 1990.

Arimoto, S.: "Passivity of robot dynamics implies capability of motor program learning", Proc. of the Workshop on Nonlinear and Adaptive Control, Applications to Robotics, Grenoble, 1990.

Arimoto, S.: "Robustness of learning control for robot manipulators", Proc. of IEEE International Conference on Robotics and Automation, Cincinnati, Ohio, pp.1528-1533, 1990.

Arimoto, S., Naniwa, T. and Suzuki, H.: "Robustness of p-type learning control with a forgetting for robotic motions", Proc. of 29th IEEE Conference on Decision and Control, Honolulu, Hawaii, 1990.

Arimoto, S.: "Learning for skill refinement in robotic systems", IEICE Transactions, Vol. E 74, pp.235-243, 1991.

Arimoto, S. and Miyazaki, F.: "Asymptotic stability of feedback control laws for robot

manipulators", IFAC Symposium on Robot Control, Barcelona, pp.447-452, 1985.

Aström, K.J., Borissonm U., Ljung, L. and Wittenmark, B.: "Theory and application of self-tuning regulators", Automatica, Vol. 13. pp.457-476, 1977.

Aström, K.J. and Wittenmark, B.: "Adaptive Control", Addison-Wesley Publishing Co., 1989.

Atkeson, C.G. and McIntyre, J.: "Robot trajectory learning through practice", Proc. of IEEE International Conference on Robotics and Automation, San Francisco, pp.1737-1742, 1986.

Bien, Z. and Huh, K.M.: "Higher-order iterative learning control algorithm", IEEE Proc., Vol. 136, pp.105-112, 1989.

Borison, U.: "Self-tuning regulator for a class of multivariable systems", Automatica, Vol. 15, pp.209-215, 1979.

Clark, D.W.: "Introduction to self-tuning controllers", in self-tuning and adaptive control: theory and applications, C.J. Harris and S.A. Billings, (Eds.), Peter Peregrinus, London, 1981.

Craig, J.J.: "Adaptive control of manipulators through repeated trials", Proc. American Control Conference, San Diego, pp.1566-1574, 1984.

Craig, J.J.: "Introduction to Robotics, Mechanics and Control", Addison-Wesley Publishing Co., Reading, 1986.

Craig, J.J.: "Adaptive Control of Mechanical Manipulators", Addison-Wesley Publishing Company, 1988.

Desoer, C.A. and Vidyasagar, M.: "Feedback Systems: Input-Output Properties", Academic Press, 1975.

Fortesque, T.R., Kersherbaum, L.S. and Yolstie, B.E.: "Implementation of self-tuning regulators with variable forgetting factors", Automatica, Vol. 17, pp.831-835, 1981.

Furuta, K. and Yamakita, M.: "Iterative generation of optimal input of a manipulator", Proc. of IEEE Conference on Robotics and Automation, San Francisco, pp.579-584, California, 1986.

Furuta, K. and Yamakita, M.: "The design of a learning control system for multivariable systems", Proc. of IEEE International Symposium on Intelligent Control, Philadelphia, Pennsylvania, pp.371-376, 1987.

Goodwin, G.C. and Sin, K.S.: "Adaptive Filtering Prediction and Control", Prentice-Hall, New Jersey, 1984.

Goldenthal, W. and Farrell, J.: "Application of neural networks to automatic control", Proc. of AIAA, Guidance, Navigation and Control Conference, Portland, Oregon, pp.1108-112, 1990.

Hara, S. and Yamarmoto, Y.: "Stability of repetitive control systems", Proc. 24th Conference on Decision and Control, Vol. 1, Ft. Lauderdale, FL, pp.326-327, 1985.

Hara, S., Yamarmoto, Y., Omata, T. and Nakano, M.: "Repetitive control systems: a

new type servo system for periodic exogenous signals", IEEE Trans. Automatic Control, Vol. 33, pp.659-668, 1988.

Hwang, D.H. Bien, Z. and Oh, S.R.: "Iterative learning control method for discrete-time dynamics systems", IEE proc., Vol. 138, pp.139-144, 1991.

Ishihara, T., Abe, K. and Takeda, H.: "A design of discrete time repetitive control system", Trans. Soc. Instrum. Contr. Eng., 21, pp.43-49, 1986.

Kawamura, S., Miyazaki, F. and Arimoto, S.: "Iterative learning control for robotic systems", Proc. of IECON '84, Tokyo, Japan, pp.393-348, 1984.

Kawamura, S. Miyazaki, F. and Arimoto, S.: "Applications of learning method for dynamic control of robot manipulators", Proc. of 24th IEEE Conference on Decision and Control, Fort Lauderdale, Florida, pp.1381-1386, 1985.

Kawamura, S., Miyazaki, F. and Arimoto, S.: "Hybrid position, force control of robot manipulators based on learning method", Proc. of '85 International Conference on Advanced Robotics, Tokyo, pp.235-242, 1985.

Kawamura, S., Miyazaki, F. and Arimoto, S.: "Intelligent control of robot motion based on learning method", Proc. of IEEE International Symposium on Intelligent Control, Philadelphia, Pennsylvania, 1987.

Kawamura, S., Miyazaki, F. and Arimoto, S.: "Realization of robot motion based on a learning method", IEE Trans. Sys. Man. and Cybern., SMC-18, 1, pp.126-134, 1988.

Kawato, M., Etoh, M., Oda, Y. and Tsukahara, N.: "A new algorithm for voltage

clamp by iteration : learning control of a nonlinear neuronal system", Biological Cybern., Vol. 53, pp.57-66, 1985.

Kawato, M., Furukawa, K. and Suzuki, R.: "A hierarchial neural-network model for control and learning of voluntary movement", Biological Cybern., Vol. 57, pp.169-185, 1987.

Kuc, T., Nam, K. and Lee, J.S.: "An iterative learning control of robot manipulators", IEEE Trans. on Robotics and Automation, Vol. 7, pp.835-842, 1991.

MacFarlane, A.G.J.: "Dynamical System Models", G.G. Harrap and Co. Ltd., 1970.

Messner, W., Horowitz, R., Kao, W.W. and Boals, M.: "A new adaptive learning rate", IEEE Trans. on Automatic control, Vol. 36, pp.188-197, 1991.

Miller III, W.T., Glanz, F.H. and Kraft III, L.G.: "Application of a general learning algorithm to the control of robot manipulators", International J. of Robotic Research, Vol. 6, pp.84-98, 1987.

Miller III, W.T.: "Sensor-based control of robotic manipulators using a general learning algorithm", IEEE J. of Robotics and Automation, Vol. RA-3, pp.157-165, 1987.

Miller III, W.T., Hewes, R.P., Glanz, F.H. and Kraft III, L.G.: "Real-time dynbamic control of an individual manipulator using a neural-network based learning controller", IEEE Trans. on Robotics and Automation, Vol. 6, pp.1-9, 1990.

Mita, T and Kato, E.: "Iterative control and its application to motion control of robot arm - a direct approach to servo-problems", Proc. of IEEE 24th Conference on

Decision and Control, Ft. Lauderdale, FL., pp.1393-1398, 1985.

Mita, T., Kato, E. and Aoki, Y.: "Iterative control and its applications to the trajectory control of robot manipulators", Proc. of 24th SICE conference, pp.1223-1230, 1985.

Oh, S-R, Bien, Z. and Suh, I.H.: "An iterative learning control method with application for the robot manipulator", IEEE J. of Robotics and Automation, Vol. 4, pp.508-514, 1988.

Petropoulakis, L.: "Design of digital trajectory tracking systems for robotic manipulators", Ph.D. Thesis, University of Salford, 1986.

Porter, B. and Mohamed, S.S.: "Iterative learning control of irregular plants with initial state shifting", Electron. Lett., Vol. 26, pp.106-107, 1990.

Porter, B. and Mohamed, S.S.: "Iterative learning control of irregular plants with initial impulsive action", Electron. Lett., Vol. 26, pp.851-852, 1990.

Porter, B. and Mohamed, S.S.: "Model-based iterative learning control of robotic manipulators", Proc. of Mathematical and Intelligent Models in System Simulation, IMACS, pp.293-297, 1990.

Porter, B. and Mohamed, S.S.: "Model-based iterative learning control of space-shuttle manipulator", Proc. of AIAA, Guidance, Navigation and Control Conference, Portland, Oregon, pp.743-746, 1990.

Porter, B. and Mohamed, S.S.: "Robustness characteristics of model-based iterative

learning controllers for robotic manipulators", Proc. of the IEEE Int. Workshop on Intelligent Motion Control, Istanbul, Turkey, pp.123-129, 1990.

Porter, B. and Mohamed, S.S.: "Iterative learning control of partially irregular multivariable plants with initial state shifting", Int. J. Systems Sci., Vol. 22, pp.229-235, 1991.

Porter, B. and Mohamed, S.S.: "Iterative learning control of partially irregular multivariable plants with initial impulsive action", Int. J. Systems Sci., Vol. 22, pp.447-454, 1991.

Porter, B. and Mohamed, S.S.: "Design of adaptive iterative learning controllers", Proc. of IFAC Int. Symposium on Intelligent Tuning and Adaptive Control, Singapore, 1991.

Porter, B. and Mohamed, S.S.: "Adaptive iterative learning control of robotic manipulators in task space", Proc. of AIAA, Guidance, Navigation and Control Conference, New Orleans, LA, pp.1614-1620, 1991.

Porter, B. and Mohamed, S.S.: "Digital iterative learning control of linear multivariable plants", Int. J. Systems Sci., (to be published) June, 1992.

Porter, B. and Mohamed, S.S.: "Learning rates in the digital iterative learning control of linear multivariable plants", Int. J. Systems Sci., (to be published) July, 1992.

Porter, B. and Mohamed, S.S.: "Digital iterative learning control of compensator linear multivariable plants", Int. J. Systems Sci., (to be published) August, 1992.

Porter, B. and Mohamed, S.S.: "Digital iterative learning control of unknown multivariable plants", to be published in Proc. of IEEE Int. Symposium on Intelligent Control, Glasgow, Scotland, 1992.

Porter, B. and Bradshaw, A.: "Multivariable time-invariant linear systems with input-derivative control : state controllability and eigenvalue assignability", Int. J. Control, Vol. 16, pp.101-104, 1972.

Porter, B. and Bradshaw, A.: "Mode controllability characteristics of multivariable time-invariant systems with input-derivative control", Int. J. Control. Vol. 16, pp.105-107, 1972.

Porter, B. and Bradshaw, A.: "Eigenvalue assignment in multivariable linear systems with input-derivative control", Int. J. Control, Vol. 16, pp.109-113, 1972.

Saelid, S. and Foss, B.: "Adaptive controllers with a vector variable forgetting factor", Proc. of 23rd IEEE Conference on Decision and Control, pp.1488-1494, 1983.

Seraji, H.: "An approach to multivariable control of manipulators", Transactions of the ASME, Vol. 109, pp.146-154, 1987.

Seraji, H., Jamshidi, M., Kim, Y. and Shahinpoor, M.: "Linear multivariable control of two-link robots", J. or Robotic Systems, Vol. 3, pp.349-365, 1986.

Seraji, H.: "Direct adaptive control of manipulators in cartesian space", J. of Robotic Systems, Vol. 4, pp.157-178, 1987.

Shoureshi, R., Evans, R. and Swedes, D.: "Learning control for autonomous

machines", ASME paper 88-WA/DSC-29, 1988.

Shoureshi, R., Evans, R. and Stevenson, W. "Optically driven learning control for industrial manipulators", presented at the 1988 American Control Conference, Atlanta, Georgia, 1988.

Spong, M.W. and Vidyasagar, M. "Robot Dynamics and Control", J. Wiley and Sons, New York, 1989.

Sugie, T. and Ono, T.: "On a learning control law" Systems and Control (Japan), Vol. 31, pp.129-135, 1987.

Togai, M. and Yamano, O. "Discrete learning control and its application to controlling industrial robots", Proc. of IEEE on Intelligent Control, pp.152-157, 1985.

Togai, M. and Yamano, O.: "Learning control of robot manipulators", SIAM Conference Geometric Modelling and Robitics, Albany, NY, 1985.

Togai, M. and Yamano, O.: "Analysis and design of an optimal learning control scheme for industrial robots: a discrete system approach", Proc. of IEEE 24th Conference on Decision and Control, Ft. Lauderdale, FL, pp.1399-1404, 1985.

Uchiyama, M.: "Formation of high-speed motion pattern of a mechanical arm by trial", Transactions of Society of Instrumentation and Control Engineers, Vol. 21, Japan, pp.706-712, 1978.

Ward, T., Ralston, P. and Stoll, K.: "Intelligent control of machines and processes", Computers Ind. Engineering, Vol. 19, pp.205-209, 1990.

Yuan, J.S-C.: "Dynamic decoupling of a remote manipulator system", IEEE Transaction in Automatic Control, pp.713-717, 1978.